

Studies Related to Tandem Reactivity of 1-Carbomethoxy-5-dicyanomethyl-1,3-cyclohexadiene

by

Anthony P. Krismanich

A thesis

Presented to the University of Waterloo

in fulfillment of the

thesis requirement for the degree of

Doctor of Philosophy

in

Chemistry

Waterloo, Ontario, Canada, 2006

© Anthony Krismanich 2006

Author's Declaration for Electronic Submission of a Thesis

I hereby declare that I am the sole author of this thesis. This is a true copy of the thesis, including any required final revisions, as accepted by my examiners.

I understand that my thesis may be made electronically available to the public.

Anthony Krismanich

Acknowledgements

I would like to thank Professor Gary Dmitrienko for his long and patient guidance in the course of this work and in the preparation of this thesis. His collaboration and great intellectual example have been a great pleasure and the better part of my total education.

I would also like to thank the succession of friends in the lab and department who have been great company and excellent and inspiring coworkers.

For academic and administrative help, thank you: Dr. Nicholas Taylor for the determination of X-ray crystal structures; Mrs. Jan Venne for advice and aid in the carrying out of NMR experiments; and Mrs. Cathy van Esch for infinite patience in the conduct of administrative affairs over the years.

Thank you as well to my advisory committee — Dr. Donald Mackay, Dr. John Honek, and Dr. Adrian Schwan — for their useful insights and suggestions in committee meetings and for their contributions in the improvement of this work.

Abstract

A set of studies centered around the reactions of the active methine compound 1-carbomethoxy-5-dicyanomethyl-1,3-cyclohexadiene (the “ring-opened adduct”), obtained by base-induced ring-opening of the Diels-Alder adduct of 5,5-dicyanocyclopentadiene and methyl acrylate, has been carried out. A plan was devised for the anionic (at the dicyanomethyl carbon) ring-opened adduct whereby its reaction with electrophiles, for example Michael reactions with double-bond acceptors, would generate reactive intermediates that would undergo cyclization by tandem conjugate addition to the $\alpha,\beta,\gamma,\delta$ -unsaturated ring π -system to generate bicyclic compounds. In practice, reaction with di-*tert*-butyl methylidenemalonate, methyl vinyl ketone, and cyclopentenone generated intermediates that exhibited greater tandem reactivity than was anticipated: the bicyclic enolates were found to cyclize further by Thorpe-Ziegler-like reaction with the proximal nitrile to generate, after facile acid hydrolysis, substituted known tricyclic skeleta termed homobrendanes, specifically, tricyclo[5.2.1.0^{4,8}]decenes. An attempt was made to generalize the reaction to other substrates, among them singly-activated Michael acceptors and 1,2-heteroatom electrophiles, but the generalization of the homobrendane forming reaction did not meet with success. Attempted functional group manipulations to probe the conversion of the homobrendane derived from di-*tert*-butyl methylidenemalonate to the homobrendane natural product 2-isocyanoallopupukeanane revealed the unreactivity of the skeletal double-bond toward electrophiles and the high reactivity of the ring ketone toward nucleophiles, among them mCPBA which brought about Baeyer-Villiger reaction, and chloride and hydroxide, which brought about addition/elimination reactions to cleave the last-formed homobrendane ring.

The ring-opened adduct was also envisaged as a potential substrate in intramolecular Heck reactions. To this end, Heck substrates were generated from the ring-opened adduct anion and iodo- and bromo-benzyl halides. A key observation at this stage pertained to the unexpected acidity of the ring-opened adduct C5 proton, which could be deprotonated by DBU to bring about allylic isomerization, a finding that would provide a key insight to the pattern of reactivity later evidenced with alkyl propiolates. Optimization of the Heck substrate-generating reaction was followed by Heck reactions under Jeffery's conditions, which generated angular tricycles as intended, accompanied by aromatic compounds generated by base-induced HCN elimination/rearrangement and dehydrogenation. The Jeffery's conditions were optimized to limit the production of aromatics.

The possibility of ring-opened adduct-derived vinyl silane intermediates undergoing cationic cyclizations led to a minor study based upon the bromination of allylsilanes and the elimination of TMSBr from 1,2-dibromo-3-trimethylsilyl compounds, accessible compounds unaccounted for in the review literature. It was determined that the combination of HBr and Br₂ (perhaps as HBr₃) was required to eliminate TMSBr, in contravention of the textbook account of electrophilic substitutions being the inherent reactions of allylsilanes and Br₂.

Unexpected tandem reactivity was observed in the reactions of the anionic ring-opened adduct and alkyl propiolates under catalytic DBU conditions. Rather than tandem cyclization or simple adduct formation, the allenolate intermediates were determined to undergo extremely facile formal allenolate Cope rearrangements involving the γ,δ -double-bond of the parent ring. Excess base intercepted the allenolate by deprotonating ring C5 and effecting 1,2-vinyl transfer by 3-*exo*-trig addition-elimination. The chemistry of the highly delocalized side-chain carbanion in the Cope product was studied in detail.

Dedicated to my long-suffering parents

Table of Contents

Chapter 1: Introduction

1.1 Purpose.	1
1.2 Cyclization Reactions.	2
1.2.1 General Introduction.	2
1.2.2 Tandem Anionic Cyclizations.	9
1.2.3 Metal-Catalyzed Cyclizations.	14
1.2.4 Cationic Cyclizations.	15
1.3 Conclusion.	16
References.	18

Chapter 2: Tandem Anionic Cyclization of the Ring-Opened Adduct

2.1 Introduction.	19
2.1.1 Project Origin.	19
2.1.2 Ilimaquinone, Puupehenone and the Entry to the Main Focus of Research.	20
2.1.3 Chemistry 5,5-Dicyanocyclopentadiene.	24
2.2 Results and Discussion.	42
2.2.1 Attempted Diels-Alder Reactions.	42
2.2.2 Reaction of Ring-Opened Adduct with Doubly-Activated Michael Acceptors.	48
2.2.3 Reaction of Ring-Opened Adduct with Singly-Activated Michael Acceptors and Heteroatom 1,2-addition Partners.	54
2.2.4 Exploratory Functional Group Manipulations Related to Conversion of Homobrendane 2-74 to 2-Isocyanoallopupukeanane.	67
2.2.4.1 General Comments.	67
2.2.4.2 Reactivity of the Ring Ketone of 2-74 Evidenced in Attempted Functional Group Conversions at Other Sites.	71
2.2.4.3 Other Attempted Functional Group Conversions.	77
2.3 Experimental.	79
2.3.1 General Experimental.	79
2.3.2 Experimental Details.	82
References.	97

Chapter 3: Intramolecular Heck Reactions of Halobenzyl Adducts of the Ring-Opened Compound

3.1 Introduction.	100
3.2 Results and Discussion.	108
3.2.1 Synthesis of Substrate for Intramolecular Heck Reaction.	108
3.2.2 Intramolecular Heck Reactions of Adducts 3-3	116
3.2.3 Conclusions and Future Work.	144
3.3 Experimental.	147
3.3.1 Supplemental General Experimental.	147
3.3.2 Experimental Details.	147
References.	162

Chapter 4: Bromination of Allyl Silanes: Insights Into Ionic and Free Radical Reaction Pathways

4.1 Introduction.	165
4.2 Results and Discussion.	166
4.3 Experimental.	187
4.3.1 Supplementary General Experimental.	187
4.3.2 Experimental Details.	188
References.	197

Chapter 5: Novel Reactivity of the Adducts of the Ring-Opened Adduct and Alkyl Propiolates

5.1 Introduction.	198
5.2 Results and Discussion.	200
5.2.1 Structure Elucidation of Novel Product.	200
5.2.2 Identification of Minor Components of Cope Product Mixture.	223
5.2.3 Cleavage and Aromatization of Cope Product 22	232
5.2.4 Reactivity of Anionic 5-32	237
5.2.5 Attempted Generalization of Allenolate Cope Reactions.	256
5.2.6 Attempted Allenolate Cope Rearrangements with Stoichiometric and Excess Base.	263

5.2.6.1 Attempted Allenolate Cope Rearrangement with Stoichiometric DBU Followed by Acidic Workup.263
5.2.6.2 Attempted Allenolate Cope Rearrangement with Stoichiometric DBU Without Acidic Workup.268
5.2.6.3 Attempted Allenolate Cope Rearrangement with Excess Base280
5.2.6.4 Attempted Allenolate Cope Rearrangements with Strong Base281
5.2.7 Mechanistic Considerations and Assessment of Reactive Species in Formal Allenolate Cope Rearrangements.288
5.2.7.1 Introduction.288
5.2.7.2 Mechanism of Cope Rearrangement and Influence of Substituents.289
5.2.7.3 Assessment of the Reactive Species.296
5.2.7.4 Other Examples of Allenolate-Based [3,3]-Rearrangements.313
5.3 Conclusions and Future Work319
5.4 Experimental.321
5.4.1 Supplementary General Experimental.321
5.4.2 Experimental Details.321
References.336

List of Schemes

Chapter 1

- Scheme 1-1.** General modes and products of cyclization. 2
- Scheme 1-2.** Robinson's synthesis of tropinone. 8
- Scheme 1-3.** Anionic cyclizations of **1-2** and general unsaturated substrates. 9
- Scheme 1-4.** Cyclization by a sequence of Michael and 1,6-conjugate addition. 10
- Scheme 1-5.** General reflexive Michael reaction of cyclohexenone and its complementarity to the Diels-Alder reaction. 11
- Scheme 1-6.** General tandem Michael cyclization to generate five-membered rings. . . . 11
- Scheme 1-7.** PGB₁ analog dimerization by tandem Michael-Michael cyclization. 12
- Scheme 1-8.** Triple Michael cyclization of enolate **1-6**. 13
- Scheme 1-9.** Synthesis of ishwarane precursor by reflexive Michael cyclization and bromide displacement. 13
- Scheme 1-10.** Alternative reflexive Michael reaction of a bifunctional donor to generate a five-membered ring. 14
- Scheme 1-11.** Intramolecular Heck reactions planned for a substrate **1-11** derived from **1-1**. 15
- Scheme 1-12.** Initial synthetic outlook for the study of cationic reactions of allylsilanes. . . 16

Chapter 2

- Scheme 2-1.** Outline of synthesis of puupehenone and related compounds. 23
- Scheme 2-2.** Ketene 2 + 2 cycloaddition in the synthesis of penicillin analogs. 25
- Scheme 2-3.** Conversion of 5-alkylated cyclopentadiene into both [1,5]-H shift products. 25
- Scheme 2-4.** 5,5-Disubstituted functional equivalent of monosubstituted cyclopentadiene. 26
- Scheme 2-5.** Rouse and Tyler's synthesis of 5,5-dimethylcyclopentadiene. 27

Scheme 2-6. Eilbracht and coworkers' route to 5,5-dialkylcyclopentadienes.	27
Scheme 2-7. Oediger and Möller's synthesis of 4,4-disubstituted cyclopentenes.	28
Scheme 2-8. Failure of attempted synthesis of 5,5-dicarboethoxycyclopentadiene.	29
Scheme 2-9. Thandi's generation of 5,5-dicyanocyclopentadiene.	30
Scheme 2-10. Diels-Alder dimerization of 2-40	30
Scheme 2-11. Generation of solely heterodimers in Diels-Alder reactions of mixed quantities of cyclopentadiene, 2-40 , and methyl acrylate.	35
Scheme 2-12. Base-induced ring opening of furan/methyl acrylate Diels-Alder adduct. . .	39
Scheme 2-13. Friesen's ring-opening of 2-49 and trapping of 2-55 with electrophiles. . .	40
Scheme 2-14. Ring-opening of 2-49 as a retro-Michael addition.	40
Scheme 2-15. Potential synthesis of "push-pull-stabilized" quinodimethanes.	41
Scheme 2-16. Two aromatizations of 2-56 carried out by R. Friesen.	42
Scheme 2-17. Epoxidation of 2-56 carried out by R. Friesen.	42
Scheme 2-18. Generation of dibromide 2-63 and tricyclic compound 2-64 by R. Friesen.	43
Scheme 2-19. Conversion of 2-49 to triester 2-67 by R. Friesen.	43
Scheme 2-20. Generation of di- <i>tert</i> -butyl methylenemalonate.	48
Scheme 2-21. Generation of tricyclic tandem conjugate addition product 2-74	50
Scheme 2-22. Generation of bicyclic bis-alkylated compound 2-76 at long reaction times in the presence of excess di- <i>tert</i> -butyl methylenemalonate.	52
Scheme 2-23. Cleavage of labile adduct 2-77 in acetone-d ₆	57
Scheme 2-24. Generation of aromatic adduct 2-78 by aromatization of adduct intermediate.	58
Scheme 2-25. Possible isomerization mechanisms following 1,4-addition to cyclopentenone.	63
Scheme 2-26. Possible isomerization mechanisms following 1,2-addition to cyclopentenone.	65
Scheme 2-27. Tandem conjugate addition products derived from 2-56 and cyclopentenone.	66

Scheme 2-28. Trost and coworkers' synthesis of hirsutic acid C via a homobrendane intermediate.	69
Scheme 2-29. Ho and coworkers' synthesis of (\pm)-2-isocyanoallopupukeanane (2-91).	70
Scheme 2-30. Generalized plan for double-bond bisfunctionalization of an appropriately substituted homobrendane derivative as part of 2-isocyanoallopupukeanane synthesis.	72
Scheme 2-31. Unexpected quantitative Baeyer-Villiger reaction of 2-74 to exclusion of double-bond epoxidation.	73
Scheme 2-32. Planned Barton decarboxylation of acid 2-115 derived from 2-74	73
Scheme 2-33. Generation of bicyclic compound 2-123 in attempted nucleophilic cleavage of carbomethoxy methyl group.	75
Scheme 2-34. Unintended reaction pathway in attempted basic hydrolysis of 2-74	77
Scheme 2-35. Failure of iodolactonization of 2-74	78
Scheme 2-36. Cleavage and decarboxylation of <i>t</i> -butyl esters of 2-74	78

Chapter 3

Scheme 3-1. General intramolecular Heck reaction.	101
Scheme 3-2. Synthesis of (\pm)-dehydrotubifoline by intramolecular Heck reaction.	107
Scheme 3-3. Substrate preparation and intramolecular Heck reactions devised for 3-2	108
Scheme 3-4. Generation of intramolecular Heck reaction substrates.	109
Scheme 3-5. Generation of deconjugated adduct isomer 3-8a by anionic site equilibration among the ring-opened adduct population prior to addition of alkylating agent.	112
Scheme 3-6. Generation of deconjugated adduct isomer 3-8a by deprotonation of adduct 3-3a	113
Scheme 3-7. Aromatized side-products in initial attempted intramolecular Heck reaction.	121
Scheme 3-8. Product distribution (^1H NMR) in attempted intramolecular Heck reaction halted prior to total consumption of starting material.	122
Scheme 3-9. Generation of phenanthrene by intramolecular aryl bromide to arene coupling under Jeffery's conditions.	123

Scheme 3-10. Heck cyclization of aromatized substrates 3-20a and 3-18a	124
Scheme 3-11. Generation of putative substituted phenanthrenes 3-21 and 3-22	126
Scheme 3-12. First instance of generation of Heck product 3-4	129
Scheme 3-13. Aromatization of Heck substrate 3-3a by base-induced HCN elimination and sigmatropic hydrogen shift.	130
Scheme 3-14. Generation of 2-iodo-benzyl bromide.	135
Scheme 3-15. Epimerization of palladated carbon to enable <i>syn</i> - β hydride elimination by oxoallyl palladium isomerization as posited by Branchaud and coworkers, or by isomerization via base-induced enolate.	137
Scheme 3-16. Base-induced epimerization of palladium-bearing carbon to permit <i>syn</i> β -hydride elimination leading to 3-4	138
Scheme 3-17. Base-induced <i>anti</i> elimination of H-PdXL _n proposed by Thal and co-workers and the analogous reaction of 3-30	138
Scheme 3-18. Predicted and observed intramolecular Heck reaction products of mixture of substrate isomers 3-3b and 3-8b	142
Scheme 3-19. Proposed mechanism of palladium reduction by dehydrogenation of Heck substrates.	143
Scheme 3-20. Conversion of nitriles to prevent HCN elimination from Heck substrates.	146
 Chapter 4	
Scheme 4-1. Proposed cationic cyclization of ring-opened adduct derivative 4-5	165
Scheme 4-2. Generation of regioisomeric trimethylsilylallyl bromides 4-4 and 4-8	166
Scheme 4-3. Results of bromination of 4-9 reported by Fleming and Au-Yeung.	167
Scheme 4-4. Results of bromination of allyltrimethylsilane with bromine reported by Sommer, Tyler, and Whitmore.	167
Scheme 4-5. Product mixtures observed by Thandi in attempted bromination of 4-9	168
Scheme 4-6. Generation of TMS dibromide 4-15 by Weeratunga in this laboratory.	168
Scheme 4-7. Repeat in this laboratory of the experiment of Sommer and co-workers.	169
Scheme 4-8. Generation of bicyclic allylsilane 4-9	170

Scheme 4-9. Generation of dibromide 4-13 and vinyl TMS allyl bromide 4-14	171
Scheme 4-10. Product distribution in bromination of 4-9 under the conditions reported by Fleming and Au-Yeung.	172
Scheme 4-11. Summary of key attempted elimination reactions of 4-15	175
Scheme 4-12. Results of Carre et al. in brominations of various allylsilanes.	176
Scheme 4-13. Unreactivity of 4-13 toward Br ₂ , HBr, and HBr/Br ₂	179
Scheme 4-14. Competing outcomes for neutralization of bromonium intermediate in bromination of 4-9	182
Scheme 4-15. Proposed mechanism for HBr ₃ catalysis of TMSBr elimination from 4-15	184
Scheme 4-16. Possible steric and electronic factors in failure of 4-13 to eliminate TMSBr.	185
 Chapter 5	
Scheme 5-1. Expected products of Michael addition of ring-opened adduct anion to propiolate esters.	199
Scheme 5-2. Allylic isomerization to the likely ring arrangement of the unidentified product.	208
Scheme 5-3. Intramolecular mechanism for ring allylic isomerization.	210
Scheme 5-4. Anionic mechanism for 1,3-nitrile migration within side-chain to establish putative structure for unknown major product.	212
Scheme 5-5. Pathway to putative identity 5-17 via side-chain vinylic deprotonation.	213
Scheme 5-6. Generation of 5-22 by formal [1,3]-alkyl shift.	218
Scheme 5-7. Anionic formal 1,3-shift of C3-C3' bond to generate identity 5-22	218
Scheme 5-8. Formal allenolate Cope rearrangement to generate 5-22	220
Scheme 5-9. Formation of deconjugated adduct 5-28	226
Scheme 5-10. Products of cleavage/aromatization of the formal Cope product.	227
Scheme 5-11. A formal mode of cleavage and aromatization of 5-22	230

Scheme 5-12. Radical mechanism for the conversion of 5-22 to methyl benzoate and 5-32232
Scheme 5-13. Generation of methyl benzoate and 5-32 from 5-22 by alternative Cope/retro-ene reaction sequences.234
Scheme 5-14. Generation of methyl benzoate and 5-32 from 5-22 by an eight-centered reaction and [1,3]-H shift.235
Scheme 5-15. Literature example of a putative vinylogous homoene reaction.236
Scheme 5-16. Resistance of methylenecyclohexadienes to aromatization by [1,3]-H shift.236
Scheme 5-17. A suprafacial, configuration-retaining [1,3]-alkyl shift.237
Scheme 5-18. Expected synthesis of 5-32237
Scheme 5-19. Available exchange pathways for exhaustive H–D exchange of 5-49 and DBU–H ⁺246
Scheme 5-20. Catalytic excess DBU permits total H–D exchange of DBU–H ⁺ counterion independent of 70 mol percent exchange of 5-49248
Scheme 5-21. Dimerization of 5-49 and 5-32 by conjugate addition during mild acid workup.253
Scheme 5-22. Continuation of Cope reaction by neutralization of Cope product enolate.256
Scheme 5-23. Planned one-pot Cope rearrangement of a model substrate derived from allyl bromide.257
Scheme 5-24. Products of initial model Cope rearrangement.258
Scheme 5-25. Mode of generation of product distribution observed in attempted one-pot model Cope rearrangement.260
Scheme 5-26. Generation of model Cope substrate 5-65261
Scheme 5-27. Attempted allenolate Cope rearrangement of preformed substrate 5-65262
Scheme 5-28. New ring-opened adduct-propiolate adduct 5-69a observed in reaction conducted with stoichiometric base.265
Scheme 5-29. Conversion of direct adducts to adduct isomer 5-69a266
Scheme 5-30. Generation of adduct isomer 5-69 by pathway involving a reverse allenolate Cope rearrangement.267

Scheme 5-31. Initial constituents of the product mixture derived from formal allenolate Cope reaction employing one equivalent of DBU without acidic workup.270
Scheme 5-32. Development of a <i>meta</i> -substituted aromatic compound through aromatization of adduct isomer 5-71b271
Scheme 5-33. Geometric isomerism within the side-chain of the Cope rearrangement product.274
Scheme 5-34. Downfield shift in protons of thermodynamically more stable side-chain isomer by possible ring-current-like effect, or by ring current established through cyclization.276
Scheme 5-35. Nearly quantitative generation of 5-71b by treatment of 5-1 with a large excess of DBU.281
Scheme 5-36. Postulated role of conformation in allenolate Cope experiments conducted with DBU.286
Scheme 5-37. Proposed steric interactions upon conjugate addition promoting conformation change to position side-chain in pseudo-axial orientation.286
Scheme 5-38. Possible conformational features at work in generation of 5-71288
Scheme 5-39. Potential reactive species in Cope rearrangement of adduct of 5-1 and alkyl propiolates.296
Scheme 5-40. Diastereomeric product ratio as possible evidence of allenolate Cope rearrangement.298
Scheme 5-41. Coupling of neutral Cope rearrangement to generation of 5-69b in LHMS experiments.301
Scheme 5-42. Reasonably expected aromatization/cleavage substrates for conversion observed during adduct formation/allenolate Cope reaction.302
Scheme 5-43. Cope product anion is not observed to generate methyl benzoate and fragment anion.303
Scheme 5-44. Processes involved in allenolate Cope rearrangement.308
Scheme 5-45. Aromatization of neutral adduct 5-4 by retro-ene reaction.309
Scheme 5-46. Processes involved in neutral Cope rearrangement.311
Scheme 5-47. Processes involved in the allenol Cope rearrangement.313
Scheme 5-48. Claisen rearrangement in the addition of allyl alcohol to DMAD.314
Scheme 5-49. Aza-Claisen rearrangements in reactions of allylamines with DMAD.315

Scheme 5-50. Minor generation of allyl transfer product without allylic isomerization. . .	.317
Scheme 5-51. Potential for allenolate Cope rearrangement from optically pure ring-opened adduct as a 1,3-chirality transfer process.320

List of Figures

Chapter 1

- Figure 1-1.** Key substrate 5-dicyanomethyl-cyclohexa-1,3-dienecarboxylic acid methyl ester.1
- Figure 1-2.** Generalized summary of cyclization reactions.4

Chapter 2

- Figure 2-1.** Ilimaquinone.19
- Figure 2-2.** Puupehenone.21
- Figure 2-3.** Spiroconjugated compound spiro[4.4]nonatetraene.32
- Figure 2-4.** Frontier orbitals of **2-42**.32
- Figure 2-5.** Energies of frontier molecular orbitals of cyclopentadiene, **2-40**, and methyl acrylate.33
- Figure 2-6.** ORTEP: Diels-Alder adduct of MVK and 5,5-dicyanocyclopentadiene.46
- Figure 2-7.** ORTEP: Diels-Alder dimer of 5,5-dicyanocyclopentadiene.47
- Figure 2-8.** ORTEP: homobrendane skeleton derived from Diels-Alder adduct **2-49** or ring-opened adduct **2-56** and di-*tert*-butyl methylenemalonate.51
- Figure 2-9.** ORTEP: bicyclic bis-alkylated compound **2-76**.53
- Figure 2-10.** ORTEP: homobrendane **2-79** derived from ring-opened adduct and MVK. . .59
- Figure 2-11.** Isomer of the ring-opened adduct produced in attempted tandem Michael reaction with cyclopentenone.62
- Figure 2-12.** Determination of relative stereochemistry of **2-83** by $^1\text{H}-^1\text{H}$ nOe difference spectroscopy.67
- Figure 2-13.** Structural relationships among several C_{10} tricyclic compounds related to 2-homobrendane.68
- Figure 2-14.** Schematic of functional group manipulations required in conversion of **2-74** to 2-isocyanoallopupukeanane.71

Chapter 3

- Figure 3-1.** “Textbook” intermolecular Heck reaction catalytic cycle with catalyst preactivation by phosphines.102
- Figure 3-2.** Common Heck reaction constituents identified as potential reducing agents for Pd(0).103
- Figure 3-3.** New catalytic cycle of intermolecular Heck reaction detailing phosphine-based palladium reduction and comprising anionic intermediates.105
- Figure 3-4.** Potential ring formulations for unknown alkylation product.110
- Figure 3-5.** Experimental 5J coupling constants among methylene protons in 2,4-dihydronaphthalene.111
- Figure 3-6.** Side-product in the alkylation of the ring-opened adduct with 2-bromobenzyl bromide.111
- Figure 3-7.** ORTEP: X-ray crystal structure of Heck product **3-4**.127
- Figure 3-8.** ORTEP: X-ray crystal structures of **3-16** (top) and **3-17** (bottom).128
- Figure 3-9.** Catalytic cycle comprising Pd(II)–Pd(IV) species posited by Yao et al. for a ligand-free Heck reaction involving Pd(OAc)₂.140
- Figure 3-10.** Postulated catalyst pre-activation and catalytic cycle in intramolecular Heck reactions of adduct **3-3**.144

Chapter 4

- Figure 4-1.** Structure of Diels-Alder dimer of 1-trimethylsilylcyclopentadiene.170
- Figure 4-2.** Potential structures of HBr₃.180

Chapter 5

- Figure 5-1.** ^1H NMR spectrum (500 MHz, CDCl₃) of product of reaction of ring-opened adduct with ethyl propiolate.201
- Figure 5-2.** ^1H NMR spectrum (bottom) of ethyl propiolate-derived Cope product, and ^1H – ^1H TOCSY spectra based upon irradiation of isolated one-proton signals at δ 7.32 (middle) and δ 7.27 (top).203
- Figure 5-3.** Scale-expanded ^1H NMR spectrum (bottom) of ethyl propiolate-derived Cope product, and ^1H – ^1H TOCSY spectra based upon irradiation of isolated one-proton signals at δ 7.32 (middle) and δ 7.27 (top).205

Figure 5-4. Initial Partial structure of novel compound.206
Figure 5-5. Expanded partial structure of novel compound.207
Figure 5-6. Determination of ring substitution pattern through observed ^1H - ^1H coupling pattern to decisive δ 6.77 resonance.209
Figure 5-7. Potential double-bond position and substitution assignment to 5-17 on the basis of side-chain vinyl proton count and vicinal proton coupling pattern.211
Figure 5-8. Observed olefinic ^{13}C resonance for side-chain C1' of novel compound and estimated resonances for side-chain bearing potential substitutions, as predicted by ChemNMR Pro functionality of CS ChemDraw Ultra®.214
Figure 5-9. Observed olefinic ^{13}C resonance for side-chain C2' of novel compound and estimated resonances for side-chain bearing potential substitutions, as predicted by ChemNMR Pro functionality of CS ChemDraw Ultra®.215
Figure 5-10. Ultimate structural assignment of novel compound as 5-22 on the basis of nitrile carbon chemical shifts.216
Figure 5-11. Fragmentation of methyl propiolate-derived rearrangement product in EI mass spectrum.217
Figure 5-12. Initial adduct intermediate.219
Figure 5-13. Set of potential reactive species in formal [3,3]-sigmatropic rearrangement.221
Figure 5-14. Numbering of allenolate Cope rearrangement product cited in Table 5-1.221
Figure 5-15. Expansion of ^1H NMR spectrum (500 MHz, CDCl_3) of ethyl propiolate Cope product mixture.223
Figure 5-16. Expansion of ^1H NMR spectrum (300 MHz, CDCl_3) of methyl propiolate Cope product mixture after several days' retention at room temp. in CDCl_3228
Figure 5-17. ^1H NMR spectral expansion reveals discrete signals of methyl benzoate and 5-32229
Figure 5-18. ^1H NMR spectrum (300 MHz, CDCl_3) of methyl propiolate Cope product after several days' aging in CDCl_3233
Figure 5-19. ^1H NMR spectra of CDCl_3 solution of DBU- H^+ salt of 5-49 . Bottom spectrum (300 MHz): initial; middle spectrum (500 MHz): 67 hours; top spectrum (500 MHz): 147 hours.241
Figure 5-20. Schematic ^1H NMR spectra for an equally-populated mixture of species 5-49 , 5-50 , and 5-51 (top); exchange product 5-50 (middle); and exchange product 5-51 (bottom).243

Figure 5-21. Resonance contributors and hybrid of fragment anion, and expected sites of D exchange at sites of electron-pair localization.244
Figure 5-22. Schematic and observed ¹ H NMR spectra reflecting conversion of species 5-49 to deuterated species 5-51245
Figure 5-23. Schematic mechanism of H–D exchange of 5-49 /DBU-H ⁺ salt. Two cycles (A→B→C) with one intervening replacement of CDCl ₃ conclude the exchange process.247
Figure 5-24. Expanded ¹ H NMR spectra (500 MHz, CDCl ₃) of the downfield region of 5-49 at the last observed stage of H–D exchange (top) and after addition of acetic acid.249
Figure 5-25. ¹ H NMR spectra (500 MHz, CDCl ₃) of neutral Cope product 5-22 (bottom) and Cope product/DBU-H ⁺ salt.251
Figure 5-26. Partial ¹ H NMR spectrum (300 MHz, CO(CD ₃) ₂) of 5-53 precipitated from CDCl ₃ solution. Broad signal superimposed upon C2-H signal at δ 3.0 is the protons of NH ₄ ⁺252
Figure 5-27. Differences in pK _a of analogous acidic protons in 5-22 and 5-57 as revealed by differential neutralization by saturated aqueous NH ₄ Cl of anions 5-24 and 5-58255
Figure 5-28. Sequential ¹ H NMR spectra of attempted stoichiometric DBU Cope reaction isolated without acidic workup. Bottom spectrum - initial; middle - 190 min.; top - 20 hrs.269
Figure 5-29. Elimination of vinyl ¹ H NMR signals upon isomerization of side-chain of Cope product anion.272
Figure 5-30. Sources of two observed signals for isomers of anionic Cope product based upon accidental chemical shift equivalence of indicated pairs of isomers.275
Figure 5-31. Generation of initial anionic side-chain <i>E</i> isomer by slight rotation of formal σ-bond in Cope enolate product derived via putative chair transition state.278
Figure 5-32. Relationship between conformation of Cope product and isomerism of side-chain anion, and tenable implication for the geometry of rearrangement.279
Figure 5-33. Temperature-dependent conformational preferences of substituted 1,3-cyclohexadienes.283
Figure 5-34. Potential relationships of ring face of anionic ring-opened adduct to counterions in the pseudoaxial conformation.285
Figure 5-35. Cope rearrangement of 1,5-cyclohexadiene.289
Figure 5-36. Transition state models for the Cope rearrangement.290

Figure 5-37. Resonance hybrid model of Cope rearrangement transition state.290
Figure 5-38. Consideration of formal allenolate Cope rearrangement in terms of substituent effects at C1, C3, C4, and C6.291
Figure 5-39. Bis-allyl radical character in the transition state of the Cope rearrangement of 3,3-dicyano-1,5-hexadiene.292
Figure 5-40. Bis-allyl radical character in the transition state of the formal allenolate Cope rearrangement.293
Figure 5-41. Delocalization of allyl radical character by C6 substituent in Cope rearrangement transition state.294
Figure 5-42. The Cope ring expansion of 1-allenyl-2-vinylcyclohexanes driven by decumulation of the allenyl subunit.295
Figure 5-43. Counterionic centers of the allenolate intermediate are at sufficient separation to provide opportunity for Cope rearrangement prior to neutralization.310

List of Tables

Chapter 2

Table 2-1. Attempted Diels-Alder reactions of 5,5-dicyanocyclopentadiene (**2-40**). 37

Table 2-2. Reactions of **2-49** and **2-56** with singly-activated Michael acceptors and heteroatom 1,2-acceptors. 55

Chapter 3

Table 3-1. Conditions and product distributions in alkylations of ring-opened adduct with halobenzyl halides. 114

Table 3-2. Conditions and product distributions in intramolecular Heck reactions of **3-3**. 131

Chapter 4

Table 4-1. TMSBr eliminations from **4-15** attempted with various reagents. 174

Chapter 5

Table 5-1. NMR spectral correlations (^1H - ^1H COSY, HMQC, HMBC) and positional assignments for formal Cope product **5-22**. 222

Table 5-2. Minor constituents of the formal allenolate Cope reaction product mixture. . . 231

Table 5-3. Product distributions in attempted one-pot model allenolate Cope reactions. 261

Table 5-4. Product distributions in allenolate Cope reaction at varied quantities of DBU. 304

Abbreviations

Δ	heated to reflux
Ac	acetyl
AgOTf	silver trifluoromethanesulfonate
br	broad
<i>t</i> -Bu	<i>tert</i> -butyl
CI	chemical ionization
COSY	correlated spectroscopy
mCPBA	<i>m</i> -chloroperbenzoic acid
d	doublet
DBU	1,8-diazabicyclo[5.4.0]undec-7-ene
DMAD	dimethyl acetylenedicarboxylate
DMF	N,N-dimethylformamide
DMSO	dimethylsulfoxide
EI	electron impact
EIMS	electron impact mass spectrometry
equiv.	equivalent(s)
Et	ethyl
g	gram
HOMO	highest occupied molecular orbital
HMBC	heteronuclear multiple bond correlation
HMQC	heteronuclear correlation through multiple quantum coherence
HPLC	high-performance liquid chromatography

HRMS	high resolution mass spectrum
Hz	Hertz
IR	infrared
JMOD	J-modulated
KHMDS	potassium hexamethyldisilazide
LDA	lithium diisopropylamide
LHMDS	lithium hexamethyldisilazide
m	multiplet
mp	melting point
Me	methyl
mmol	millimole
NBS	N-bromosuccinimide
NMR	nuclear magnetic resonance
nOe	nuclear Overhauser effect
py	pyridine
q	quartet
qn	quintet
RT	room temperature
s	singlet
t	triplet
TFA	trifluoroacetic acid
THF	tetrahydrofuran
TLC	thin layer chromatography

TMS	trimethylsilyl or trimethylsilane
TOCSY	totally correlated spectroscopy
Ts	<i>p</i> -toluenesulfonyl, tosyl
TsOH	toluenesulfonic acid

Chapter 1

Introduction

1.1 Purpose

This thesis comprises studies of cyclizations stemming from the formation of adducts of a substrate, previously developed and partially elaborated in our laboratory, with various classes of electrophiles such that the adducts are suited to ring closures upon the substrate moiety. Specifically, the dicyanomethyl-substituted conjugated carbomethoxycyclohexadiene **1-1** (Figure 1-1) was deemed a promising candidate for cyclization chemistry, possessing the potential for regiochemically controlled introduction of groups and a suitably disposed synthetic handle to accept ring closure.

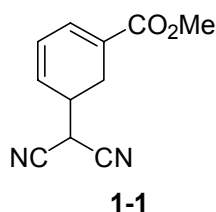
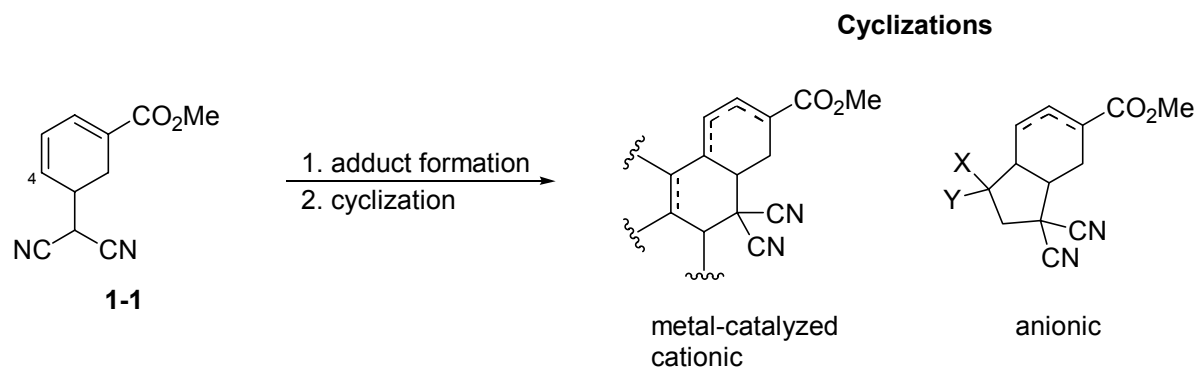


Figure 1-1. Key substrate 5-dicyanomethylcyclohexa-1,3-dienecarboxylic acid methyl ester.

Upon deprotonation of its reasonably acidic proton, the dicyanomethyl carbon of **1** furnishes a nucleophilic site capable of adduct formation with electrophiles to establish cyclization substrates. The ring C4 situates an electrophilic position appropriately for the ring-closing reaction. On this basis, **1-1** was envisioned as forming the basis of study of cyclization reactions of adducts by anionic conjugate addition, cationic cyclization, and metal-catalyzed intramolecular coupling (Scheme 1-1). In addition, observations stemming

from the expansion of the tandem anionic cyclization reaction to acetylenic substrates, and from the preparation of cationic cyclization substrates from **1-1**, led to substantial studies unrelated to ring closures upon **1-1** and constitute the concluding chapters of this work.



Scheme 1-1. General modes and products of cyclization.

1.2 Cyclization Reactions

1.2.1 General Introduction

Cyclization reactions constitute a cornerstone of organic synthesis. Innumerable examples abound in the literature of structures comprising cyclic structures, including the majority of natural compounds. The centrality of natural products to organic chemistry, as the direct targets of synthesis for medicinal or exploratory purposes, or for experimental purposes reaching into multiple avenues of the physical sciences, as well as into the biochemical, biophysical, molecular biological, and physiological fronts, presents synthetic chemistry with the ongoing challenges of determining and realizing routes to the synthesis of an ever-expanding population of novel designed and discovered molecules. The development of reagents and conditions to effect syntheses with the highest efficiencies in all aspects susceptible to the term — selectivity, time, number of steps, material expenditures —

represents a governing feature of the approach to new compounds, and presents the opportunity for the refinement of existing syntheses. These considerations are of particular significance in the commercial realm, which bridges the contributions of pure research and the needs of society. All that can be said of synthesis necessarily applies to its constituents, making the discovery of new cyclization reactions of high selectivity, ease, and atom efficiency a continuous pursuit.

The ring closures and related studies with which this work is concerned belong to three of the four main modes, defined by their intermediates, as anionic, metal complex (metal-catalyzed), cationic, and radical cyclizations. Figure 1-2 depicts these categories in general terms.

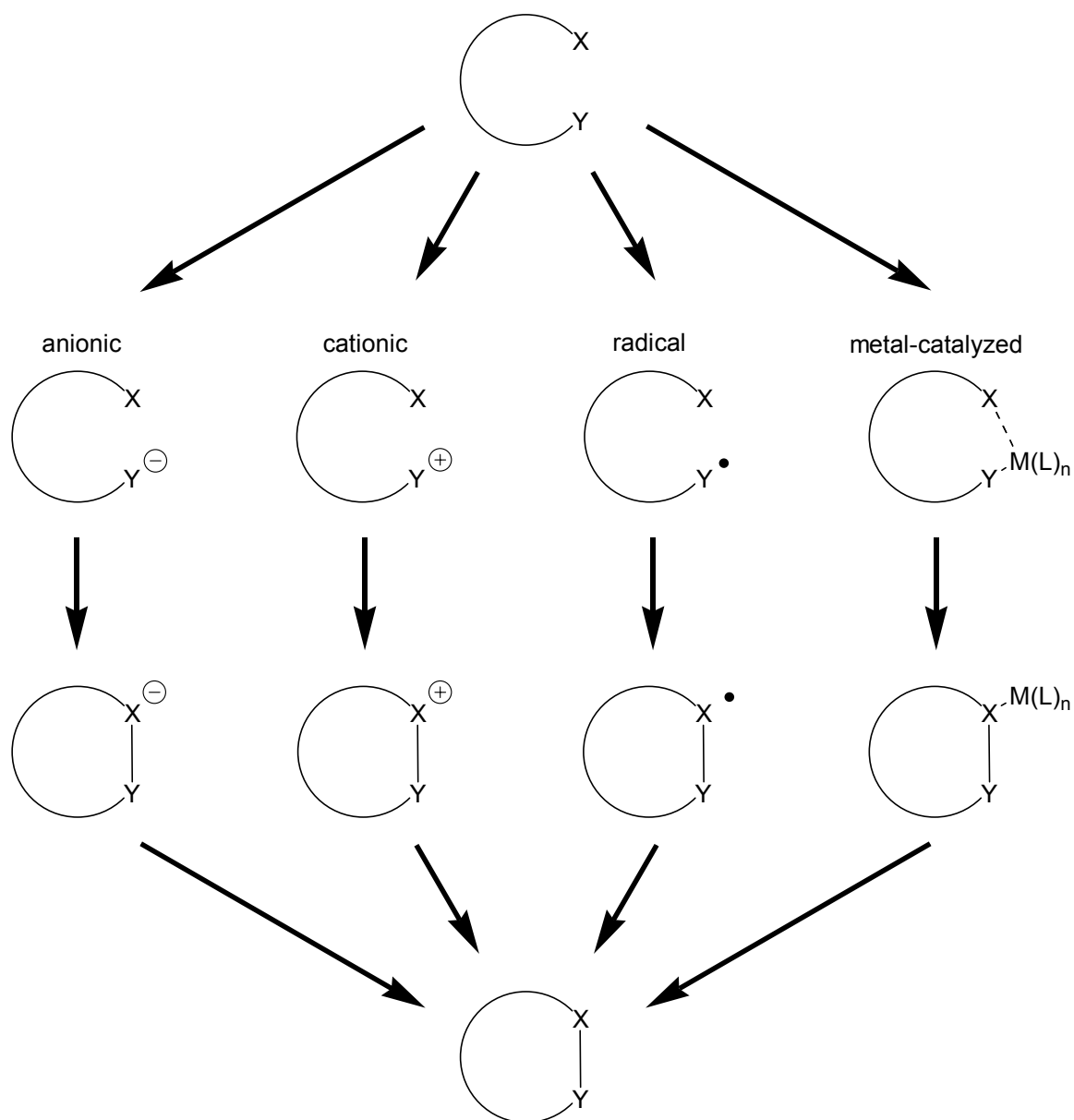


Figure 1-2. Generalized summary of cyclization reactions.¹

A striking instance of synthetic efficiency is that broad and rapidly expanding class of processes variously referred to as tandem, cascade, and domino reactions, terms which, along with polycyclization, also refer to ring closures. These terms are frequently used synonymously in the literature, although individual authors reviewing the field and the researchers publishing primary literature have enjoyed considerable latitude in deploying

varied definitions of the processes and in discriminating between the terms. The most permissive formulation equates the terms domino, tandem, and cascade and offers the least constrictive definition of the processes to which the terms apply. Parsons and co-authors reviewed tandem reactions as applied to natural product elaboration and the discovery of new synthetic methodology, using “tandem” in the title and “cascade” in the first sentence, offering the brief definition of these processes as ones that combine a series of reactions in one synthetic operation.²

Tietze³ simultaneously published a more extensive review that offered a strict definition of a domino reaction as, “a process involving two or more bond-forming reactions (usually C–C bonds) which take place under the same reaction conditions without adding additional reagents and catalysts, and in which the subsequent reactions result as a consequence of the functionality formed in the previous step.” Several clarifications are offered which further limit the definition and the acceptable terms. A substrate with several functionalities that undergo simultaneous individual transformations would not be undergoing a domino reaction. The author considers the term domino apt because of its close analogy to the tumbling of a line of standing dominos upon the tipping of the first, which brings down every piece without changing any conditions. Also, the “time-resolved” aspect of falling dominos correlates closely with the succession of reactions. For this reason, it is suggested that the term “tandem” be eliminated from future discourse because it suggests simultaneity rather than an uninterrupted sequence. Tietze also rejects “cascade” as not describing the “real meaning” of the process and because it already has widespread use in science to describe other phenomena.³

Tietze's review goes on to introduce a classification of the types of domino reactions based on the mechanisms of the steps, assigning number-letter codes to abbreviate the combined terms. The scheme is a generalization of the already universal naming of domino sequences as a hyphenated combination of the individual reactions. Using the general mechanistic categories of anionic, cationic, radical, pericyclic, photochemical, carbenoid, transition metal-catalyzed, and oxidation/reduction, assigned respective letters a to h, and numbers for the step of the sequence, a Michael-aldol domino reaction would be labelled as 1a/2a, and in general terms, an anionic-pericyclic-pericyclic sequence would be 1a/2d/3d.

A more recent review by Nicolaou and co-authors referred to tandem sequences and reaction cascades in different senses without defining the difference, although an implicit distinction emerges in the examples cited for the two types of reactions.⁴

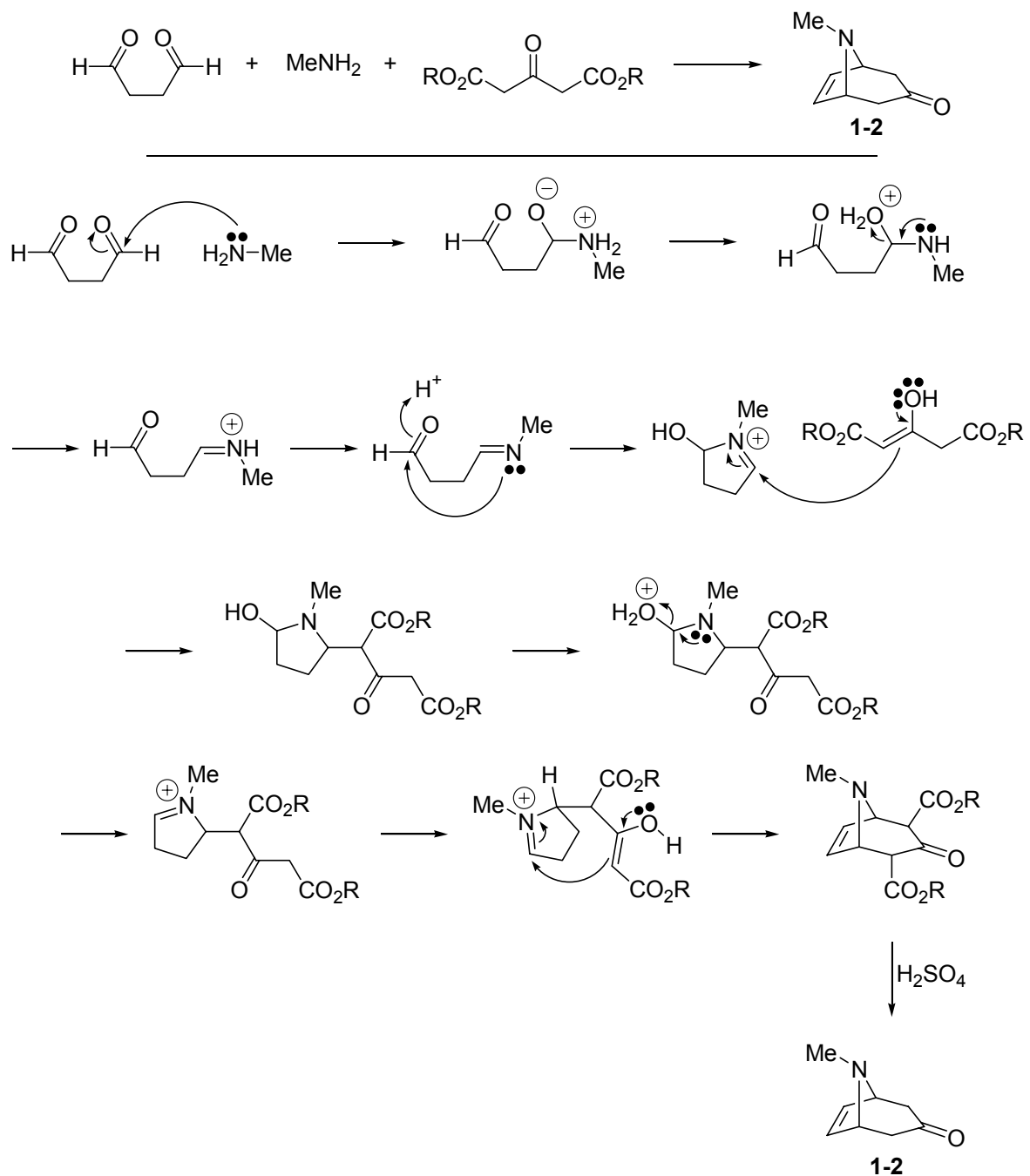
Tietze's exclusion of cascade and tandem from the permitted terminology does not withstand scrutiny. Multiple dictionary definitions of cascade include the concept of successive events, making it synonymous with this sense of "domino." The term tandem comprises a variety of definitions including ones based on simultaneity, the grounds of Tietze's objection, but crucially includes the idea of objects placed "one after the other," which allies it to both cascade and domino. It would therefore appear reasonable for all three common terms to persist for these reactions.

A reasonable definition of a tandem reaction is one in which multiple transformations which would individually be recognized as discrete reactions occur in a single experimental process, which may involve multiple introductions of reagents and changes of conditions, but which passes from substrate to terminal product via a chain of reactive intermediates that are the reactants for each successive step. Under this definition, a reaction process involving a

quench or the generation of an isolable product preceding submission to new conditions would not qualify as a tandem process. Furthermore, a reaction involving multiple alterations that are understood to constitute a single transformation would not represent a tandem reaction. For example, a Diels-Alder reaction divorced from mechanistic understanding and viewed in purely schematic terms involves ring closure by the creation of two bonds, along with drastic alteration in the unsaturation pattern among the reactants, but is obviously not a tandem process.

Common to reviewers of tandem chemistry is the high esteem for reactions, whether tandem or sequential, that rapidly advance molecular complexity. The efficient introduction of structural complexity is seen as a worthy aim insofar as it increases economies of time, labour, and material and energy consumption, and limits losses incurred at every isolation and purification process. Recent reviews also highlight environmental considerations in the drive to condense syntheses by the deployment of tandem sequences. Not least among the features cited by reviewers as recommending tandem sequences is the considerable aesthetic appeal of single procedures effecting large gains in connectivity. This appeal also comprises the elegance inherent to the impressive regio-, chemo-, and stereoselectivities exhibited by many tandem processes.

The Mannich reaction may be the first tandem reaction, and its application to Robinson's⁵ synthesis of tropinone (**1-2**, Scheme 1-2) may be the first tandem synthesis in organic chemistry. It employs a double Mannich reaction in three syntheses all involving succindialdehyde and methylamine, and separately employing acetone, ethyl acetonedicarboxylate, and calcium acetonedicarboxylate (in aqueous solution).



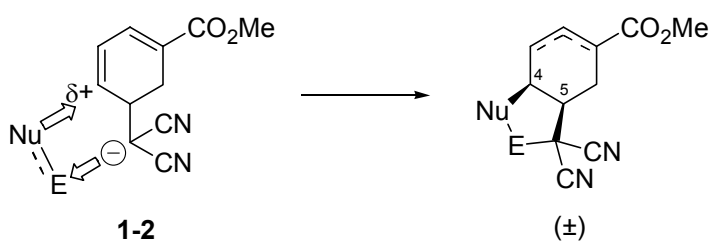
Scheme 1-2. Robinson's synthesis of tropinone.

Since those beginnings, and with increasing pace in recent years, tandem reactivity across multiple categories of reactivity has been explored and exploited to remarkably elegant and efficient effect. In addition to those instances cited in the realm of cascade conjugate additions that especially pertain to this work, wide application of tandem metal-

catalyzed couplings has been achieved, and these are briefly described in Chapter 3 in the context of the intramolecular Heck reaction.

1.2.2 Tandem Anionic Cyclizations

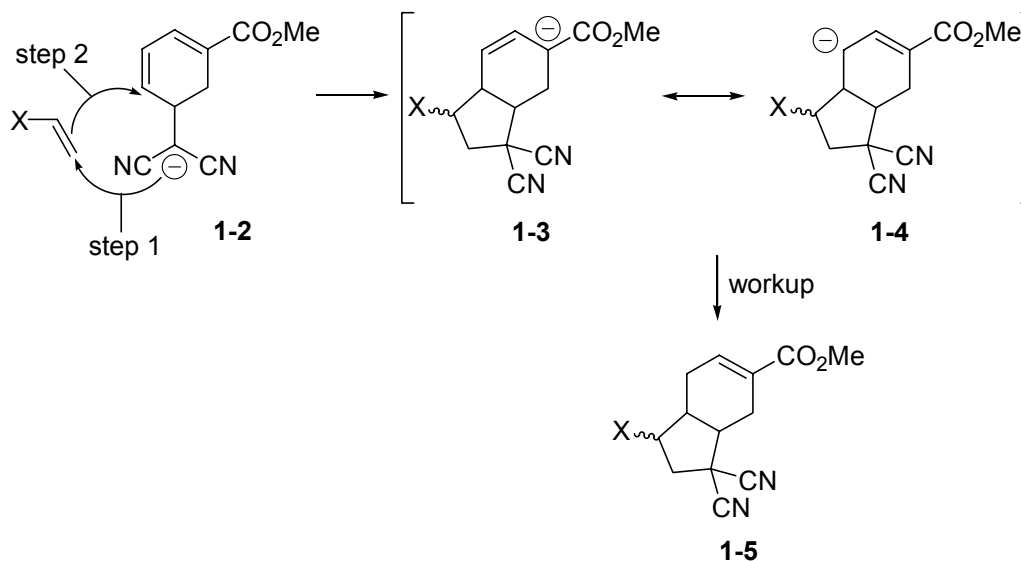
The anionic cyclizations envisaged for **1-1** were to capitalize upon the latent nucleophilic and electrophilic sites present at the dicyanomethyl and ring-C4 positions, respectively. The 1,3-disposition of these sites made possible anionic cyclization schemes incorporating coupling partners bearing complementary electrophilic and nucleophilic sites to generate five-membered rings as depicted in Scheme 1-1. One avenue of inquiry was that the polar complementarity would be initiated by the reaction itself: for example, addition of **1-2** to a general unsaturated reagent (Scheme 1-3) at the electrophilic site E would set up the adduct for cyclization by the incipient nucleophile Nu onto the parent ring. The potential for this two-step sequence to occur *in situ* qualifies the general transformation as a domino reaction. Anion **1-2** also represents a chiral synthon offering stereocontrol in the formation of five-membered rings, as indicated in the relative stereochemistry of parent ring C4 and C5 in Scheme 1-3.



Scheme 1-3. Anionic cyclizations of **1-2** and general unsaturated substrates.

The possibility of realizing tandem reactivity in cyclizations of **1-1** through anionic chemistry led to the decision to restrict the adduct formation to nucleophilic attack of anion **1-2** upon unsaturated compounds, for example Michael additions to conjugated vinyl

systems. These reactions would establish the substrate for a second conjugate addition to the $\alpha,\beta,\gamma,\delta$ -unsaturated system of **1-1** (Scheme 1-4). The intermediate **1-3** \leftrightarrow **1-4** would be expected to predominantly neutralize as conjugated vinyl regioisomer **1-5**. The initiation of a tandem cyclization by a Michael addition in the adduct-forming step is a sufficiently widespread process that it has been designated the Michael-initiated ring closure (MIRC).⁶

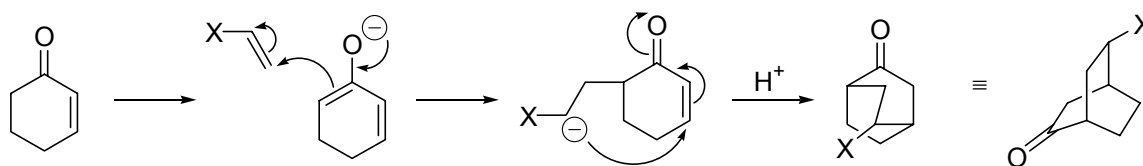


Scheme 1-4. Cyclization by a sequence of Michael and 1,6-conjugate addition.

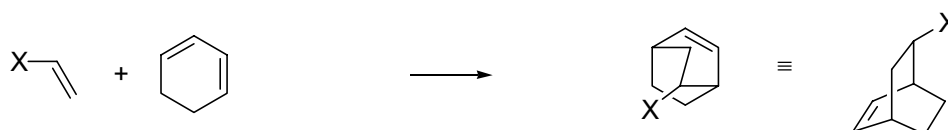
These planned tandem Michael-intramolecular Michael cyclizations are closely related to “reflexive Michael reactions” a term applied to a specific class of MIRCs in which both components sequentially play both roles of donor and acceptor and in which the defining aspect is the deployment of a cross-conjugated kinetic enolate of an enone as the initial donor (Scheme 1-5). In the reactions of this class, the adduct enolate attacks the restored Michael acceptor of the initial donor, bringing about a six-*endo*-trig closure that exhibits functional complementarity to the Diels-Alder reaction, establishing the same carbon connectivity but bearing a product ketone rather than a double-bond.¹ A representative

instance is the reflexive Michael reaction of cyclohexenone with a general Michael acceptor, illustrative of instances in which cyclic dienolates give rise to bridged ring systems.

Reflexive Michael reaction

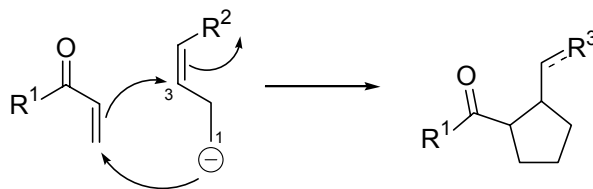


Diels-Alder reaction



Scheme 1-5. General reflexive Michael reaction of cyclohexenone and its complementarity to the Diels-Alder reaction.¹

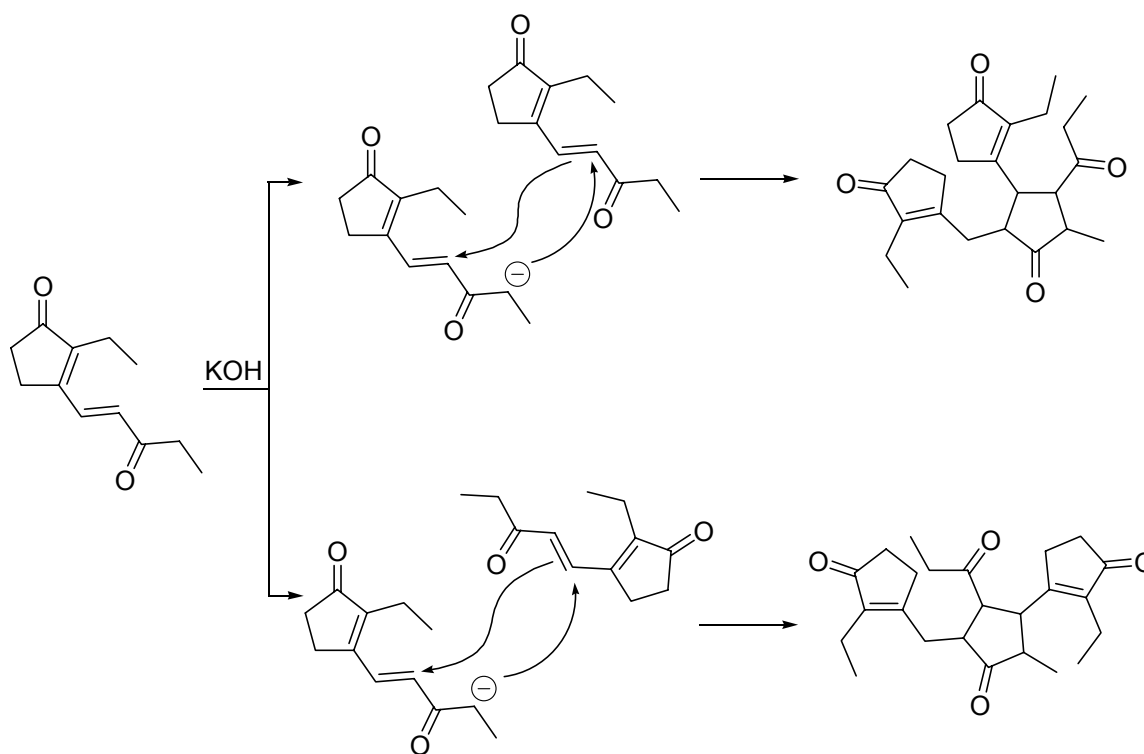
Tandem Michael-intramolecular Michael reactions of this type that bring about cyclizations wherein the initial donor's subsequent acceptor site is in the three-position, such that reaction with a Michael acceptor/donor (specifically unsaturated carbonyl compounds) generates a five-membered ring by 5-*exo*-trig cyclization (Scheme 1-6) have been little reported in the literature, but several of those that are known exhibit additional tandem reactivity. Of the reactions that adhere to Scheme 6, none has a substituent at the position three of the initial donor.



Scheme 1-6. General tandem Michael cyclization to generate five-membered rings.

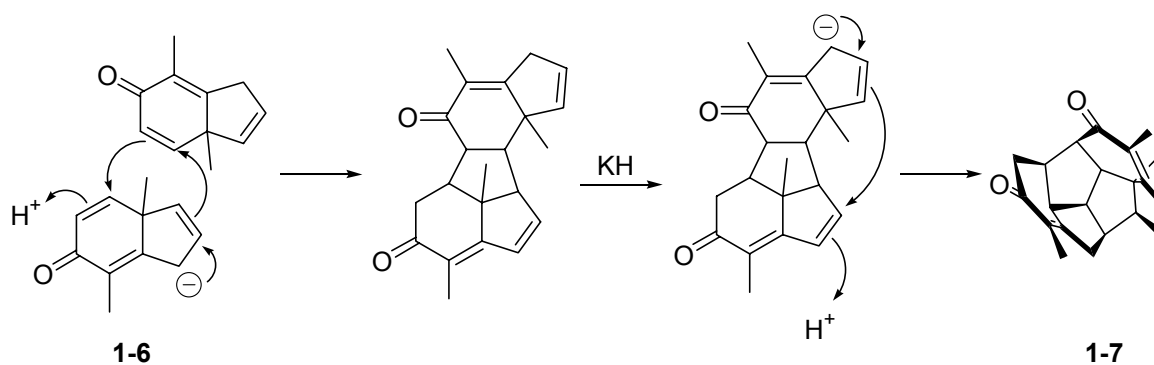
Nelson and Verdine reported the generation and separation of a simpler analog of a medically significant complex mixture termed PGB_x, obtained by treatment of a particular

prostaglandin with 1 M ethanolic KOH.⁷ Two of the six analog dimers were determined to have arisen by tandem Michael 5-*exo*-trig cyclization (Scheme 1-7)



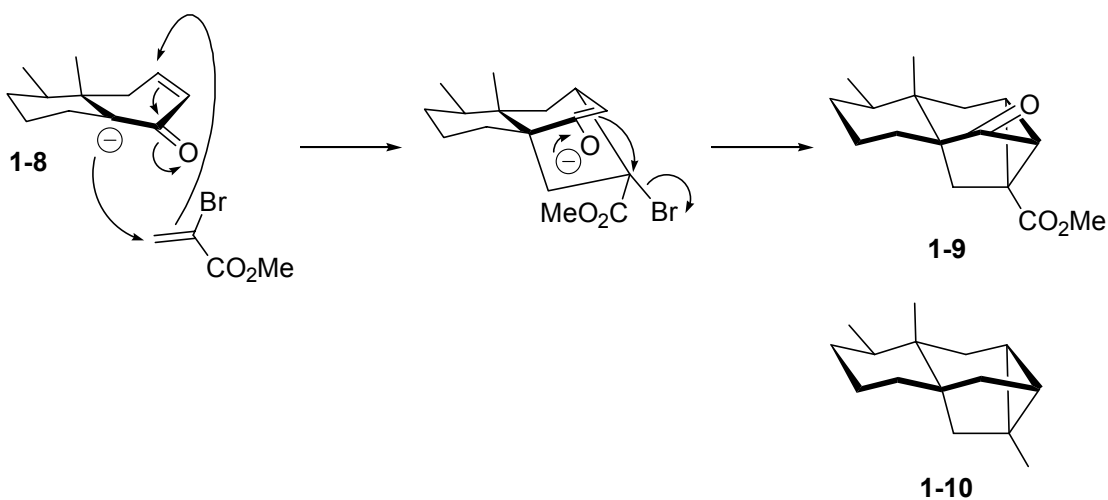
Scheme 1-7. PGB₁ analog dimerization by tandem Michael-Michael cyclization.

In studying the enolate of 3a-methyl-3a*H*-indene (**1-6**, Scheme 1-8), Foster et al. observed an unexpected triple Michael addition resulting in two cyclizations to yield the highly concave hexacyclic adduct **1-7**, the anion of which had a persistent blue colour attributed to intramolecular charge transfer across the central cavity between the nearly parallel sides.⁸



Scheme 1-8. Triple Michael cyclization of enolate **1-6**.⁸

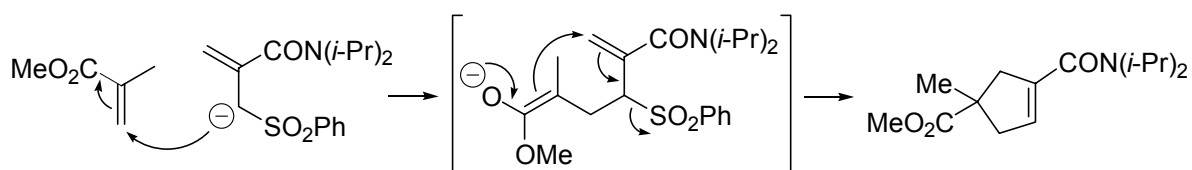
Hagiwara and coworkers were able to synthesize the carbon framework **1-9** of ishwarane (**1-10**), a hydrocarbon related to the eremophilane family of sesquiterpenes, from the kinetic enolate **1-8** of dimethyloctalone (Scheme 1-9) and methyl α -bromoacrylate by a reflexive Michael addition in tandem with displacement of the secondary bromide.⁹ This method has also been used with the related 3-substituted α -halo acrylate, methyl 2-chloro-2-cyclopropylidene acetate, in the synthesis of terpenoid frameworks.^{10,11}



Scheme 1-9. Synthesis of ishwarane precursor by reflexive Michael cyclization and bromide displacement.⁹

In his monograph on tandem chemistry, Ho¹² permits a contradiction to his definition of reflexive Michael reactions to include mutual double Michael reactions to generate five-

membered rings, which allies these transformations to those which were planned for the current research. A five-membered ring closure is made possible in reflexive reactions of bifunctional initial donors. Of particular interest are reactions in which initial donor activating groups are simultaneously good leaving groups for the ring closure step (Scheme 1-10). Such reactions generate cyclopentenes by apparent 5-*endo*-trig closures, through the 1,3-disposition of donor and acceptor sites, as in this proposed work, which alternatively proceeds by 5-*exo*-trig closures.

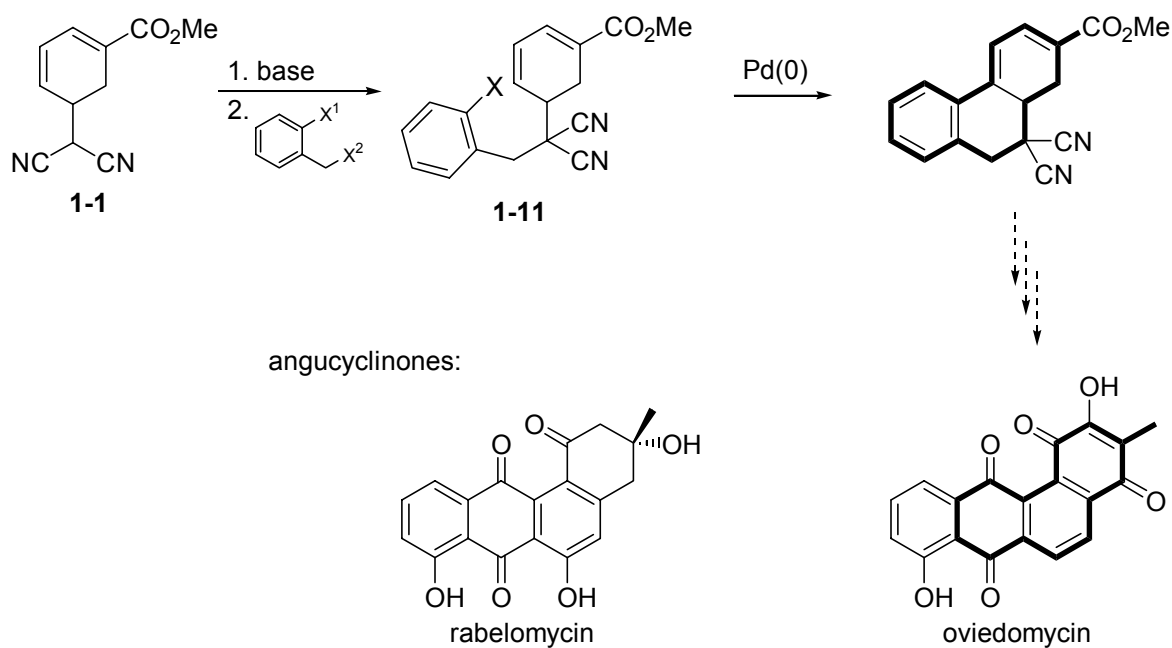


Scheme 1-10. Alternative reflexive Michael reaction of a bifunctional donor to generate a five-membered ring.

1.2.3 Metal-Catalyzed Cyclizations

The same functional disposition in **1-1** that was observed to make it amenable to tandem conjugate addition chemistry was noted to afford other routes to cyclization. The potential to expand upon the cyclopentyl-forming anionic cyclizations by forming six-membered rings through metal-catalyzed coupling was seen as a useful complement and would establish the versatility of the ring-opened adduct. Specifically, the C3-C4 double-bond was seen as an intramolecular coupling partner in Heck reactions of appropriately prepared substrates **1-11** (Scheme 1-11). Granted the establishment of the intramolecular Heck reaction as viable for this system, a long term view toward its application to natural product synthesis was envisioned, for example to the angucyclinone^{13,14} family of natural

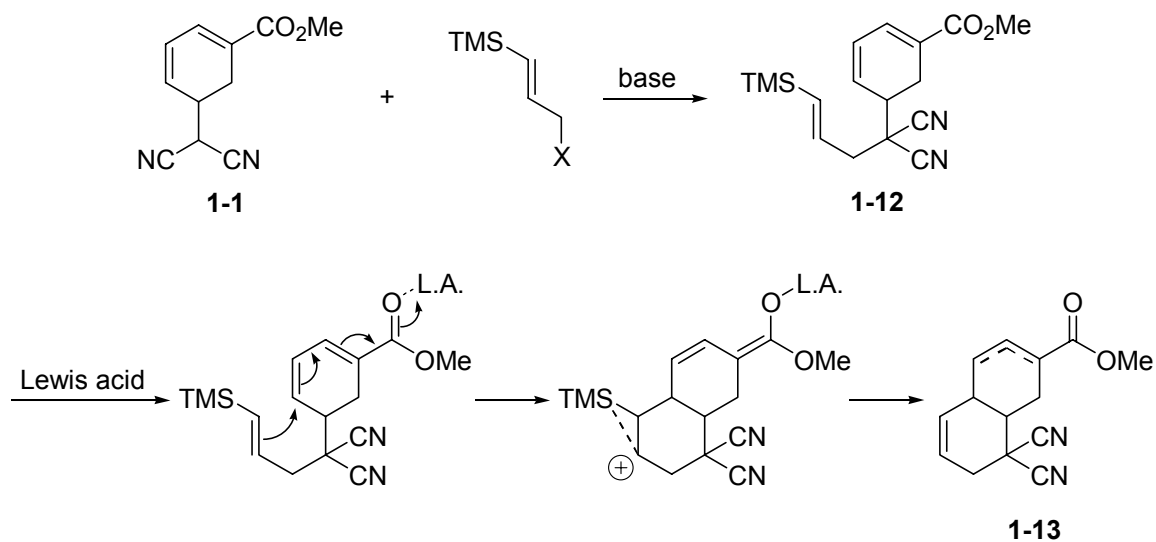
products. The Heck reaction and its intramolecular application are given detailed treatment in Chapter 3.



Scheme 1-11. Intramolecular Heck reactions planned for a substrate **1-11** derived from **1-1**.

1.2.4 Cationic Cyclizations

It was envisaged that **1-1** would again serve at the same sites as a useful cyclization substrate, this time to effect cationic ring closures of appropriate vinylsilane precursors of type **1-12** to generate products **1-13** (Scheme 1-12). The study that materialized diverged vastly from this plan and the introductory groundwork for this alternative study, which is unrelated to the use of cationic cyclization in synthesis, is more appropriately laid in Chapter 4.



Scheme 1-12. Initial synthetic outlook for the study of cationic reactions of allylsilanes.

1.3 Conclusion

Each of the aforementioned modes of cyclization — tandem anionic, metal-catalyzed (intramolecular Heck reaction), and cationic — is the subject of a chapter. Chapter 2, which was to probe the possibility of one degree of tandem anionic reactivity, details the fortuitous discovery of the continuation of the first tandem event, a Michael-Michael cyclization, to include a second cyclization by Thorpe-Ziegler-like reaction that furnished the tricyclic homobrendane skeleton with potential application to the synthesis of the natural product 2-isocyanoallopupukeanane. In addition to a brief exploration of the Diels-Alder reactions of a diene (5,5-dicyanocyclopentadiene) previously developed in this laboratory that was hoped would lead to adducts like the source of ring-opened adduct **1-1**, several Michael acceptors and heteroatom 1,2-addition substrates were tested for the same tandem reactivity that was revealed with the initial doubly-activated Michael acceptor di-*tert*-butyl methylenemalonate. In addition, preliminary attempts at the functional manipulation of the

tricyclic homobrendane system applicable to its conversion to 2-isocyanoallopupukeanane were undertaken.

Chapter 3 concerns attempts at intramolecular Heck reactions of halobenzyl adducts of **1-1** that were ultimately optimized for the chosen catalytic conditions. Base-induced reactions upon the parent cyclohexadiene ring of **1-1** in the context of both substrate preparation and of the Heck reactions provided insights into the acidic characteristics of **1-1** that would inform the findings of the other studies.

The potential for cationic cyclization of **1-1**-derived compounds was the gateway to a separate study derived from observations made in the preparation from **1-1** of the cyclization substrate and related to the radical and polar brominations of allylsilanes, a subject significantly advanced in previous years in this laboratory that still demanded further scrutiny. A mechanistic study was undertaken that has shed light upon influential literature experiments in this area and has resulted in a new mechanistic suggestion for the electrophilic substitution reactions of these systems.

The extension of the tandem anionic reactions of **1-1** to multiple Michael acceptors revealed an interesting alternative tandem mode of reactivity in the case of alkyl propiolates that was of sufficient novelty and subtlety that its thorough treatment required a separate chapter. Chapter 5 details the structural characterization of the unexpected compounds and explores the mechanistic facets of the reactions.

References

1. Thebtaranonth, C.; Thebtaranonth, Y. *Cyclization Reactions*; CRC Press: Boca Raton, 1994.
2. Parsons, P. J.; Penkett, C. S.; Shell, A. J. *Chem. Rev.* **1996**, *96*, 195-206.
3. Tietze, L. F. *Chem. Rev.* **1996**, *96*, 115-136.
4. Nicolaou, K. C.; Montagnon, T.; Snyder, S. A. *Chem. Commun.* **2003**, 551-564.
5. Robinson, R. J. *J. Chem. Soc., Trans.* **1917**, *11*, 762-768.
6. Bey, P.; Gerhart, F.; Van Dorsselaer, V.; Danzin, C. *J. Med. Chem.* **1983**, *26*, 1551-1556.
7. Nelson, G. L.; Verdine, G. L. *Tetrahedron Lett.* **1982**, *23*, 1967-1970.
8. Foster, S. J.; Rees, C. W.; Williams, D. J. *J. Chem. Soc., Perkin Trans. 1* **1985**, 711-717.
9. Hagiwara, H.; Uda, H.; Kodama, T. *J. Chem. Soc., Perkin Trans. 1* **1980**, 963-977.
10. Spitzner, D.; Engler, A.; Liese, T.; Splettstösser, G.; de Meijere, A. *Angew. Chem., Int. Ed. Engl.* **1982**, *21*, 791.
11. Spitzner, D.; Engler, A.; Wagner, P. *Tetrahedron* **1987**, *43*, 3213-3223.
12. Ho, T.-L. *Tandem Organic Reactions*; Wiley: New York, 1992.
13. Méndez, C.; Künzel, E.; Lipata, F.; Lombó, F.; Cotham, W.; Walla, M.; Bearden, D. W.; Braña, A. F.; Salas, J. A.; Rohr, J. *J. Nat. Prod.* **2002**, *65*, 779-782.
14. Krohn, K.; Böker, N.; Flörke, U.; Freund, C. *J. Org. Chem.* **1997**, *62*, 2350-2356.

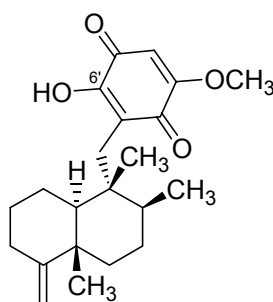
Chapter 2

Tandem Anionic Cyclization of the Ring-Opened Adduct

2.1 Introduction

2.1.1 Project Origin

The work detailed in this thesis deviated sharply from the clearly defined goals at its inception, which were instigated by the discovery by Loya and Hizi^{1,2} of the activity against the Human Immunodeficiency Virus (HIV) of the marine sponge-derived quinone sesquiterpene ilimaquinone, originally isolated from *Hippiospongia metachromia*³ (Figure 2-1).



2-1

Figure 2-1. Ilimaquinone.

The exploration of ilimaquinone-guided chemistry toward *in vitro* antiviral compounds was to constitute one line of research in a three-pronged investigation by this group into potential anti-HIV compounds, each capitalizing on discoveries of the potency of a different natural product against various specific biochemical functionalities within the viral life cycle. The pharmacological potential of ilimaquinone-based derivatives ultimately

prompted a synthetic scheme toward a related class of marine quinones about whose interaction with the target of ilimaquinone nothing was known, but which promisingly contained the structural motif that proved essential to ilimaquinone's antiviral effect. This plan would not be explored, as early fortuitous discoveries of the reactivity of a key synthetic intermediate, which had previously been generated and partially developed in our group for other purposes, led to vastly divergent chemistry centered upon its synthetic potential. When our ilimaquinone-based investigation encountered persistent difficulties at a late intermediate, this new chemistry had increasingly captured our interest and had proved sufficiently promising to sustain itself as the sole focus of our experiments; the original project defined by ilimaquinone and the speculative synthetic offshoot based on its marine natural product congener were therefore suspended.

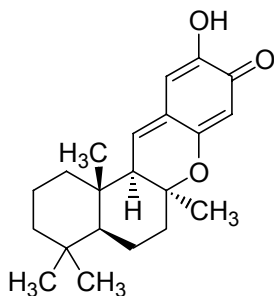
2.1.2 Ilimaquinone, Puupehenone and the Entry to the Main Focus of Research

Ilimaquinone had demonstrated *in vitro* activity against the HIV reverse transcriptase (RT) enzyme, the protein with the task of transcribing retroviral RNA into DNA that could be incorporated into the host cell's genome.⁴ The RT enzyme bears several structural regions, each responsible for carrying out a specific catalytic function: an RNA-dependent DNA polymerase, which uses the viral single-stranded RNA as a template to transcribe a complementary strand of DNA; the DNA-dependent DNA polymerase, which assembles the DNA strand complementary to the first, forming the duplex DNA that, upon integration into the host genome, represents the latent identity of the virus within the host cell, a form termed the provirus;⁴ and the RNase-H domain, which serves to degrade the RNA strand of the RNA-DNA heteroduplex after the first round of polymerase activity, opening the way for the

anticoding strand.⁵ It was the RNase-H domain that ilimaquinone was found to inhibit.⁶ In the intervening period, ilimaquinone has also been demonstrated to have a range of biochemical effects, including antimicrobial, antimitotic and anti-inflammatory activities;⁷ the promotion of the reversible vesiculation of the Golgi apparatus and interference with intracellular protein trafficking;⁷⁻⁹ and inhibition of the cytotoxicity of ricin and diphtheria toxins.¹⁰

It was our intention to synthesize simple analogs of ilimaquinone to determine the minimal and most easily incorporated structural features required of compounds for the retention of the inhibition, and to improve upon the potency of the parent compound. As a starting point, we planned the synthesis of an analog that retained the quinone moiety of ilimaquinone but that bore a naphthyl unit in place of the bicyclic terpenoid skeleton. The synthesis stalled at a late stage oxidation to unmask the quinone.

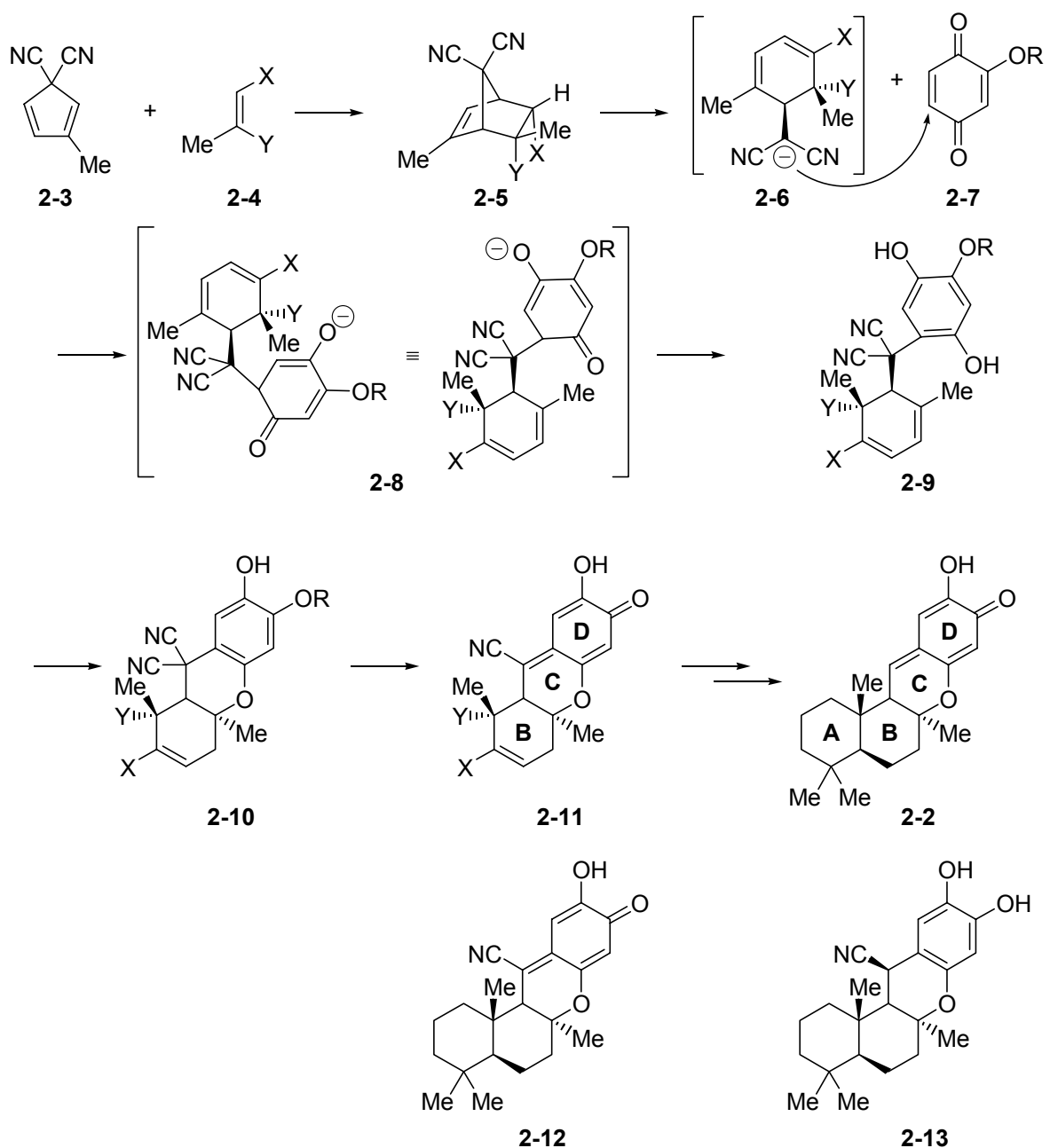
Whereas the frustration of the synthesis at this stage need not have proved insurmountable, solutions were not explored at length, and the originally planned project was ultimately suspended, as a productive line of research prompted by ideas related to the tetracyclic paraquinone-methide puupehenone (**2-2**, Figure 2-2), led us toward unrelated investigations that would solely command our attention for the duration of our research.

**2-2****Figure 2-2.** Puupehenone.

First discovered by Scheuer and co-workers in the marine sponge tentatively identified as *Chondrosia chucalla*,¹¹ and later from many marine sponges such as *Heteronema*, *Hyrtios*, *Strongylophora* sp., and *Psammalplysilla purpurea*,¹² puupehenone possesses antitumour, antifungal, antimalarial, and antibiotic (against Gram-positive bacteria) activities.¹³ It has also been demonstrated to completely inhibit the growth of *Mycobacterium tuberculosis* at a 12.5 $\mu\text{g/mL}$ concentration, and to possess activity against Herpes simplex virus II, but nothing was known at the outset of our research about its interaction with RNase H.¹² It came to our attention in the context of our RNase-H-related research plan because it shared the α -hydroxy quinone carbonyl relationship of ilimaquinone, whose 6'-hydroxyl had been established as crucial to its antiviral activity.¹ With the goal of synthesizing close mimics, or of effecting total syntheses, of the puupehene class of quinone methides, we intended to capitalize on chemistry previously developed in our laboratory that seemed suited to the efficient elaboration of the B, C, and D rings of puupehene-related compounds (Scheme 2-1).

Steps similar to those at the opening of the synthetic plan, directed toward the generation of the anionic dicyanomethyl-substituted cyclohexadiene **2-6** (parent to the B ring of puupehenone **2-2**), were accomplished years earlier in our lab for other purposes (*vide infra*) with the simpler substrates 5,5-dicyanocyclopentadiene and a small set of electron-poor monosubstituted dienophiles. It was found that treatment of the Diels-Alder adduct analogous to **2-5** (methyl acrylate dienophile) with strong base was able to effect ring-opening following from deprotonation of the methine proton α to the carbonyl. For the purpose at hand, a 3-methyl-substituted dicyanocyclopentadiene **2-3** was envisioned as forming a Diels-Alder adduct with a dienophile **2-4** appropriately substituted for both the

ring-opening reaction and for the immediate incorporation of the nascent B-C ring angular methyl and a synthetic handle (Y) for later installation of the A ring.



Scheme 2-1. Outline of synthesis of puupehenone and related compounds.

The elements of the C and D rings would be in place upon conjugate addition of **2-6** to the 2-alkoxybenzoquinone **2-7**, which would furnish via adduct intermediate **2-8** the

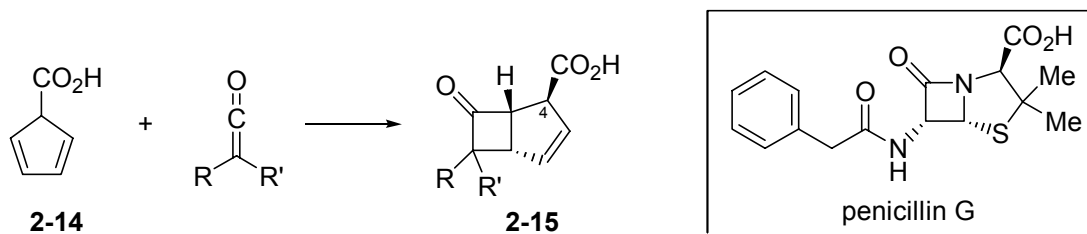
hydroquinone adduct **2-9** after workup and tautomerization. Deprotonated **2-9** was reasonably expected to cyclize onto the δ carbon of the conjugated double-bond system of the cyclohexadiene ring in a 5-exo-trig conjugate addition to furnish **2-10**. Oxidation to reveal the quinone-cyanomethide **2-11** would bring the synthesis close to conclusion, requiring the introduction of a moiety that could provide closure of the A ring, either through involvement of the X and Y functions, or by a route that attended to their scission from the final compound, as well as reduction of the A ring unsaturation. In connection with this potential route to puupehenone, the nitrile-bearing naturally occurring puupehenone derivatives 15-cyanopuupehenone **2-12** and 15-cyanopuupehenol **2-13** are noteworthy in light of the fortuitous presence of the nitrile in synthetic **2-11**.

Our investigation of the Diels-Alder/base-induced ring-opening sequence centered around the chemistry of 5,5-dicyanocyclopentadiene was diverted away from synthesis in the puupehenone family; our initial foray into conjugate addition of a simpler analog of **2-6** to various acceptors disclosed promising reactivity in carbocyclizations analogous to the heterocycle-forming conversion **2-9**→**2-10**. Exploitation of the ring-opened adduct in the generation of polycyclic compounds, and in the exploration of novel reactivity uncovered in relation to that goal, form the basis of this report.

2.1.3 Chemistry 5,5-Dicyanocyclopentadiene

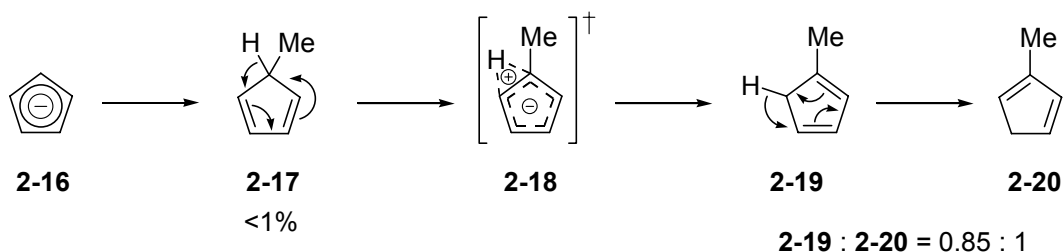
Our lab's previous development of the ring-opening of the Diels-Alder adducts of 5,5-dicyanocyclopentadiene was founded in the generation of the novel diene to circumvent the inaccessibility of 5-monosubstituted cyclopentadienes. It had been intended that a synthetic equivalent of 5-carboxycyclopentadiene **2-14** be coupled with a substituted ketene

in a $[\pi 2s + \pi 2a]$ cycloaddition directed toward the preparation of carbocyclic penicillin analogs **2-15** that would serve as potential β -lactamase inhibitors (Scheme 2-2).



Scheme 2-2. Ketene 2 + 2 cycloaddition in the synthesis of penicillin analogs.

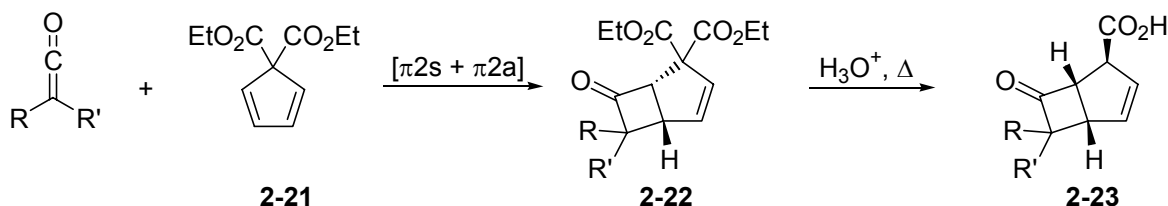
Reported attempted syntheses of 5-monosubstituted cyclopentadienes had established the system as prone to furnish little of the desired product, providing instead double-bond regioisomers that carried substituents at vinylic positions. For example, McLean had failed to realize the synthesis of 5-methylcyclopentadiene through the reaction of cyclopentadienide **2-16** with methyl iodide, obtaining instead a mixture of 1- and 2-methylcyclopentadiene (**2-19** and **2-20**, 57% combined yield) that contained less than one percent of the intended compound.¹⁴ The main constituents were proposed to arise from the initially formed 5-methyl product **2-17** by a sequence of [1,5]-sigmatropic hydrogen shifts passing through the postulated polar transition state **2-18** (Scheme 2-3).



Scheme 2-3. Conversion of 5-alkylated cyclopentadiene into both [1,5]-H shift products.

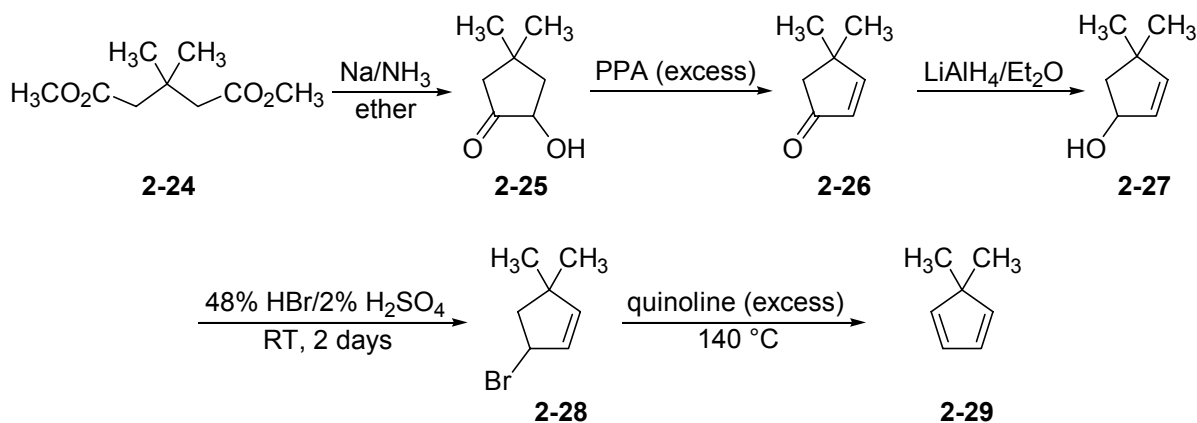
To avoid the impediment raised by sigmatropic shifts, it was decided that 5,5-disubstituted cyclopentadienes be synthesized that were properly functionalized for

conversion to the C4 *exo*-carboxy substituent of **2-15**. For example, the [2 + 2] adduct **2-22** of a suitable ketene and 5,5-dicarboethoxycyclopentadiene **2-21** would be expected, after cycloaddition, to undergo facile hydrolysis and decarboxylation to furnish an intermediate **2-23** with the properly established carboxyl stereochemistry (Scheme 2-4).



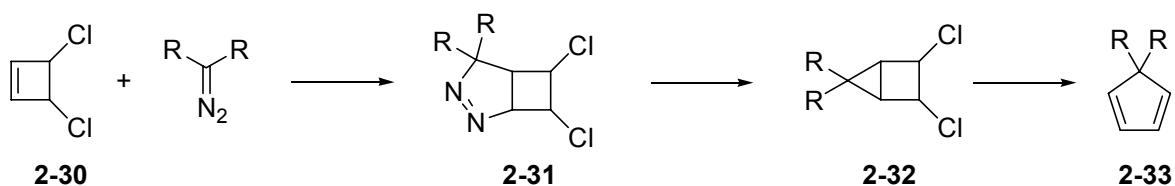
Scheme 2-4. 5,5-Disubstituted functional equivalent of monosubstituted cyclopentadiene.

At that stage, routes to 5,5-disubstituted cyclopentadienes had been reported, but none with C5 substituents that could be converted to a carboxylic acid; therefore, a survey of the literature methods was made to assess the adaptability of existing syntheses to that goal. Rouse and Tyler had published a synthesis of 5,5-dimethylcyclopentadiene dependent upon an acyloin condensation of 3,3-disubstituted glutaric acid esters **2-24** to close the cyclopentane ring and sequential dehydrations to establish the double bonds (Scheme 2-5).¹⁵ Specifically, the cyclic α -hydroxy acid condensation product **2-25** was dehydrated to install the C1–C2 unsaturation, followed by carbonyl reduction to allylic alcohol **2-27** to set up a second dehydration via allylic bromide **2-28** that furnished 5,5-dimethylcyclopentadiene **2-29**. Whereas Rouse and Tyler had generated the dimethyl compound, the requirement of C5 diesters was incompatible with these conditions.



Scheme 2-5. Rouse and Tyler's synthesis of 5,5-dimethylcyclopentadiene.

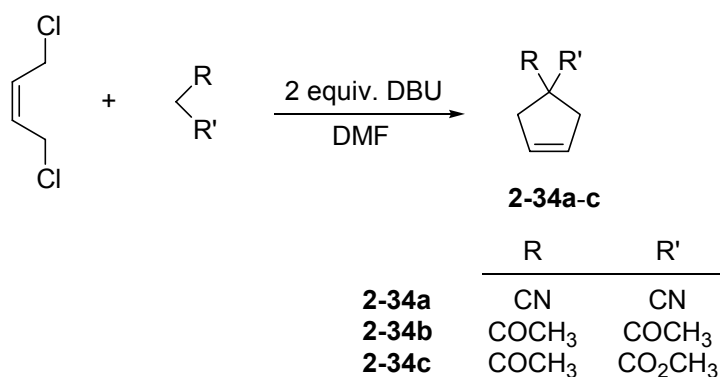
Eilbracht and coworkers¹⁶ had reported an alternative route which employed 3,4-dichlorocyclobut-1-ene **2-30** in a dipolar cycloaddition with diazo ketones to furnish bicyclo[2.1.0] cycloadducts **2-31** prone to rearrangement via nitrogen elimination product **2-32** to the desired cyclopentadienes **2-33** (Scheme 2.6). The requirement for **2-30**, which was not readily available, and the use of relatively large quantities of hazardous diazoalkanes made this approach unattractive.



Scheme 2-6. Eilbracht and coworkers' route to 5,5-dialkylcyclopentadienes.

The possibility of introducing the desired substituents by stepwise introduction of the appropriate electrophiles to cyclopentadienide **2-16** was foreclosed by Webster's earlier report¹⁷ that, whereas nitriles can be introduced sequentially by treatment of **2-16** with cyanogen chloride, the process furnishes all carbon-monosubstituted congeners, and no products with substitution twice at one carbon. The products of dicyanation were all 1,2- and 1,3-dicyano isomers.

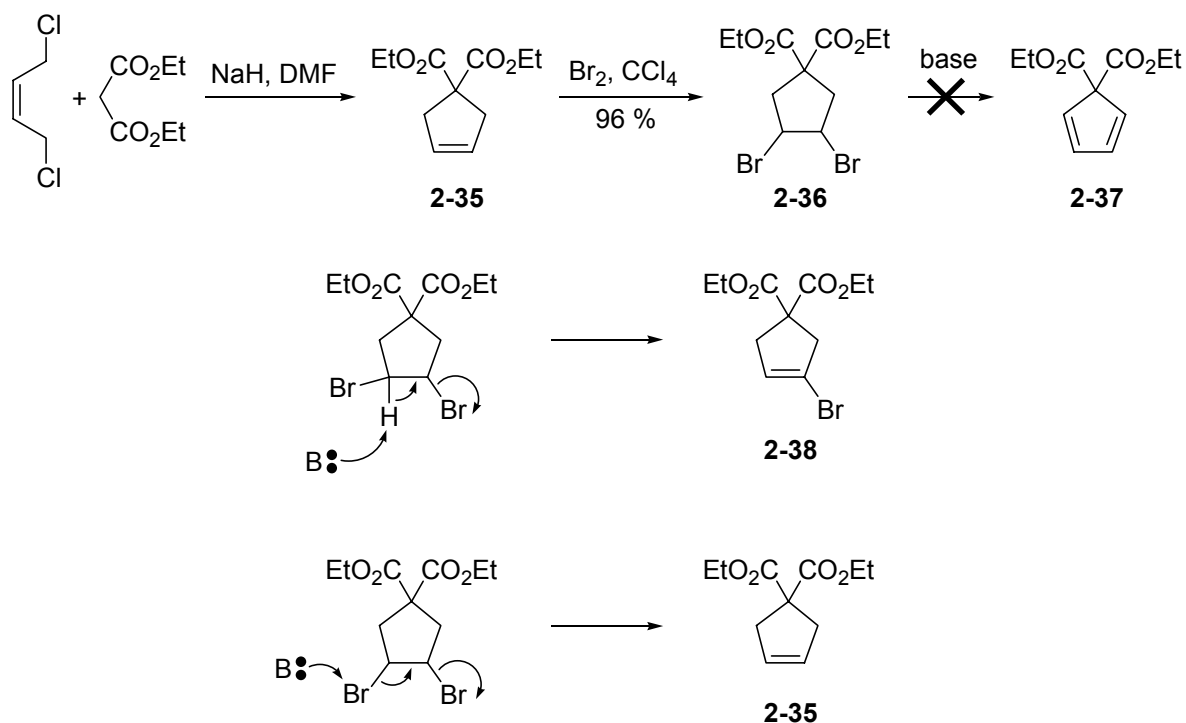
Although it had not been employed in the synthesis of 5,5-disubstituted cyclopentadienes, the potential implicit in Oediger and Möller's generation of 4,4-disubstituted cyclopentenes¹⁸ **2-34** was noted by our group and this intermediate would ultimately serve in the successful synthesis of the required dienes. The authors had demonstrated that bis-alkylation of a small series of malonyl compounds by *cis*-1,4-dichloro-2-butene could be realized by treatment with two equivalents of DBU in DMF (Scheme 2-7).



Scheme 2-7. Oediger and Möller's synthesis of 4,4-disubstituted cyclopentenes.

A scheme to doubly unsaturate the ring was devised which would follow bromination of the ring double-bond with base-induced bis-dehydrobromination. In M.S. Thandi's hands, the first attempt uneventfully produced, by the literature method, 4,4-dicarboethoxycyclopent-1-ene (**2-35**), which was then treated with molecular bromine in CCl₄ to furnish the dibromide **2-36** in 96 % yield.¹⁹ At this stage, the failure of DBU in either room temperature Et₂O or in refluxing benzene to induce the desired eliminations to furnish **2-37** instigated a mounting series of trials with varied reagents and conditions, none of which delivered the cyclopentadiene. It was thought that the size of the carboethoxy substituents made the vicinal hydrogens sterically inaccessible, favouring the eliminations that were observed in some cases: 1,2-HBr eliminations to give vinyl bromide **2-38** and bromine displacement-eliminations to return cyclopentene **2-35**, presumably

effected by base acting as a nucleophile (Scheme 2-8).

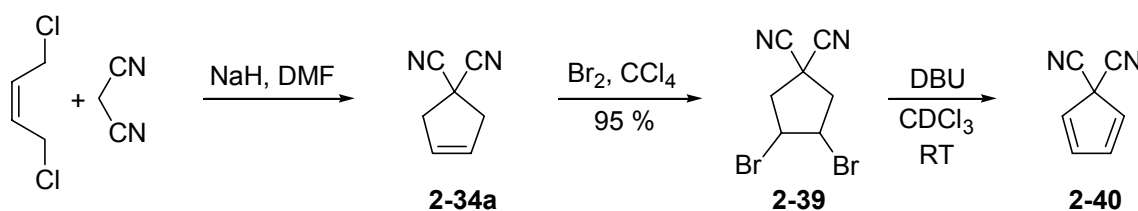


Scheme 2-8. Failure of attempted synthesis of 5,5-dicarboethoxycyclopentadiene.

Thandi abandoned this synthetic target and succeeded in the synthesis of the acceptable alternative, 5,5-dicyanocyclopentadiene, by the same method (*vide infra*), but in later years, J. Venkat Raman of this lab returned to the failed 5,5-dicarboalkoxy case with attempts to realize its synthesis by alternative means. To this end, the generation of 5,5-dicarbomethoxycyclopentadiene was undertaken to probe the possibility that less steric interference in the vicinity of the C3- and C5-protons of the diene precursor 1,2-dibromide by the smaller ester groups might permit deprotonation. Attempted bis-HBr elimination by potassium *t*-butoxide brought about no reaction, and in the interests of advancing other synthetic goals, a more detailed study was not made.²⁰

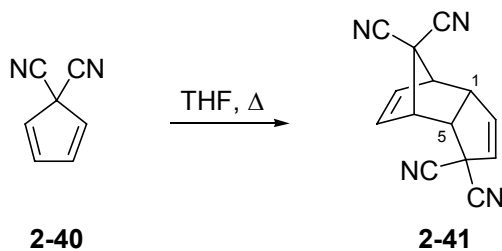
Thandi's successful preparation of 5,5-dicyanocyclopentadiene proceeded along the scheme laid down by Oediger and Möller for 4,4-disubstituted cyclopentenes, although in the

initial experiment, Thandi employed NaH to effect the bis-alkylation of malononitrile. Bromination of **2-34a** with Br₂ in CCl₄ afforded the dibromide **2-39** in 95 % yield. A ¹H NMR experiment was the first performed to assess the generation of 5,5-dicyanocyclopentadiene. Dibromide **2-39**, dissolved in CDCl₃ and treated with DBU at room temperature, was examined periodically at 60 MHz over the course of three hours, which revealed the conversion of the substrate to **2-40** by the appearance of the ¹H multiplets (δ 6.85 and δ 6.50) expected of the AA'BB' spin system.



Scheme 2-9. Thandi's generation of 5,5-dicyanocyclopentadiene.

The NMR sample was not monitored beyond the production of **2-40** and so was not noted to reveal the marked tendency of the diene to form the Diels-Alder dimer **2-41**. At a later stage, **2-40** was generated and then refluxed in THF for 4.3 hours and produced **2-41** (Scheme 2-10), which was recrystallized and analyzed by ¹H NMR spectroscopy to determine the relative stereochemistry of the sole diastereomer obtained.

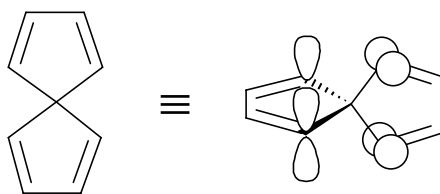


Scheme 2-10. Diels-Alder dimerization of **2-40**.

The Karplus relationship was invoked to assign the product as having *endo* adduct stereochemistry, based upon the observation of a significant coupling (4 Hz) between the

bridgehead protons of the diene fragment and the respective dienophile-derived vicinal protons at C1 and C5, which would not have been observed had the protons taken up the *endo* position and so brought about a 90° dihedral angle among the vicinal proton pairs. The self-reactivity of **2-40** was sufficient to complicate its synthetic use if measures weren't taken to limit the production of **2-41** during workup. Thandi established that a useful method was to work up the didehydrobromination reaction (**2-39**→**2-40**) with cold, dilute aqueous HCl and to carry out *in vacuo* solvent removal at 0°C, subjecting isolated **2-40** to the subsequent reaction conditions without delay.

Thandi pressed on with the synthetic applications of **2-40**, but during Raman's later tenure, it was deemed valuable to undertake a closer experimental and theoretical examination of the dimerization reaction. Specifically, the relative ease of the dimerization compared to the sluggishness of the reaction of **2-40** with dienophiles was examined in terms of the well-established predictions of qualitative perturbation theory for 5-substituted cyclopentadienes. These predictions arise from the extension of the claims made by perturbation theory for systems exhibiting spiroconjugation to qualitatively similar systems bearing substituents with p orbitals capable of taking up orientations like those observed in spiroconjugated systems. Spiroconjugation describes a form of homoconjugation which is established when the termini of orthogonal π systems are held in mutual proximity as a consequence of their linkage by a common spiro carbon. An example of these so-called spirarenes is spiro[4.4]nonatetraene **2-42** (Figure 2-3).



2-42

Figure 2-3. Spiroconjugated compound spiro[4.4]nonatetraene.

Qualitative perturbation theory offers predictions of the influence of spiroconjugative interactions on the frontier molecular orbitals of the isolated π systems. It is predicted that the HOMO of **2-42** will be raised in energy as a result of the antibonding interaction between the terminal p orbitals of the two π systems. Alternatively, the LUMO of **2-42** is expected to be unaffected because the LUMO of the cyclopentadiene fragment is symmetric with respect to the ring-orthogonal symmetry plane whereas the p orbitals of the orthogonal π system are anti-symmetric about the same plane (Figure 2-4)

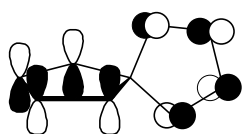
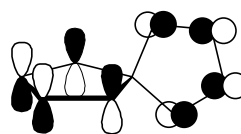
HOMO for **2-42**LUMO for **2-42**

Figure 2-4. Frontier orbitals of **2-42**.

It has been pointed out that the predictions of perturbation theory for spirarenes can be applied to 5-substituted cyclopentadienes in which the C5 substituent contains a p orbital that can be oriented orthogonally to the ring π system. An implication of the spiroconjugation-like interaction is that the raising of the HOMO energy level toward the unaffected LUMO energy level decreases the energy gap and can be invoked to explain the tendency of 5-substituted cyclopentadienes such as cyclopentadienone ketals and 5-halocyclopentadienes to dimerize in preference to undergoing Diels-Alder reactions with

other dienophiles.

In this group, *ab initio* calculations (3-21G basis set) were carried out to determine whether the Diels-Alder reactivity of **2-40** is explicable by spiroconjugation arguments. The computational study determined that both the HOMO and LUMO energies of 5-substituted cyclopentadienes can be lowered by substitution with respect to cyclopentadiene, in contradiction to the predictions of perturbation theory for spiroconjugated systems. The influence of spiroconjugation was found to be weak relative to the consequences of the electron-withdrawing effects of the C5 substituents, and for **2-40**, the HOMO and LUMO energy levels were found to be lowered with respect to the corresponding orbitals in cyclopentadiene by comparable amounts (Figure 2-5).²¹

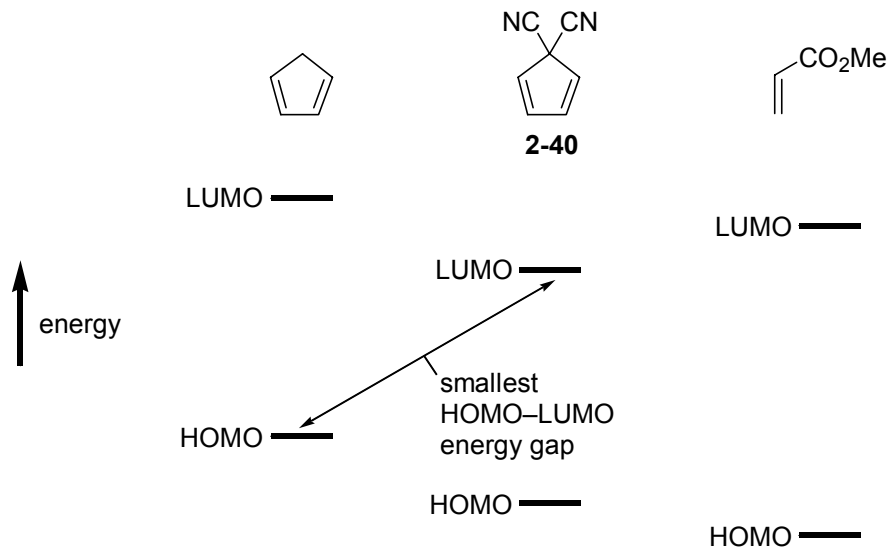
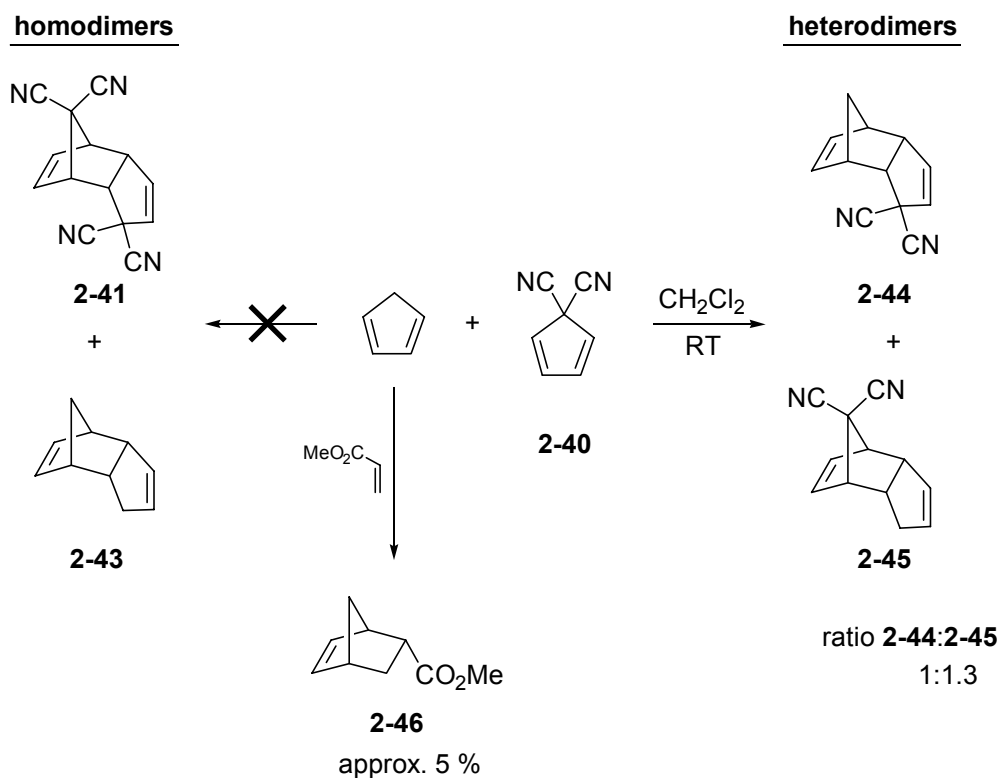


Figure 2-5. Energies of frontier molecular orbitals of cyclopentadiene, **2-40**, and methyl acrylate.

The relatively low reactivity of **2-40** toward typical dienophiles was accounted for by reference to the energy scale for the frontier molecular orbitals (Figure 2-5) in which it is apparent that there is an enlarged HOMO_{diene}-LUMO_{dienophile} energy gap, as compared to the diene-dienophile relationship for the relatively reactive cyclopentadiene, which reduces the

degree of stabilizing frontier orbital interaction in the beginning of cycloaddition. The orbital energy diagram reveals that the smallest energy gap is between the HOMO of cyclopentadiene and the LUMO of **2-40**. If this energy relationship was predictive, then a mixture of cyclopentadiene and **2-40** would be expected to yield predominately the Diels-Alder heterodimers. To test this prediction, two competition experiments were carried out: the first employing an equimolar mixture of cyclopentadiene and **2-40**, measuring by ^1H NMR spectroscopy the proportion of production of the four possible Diels-Alder dimers; the second employing an equimolar mixture of cyclopentadiene, **2-40**, and methyl acrylate as a competitive dienophile. In both cases, the dienes were prepared for immediate use, and the reactants were dissolved in CH_2Cl_2 at room temperature. In each experiment, heterodimers were produced exclusively. In the experiment that included methyl acrylate, a small quantity of adduct **2-46** was generated (5 %), along with the diene heterodimers.



Scheme 2-11. Generation of solely heterodimers in Diels-Alder reactions of mixed quantities of cyclopentadiene, **2-40**, and methyl acrylate.

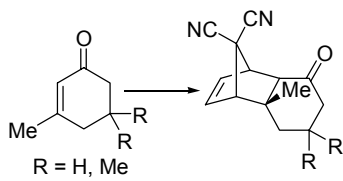
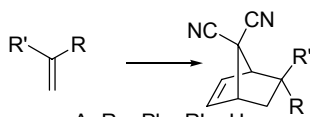
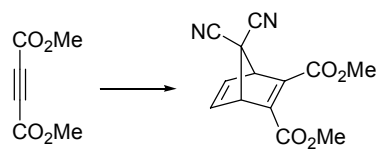
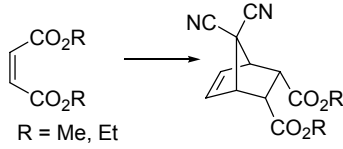
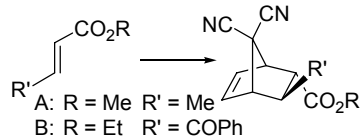
With a reliable means to generate 5,5-dicyanocyclopentadiene in hand, Thandi submitted it to the planned [2 + 2] cycloaddition with dichloroketene, chosen for its reactivity and ease of preparation. After a varied series of attempts, no [2 + 2] cycloaddition products were obtained, the Diels-Alder dimer **2-41** being the only product isolated. The failure of the [2 + 2] cycloaddition was attributed to electronic effects, as successful ketene cycloadditions had been reported with more sterically hindered 5,5-disubstituted cyclopentadienes. The ability of **2-40** to undergo [4 + 2] dimerization prompted an alternative examination of the diene in the Diels-Alder reaction. Thandi didn't observe Diels-Alder adducts with his chosen set of dienophiles, in each case obtaining dimer **2-41**, and so returned to experiments related to substituted bicyclo[3.2.0]heptanes in the context of β -lactamase inhibition; however, the seeming promise of **2-40** as a Diels-Alder diene compelled further exploration.

Undergraduate researcher R. Friesen successfully implemented **2-40** in Diels-Alder reactions with a set of electron-poor dienophiles,²² and J.V. Raman would later attempt to expand the set of adducts, employing, among others, more highly substituted dienophiles.⁷ The set of attempted Diels-Alder reactions of **2-40**, carried out across the three discontinuous research projects in advance of the current work, is summarized in Table 2-1.

Table 2-1. Attempted Diels-Alder reactions of 5,5-dicyanocyclopentadiene (**2-40**).

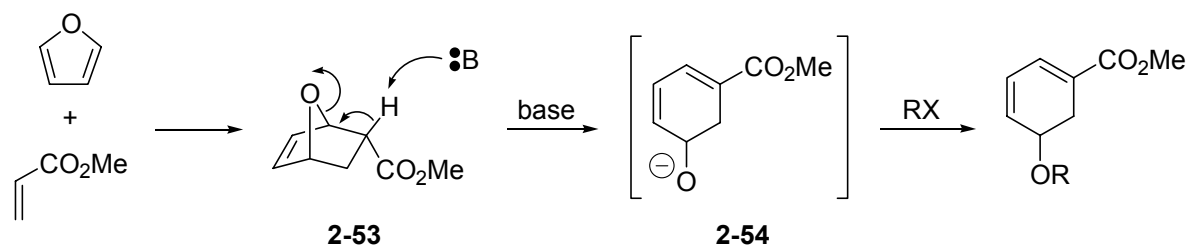
Entry	Attempted 2-40 + dienophile → adduct	Dienophile Quantity (equiv.)	Conditions	Result	Ref.
1		Expt. 1: 20	1: CDCl ₃ RT 26 hrs.		A
		Expt. 2: 10	2: CH ₂ Cl ₂ RT 17 hrs.		
2		"excess"	THF RT 24 hrs.	2-41	A
3		1	THF RT 63 hrs.	2-41	A
4		1	CH ₂ Cl ₂ RT 5 hrs.	2-41	A
5		25 (as solvent)	RT 22 hrs.	67%	B
6		25 (as solvent)	RT 22 hrs.	76%	B
7		25 (as solvent)	RT 22 hrs.	63%	B
8		25 (as solvent)	RT 22 hrs.	37%	B

Table 2-1. (Continued)

Entry	Attempted 2-40 + dienophile → adduct	Dienophile Quantity (equiv.)	Conditions	Result	Ref. ¹
9		not given	not given	“unsuccessful”	C
10		A: 25 (as solvent)	A: RT 20 hrs.	2-51 : “13-18%”	D
		B: 25 (as solvent)	B: RT ²	B: 2-41	
11		25 (as solvent)	RT “12-15 hrs.”	2-52 : “75-80%”	D
12		25 (as solvent)	RT ²	2-41	D
13		25 (as solvent)	RT ²	2-41	D

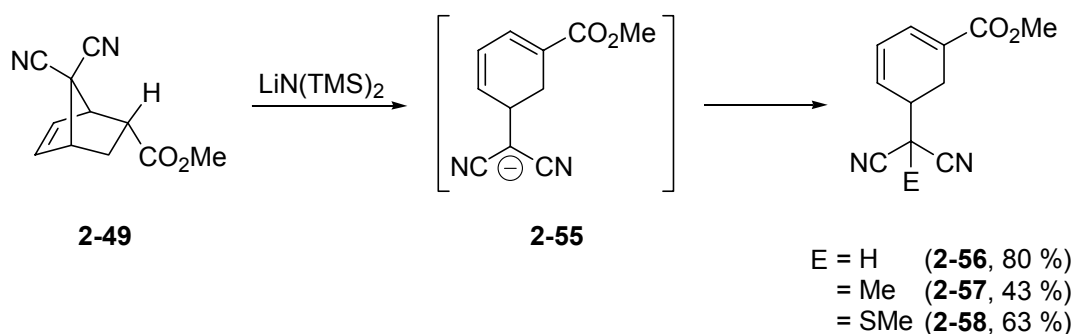
¹ References: A, M.S. Thandi M.Sc. Thesis (1981); B, R.W. Friesen Chem 492 report (1984), and Dmitrienko, G.I., Savard, M.E., Friesen, R.W., Thandi, M.S. *Tetrahedron Lett.* **1985**, 26, 1691-1694.; C, R.W. Friesen Chem 492 report (scheme), lab book (experimental details; applies to both R = H and R = Me); D, J.V. Raman M.Sc. Thesis (1986). ² No time given.

As the first successes with the Diels-Alder reaction of **2-40** were being achieved with the syntheses of adducts **2-47–2-50**, some thought was directed toward synthetic applications of their further elaboration. A number of reports had appeared concerning the ring-opening of Diels-Alder adducts of furan and dienophiles bearing electron-withdrawing groups by treatment with base, which deprotonated the methine protons α to the carbonyl in the respective compounds (Scheme 2-12).^{23,24}



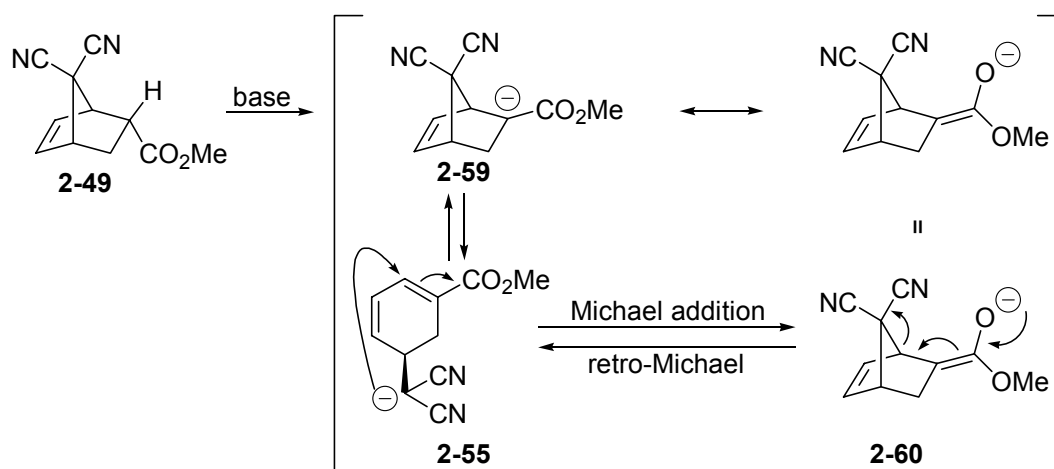
Scheme 2-12. Base-induced ring opening of furan/methyl acrylate Diels-Alder adduct.

The formal reversion of a conjugate alkoxide addition which resulted (**2-53**→**2-54**) furnished 5-oxa-substituted cyclohexadienes, specific instances of which had been incorporated into total syntheses of significant carbocyclic natural products. It was reasoned that the malononitrile moiety of our carbobicyclic [2.2.1] cycloadducts might be able to stabilize the negative charge resultant upon, and so permit, the conversion to a 1,5-disubstituted cyclohexadienyl carbanion generated analogously to **2-54**. Treatment of **2-48** (methylvinylketone dienophile) with alkoxide bases in alcohol in temperature-varied experiments resulted either in no reaction or decomposition, as did DBU in THF. Reasoning that the lack of success could be attributed to deprotonation of the methyl group of **2-48**, deprotonation of **2-49** (methyl acrylate dienophile) was attempted, this time with LDA, which furnished, after acid workup, the neutral ring-opened adduct in modest yields (20-35%). Encouraged by a report that ring-opening of furan adducts could be effected at higher, though unspecified, yields with lithium hexamethyldisilazide, Friesen treated **2-49** with $\text{LiN}(\text{TMS})_2$ in THF at low temperature (obtaining **2-56**, after acidic workup, in 80% yield), and was able to trap the ring-opened anion *in situ* with electrophiles to obtain methylated and sulfonylated products (Scheme 2-13).



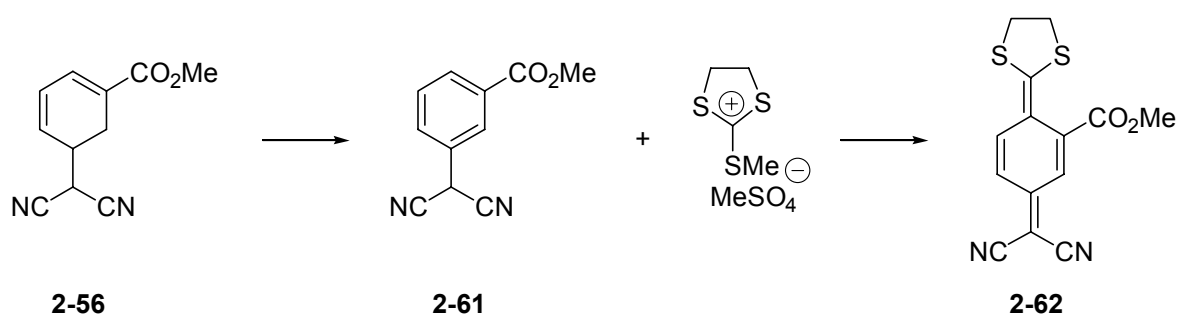
Scheme 2-13. Friesen's ring-opening of **2-49** and trapping of **2-55** with electrophiles.

The Diels-Alder adduct **2-49** could formally be viewed as having formed by intramolecular Michael addition of the anion **2-55** of the anionic active methine compound **2-55** to the β carbon of the ring π system (Scheme 2-14). The reaction would be a favourable 5-*exo*-trig cyclization with respect to the so-formed diene-derived ring of **2-49**, but would be an unfavourable 5-*endo*-trig cyclization with respect to the second five-membered ring. The reverse, or retro-Michael, reaction (**2-55** \rightarrow **2-59/2-60**) would be driven by the greater stability of the ring-opened dinitrile-stabilized carbanion with respect to the ester enolate **2-59**, the formation of the extended conjugated system upon introduction of the α,β unsaturation, and the relief of the ring strain in the bicyclo[2.2.1]heptene ring system.



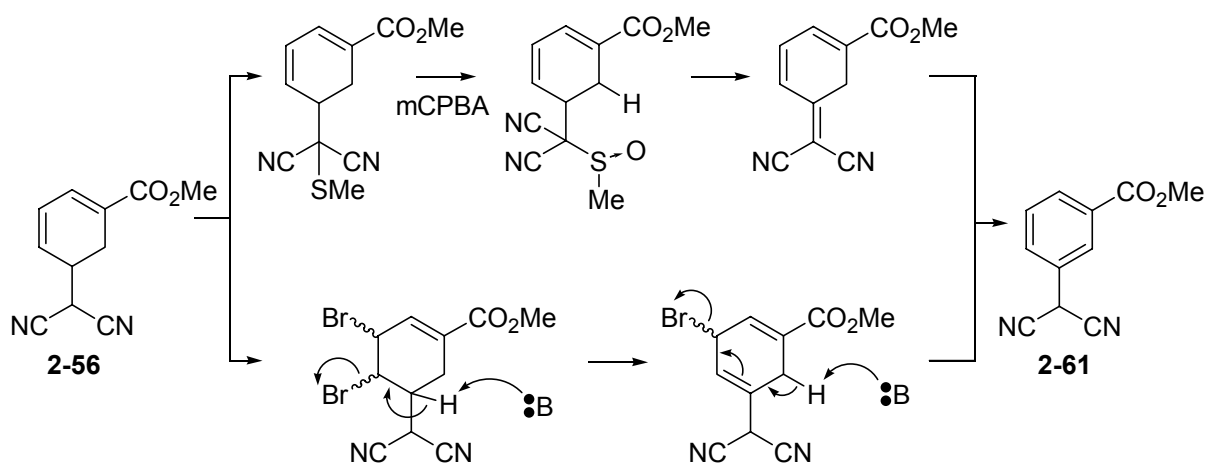
Scheme 2-14. Ring-opening of **2-49** as a retro-Michael addition.

Two applications for the ring-opened adduct **2-56** were conceived of in the early going. The aromatic *meta*-substituted arylmalononitrile obtained by dehydrogenation of **2-56** would have been of use in the synthesis of substituted examples of the “push-pull” stabilized quinodimethanes then being explored for use as semiconductors. The relative inaccessibility of *meta*-substituted benzyl cyanides presumably accounted for the sparse occurrence of the resultant *meta*-substituted arylmalononitriles reported by Davis and Cava in their route to the desired quinodimethanes (Scheme 2-15).²⁵



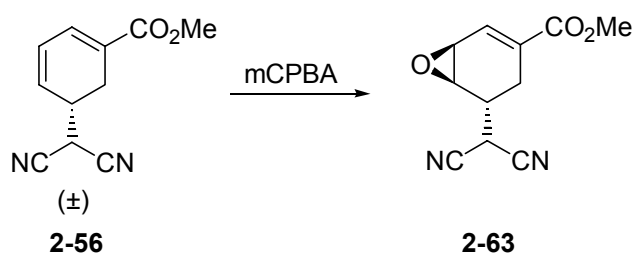
Scheme 2-15. Potential synthesis of “push-pull-stabilized” quinodimethanes.

The typical method of aromatizing cyclohexadienes with 2,3-dichloro-5,6-dicyanobenzoquinone (DDQ) failed in the case of **2-56**, but the conversion was easily accomplished by two means: treatment of the sulfoxide derived from **2-56** with mCPBA; and by regioselective bromination of **2-56**, followed by treatment with two equivalents of DBU, both via the posited intermediates shown (Scheme 2-16).



Scheme 2-16. Two aromatizations of **2-56** carried out by R. Friesen.

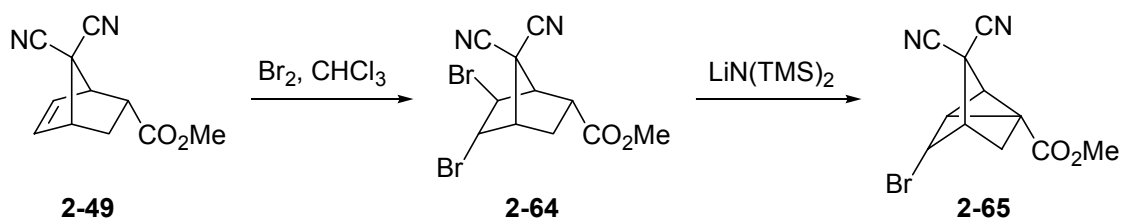
A more involved use devised for the ring-opened adduct was in its possible applicability to the synthesis of eremophilane sesquiterpenoids. As a preliminary functional manipulation devised for the synthetic study, the epoxidation of the ring C3–C4 bond was undertaken. Friesen was able to epoxidize **2-56**, and although determination of the relative stereochemistry of the sole epoxide diastereomer proved elusive by ^1H NMR experiments, a *trans* relationship to the dicyanomethyl moiety was reasonably assumed (Scheme 2-17).



Scheme 2-17. Epoxidation of **2-56** carried out by R. Friesen.

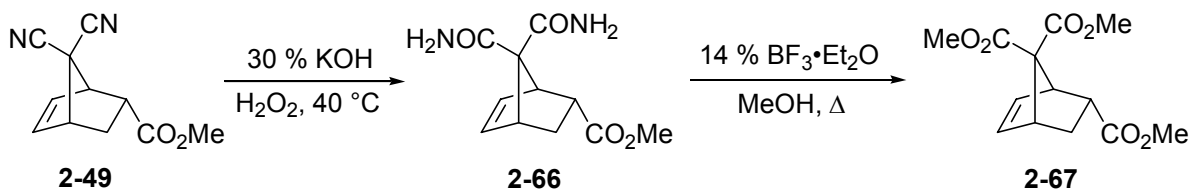
Functionalization of the double-bond of Diels-Alder adduct **2-49** was also attempted, first by epoxidation and then by halolactonization, osmylation, bromination, and halohydrin formation, with the thought that appropriate addition products could be obtained prior to ring-opening. Only bromination, which was carried out in refluxing CHCl_3 , succeeded. The reaction was concluded to have occurred by a radical mechanism, because experiments in

polar solvents such as acetic acid and methanol had failed. The bromination was formulated as having furnished the trans-dibromide **2-64**. Treatment of **2-64** with base did not furnish the ring-opened product, instead generating the tricyclic bromide displacement product **2-65** (Scheme 2-18), which offered support to the stereochemical assignment, since backside displacement of the C3-bromide would only be possible if it occupied the *exo* face of the adduct.



Scheme 2-18. Generation of dibromide **2-63** and tricyclic compound **2-64** by R. Friesen.

With epoxide **2-63** in hand, Friesen undertook other functional manipulations, now focussing on **2-49**, with the expectation that functional conversions could precede ring-opening and so increase the versatility of the Diels-Alder/ring-opening sequence. A survey of the literature for the hydrolysis of the geminal nitriles uncovered various harsh methods. After some unsuccessful experiments employing HCl and H₂SO₄ in methanol at room temp. and at reflux, **2-49** was treated with 30% KOH and stoichiometric H₂O₂ at 40 °C. The reaction produced not the acid but the intermediate malonamide **2-66**, which was hydrolyzed and esterified in a refluxing solution of 14% boron trifluoride etherate in methanol according to the method of Harley-Mason and coworkers (Scheme 2-19).²⁶



Scheme 2-19. Conversion of **2-49** to triester **2-67** by R. Friesen.

Still with a view to the use of the Diels-Alder/ring-opening sequence in natural product synthesis, Friesen carried out unsuccessful model experiments with 5,5-dicyanocyclopentadiene and substituted cyclohexenones in an attempt to extend the generality of the Diels-Alder reaction to more complex dienophiles that would give more elaborate synthetic intermediates (Table 2-1, entry 9). The potential for derivatives of the ring-opened adduct to behave as dienophiles prompted an attempted Diels-Alder reaction between 2-trimethylsiloxy-1,3-butadiene and epoxide **2-63**, which was unsuccessful.

The generation of 5,5-dicyanocyclopentadiene and its Diels-Alder reactions with monosubstituted dienophiles, the subsequent base-induced ring-opening of the adduct with methyl acrylate (**2-49**), and the trapping of the intermediate anion **2-55** with a small set of electrophiles, provided the basis for the current study, which set out to expand the reaction of **2-55** with acceptor electrophiles potentially capable of exhibiting tandem reactivity. Prior to the study of the planned tandem reactions, attention was briefly returned to the problem of carrying out successful Diels-Alder reactions with more highly substituted dienophiles.

2.2 Results and Discussion

2.2.1 Attempted Diels-Alder Reactions

Though the main focus of this work took as its starting point the ring-opened adduct, some preliminary attempts were made to further the goal of expanding the set of dienophiles capable of undergoing Diels-Alder reaction with 5,5-dicyanocyclopentadiene to include *trans*-disubstituted dienophiles. More complex Diels-Alder adducts would represent efficiently realized synthetic intermediates in any future use of the ring-opened adduct in

natural products synthesis. Indeed, a trisubstituted dienophile was the basis of the synthesis planned for puupehenone analogs. Numerous experiments were conducted with methyl crotonate and methyl methacrylate under a variety of conditions including greater excesses of dienophile as solvent and Lewis acid catalysis (AlCl_3 , BF_3 -etherate), but in all cases only 5,5-dicyanocyclopentadiene Diels-Alder dimer **2-41** was isolated. In the early going, several Diels-Alder adducts previously made by R.W. Friesen (Table 2-1: from dienophiles acrolein, methyl vinyl ketone (MVK), methyl acrylate) were replicated. Of the three, the two adducts derived from acrolein and methyl acrylate were oils, but the MVK-derived adduct (**2-48**) was crystalline. A slowly-grown crystal was submitted to analysis by single crystal X-ray diffraction (Figure 2-6).

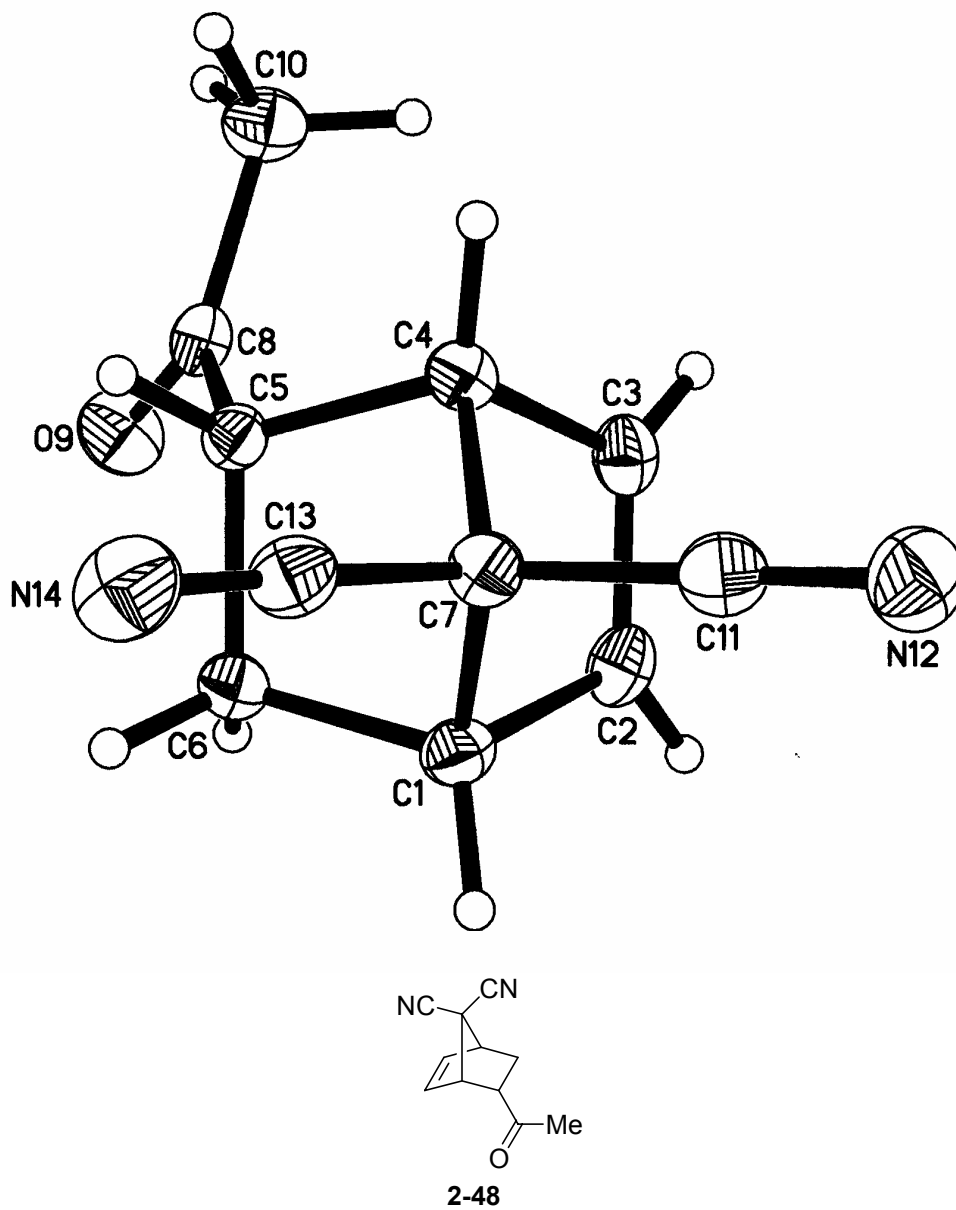


Figure 2-6. ORTEP: Diels-Alder adduct of MVK and 5,5-dicyanocyclopentadiene. (See Appendix page 339 for full crystallographic data)

From the supply of high-purity **2-41** derived from unsuccessful Diels-Alder reactions, a sample was crystallized and studied by single crystal X-ray diffraction (Figure 2-7).

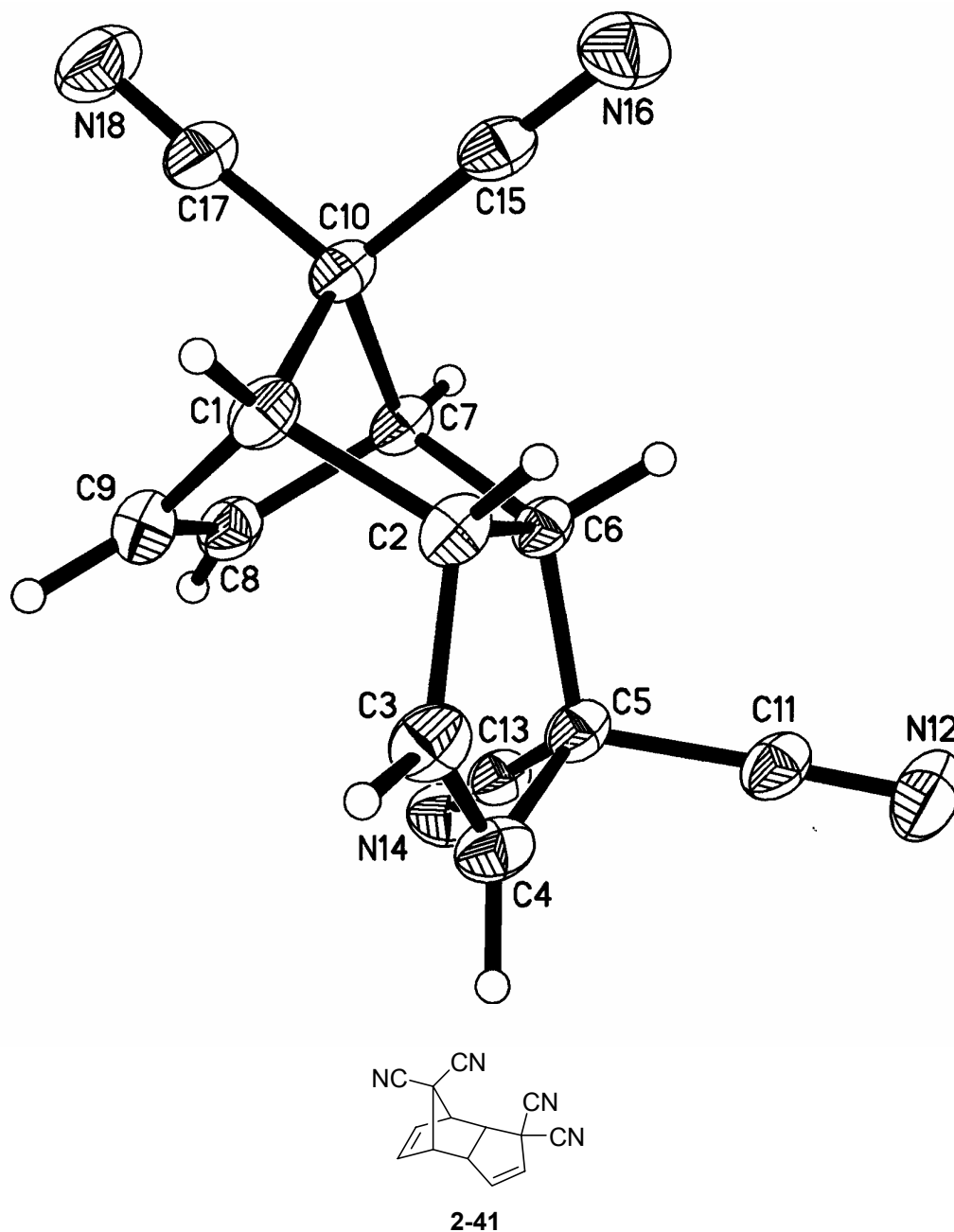


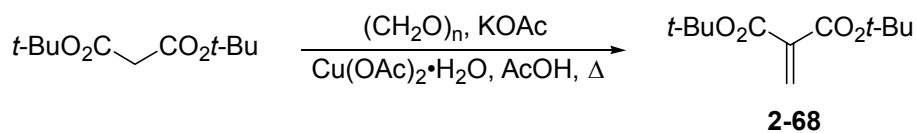
Figure 2-7. ORTEP: Diels-Alder dimer of 5,5-dicyanocyclopentadiene. (See Appendix page 343 for full crystallographic data)

Some variations were introduced to Friesen's established method of forming the Diels-Alder adduct **2-49** (dienophile = methyl acrylate) to make the process simpler and to

limit the extent of diene dimerization. To avoid the potential for dimerization in the workup of the newly generated 5,5-dicyanocyclopentadiene, it was thought that the didehydrohalogenation of **2-39** could be effected in the dienophile solvent at room temperature without workup, and that the Diels-Alder reaction would occur uneventfully in the presence of spectator ion pair $\text{DBU}^+\text{-H}$. In practice, the addition at small scale of neat DBU to a solution of dibromide **2-39** in acrolein resulted in a violent exothermic polymerization of the solvent. Greater success was achieved with solutions of the dibromide dissolved in methyl acrylate at $-78\text{ }^\circ\text{C}$ and slow addition of DBU, followed by warming to room temperature over the course of the overnight reaction. Workup entailed filtration of the DBU-H^+ precipitate and removal of methyl acrylate *in vacuo*.

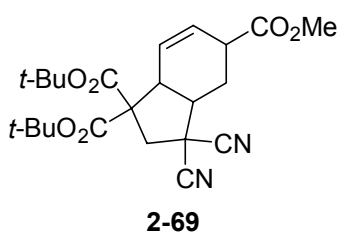
2.2.2 Reaction of Ring-Opened Adduct with Doubly-Activated Michael Acceptors

The initial Michael acceptor designated for this study was di-*tert*-butyl methylenemalonate (**2-68**), chosen to chemically distinguish the acceptor-derived esters from the carbomethoxy group of the parent ring in any later manipulations. According to a literature precedent, di-*tert*-butyl malonate was treated with paraformaldehyde, potassium acetate and cupric acetate monohydrate in acetic acid and refluxed for several hours. Removal of the acetic acid *in vacuo* and distillation provided material of acceptable purity (Scheme 2-20).

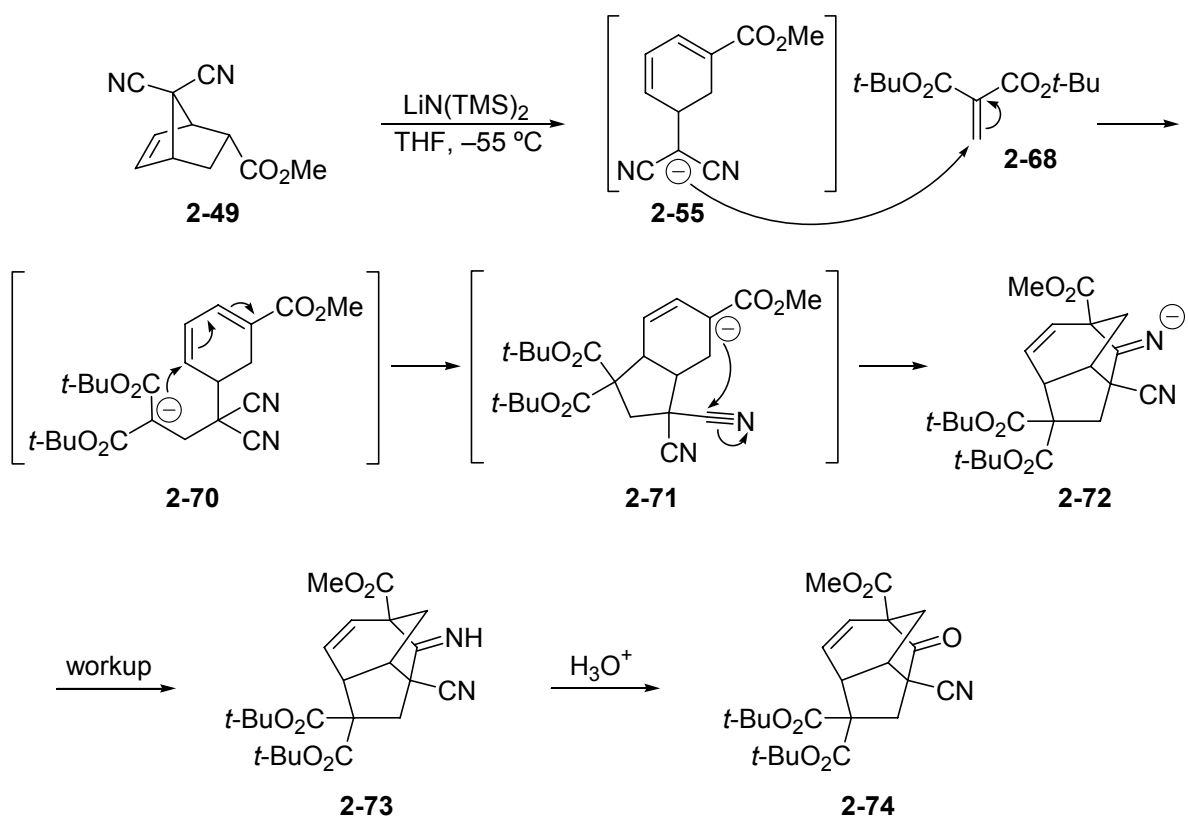


Scheme 2-20. Generation of di-*tert*-butyl methylenemalonate.

In our initial attempts to employ **2-68** as a tandem conjugate addition substrate, the ring-opened adduct anion was generated by treatment of Diels-Alder adduct **2-49** with $\text{LiN}(\text{TMS})_2$ in THF at $-50\text{ }^\circ\text{C}$, followed by the slow addition of a THF solution of **2-68**. After 30 min. at $-50\text{ }^\circ\text{C}$ and 30 min. at room temp., the reaction was worked up by partition between CH_2Cl_2 and saturated aqueous NH_4Cl .

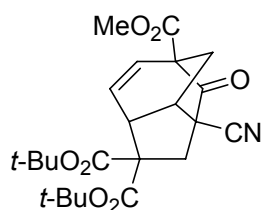
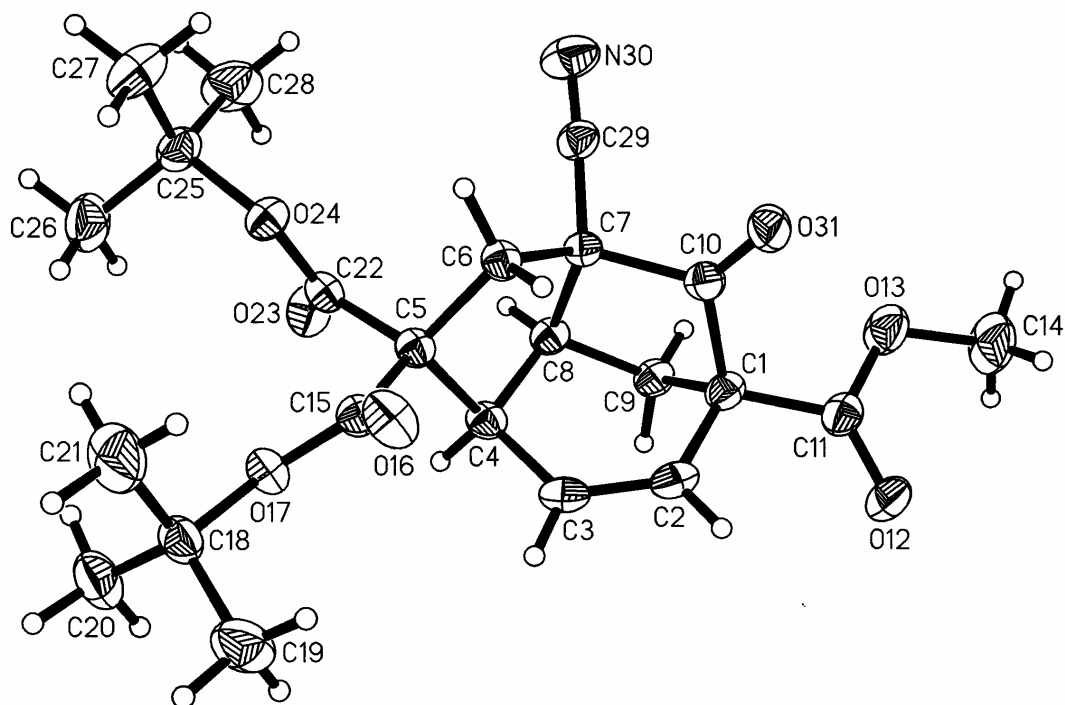
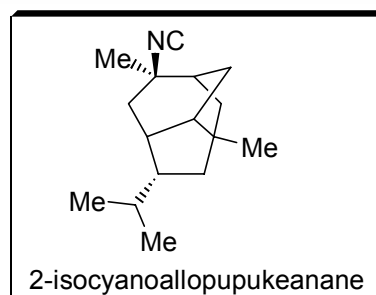


The crude reaction mixture furnished a ^1H NMR spectrum whose two vinyl proton signals indicated the disruption of the parent ring vinyl system, and therefore that further reaction had occurred after generation of the adduct. The signals seemed consistent with those of a bicyclic compound **2-69** expected as the outcome of tandem addition/cyclization, but the spectrum also contained a broad signal at δ 9.95 that was not expected. It was reasoned that the tandem cyclization product enolate **2-71** (Scheme 2-21), resulting from conjugate addition of the stabilized adduct enolate **2-70** to the δ -carbon of the parent ring unsaturated system, was sufficiently close to the proximate nitrile to bring about a second tandem addition to generate the imine anion **2-72**, and, after workup, the tricyclic imine **2-73**. Hydrolysis of the putative imine with aqueous HCl in EtOAc at room temperature furnished a compound with separated vinyl proton signals and IR (1723 cm^{-1}) and ^{13}C NMR (δ 198.1) spectra consistent with the presence of a ketone. Ultimately, structural confirmation was achieved when a crystal suitable for study by X-ray diffraction was obtained (Figure 2-8). Anion **2-55** was unreactive toward diethyl isopropylidene malonate, presumably for steric reasons.



Scheme 2-21. Generation of tricyclic tandem conjugate addition product **2-74**.

The fortuitous high extent of tandem reactivity that generates **2-74** is significant insofar as the carbocyclic homobrendane skeleton generated is present in the marine natural product 2-isocyanoallopupukeanane (Figure 2-8), one of seven sesquiterpene isonitriles isolated from the marine nudibranch *Phyllidia pustulosa*.²⁷

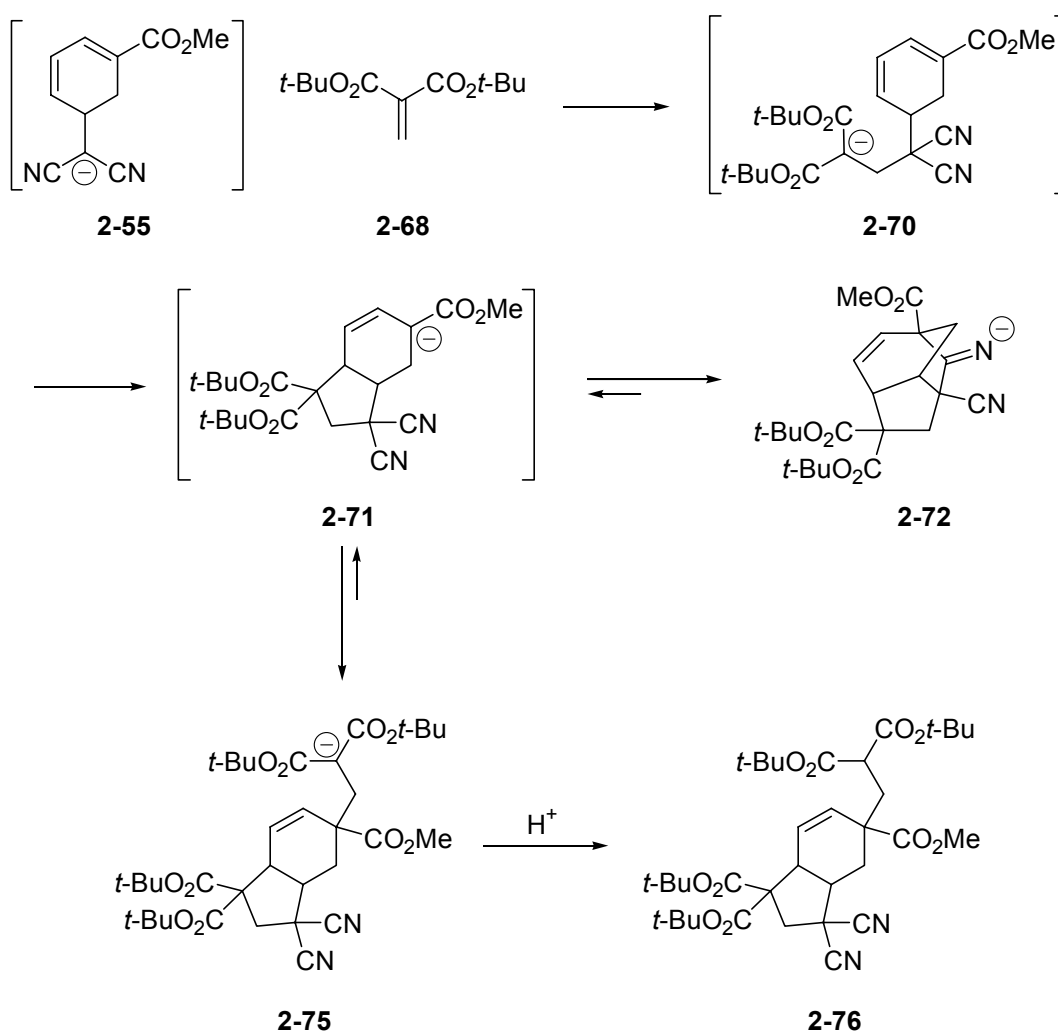
**2-74**

2-isocyanoallopupukeanane

Figure 2-8. ORTEP: homobrendane skeleton derived from Diels-Alder adduct **2-49** or ring-opened adduct **2-56** and di-*tert*-butyl methylenemalonate. (See Appendix page 347 for full crystallographic data)

An interesting result was uncovered when the reaction of **2-49** was carried out with excess di-*tert*-butyl methylenemalonate and permitted to continue beyond the time necessary to consume the starting material. Specifically, when **2-49** and 2.5 equivalents of di-*tert*-butyl methylenemalonate were reacted at $-60\text{ }^{\circ}\text{C}$ for 30 min. followed by stirring overnight at room temp., the ^1H NMR spectrum of the resulting rather complex crude product evidenced four peaks for *t*-butyl protons and vinyl protons at different chemical shifts than

were observed for the homobrendane system. Column chromatography and careful crystallization furnished a crystal suitable for assessment by single crystal X-ray diffraction that confirmed the structure as bicyclic bis-alkylated adduct **2-76** (Figure 2-9). It was reasoned that, whereas tricyclic imine anion **2-72** represents the kinetic product of the tandem sequence, prolonged exposure to excess Michael acceptor permits slow equilibration to the thermodynamically more stable bicyclic bis-alkylated stabilized enolate **2-75**, via bicyclic enolate **2-71**.



Scheme 2-22. Generation of bicyclic bis-alkylated compound **2-76** at long reaction times in the presence of excess di-*tert*-butyl methylidenemalonate.

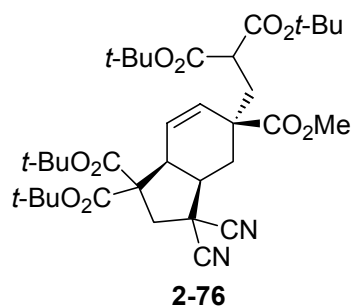
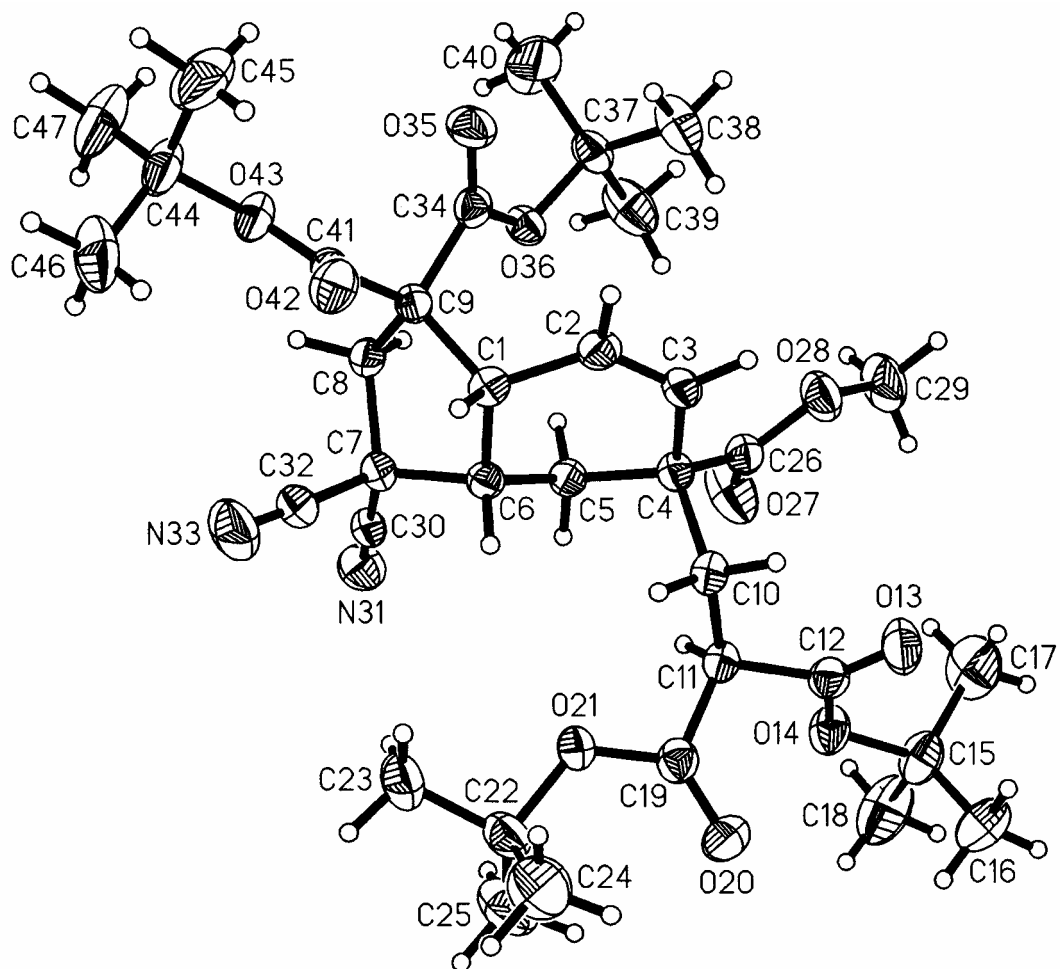
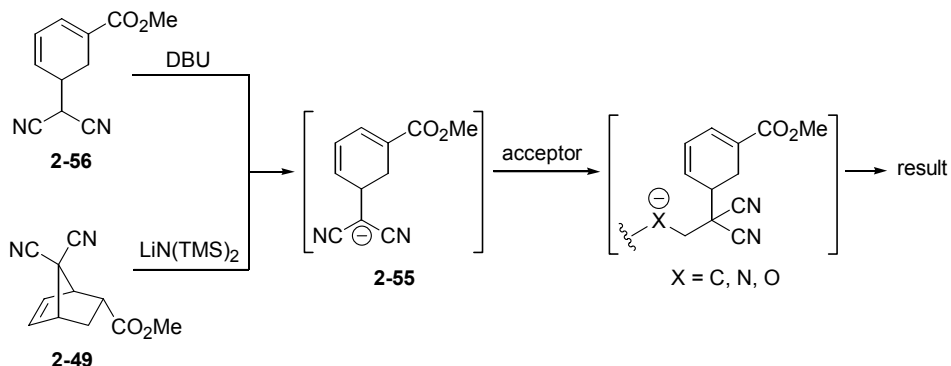


Figure 2-9. ORTEP: bicyclic bis-alkylated compound **2-76**. (See Appendix page 352 for full crystallographic data)

2.2.3 Reaction of Ring-Opened Adduct with Singly-Activated Michael Acceptors and Heteroatom 1,2-Addition Partners

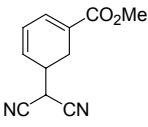
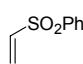
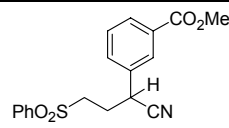
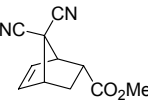
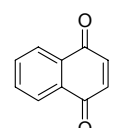
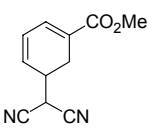
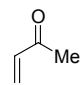
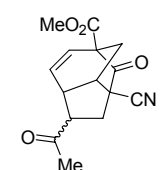
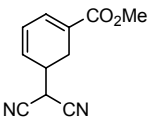
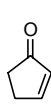
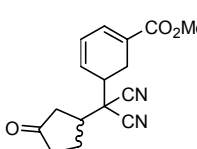
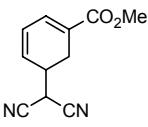
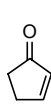
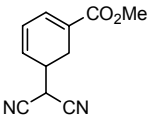
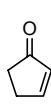
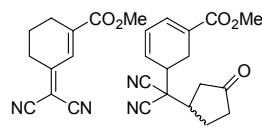
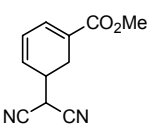
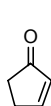
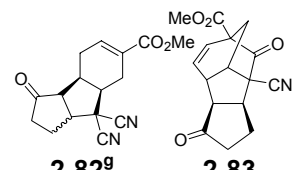
Several unsaturated compounds, among them vinyl reagents, carbonyl compounds, isocyanates, and others were tested for their ability to undergo conjugate or 1,2-addition with the ring-opened adduct anion to yield intermediates capable of undergoing the tandem conjugate addition. With the heteroatom reagents, it was hoped that efficient syntheses of heterocycles could be achieved, for example hexahydrobenzofurans from aldehydes. Reactions were conducted starting with either the Diels-Alder adduct **2-49** or the ring-opened adduct **2-56**, and employing either LHMDS or DBU, respectively. Table 2-2 summarizes these experiments.

Table 2-2. Reactions of **2-49** and **2-56** with singly-activated Michael acceptors and heteroatom 1,2-acceptors.



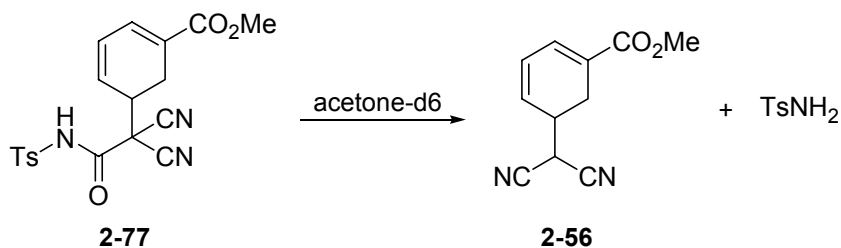
Entry	Substrate	Acceptor	Conditions	Duration (hrs.) ^a	Result
1			1.1 equiv. LHMDS, THF 2 equiv. acceptor $-60\text{ }^\circ\text{C} \rightarrow \text{room temp.}$	19	no reaction
2			1.1 equiv. DBU, CH_3CN 1 equiv. acceptor room temp.	27	complex mixture
3			1 equiv. DBU, CH_3CN 1 equiv. acceptor room temp.	7	complex mixture
4			1 equiv. DBU, CH_3CN 1 equiv. acceptor $0\text{ }^\circ\text{C}$	2.33	 2-77 labile adduct ^b
5			1.2 equiv. DBU, CH_3CN 1.2 equiv. acceptor room temp.	93	complex mixture
6			1 equiv. DBU, CH_3CN 1 equiv. acceptor room temp.	29	complex mixture
7			1.1 equiv. LHMDS, THF 2 equiv. acceptor $-60\text{ }^\circ\text{C} \rightarrow \text{room temp.}$	19	complex mixture

Table 2-2 (continued)

Entry	Substrate	Acceptor	Conditions	Duration (hrs.)	Result
8			1 equiv. DBU, CH ₃ CN 1 equiv. acceptor room temp.	28	 2-78 (16 %)
9			1.1 equiv. LHMDS, THF 2.5 equiv. acceptor -60 °C → room temp.	4	complex mixture
10			1 equiv. DBU, CH ₃ CN 1.1 equiv. acceptor 0 °C, aq. NH ₄ Cl workup then 6 % HCl hydrolysis for 1 hr.	1.66 ^c	 2-79 (42 %)
11			0.1 equiv. DBU, CH ₃ CN 1 equiv. acceptor -10 °C → room temp.	0.5	 2-80 (quant.)^d
12			1 equiv. LHMDS, THF 1.13 equiv. acceptor -60 °C → room temp.	19	no reaction
13			1 equiv. DBU, CH ₃ CN 1 equiv. acceptor -10 °C	3	 2-81 (14 %)^e 2-80 (39 %)^f
14			1 equiv. DBU, CH ₃ CN 1 equiv. acceptor -10 °C → room temp. then 6 % HCl hydrolysis for 30 min.	26 ^c	 2-82^g (8 %)^h 2-83 (5 %)^h

^a Short duration reactions (> 7 hrs.) were monitored by TLC. Longer reactions may have consumed starting material prior to cited durations. ^b Adduct reverted to ring-opened adduct and generated white precipitate upon dissolution in CDCl₃ and acetone-d₆. ^c Duration of initial conjugate addition reaction. Hydrolysis of homobrendane imine in EtOAc/aq. 6 % HCl emulsion was carried out for 1 hour (entry 10) or for 30 min. (entry 14). ^d Reaction monitored by aliquot removal and workup. Quantitative yield cited based on ¹H NMR spectrum. ^e ¹H NMR yield within impure column fraction set contaminated with 40 mol % of **2-56**. ^f Isolated yield. ^g Putative structure only, based upon CO₂CH₃ ¹H NMR signals and broad singlet for each racemic diastereomer at approx. δ 7. ^h ¹H NMR yields within mixed column fraction set: **2-82** a racemic mixture of diastereomers; **2-83** racemic single diastereomer.

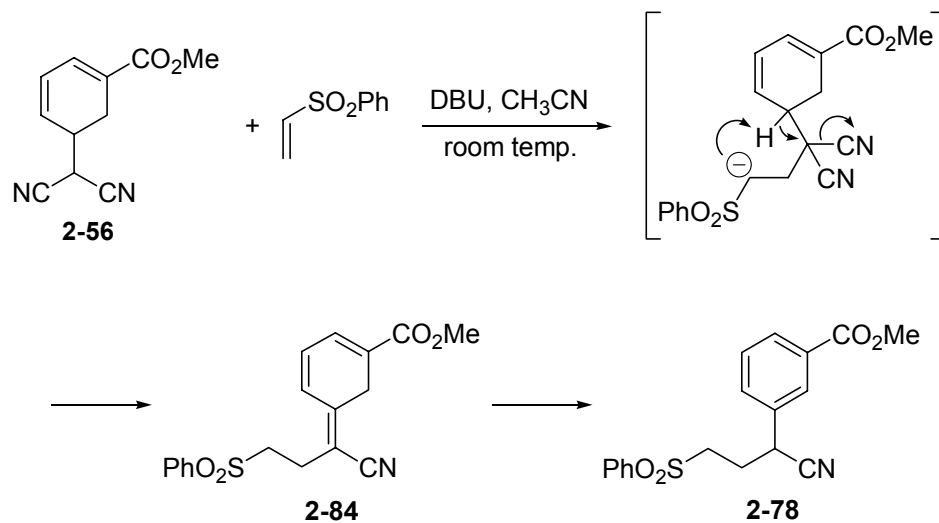
Attempted addition to benzaldehyde was expected to furnish heterocyclic tandem reaction products, but strong base conditions, starting from **2-49** (entry 1) brought about no reaction, and an experiment starting from the ring-opened adduct (entry 2) produced a complex mixture. The result was the same for the remainder of the aza heterocycle-directed experiments. Treatment of **2-56** with base and *N*-benzylidene-benzenesulfonamide (entry 3) generated a complex mixture. Reaction of anion **2-55** with TMS isocyanate (entry 5) produced a complex mixture. The analogous reaction with tosyl isocyanate (entry 4) apparently generated adduct **2-77** that could partially survive column chromatography on silica but that formed extensive white precipitate of what appeared by ^1H NMR spectroscopy to be tosyl amide, and returned the ring-opened adduct (Scheme 2-23). Evidently, reversal of adduct formation regenerated tosyl isocyanate which was easily hydrolyzed to tosyl amine.



Scheme 2-23. Cleavage of labile adduct **2-77** in acetone-d₆.

An experiment conducted with phenyl vinyl sulfoxide (entry 6) generated a complex mixture, as did that conducted with phenyl vinyl sulfone and starting from **2-49**. The reaction of **2-56** with phenyl vinyl sulfone (entry 8) furnished a crude sample of high mass recovery and a crude ^1H NMR spectrum that contained aromatic proton signals but no vinyl signals. The product, purified by column chromatography, furnished a ^1H NMR spectrum that revealed the crude sample to have been fairly pure, but the recovery was sufficiently poor that the isolated yield of aromatic adduct **2-78** was only 16.4 %. An explanation is not readily devised for the disparity between the high mass balance and reasonable purity of the

crude sample along with its apparent stability with respect to TLC and the minimal isolated yield. The aromatization is rationalized as being a consequence of the reluctance of the adduct intermediate to undergo further conjugate addition. Evidently, intramolecular deprotonation of the ring C5-proton by the anionic carbon causes CN elimination to intermediate **2-84** and aromatization by base-induced rearrangement (Scheme 2-24).



Scheme 2-24. Generation of aromatic adduct **2-78** by aromatization of adduct intermediate.

A series of singly-activated 1,4-acceptors was next examined. A poorly soluble purple complex mixture was obtained from reaction of **2-49** with 1,4-naphthoquinone (entry 9) under strong base conditions. Ring-opened adduct (with DBU) furnished the second observed homobrendane upon reaction with methyl vinyl ketone (entry 10) at 0 °C for 1 hr. 40 min., followed by acid hydrolysis of the homobrendane imine. Column chromatography to separate the racemic diastereomers of **2-79** and crystallization furnished a crystal of the *endo*-acetyl isomer suitable for single-crystal X-ray analysis (Figure 2-10).

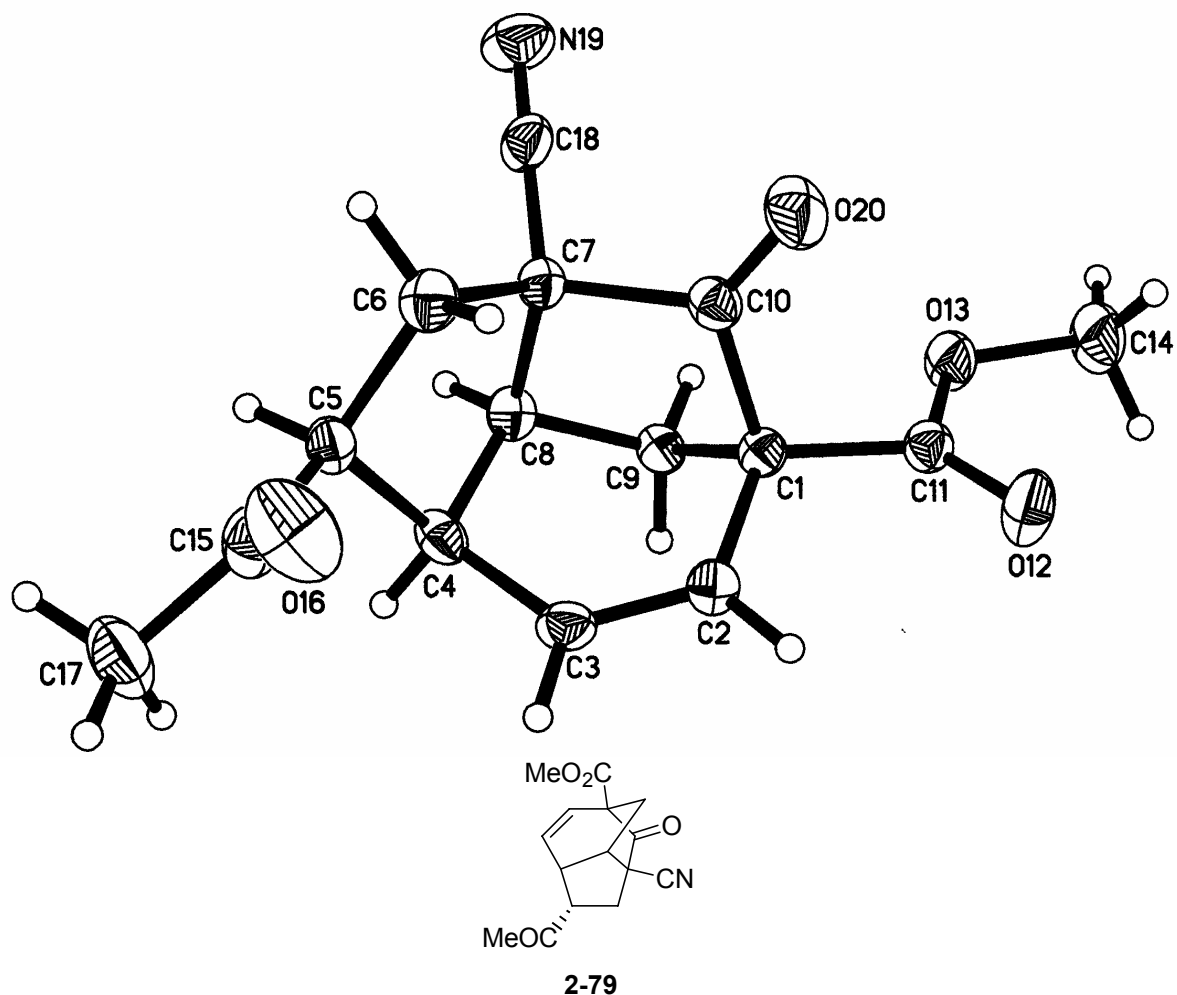


Figure 2-10. ORTEP: homobrendane **2-79** derived from ring-opened adduct and MVK. (See Appendix page 358 for full crystallographic data)

A series of experiments was conducted with cyclopentenone as acceptor (entries 11–14). Catalytic DBU acting upon **2-56** in the presence of one equiv. of cyclopentenone (entry 11) smoothly gave the adduct **2-80** as a diastereomeric mixture within 30 minutes. Overlap of ^1H NMR spectral signals made it difficult to determine whether any facial selectivity in the conjugate addition had occurred, but the partially resolved methyl ester proton singlets appeared to have similar intensities, suggesting that diastereoselectivity was at best minimal. The reaction was permitted to continue for 25 hours, at which time the ^1H NMR spectrum of the crude material revealed the persistence of pure adduct and the

occurrence of no side reactions, a valuable observation in the further experimental examination of cyclopentenone as a conjugate acceptor.

It was concluded that the anionic adduct intermediate in the catalytic DBU experiment had proved too kinetically basic to survive long enough to undergo tandem conjugate addition. It was thought that stoichiometric strong base would generate a persistent intermediate that would conclusively demonstrate whether the tandem reaction was possible for cyclopentenone. Treatment of **2-56** with LHMDS and a slight excess of cyclopentenone for 19 hours brought about no reaction aside from the generation of a trace of ring-opened adduct-derived tertiary alcohol due to attack of the ester carbonyl by an inadvertent slight excess of BuLi. The low reactivity of **2-56** in this case was puzzling and had an apparent counterpart in the reaction of lithiated **2-56** with alkyl propiolates (see chapter 5). This feature is difficult to account for as the same intermediate has generally demonstrated reactivity toward electrophiles. A remarkable possibility entails the determination of the reactivity of the lithiated **2-55** by the choice of substrate. The failed conjugate addition reactions involved treatment of the ring-opened adduct with LHMDS, whereas, aside from benzaldehyde, anion **2-55** derived from the Diels-Alder adduct **2-49** has proved invariably reactive toward electrophiles. If valid, the differing reactivity of formally the same counterion pair from the two different substrates would presumably be accounted for by a crucial difference in the structure of the counterion association that could drastically influence the anionic reactivity. Unfortunately, in the data at hand there is no direct comparison available of **2-49** and **2-56** in reaction with LHMDS and the same acceptor, and so further study is required to account for this observation. It is quite possible and certainly expected that the anion is indeed identical in all features, irrespective of the source, and that

in the case of the acceptors in question, the equilibrium so favours the malonyl anion/lithium cation over the adduct lithium enolate that no appreciable extent of reaction is seen.

Two experiments involving cyclopentenone were conducted with stoichiometric DBU. In a carefully monitored experiment (entry 13), the ring-opened adduct and stoichiometric cyclopentenone were pre-incubated at 0 °C and one equivalent of DBU in CH₃CN solution was added slowly. Periodic examination by TLC and ¹H NMR spectrometry of small quenched aliquots revealed the formation of a diastereomeric mixture of the expected adduct (**2-80**), as well as an unknown compound evidencing one vinylic proton triplet (1.9 Hz *J*) signal at δ 7.59. The reaction was halted when the consumption of starting material had seemed to cease, while the side-product was increasing in intensity. The ¹H NMR spectrum of the crude mixture revealed a considerable quantity of the unknown side-product (approx. 1:3 with respect to adduct). Column chromatography was performed and although the side-product proved inseparable from the slight quantity of remaining starting material, the sample was sufficiently enriched in the unknown to permit assessment over the entire proton spectral region. Three symmetrical two-proton signals — at δ 2.81, δ 2.62 (a 6.3 Hz quintet), and δ 1.93 — and the methyl ester protons were the only signals in evidence, aside from the previously isolated vinyl signal. A ¹³C JMOD spectrum was obtained and the known signals of the ring-opened adduct eliminated, leaving side-product signals for two nitrile carbons and four vinyl carbons (one down signal and three up), which suggested the presence of three vinylic quaternary carbons. The overall carbon count matched that of the ring-opened adduct; coupled with the remarkably downfield chemical shift for the sole vinyl proton, these data allowed us to tentatively assign the structure as a conjugated 3-dicyanomethylidanyl isomer of the ring-opened adduct (**2-81**, Figure 2-11).

The yield was calculated as approximately 15 % by ^1H NMR integration of the impure chromatography fraction.

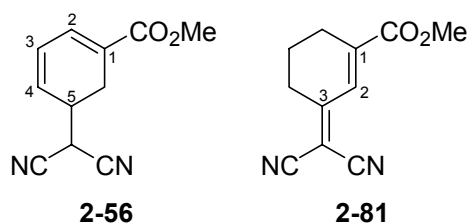
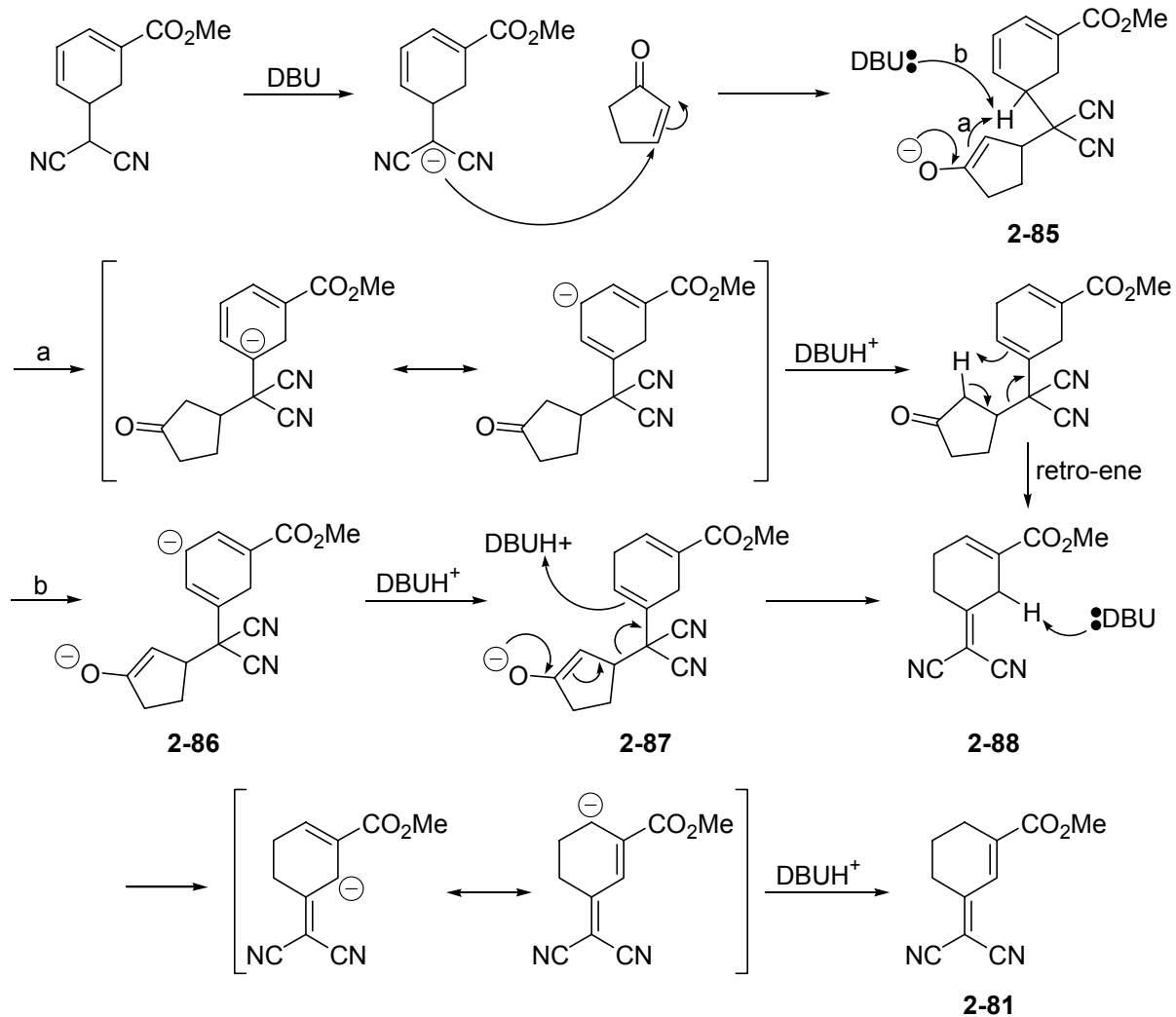


Figure 2-11. Isomer of the ring-opened adduct produced in attempted tandem Michael reaction with cyclopentenone.

The critical step in formulating a mechanism for the two-bond isomerization is establishing a pathway to the C3 methylenidyl double-bond. A base-induced isomerization of the ring-opened adduct C1–C2 double bond to the isomer C1–C2 double bond position is easily conceived, beginning with allylic deprotonation; however, the establishment of the methylenidyl double bond seems to demand initial deconjugation of the ring-opened adduct to a C4–C5 double-bond species: recourse to a C5-deprotonation-induced elimination with retention of both nitriles makes the impossible demand of a C3-carbanionic cyclopentanone leaving group. Mechanistic speculation that offers routes to an unsubstituted, dicyanomethylenidyl ring-opened adduct is offered in Schemes 2-25 and 2-26. The long-duration experiment involving catalytic DBU (Table 2-2, entry 11) provides the valuable observation that generation of **2-81** is not due to base reaction upon adduct **2-80**.



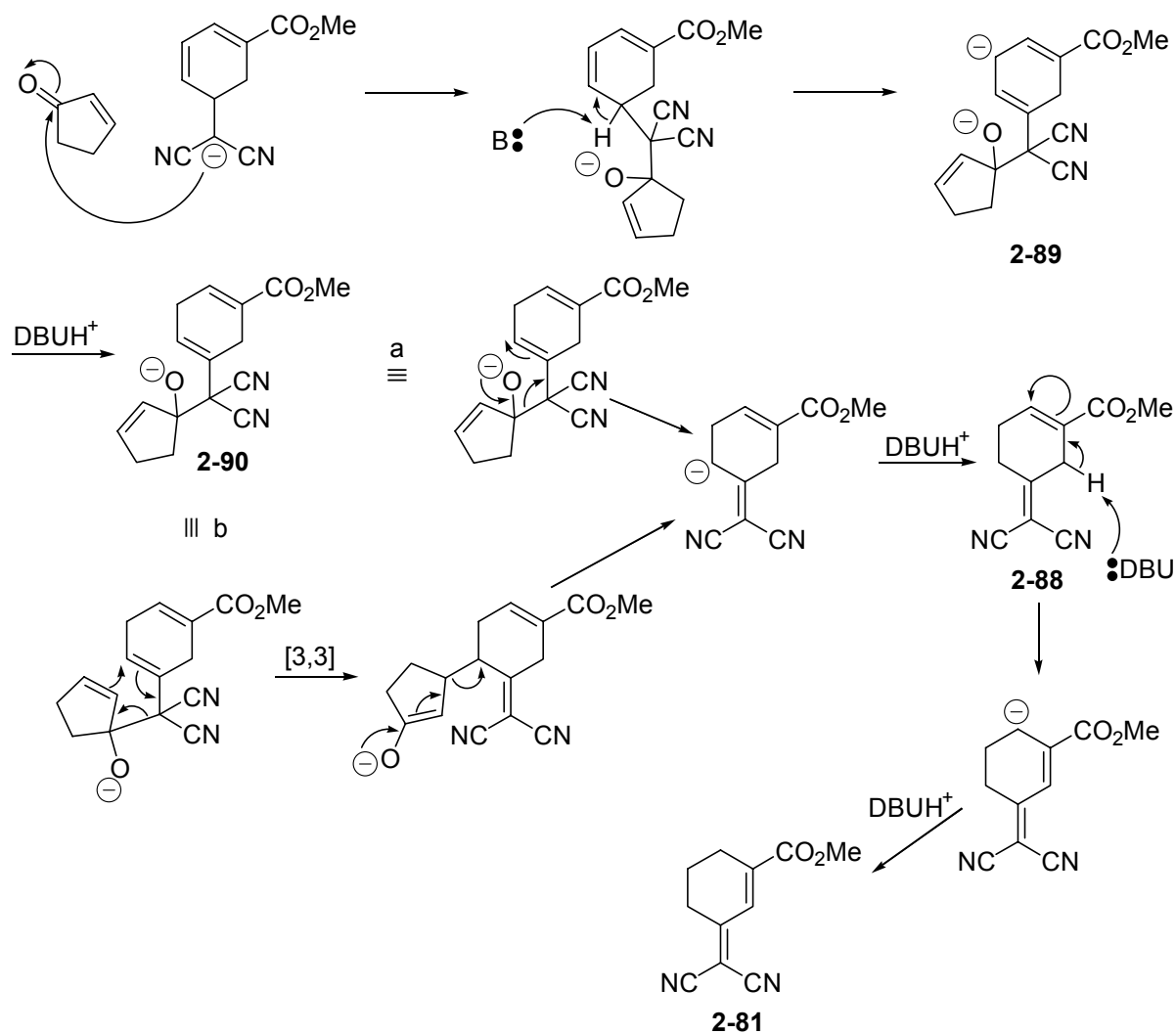
Scheme 2-25. Possible isomerization mechanisms following 1,4-addition to cyclopentenone.

In Scheme 2-25, initial 1,4-addition to cyclopentenone sets up two alternative pathways: in one, intramolecular neutralization of the adduct enolate by the allylic C5 proton of the parent ring, followed by isomerization and reprotonation, establishes the neutral deconjugated adduct that undergoes a retro-ene reaction; in the other, base-induced isomerization of the parent ring occurs during the lifetime of the adduct enolate, followed by reversal of the adduct-forming addition, followed by ring-C4 protonation that establishes the exocyclic double bond. The possibility of a retro-ene-based mechanism appears remote in

light of the long persistence of **2-80** in the catalytic DBU reaction. The ability of stoichiometric DBU to support reaction from the adduct would be difficult to explain. The reversibility of the reaction following from formation of dianion **2-86** and the subsequent cyclopentene elimination and isomerization to **2-88** seems reasonable since the generation of the dianion would occur more readily in an environment of high base concentration, which could explain the smooth generation of adduct **2-80** with catalytic DBU and the absence of **2-81**.

Scheme 2-26 depicts 1,2-addition to the carbonyl of cyclopentenone, followed by deprotonation of the allylic alkoxide at the proximal ring-C5 proton by base, leading to ring deconjugated anion **2-90** via dianion **2-89**. The deconjugated adduct allylic alkoxide could then reverse the 1,2-addition and protonation would furnish the exocyclic double bond. Alternatively, the cyclopentene and ring-C4–C5 double bonds are suitably positioned for anionic oxy-Cope reaction, followed by elimination of cyclopentenone and protonation to establish the exocyclic double bond, as in the anionic pathway shown in Scheme 2-25. Having converged at the exocyclic double bond isomer by all four pathways derived from either 1,2- or 1,4-addition, the concluding step is base-induced allylic isomerization of the methoxycarbonyl-substituted double bond in **2-88**. That smooth 1,4-addition is observed in the catalytic DBU experiment, whereas a slight extent of 1,2-addition is called for in the posited mechanism, would have to be accounted for either by the influence of a stoichiometric quantity of anion **2-55** on the regiochemical course of the addition, or by the occurrence of a slight extent of 1,2-addition in both catalytic and stoichiometric DBU reactions. In this case it would be argued that the adduct allylic alcohol is not deprotonated by DBU and that whereas in the catalytic DBU experiment, there is not enough base to

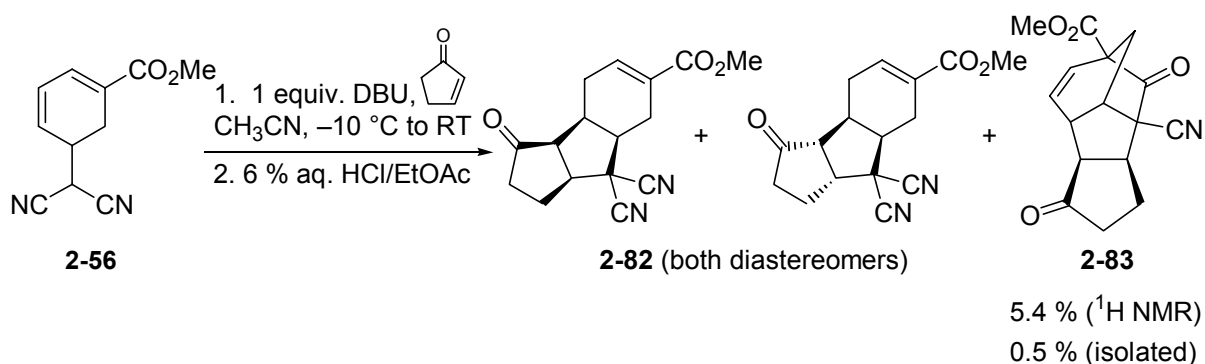
generate the dianion (**2-89**) that can eliminate cyclopentenone via ring-deconjugated allylic alkoxide **2-90**, in the case of stoichiometric DBU, an appreciable extent of 1,2-addition is attended by dianion formation by the deprotonation of ring-C5.



Scheme 2-26. Possible isomerization mechanisms following 1,2-addition to cyclopentenone.

Among the reactions of cyclopentenone as acceptor, the sole instance of generation of a homobrendane congener (Table 2-2, entry 14) was accomplished by treatment of **2-56** with stoichiometric DBU at $-10\text{ }^{\circ}\text{C}$, followed by warming to room temp. stirring overnight. Column chromatography of the complex mixture (TLC: ten discrete spots) furnished a mixed

sample whose ^1H NMR spectrum contained signals reminiscent of homobrendanes **2-74** (from di-*tert*-butyl methylenemalonate) and **2-79** (from methyl vinyl ketone), as well as two additional components with methyl ester proton resonances at δ 3.80 and δ 3.78 and separate broad singlets at δ 7.16 and δ 7.04 that were accepted as diagnostic of vinyl protons at carbomethoxy-conjugated positions, suggesting the diastereomeric products of single conjugate cyclization (**2-82**, Scheme 2-27). The apparent tricyclic compounds were in a ratio of 1 and 0.4 to one with respect to the tetracyclic homobrendane (**2-83**), which was present as only a single racemate of diastereomers. The sample of **2-83** (0.5 % after HPLC) furnished only microcrystals unsuitable for X-ray analysis in multiple attempted crystallizations.



Scheme 2-27. Tandem conjugate addition products derived from **2-56** and cyclopentenone.

The homobrendane-appended ring was determined as *exo* to the concave surface of the homobrendane by ^1H - ^1H nOe difference spectroscopic analysis. Irradiation of the vinyl signal at δ 5.83 elicited resonances at δ 3.44 (a triplet) and δ 2.62 (a doublet). An *exo* proton corresponding to the δ 2.62 resonance would have been too distant to exhibit an nOe relationship to the δ 5.83 proton (Figure 2-12).

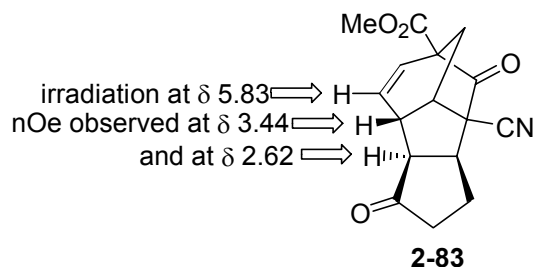


Figure 2-12. Determination of relative stereochemistry of **2-83** by ^1H - ^1H nOe difference spectroscopy.

2.2.4 Exploratory Functional Group Manipulations Related to Conversion of Homobrendane 2-74 to 2-Isocyanoallopupukeanane

2.2.4.1 General Comments

The fully saturated parent 2-homobrendane system (**2-92**) found in 2-isocyanoallopupukeanane (**2-91**) and named as a C_{10} homolog of brendane (**2-93**) is one member of a family of tricyclic decanes related to adamantane (**2-94**) through carbocation rearrangements. Specifically, 2-homobrendane is derived by 1,2-carbon shift from 2-protoadamantane (**2-95**),²⁸ itself derived from adamantane by 1,2-carbon shift, in practice through carbocation rearrangements attending solvolysis, but here (Figure 2-13) viewed formally as via 1,2-hydrogen/carbon exchanges. Experimentally, 6-*exo*-substituted homobrendanes were obtained as minor products in several solvolyses of *endo*- and *exo*-2-protoadamantyl *p*-bromobenzene sulfonates that produced as many as eight constitutional isomers.²⁹

realistic conformations:

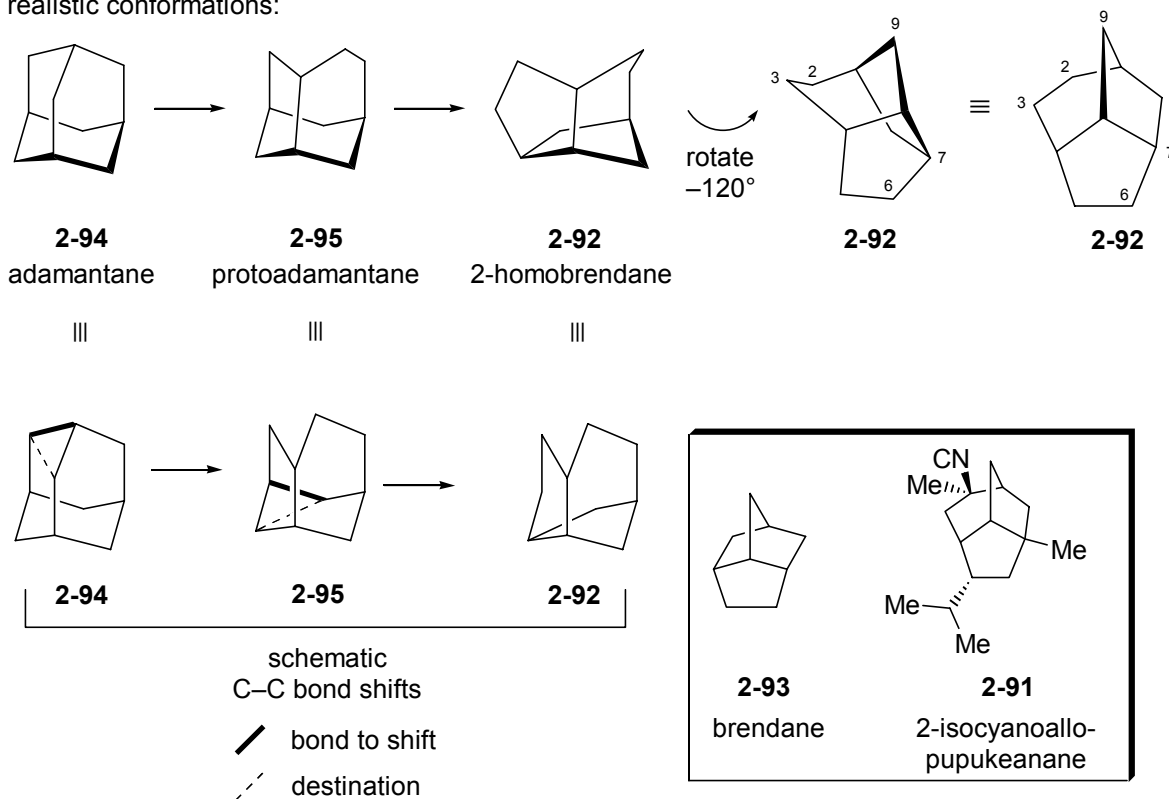
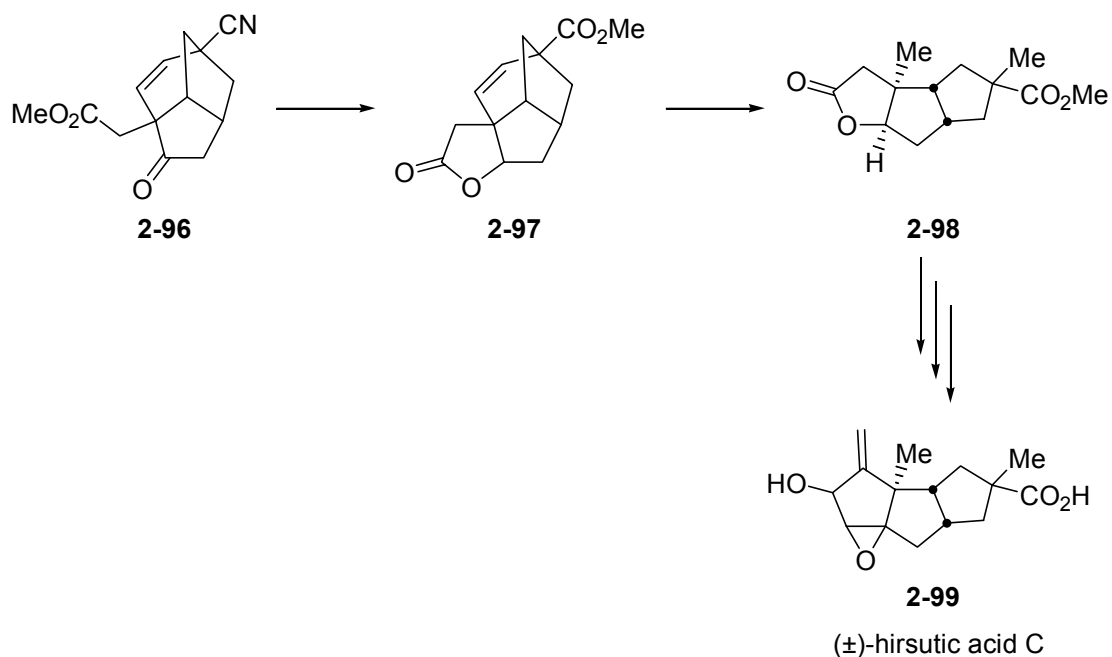


Figure 2-13. Structural relationships among several C_{10} tricyclic compounds related to 2-homobrendane

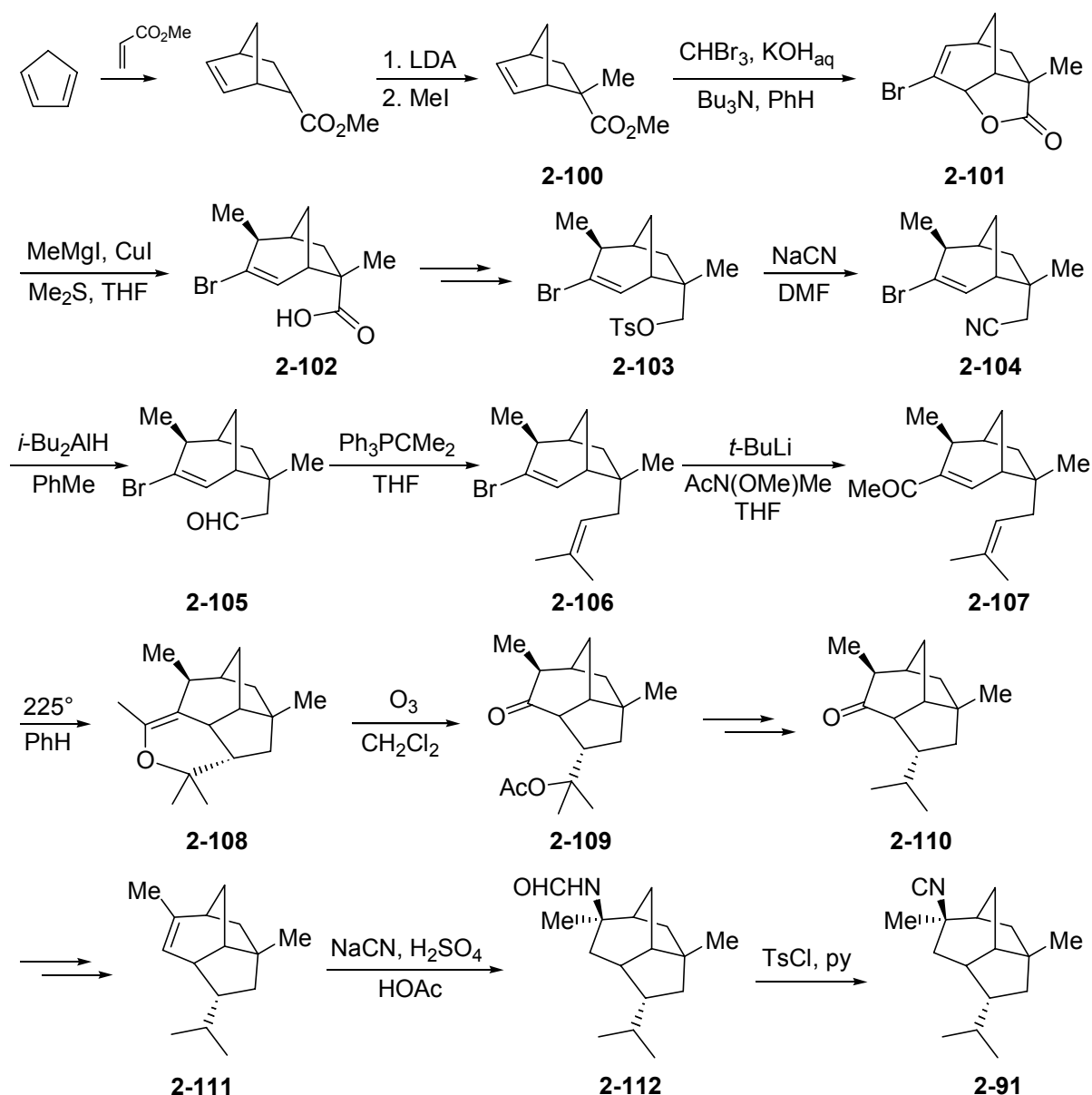
In addition to their involvement in the study of carbocation rearrangements, more highly substituted 2-homobrendanes have found applications as advanced intermediates in the synthesis of other polycyclic systems found in natural products. For example, Trost et al. generated homobrendane system **2-96** as precursor to tetracyclic lactone **2-97**. The homobrendane skeleton was then cleaved at the double-bond by ozonolysis and reduction to generate the linear tricycle **2-98** in the course of synthesizing racemic hirsutic acid C (**2-99**) (Scheme 2-28).³⁰



Scheme 2-28. Trost and coworkers' synthesis of hirsutic acid C via a homobrendane intermediate.

The pupukeananes are a novel family of marine sesquiterpenoid isonitriles comprising three groups defined by differing carbocyclic frameworks. Ho and coworkers have disclosed a synthesis of racemic **2-91** (Scheme 2-29) that delivered the natural product in 5 % yield over 19 steps.^{31,32} The synthesis progressed from the methylated Diels-Alder adduct **2-100** by ring-expansion/lactonization under phase-transfer conditions to give vinyl bromide **2-101**, which suffered S_N2' displacement of the carboxylate oxygen by treatment with MeMgI to give **2-102**. The acid was reduced and the tosylate **2-103** generated as a preamble to chain elongation by displacement by cyanide (→ **2-104**) and conversion to aldehyde **2-105**. Wittig reaction gave isopropylidene compound **2-106** that was converted to enone **2-107**, the substrate for a hetero-Diels-Alder reaction (→ **2-108**) that furnished the homobrendane skeleton. Ozonolysis to **2-109** set up a two step elimination and reduction to give **2-110**, which contained the properly disposed isopropyl group. Reduction and

elimination furnished **2-111**, substrate to the two step sequence that delivered **2-91**, involving a Ritter reaction (\rightarrow **2-112**) and dehydration to complete the total synthesis.



Scheme 2-29. Ho and coworkers' synthesis of (\pm)-2-isocyanoallopupukeanane (**2-91**).

Our fortuitous generation of the homobrendane ring system present in 2-isocyanoallopupukeanane (**2-91**), and the apparent promise of its functional group array as an exploitable set of synthetic handles for the elaboration of the natural product, offered the reasonable

possibility of a total synthesis of **2-91** alternative to Ho's. Furthermore, whereas in the existing total synthesis the final establishment of the complete tricyclic ring system is accomplished in the late stages (eleven steps, including ozonolysis of a tetracyclic vinyl ether to deliver the homobrendane skeleton), our homobrendane is delivered in five steps (including the facile hydrolysis of the crude homobrendane imine **2-73**). This efficiency makes our route attractive with respect to any future generation of analogs that seek to capitalize upon biological activity potentially reliant upon the tricyclic skeleton.

Whereas some of the functional appendages of the homobrendane **2-74** seemed well-suited to the total synthesis of **2-91**, a considerable portion of the task of conversion to the natural product lay in reduction and reductive cleavage of functional groups (Figure 2-12).

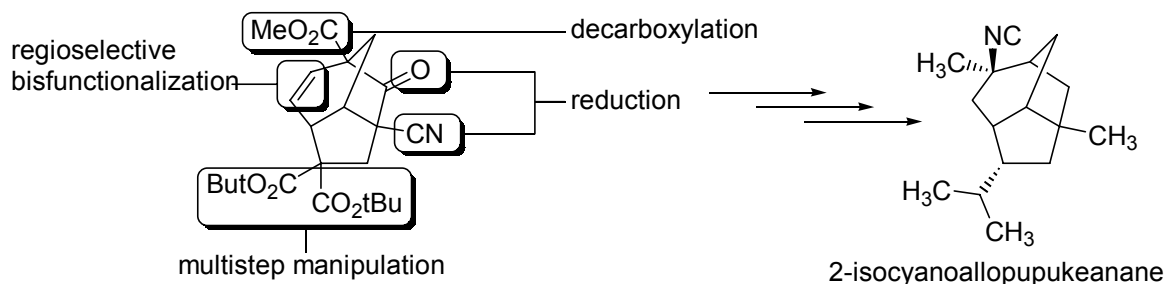
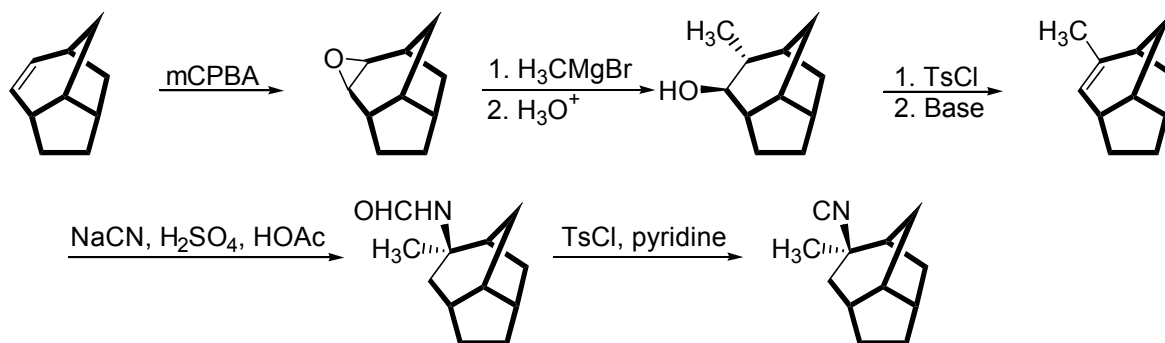


Figure 2-14. Schematic of functional group manipulations required in conversion of **2-74** to 2-isocyanoallopupukeanane.

2.2.4.2 Reactivity of the Ring Ketone of **2-74** Evidenced in Attempted Functional Group Conversions at Other Sites

Our initial attempt to functionalize the ring C4–C5 double-bond involved mCPBA epoxidation, presumably from the *exo* face, envisioned as part of a sequence leading eventually to regioselective methylation at C5 with restoration of the double-bond. This would leave the system poised for the appropriation of the terminal steps of Ho's synthesis

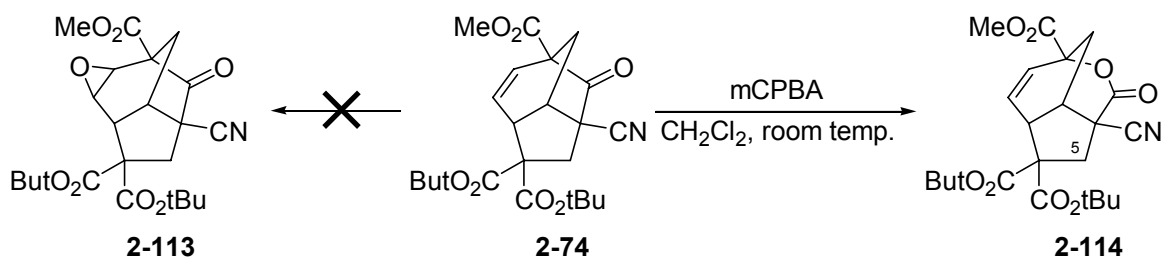
for the introduction of the isocyano group: a modified Ritter reaction (NaCN, H₂SO₄, HOAc), and dehydration by tosyl chloride in pyridine. Specifically, a potential scheme following from epoxidation, and given the compatible functional pattern already established for the remainder of the molecule, would involve regioselective nucleophilic opening of the epoxide by a methyl Grignard reagent, followed by dehydration (Scheme 2-30).



Scheme 2-30. Generalized plan for double-bond bisfunctionalization of an appropriately substituted homobrendane derivative as part of 2-isocyanoallopupukeanane synthesis.

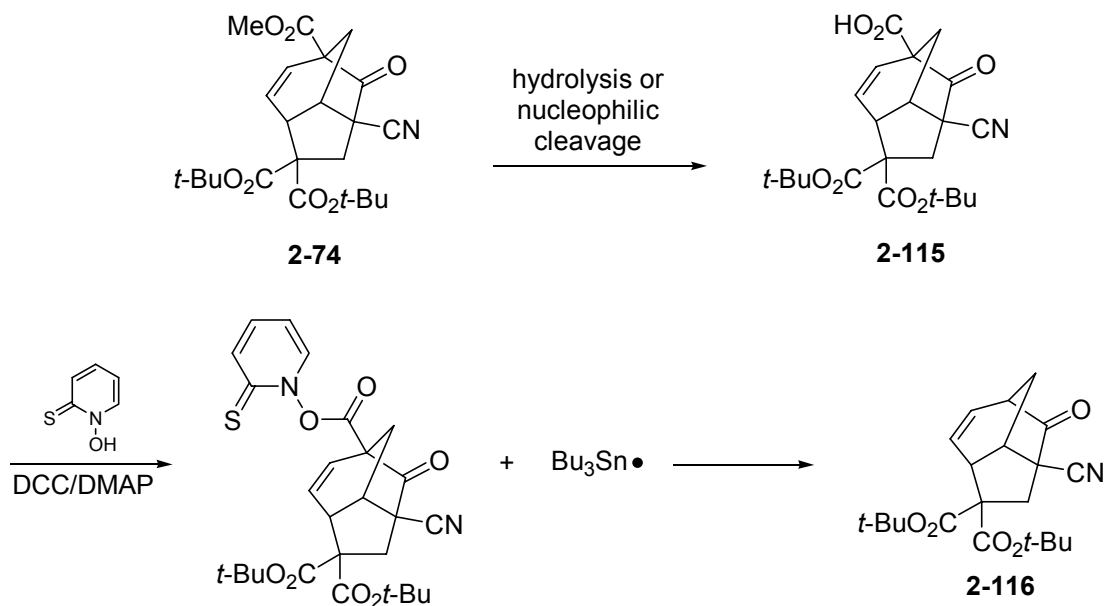
Treatment of **2-74** with slightly greater than two equivalents of mCPBA overnight in CH₂Cl₂ at room temperature did not furnish a compound whose ¹H NMR spectrum was absent vinyl protons, although spectral differences were evident in the cleanly generated new compound. The ¹³C NMR spectrum revealed the absence of a resonance appropriate for a ketone carbon, but did reveal the presence of four ester carbonyl carbon signals, indicating that a Baeyer-Villiger reaction to generate **2-114** had completely superseded any double-bond epoxidation (→ **2-113**). Despite the long reaction time (overnight) and the ample quantity of mCPBA, no evidence of epoxidation was detected. HMBC spectroscopy was performed to determine the regioselectivity of oxygen insertion into the homobrendane skeleton. A correlation was detected between the C5-methylene protons at δ 3.03 and δ 2.90 and three ester carbonyls, indicating that they are proximal to both *t*-butyl ester carbonyl

carbons, and the now ester-situated carbonyl carbon, which demonstrates that no intervening ester oxygen atom is present and prescribing the regiochemistry indicated (Scheme 2-31).



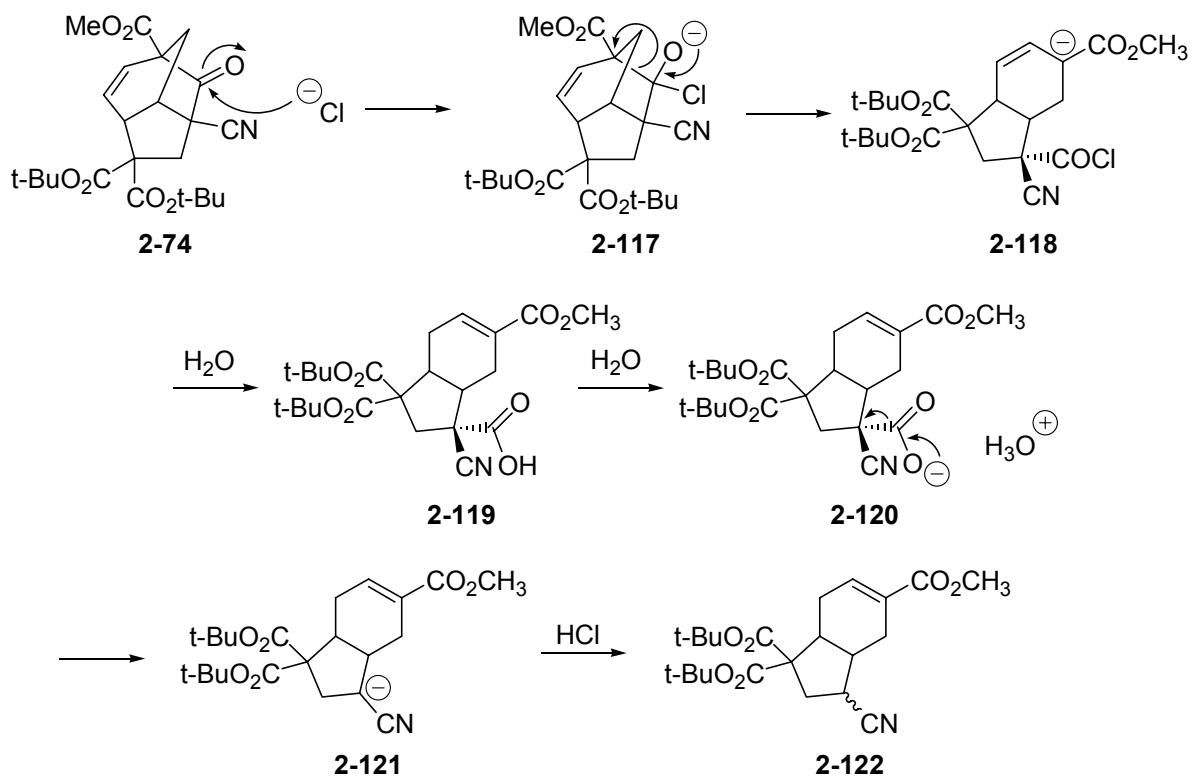
Scheme 2-31. Unexpected quantitative Baeyer-Villiger reaction of **2-74** to exclusion of double-bond epoxidation.

Further evidence for the high reactivity of the ring ketone was provided by our attempts to nucleophilically cleave the carbomethoxy group, as preparation for a planned Barton radical decarboxylation necessary to the synthesis of **2-91**. Thus, generation of carboxylic acid **2-115** would set up decarboxylation to give **2-116** (Scheme 2-32).



Scheme 2-32. Planned Barton decarboxylation of acid **2-115** derived from **2-74**.

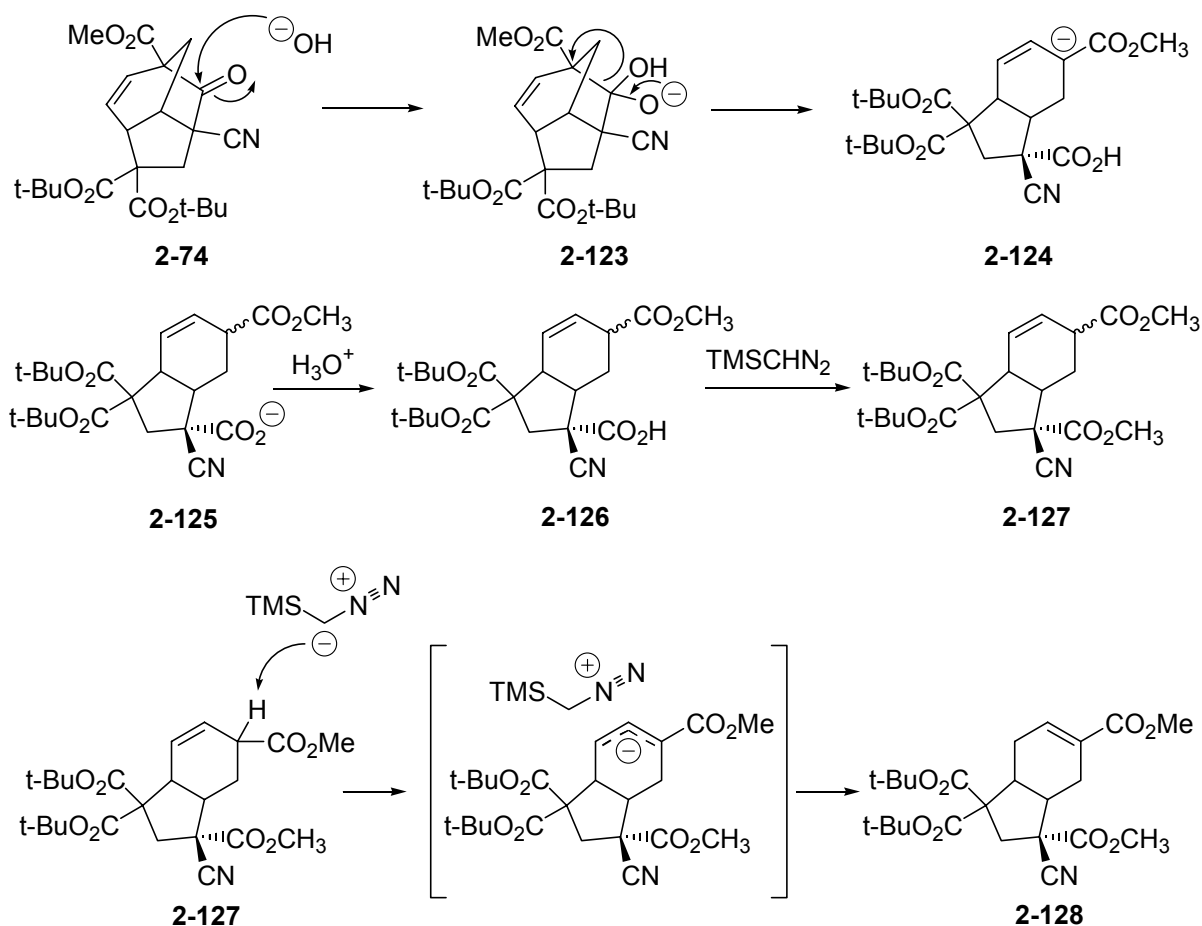
In practice, when homobrendane **2-74** was treated with excess NaCl in water-DMF at 160 °C for 24 hours, the ¹H NMR spectrum of the crude product revealed no acid proton signal. Furthermore, TLC demonstrated remarkable mobility of the two main products in a mildly polar eluent mixture, which was inconsistent with a carboxylic acid. Broad singlets at δ 6.99 and δ 6.93 were consistent with vinyl protons on double bonds in conjugation with carbonyls. In addition, two methyl ester proton singlets were present at δ 3.75 and 3.73. The two pairs of associated signals suggested diastereoisomerism. We suspected a cleavage reaction as being capable of generating a new stereocenter. Examination of the X-ray crystal data for **2-74** indicated that the angle between the σ-bonds at the ring ketone carbon (C1–C10–C7) is 106.83°, which suggested sufficient angle strain that the carbonyl would be highly electrophilic. A CI mass spectrum provided a molecular ion at *m/z* 423 (405 + NH₄⁺), a loss of 26 u from **2-73** consistent with loss of CO and addition of H₂. Together, the mass data and anticipated reactivity of the ketone toward nucleophiles suggested the outcome of Scheme 2-33. It was surmised that chloride had attacked **2-74**, freeing bicyclic enolate **2-118** (via tetrahedral intermediate **2-117**), which is depicted as undergoing hydrolysis of the acyl chloride and neutralization to give α-cyano acid **2-119**. Decarboxylation of carboxylate **2-121** generates α-cyano carbanion **2-121** which neutralizes to give **2-122** as a mixture of diastereomers.



Scheme 2-33. Generation of bicyclic compound **2-123** in attempted nucleophilic cleavage of carbomethoxy methyl group.

Basic hydrolysis of the methyl ester was next attempted in light of the expected stability of the *t*-butyl esters to basic conditions. Initially, **2-74** was subjected to hydrolysis by aqueous methanolic NaOH solution at room temperature for two hours, which, as evidenced in the ^1H NMR spectrum, had hydrolyzed the methyl ester and appeared to have resulted in the generation of two carboxylic acid protons (precluding decarboxylation), as well as the collapse of the formerly resolved ring vinyl protons to a multiplet at δ 5.93. A second attempt of much shorter duration (two minutes) was made, which resulted in complete consumption of the starting material, but retention of the ester methyl proton signal in the ^1H NMR spectrum, and the generation of only one carboxylic acid proton. The two samples were separately esterified by treatment with trimethylsilyldiazomethane in methanol-benzene solution and combined for column chromatography to separate the two

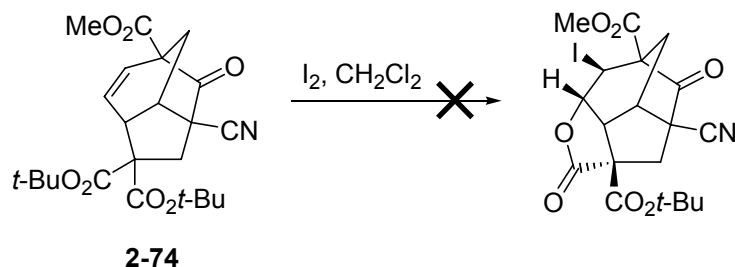
major compounds, which were concluded to be diastereomers based on the doubling of diagnostic proton signals. A single column fraction which appeared to be pure by TLC was assessed by ^1H NMR spectroscopy. Methyl ester proton signals appeared at δ 3.87 and δ 3.68. The generation of two carboxylic acid sites in the long-duration hydrolysis, and the simultaneous presence of an ester and a carboxylic acid in the short-duration hydrolysis, prompted a structural formulation resulting from nucleophilic attack of hydroxide at the ring carbonyl (\rightarrow **2-123**, Scheme 2-34), resulting in ring-cleavage by addition-elimination as in the attempted nucleophilic cleavage with chloride. The regioselectivity of the elimination reaction, amounting to the release of either the α -cyano carbanion or the ester enolate, was reasonably resolved by consideration of the shift positions of the two ester methyl proton singlets. The downfield shift of the signal at δ 3.87 suggested the influence of an electron-withdrawing group, whereas the upfield ester signal was consistent with alkyl substitution. It was therefore concluded that the ester enolate **2-124** was eliminated from the addition intermediate, and that the anion **2-125** was most likely the species present upon workup. The α -cyano acid **2-126** was esterified to give **2-127** as a mixture of diastereomers. The regioselectivity of the elimination was further evidenced during the esterification, during which a small quantity was generated of a compound bearing a vinyl proton (δ 6.89) on an apparently now ester-conjugated double-bond as well as two associated methyl ester proton singlets. Whereas the compound was not isolated and rigorously identified, it is reasonable to suggest that TMSCHN_2 had acted as a base and brought about isomerization to the more stable conjugated double-bond isomer (Scheme 2-34).



Scheme 2-34. Unintended reaction pathway in attempted basic hydrolysis of **2-74**.

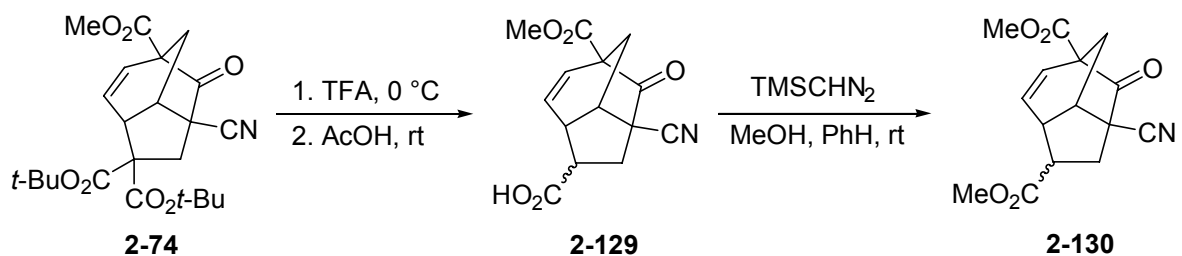
2.2.4.3 Other Attempted Functional Group Conversions

The high reactivity of the C10 carbonyl of **2-74** may represent a considerable obstacle in the conversion of the homobrendane to the natural product **2-91**. The challenge is compounded by the apparent unreactivity of the ring double-bond toward electrophiles. For example, **2-74** proved inert to attempted iodolactonization (Scheme 2-35) and bromohydrin formation (DMSO/ H_2O /NBS, RT, 24 hours: no reaction; and 72 hours at RT, then reflux 72 hours: no reaction).



Scheme 2-35. Failure of iodolactonization of **2-74**.

Apparent success was achieved in the TFA cleavage/decarboxylation of **2-74**. Treatment of **2-74** with TFA at 0 °C, followed by removal of the acid *in vacuo* and stirring of the residue in AcOH at room temperature overnight furnished a crude product whose ¹H NMR spectrum evidenced the loss of the *t*-butyl groups, indicating successful generation of **2-129** (Scheme 2-36). The ¹H NMR spectrum was otherwise so poorly resolved that little interpretation was possible. The cleavage and decarboxylation were repeated to the same effect. Separate esterification of both samples again generated very poor ¹H NMR spectra in which four methyl ester proton signals were evident, indicating the presence of two diastereomers of **2-130**. The full characterization of **2-130**, generated at very small scale, was not pursued.



Scheme 2-36. Cleavage and decarboxylation of *t*-butyl esters of **2-74**.

2.3 Experimental

2.3.1 General Experimental

All glassware required for dry reactions was either flame-dried (and then brought down to manageable temperature in a 140 °C oven) or oven-dried (at least 4 hours), and either partially cooled in a nitrogen-flushed desiccator cabinet prior to assembly, or assembled hot, both under flow of dry inert gas (nitrogen or argon). Teflon-containing and other oven-sensitive implements (e.g. Gas-Tight™ and polypropylene syringes, stopcock keys) were warmed by heat gun and stored under high vacuum until needed. Solvents that were required to be rigorously dried were refluxed in a nitrogen atmosphere over appropriate drying agents: tetrahydrofuran over sodium wire–benzophenone to the deep purple endpoint; dichloromethane over calcium hydride; carbon tetrachloride over phosphorus pentoxide. The dry solvents were then either distilled directly into reaction flasks, into intermediate vessels pending transfer by syringe or cannula, or into storage vessels over 4 Å molecular sieves (generally stored for less than one week). Reagent grade solvents were used as received for reactions that didn't require rigorous exclusion of water. DMF was degassed by multiple freeze–thaw cycles under constant high vacuum, concluding with argon backfill. Unless otherwise stated, all organic reagents were purchased from Aldrich Chemical Company and were used as received after assessment for purity by ¹H NMR spectroscopy.

Unless otherwise stated, all reactions were carried out under dry nitrogen (house line), or dry argon (cylinder, Praxair Canada Inc.). Low reaction temperatures were reached by submersion in various cooling baths: ice–water mixture for 0 °C; ice–water temperature-adjusted with NaCl for 0 to –20 °C; chloroform–dry ice mixture for –50 °C; acetone–dry ice

slurry for $-78\text{ }^{\circ}\text{C}$. Thin-layer chromatographic (TLC) analyses were carried out on aluminum-backed F₂₅₄ silica gel 60 plates from EM Science, with compound visualization by UV lamp, or by staining with one of I₂, basic KMnO₄, or ethanolic phosphomolybdic acid. In some cases, reactions were monitored by ¹H NMR spectroscopy of suitably quenched and isolated small aliquots. Removal of solvent “*in vacuo*” refers to bulk solvent removal by rotary evaporator (Büchi) at water aspirator pressure with mild warming by water bath (exceptions noted), followed by rigorous evacuation by high vacuum pump (BOC Edwards) to trace levels of solvent (NMR) or constant weight.

Preparative-layer chromatography was performed on Whatman glass-backed 20 × 20 cm plates bearing 1000 μm layers of PK6F 60 Å silica. Column chromatography was carried out on either 70–230 (gravity elution) or 230–400 (slight air or nitrogen gas pressure) mesh silica from Merck. Preparative HPLC was performed with equipment by Waters Corporation: solvent controlled by Waters 600E Multisolute Delivery System; detection by Waters 2996 Photodiode Array Detector; columns and packings described in individual experiments.

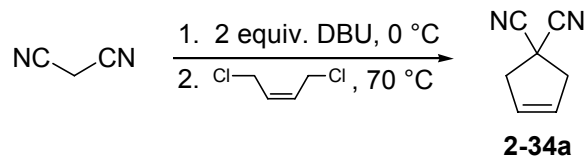
¹H NMR and ¹³C NMR spectra were recorded on Bruker AC 200, AM 250, and on AVANCE 300, 500, and 600 spectrometers. In ¹H spectra, chemical shifts are reported as parts per million (ppm) downfield of 0 ppm for tetramethylsilane (TMS). Peak multiplicities for proton signals are defined with the following abbreviations: s, singlet; d, doublet; t, triplet; dd, doublet of doublets; ddd, doublet of doublet of doublets; q, quartet; qn, quintet; m, multiplet for which first-order or symmetrical line spacings are not discerned; br, broad. For spin systems that do not exhibit first-order coupling, the chemical shifts and coupling constants cited are the centers and line spacings, respectively, of the observed signals. In ¹³C

NMR spectra, chemical shifts are reported with respect to 77.0 ppm for the center of the ^{13}C triplet of CDCl_3 . Letter designations following ^{13}C chemical shifts in the JMOD spectrum refer to upward-pointing (u) peaks for carbons bearing either 0 or 2 hydrogen atoms, or to downward-pointing (d) peaks for carbons bearing 1 or 3 hydrogen atoms. ^1H - ^1H COSY, HMQC, HMBC, TOCSY, and NOE difference spectra were obtained on AVANCE 300, 500, and 600 spectrometers. HMQC and HMBC spectra, where cited in the experimental characterization data, report ^{13}C resonances followed by the correlated ^1H resonances in brackets.

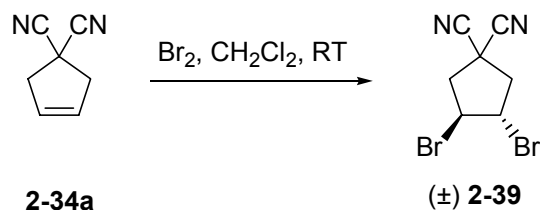
Melting points were determined on a MEL-TEMP melting point apparatus and are uncorrected. IR spectra were recorded from compressed KBr discs, or from thin films deposited from dichloromethane solutions on single NaCl plates, on either a Perkin Elmer 1600 FT-infrared or a Bomem MB-100 spectrophotometer. Mass spectra were recorded at the McMaster Regional Centre for Mass Spectrometry, (Hamilton, Ontario), at the University of Ottawa Mass Spectrometry Centre, and at the WATSPEC Mass Spectrometry Facility (University of Waterloo). X-ray crystallographic analyses were performed by Dr. Nicholas J. Taylor at the University of Waterloo. Elemental analyses were carried out by M-H-W Laboratories of Phoenix, Arizona, U.S.A.

2.3.2 Experimental Details

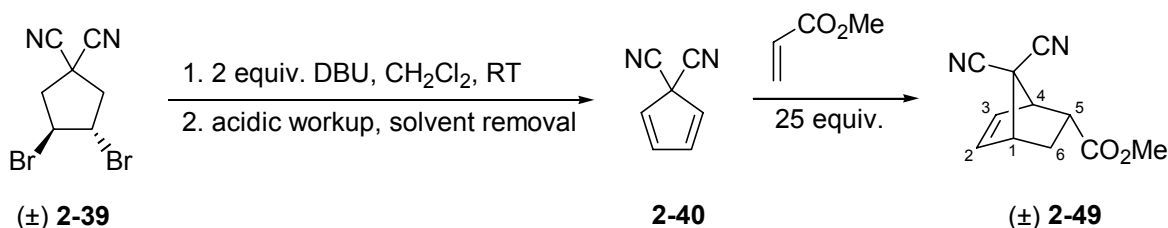
4,4-Dicyano-cyclopent-1-ene



To stirred DMF (40 mL) at 0 °C under Ar was added malononitrile (3.3 g, 49.9 mmol) and DBU (16.6 mL, 16.9 g, 110 mmol, 2.22 equiv.). The solution was stirred at room temp. for 30 min. and then cooled to -20 °C, at which point *cis*-1,4-dichlorobutene (5.54 mL, 6.58 g, 52.6 mmol, 1.05 equiv.) was added dropwise. The solution was stirred at room temp. for 15 min., heated to 70 °C for 30 min., and then cooled to room temp. and poured into water (150 mL). The mixture was extracted with Et₂O (4 × 30 mL), and the combined organics were partitioned against brine (2 × 30 mL), dried (Na₂SO₄), and concentrated *in vacuo* to give **2-34a** as a brown oil (5.01 g, 85 %) that was of sufficient purity to use directly in the subsequent reaction. The material was spectroscopically identical to material prepared by R. Friesen.²² ¹H NMR (CDCl₃, 300 MHz) δ 5.83 (2 H, s, C1-H, C2-H), 3.22 (4 H, s, CH₂).

1,2-dibromo-4,4-dicyanocyclopentane

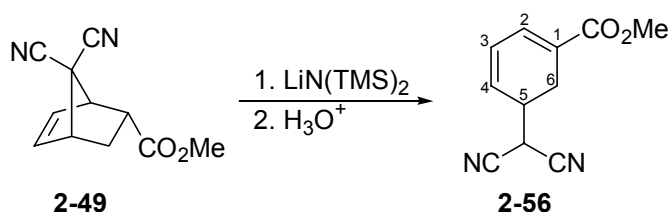
Crude **2-34a** (5.01 g, 42.4 mmol) was dissolved in CH_2Cl_2 (50 mL) and stirred at room temp. under Ar. A solution of Br_2 (7.45 g, 2.40 mL, 46.6 mmol, 1.1 equiv.) in CH_2Cl_2 (20 mL) was added slowly by addition funnel and the mixture was stirred for an additional 3 hours. The mixture was washed with 20 % aqueous NaHSO_3 , brine, dried (Na_2SO_4) and concentrated *in vacuo* to give **2-39** as a yellow-brown solid (9.57 g, 81 %) that was sufficiently pure to use in subsequent reactions. The material was spectroscopically identical to material prepared by R. Friesen²² and to that reported by Dmitrienko et al.³³

7,7-Dicyano-bicyclo[2.2.1]hept-5-ene-2-carboxylic acid methyl ester

To a room temp., stirred solution of dibromide **2-39** (9.48 g, 34.1 mmol) in CH_2Cl_2 (300 mL) was added DBU (10.39 g, 10.2 mL, 68.2 mmol, 2 equiv.) and the reaction was stirred for 60 min. The reaction was diluted with ice-cold CH_2Cl_2 (100 mL), washed with ice-cold 6 % aq. HCl, ice-cold brine, dried (Na_2SO_4), and concentrated *in vacuo* in an ice bath to furnish a brown oil that was added to methyl acrylate (approx. 77 mL, 850 mmol, 25 equiv.). The reaction was stirred for 48 hours and concentrated *in vacuo*. Silica flash column chromatography (230–400 mesh silica) eluting with 15:85 EtOAc:hexanes gave **2-49**

(4.14 g, 60 %) as a mobile clear yellow oil that turned to a glass upon refrigeration. The material was spectroscopically identical to material reported by R. Friesen.²² ¹H NMR (CDCl₃, 500 MHz) δ 6.34 (1 H, dd, $J = 5.6, 3.0$ Hz, C3-H), 6.15 (1 H, dd, $J = 5.6, 2.7$ Hz, C2-H), 3.81 (1 H, br s, C4-H), 3.67 (3 H, s, CO₂CH₃), 3.55 (1 H, br s, C1-H), 3.43 (1 H, dt, $J = 9.2, 3.9$ Hz, C5-H), 2.41 (1 H, ddd, $J = 13.1, 9.3, 3.8$ Hz, C6-*exo*-H), 1.78 (1H, dd, $J = 13.1, 4.1$ Hz, C6-*endo*-H).

5-Dicyanomethyl-cyclohexa-1,3-dienecarboxylic acid methyl ester

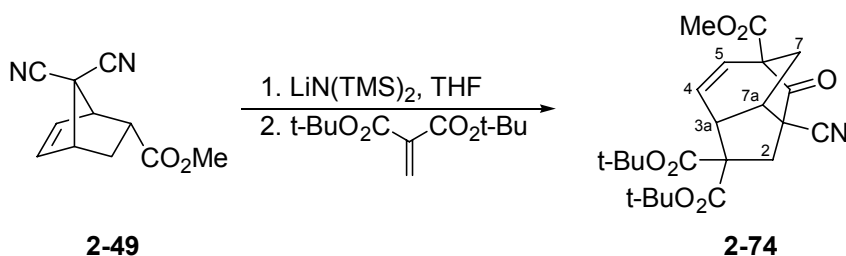


A flame-dried 100 mL round-bottom flask containing a stir bar and fitted with a rubber septum and a dry N₂ line was mounted in a -60 °C CHCl₃/dry ice bath. Successively, dry THF (50 mL), HN(TMS)₂ (3.12 mL, 14.8 mmol), and n-BuLi (1.44 M in hexanes, 10.3 mL, 14.8 mmol) were added, and the mixture was stirred in a 0 °C ice/water bath for 15 minutes. Return to the -60 °C bath preceded dropwise addition of the Diels-Alder adduct **2-49** (1.5 g, 7.4 mmol) dissolved in dry THF (10 mL) over 7 minutes. After stirring for 75 min. at -60 °C, the reaction was acidified (6% aq. HCl, 30 mL) and added to a separatory funnel with EtOAc (60 mL) and water (50 mL). After extraction, the phases were separated and the aqueous phase was further extracted with EtOAc (2 × 20 mL). The combined organics were dried (Na₂SO₄) and the solvent was removed, leaving a brown oil. A silica plug (40:60 EtOAc:hexanes) furnished a yellow oil (1.16 g, 78%): ¹H NMR (CDCl₃, 300 MHz) δ 7.07 (1H, d, $J = 5.5$ Hz, C2-H), 6.38 (1H, ddd, $J = 9.5, 5.5, 1.4$ Hz, C4-H), 6.12 (1H, dd, $J = 9.5,$

4.5 Hz, C3-H), 3.78 (3H, s, CO₂CH₃), 3.69 (1H, d, *J* = 8.1 Hz, (NC)₂CH), 3.11 (1H, m, C5-H), 2.79 (2H, dd, *J* = 8.4, 1.6 Hz, C6-H₂); ¹³C NMR (CDCl₃, 50 MHz) δ 166.3, 132.1, 128.12, 128.09, 126.3, 111.5, 111.4, 52.1, 35.3, 25.9, 25.0; LRMS *m/z* 202 (M⁺); Anal Calcd for C₁₁H₁₀N₂O₂: C, 65.34; H, 4.98; N, 13.85. Found: C, 65.40; H, 5.11; N, 14.17.

1-Cyano-8-oxo-1,2,7,7a-tetrahydro-3aH-1,6-methano-indene-3,3,6-tricarboxylic acid di-tert-butyl ester methyl ester

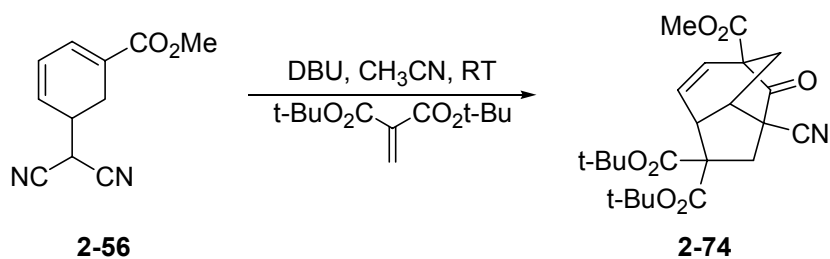
Method 1:



An oven-dried 25 mL round-bottom flask containing a magnetic stir bar was fitted with a rubber septum, purged with dry N₂ and placed in a -56 °C dry ice/CHCl₃ bath. To the flask were successively added by syringe dry THF (10 mL), HN(TMS)₂ (0.31 mL, 1.47 mmol), and n-BuLi (0.59 mL, 1.47 mmol). The mixture was stirred at 0 °C for 15 minutes, then returned to the -56 °C bath. Diels-Alder adduct **2-49** (0.2724 g, 1.35 mmol), dissolved in dry THF (2 mL), was added dropwise by syringe over 8 min., during which the solution turned clear yellow, followed by a 0.5 mL THF rinse of the originating flask. Once the reaction had stirred for 30 minutes at -55 to -60 °C, di-*tert*-butylmethylidene malonate (0.77 g, 3.4 mmol) dissolved in dry THF (2 mL) was added dropwise by syringe over 7 minutes. The reaction stirred for thirty minutes at -55 to -60 °C, and then for 1 hour at room temperature, at which time it was diluted with CH₂Cl₂ (40 mL), washed with water (2 × 40

mL) and brine (50 mL), dried (Na₂SO₄), and the solvent was removed under reduced pressure. The residue was dissolved in EtOAc (40 mL), 6% aq. HCl (30 mL) was added and the mixture was stirred vigorously at room temp. for 2 hours, at which time the phases were separated and the aqueous acidic phase was extracted with EtOAc (3 × 20 mL). The combined EtOAc portions were dried (Na₂SO₄) and concentrated *in vacuo*. The resultant oil was chromatographed on silica (20:80 EtOAc:hexanes), furnishing an off-white solid (0.216 g, 37%). Slow crystallization from ether produced clear, colourless crystals suitable for X-ray analysis: mp 155-158 °C; ¹H NMR (CDCl₃, 300 MHz) δ 6.33 (1H, d, *J* = 9.6 Hz, C4-H), 5.72 (1H, ddd, *J* = 9.6, 3.5, 0.9 Hz, C5-H), 3.84 (3H, s, CO₂CH₃), 3.66 (br), 3.47 (1H, br t, *J* = 5.2 Hz), 2.87 (1H, d, *J* = 15.4 Hz, C2-H), 2.67 (1H, ddd, *J* = 12.5, 5.0, 1.4 Hz, C7-H), 2.65 (1H, d, *J* = 15.4 Hz, C2-H), 2.02 (1H, d, *J* = 12.5 Hz, C7-H), 1.51 (9H, s, CO₂C(CH₃)₃), 1.46 (9H, s, CO₂C(CH₃)₃); ¹³C NMR (CDCl₃, 50 MHz) δ 198.1, 168.6, 168.3, 166.5, 129.4, 128.2, 118.1, 83.3, 82.8, 64.8, 58.2, 52.9, 49.6, 47.7, 47.0, 41.0, 31.6, 27.7, 27.6; IR (thin film, NaCl) 2238, 1763, 1743, 1723 cm⁻¹; LRMS (EI) *m/z* 432 (M + H); Anal Calcd for C₂₃H₂₉NO₇: C, 64.02; H, 6.77; N, 3.25. Found: C, 63.91; H, 6.69; N, 3.33.

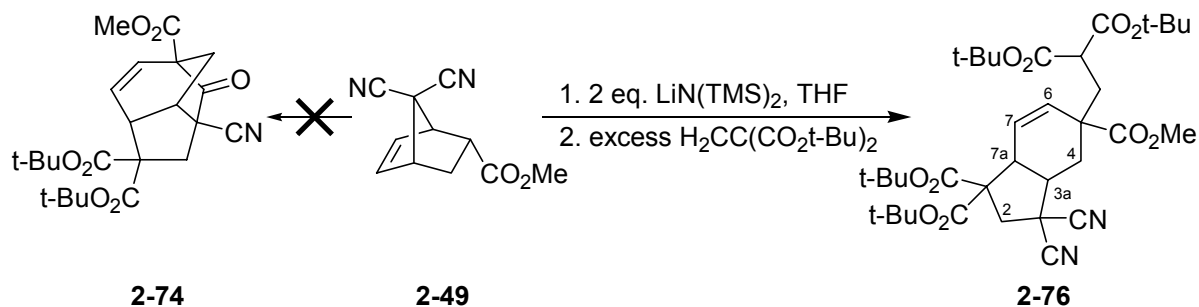
Method 2:



To a 25 mL round bottom flask were added 5-dicyanomethyl-cyclohexa-1,3-diene carboxylic acid methyl ester (0.1188 g, 0.587 mmol), acetonitrile (5 mL), di-*tert*-butylmethylidene malonate (0.136 g, 0.598 mmol), and DBU (0.088 mL, 0.588 mmol). The

mixture was stirred for 2 hours at room temp. under Ar, lightening from orange to faint clear yellow. The reaction was diluted with EtOAc (25 mL), and extracted with saturated aqueous NH_4Cl (25 mL), and the aqueous extract was washed with EtOAc (2×10 mL). The combined EtOAc extracts were dried (Na_2SO_4) and the solvent was removed under reduced pressure. The crude product was dissolved in EtOAc (5 mL), 6% aq. HCl (10 mL) was added, and the mixture was stirred vigorously at room temp. for 3 hours, after which it was diluted with EtOAc (25 mL), and extracted with water (25 mL). The aqueous extract was washed with 2 portions of EtOAc (10 mL), and the combined EtOAc extracts were dried (Na_2SO_4) and evaporated under reduced pressure, furnishing a dark yellow oil which was purified by silica flash column chromatography (230-400 mesh silica, 20:80 EtOAc:hexanes) to provide a white solid (0.1773g, 70%).

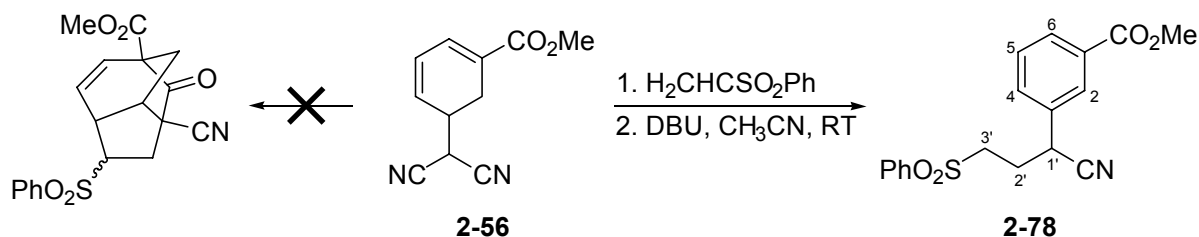
5-(2,2-Bis-tert-butoxycarbonyl-ethyl)-3,3-dicyano-2,3,3a,4,5,7a-hexahydro-indene-1,1,5-tricarboxylic acid di-tert-butyl ester methyl ester



To an oven-dried 50 mL round bottom flask mounted in a dry ice/chloroform bath (-50 to -60 °C), containing a magnetic stir bar and fitted with a rubber septum, were added successively by syringe dry THF (15 mL), $\text{HN}(\text{TMS})_2$ (0.84 mL, 3.98 mmol), and n-BuLi (2.5 M, 1.58 mL, 3.95 mol). After transfer to a 0°C ice bath for 15 minutes and return to the -60 °C bath, Diels-Alder adduct **2-49** (0.401 g, 1.98 mmol), dissolved in dry THF (4 mL),

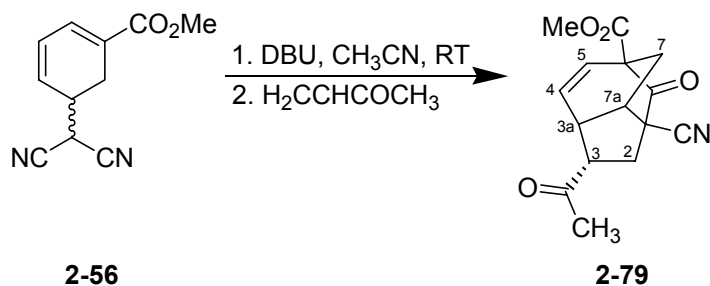
was added slowly by syringe over 9 minutes. The reaction mixture was stirred at $-60\text{ }^{\circ}\text{C}$ for 2 hours, at which time di-*tert*-butylmethylidene malonate (1.13 g, 4.95 mmol), dissolved in dry THF (3 mL), was added dropwise by syringe over 10 minutes. After stirring for 30 minutes at $-60\text{ }^{\circ}\text{C}$, the reaction was warmed to room temp. and allowed to stir overnight. The reaction was diluted with CH_2Cl_2 (50 mL), washed with 6% aq. HCl (20 mL), and the aqueous acidic extract was washed with two portions of CH_2Cl_2 (10 mL each). The combined organics were dried (Na_2SO_4), and the solvent was removed under reduced pressure. Flash column chromatography on silica (230-400 mesh, 20:80 EtOAc:hexanes) yielded a clear, yellow oil (0.3297 g, 25%) that turned into a glass upon complete solvent removal: ^1H NMR (CDCl_3 , 300 MHz) δ 6.02 (1H, d, $J = 1.2$ Hz, C6-H), 5.82 (1H, dd, $J = 10.2, 5.1$ Hz, C7-H), 3.82 (1H, br t, C7a-H), 3.69 (3H, s, CO_2CH_3), 3.42 (1H, d, $J = 14.8$ Hz, C2-H), 3.18 (1H, t, $J = 5.2$ Hz, $(\text{t-BuO}_2\text{C})_2\text{CH}$), 3.06–2.99 (1H, m, overlaps with δ 2.96 doublet, C3a-H), 2.96 (1H, d, $J = 14.8$ Hz, C2-H), 2.31–2.16 (2H, m, side-chain CH_2), 2.02–1.81 (2H, m, C4-H₂), 1.50 (9H, s, $\text{CO}_2\text{C}(\text{CH}_3)_3$), 1.47 (9H, s, $\text{CO}_2\text{C}(\text{CH}_3)_3$), 1.45 (9H, s, $\text{CO}_2\text{C}(\text{CH}_3)_3$), 1.39 (9H, s, $\text{CO}_2\text{C}(\text{CH}_3)_3$); ^{13}C NMR (CDCl_3 , 75 MHz) δ 173.8, 168.6, 168.3, 168.2, 167.4, 130.7, 124.6, 115.5, 113.0, 83.7, 83.0, 82.2, 81.8, 63.2, 52.4, 50.3, 46.3, 44.2, 43.0, 42.0, 37.6, 35.4, 27.9, 27.8, 27.7; IR (thin film, NaCl) 2360, 2342, 1728 cm^{-1} ; LRMS (ESI) m/z 681 ($\text{M} + \text{Na}$); Anal Calcd for $\text{C}_{35}\text{H}_{50}\text{N}_2\text{O}_{10}$: C, 63.81; H, 7.65; N, 4.25. Found: C, 63.63; H, 7.60; N, 4.30.

3-(3-Benzenesulfonyl-1-cyano-propyl)-benzoic acid methyl ester



5-Dicyanomethylcyclohexa-1,3-diene carboxylic acid methyl ester (0.1059 g, 0.524 mmol) and phenyl vinyl sulfone (0.088 g, 1 equiv.) were dissolved in acetonitrile (5 mL), and the solution was stirred at room temp. under Ar. DBU (0.078 mL, 1 equiv.) was added slowly dropwise, causing the reaction mixture to turn orange, and the reaction was stirred at room temp. overnight. The reaction was diluted with EtOAc (40 mL), extracted with saturated aqueous NH_4Cl (40 mL), and the aqueous extract was washed with two portions of EtOAc (10 mL). The combined EtOAc portions were dried (Na_2SO_4) and the solvent was removed under reduced pressure to give a brown oil. Flash column chromatography (230–400 mesh silica, 30:70 EtOAc:hexanes) furnished a clear, yellow oil as the major isolable product (0.0295 g, 15%): ^1H NMR (CDCl_3 , 300 MHz) δ 8.00 (1H, dt, $J = 6.8, 1.8$ Hz, C6-H), 7.95 (br s, C2-H, Ph-H), 7.90–7.85 (2H, m, Ph-H), 7.71–7.42 (5H, m, Ar-H), 4.16 (1H, t, $J = 7.5$ Hz, C1'-H), 3.91 (3H, s, CO_2CH_3), 3.32–3.06 (2H, m, C3'-H), 2.41–2.29 (2H, m, C2'-H); ^{13}C NMR (CDCl_3 , 75 MHz) δ 166.0, 138.5, 134.4, 134.2, 131.6, 131.4, 129.9, 129.6, 129.5, 128.3, 127.9, 118.9, 52.8, 52.4, 35.5, 28.6; IR (thin film, NaCl) 2247, 1725, 1308, 1152 cm^{-1} ; LRMS (EI) m/z 343 (M^+ , 1%).

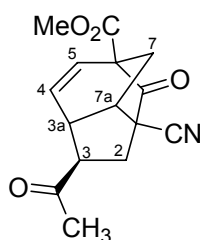
3-Acetyl-1-cyano-8-oxo-1,2,3,3a,7,7a-hexahydro-1,6-methano-indene-6-carboxylic acid methyl ester



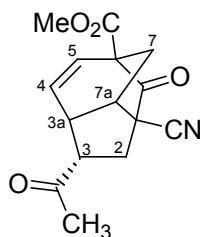
To 5-dicyanomethylcyclohexa-1,3-diene carboxylic acid methyl ester (0.0958 g, 0.474 mmol), dissolved in CH₃CN (6 mL) and cooled to 0 °C was added DBU (1.4 mL of a 0.0516 g/mL solution, 0.474 mmol), followed immediately by methyl vinyl ketone (0.9 mL of a 0.0407 g/mL solution, 0.522 mol), and the reaction mixture was stirred at 0 °C for 1 hour, 40 minutes under Ar. The reaction mixture was diluted with EtOAc (40 mL) and washed with saturated aqueous NH₄Cl (40 mL). The aqueous phase was washed with EtOAc (2 × 20 mL) and the combined portions of EtOAc were dried (Na₂SO₄). Removal of solvent *in vacuo* furnished a dark yellow oil which was then dissolved in EtOAc (6 mL) and stirred vigorously with 6% aqueous HCl (6 mL) at room temp. under Ar for 1 hour, 20 minutes. The mixture was diluted with EtOAc (40 mL) and washed with water (40 mL), followed by extraction of the water with further EtOAc (2 × 20 mL), drying of the combined EtOAc extracts (Na₂SO₄), and removal of the solvent *in vacuo*, leaving a dark yellow oil. Silica column flash chromatography (230–400 mesh, 40:60 EtOAc:hexanes) provided a 1.2:1 mixture of diastereomers of the title compound as a thick, light yellow oil (0.100 g, 42%): IR (thin film, NaCl) 2238, 1761, 1737, 1712 cm⁻¹; LRMS (EI) *m/z* 274 (M + H).

A portion of the pure mixture of diastereomers was subjected to preparative HPLC (25 × 100 mm μPorasil™ RCM silica column; gradient elution from 40:60 to 50:50 (25

minutes) to 100:0 (5 minutes) EtOAc:hexanes; 600 μ L sample injection in CH_2Cl_2 solution), which afforded a pure sample of the less polar racemic 3-exo acetyl diastereomer, followed by the 3-endo acetyl diastereomer slightly contaminated with the 3-exo diastereomer. After slow crystallization from an acetone–ether–hexanes solution, the later-eluting material produced a crystal of sufficient quality to permit study by single-crystal X-ray diffraction (aforementioned stereochemical assignments based on correlation of crystal structure to ^1H NMR spectra).



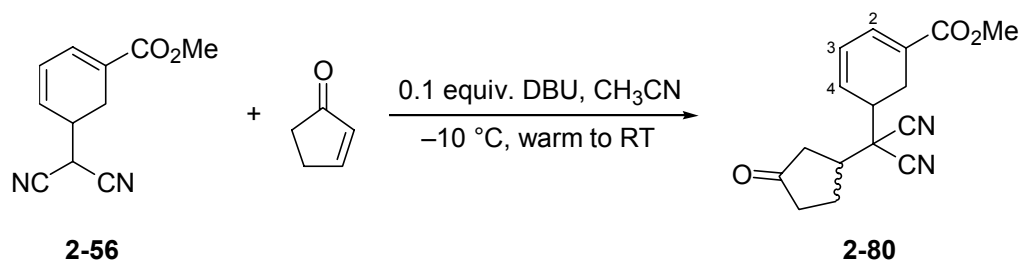
^1H NMR (CDCl_3 , 300 MHz) δ 6.27 (1H, dt, $J = 9.4, 1.6$ Hz, C4-H), 5.76 (1H, ddd, $J = 9.43, 3.8, 1.2$ Hz, C5-H), 3.84 (3H, s, CO_2CH_3), 3.37 (1H, m, C3a-H), 3.17 (1H, m, C7a-H), 3.02 (1H, d, $J = 8.1$ Hz, C3-H), 2.75–2.69 (2H, m, C2-H, C7-H), 2.28 (3H, s, COCH_3), 2.23 (1H, dd, $J = 14.7, 8.3$ Hz, C2-H), 2.02 (1H, d, $J = 12.4$ Hz); ^{13}C JMOD (CDCl_3 , 75 MHz) δ 206.6 (u), 198.7 (u), 168.5 (u), 131.8 (d), 127.8 (d), 118.0 (u), 57.9 (u), 55.1 (d), 53.1 (d), 51.4 (u), 46.3 (d), 45.1 (d), 35.9 (u), 31.6 (u), 28.5 (d).



^1H NMR (CDCl_3 , 300 MHz) δ 6.27 (1H, dt, $J = 9.6, 1.5$ Hz, C4-H), 5.60 (1H, ddd, $J = 9.6, 3.3, 1.0$ Hz, C5-H), 3.83 (3H, s, CO_2CH_3), 3.49 (1H, m, C3a-H), 3.38–3.31 (1H, m, C3-H), 3.24 (1H, br t, $J = 5.2$ Hz, C7a-H), 2.71 (1H, ddd, $J = 12.5, 4.9, 1.7$ Hz, C7-H), 2.55 (1H, dd,

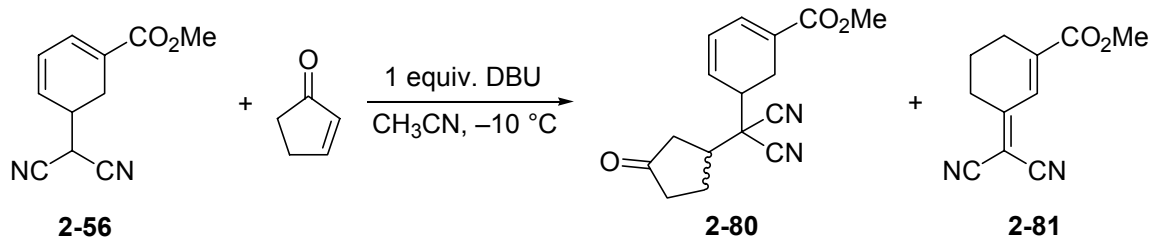
$J = 14.6, 8.3$ Hz, C2-H), 2.39 (1H, dd, $J = 14.6, 11.0$ Hz, C2-H), 2.24 (3H, s, COCH₃), 2.03 (1H, d, $J = 12.5$ Hz, C7-H); ¹³C NMR (CDCl₃, 75 MHz) δ 204.7, 197.6, 168.3, 129.0, 127.6, 118.5, 58.3, 55.4, 53.1, 50.0, 48.4, 44.5, 35.5, 31.6, 29.7.

5-[Dicyano-(3-oxo-cyclopentyl)-methyl]-cyclohexa-1,3-dienecarboxylic acid methyl ester

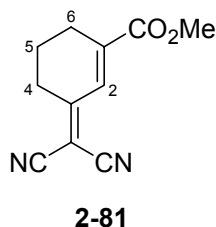


To a stirred solution of **2-56** (179.1 mg, 0.886 mmol) and 3-oxo-cyclopentene (2.16 mL of a 33.8 mg/mL CH₃CN solution, 0.886 mmol, 1 equiv.) in CH₃CN (additional 4 mL) at -10 °C was added DBU (0.35 mL of a 38.1 mg/mL solution, 0.086 mmol, 0.1 equiv.). An aliquot removed at 30 min. revealed complete consumption of the starting material. The reaction was allowed to continue overnight to test further reaction of the adduct with DBU, and was then partitioned between saturated aqueous NH₄Cl (50 mL) and CH₂Cl₂ (3 \times 30 mL). The combined organics were dried (Na₂SO₄) and concentrated *in vacuo* to give a red-brown oil whose ¹H NMR spectrum was consistent with the generation of **2-80** as a mixture of diastereomers. ¹H NMR (CDCl₃, 300 MHz) δ 7.08[†] (2 H, d, $J = 5.3$ Hz, C2-H), 6.42[†] (2 H, m, C4-H), 6.13 (1H, dd, $J = 9.6, 3.4$ Hz, C3-H), 6.09 (1 H, dd, $J = 9.6, 3.6$ Hz, C3-H), 3.82 (3 H, s, CO₂CH₃), 3.81 (3 H, s, CO₂CH₃), 3.05–1.95[†] (20 H, m). [†] combined signals from both diastereomers.

3-Dicyanomethylene-cyclohex-1-enecarboxylic acid methyl ester



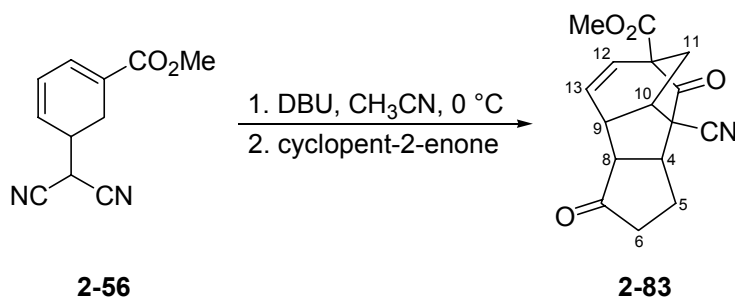
To a stirred solution of **2-56** (124.5 mg, 0.616 mmol) and 3-oxo-cyclopentene (1.50 mL of a 33.8 mg/mL CH₃CN solution, 0.616 mmol, 1 equiv.) in CH₃CN (additional 4 mL) at -10 °C was added DBU (2.46 mL of a 38.1 mg/mL CH₃CN solution, 0.616 mmol, 1 equiv.) over 4 min. 20 sec., which caused the reaction to turn yellow and finally orange. At 3 hrs., TLC indicated an increase in the quantity of a side-product and the persistence of starting material, so the reaction was partitioned between saturated aqueous NH₄Cl (60 mL) and EtOAc (40 mL + 2 × 25 mL), and the combined organics were dried (Na₂SO₄) and concentrated *in vacuo* to give a yellow oil that darkened at room temperature while at high vacuum. Column chromatography on silica (230–400 mesh, 11.5 g) by elution with 40:60 EtOAc:hexanes furnished first **2-81** (14 %: 31.2 mg sample contaminated with 40 mol % **2-56**) and then **2-80** (67.7 mg, 39 %).



¹H NMR (CDCl₃, 300 MHz) δ 7.59 (1 H, t, *J* = 1.9 Hz, C2-H), 3.86 (3 H, s, CO₂CH₃), 2.81 (2 H, t, *J* = 6.5 Hz, C4-H₂), 2.62 (2 H, td, *J* = 6.0, 1.9 Hz, C6-H₂), 1.93 (2 H, qn, *J* = 6.3 Hz, C5-H₂); ¹³C NMR (CDCl₃, 75 MHz) δ 168.3 (u, CO₂CH₃), 146.2 (u, C1), 129.5 (d, C2),

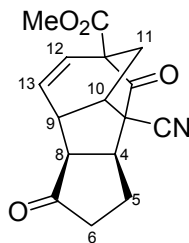
126.2 (u, C3), 111.9 (u, CN), 111.1 (u, CN), 84.9 (u, NC–C–CN), 35.3 (d, CH₃), 29.1 (u, CH₂), 25.1 (u, CH₂), 20.9 (u, CH₂).

3-Cyano-2,7-dioxo-tetracyclo[7.2.2.0^{3,8}.0^{4,10}]tridec-12-ene-1-carboxylic acid methyl ester



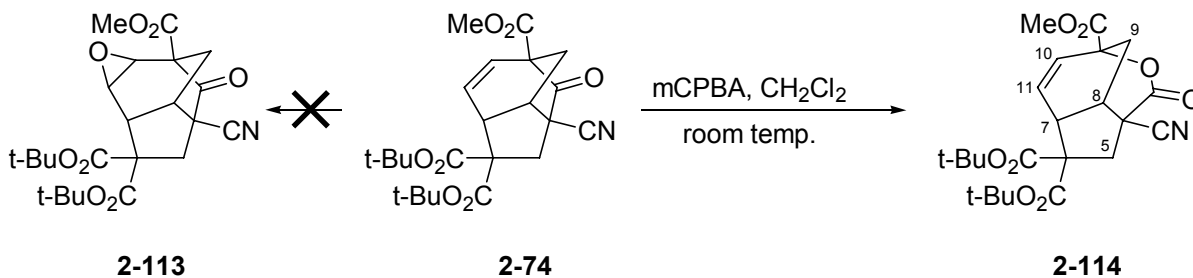
To a stirred, 0 °C solution of the ring-opened adduct **2-56** (0.1010 g, 0.500 mmol) in CH₃CN (5 mL) was quickly added (approx. 5 sec.) a CH₃CN solution of DBU (0.0332 g/mL, 2.293 mL, 0.500 mmol) measured by 5 mL gas-tight™ syringe, which caused the solution to turn orange. Immediately, a similarly dispensed CH₃CN solution of cyclopent-2-enone (0.0188 g/mL, 2.185 mL, 0.500 mmol) was added (approx. 5 sec.). The reaction was arbitrarily allowed to slowly reach room temp. and stir overnight to a total of 25 hours. The reaction mixture was added to saturated aq. NH₄Cl (40 mL) and extracted with CH₂Cl₂ (3 × 30 mL), after which the combined organic extracts were dried (Na₂SO₄) and the solvent was removed *in vacuo*, depositing a thick brown oil. The crude mixture was dissolved in EtOAc (5 mL) and rapidly stirred to form an emulsion with 6% aq. HCl (8 mL) in a stoppered flask at room temp. for 30 minutes. The reaction was added to a sep. funnel with water (35 mL) and EtOAc (25 mL), partitioned, and the organic phase was washed with water (25 mL). The dried (Na₂SO₄) EtOAc solution was dried *in vacuo*, expanding into a golden foam at high vacuum. Flash column chromatography on silica (230–400 mesh, 11.6 g, 1.43 ID × 17 cm stationary phase, six-stage EtOAc:hexane elution gradient from 10:90 to 60:40) furnished a

small quantity of promising contaminated material. Preparative normal phase HPLC (25 × 100 mm μ Porasil™ RCM silica column; gradient elution from 20:80 to 50:50 (25 minutes) to 100:0 (5 minutes) EtOAc:hexanes; 5 mL/min. flow rate; 600 μ L sample injection in CH_2Cl_2 solution) furnished a single diastereomer of the title compound (0.7 mg, 0.5%). ^1H - ^1H nOe spectroscopy established the relative stereochemistry depicted below.



^1H NMR (CDCl_3 , 300 MHz) δ 6.22 (1H, d, $J = 9.5$ Hz, C12-H), 5.82 (1H, dd, $J = 9.5, 3.5$ Hz, C13-H), 3.85 (3H, s, CO_2CH_3), 3.44 (1H, br t, $J = 4.0$ Hz, C9-H), 3.07 (1H, br t, $J = 7.0$ Hz, C4-H), 2.95 (1H, br t, $J = 5.1$ Hz, C10-H), 2.76 (1H, dd, $J = 12.3, 4.4$ Hz, C11-H), 2.64 (1H, d, $J = 7.3$ Hz, C8-H), 2.60–2.47 (2H, m, C6-H₂), 2.40–2.19 (2H, m, C5-H₂), 2.05 (1H, d, $J = 12.3$ Hz, C11-H).

4-Cyano-3-oxo-2-oxa-tricyclo[5.2.2.0^{4,8}]undec-10-ene-1,6,6-tricarboxylic acid di-tert-butyl ester methyl ester



To a solution of **2-74** (11.4 mg, 0.0264 mmol) dissolved in CH₂Cl₂ (2 mL) was added m-CPBA (9.3 mg, 0.0539 mmol, 2.04 equiv.) and the stoppered mixture was stirred at room temperature overnight, resulting in inadvertent total loss of solvent. The mixture was dissolved in CH₂Cl₂ and washed with saturated aqueous NaHCO₃ (30 mL). The aqueous phase was extracted with CH₂Cl₂ (20 mL), the combined organic portions were dried (Na₂SO₄), and the solvent was removed *in vacuo*, furnishing **2-114** as a clear colourless oil (11.4 mg, 96%) requiring no purification: ¹H NMR (CDCl₃, 500 MHz) δ 6.35 (1H, dt, *J* = 10.1, 1.7 Hz, C10-H), 5.79 (1H, ddd, *J* = 10.1, 2.7, 1.3 Hz, C11-H), 3.87 (3H, s, CO₂CH₃), 3.56 (2H, m, C7-H, C8-H), 3.03 (1H, dd, *J* = 15.2, 1.2 Hz, C5-H), 2.90 (1H, d, *J* = 15.2 Hz, C5-H), 2.48 (1H, ddd, *J* = 14.4, 3.6, 1.6 Hz, C9-H), 2.31 (1H, dd, *J* = 14.4, 2.6 Hz, C9-H), 1.53 (9H, s, CO₂C(CH₃)₃), 1.48 (9H, s, CO₂C(CH₃)₃); ¹³C NMR (CDCl₃, 125 MHz) δ 168.7 (u), 167.8 (u), 165.8 (u), 164.9 (u), 130.6 (d), 130.1 (d), 119.3 (u), 83.9 (u), 83.4 (u), 77.4 (u), 64.7 (u), 53.5 (d), 45.8 (d), 44.4 (u), 43.3 (u), 40.7 (d), 27.9 (u), 27.8 (d), 27.7 (d); HMBC (500 MHz) δ 168.7 (6.35, 3.87), 167.8 (3.03, 2.90), 165.8 (2.90), 164.9 (3.03, 2.90), 130.6 (3.56), 130.1 (2.48), 119.3 (3.03, 2.90), 83.9 (1.53), 83.4 (1.48), 77.4 (6.35, 5.79, 2.48), 64.7 (3.03, 2.90), 45.8 (6.35, 5.79, 3.56, 3.03, 2.48), 44.4 (3.56, 3.03, 2.90, 2.48, 2.31), 40.7 (5.79, 3.03, 2.48, 2.31), 27.9 (6.35).

References

1. Loya, S.; Tal, R.; Kashman, Y.; Hizi, A. *Antimicrob. Agents Chemother.* **1990**, *34*, 2009-2012.
2. Loya, S.; Hizi, A. *J. Biol. Chem.* **1993**, *268*, 9323-9328.
3. Luibrand, R. T.; Erdman, T. R.; Vollmer, J. J.; Scheuer, P. J.; Finer, J.; Clardy, J. *Tetrahedron* **1979**, *35*, 609-612.
4. Steitz, T. A. *Curr. Opin. Struct. Biol.* **1993**, *3*, 31-38.
5. Starnes, M. C.; Cheng, Y.-c. *J. Biol. Chem.* **1989**, *264*, 7073-7077.
6. Hafuri, Y.; Takemori, E.; Oogose, K.; Inouye, Y.; Nakamura, S.; Kitahara, Y.; Nakahara, S.; Kubo, A. *J. Antibiot.* **1988**, *41*, 1471-1478.
7. Radeke, H. S.; Digits, C. A.; Bruner, S. D.; Snapper, M. L. *J. Org. Chem.* **1997**, *62*, 2823-2831.
8. Takizawa, P. A.; Yucel, J. K.; Veit, B.; Faulkner, D. J.; Deerinck, T.; Soto, G.; Ellisman, M.; Malhotra, V. *Cell (Cambridge, Massachusetts)* **1993**, *73*, 1079-1090.
9. Cruciani, V.; Leithe, E.; Mikalsen, S.-O. *Exp. Cell Res.* **2003**, *287*, 130-142.
10. Nambiar, M. P.; Wu, H. C. *Exp. Cell Res.* **1995**, *219*, 671-678.
11. Ravi, B. N.; Perzanowski, H. P.; Ross, R. A.; Erdman, T. R.; Scheuer, P. J.; Finer, J.; Clardy, J. *Pure Appl. Chem.* **1979**, *51*, 1893-1900.
12. Quideau, S.; Lebon, M.; Lamidey, A.-M. *Org. Lett.* **2002**, *4*, 3975-3978.
13. Piña, I. C.; Sanders, M. L.; Crews, P. *J. Nat. Prod.* **2003**, *66*, 2-6.
14. McLean, S.; Haynes, P. *Tetrahedron* **1965**, *21*, 2343-2351.

15. Rouse, R. S.; Tyler, W. E., III *J. Org. Chem.* **1961**, *26*, 3525-3527.
16. Eilbracht, P.; Dahler, P.; Totzauer, W. *Tetrahedron Lett.* **1976**, *17*, 2225-2228.
17. Webster, O. W. *J. Am. Chem. Soc.* **1966**, *88*, 4055-4060.
18. Oediger, H.; Möller, F. *Liebigs Ann. Chem.* **1976**, 348-351.
19. Thandi, M. S. Master of Science, University of Waterloo, 1981.
20. Raman, J. V. Master of Science, University of Waterloo, 1986.
21. Raman, J. V.; Nielsen, K. E.; Randall, L. H.; Burke, L. A.; Dmitrienko, G. I. *Tetrahedron Lett.* **1994**, *35*, 5973-5976.
22. Friesen, R. W. Chemistry 492 Report, University of Waterloo, 1984.
23. Brion, F. *Tetrahedron Lett.* **1982**, *23*, 5299-5302.
24. Guildford, A. J.; Turner, R. W. *J. Chem. Soc., Chem. Commun.* **1983**, 466-467.
25. Davis, W. A.; Cava, M. P. *J. Org. Chem.* **1983**, *48*, 2774-2775.
26. Calverley, M. J.; Banks, B. J.; Harley-Mason, J. *Tetrahedron Lett.* **1981**, *22*, 1635-1638.
27. Fusetani, N.; Wolstenholme, H. J.; Matsunaga, S.; Hirota, H. *Tetrahedron Lett.* **1991**, *32*, 7291-7294.
28. Battiste, M. A.; Coxon, J. M.; Posey, R. G.; King, R. W.; Mathew, M.; Palenik, G. J. *J. Am. Chem. Soc.* **1975**, *97*, 945-947.
29. Spurlock, L. A.; Clark, K. P. *J. Am. Chem. Soc.* **1972**, *94*, 5349-5360.
30. Trost, B., M.; Shuey, C. D.; DiNinno, F., Jr.; McElvain, S. S. *J. Am. Chem. Soc.* **1979**, *101*, 1284-1285.

31. Ho, T.-L.; Kung, L.-R.; Chein, R.-J. *J. Org. Chem.* **2000**, *65*, 5774-5779.
32. Ho, T.-L.; Kung, L.-R. *Org. Lett.* **1999**, *1*, 1051-1052.
33. Dmitrienko, G. I.; Savard, M. E.; Friesen, R. W.; Thandi, M. S. *Tetrahedron Lett.* **1985**, *26*, 1691-1694.

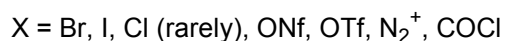
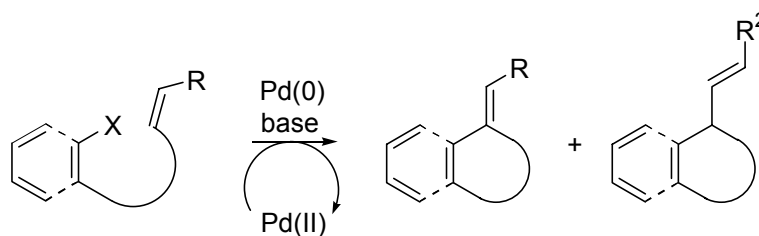
Chapter 3

Intramolecular Heck Reactions of Halobenzyl Adducts of the Ring-Opened Compound

3.1 Introduction

The Heck¹ reaction, also frequently credited as the Mizoroki²-Heck reaction in light of its simultaneous independent discovery by the two named researchers, has proven itself as a member of the top rank of versatile and reliable carbon-carbon bond-forming reactions. The palladium-catalyzed arylation or vinylation of vinyl groups by mainly aryl or vinyl halides, respectively, and occasionally of aryl carbon centers, has enjoyed a use sufficiently widespread that its application has been fine-tuned to effect the desired coupling of a vast collection of substrates. Indeed, as noted by Beletskaya and Cheprakov in a review focussed on features of the Heck reaction that make it so adaptable and unpredictable, “The limits of scope are blurred, the substrates which yesterday had been considered as *unheckable* are being cracked on need with yet another improvement.”³ The reaction has witnessed an evolution in catalysts, reagents, additives, conditions, and leaving groups that has realized a drive toward its deployment in sensitive and demanding applications involving a need for lower temperatures or in the successful coupling of less reactive substrates. The great interest in the Heck reaction in recent years, from both preparative and mechanistic standpoints, has resulted in the generation of an overwhelming body of literature that has supported the publication of numerous reviews and monographs.⁴⁻¹³ Among these manifold advances, the concern of the present study, the intramolecular Heck reaction (Scheme 3-1),

has been established as a powerful cyclization tool in synthesis and has witnessed the broadening of its scope to include tandem and asymmetric reactions.



Scheme 3-1. General intramolecular Heck reaction.

The Heck reaction has long been described by the ubiquitous catalytic cycle¹² depicted in Figure 3-1 as involving six steps that comprise: catalyst reduction from Pd(II) to Pd(0), also referred to as preactivation; oxidative addition to an aryl or vinyl carbon–halogen bond; complexation with the π -bond of the coupling partner; migratory insertion that establishes the new carbon–carbon linkage; a sequence of rotation to coplanarize the palladium and β -hydrogen atom and reductive elimination to conclude the coupling; and base-induced α -elimination of hydrogen halide from the Pd(II) species to conclude the catalytic cycle and deliver reduced palladium for the next turnover.

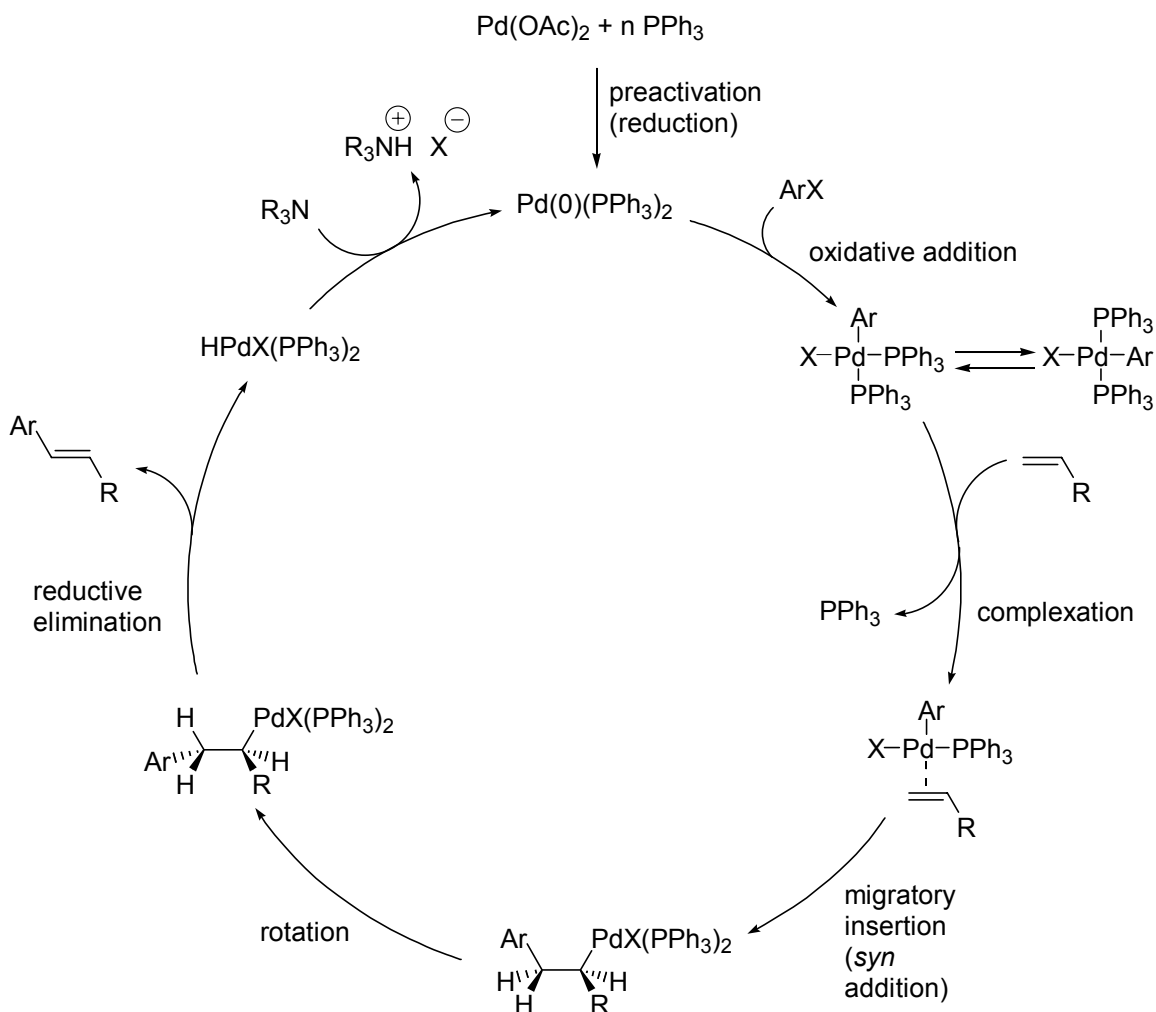


Figure 3-1. “Textbook” intermolecular Heck reaction catalytic cycle with catalyst preactivation by phosphines.

In addition to its great usefulness in synthesis, the Heck reaction is an open field of mechanistic research. Each step of the catalytic cycle has been closely scrutinized and the result of this long and varied study has been a more complex view of the process, which is sufficiently subtle that in some issues there is still disagreement. The nature of the catalytic species emerging from pre-activation (reduction) and involved in oxidative addition to the carbon–halogen bond has been the subject of lengthy study.

The reduction of Pd(II) to Pd(0) in situ, generally from Pd(OAc)₂, has received considerable attention, and a variety of reducing agents better known for their involvement in the catalytic cycle with existing Pd(0) have been identified (Figure 3-2). Among them, the added phosphine is the best known species capable of reducing palladium. A portion of phosphine is oxidized by an inner-sphere reduction of palladium to the corresponding phosphine oxide.^{14,15}

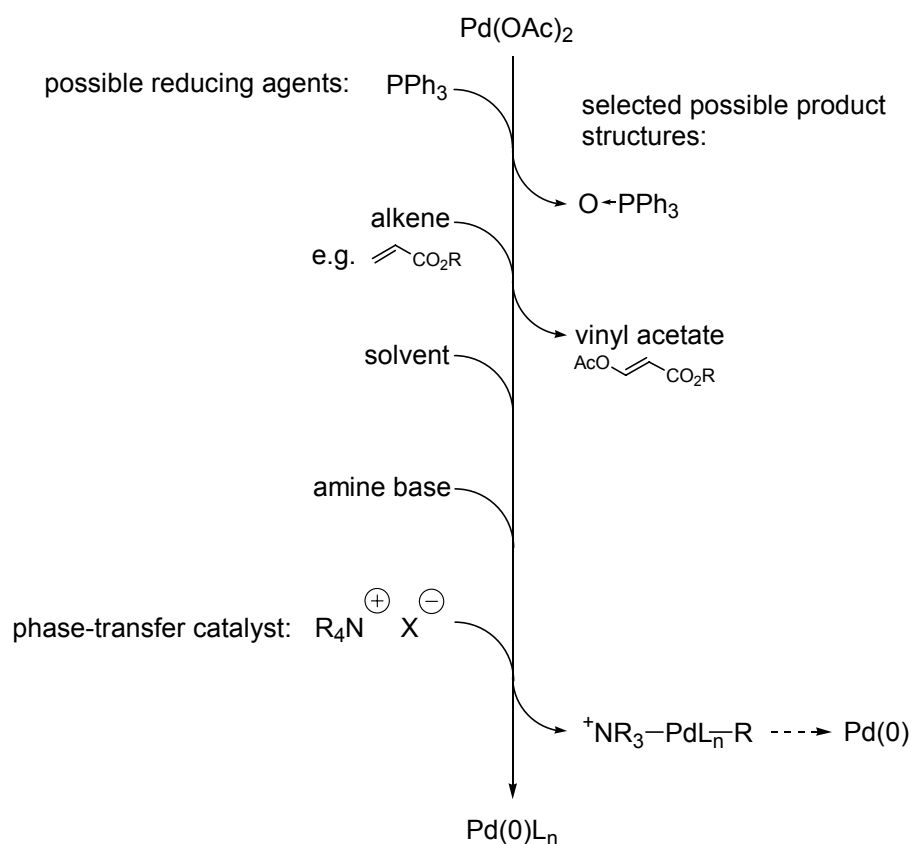


Figure 3-2. Common Heck reaction constituents identified as potential reducing agents for Pd(0).

It has generally been held that the purpose of the phosphine ligands is to stabilize the Pd(0) atom in solution to prevent precipitation of palladium black and a drastic reduction in rate.³ A problem perceived in reactions mediated by monodentate phosphine ligands centers around the equilibria involving the degree of coordinative unsaturation of palladium. The

conventional view has been that a dicoordinated Pd species, retaining two open sites in its coordination sphere and adhering to the 18 electron rule for transition metals, is the form available for oxidative addition to the carbon–halogen bond, where the addition saturates the coordination sphere and moves the complex toward association and migratory insertion of the alkene. The equilibrium between PdL_3 and PdL_2 , which favours PdL_3 , retards the formation of a large catalytically active population. The problem is compounded by excess phosphine ligand. On the other hand, the use of just two equivalents of phosphine leads to disproportionation to a tricoordinated and stable complex and a low-ligated species that aggregates and precipitates as palladium metal. This account of the extent and role of ligand coordination resides in the center of the range of opinion: there are significant bodies of findings that argue for lower degrees of ligation¹⁶ and even for the absence of ligands to the catalytic species in certain cases, as well as for higher degrees of coordination, including tricoordinate species leading to anionic pentacoordinate species.^{15,17,18}

Electrochemical studies by Amatore and Jutand have identified the catalytically active oxidative addition product in $\text{Pd}(\text{OAc})_2$ /phosphine catalytic systems as an anionic pentacoordinate complex of palladium involving trialkyl phosphine ligands and a previously unappreciated acetate ligand that imparts the negative charge. The anionic catalytic cycle (Figure 3-3) that has emerged from these studies has come to augment and increasingly to supplant the simpler textbook version of the catalytic cycle in the secondary literature.¹⁷⁻¹⁹ Whereas the catalytic activity of the anionic tricoordinate species is well-documented, computational studies have found the existence of Amatore and Jutand's postulated pentacoordinate oxidative addition species to be controversial.^{19,20}

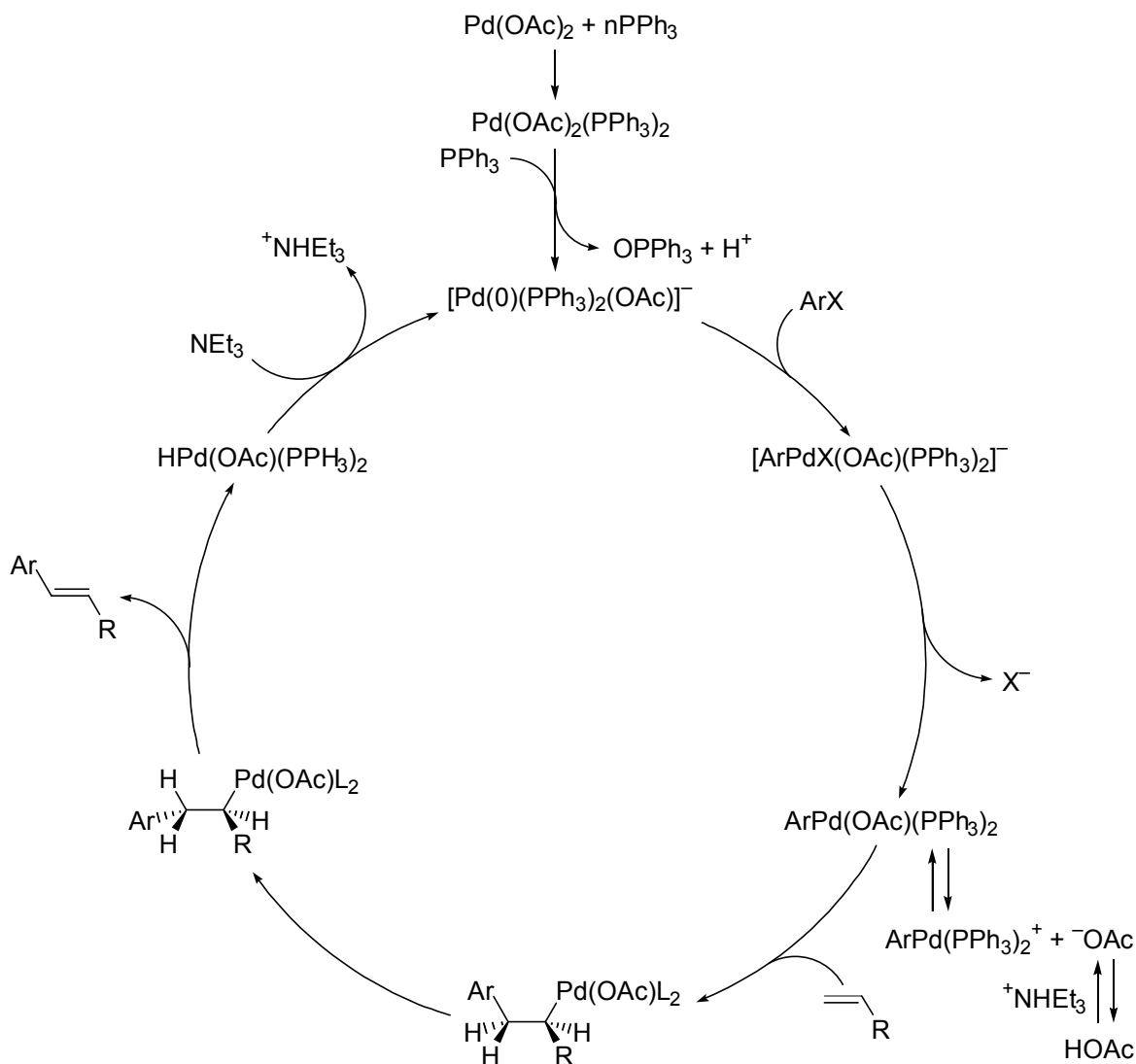


Figure 3-3. New catalytic cycle of intermolecular Heck reaction detailing phosphine-based palladium reduction and comprising anionic intermediates.

In contention with the determination of overligated palladium, a recent theoretical study has adduced low-ligated palladium as the catalytically relevant species.¹⁶ The DFT study by Norrby and coworkers of the oxidative addition of PhI to $\text{Pd}(0)$ determined that the species obtained is ArIPdL , derived from Pd-L . The authors indicate that the foundation is weak for the consideration of Pd -catalyzed reactions as adhering to the 18-electron rule, and that kinetic studies which have determined the oxidative addition to be of negative reaction

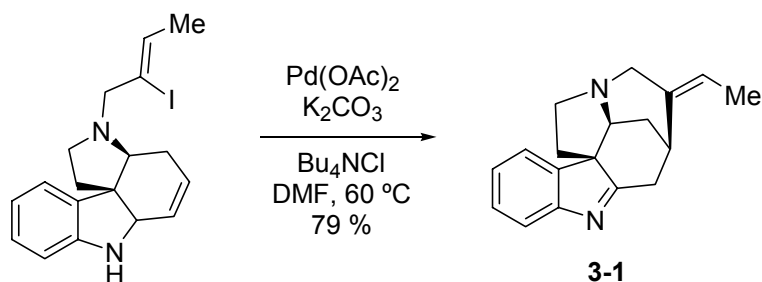
order are incorrectly interpreted in light of the 18-electron rule as involving the equilibria between a tricoordinate resting state and a catalytically active PdL_2 species. Instead, a lower order equilibrium between PdL_2 and Pd-L is proposed.

Of increasing significance are ligand-free Heck reaction systems, especially in light of their potential industrial applications. Studies related to supported palladium catalysts, palladacycles, and ligand-free heterogeneous catalyst systems, all with the implication of unligated palladium nanoparticles and colloids as the catalytic species, have increased significantly in recent years. Supported catalysts are frequently determined to be reservoirs for desorption of catalytically active palladium species. In a study of Heck reactions with catalytic palladium supported on metal oxides, it was determined that solution concentrations of palladium of less than one ppm arose upon heating of the system to 140 °C, ultimately leading to the leaching of one-third of the palladium. The system, which successfully catalyzed Heck reactions of aryl chlorides, was found to rely on the equilibrium between dissolved species and reprecipitation onto the support. It was felt that the availability of this phase change suppressed agglomeration of the palladium and formation of palladium black.²¹ Davies and coworkers performed “three-phase tests” of Heck reactions of aryl halides with butyl acrylate in the presence of resin-bound aryl iodides to determine that palladium supported on alumina is also a source of homogeneous catalyst.²² Oxidative addition of aryl iodides at the heterogeneous surface of supported palladium has been found to cause desorption, and coordinating base (e.g. NaOAc) to assist the process.²³

Ligand-free systems of Pd(II) precatalysts have also been shown to produce catalytically active nanoparticles and colloids, among them $\text{PdCl}_2(\text{SEt}_2)_2$ /tetrabutyl ammonium bromide²⁴ (in a study in which even washed glassware was found to retain

catalytic activity), $\text{PdCl}_2(\text{C}_6\text{H}_5\text{CN})_2/\text{NaOAc}$,²⁵ and $\text{Pd}(\text{OAc})_2/\text{NaOAc}/\text{NMP}$ ²⁶. In the latter study, the catalytic system was tested against Herrmann's palladacycle²⁷ and determined to exhibit similar kinetics. In addition, an MS study of the palladacycle-catalyzed Heck reaction indicated that palladacycles may be sources of ligand-free palladium as the catalytic species. These findings were supported by a study of a thermomorphic (i.e. temperature-dependent solubility changes in fluorous versus organic solvents) fluorous palladacycle in which the palladacycle was found to release highly reactive palladium nanoparticles that were the catalytic species.²⁸

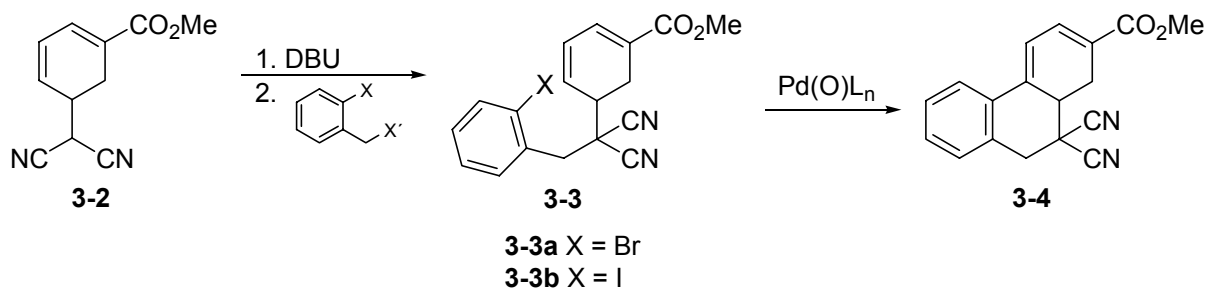
The Heck reaction has proven so valuable in synthesis partially because of its tolerance of a variety of functional groups (e.g. $-\text{CHO}$, COR , $-\text{CO}_2\text{R}$, $-\text{COOH}$, $-\text{CN}$, $-\text{NO}_2$, $-\text{OH}$, $-\text{OR}$, amines), which permits its deployment to establish bonds to and within advanced and functionally relatively ornate intermediates. The intramolecular Heck reaction has frequently been applied in natural product synthesis, a viable future prospect for the outcome of the present study. For example, Rawal et al. concluded the synthesis of *Strychnos* alkaloid (\pm)-dehydrotubifoline (**3-1**, Scheme 3-2) with an intramolecular Heck reaction and enamine tautomerization.⁵



Scheme 3-2. Synthesis of (\pm)-dehydrotubifoline by intramolecular Heck reaction.

The intramolecular Heck reaction of substrates derived from **1** was undertaken with the goal of expanding the ring-closure scheme to include six-membered rings, an outcome

not open to the tandem conjugate addition–conjugate addition mode of cyclization detailed in Chapter 2. To this end, it was devised that **3-2** would be alkylated with 2-halobenzyl halides to provide substrates **3-3** for the palladium-catalyzed ring closure onto ring C4 of the parent ring to furnish Heck product **3-4** (Scheme 3-3).

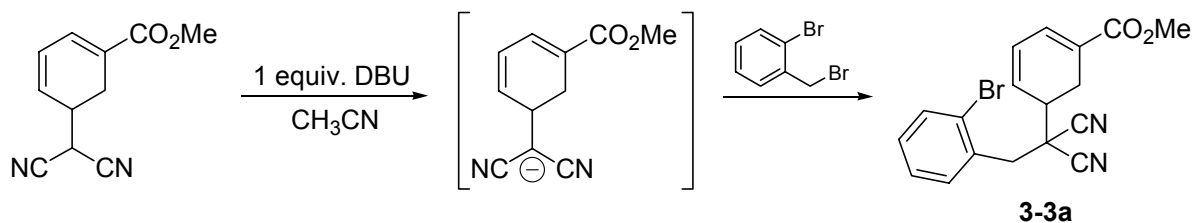


Scheme 3-3. Substrate preparation and intramolecular Heck reactions devised for **3-2**.

3.2 Results and Discussion

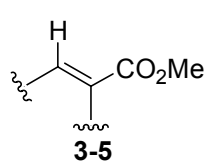
3.2.1 Synthesis of Substrate for Intramolecular Heck Reaction

For the initial attempts at the intramolecular Heck reaction, commercial 2-bromobenzyl bromide was used to alkylate the ring-opened adduct (**3-2**) treated with a stoichiometric amount of DBU (Scheme 3-3). The initial adduct-forming reactions did not proceed smoothly, although the generation of the main side-product provided insight into the properties of the ring-opened adduct that were more readily apparent absent the further reactivity available to conjugate adduct intermediates described earlier in this thesis (see Chapter 2).



Scheme 3-4. Generation of intramolecular Heck reaction substrates.

In the first experiment, the ring-opened adduct in CH_3CN was treated at room temperature with neat DBU added over the course of one minute. Fifteen minutes were allowed to elapse prior to the addition, also over the course of one minute, of neat stoichiometric 2-bromobenzyl bromide. After 20 minutes, TLC revealed the complete consumption of the starting material. The ^1H NMR spectrum of the crude product mixture evidenced the presence of the desired product and a greater quantity of an unknown compound. The side-product co-migrated with the intended adduct on TLC and proved inseparable by column chromatography and HPLC. Recrystallization of a later sample with a more favourable product ratio was also unsuccessful. The significant excess of the unknown



(2:1 with respect to **3-3a**) simplified the mutual association of all its ^1H NMR signals. In addition, several key signals were isolated. Of particular significance were two broad, very finely and multiply coupled vinyl proton signals (δ 6.96 and δ 6.03) which represented all of the vinyl resonances. Their lineshapes, essentially broad singlets with barely discernable multiple shoulders (multiple fine splittings of ca. 1.3 Hz resolved at high expansion), indicated both the residence of the protons on separate double-bonds, and the mutual isolation of the double-bond protons. The downfield vinyl signal (δ 6.96) was sufficiently deshielded that its residence at the carbomethoxy-substituted vinyl group of the parent ring was suggested (fragment **3-5**).

The signal pattern of the second vinyl proton (δ 6.03) was identical to the first, indicating its attachment to a substituted double-bond. Two two-proton multiplets (δ 3.19 and δ 2.99) with large and small couplings were also in evidence, representing the apparent balance of the parent ring protons. The absence of a signal for a single proton at an sp^3 carbon was consistent with the ring-formulations that pair the non-vinyl protons as ring methylene groups and keep the ring vinyl protons out of vicinal relationship (Figure 3-4). The situation of side-chain R on a double-bond was further supported by the appearance as a two-proton singlet of the benzylic methylene protons of the halobenzyl group, indicating an accessible planar conformation for the compound.

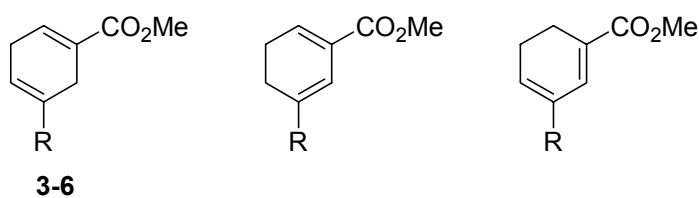
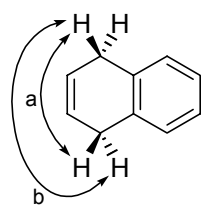


Figure 3-4. Potential ring formulations for unknown alkylation product.

The most sensible ring assignment is **3-6**, which accounts for the matching lineshapes of the two vinyl protons if the ring substituents are considered general groups, insofar as both protons then share a nominally symmetrical relationship to each other and the other ring protons. Moreover, **3-6** is the most reasonably accessed arrangement, requiring a single double-bond isomerization that is easily envisioned. The large mutual coupling of the ring methylene protons is a striking and well-established feature of cyclohexa-1,4-diene systems, in which the five-bond homoallylic coupling exceeds the allylic couplings. Experimental values for the *cis* and *trans* homoallylic couplings in 2,4-dihydronaphthalene are 9.63 and 8.04 Hz, respectively (Figure 3-5).



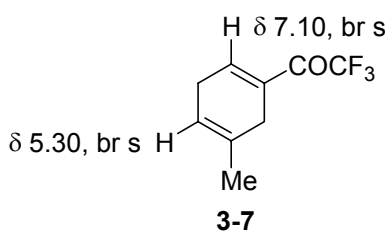
5J methylene proton couplings

a) *cis* homallylic: 9.63 Hz

b) *trans* homallylic: 8.04 Hz

Figure 3-5. Experimental 5J coupling constants among methylene protons in 2,4-dihydronaphthalene.

Precedent for the coupling patterns of the vinyl protons in **3-6** has been observed in a similarly 1,5-disubstituted cyclohexa-1,4-diene system described in Nenajdenko and



coworkers' study of the Diels-Alder reactions of β -trifluoroacetylvinyl-sulfones and the subsequent DBU-induced eliminations of the sulfonyl groups, in which compound **3-7** was encountered.²⁹ Their ^1H NMR

characterization of the compound cites a 120 Hz-wide four proton multiplet for the methylene protons, consistent with homoallylic couplings of considerable magnitude. Their description of the two vinyl protons as broad singlets is in accord with our observation and constrains the source of the large J line splittings to the mutually remote methylenes. Cumulatively, the data strongly support the formulation **3-8a** as the identity of the side-product in alkylations of the ring-opened adduct (Figure 3-6). The alkylation is reasonably assigned as having proceeded according to expectation at the dicyanomethyl carbon.

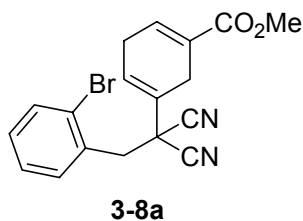
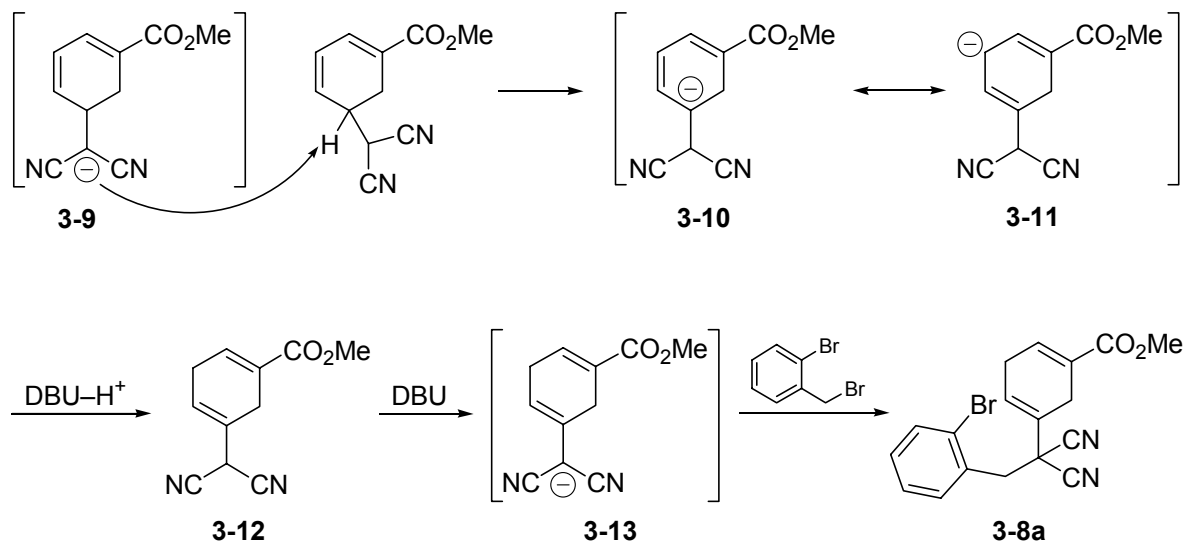


Figure 3-6. Side-product in the alkylation of the ring-opened adduct with 2-bromobenzyl bromide.

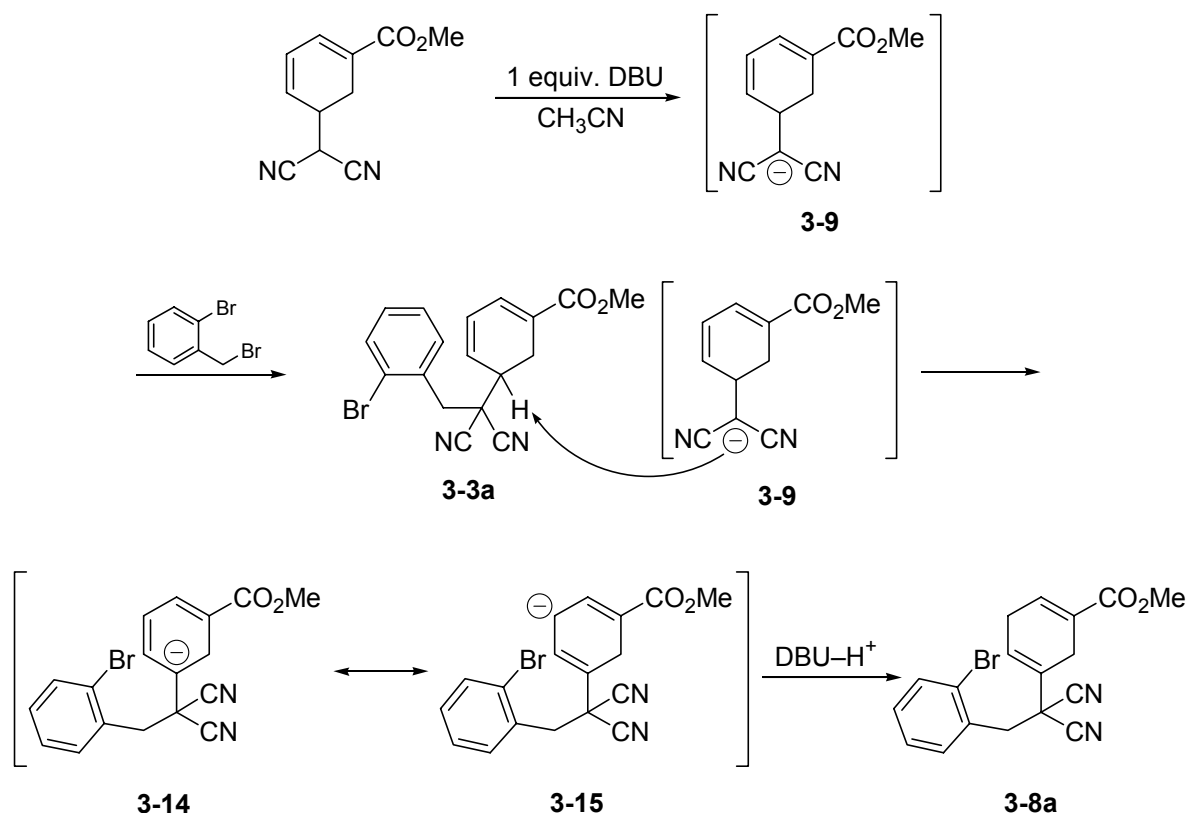
Two opportunities for double-bond isomerization are available to the parent ring under the conditions employed. Prior to the conclusion of the addition, the slow introduction of base to the substrate solution formed a mixed population of deprotonated and neutral ring-opened adduct. Under these conditions, it is possible that the ring-opened adduct anion **3-2** deprotonated the ring C5 of the neutral adduct, generating the resonance pair **3-10**↔**3-11**, which neutralized as deconjugated isomer **3-12** (Scheme 3-5). The side-chain alkylation would then proceed via anion **3-13** as expected to furnish **3-8a**. Under the operation of this process, the twofold excess of **3-8a** over the expected adduct would indicate that the dicyanomethyl carbon is the kinetically deprotonated site, whereas the ring-C5 is the thermodynamically favoured anion.



Scheme 3-5. Generation of deconjugated adduct isomer **3-8a** by anionic site equilibration among the ring-opened adduct population prior to addition of alkylating agent.

Alternatively, the stoichiometric quantity of base may reliably be introduced with the sole deprotonation of the dicyanomethyl group. In this case, the dropwise addition of the alkylating agent and the non-diffusion-controlled rate of alkylation would afford the opportunity for neutral adduct **3-3a** (Scheme 3-6) to be ring-C5-deprotonated by anionic

ring-opened adduct, with neutralization of anion **3-14**↔**3-15** furnishing a large extent of deconjugated isomer **3-8a** (Scheme 3-6). Both processes are potentially at work at their respective stages.

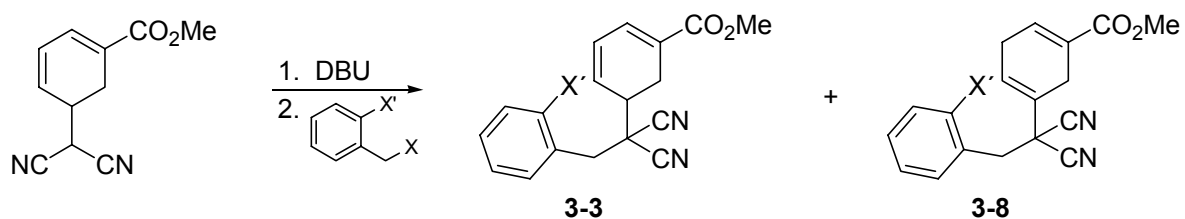


Scheme 3-6. Generation of deconjugated adduct isomer **3-8a** by deprotonation of adduct **3-3a**.

In attempting to optimize the synthesis of **3-3a**, several refinements were introduced that ultimately reduced the extent of the generation of deconjugated isomer **3-8a** to trace levels. An initial concern with respect to the isomerization was that the dispensing of small neat quantities of DBU might decrease the accuracy of their measurement. Of particular significance was the potential to inadvertently dispense greater than stoichiometric quantities of base, which would hasten the isomerization process. After the earliest experiments, CH_3CN solutions of both DBU and the alkylating agents were used to maximize accuracy,

with the attendant benefit of eliminating the inconvenient viscosity of neat DBU. Table 3-1 details the most informative alkylation experiments conducted.

Table 3-1. Conditions and product distributions in alkylations of ring-opened adduct with halobenzyl halides.



Entry	Temp.	DBU conc. (M) ^a	Duration of base addition (sec.)	Base incubation (min.) ^b	Alkylating agent		Alkylating agent conc. (M)	Alkylating agent addition (sec.)	Reaction time (min.)	Result (%)	
					X	X'				3-3	3-8
1	RT	neat	60	15	Br	Br	neat	60	20	34	66
2	RT	0.149	140	15	Br	Br	0.167	375	50	51	49
3	0 °C	0.152	10	1	Br	Br	0.147	20	40	>95	tr. ^c
4	0 °C ^d	0.056	20	1	Cl	I	0.042	20	456	34	66
5	0 °C	0.339	15	1	Br	I	ca. 0.46 ^e	unknown ^f	53	82	18
6	0 °C	0.339	20	1	Br	I	ca. 0.48 ^e	unknown ^f	82	>95	tr. ^c

^a Solutions in CH₃CN. ^b Period from end of DBU addition to start of addition of alkylating agent. ^c trace: minor product signal not integrated. ^d Allowed to warm to room temperature overnight. ^e Stoichiometric samples weighed and dissolved in known solvent volume. ^f Reasonably assumed as 15–20 seconds.

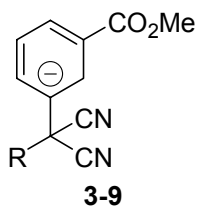
Of particular interest is the comparison of entries 3 and 4 in Table 1. The less reactive alkylating agent 2-iodobenzyl chloride required ten times the duration of 2-bromobenzyl bromide to complete the alkylation of **3-2**. Whereas the benzyl bromide alkylation produced only trace ring-deconjugated adduct, in the benzyl chloride alkylation it represented the major product (66:34 with respect to intended adduct **3-3**). The base addition durations and intervals prior to introductions of the alkylating agent solution were comparable in the two cases, indicating that the propensity of the benzyl chloride alkylation

to produce **3-8** was realized once the reactants were combined. This indicates that in this case the major route to the ring-deconjugated adduct **3-8** was that depicted in scheme 3-6, in which the slowly accumulating quantity of adduct **3-3** is deprotonated at ring-C5 by ring-opened adduct anion **3-2**.

It is noteworthy that adduct **3-3**, given prolonged exposure to base in the form of persistent ring-opened adduct anion will slowly convert to the ring-deconjugated isomer **3-8**, indicating that it is the product thermodynamically favoured over the desired isomer **3-3**. This effect may be ascribed to the generation of a more highly substituted double-bond. It is also possible that the contiguous π system of the ring does not experience the full stabilizing effect of conjugation due to the conformation of the ring: whether the substituted dicyanomethyl substituent is positioned in the pseudo-axial or the pseudo-equatorial position is immaterial to the mutual relationship of the ring double-bonds, which in either case results in non-parallel p orbitals. The generation of a more highly substituted double-bond, and perhaps a more stable conformation available to a 1,4-cyclohexadiene system, are sufficient to drive deconjugation. This effect was repeated when a sample of **3-3b**, contaminated with 16.7 mol % of **3-8b** was treated with 0.1 equivalents of DBU in CH₃CN at room temp. for two hours. When the reaction was arbitrarily concluded the quantity of **3-8b** had increased to 34.1 mole % of the mixture.

The practical recommendations that emerged from the series of alkylations of **3-2** with 2-halobenzyl halides were twofold: first, that the base should be introduced at low temperature as quickly as possible to lessen the length of time during which there is a mixed population of neutral **3-2** and anionic **3-9**, thereby limiting the opportunity for ring double-bond isomerization prior to alkylation; and second, that the alkylating agent should be as

reactive as possible (benzyl bromide favoured over benzyl chloride) so that alkylation concludes quickly to limit the lifetime of a mixed population of neutral adduct **3-3** and ring-



opened adduct anion **3-9**. Nucleophilic reaction of **3-9** without the possibility of tandem reactivity afforded a valuable insight into the acid-base behaviour of **3-2** that would especially inform the detailed study of the tandem reactive qualities of **3-2** toward alkyl propiolates (Chapter 5). The

deprotonation of adduct **3-3**, necessarily by anion **3-9**, gave the first indication of the unexpectedly high acidity of the ring C5-proton and demonstrated that, given a thermodynamically favourable fate for the general anion **3-14**, and the finding that anion **3-9** can deprotonate ring C5 in a reasonable length of time, the acidities of the two vicinal protons of **3-2** are comparable.

3.2.2 Intramolecular Heck Reactions of Adducts 3-3

A preliminary search of the literature regarding Heck and specifically intramolecular Heck reactions was undertaken to select as a starting point an appropriate catalyst and set of conditions. The literature revealed a variety of reagent sets and conditions that frequently involved high temperatures. Because the lability of the ring-opened compound, particularly its marked ability to aromatize by multiple pathways to generate product mixtures, even due to careless storage, had been well established, it was deemed especially desirable to select as mild a set of reaction conditions as possible. The reagent system disclosed and studied by Jeffery,³⁰⁻³⁶ comprising Pd(OAc)₂, carbonate base, and a phase-transfer catalyst, originally in DMF, was considered for its reported ability to catalyze the intermolecular Heck reactions of aryl halides and alkyl acrylates at room temperature. Prior to the report of this remarkably

gentle reagent set that would prove sufficiently versatile to take on the recognized term “Jeffery’s conditions,” a notable precedent for lower temperature Heck reactions in the generation of carbomycin model compounds (e.g. $\text{PdCl}_2(\text{CH}_3\text{CN})_2/\text{CH}_3\text{CN}/55\text{ }^\circ\text{C}$) was reported by Ziegler et al.,³⁷ but these conditions were superseded in mildness with the report by Jeffery.

Jeffery’s conditions were also thought attractive because in using $\text{Pd}(\text{OAc})_2$, palladium is introduced as in its Pd(II) oxidation state, and is easily handled without risk to the reagent in the air and light. Conversely, a Pd(0) reagent such as tetrakis(triphenylphosphine)palladium(0) ($\text{Pd}(\text{PPh}_3)_4$) is sensitive to light and is unstable in air. Furthermore, the complete set of Jeffery’s reagents can be handled without stringent exclusion of atmospheric moisture, as water has been demonstrated to be beneficial to the progress of the catalyzed Heck reaction: this convenience particularly applies to the handling of the extremely hygroscopic tetraalkyl ammonium halide phase-transfer catalysts.

A final factor to recommend the use of Jeffery’s conditions was revealed in analyzing the cost of various palladium reagents. Using recent catalogue prices for comparable 99.9% purity reagents, $\text{Pd}(\text{PPh}_3)_4$ was determined to be 3.29 times more costly per mole of palladium than $\text{Pd}(\text{OAc})_2$. Assuming potentially equal catalyst loadings in practice, the combination of the cost and relative ease of handling of $\text{Pd}(\text{OAc})_2$ and the relatively low temperatures employed in Heck reactions with this reagent set led to the selection of Jeffery’s conditions for the initial attempts at the ring closure of **3-3**.

Prior to the ultimate refinement of the reaction conditions in the course of these experiments, several attempts at the intramolecular Heck reaction were made that resulted in mixtures of compounds, some of them containing none of the intended product. In the early

going, side-products were isolated whenever possible and their ^1H NMR spectra were recorded for future use in determination of the identities and relative quantities of the constituents of product mixtures solely by the discernment of their diagnostic ^1H NMR signals in the crude reaction spectra.

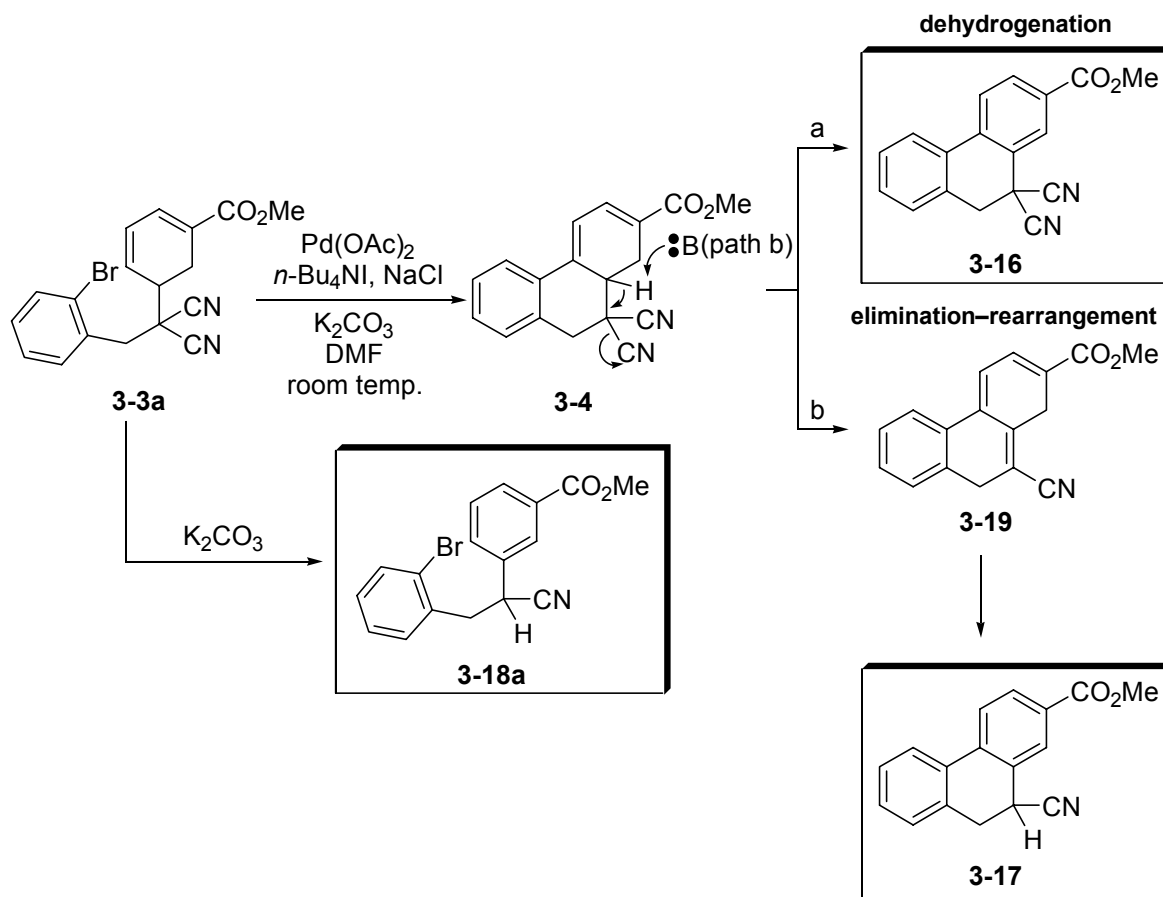
At the beginning of the present study, intramolecular Heck reactions were attempted prior to the arrival of commercial BnEt_3NCl in the interests of quickly advancing the work. Whereas Jeffery reported a catalytic system comprising the reagents that were in our possession, namely $\text{Pd}(\text{OAc})_2$ and K_2CO_3 , his system included the phase-transfer catalyst $n\text{-Bu}_4\text{NCl}$. The tetraalkyl ammonium halide phase-transfer catalyst on hand at the time was $n\text{-Bu}_4\text{NI}$, and so this was employed for the initial Heck reaction attempts along with NaCl in the hopes of halide exchange furnishing *in situ* the desired phase-transfer species. The substrate **3-3a** (the 2-bromoaryl substrate was used for the majority of experiments in the present study) was dispensed along with $\text{Pd}(\text{OAc})_2$ (approximately 0.2 equivalents), K_2CO_3 (three equivalents), and the cooperative pair of phase-transfer additives $n\text{-Bu}_4\text{NI}$ (one equivalent) and NaCl (approximately 1.3 equivalents). To the mixture was added DMF, and the reaction was set to stir overnight to a total of 22 hours, after which TLC revealed the absence of starting material. The crude reaction mixture, observed by ^1H NMR spectroscopy, evidenced none of the vinyl proton signals that would be expected for the Heck ring-closure product **3-4**, instead evidencing for downfield signals solely a complex array of aromatic proton resonances. The mixture was determined by the presence of three methyl ester proton singlets to comprise three constituents; indeed, ^1H NMR spectroscopy represented a generally useful supplement to the sometimes inconclusive TLC data, owing to the close migration of various species, including co-migration in certain cases. Whereas the

Careful separation of product mixture components from later reactions would allow for the identification of the constituents of the product mixtures for every reaction of the study, at the time it sufficed to conclude that the reaction had not delivered any of the desired product, although further structural conclusions were permitted by the data in hand.

Close study of the aromatic region of the ^1H NMR spectrum of the initial experiment allowed for the association of some of the various signals with the respective compounds. The crude sample soon deposited a small quantity of crystals while stored in the freezer. The crystals were partially isolated by rapidly dissolving the crude oil and carefully drawing the solution away from the remaining solid. A ^1H NMR spectrum of the dissolved crystals, while still comprising the three constituents of the original sample, was heavily enriched in the minor constituent of the total crude sample, which greatly aided in the discernment of assignable protons in the complex aromatic region. The assignment of all terminal ring positions to aromatic protons indicated that the cyclohexadiene ring present in **3-3a** had aromatized in all three compounds. The remaining aliphatic proton signals were necessarily derived from the benzylic positions, that is, from saturated B ring sites in the case of ring-closed compounds. The major component of the crystalline mixture revealed a two proton singlet at δ 3.61, a signal that in the original sample was not easily appreciated. This signal was the type expected for a benzylic methylene proton pair ($\text{ArCH}_2\text{C}(\text{CN})_2\text{Ar}$) in an aromatized compound exhibiting planar symmetry. Scrupulous comparison of the aromatic signals between the two spectra suggested that the planar symmetric compound contained seven aromatic protons, which indicated substitution of a proton of the substrate, that is, successful ring closure. This finding was later confirmed with a pure sample of what was at

the time tentatively formulated as a 9,10-dihydrophenanthrene 10,10-dinitrile **3-16** (Scheme 3-7).

The presence in the upfield region of three additional mutually coupled protons for each of the two remaining compounds suggested ABX arrangements of three aliphatic protons for each species, especially owing to the two doublets of doublets at δ 4.23 and δ 4.09. These arrangements would have derived from HCN elimination–aromatization, as had been observed for attempted tandem conjugate addition reactions of the ring-opened compound anion and phenyl vinyl sulfone (Chapter 2). The presence of two ABX systems was strongly suggestive of the presence of cyclized and uncyclized aromatized compounds. Reasonable initial structural assignments were: for the cyclized compound, a 10-cyano-9,10-dihydrophenanthrene **3-17**; and, for the uncyclized compound, the 2-aryl-1-cyanoethyl-substituted aromatized ring-opened compound **3-18a** (Scheme 3-7).

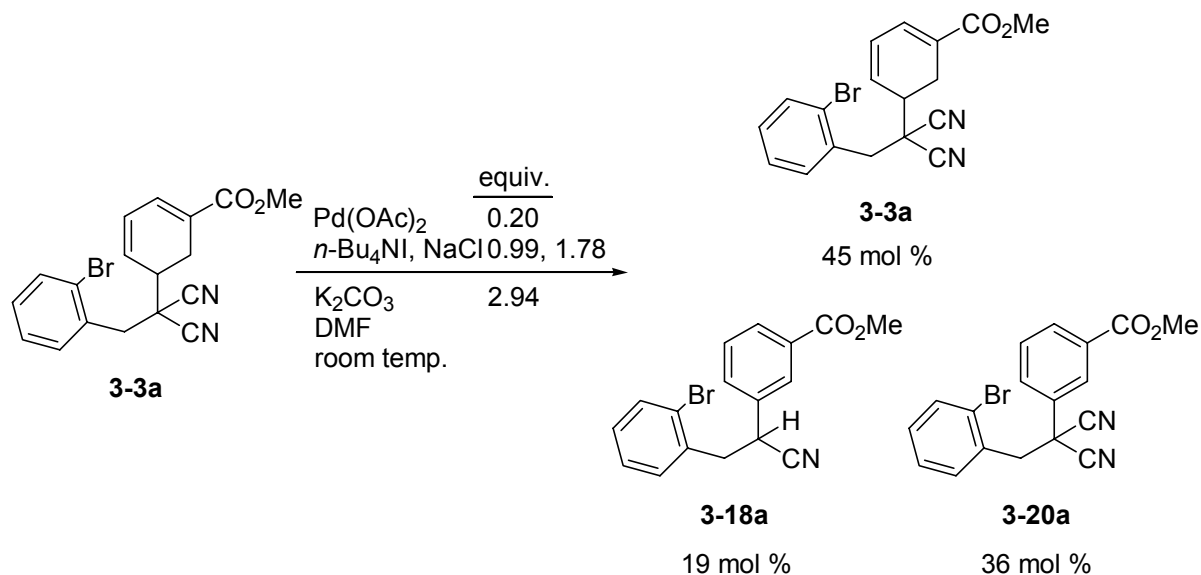


Scheme 3-7. Aromatized side-products in initial attempted intramolecular Heck reaction.

The ring-closed dihydrophenanthrene **3-17** was presumed to have arisen from an initial quantity of successfully ring-closed product **3-4** by the depicted elimination–rearrangement pathway ($3-4 \rightarrow 3-19 \rightarrow 3-17$). The aromatized decyanated compound **3-18a** would arise in the same fashion. Of special significance is the dehydrogenated compound **3-16**. The oxidation of the cyclohexadiene ring by direct dehydrogenation must involve palladium, and could have a crucial bearing on the progress of the reaction in terms of the generation of catalytically active palladium (*vide infra*).

The experiment was repeated under the same conditions, but the reaction was closely monitored by TLC. Because the first experiment had furnished cyclized aromatic material that was concluded to have derived from an initial quantity of Heck product, it was deemed

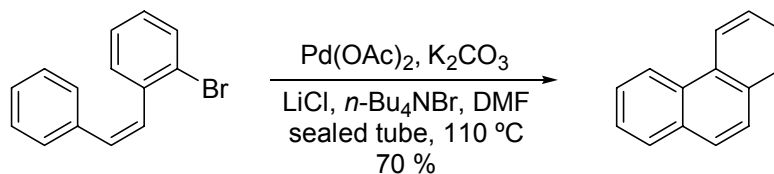
potentially instructive to halt the second reaction when starting material had been consumed to generate new compounds, but before, it was hoped, any extant Heck product had been converted to the two aromatic compounds **3-16** and **3-17**. In the event, after six hours TLC revealed products and the persistence of starting material, and so the reaction was worked up by aqueous/organic partition and the crude mixture was assessed by ^1H NMR spectroscopy. As indicated by TLC, a considerable quantity of starting material remained, but significantly, the balance of the product distribution comprised two uncyclized and aromatized species, one generated by dehydrogenation (**3-20a**) and the other (**3-18a**), as in the initial experiment, by base-induced elimination–rearrangement (Scheme 3-8). The structure of the uncyclized dehydrogenated material was determined by comparison of the crude ^1H NMR spectrum to that of an isolated sample generated in a later experiment.



Scheme 3-8. Product distribution (^1H NMR) in attempted intramolecular Heck reaction halted prior to total consumption of starting material.

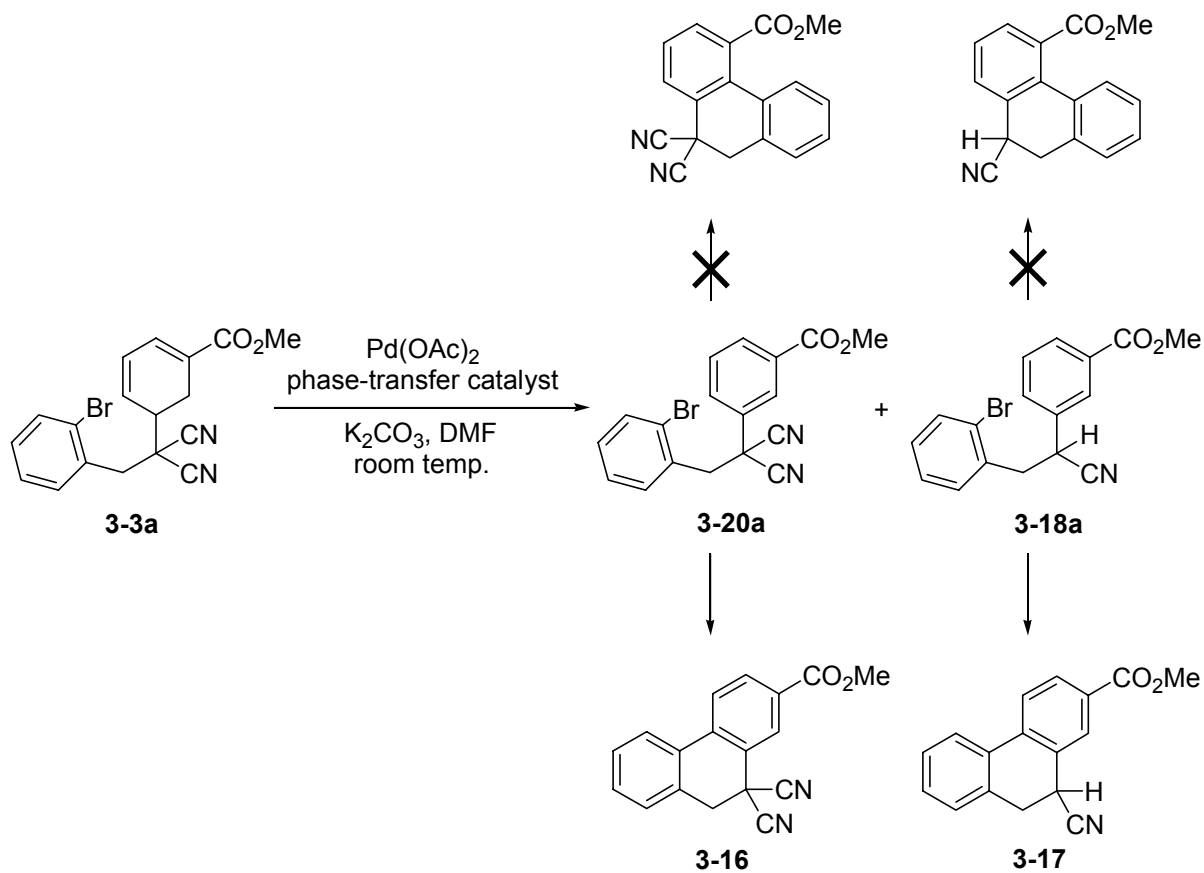
The initial longer-duration experiment under these conditions was able to generate cyclized, albeit completely aromatized, material. The shorter experiment revealed conversion of the substrate to uncyclized material aromatized by the two available pathways.

Crucially, the absence of the dehydrogenated substrate **3-20a** in the first experiment and its presence in the second indicates its reactivity at prolonged reaction times. Because its base-induced conversion to decyanated compound **3-18a** is already foreclosed by its aromaticity, its consumption indicates successful cyclization after aromatization. Similarly, the presence of cyclized and decyanated compound **3-17** indicates that the corresponding uncyclized compound **3-18a** is also a viable substrate for palladium-catalyzed cyclization. Whereas intermolecular Heck-like reactions to effect aryl-aryl coupling are relatively rare and require the presence of a hydroxyl group on the ring undergoing substitution, intramolecular reactions proceed under mild conditions without functional group requirements. For example, de Meijere et al. observed that *cis-ortho*-bromostilbene undergoes intramolecular linkage under Jeffery's conditions to give phenanthrene (Scheme 3-9).



Scheme 3-9. Generation of phenanthrene by intramolecular aryl bromide to arene coupling under Jeffery's conditions.

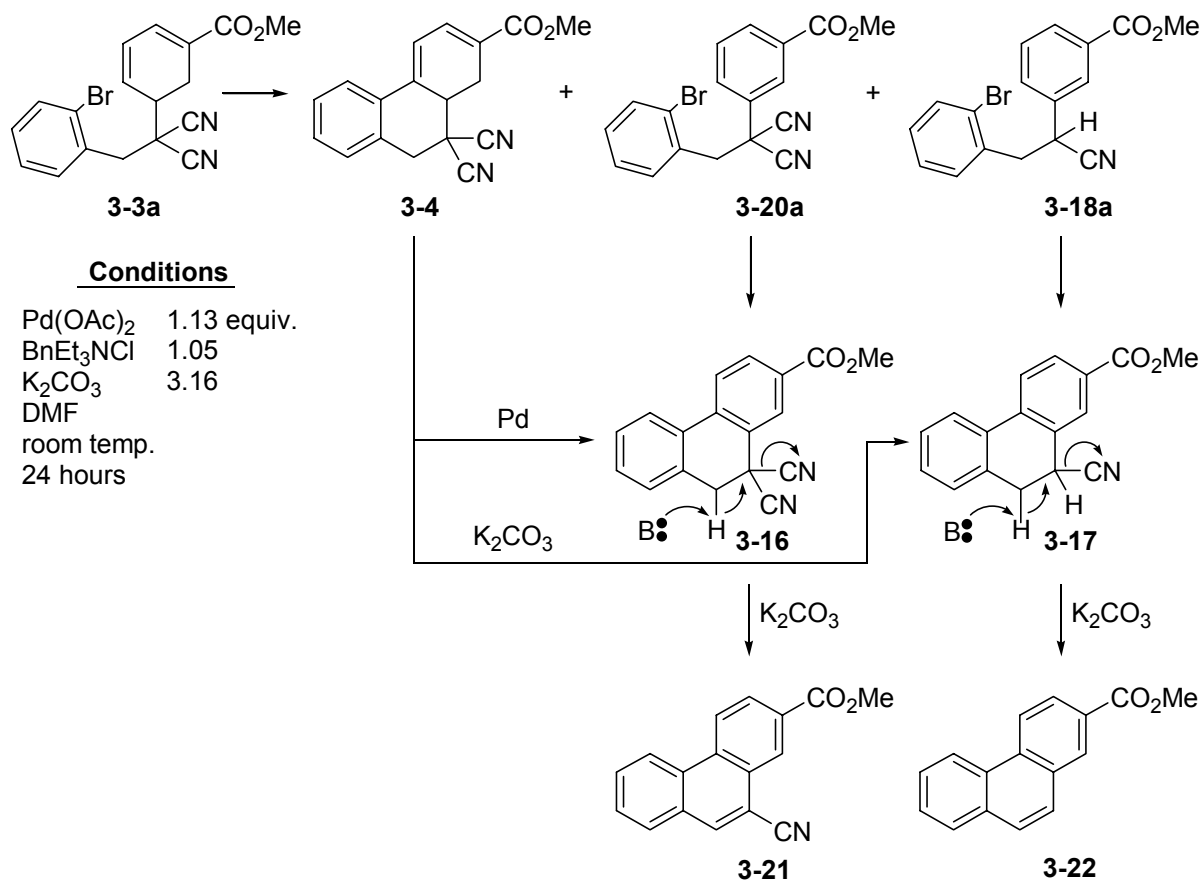
The possibility of successful Heck reactions to link aryl compounds in the present study includes the potential for two regiochemical outcomes not available prior to aromatization. The absence of the 4-carbomethoxy dihydrophenanthrene regioisomers is presumably due to the steric influence of the carbomethoxy substituent (Scheme 3-10).



Scheme 3-10. Heck cyclization of aromatized substrates **3-20a** and **3-18a**.

At this stage, it was evident that substoichiometric quantities of palladium were not sufficient to effect successful Heck couplings of the desired substrate at a rate greater than that of the generation of aromatic species. Therefore, an experiment was conducted with approximately (1.13 equivalents) stoichiometric Pd(OAc)_2 . Conducted at room temperature and this time with BnEt_3NCl rather than the provisional phase-transfer catalyst of the prior experiments, the reaction was permitted to continue for 24 hours. The crude mixture's ^1H NMR spectrum contained none of the desired ring-closure product **3-4**, and only aromatic region signals, three carbomethoxy methyl proton singlets, and the methylene proton singlet of **3-16** at δ 3.61. No other upfield signals were observed, which indicated that the two previously unobserved compounds were entirely aromatic substituted phenanthrenes. A

singlet at δ 8.94 represented the farthest downfield signal encountered in the study. The generally most downfield aromatic ring proton signals seen among these compounds are the protons *ortho* to the carbomethoxy group. It was reasonably surmised that the singlet at δ 8.94 also experienced its shift to low field due to the inductive effect of an *ortho* substituent and that the neighbouring functionality would have to be the nitrile. The compound was formulated, solely on the basis of the ^1H NMR spectrum, as 2-carbomethoxy-10-cyanophenanthrene (Scheme 3-11, compound **3-21**). Such a decyanated aromatic compound was envisioned to have arisen by HCN elimination, in this instance by deprotonation of the benzylic proton derived from the halobenzyl moiety. The remaining ^1H NMR signals were grouped upfield of the several in the region δ 9-8.2 that could be assigned to **3-21** and **3-16**. Whereas the remainder of signals were of lower intensity and were not as isolated as those of the novel phenanthrene **3-21**, they were nevertheless suggestive of compound **3-22**, the result of another HCN elimination from **3-17** (Scheme 3-11). The generation of **3-21** and **3-22** would share as their terminal steps base-induced elimination. The respective substrates, **3-16** and **3-17**, would arise either by dehydrogenation and base-induced elimination and rearrangement, respectively, of Heck product **3-4**, or by Heck aryl–aryl coupling of the aromatized substrates **3-20a** and **3-18a**. As they were not central to the purpose of effecting successful Heck ring closure of **3-3** without product consumption by aromatization reactions, unambiguous formulations of the novel structures were not undertaken.



Scheme 3-11. Generation of putative substituted phenanthrenes **3-21** and **3-22**.

A closely monitored reaction was carried out with the goal of observing the product distribution immediately upon complete consumption of the starting material under conditions nearly identical to the experiment just described. After 1 hour 23 minutes, TLC indicated the absence of starting material. The ¹H NMR spectrum of the crude mixture contained new signals, including a promising vinyl proton signal at δ 6.87. The mixture was separated by preparative layer chromatography. The lowest *R_f* band was somewhat enriched in the compound that evidenced the δ 6.87 ¹H NMR signal. The same compound was isolated in pure form from a later reaction and was crystallized suitably for analysis by X-ray diffraction, confirming its structure as Heck product **3-4** (Figure 3-7).

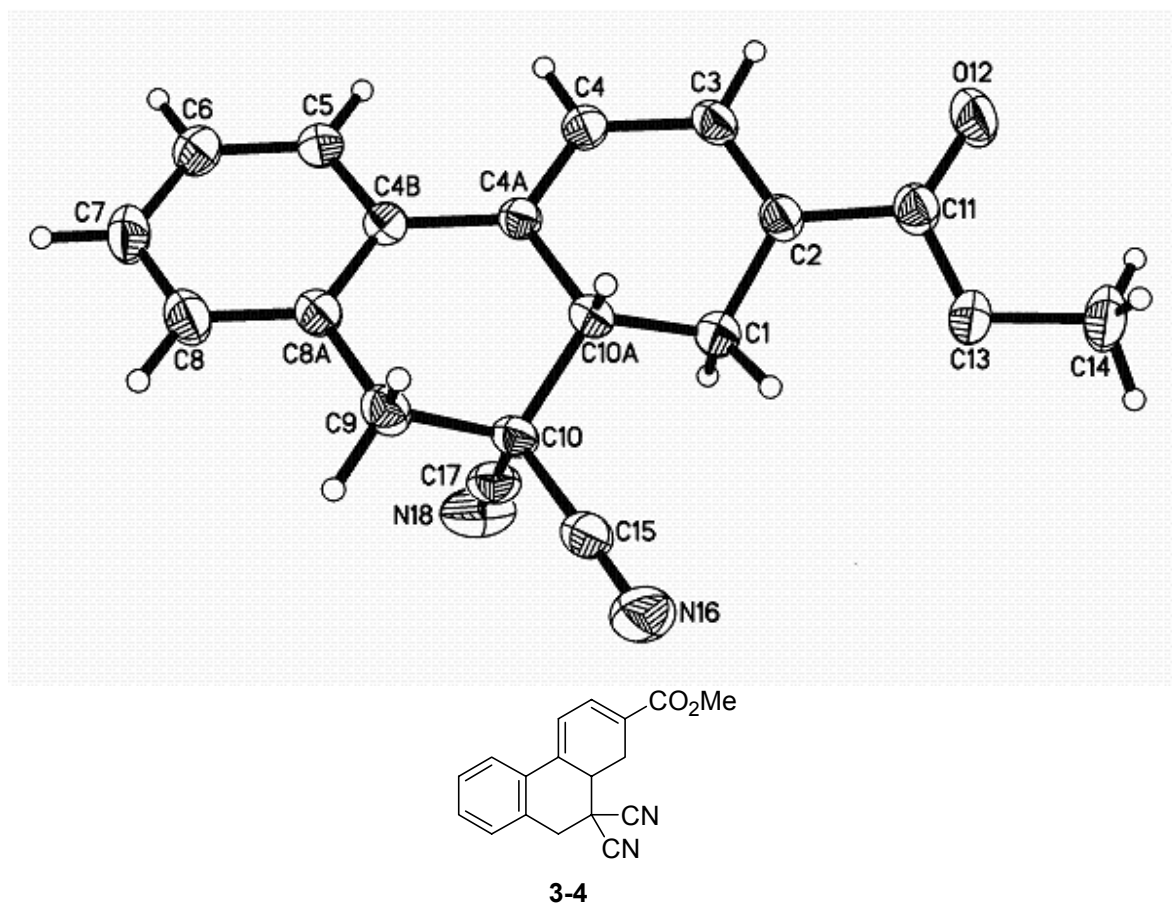


Figure 3-7. ORTEP: X-ray crystal structure of Heck product **3-4**. (See Appendix page 362 for full crystallographic data.)

A crystal grown from another chromatographic band was also amenable to X-ray diffraction study: this sample was determined to be a co-crystal of **3-16** and **3-17** (Figure 3-8). A ^1H NMR spectrum of another crystal from the same crystallization revealed it to be a nearly pure sample of dicyano dihydrophenanthrene compound **3-16**. The mother liquor furnished a ^1H NMR spectrum of decyanated and cyclized **3-17**, which included minor unidentified impurities. The later reaction that furnished the Heck product crystal also produced a mixed chromatographic fraction of nearly equimolar cyclized aromatics **3-16** and **3-17**, the ^1H NMR spectrum of which was of a higher quality than that of purer **3-17**, and so proved useful in product mixture analysis.

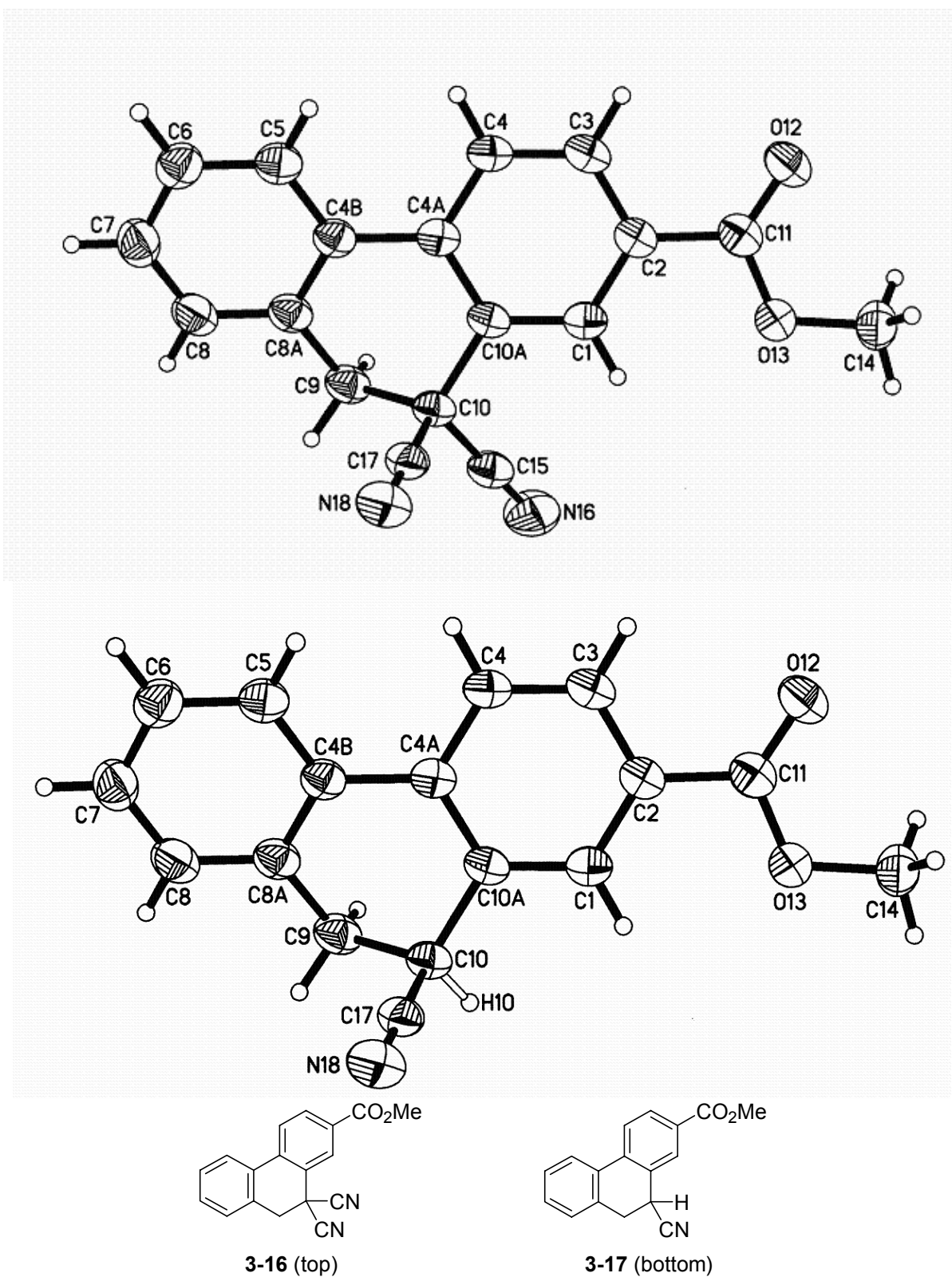
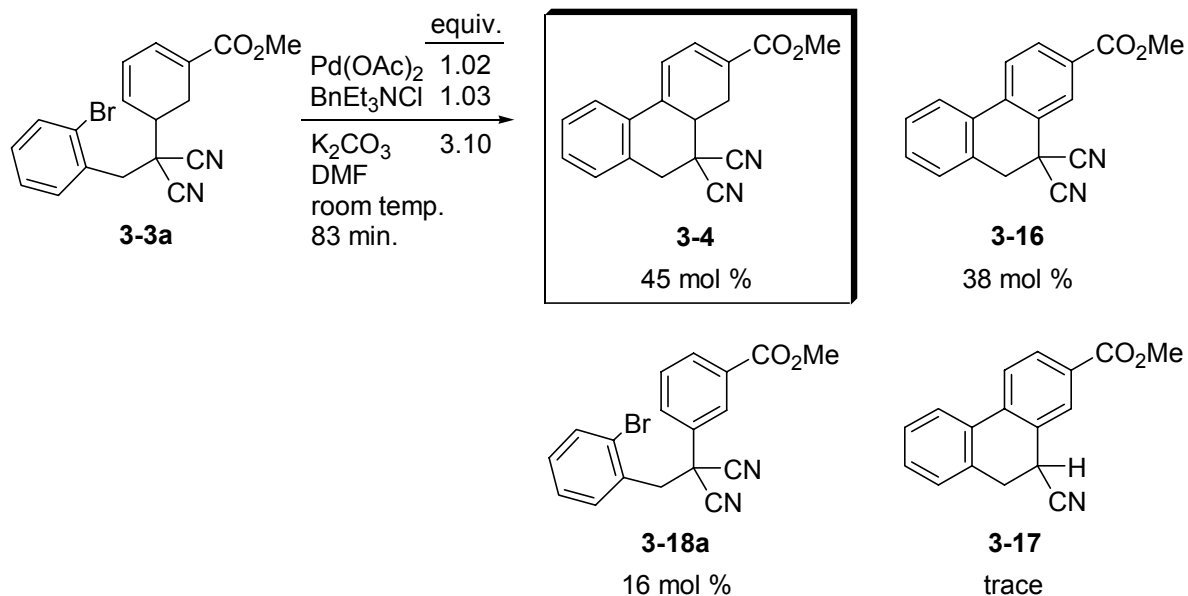


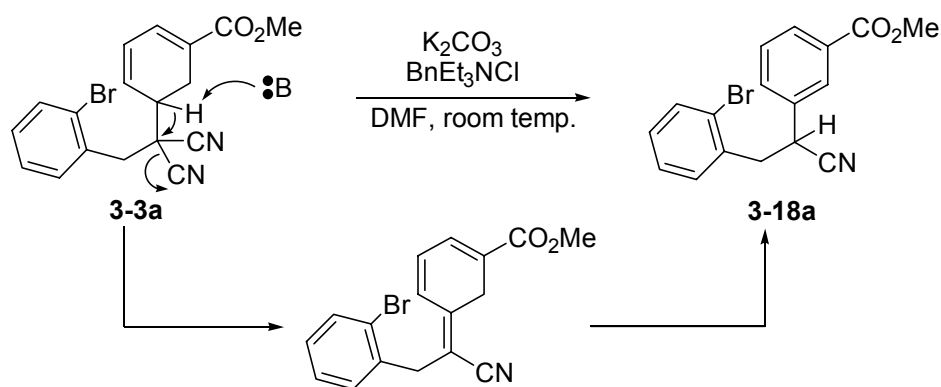
Figure 3-8. ORTEP: X-ray crystal structures of **3-16** (top) and **3-17** (bottom). (See Appendix page 366 for full crystallographic data.)

A final chromatographic sample contained aromatized substrate **3-20a**. Scheme 3-12 depicts the result and molar ratio as determined by ^1H NMR of the products of the first reaction to generate **3-4**.



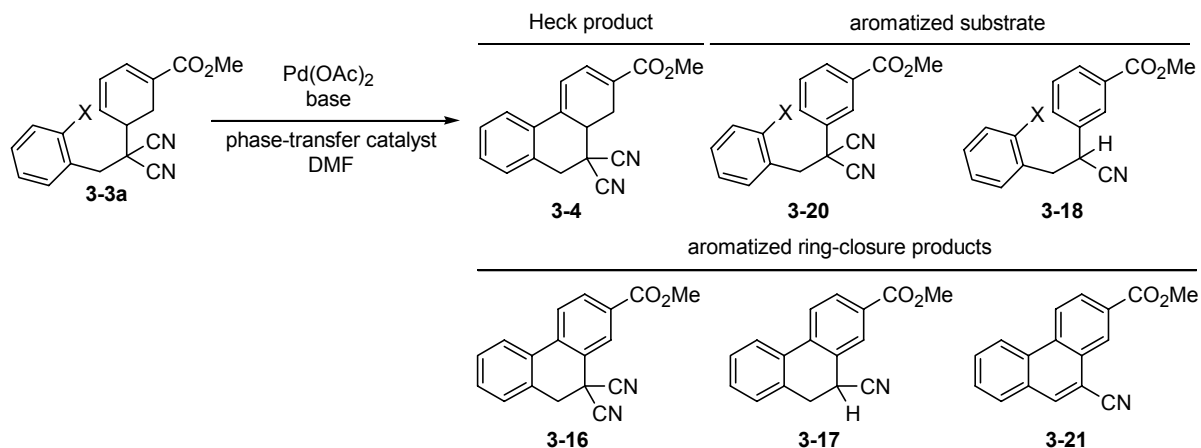
Scheme 3-12. First instance of generation of Heck product **3-4**.

The base-induced elimination–rearrangement pathway to decyanated aromatics was confirmed by a “palladium-free” experiment in which **3-3a** was treated only with approximately three equivalents each of K_2CO_3 and BnEt_3NCl , Jeffery’s conditions absent $\text{Pd}(\text{OAc})_2$. After stirring overnight at room temperature, the crude product furnished a ^1H NMR spectrum consistent with **3-18a**. Especially useful as a diagnostic peak in the analysis of mixtures was the doublet of doublets centered at δ 4.25, part of the acyclic ABX system and downfield of the analogous doublet of doublets for the cyclized and aromatized compound **3-17**.



Scheme 3-13. Aromatization of Heck substrate **3-3a** by base-induced HCN elimination and sigmatropic hydrogen shift.

With the first successful generation of **3-4**, the complete set of bromoaryl-containing and cyclized products that would be observed in this study was in hand. The X-ray crystal structures for the three main cyclized compounds (**3-4**, **3-16**, and **3-17a**) certified the use of the corresponding ¹H NMR spectra in the analysis of product mixtures. Table 3-2 details the results of the most informative experiments, including both those that led chronologically to the first generation of **3-4** (entries 1 to 5), and the remainder of the study that sought to optimize its yield.

Table 3-2. Conditions and product distributions in intramolecular Heck reactions of **3-3**.

		Reaction conditions						Product distribution ^a						
Entry	X	Substrate conc. (mM) ^b	Reagent distribution (equivalents)					3-3	3-4	3-20	3-18	3-16	3-17	3-21
			Pd(OAc) ₂	PTC ^c	Base ^d	Time (h) ^e	Temp.							
1	Br	43.68	0.195	1.06 ^c	3.01	22	RT	0	0	0	1.59	1	2.83	0
2	Br	12.35	0.195	0.99 ^c	2.94	6.25	RT	2.38	0	1.90	1	0	0	0
3	Br	15.15	1.130	1.05	3.16	24	RT	0	0	0	0	1	0	1.33
4	Br	20.74	1.009	1.12	1.28	1.00	-10 °C	12.5	0	1	0	0	0	0
5	Br	18.65	1.015	1.03	3.10	1.38	RT	0	2.94	1	0	2.50	trace ^f	0
6	Br	16.70	1.060	2.92	3.47	1.40	RT	0	10.75	0	0	1	9.57	0
7 ^g	Br	16.50	1.147	1.27	3.84	1.33	RT	1.36	1	1.43	0	trace	trace	0
8	Br	13.30	1.194	3.03	3.79 ^d	22	RT	0	1.26	0	0	1	1.58	0
9	I	17.70	0.208	3.07	2.98	1.66	RT	0	0	trace	1	0	0	0
10	I	18.47	1.442	1.06	3.17	1.00	RT	0	1	0	0	trace	trace	0

^a Determined from relative ¹H NMR signal intensities of isolated diagnostic peaks. ^b Approximate concentration of substrate alone with respect to added solvent volume. ^c Phase-transfer catalyst: BnEt₃NCl in entries 3 to 8. *n*-Bu₄I + NaCl (1.27 and 1.78 equivalents, respectively) in entries 1 and 2. ^d K₂CO₃, except NaHCO₃ for entry 8. ^e Arbitrary reaction durations: entries 1, 3, 4, 6, 7, and 8. Entry 2 worked up despite known persistence of starting material. Close monitoring of reaction progress (total consumption of starting material) by TLC: entries 5, 9, and 10. ^f Visible small signals not integrated. ^g Entry 7 included approx. 0.02 mL of D₂O.

Entry 5 informs the product distribution of entry 3. Long reaction times with stoichiometric Pd(OAc)₂ gave all cyclized products and a large quantity of **3-21** derived from **3-16**. Worked up upon starting material consumption, entry 5 reveals Heck product **3-4** and dehydrogenated compounds **3-20a** and **3-16**. Cumulatively, this indicates that the Heck product is a substrate for dehydrogenation. Furthermore, the presence of **3-20a** in the product mixture of entry 5 confirms the findings of entries 1 and 2 (cat. Pd(OAc)₂ and provisional phase-transfer system *n*-Bu₄NI/NaCl, described above) that aromatized substrates are susceptible to ring-closure under these Heck conditions. Given a longer reaction time, as in entry 3, **3-20a** would be consumed to furnish **3-16**. The readiness of Jeffery's conditions to convert **3-3a** to **3-20a** was most clearly displayed in a low temperature reaction of short duration (entry 4). Conducted at -10 °C for one hour, with slightly greater than stoichiometric quantities of Pd(OAc)₂, K₂CO₃, and BnEt₃NCl, the reaction generated solely a slight quantity (7.4 mol %; remainder the starting material) of **3-20a**. The ease of dehydrogenation of the cyclohexadiene ring of both the substrate and the product of this conversion has significant implications for the operation of the overall catalytic cycle and will receive greater attention below.

A striking difference was observed between the experiment that first furnished **3-4** (entry 5) and the subsequent experiment in which the role of the quantity of BnEt₃NCl was probed (entry 6). Conducted under the same conditions, except for the increase of BnEt₃NCl to nearly three equivalents, experiment 6 in fact produced a slightly greater proportion of **3-4** (50.4 mol %) than did experiment 5 (45 mol %), but the remainder of the product distribution was in this case dominated by HCN elimination product **3-17**, and included only a small quantity of **3-16**, a reversal of the balance of **3-16** and **3-17** in entry 5. It is likely that a

greater quantity of BnEt_3NCl increases the active concentration of K_2CO_3 and so increases the rate of HCN elimination.

More difficult to discern at this stage was the effect of increased BnEt_3NCl on the catalytic palladium species. In entry 5, a great deal of dehydrogenation is observed to generate **3-20a** (16 mol %) and **3-16** (38 mol %); conversely, in entry 6, dehydrogenation is reduced to the extent of 4.7 mol % generation of **3-16**. One possibility is that both the rate of base-induced reaction and of palladium-catalyzed coupling are increased with greater BnEt_3NCl , and so **3-3a** is quickly converted to Heck product **3-4**, which is then converted at a high rate by base to **3-17**, both reactions vastly outpacing dehydrogenation either of substrate or of Heck product. Alternatively, the higher concentration of BnEt_3NCl could inhibit the dehydrogenation reaction, irrespective of its influence on base solubility.

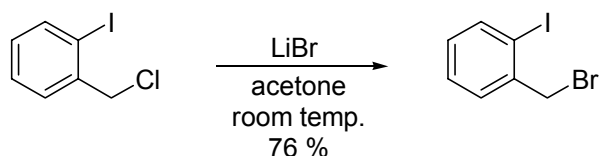
Entry 7 was conducted with reagent concentrations near those employed in entry 5, but approximately 0.02 mL of D_2O was added. Water has proven a useful additive in Heck reactions run under Jeffery's conditions with K_2CO_3 , but in this instance, the added water significantly slowed the reaction, to the extent that at a reaction time comparable to those sufficient to consume **3-3a** in other experiments, it persisted at 35 mol %. A noteworthy aspect of this experiment is that the added water did not hasten base-induced reactions.

The propensity of these systems to undergo base-induced elimination prompted an experiment in which K_2CO_3 was replaced with NaHCO_3 . It was hoped that the weaker base, while known³⁰ to possess sufficient basicity for the reductive elimination of HBr from the hydridopalladium halide complex to permit catalytic turnover, would effect an elimination of HCN sufficiently slow that a high yield of product could be obtained from reactions halted in a timely fashion. Jeffery's initial disclosure of his conditions involved the use of NaHCO_3 in

couplings of phenyl iodide and methyl acrylate at yields of up to 97 %. In the context of this study, NaHCO₃ was initially thought to have a deleterious effect upon the yield of **3-4** (entry 8), and so the optimization ultimately and successfully focussed elsewhere, but a retrospective consideration of the result leaves open the possibility that NaHCO₃ could prove a valuable reagent in these ring closures. A long reaction time (22 hours) with greater than three equivalents each of NaHCO₃ and BnEt₃NCl furnished 32.8 mol % of **3-4**, and respective 26.0 and 41.1 mol % yields of **3-16** and **3-17**. A reliable parallel can be drawn with entry 3, also a long reaction (24 hours), but with K₂CO₃ and in fact less BnEt₃NCl (1.05 equivalents). Under those conditions, the base proved reactive enough to carry out further conversions upon the initial ring-closure products, respectively converting **3-16** and **3-17** to **3-21** and putative 2-carbomethoxyphenanthrene. The persistence of **3-16** and **3-17** in the NaHCO₃ reaction and the long reaction time cumulatively suggest that a more closely monitored reaction might have been observed to provide a high initial yield of **3-4**, prior to the ample time provided for dehydrogenation (**3-4** → **3-16**) and HCN elimination (**3-4** → **3-17**).

The concluding steps in the optimization were carried out in light of the guidelines established in the preceding work. It was clear that high quantities of Pd(OAc)₂ were required in conjunction with short reaction times to limit the extent of dehydrogenation and HCN elimination. It was felt that a switch to the more reactive aryl iodide would increase the rate of oxidative insertion of palladium and so realize the shortest reaction times possible. To this end, 2-iodo-benzyl chloride was converted to the benzylic bromide by treatment with lithium bromide in acetone (Scheme 3-14). As discussed above (Section 3.2.1), attempted

benzylation of the ring-opened adduct with the chloride was sufficiently slow that side-product formation dominated.



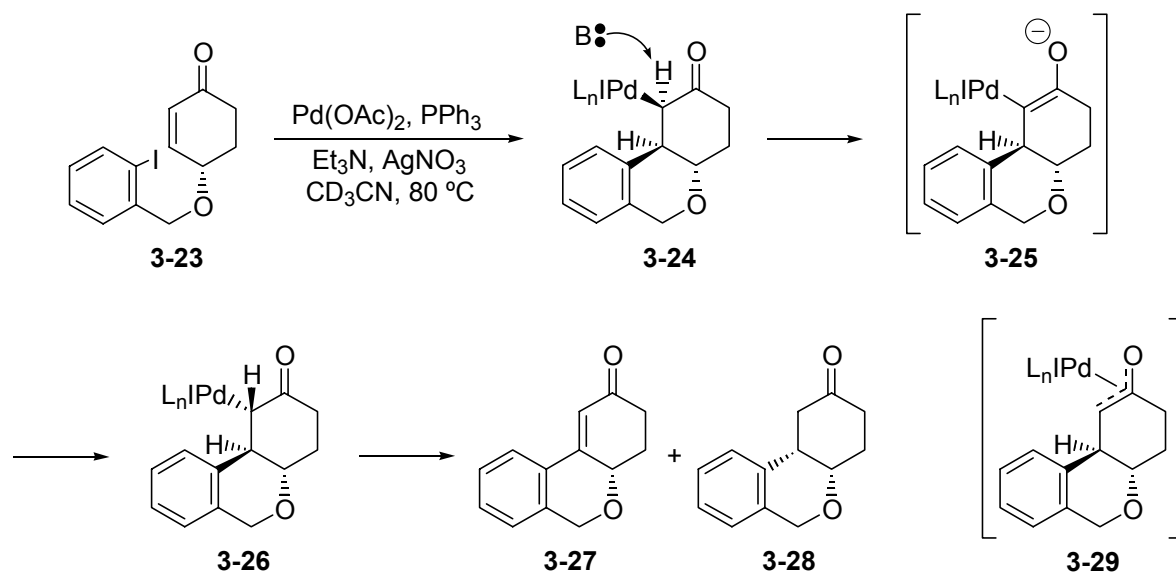
Scheme 3-14. Generation of 2-iodo-benzyl bromide.

Coupling of **3-2** and 2-iodobenzyl bromide proceeded in greater than 95 % yield. With the aryl iodide in hand, the penultimate Heck reaction was conducted (entry 9), employing approximately three equivalents each of K₂CO₃ and BnEt₃NCl. It was hoped that the more reactive iodide would permit the use of a substoichiometric quantity of Pd(OAc)₂, in this case 0.21 equivalents. The reaction was determined by TLC to have consumed the starting material within 100 minutes. The only products were a trace of **3-20a** and otherwise complete conversion to uncyclized HCN elimination product **3-18a**. This was viewed as another instance in which dehydrogenation and base-induced elimination, aided by the higher concentration of BnEt₃NCl, completely outpaced Heck cyclization.

High amounts of Pd(OAc)₂ were viewed as an apparent necessity in this system, and so the reaction was repeated with 1.44 equivalents of Pd(OAc)₂. The quantity of BnEt₃NCl was reduced to one equivalent, and the reaction was again monitored for completion. Workup after one hour and assessment by ¹H NMR spectroscopy revealed nearly complete conversion to Heck product **3-4**, with only trace quantities of **3-16** and **3-17** present. Accepting the considerable consumption of Pd(OAc)₂, these conditions were viewed as a tolerable investment in the high-yielding ring-closure of a reasonably advanced substrate. The dramatic reversal of outcomes between entries 9 and 10, namely the respective aromatization of uncyclized substrate versus the complete cyclization of the substrate and

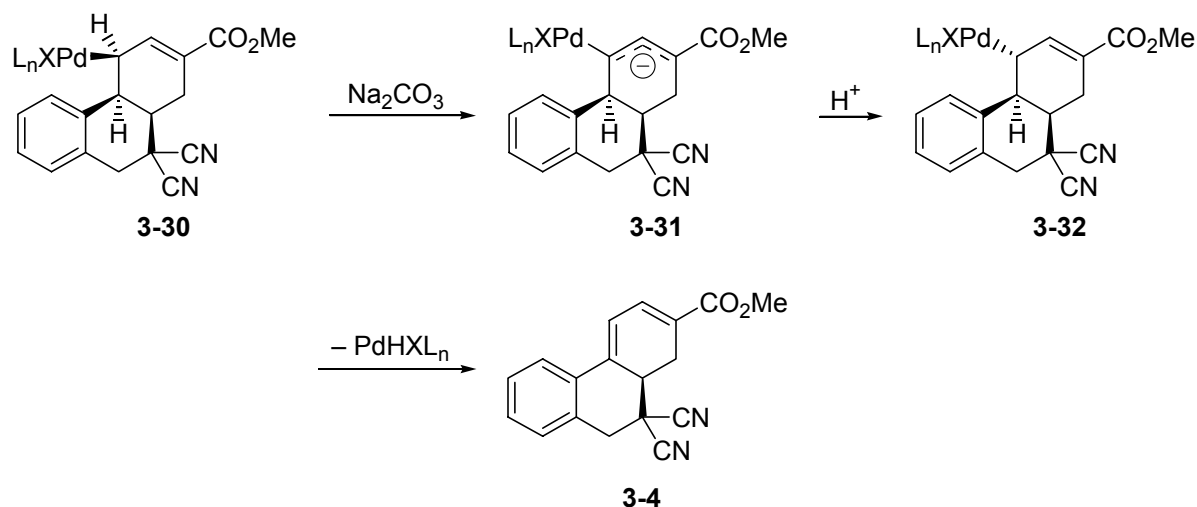
limited aromatization, highlights the combined influence of the quantity of BnEt_3NCl on the rate of base-induced elimination and of the quantity of $\text{Pd}(\text{OAc})_2$ on the rate of generation of catalytic palladium.

The selection of the intramolecular Heck reaction for this system raises the question of the means of hydridopalladium halide elimination from the ring-closed migratory insertion product, given the well-established requirement for a *syn* β -hydrogen with respect to palladium. In this and other systems lacking vicinal hydrogen atoms other than at the site of substitution, the only candidate for elimination is the *anti* β -hydrogen. Either epimerization or *anti*-elimination is necessary to free the reaction product from the metal center. The existence of literature precedent for epimerization of the palladium-bearing carbon in intramolecular Heck reactions indicated the likelihood of success of the present conversion, granted successful migratory insertion. For example, Branchaud and coworkers reported the intramolecular Heck reaction of **3-23** to give **3-27**, which apparently required an *anti*-elimination of HPdIL_n .³⁸ It was suggested that the σ -palladium complex **3-24** would be long-lived enough to epimerize to **3-26** via the oxo- π -allylpalladium complex **3-29**, which would presumably involve C–O bond rotation in the palladium enolate tautomer (Scheme 3-15). It is also reasonable to suggest base-induced epimerization via the enolate and a discrete vinyl carbon–palladium bond (**3-24** \rightarrow **3-25** \rightarrow **3-26**) followed by the standard *syn*-elimination (**3-26** \rightarrow **3-27**).



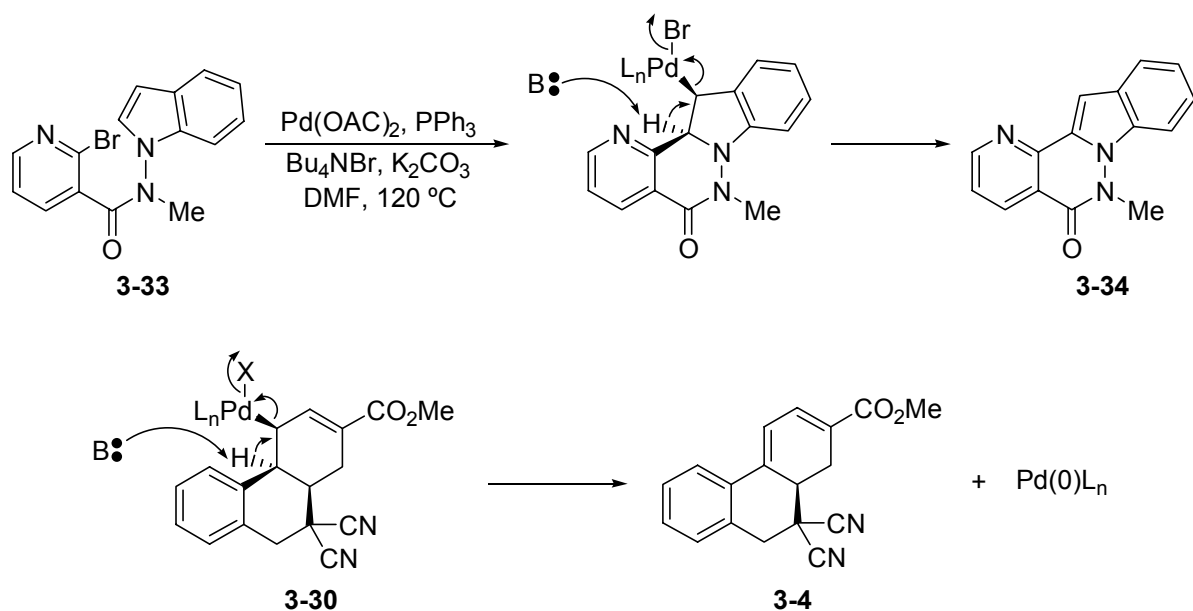
Scheme 3-15. Epimerization of palladated carbon to enable *syn*- β hydride elimination by oxoallyl palladium isomerization as posited by Branchaud and coworkers, or by isomerization via base-induced enolate. (Reduction product **3-28** is common feature of Heck reactions of enones proceeding via conjugate addition.)

The analogous mode of epimerization may be at work in the intramolecular Heck reactions of **3-4** (Scheme 3-16). Thus, σ -palladated complex **3-30** would give conjugated enolate **3-31**, which would neutralize to **3-32** with the appropriate stereochemistry for elimination.



Scheme 3-16. Base-induced epimerization of palladium-bearing carbon to permit *syn* β -hydride elimination leading to **3-4**.

An alternative elimination was posited by Thal and coworkers in the intramolecular Heck reaction of **3-33** to generate pyrido[2',3'-d']pyridazino[2,3-a]indole **3-34**.³⁹ Rather than epimerization, a simultaneous E2/reductive elimination is suggested (Scheme 3-17). The extension of this possibility to the present system is also depicted (**3-30** \rightarrow **3-4**).



Scheme 3-17. Base-induced *anti* elimination of H-PdXL_n proposed by Thal and co-workers and the analogous reaction of **3-30**.

A question that requires consideration in such a ligand-free system is the means of generation of the catalytically active Pd(0) species. Whereas phosphine-containing systems are well known to accomplish reduction of the metal center by a process culminating in the generation of phosphine oxides, the process isn't so clear in variations of Jeffery's conditions. In a study of ligand-free Heck reactions of phenyl bromide and styrene, Yao et al.⁴⁰ employed a system comprising Pd(OAc)₂ and K₃PO₄ in dimethylacetamide that was optimized for base and solvent and achieved catalytic turnover numbers in the range of 3.85×10^4 . Because no black precipitate was noted, which was considered a standard feature of Heck reactions carried out at the cited temperature, the authors invoked the operation of a Pd(IV)–Pd(II) catalytic cycle. This was suggested to involve a reversal of the involvement of the coupling partners, in which Pd(OAc)₂ added to the alkene initially, followed by oxidative insertion into the Ar–X bond and base-induced elimination of acetic acid (Figure 3-9). The resulting intermediate would be concluded in another context to arise from the attempted coupling of a vinyl halide and an arene.

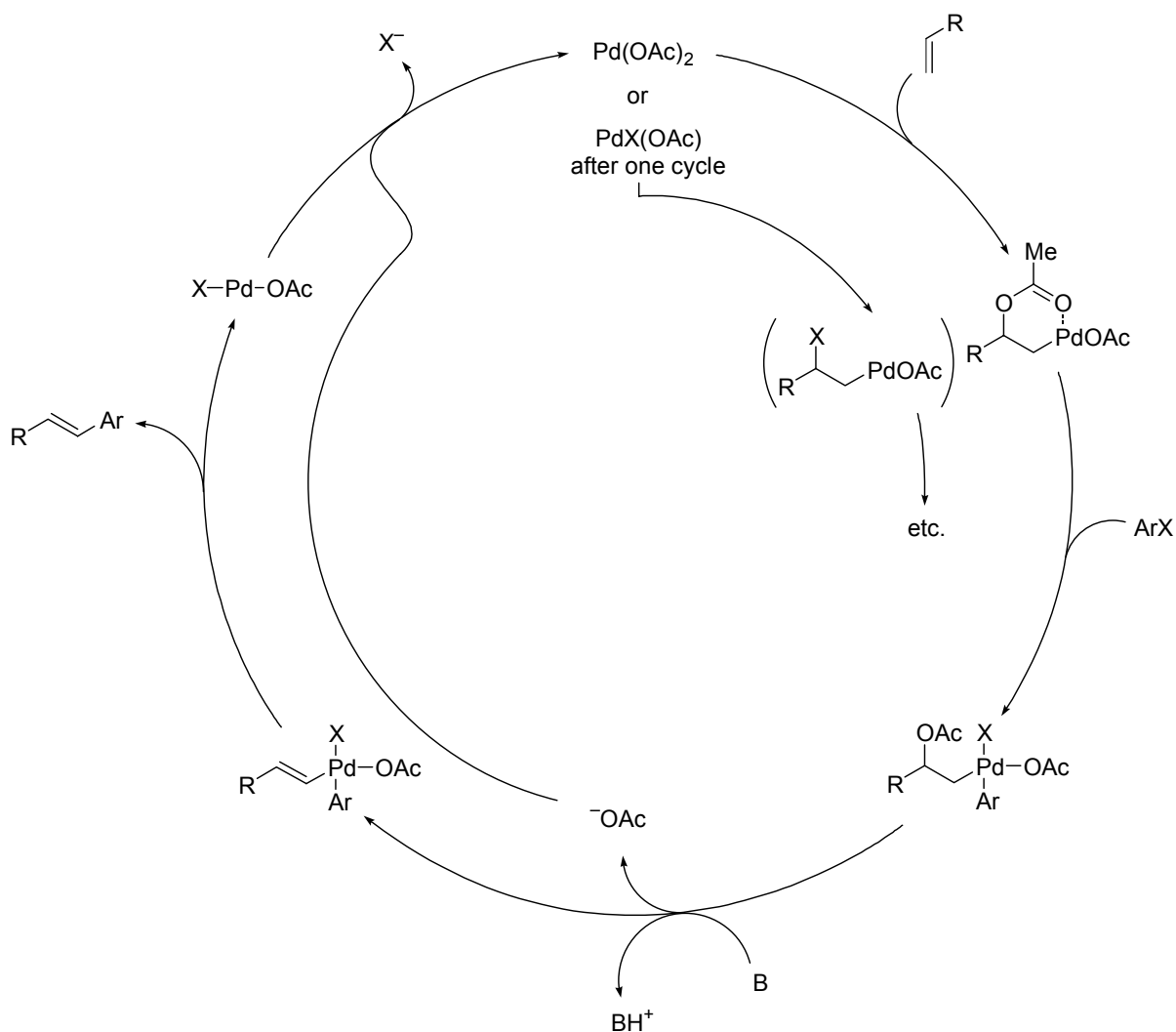


Figure 3-9. Catalytic cycle comprising Pd(II)–Pd(IV) species posited by Yao et al. for a ligand-free Heck reaction involving $\text{Pd}(\text{OAc})_2$.

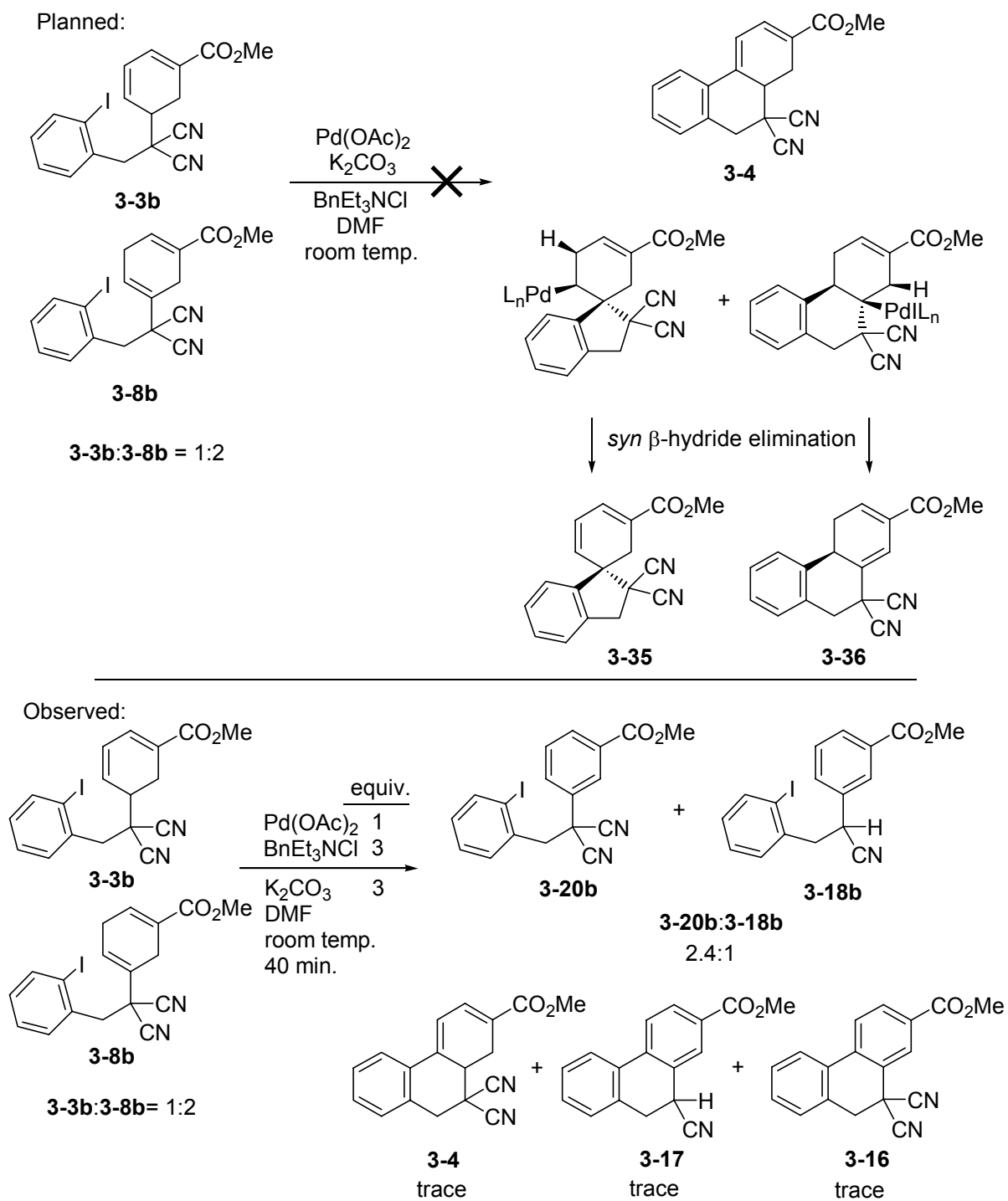
The operation of the generally accepted $\text{Pd}(0)$ as catalyst in ligand-free systems has also been accounted for by thermolysis of $\text{Pd}(\text{OAc})_2$ to give neutral palladium atoms that form nanoparticles in solution, along with CO_2 and either methane or ethane.²⁵

In the current study, the opacity of the reaction media and the observation of black emulsions at the phase boundaries in the extractions of the reaction mixtures prompt the conclusion that the catalytic species is $\text{Pd}(0)$. Furthermore, the known ability of alkenes to reduce palladium and the inevitable dehydrogenation of a small amount of substrate or

product in these Heck reactions indicate that the cyclohexadiene rings of the respective species are the reducing agents.

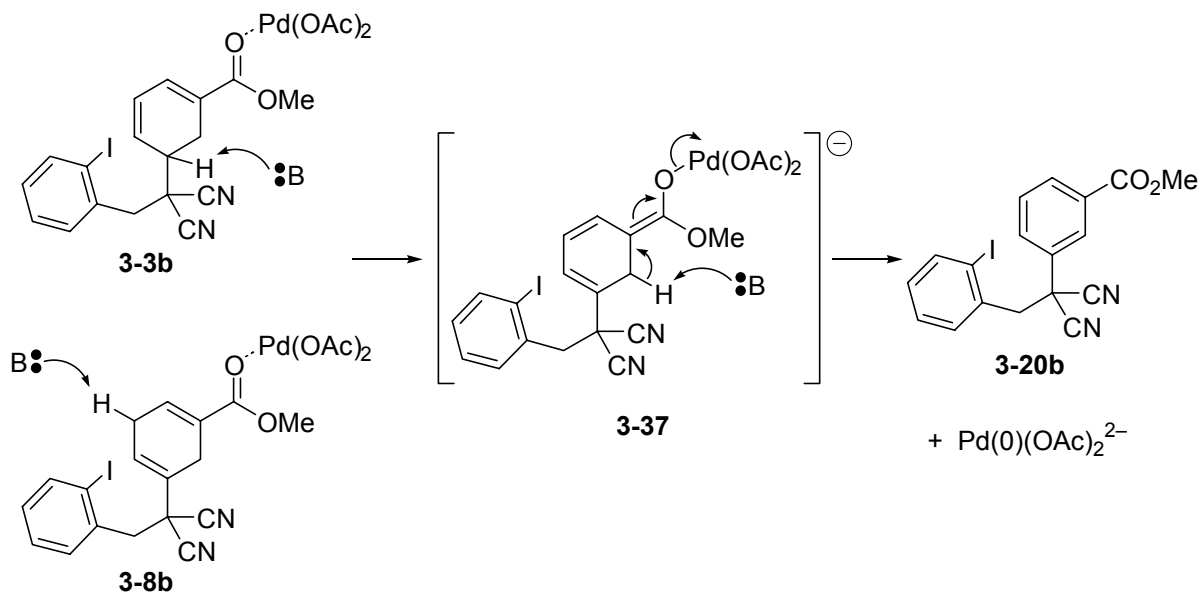
A revealing experiment in this context is the attempted intramolecular Heck reaction conducted on the 2:1 mixture of **3-8b** and **3-3b**, obtained from the slow benzylation of **3-2** with 2-iodobenzyl chloride, which witnessed a great deal of base-catalyzed ring-deconjugation. The mixture proved inseparable either by crystallization or chromatography. For interest's sake, the mixture was submitted to Jeffery's conditions for 40 minutes in the hopes of deriving novel ring-closure products **3-35** and **3-36** from isomer **3-8b**. The outcome involved none of the two potential novel Heck products, instead furnishing a trace of Heck product **3-4**, the variously aromatized substrates **3-20** and **3-18b**, and only traces of the corresponding cyclized compounds **3-16** and **3-17**.

A valuable comparison can be drawn with entry 6 in Table 3-2. In that experiment, conducted under comparable conditions, excepting bromide in place of iodide and a longer reaction time, all of the substrate was cyclized and, aside from Heck product, the ratio of cyclized HCN elimination product **3-17** to dehydrogenated cyclization product **3-16** was 9.6:1. In the present experiment, there is almost no cyclization and the ratio of dehydrogenated to decyanated uncyclized substrates is 2.4:1. This strongly suggests that **3-8b** is a better dehydrogenation substrate than **3-3b** and that the dehydrogenation of **3-8b** is extremely rapid and favoured over HCN elimination, whereas perhaps **3-3b** is prone to a mixed outcome of dehydrogenation and HCN elimination, which cumulatively afford a ratio of corresponding aromatic products greater than the initial ratio of isomers.



Scheme 3-18. Predicted and observed intramolecular Heck reaction products of mixture of substrate isomers **3-3b** and **3-8b**.

Reduction of palladium by alkenes has been proposed to occur by a process akin to the first turn of a Wacker-type catalytic cycle,³ although this is precluded by the absence of oxygenation of the aromatized rings. Whereas complex and subtle redox processes involving multiple components (e.g. water and molecular oxygen) cannot be ruled out, a polar mechanism involving base and palladium enolate **3-37** is readily conceived (Scheme 3-19).



Scheme 3-19. Proposed mechanism of palladium reduction by dehydrogenation of Heck substrates.

With the conclusion that the substrate **3-3**, trace levels of **3-8**, and product **3-4** are reducing agents for $\text{Pd}(\text{OAc})_2$, a catalytic cycle (Figure 3-10) can be devised that accounts for the intramolecular Heck reactions in this study and that comprises catalyst pre-activation, progress to the palladated ring-closure product, epimerization, and reductive elimination.

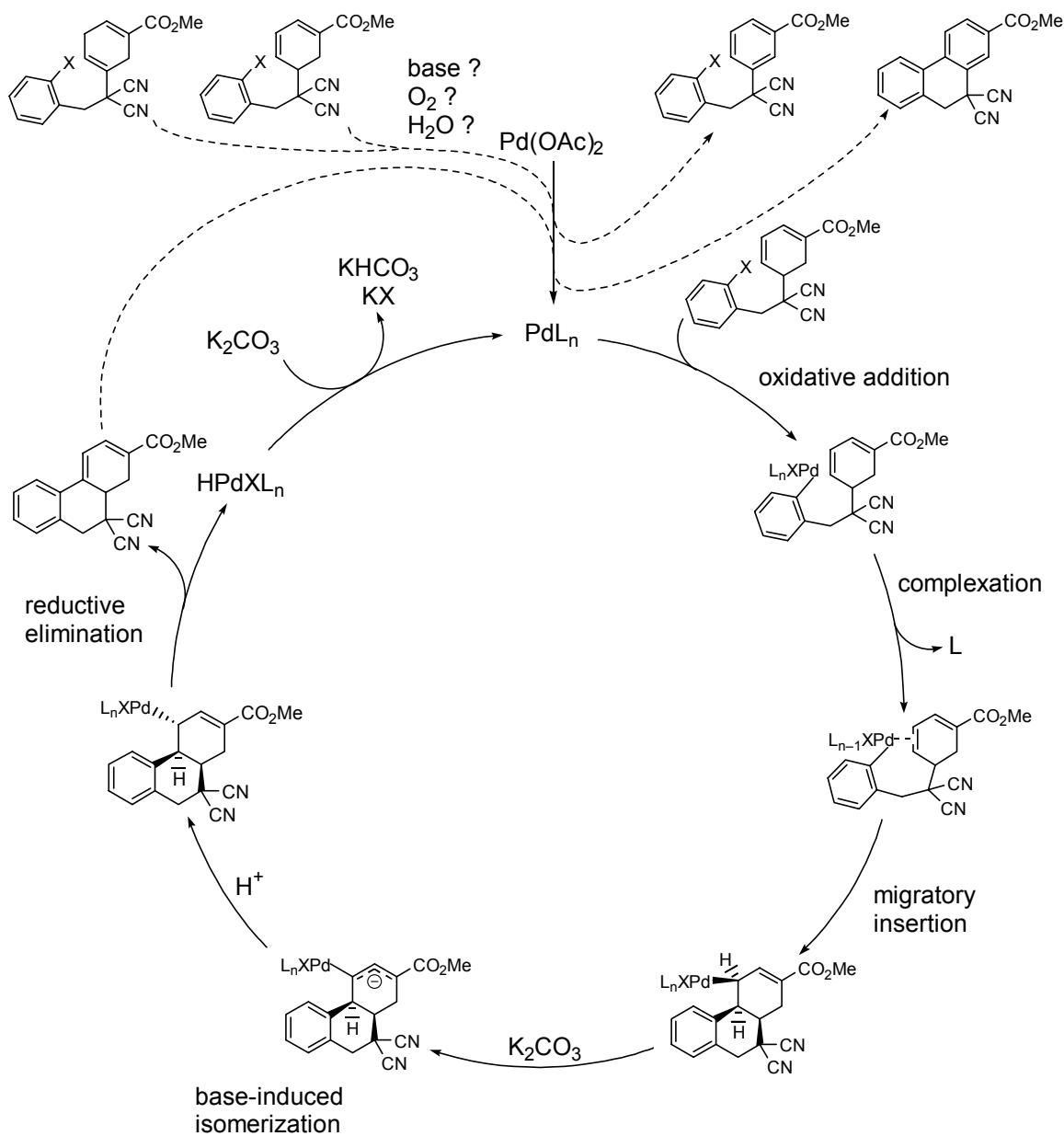


Figure 3-10. Postulated catalyst pre-activation and catalytic cycle in intramolecular Heck reactions of adduct 3-3.

3.2.3 Conclusions and Future Work

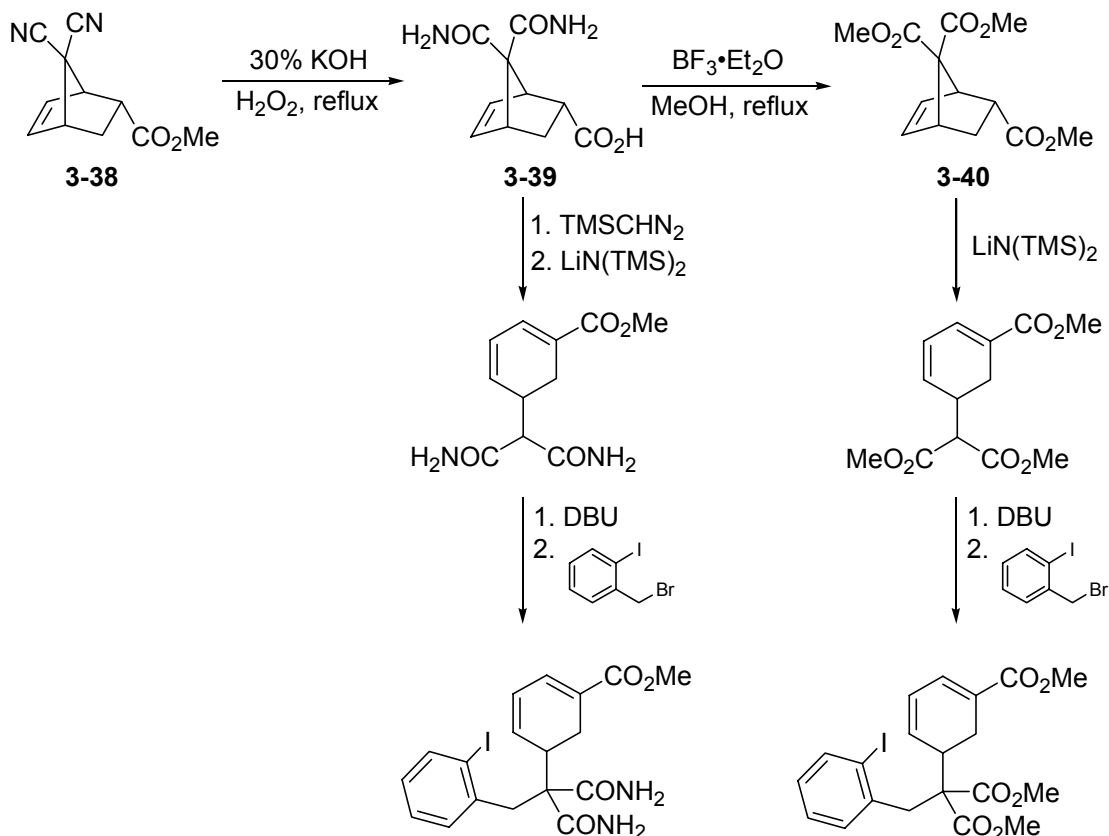
The present study has, in the otherwise trivial step of substrate preparation, afforded a useful insight into the acid-base characteristics of the ring-opened adduct. Ring C5-deprotonation was previously invoked to explain the low-recovery generation of an aromatic

side product in the attempted tandem reaction of **1** with phenyl vinyl sulfone (Chapter 2), but the findings in this context more clearly revealed the comparable acidities of the dicyanomethyl and ring C5 protons, and so would prove valuable in the interpretation of the data presented in Chapter 5.

Successful intramolecular Heck reactions have been carried out and optimized for Jeffery's conditions at high catalyst loadings. The optimal conditions of at least stoichiometric Pd(OAc)₂, as well as excess K₂CO₃ and approximately stoichiometric BnEt₃NCl, and prompt workups, would most obviously be improved by reducing the quantity of palladium catalyst. This would both reduce costs and limit the extent of dehydrogenation of **3-4**, which has been linked to the generation of Pd(0). It has been found³ that quaternary ammonium phase-transfer catalysts can reduce Pd(OAc)₂. It is therefore possible that reduction of Pd(OAc)₂ in these reactions is being carried out in parallel by BnEt₃NCl and by the cyclohexadiene ring of substrate and product. Rather than sacrificing starting material to initiate catalysis, this possibility merits an experiment in which Pd(OAc)₂ and BnEt₃NCl are pre-incubated prior to the addition of substrate in the hope that Pd(0) will be generated so that no induction period is experienced and the vulnerability of the substrate can be reduced.

Limitation of the consumption of starting material and product by HCN elimination would also serve the goal of reducing the catalyst loading, as it would make protracted exposure of the substrate to the reaction conditions more benign, permitting longer reaction times at substoichiometric quantities of Pd(OAc)₂. Furthermore, it is possible that cyanide poisons the catalyst, so reduced HCN elimination would be beneficial in this regard as well. As previously mentioned, renewed attention to the use of NaHCO₃ might serve this goal. Alternatively, the nitriles of the substrate might be converted to poor leaving groups. A

precedent was established in this lab for the conversion by R.W. Friesen and involves treatment of Diels-Alder adduct **3-38** with KOH and H₂O₂ at reflux to furnish diamide **3-39**.⁴¹ Further solvolysis to **3-40** was achieved with BF₃ etherate in refluxing methanol. Two ring-opened compounds could be derived from these products and converted to intramolecular Heck reaction substrates (Scheme 3-20).



Scheme 3-20. Conversion of nitriles to prevent HCN elimination from Heck substrates.

With HCN elimination prevented, and if indeed phase-transfer catalyst can act as a reductant toward Pd(OAc)₂, then increased quantities of BnEt₃NCl could be employed to improve the generation of Pd(0) without the attendant great extent of HCN elimination observed with the present substrate. As indicated in Chapter 1, the optimization of the intramolecular Heck reaction at lower catalyst loadings and permissible lengthier reaction

times should pave the way for the generation and ring-closure of more complex substrates analogous to **3-3** in a fashion applicable to natural product synthesis.

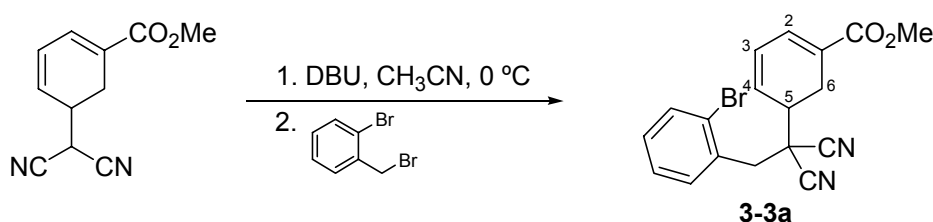
3.3 Experimental

3.3.1 Supplemental General Experimental

Commercial Pd(OAc)₂ (Aldrich), BnEt₃NCl (Aldrich), 1-chloromethyl-2-iodobenzene (Aldrich), K₂CO₃, Bu₄NI, NaCl, and DMF were used as received. The Aldrich reagents were newly purchased for the reported study. For a single experiment, DMF was degassed by passage through several cycles of freeze–pump–thaw under continuous high vacuum.

3.3.2 Experimental Details

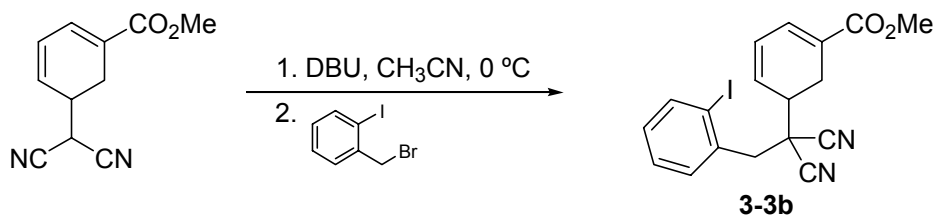
5-[2-(2-Bromophenyl)-1,1-dicyanoethyl]-cyclohexa-1,3-dienecarboxylic acid methyl ester



To a stirred CH₃CN (4 mL) solution of **3-2** (108.1 mg, 0.535 mmol) at 0 °C was added DBU (3.52 mL of a 23.1 mg/mL solution, 0.535 mmol, 1 equivalent) by syringe over ten seconds, which caused the reaction mixture to turn faintly orange. To this solution was added 2-bromobenzyl bromide (3.63 mL of a 36.8 mg/mL solution, 0.535 mmol, one equivalent) by syringe over twenty seconds and the reaction was maintained at 0 °C until

TLC at 40 minutes revealed it to be complete. The reaction mixture was partitioned between saturated aqueous NH_4Cl (40 mL) and EtOAc (40 mL + 2 × 20 mL), and the combined organic portions were dried (Na_2SO_4) and concentrated *in vacuo* to give a light yellow oil. The trace quantities of the isomer **3-8a** and 2-bromobenzyl bromide were reduced by trituration with hexane, and the parent material was filtered through a silica plug. Concentration furnished 173.9 mg of a clear faint yellow oil (87.8 %). ^1H NMR (CDCl_3 , 300 MHz) δ 7.63 (1 H, dd, $J = 7.7, 1.2$ Hz, ArH), 7.54 (1 H, dd, $J = 7.7, 1.6$ Hz, ArH), 7.35 (1 H, td, $J = 7.7, 1.2$ Hz, ArH), 7.22 (1 H, td, $J = 7.7, 1.6$ Hz, ArH), 7.07 (1 H, br d, $J = 5.5$ Hz, C2-H), 6.43 (1 H, ddd, $J = 9.6, 5.5, 2.2$ Hz, C3-H), 6.20 (1 H, dd, $J = 9.6, 3.6$ Hz, C4-H), 3.79 (3H, s, $-\text{CO}_2\text{CH}_3$), 3.47 (1 H, d, $J = 14.07$ Hz, $\text{ArCH}_2\text{C}(\text{CN})_2\text{R}$), 3.42 (1 H, d, $J = 14.07$ Hz, $\text{ArCH}_2\text{C}(\text{CN})_2\text{R}$), 3.18 (1 H, m, C5-H), 3.01 (1 H, ddd, $J = 17.7, 9.3, 1.4$ Hz, C6-H), 2.84 (1 H, ddd, $J = 17.7, 12.1, 2.0$ Hz, C6-H); ^{13}C NMR (CDCl_3 , 75 MHz) δ 166.5, 133.8, 132.4, 132.1, 131.6, 130.6, 128.6, 128.2, 127.2, 127.0, 125.9, 114.2, 113.9, 52.2, 42.8, 41.4, 38.5, 24.0.

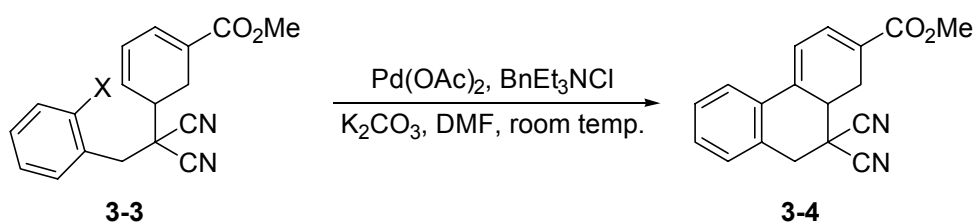
5-[1,1-Dicyano-2-(2-iodo-phenyl)-ethyl]-cyclohexa-1,3-dienecarboxylic acid methyl ester



To a stirred CH_3CN (10 mL) solution of **1** (273.9 mg, 1.35 mmol) at $0\text{ }^\circ\text{C}$ was added DBU (3.99 mL of a 51.6 mg/mL solution, 1.35 mmol, 1 equivalent) by syringe over twenty seconds, which caused the reaction mixture to turn faintly orange. To this solution was added 2-iodobenzyl bromide (428.2 mg dissolved in 3 mL of CH_3CN) by syringe and the

reaction was maintained at 0 °C until TLC at 1 hour 22 minutes revealed it to be complete. The reaction mixture was partitioned between saturated aqueous NH₄Cl (100 mL) and EtOAc (100 mL + 2 × 40 mL), and the combined organic portions were dried (Na₂SO₄) and concentrated *in vacuo* to give 544.8 mg (96 %) of a light yellow oil with acceptable trace quantities of isomer **3-8b** and Diels-Alder adduct **3-38**. The sample purity was improved slightly by column chromatography on 230–400 silica (20 g, 8 cm), eluting with 20:80 EtOAc:hexanes. The best fraction pool (135.6 mg) was selected for use in subsequent reactions. ¹H NMR (CDCl₃, 500 MHz) δ 7.96 (1 H, dd, *J* = 7.8, 1.1 Hz, ArH), 7.61 (1 H, dd, *J* = 7.8, 1.5 Hz, ArH), 7.44 (1 H, td, *J* = 7.8, 1.1 Hz, ArH), 7.13 (1 H, br d, *J* = 5.6 Hz, C2-H), 7.10 (1 H, td, *J* = 7.8, 1.5 Hz, ArH), 6.49 (1H, ddd, *J* = 9.6, 5.6, 2.2 Hz, C5-H), 6.28 (1 H, dd, *J* = 9.6, 3.6 Hz, C4-H), 3.84 (3 H, s, CO₂CH₃), 3.51 (1 H, d, *J* = 14.1, ArCH₂C(CN)₂R), 3.47 (1 H, d, *J* = 14.1 Hz, ArCH₂C(CN)₂R), 3.24 (1 H, m, C5-H), 3.07 (1 H, ddd, *J* = 17.9, 9.4, 1.4 Hz, C6-H), 2.93 (1 H, ddd, *J* = 17.9, 11.8, 2.0 Hz, C6-H); ¹³C NMR (CDCl₃, 125 MHz) δ 166.2, 140.5, 135.3, 132.2, 130.5, 129.0, 128.6, 127.1, 127.0, 114.6, 113.8, 102.3, 52.1, 42.9, 42.8, 41.5, 23.9.

General method for intramolecular Heck reactions of substrates 3-3

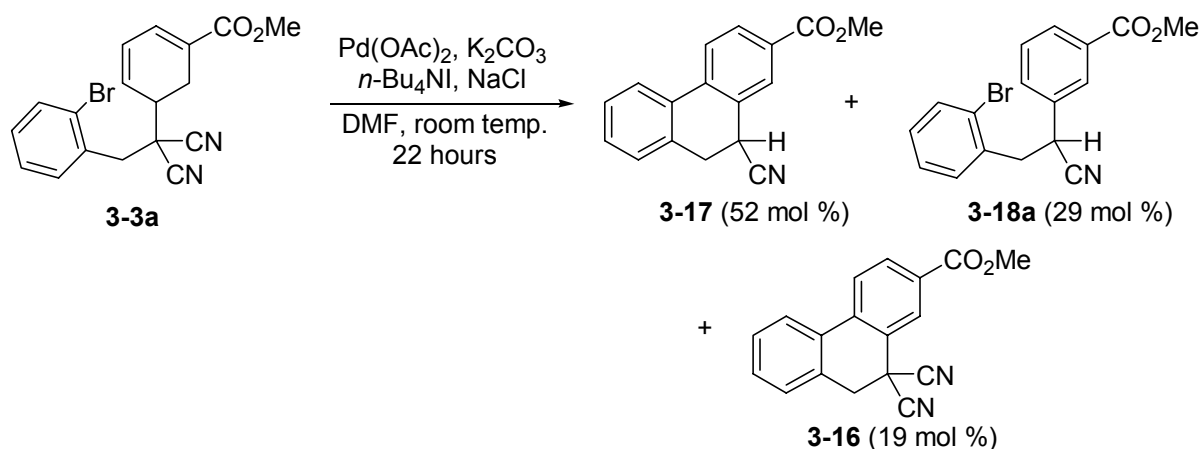


Solid reagents were weighed in the air and generally stored in capped vials for several minutes until use. This precaution was especially adhered to for the weighing and handling of the extremely hygroscopic phase-transfer catalyst BnEt₃NCl. The neat substrate **3-3** was dispensed into the reaction vessel as a thick oil and was dissolved in DMF and set up for

magnetic stirring under Ar. The solid reagents were added in rapid succession to the briefly opened mouth of the reaction vessel and then the argon atmosphere was restored. In several cases the solid reagents were poured directly into the substrate-containing reaction vessel in advance of solvent which immediately followed. The reactions were stirred at room temperature (one exception was carried out at $-10\text{ }^{\circ}\text{C}$) and were then poured into an appropriate partition mixture in a separatory funnel and multiply extracted into the organic solvent (saturated aqueous NH_4Cl and either EtOAc or CH_2Cl_2). Variations to the workup scheme are noted. The combined organic solutions were dried (Na_2SO_4) and concentrated *in vacuo*. Numerous experiments were conducted without product isolation: baseline-resolved diagnostic ^1H NMR signals for the complete set of compounds permitted the determination of product distributions in crude mixtures. Purification methods are described in specific experiments.

Intramolecular Heck reactions

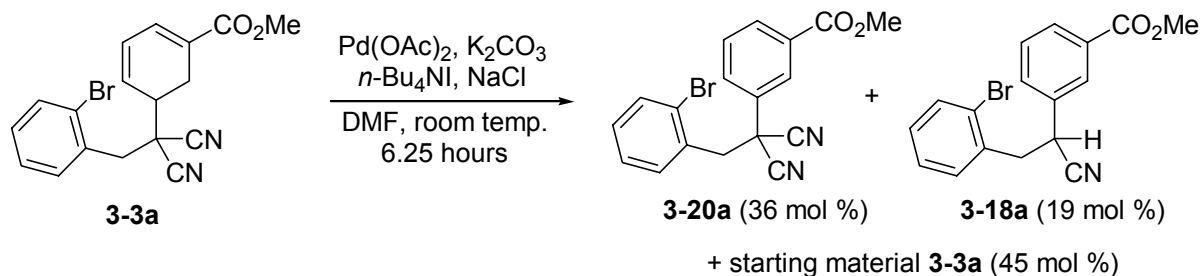
Table 3-2, entry 1



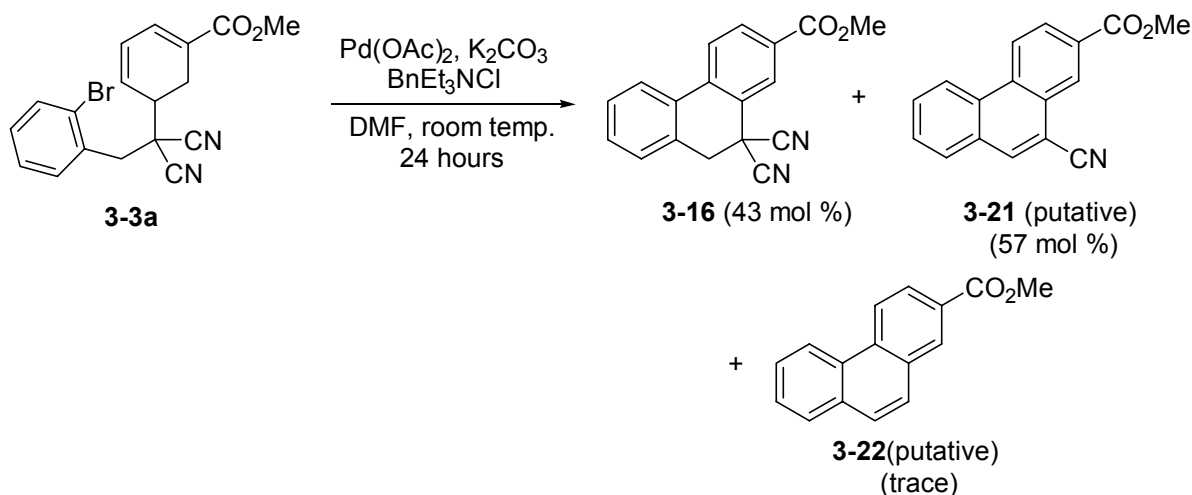
To **3-3a** (97.3 mg, 0.262 mmol) were added $\text{Pd}(\text{OAc})_2$ (10.2 mg, 0.0454 mmol, 0.195 equivalents), K_2CO_3 (109.2 mg, 0.790 mmol, 3.01 equivalents), NaCl (19.5 mg, 0.333 mmol, 1.27 equivalents), $n\text{-Bu}_4\text{NI}$ (102.6 mg, 0.277 mmol, 1.06 equivalents), and DMF (6 mL).

The reaction was stirred for 22 hours. Partition mixture: saturated aqueous NH_4Cl (40 mL), EtOAc (3×20 mL). The combined organics were dried (Na_2SO_4) and concentrated *in vacuo* to give a yellow oil (77.6 mg).

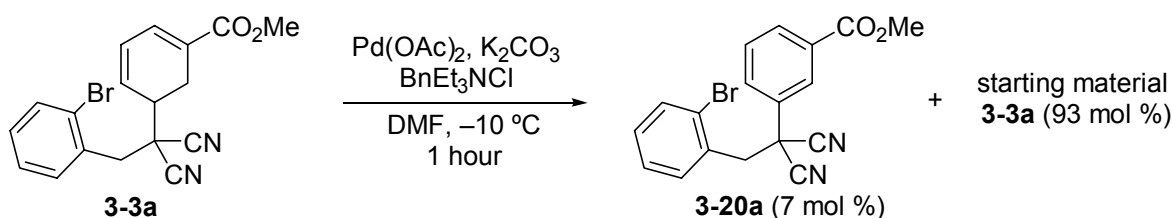
Table 3-2, entry 2



To **3-3a** (32.1 mg, 0.0864 mmol) were added Pd(OAc)_2 (3.8 mg, 0.0169 mmol, 0.195 equivalents), K_2CO_3 (35.1 mg, 0.254 mmol, 2.94 equivalents), NaCl (9.0 mg, 0.154 mmol, 1.78 equivalents), $n\text{-Bu}_4\text{NI}$ (31.7 mg, 0.0858 mmol, 0.99 equivalents), and DMF (7 mL). The reaction was stirred for 6.25 hours and worked up despite the persistence of starting material. Partition mixture: saturated aqueous NH_4Cl (40 mL), EtOAc (2×20 mL). The combined organics were dried (Na_2SO_4) and concentrated *in vacuo* to give a thick brown oil (27.7 mg).

Table 3-2, entry 3

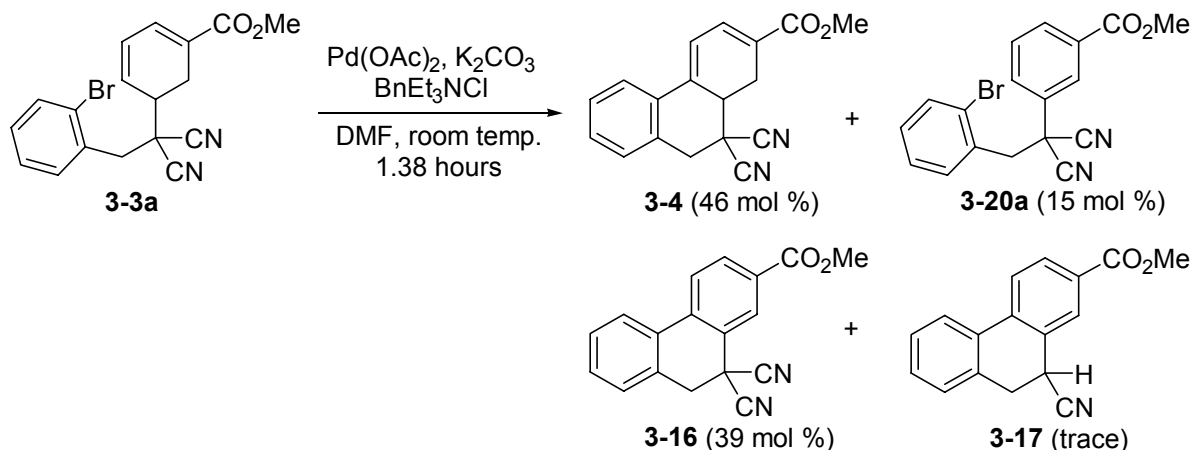
To **3-3a** (22.5 mg, 0.0606 mmol) were added $\text{Pd}(\text{OAc})_2$ (15.4 mg, 0.0686 mmol, 1.13 equivalents), K_2CO_3 (26.5 mg, 0.192 mmol, 3.16 equivalents), BnEt_3NCl (14.5 mg, 0.0637 mmol, 1.05 equivalents), and DMF (4 mL). The reaction was stirred for 24 hours. Partition mixture: saturated aqueous NH_4Cl (40 mL), EtOAc (40 mL + 2 × 20 mL). The combined organics were dried (Na_2SO_4) and concentrated *in vacuo* to give a yellow and white film (18.4 mg).

Table 3-2, entry 4

To **3-3a** (30.8 mg, 0.0829 mmol) were added $\text{Pd}(\text{OAc})_2$ (18.8 mg, 0.0838 mmol, 1.00 equivalents), K_2CO_3 (14.7 mg, 0.106 mmol, 1.28 equivalents), BnEt_3NCl (21.1 mg, 0.0926 mmol, 1.12 equivalents), and DMF (4 mL). The reaction was cooled to $-10\text{ }^\circ\text{C}$ (ice-salt bath) and stirred for one hour. Partition mixture: saturated aqueous NH_4Cl (40 mL), EtOAc

(40 mL + 2 × 20 mL). The combined organics were dried (Na₂SO₄) and concentrated *in vacuo* to give a thick clear yellow oil that developed a fine white suspension at high vacuum.

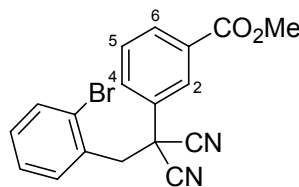
Table 3-2, entry 5



To **3-3a** (27.7 mg, 0.0746 mmol) were added Pd(OAc)₂ (17.0 mg, 0.0757 mmol, 1.02 equivalents), K₂CO₃ (32.0 mg, 0.2315 mmol, 3.10 equivalents), BnEt₃NCl (17.5 mg, 0.0768 mmol, 1.03 equivalents), and DMF (4 mL). The reaction was stirred for 83 minutes and worked up when TLC revealed total consumption of starting material. Partition mixture: saturated aqueous NH₄Cl (40 mL), EtOAc (40 mL + 2 × 20 mL). The combined organics were dried (Na₂SO₄) and concentrated by rotary evaporator to a small volume of DMF, and then taken up in CH₂Cl₂, passed through a silica plug (70–230 mesh) and concentrated *in vacuo* to give a 22.4 mg of a clear yellow oil that developed a fine white precipitate at high vacuum (cf. entry 4). The crude sample was dissolved in EtOAc, applied to a preparative chromatography plate (Whatman PK6F, 1000 μm thickness, 60 Å), and developed with a 65:25:10 solution of hexane:diethyl ether:acetone. Bands of useful degrees of purity included one at intermediate R_f that contained a 2.3:1 ratio of **3-16** and **3-17**, the crystallization of which furnished a co-crystal as determined by an X-ray diffraction study, and the highest R_f band, which furnished pure **3-20a** (3.5 mg). Another crystal from the

sample that furnished that used for the X-ray diffraction comprised nearly pure **3-16**. The mother liquor furnished **3-17**.

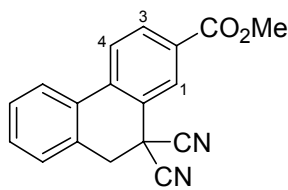
3-[2-(2-Bromo-phenyl)-1,1-dicyano-ethyl]-benzoic acid methyl ester



3-20a

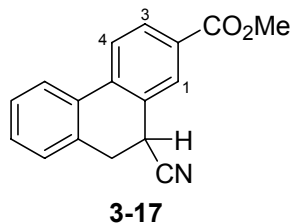
$^1\text{H NMR}$ (CDCl_3 , 300 MHz) δ 8.19 (1 H, m, C2-H), 8.14 (1 H, dt, $J = 7.8, 1.2$ Hz, C6-H), 7.65 (1H, ddd, $J = 7.8, 2.1, 1.2$ Hz, C4-H), 7.56 (1 H, dd, $J = 7.6, 1.2$ Hz, ArH), 7.53 (1 H, t, $J = 7.8$ Hz, C5-H), 7.44 (1 H, dd, $J = 7.6, 1.7$ Hz, ArH), 7.34 (1 H, td, $J = 7.6, 1.2$ Hz, ArH), 7.22 (1 H, td, $J = 7.6, 1.7$ Hz, ArH), 3.94 (3 H, s, CO_2CH_3), 3.73 (2 H, s, $\text{ArCH}_2\text{C}(\text{CN})_2\text{Ar}$).

10,10-Dicyano-9,10-dihydro-phenanthrene-2-carboxylic acid methyl ester

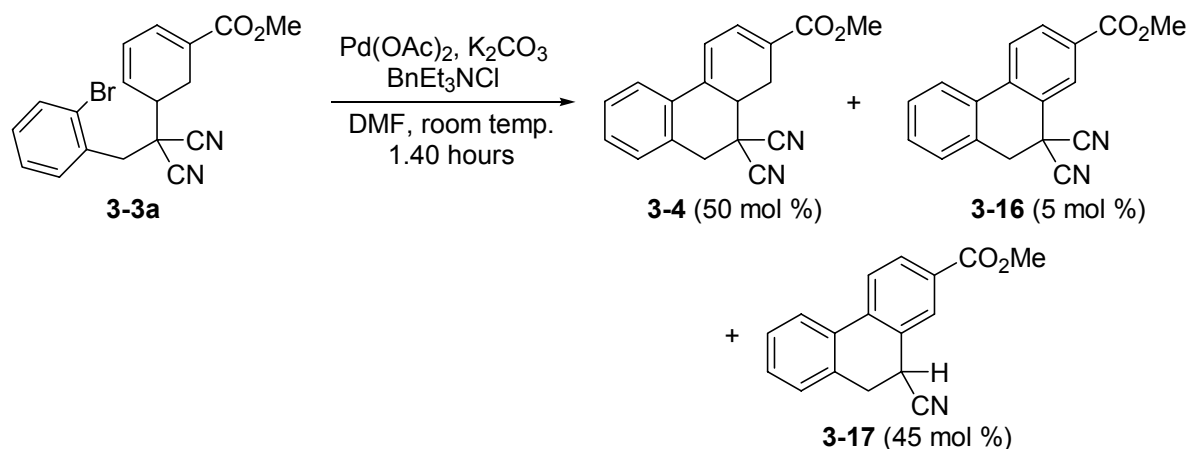


3-16

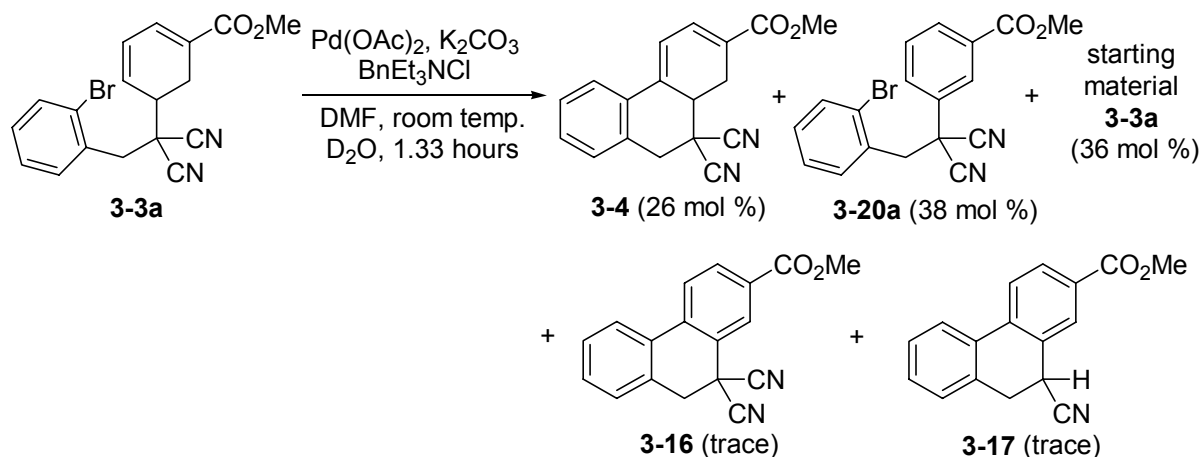
$^1\text{H NMR}$ (CDCl_3 , 300 MHz) δ 8.43 (1 H, d, $J = 1.6$ Hz, C1-H), 8.24 (1 H, dd, $J = 8.2, 1.6$ Hz, C3-H), 7.94 (1 H, d, $J = 8.2$ Hz, C4-H), 7.86 (1 H, br d, $J = 7.4$ Hz, ArH), 7.50 (1 H, td, $J = 7.4, 1.7$ Hz, ArH), 7.44 (1 H, td, $J = 7.4, 1.3$ Hz, ArH), 7.37 (1 H, br d, $J = 7.4$ Hz, ArH), 3.97 (3 H, s, CO_2CH_3), 3.61 (2 H, s, ArCH_2).

10-Cyano-9,10-dihydrophenanthrene-2-carboxylic acid methyl ester

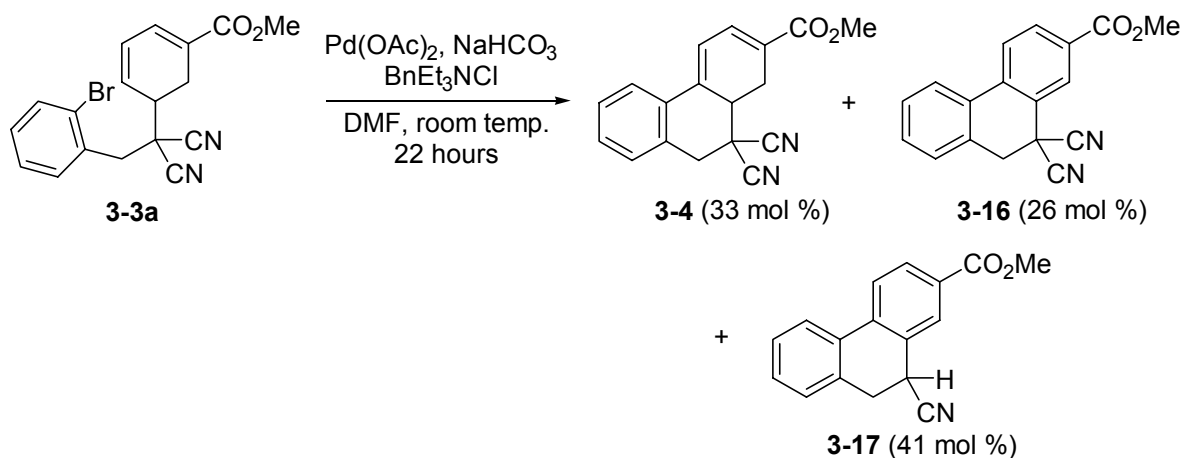
^1H NMR (CDCl_3 , 300 MHz) δ 8.20 (1 H, br s, C1-H), 8.10 (1 H, dd, $J = 8.2, 1.7$ Hz, C3-H), 7.85 (1 H, d, $J = 8.2$ Hz), 7.81 (1 H, d, $J = 7.4$ Hz, ArH), 7.46–7.27 (3 H, m, ArH), 4.11 (1 H, t, $J = 7.4$ Hz, ArCHCNCH₂Ar), 3.23 (2 H, d, $J = 7.4$ Hz, ArCH₂CCNHA_r).

Table 3-2, entry 6

To **3-3a** (24.8 mg, 0.0668 mmol) were added Pd(OAc)_2 (15.9 mg, 0.0708 mmol, 1.06 equivalents), K_2CO_3 (32.1 mg, 0.232 mmol, 3.47 equivalents), BnEt_3NCl (44.4 mg, 0.195 mmol, 2.92 equivalents), and DMF (4 mL). The reaction was stirred for 84 minutes. Partition mixture: saturated aqueous NH_4Cl (40 mL), EtOAc (40 mL + 2 \times 20 mL). The combined organics were dried (Na_2SO_4) and concentrated *in vacuo*, giving 24.4 mg of thick yellow oil containing a fine white suspension.

Table 3-2, entry 7

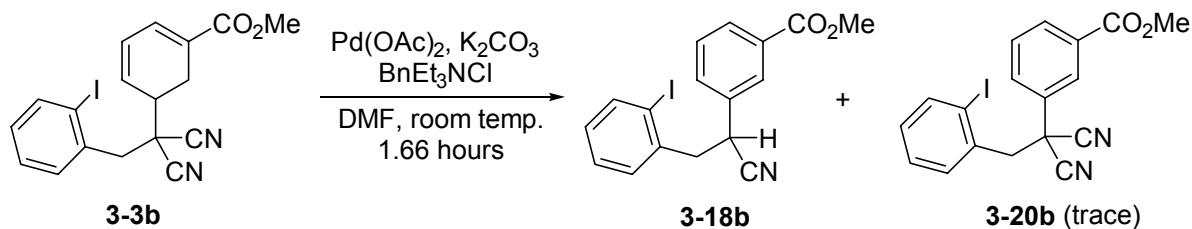
To **3-3a** (24.5 mg, 0.0659 mmol) were added Pd(OAc)₂ (17.0 mg, 0.0757 mmol, 1.15 equivalents), K₂CO₃ (35.0 mg, 0.253 mmol, 3.84 equivalents), BnEt₃NCl (19.1 mg, 0.0838 mmol, 1.27 equivalents), DMF (4 mL), and D₂O (approximately 20 μL). The reaction was stirred for 80 minutes. Partition mixture: saturated aqueous NH₄Cl (40 mL), EtOAc (40 mL + 2 × 20 mL). The combined organics were dried (Na₂SO₄) and concentrated *in vacuo* to give 24.5 mg of a yellow oil.

Table 3-2, entry 8

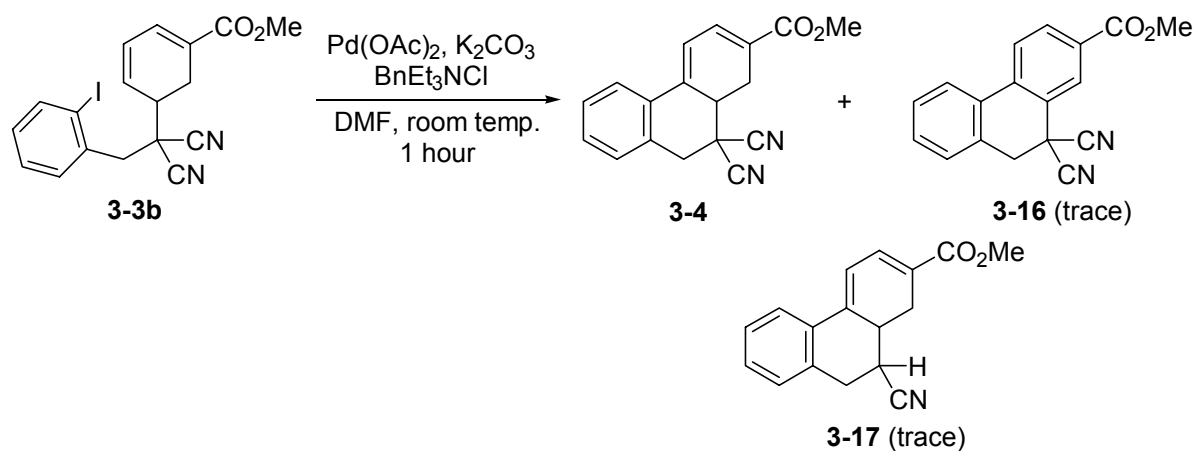
To **3-3a** (19.8 mg, 0.0533 mmol) were added Pd(OAc)₂ (14.3 mg, 0.0637 mmol, 1.19 equivalents), NaHCO₃ (17.0 mg, 0.202 mmol, 3.79 equivalents), BnEt₃NCl (36.8 mg, 0.162

mmol, 3.03 equivalents), and DMF (4 mL). The reaction was stirred for 21 hours 10 minutes. Partition mixture: saturated aqueous NH_4Cl (40 mL), EtOAc (40 mL + 2 × 20 mL). The combined organics were dried (Na_2SO_4) and concentrated *in vacuo* to give 18.8 mg of a yellow oil with finely dispersed white material.

Table 3-2, entry 9

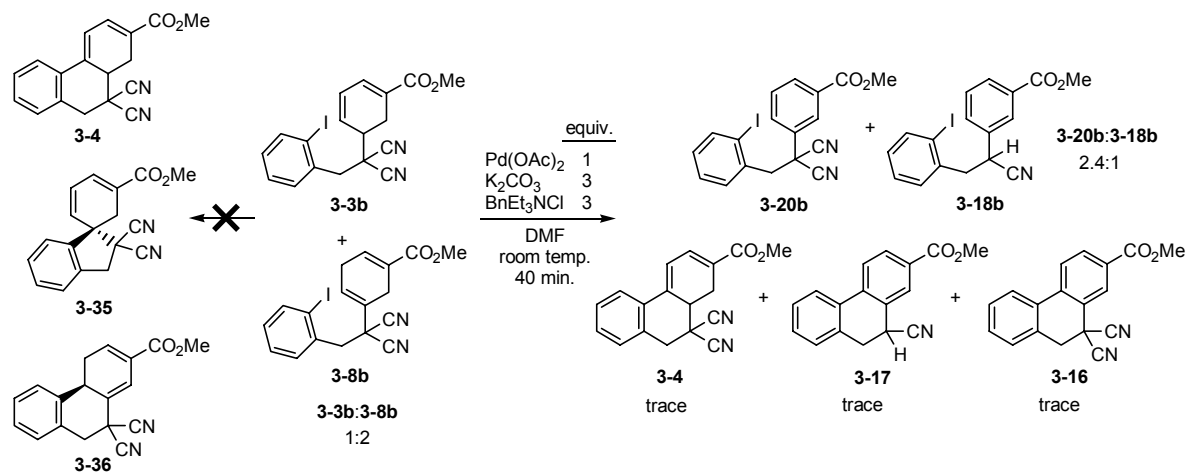


To **3-3b** (29.6 mg, 0.0707 mmol) were added $\text{Pd}(\text{OAc})_2$ (3.3 mg, 0.0147 mmol, 0.208 equivalents), K_2CO_3 (29.2 mg, 0.211 mmol, 2.98 equivalents), BnEt_3NCl (49.5 mg, 0.217 mmol, 3.07 equivalents), and DMF (4 mL). The reaction was stirred for 100 minutes, closely monitored by TLC. Partition mixture: saturated aqueous NH_4Cl (40 mL), CH_2Cl_2 (40 mL + 2 × 20 mL). The combined organics were dried (Na_2SO_4) and concentrated *in vacuo* to give a yellow oil that comprised **3-18b** and only a trace quantity of **3-20b**. ^1H NMR (CDCl_3 , 300 MHz) δ 8.08 (1 H, s, C2-H), 8.01 (1 H, d, $J = 7.9$ Hz, C6-H), 7.84 (1 H, d, $J = 7.7$ Hz, ArH), 7.56 (1 H, d, $J = 7.9$ Hz, C4-H), 7.45 (1 H, t, $J = 7.9$ Hz, C5-H), 7.30 (1 H, d, $J = 7.7$ Hz, ArH), 7.23 (1 H, td, $J = 7.7, 1.5$ Hz, ArH), 6.97 (1 H, td, $J = 7.7, 1.5$ Hz, ArH), 4.23 (1 H, dd, $J = 9.4, 6.4$ Hz, $\text{ArCHCNCH}_2\text{Ar}$), 3.92 (3H, s, CO_2CH_3), 3.30–3.15 (2 H, m, $\text{ArCH}_2\text{CCNHAr}$).

Table 3-2, entry 10

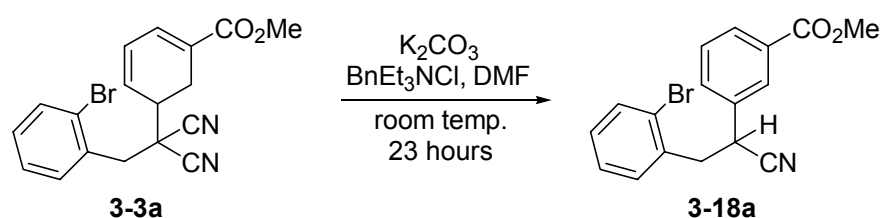
To **3-3b** (30.9 mg, 0.0739 mmol) were added Pd(OAc)₂ (23.9 mg, 0.107 mmol, 1.44 equivalents), K₂CO₃ (32.4 mg, 0.234 mmol, 3.17 equivalents), BnEt₃NCl (17.8 mg, 0.0782 mmol, 1.06 equivalents), and DMF (4 mL). The reaction was stirred for one hour, closely monitored by TLC. Partition mixture: saturated aqueous NH₄Cl (40 mL), CH₂Cl₂ (40 mL + 2 × 20 mL). The combined organics were dried (Na₂SO₄) and concentrated *in vacuo* to give **3-4** (ca. 90 % ¹H NMR spectral yield) contaminated with DMF as an amorphous brown solid (24.0 mg). Column chromatography was performed (230–400 mesh silica, 6.5 g, 6.5 cm), eluting with a stepped gradient of EtOAc:hexanes (1:99, 2:98, 4:96, 8:92, 16:84, 20:80). A well-resolved fraction was selected and slowly crystallized from acetone solution by diffusion of hexane vapour, yielding a crystal suitable for a single crystal X-ray diffraction study. ¹H NMR (CDCl₃, 500 MHz) δ 7.80 (1 H, d, *J* = 7.5 Hz, ArH), 7.40–7.35 (2H, m, ArH), 7.26 (1H, dd, *J* = 6.2, 3.1 Hz, C3-H), 7.23 (1H, d, *J* = 7.2 Hz, ArH), 6.92 (1 H, d, *J* = 6.2 Hz, C2-H), 3.87 (3 H, s, CO₂CH₃), 3.65 (1H, d, *J* = 15.34 Hz, ArCH₂C(CN)₂R), 3.49 (1H, d, *J* = 15.34 Hz, ArCH₂C(CN)₂R), 3.36–3.28 (2H, m, C6-H₂), 2.71 (1 H, m, C5-H).

Attempted intramolecular Heck reaction of mixture of **3-3b** and **3-8b**



To the mixture of **3-3b** and **3-8b** (17.3 mg, 0.0414 mmol) were added approximately one equivalent of $\text{Pd}(\text{OAc})_2$, three equivalents each of K_2CO_3 and BnEt_3NCl , and DMF (4 mL). The reaction was stirred at room temperature for 40 minutes and worked up when indicated by TLC. The reaction mixture was partitioned between saturated aqueous NH_4Cl (40 mL) and CH_2Cl_2 (40 mL + 2 × 20 mL), and the combined organics were dried (Na_2SO_4) and concentrated *in vacuo*, furnishing 15.1 mg of a dark oil.

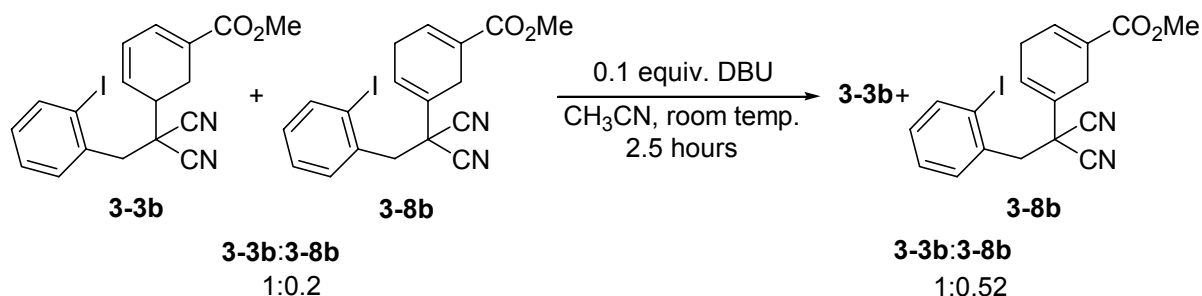
Base-induced HCN elimination and aromatization of **3-3a**



To 4.9 mg of **3-3a** (0.0132 mmol) were added K_2CO_3 (5.0 mg, 0.0362 mmol, 2.74 equivalents), BnEt_3NCl (10.0 mg, 0.0439 mmol, 3.36 equivalents), and DMF (3 mL) and the reaction was stirred overnight at room temperature under Ar to a total of 23 hours. The mixture was partitioned between saturated aqueous NH_4Cl (30 mL), and EtOAc (30 mL + 2 × 20 mL) and the combined organics were dried (Na_2SO_4) and concentrated *in*

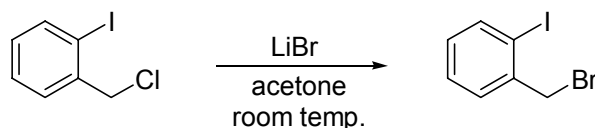
vacuo to furnish 6.2 mg (contaminated with DMF) of a yellow residue. ^1H NMR (CDCl_3 , 300 MHz) δ 8.04 (1H, s, C2-H), 8.01 (1 H, br d, $J = 7.8$ Hz, C6-H), 7.6–7.5 (3 H, m, ArH, C4-H), 7.45 (1 H, t, $J = 7.8$ Hz, C5-H), 7.30–7.10 (2 H, m, ArH), 4.24 (1 H, dd, $J = 9.4, 6.4$ Hz ArCHCCNCH₂Ar), 3.92 (3 H, s, CO₂CH₃), 3.35–3.18 (2 H, m, ArCH₂CCNHAr).

Base-catalyzed ring deconjugation of **3-3b**



To **3-3b/3-8b** (58.0 mg, 0.139 mmol) dissolved in CH_3CN (5 mL) was added DBU (64 μL of a 331.6 mg/mL CH_3CN solution, 0.0138 mmol, 0.1 equivalents) and the reaction was stirred at room temperature under Ar for two hours. The mixture was partitioned between saturated aqueous NH_4Cl (30 mL) and CH_2Cl_2 (30 mL + 2 \times 25 mL) and the combined organics were dried (Na_2SO_4) and concentrated *in vacuo* to give 56.4 mg of a golden oil. ^1H NMR spectrum revealed the quantity of **3-8b** to have increased from 16.6 mol % to 34.2 mol %.

1-Bromomethyl-2-iodobenzene



Following a published method:⁴² to an acetone (30 mL) solution of 1-chloromethyl-2-iodobenzene (2.759 g, 10.9 mmol) was added LiBr (10.13 g, 116.0 mmol, 10.7 equivalents) and the reaction was stirred overnight at room temperature under Ar. Monitoring by TLC proved misleading, prompting premature workup. Assessment by ^1H NMR spectroscopy

revealed 28 mole percent of starting material, so the crude material was again subjected to the reaction conditions (40 mL acetone; LiBr: 14.42 g, 166.0 mmol, 15.2 equivalents) for 25 hours. The reaction mixture was concentrated by rotary evaporator and partitioned between water (70 mL) and CH₂Cl₂ (2 × 60 mL). The combined CH₂Cl₂ portions were dried (Na₂SO₄) and concentrated *in vacuo*, giving a heterogeneous mixture of needles and slightly pink amorphous solid that was revealed by ¹H NMR spectroscopy to contain an acceptable trace quantity of starting material. The product (2.46 g, 76%) was used without purification. ¹H NMR (CDCl₃, 300 MHz) δ 7.84 (1 H, dd, *J* = 7.7, 1.2 Hz), 7.45 (1 H, dd, *J* = 7.7, 1.7 Hz), 7.31 (1 H, td, *J* = 7.7, 1.2 Hz), 6.96 (1 H, td, *J* = 7.7, 1.7 Hz), 4.58 (1 H, ArCH₂Br).

References

1. Heck, R. F.; Nolley, J. P. *J. Org. Chem.* **1972**, *37*, 2320.
2. Mizoroki, T.; Mori, K.; Ozaki, A. *Bull. Chem. Soc. Jpn.* **1971**, *44*, 581.
3. Beletskaya, I. P.; Cheprakov, A. V. *Chem. Rev.* **2000**, *100*, 3009-3066.
4. Heck, R. F. *Palladium Reagents in Organic Synthesis*; Academic Press, Inc.: Orlando, 1985.
5. de Meijere, A.; Meyer, F. E. *Angew. Chem., Int. Ed. Engl.* **1994**, *33*, 2379-2411.
6. Cabri, W.; Candiani, I. *Acc. Chem. Res.* **1995**, *28*, 2-7.
7. Crisp, G. T. *Chem. Soc. Rev.* **1998**, *27*, 427-436.
8. Amatore, C.; Jutand, A. *J. Organomet. Chem.* **1999**, *576*, 254-278.
9. Biffis, A.; Zecca, M.; Basato, M. *J. Mol. Catal. A – Chemical* **2001**, *173*, 249-274.
10. Whitcombe, N. J.; Hii, K. K.; Gibson, S. E. *Tetrahedron* **2001**, *57*, 7449-7476.
11. de Vries, J. G. *Can. J. Chem.* **2001**, *79*, 1086-1092.
12. Link, J. T. In *Organic Reactions*; Overman, L. E., Ed.; John Wiley & Sons, Inc.: 2002; Vol. 60, p 157-213.
13. Jutand, A. *Eur. J. Inorg. Chem.* **2003**, 2017-2040.
14. Amatore, C.; Jutand, A.; M'Barki, M. A. *Organometallics* **1992**, *11*, 3009-3013.
15. Amatore, C.; Carré, E.; Jutand, A.; M'Barki, M. A. *Organometallics* **1995**, *14*, 1818-1826.
16. Ahlquist, M.; Fristrup, P.; Tanner, D.; Norrby, P.-O. *Organometallics* **2006**, *25*, 2066-2073.
17. Amatore, C.; Carré, E.; Jutand, A.; M'Barki, M. A.; Meyer, G. *Organometallics* **1995**, *14*, 5605-5614.
18. Amatore, C.; Jutand, A. *Acc. Chem. Res.* **2000**, *33*, 314-321.
19. Goossen, L. J.; Koley, D.; Hermann, H. L.; Thiel, W. *Organometallics* **2005**, *24*, 2398-2410.

20. Gooßen, L. J.; Koley, D.; Hermann, H.; Thiel, W. *Chem. Commun.* **2004**, 2141-2143.
21. Pröckl, S. S.; Kleist, W.; Gruber, M. A.; Köhler, K. *Angew. Chem. Int. Ed. Engl.* **2004**, *43*, 1881-1882.
22. Davies, I. W.; Matty, L.; Hughes, D. L.; Reider, P. J. *J. Am. Chem. Soc.* **2001**, *123*, 10139-10140.
23. Biffis, A.; Zecca, M.; Basato, M. *Eur. J. Inorg. Chem.* **2001**, 1131-1133.
24. Gruber, A. S.; Pozebon, D.; Monteiro, A. L.; Dupont, J. *Tetrahedron Lett.* **2001**, *42*, 7345-7348.
25. Reetz, M. T.; Westermann, E. *Angew. Chem., Int. Ed. Engl.* **2000**, *39*, 165-168.
26. de Vries, A. H. M.; Mulders, J. M. C. A.; Mommers, J. H. M.; Henderickx, H. J. W.; de Vries, J. G. *Org. Lett.* **2003**, *5*, 3285-3288.
27. Herrmann, W. A.; Brossmer, C.; Öfele, K.; Reisinger, C.-P.; Priermeier, T.; Beller, M.; Fischer, H. *Angew. Chem., Int. Ed. Engl.* **1995**, *34*, 1844-1848.
28. Rocaboy, C.; Gladysz, J. A. *Org. Lett.* **2002**, *4*, 1993-1996.
29. Krasovsky, A. L.; Nenajdenko, V. G.; Balenkova, E. S. *Tetrahedron* **2001**, *57*, 201-209.
30. Jeffery, T. *J. Chem. Soc. Chem. Commun.* **1984**, 1287-1289.
31. Jeffery, T. *Tetrahedron Lett.* **1985**, *26*, 2667-2670.
32. Jeffery, T. *J. Chem. Soc. Chem. Commun.* **1991**, 324-325.
33. Jeffery, T. *Tetrahedron Lett.* **1991**, *32*, 2121-2124.
34. Jeffery, T. *Tetrahedron Lett.* **1994**, *35*, 3051-3054.
35. Jeffery, T.; Galland, J.-C. *Tetrahedron Lett.* **1994**, *35*, 4103-4106.
36. Jeffery, T. *Tetrahedron* **1996**, *52*, 10113-10130.
37. Ziegler, F. E.; Chakraborty, U. R.; Weisenfeld, R. B. *Tetrahedron* **1981**, *37*, 4035-4040.
38. Ikeda, M.; El Bialy, S. A. A.; Yakura, T. *Heterocycles* **1999**, *51*, 1957-1970.
39. Melnyk, P.; Gasche, J.; Thal, C. *Tetrahedron Lett.* **1993**, *34*, 5449-5450.
40. Yao, Q.; Kinney, E. P.; Yang, Z. *J. Org. Chem.* **2003**, *68*, 7528-7531.

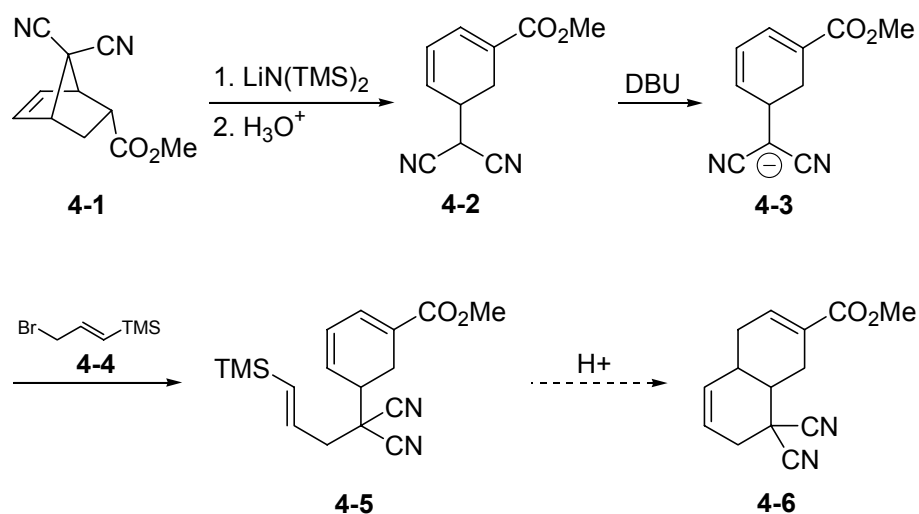
41. Friesen, R. W. Chem. 492 Report, University of Waterloo, 1984.
42. Levacher, V.; Adolfsson, H.; Moberg, C. *Acta Chem. Scand.* **1996**, *50*, 454-457.

Chapter 4

Bromination of Allyl Silanes: Insights Into Ionic and Free Radical Reaction Pathways

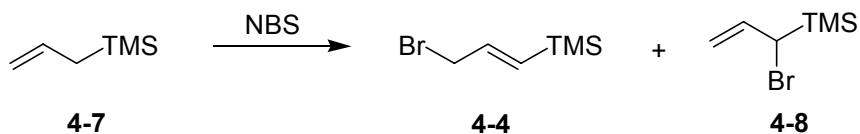
4.1 Introduction

Among the possible synthetic elaborations of the ring-opened Diels-Alder adduct **4-1** that were considered was the alkylation of the anion **4-3** by the trimethylsilylallyl bromide **4-4** followed by acid-induced cyclization as shown in Scheme 4-1 below.



Scheme 4-1. Proposed cationic cyclization of ring-opened adduct derivative **4-5**.

In order to generate **4-5**, a free-radical bromination of commercially available allyltrimethylsilane (**4-7**) was carried out with NBS to produce a mixture of the allyl bromides **4-4** and **4-8** (Scheme 4-2).

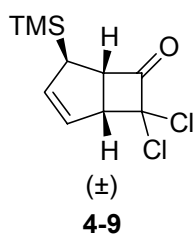


Scheme 4-2. Generation of regioisomeric trimethylsilylallyl bromides **4-4** and **4-8**.

The mixture of allyl bromides **4-4** and **4-8** reacted with the anion **4-3** in $\text{S}_{\text{N}}2$ and $\text{S}_{\text{N}}2'$ processes to yield the desired compound **4-5**. For a variety of reasons associated with other aspects of the project, which were deemed to be more promising research directions, the further conversion of **4-5** to **4-6** was not pursued, although future studies of this process should certainly be encouraged.

4.2 Results and Discussion

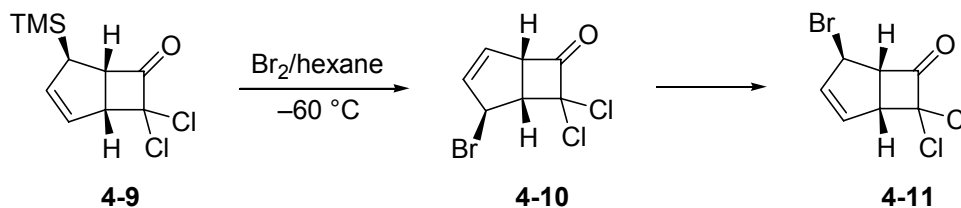
A brief study of the chemistry associated with the bromination of the parent allyltrimethylsilane and the bicyclic derivative **4-9** was carried out. The interest in this



chemistry had an origin in previous investigations in this laboratory which yielded results which were somewhat puzzling and not readily explicable in mechanistic terms and which remained unpublished. The chlorination of **4-7**, carried out by Sommer, Tyler, and Whitmore¹ in 1948, was one of the

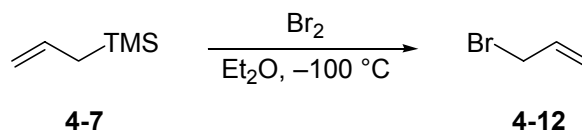
earliest reactions of allylsilanes on record and the reaction of molecular bromine with **4-7**¹ and of **4-9**² have become, literally, the “textbook” examples (e.g. see Introduction to Organic Chemistry 4th Edition by A. Streitwieser, C.H. Heathcock and E. M. Kosower, page 846) to illustrate the general allylic substitution process observed in reactions of allylsilanes with appropriate electrophiles.

The reaction of **4-9** with molecular bromine was reported by Fleming and Au-Yeung² to provide a 60% yield of the allylic bromide **4-10**, which was apparently prone to rearrangement to the isomeric allylic bromide **4-11** (Scheme 4-3).



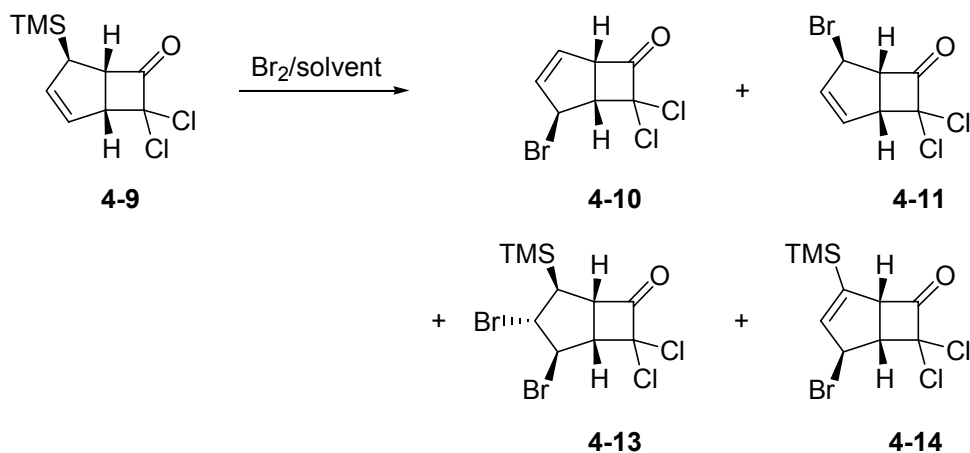
Scheme 4-3. Results of bromination of **4-9** reported by Fleming and Au-Yeung.

The prior study by Sommer et al. had reported the formation of allyl bromide (**4-12**) upon reaction of allyltrimethylsilane (**4-7**) with molecular bromine (Scheme 4-4).



Scheme 4-4. Results of bromination of allyltrimethylsilane with bromine reported by Sommer, Tyler, and Whitmore.

A previous researcher in this group, Mibbo Thandi,³ and later another student, undergraduate researcher Vernon Freer, had difficulty in reproducing the formation of **4-11** as reported by Fleming. In Thandi's work, mixtures of the allyl bromides **4-10** and **4-11** were obtained along with the dibromide **4-13** and the trimethylsilylallyl bromide **4-14** in varying amounts dependent on reaction conditions (Scheme 4-5).

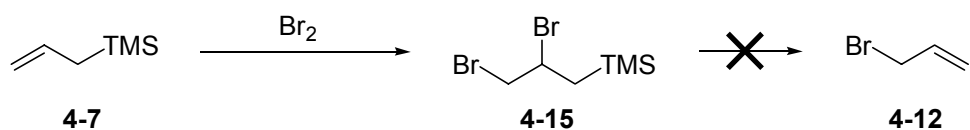


Scheme 4-5. Product mixtures observed by Thandi in attempted bromination of **4-9**.

The formation of the dibromide **4-13** was unexpected given the earlier report by Fleming² and the subsequent review of allylsilane chemistry by Chan and Fleming,⁴ in which it is stated that such TMS dibromides are intrinsically very unstable with respect to formation of the corresponding allyl bromide and TMSBr.

Experiments carried out in this laboratory at 0° in CCl₄ were found to yield **4-13** and **4-14** in the presence of light, but no reaction was observed in the absence of light. This led to the conclusion that formation of **4-13** and **4-14** was a free radical process.

Later work by G. Weeratunga in this laboratory demonstrated that reaction of **4-7** with molecular bromine in dichloromethane also provided a dibromide product **4-15**, which was perfectly stable to heat and not prone to facile conversion to allyl bromide as suggested by comments in the review by Chan and Fleming.

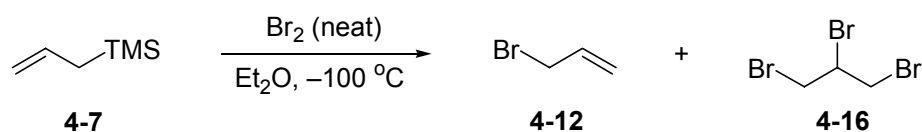


Scheme 4-6. Generation of TMS dibromide **4-15** by Weeratunga in this laboratory.

Furthermore it was shown that formation of the dibromide occurred both in the presence and in the absence of light, suggesting that, unlike the situation with **4-9**, the reaction of **4-7** to form **4-15** was not a free radical chain addition reaction.

A more thorough search of the literature revealed the existence of a previous report in French by Henner and co-workers⁵ of the detection of **4-15** in a bromination of **4-7** which had not been referenced in the review by Chan and Fleming. Although **4-15** was not fully characterized in that study, it was reported that the formation of **4-15** was favoured in less polar solvents and that formation of **4-12** could be demonstrated in polar solvents such as methanol.

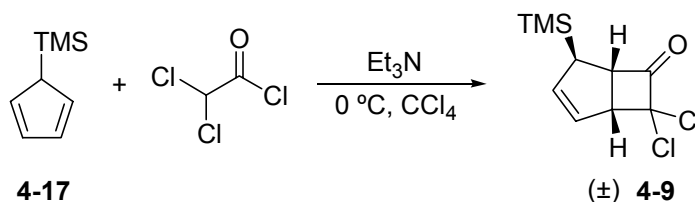
Further work in this laboratory by Weeratunga showed that effecting the reaction of **4-7** with molecular bromine under the conditions reported by Sommer and co-workers, in which neat molecular bromine is added to an ether solution of **4-7**, produced an exothermic reaction from which allyl bromide (**4-12**) and the tribromide **4-16** could be isolated in agreement with the original report.



Scheme 4-7. Repeat in this laboratory of the experiment of Sommer and co-workers.

Initially it was felt that the exothermicity of the reaction done under these conditions may have led to a thermal conversion of the dibromide **4-15** to **4-12** which then reacted with Br_2 to give **4-16**. It did not prove possible, however, to demonstrate formation of **4-12** upon heating pure dibromide **4-15**.

The present study was undertaken to shed some light on the factors which might explain the somewhat confusing observations outlined above. A sample of the bicyclic allylsilane **4-9** was generated by reaction of commercial 5-trimethylsilylcyclopentadiene with dichloroketene generated in situ by reaction of dichloroacetyl chloride with triethyl amine.



Scheme 4-8. Generation of bicyclic allylsilane **4-9**.

In the present study, the allyl silane **4-17** was found to be contaminated with an unknown compound. The source of this problem was eventually traced to the presence of this compound in the commercial sample of 5-trimethylsilylcyclopentadiene. Detailed spectroscopic analysis of this impurity led to the conclusion that the contaminant was the Diels-Alder dimer **4-18** of trimethylsilylcyclopentadiene. No previous reports of this dimer have been found in the literature and the conditions which led to its formation in the commercial preparation of 5-trimethylcyclopentadiene are unknown.

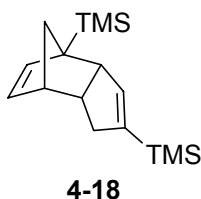
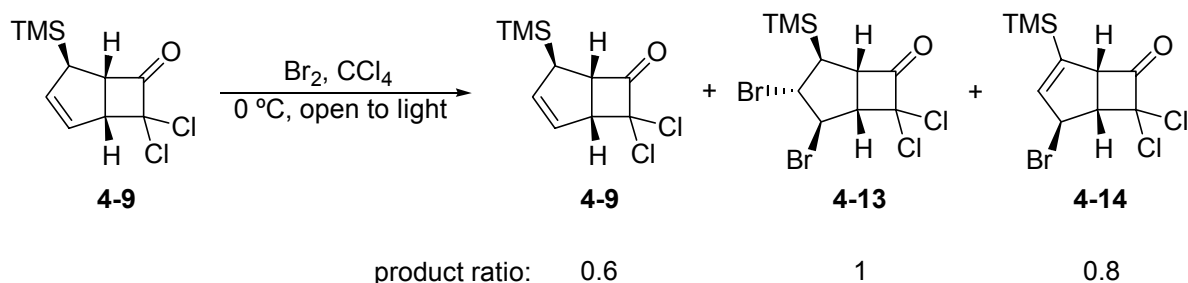


Figure 4-1. Structure of Diels-Alder dimer of 1-trimethylsilylcyclopentadiene.

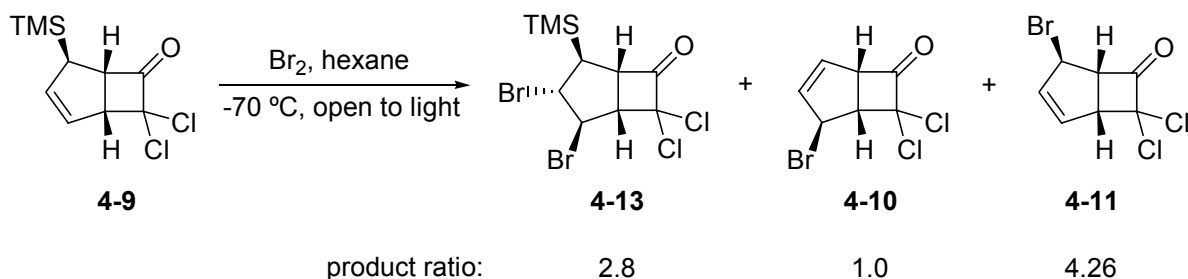
Reaction of **4-9** with molecular bromine at 0 °C in CCl₄ open to light gave a mixture of the starting material, the TMS allyl bromide **4-14** and the dibromide **4-13**. Column chromatography and recrystallization yielded a pure sample of the dibromide **4-13** and of the vinyl TMS allyl bromide **4-14**. Another experiment carried out under ostensibly the same

reaction conditions furnished **4-13** contaminated with trace quantities of at least two unknown compounds and none of either of the known allylic bromides **4-10** and **4-11** or of vinyl TMS compound **4-14**.

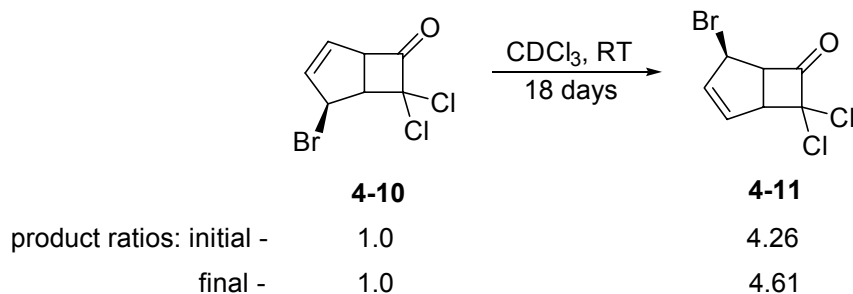


Scheme 4-9. Generation of dibromide **4-13** and vinyl TMS allyl bromide **4-14**.

Attention was then turned to reexamination of the bromination of **4-9** in hexane as described by Fleming and Au-Yeung. In the study by Thandi in this group, it had been noted that in creating solutions of bromine in hexane it was difficult to avoid reaction of Br_2 with apparent formation of HBr as indicated by generation of white fumes even when the hexane had been purified to remove any contaminating peroxides. In the present repetition of this work, the hexane was distilled from sodium prior to use. It was found that the stock solution of bromine in hexane, prepared at room temperature, became opaque and deposited a brown film on the flask walls. A freshly prepared stock solution of bromine in hexane was added by syringe pump over 30 minutes to a cooled ($-70\text{ }^\circ\text{C}$) solution of **4-9** in hexane. A sampling of the vapour above the reaction mixture by withdrawal by syringe followed by expulsion on to wet pH paper indicated that presence of acid, presumably HBr . Storage of the solution in a freezer overnight produced a deposit of white crystals which were collected and washed with hexane as described by Fleming and Au-Yeung.²



Continued NMR monitoring:



Scheme 4-10. Product distribution in bromination of **4-9** under the conditions reported by Fleming and Au-Yeung.

The solid was found to contain **4-13**, **4-10** and **4-11** in the ratios shown as indicated as indicated by ^1H NMR analysis (Scheme 4-10). After 18 days in CDCl_3 , a slight change in the proportion of **4-10** to **4-11** was observed but no indication of the conversion of the dibromide **4-13** to either of the allyl bromides was noted.

The apparent conversion of the TMS dibromides to TMSBr and the respective allyl bromides was systematically examined for the possibility that reactive species in the reaction and product mixtures were implicated. Experiments were conducted with **4-15**, involving its attempted conversion to TMSBr and allyl bromide under various conditions, beginning with control experiments in which the conversion was tested without additives. Subsequent experiments explored the role of the added reagents TMSBr, to examine the potentially autocatalytic nature of the conversion, and Br_2 , to examine the possibility that, under the

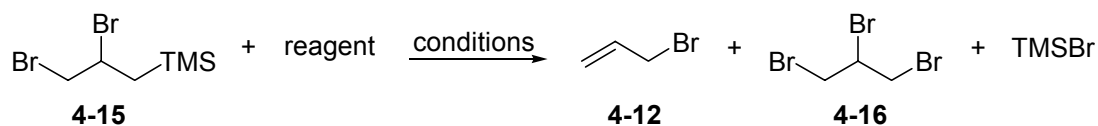
appropriate conditions, electrophilic substitution begins to compete with bromine addition to allyltrimethylsilane as the supply of the TMS dibromide increases.

The apparent formation of HBr under the conditions reported by Fleming and Au-Yeung, as well as the possibility that HBr was generated, by free radical chain reaction with the ether solvent in the exothermic reaction observed with allyltrimethylsilane **4-7**, suggested that the possible role of HBr in the conversion of the TMS dibromides to the allyl bromides should also be explored. The generation of HBr in Et₂O was confirmed in the present study in a modified version of the reaction disclosed by Sommer et al., in which a solution of Br₂ was prepared in Et₂O for addition to a cooled solution of allyltrimethylsilane. Introduction of Br₂ to freshly distilled Et₂O in an addition funnel mounted above the substrate solution immediately produced a violent exothermic reaction that vented a great deal of white acidic vapor.

Quantities of **4-15** and **4-13** were synthesized according to the optimized procedures respectively determined by Thandi and Weeratunga and submitted to the test conditions outlined in Table 4-1. Experiments were conducted in CDCl₃ to permit direct assessment by ¹H NMR spectroscopy of reaction mixture aliquots, which were generally saved for prolonged monitoring (room temp. experiments), or removed from the reaction mixture for each assessment (refluxing experiments). Product mixtures were assessed by comparison of their ¹H NMR spectra in CDCl₃ with reference spectra of commercial samples of allyl bromide (isolated diagnostic signals at δ 6.03, δ 5.31, and δ 5.14), 1,2,3-tribromopropane (isolated C2-H multiplet at δ 4.39), and TMSBr (nine proton singlet at δ 0.52). In experiments involving HBr, the acid was supplied from a stock saturated solution in CDCl₃,

which was generated by bubbling of HBr gas (Aldrich) through the ice bath-cooled solvent. Molecular bromine stock solutions were prepared in CDCl₃ and CCl₄.

Table 4-1. TMSBr eliminations from **4-15** attempted with various reagents.



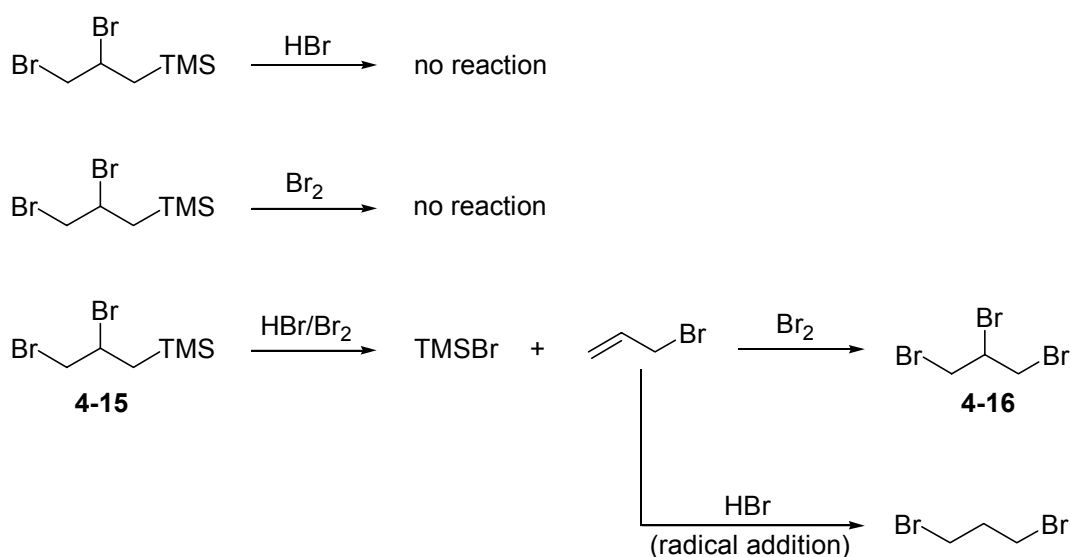
Entry	Reagent(s)	Conditions ^a	Duration (hrs.)	Products
1	none	CDCl ₃ , room temp.	389	4-15
2	none	CDCl ₃ , reflux	47	4-15
3	TMSBr (0.30 equiv.)	CDCl ₃ , reflux	47	4-15 , 4-12 (trace)
4	Br ₂ (0.2 equiv.)	CDCl ₃ , room temp.	70	4-15
5	Br ₂ (0.25 equiv.)	CCl ₄ , room temp.	163	4-15
6	HBr (catalytic) ^b	CDCl ₃ , room temp.	68	4-15
7	HBr (excess) ^c	CDCl ₃ , reflux	71	4-15 , 4-12 (trace)
8	HBr (catalytic) Br ₂ (catalytic)	CDCl ₃ , room temp.	71	4-15 (17.3 mol %) ^d 4-12 (16.0 mol %) 4-16 (66.7 mol %)

^a CDCl₃ from Ar-purged bottles, stored over K₂CO₃. CCl₄ freshly distilled from P₂O₅. ^b One drop of saturated solution in CDCl₃. ^c Substrate dissolved in saturated HBr solution in CDCl₃. ^d Complete consumption of **4-15** occurred between 71 and 145 hours. Allyl bromide (**4-12**) cited as electrophilic substitution product for convenience. All allyl bromide generated and not converted to **4-16** was converted to 1,3-dibromopropane by radical HBr addition (16 mol % at 71 hours, 30.8 mol % at 145 hours).

The persistence of **4-15** was first confirmed by prolonged aging in CDCl₃ at room temperature (entry 1) and at reflux (entry 2). In neither case was any consumption of **4-15** observed. It was thought that any trace quantity of TMSBr, produced by whatever means, might bring about TMSBr elimination from **4-15** in an autocatalytic fashion. To test this possibility, **4-15** was combined with a substoichiometric quantity of TMSBr in CDCl₃ at reflux (entry 3). Whereas a trace quantity of allyl bromide was generated, the reaction had required a great deal of time at elevated temperature; therefore, TMSBr was not considered a prime candidate for the short-duration electrophilic substitution processes to which **4-15** was

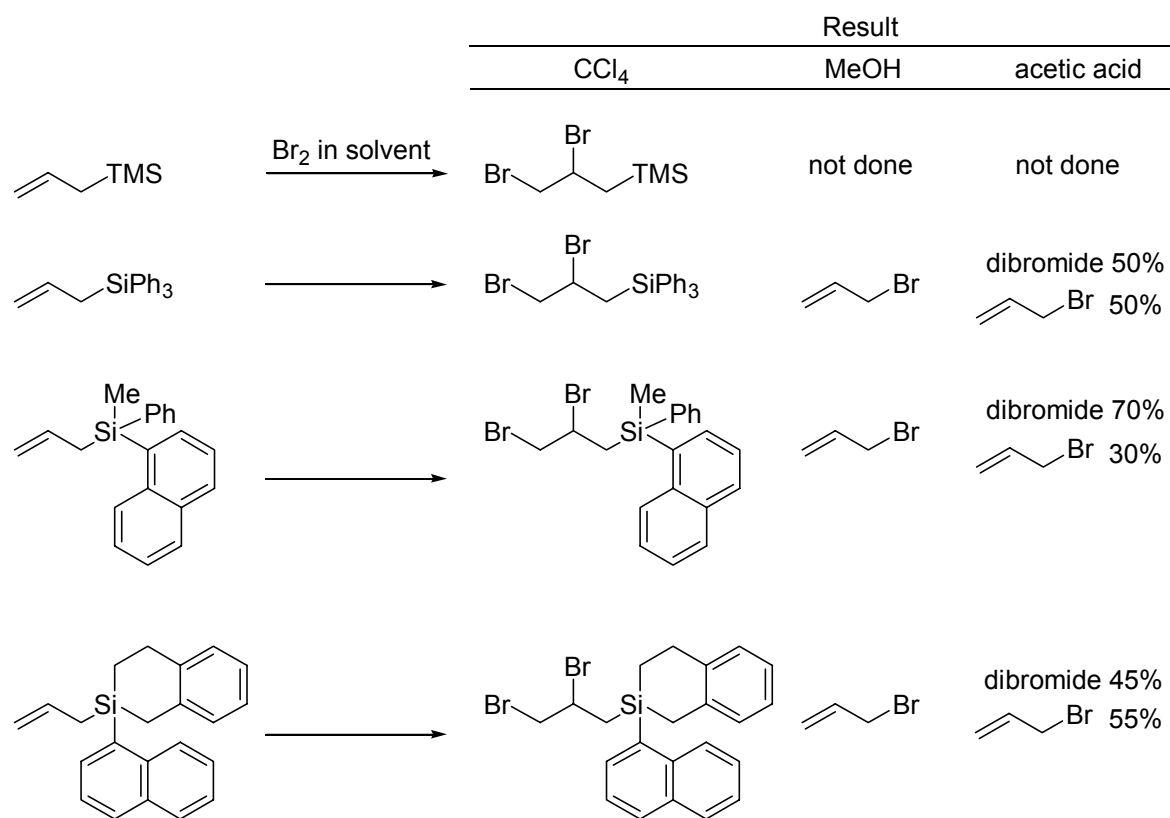
prone under the appropriate conditions. Molecular bromine at room temperature in both CDCl_3 and CCl_4 was also unreactive toward **4-15**.

Treatment of the dibromide **4-15** with HBr under various conditions (entries 6 and 7) in CDCl_3 for prolonged durations did not lead to conversion to allyl bromide. Eventually, the possibility was considered that the implication of HBr in the elimination of TMSBr involved an additional additive. Because the generation of allyl bromide occurred during bromine addition, Br_2 was the obvious candidate for combination with HBr. A room temperature experiment in which **4-15** was treated in CDCl_3 with solutions containing HBr and Br_2 yielded very interesting results. Within 23 hours (the first ^1H NMR assessment), a considerable quantity of 1,2,3-tribromopropane (**4-16**) had appeared, followed upon the second observation by the appearance of 1,3-dibromopropane, also an allyl bromide-derived product (Scheme 4-11). By 71 hours, **4-15** had declined to 17.3 mol % of the mixture (entry 8), at dramatic variance with the separate HBr and Br_2 experiments, which returned only starting material.



Scheme 4-11. Summary of key attempted elimination reactions of **4-15**.

The experiments of Carre et al.,⁵ in which TMS dibromides had been obtained from a number of allylsilanes, including allyltrimethylsilane, allyltriphenylsilane, methylphenyl-1-naphthylallylsilane, and 2-(1-naphthyl)-2-allyl-1,2,3,4-tetrahydro-2-silanaphthalene, were examined within the context of the conversion of TMS dibromides to TMSBr and allylsilanes. The authors determined that Br₂ addition occurred to a greater extent in less polar solvents: they were able to effect bromine addition in CCl₄, but observed increasing extents of Si–C cleavage in acetic acid and methanol (Scheme 4-12).



Scheme 4-12. Results of Carre et al. in brominations of various allylsilanes.

The authors determined that the TMS dibromides were not intermediates in the cleavage of the TMS groups by dissolving their triphenylsilyl dibromide (Ph₃SiCH₂CHBrCH₂Br) in methanol in the presence of Br₂ for 30 minutes, during which no reaction was observed. In our hands, the TMS dibromide **4-15** was converted to allyl bromide

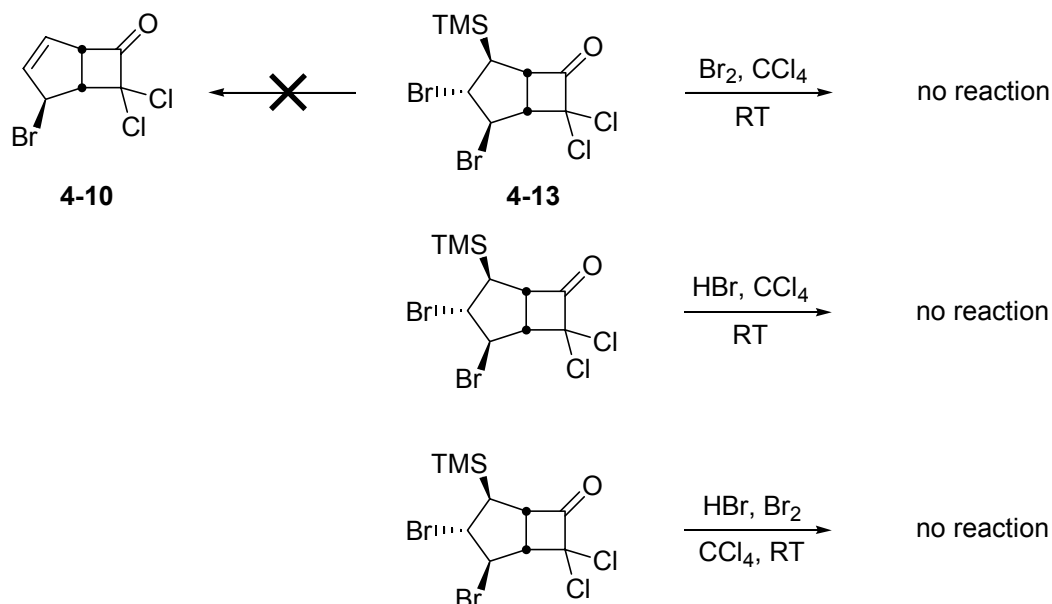
within less than 19 hours in methanol-d₄ solution at room temperature; that is, **4-15** had declined to less than 5 mol % of the mixture (**4-15** + allyl bromide) within 2 hours 48 minutes, and had disappeared by the next assessment at 19 hours. The conversion proceeded more slowly in acetic acid-d₄: at 3 hours, **4-15** had only declined to 79 mol % of the mixture, and to 52 mol % after 8 hours. By the next assessment after three days, the smooth conversion to allyl bromide was complete. The greater time required for the conversion in acetic acid correlates with the greater extent of cleavage observed by Carre et al. in brominations carried out in methanol (no addition product observed) than in acetic acid (50 % addition product). Whereas they cite precoordination of polar solvents to the silicon atom, and cleavage from the bromonium intermediate, our cleavages from the TMS dibromide confirm it as a TMSBr elimination substrate. The complete cleavage in methanol and the partial cleavage in acetic acid may reflect the differing reactivities of the two solvents toward the silyl dibromide, although combined reaction from both the bromonium ion and the dibromide cannot be ruled out.

Given their apparent finding that the triphenylsilyl dibromide is not the substrate that gives allyl bromide, combined with their determined trend of increasing extents of allyl bromide generation in more polar solvents, Carre et al. advance an explanation of Br₂ addition versus TMS/ β -bromonium elimination (to give allyl bromide) whose relative extents are determined by the nucleophilicity of the solvent. Whereas they obtain dibromides in non-polar CCl₄, they account for the observations of exclusive allyl bromide generation in Et₂O by Sommer et al. as being due to precoordination of the nucleophilic oxygen of Et₂O with the silicon atom, which brings about elimination of R₃Si--OEt₂⁺ from the bromonium intermediate. Likewise, the more highly nucleophilic methanol provides for a greater extent

of cleavage than the less nucleophilic acetic acid in their own experiments. The authors cite steric crowding of the silicon atom as a second factor influencing the course of these reactions, as they were able to generate the triphenylsilyl dibromide in Et₂O, whereas Sommer et al. obtain solely allyl bromide with allyltrimethylsilane. This account, reliant upon the extension of solvent nucleophilicity trends to the competition between addition and elimination in allylsilane brominations, is at odds with the findings of this study and of previous work in this laboratory and with Fleming's result in brominations in hexane. The attempted bromination of **4-9** in non-nucleophilic hexane generates a great deal of the corresponding allyl bromide. Weeratunga in this laboratory noted the generation of allyl bromide as the major product in the attempted bromination of **4-7** in CCl₄ when neat molecular bromine was employed at room temperature, in an experiment in which the temperature quickly rose to 78 °C. The implication of the combined involvement of HBr and Br₂ in the known elimination of TMSBr from **4-15** is developed into a mechanistic account below, but it suffices at this stage to note that solvent nucleophilicity does not account for the generation of allyl bromide in hexane and CCl₄. The observation of HBr generation from ether and hexane in exothermic reactions with Br₂ may also comport with the result in CCl₄: it is reasonable to surmise that the high temperature, perhaps resulting from rapid and exothermic dibromide generation, thermally generated radical bromine species that abstracted hydrogen atoms from either **4-7** or **4-15** to generate HBr, which acted in concert with Br₂ to effect the generation of allyl bromide.

In the present study, experiments were then conducted to extend the confirmation of the combined role of HBr and Br₂ in the elimination of TMSBr from the linear TMS dibromide to the bicyclic analog **4-13**. In this case, as reasonably expected, **4-13** proved

unreactive toward molecular bromine and HBr, in experiments conducted in CCl_4 . Unexpectedly, the combination of HBr and Br_2 was, in this case, unable to effect the conversion of the TMS dibromide to the allyl bromide **4-10** (Scheme 4-13).



Scheme 4-13. Unreactivity of **4-13** toward Br_2 , HBr, and HBr/ Br_2 .

This key set of observations allows the creation of a mechanistic construct which rationalizes the previously confusing observations concerning the bromination of the allylsilanes **4-7** and **4-9** based on the involvement, under certain reaction conditions, of both HBr and Br_2 . In this context, it is worth pointing out that complexes of HBr and Br_2 , loosely referred to as HBr_3 , have been proposed previously as key intermediates in various bromination reactions,^{6,7} although the possible significance of such species in the bromination of allyl silanes has not been reported. Interestingly, a search of the literature has failed to yield any references to either experimental or computational evidence for the structure of HBr_3 . The conjugate base of HBr_3 , Br_3^- , on the other hand, is well characterized, by crystallographic analysis of certain of its salts, in some of its many recorded crystal structures

as a linear rod with equivalent Br–Br bond lengths. In other instances, the tribromide exhibits asymmetry of its bond lengths and a slight angle at the central Br atom.⁸

Formally, protonation of Br_3^- (**4-19**) to form HBr_3 might occur on the internal Br atom or at a terminal Br atom as shown below. Additionally, it is possible that HBr_3 can be thought of as a complex (**4-22**) of Br_2 and HBr linked via a hydrogen bond (Figure 4-2).

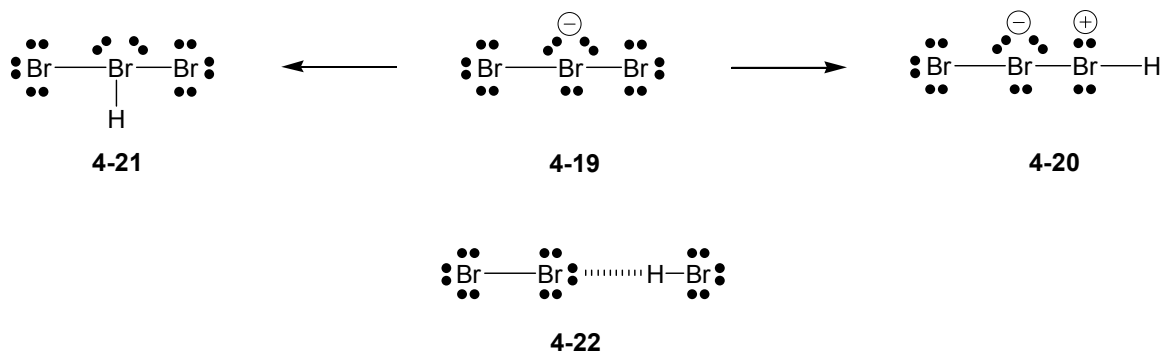


Figure 4-2. Potential structures of HBr_3 .

Ab initio molecular orbital calculations find energy minima for each of these possibilities. In the case of **4-20** and **4-22**, both linear and bent geometries are found (all Br atoms linear and a bent Br–Br–H bond for **4-20**; and Br–Br–H linear and a bent Br–H–Br bond for **4-22**). For **4-21**, a trigonal bipyramidal arrangement is predicted with the H atom and central Br atom lone pairs in the equatorial orientation and the terminal Br atoms in apical positions. The bond lengths in **4-20** are such that such a structure should be thought of as a complex in which Br_2 is acting as a Lewis acid and the Br atom of HBr is acting as a Lewis base.

The present observations do not provide any experimental indication as to the nature of the HBr/Br_2 species which is responsible for the observed catalysis of conversion of the TMS dibromide **4-15** to allyl bromide. Indeed, it might be argued that the mechanism may

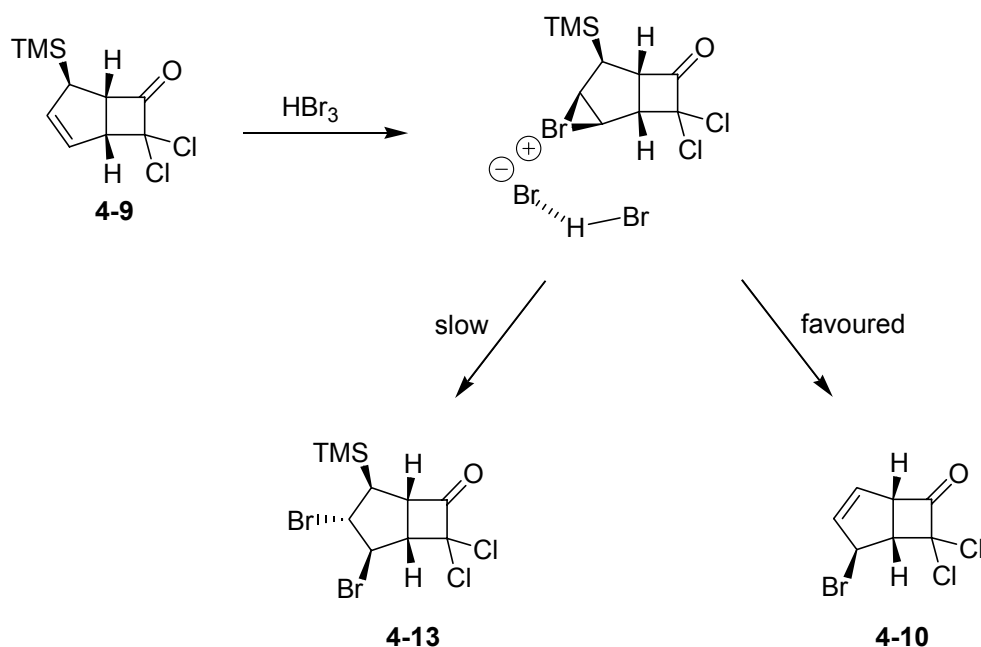
involve a transition state which is a ternary complex of **4-15** with both HBr and Br₂ wherein the HBr and Br₂ entities do not interact with one another in any direct way.

Taken together, the above observations suggest the following mechanistic interpretations. In solvents such as CCl₄ or CH₂Cl₂, bromination of allyltrimethylsilane gives the dibromide **4-15**. Since the reaction occurs with equal ease in the presence or in the absence of light, the process is likely ionic rather than a free radical chain reaction. The bromination of allyltrimethylsilane, with neat Br₂ in ether, as described in the original study by Sommer, Tyler, and Whitmore, leads to allyl bromide and 1,2,3-tribromopropane because of the presence of both Br₂ and HBr (generated by free radical reaction with the ether solvent) which induce the conversion of the initially formed TMS dibromide **4-15** to allyl bromide.

In the case of the bicyclic system **4-9**, steric and electronic factors appear to combine to make the system inert towards ionic addition of Br₂. The dibromide **4-13** is formed only in the presence of light in CCl₄, indicating that a free radical chain addition process is occurring.

The formation of the allyl bromide **4-10** appears to not occur via the dibromide **4-13**, since the HBr/Br₂ combination does not induce formation of **4-10** from **4-13**. A possible explanation for the formation of the allylic bromide is that the simultaneous presence of HBr and Br₂ makes possible a direct ionic pathway from the allyl TMS system **4-9** to the allylic bromide **4-10**. In the case of reactions in CCl₄ or CH₂Cl₂, the H in the HBr may arise via free radical chain allylic bromination which produces the vinyl TMS allyl bromide system **4-14**. In the case of the reactions in hexane, there is good reason to believe that substantial amounts of HBr may arise by free radical chain bromination of the solvent induced by light or by peroxides present as impurities in the hexane. Thus, the success of the Fleming conversion of

4-9 to **4-10** is explicable on the basis of the presence of a substantial quantity of HBr in solution from reaction of Br₂ with hexane before reaction with **4-9**. The ionic bromination of **4-9** may then proceed by its reaction with HBr₃ or some higher order complex HBr_n to yield **4-9** may then proceed by its reaction with HBr₃ or some higher order complex HBr_n to yield **4-10** directly without formation of the dibromide **4-13**. Ionic addition to form the TMS dibromide **4-13** is presumably discouraged by the steric demands of the bicyclic system. Bromonium ion formation from the exo face would seem to be the most reasonable pathway and if ring opening of the bromonium ion by Br⁻ is slow, then Br⁻ attack on silicon predominates to give the allyl bromide **4-10** without the intermediacy of the dibromide **4-13**. This hypothetical mechanism is illustrated below (Scheme 4-14).

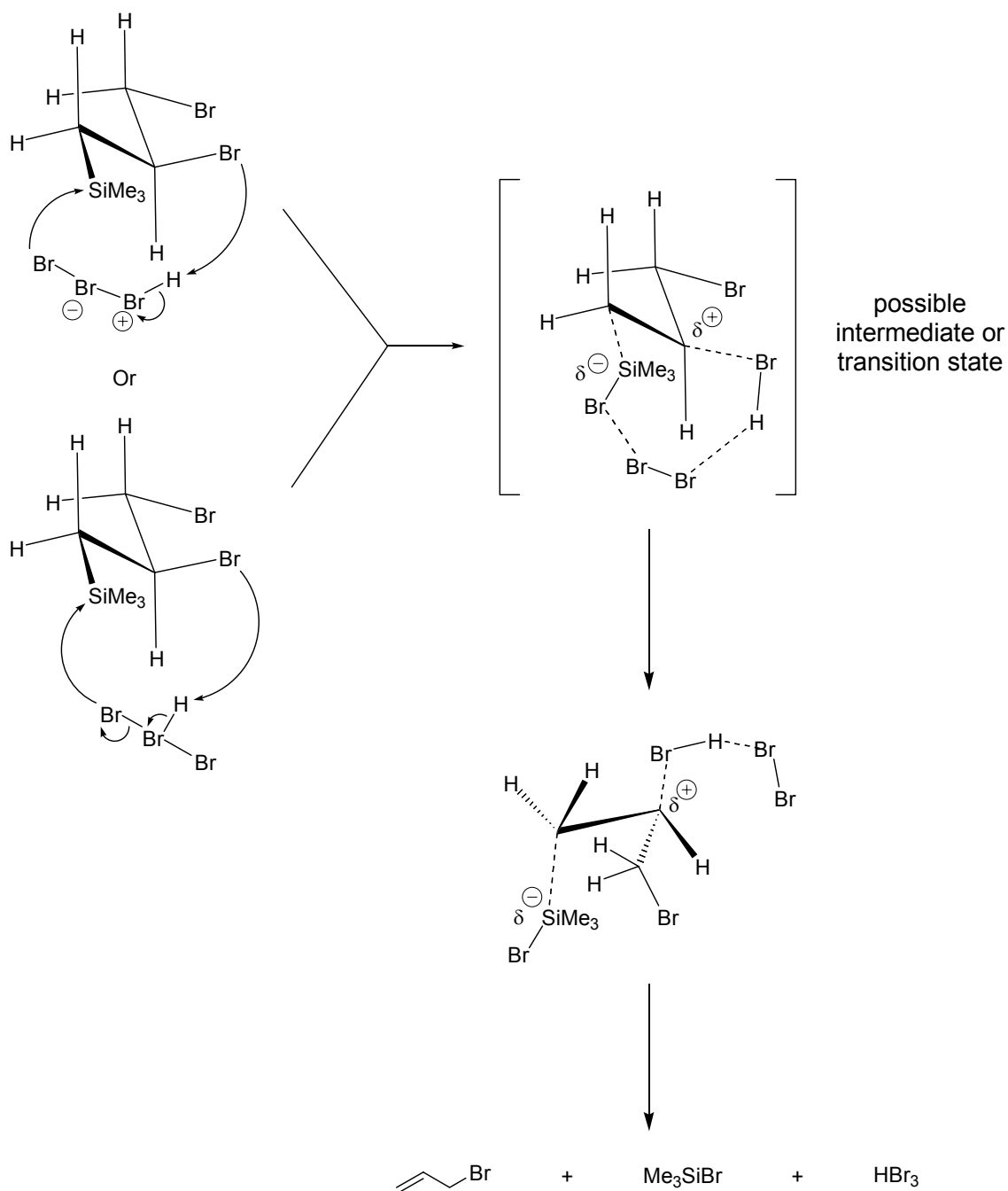


Scheme 4-14. Competing outcomes for neutralization of bromonium intermediate in bromination of **4-9**.

The difficulty in duplicating the observations of the Fleming group is explicable on the basis of a failure to generate just the correct amount of HBr in the Br₂ solution prior to reaction with **4-9**. In addition, the formation of substantial amounts of the dibromide **4-13** in this laboratory under conditions which were thought to be comparable to those in the

Fleming study is worthy of comment. Since the dibromide formation appears to be a free radical chain process for **4-9**, it is likely that light exposure of the reaction vessel was greater in the present work than in the work reported by Fleming.

The recognition of the significance of catalysis of TMS dibromide conversion to allyl bromide thus provides a very plausible explanation for the previously very confusing set of observations in the bromination of allyl silanes. A hypothetical mechanism whereby HBr_3 might catalyze the conversion of the TMS dibromide **4-15** into allyl bromide is presented below (Scheme 4-15)

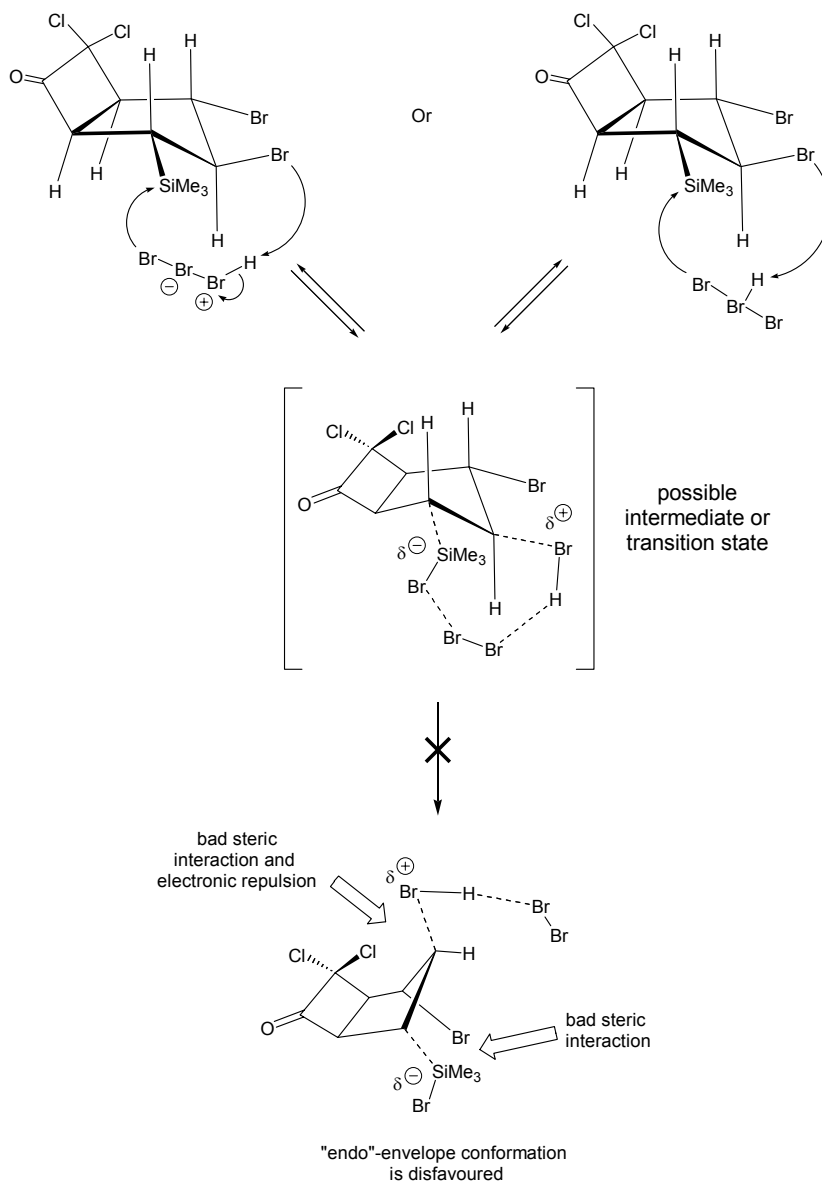


Scheme 4-15. Proposed mechanism for HBr_3 catalysis of TMSBr elimination from **4-15**.

In this mechanism, the terminal Br atom of HBr_3 acts as a nucleophile towards the silicon atom and the proton associated with HBr_3 functions as an acid to induce the ionization of the bromide. The carbocation character in the intermediate formed would be expected to be somewhat stabilized by the relatively electropositive silicon atom. In this hypothetical

scheme, it is assumed that formation of allyl bromide and TMSBr requires a conformational change to achieve an anti-coplanar arrangement of the leaving groups.

If this is correct, then it might be argued that the failure of the bicyclic TMS dibromide **4-13** to undergo TMSBr elimination is a consequence of the fact that the formation of the corresponding anticoplanar arrangement of leaving groups yields the *endo*-envelope, which is strongly disfavoured for stereoelectronic reasons (Scheme 4-16).



Scheme 4-16. Possible steric and electronic factors in failure of **4-13** to eliminate TMSBr.

Further mechanistic study employing more carefully controlled conditions which might allow meaningful kinetic studies and ab initio molecular orbital investigations of the possible mechanistic pathways are recommended.

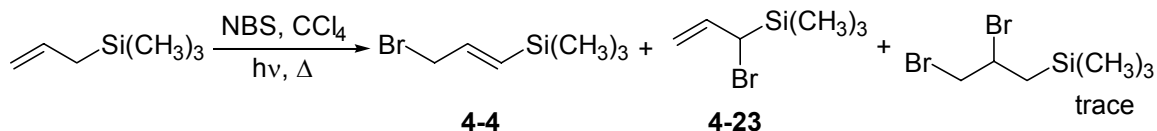
4.3 Experimental

4.3.1 *Supplementary General Experimental*

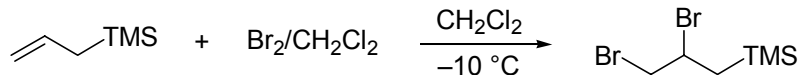
Solvents were dried by prolonged reflux over appropriate drying agents: hexane and Et₂O were distilled from sodium; CCl₄ was distilled from P₂O₅; and CH₂Cl₂ was distilled from CaH₂. Freshly opened CDCl₃ was sparged with Ar and stored over K₂CO₃. Carbon tetrachloride was distilled and stored. All other solvents were used immediately upon distillation. HBr (Aldrich) from a newly purchased Lecture bottle was passed through an all Teflon® and glass pathway and bubbled through CDCl₃ and CCl₄ in round-bottom flasks mounted in ice-water baths with a trap in line between the gas lecture bottle and the solvent flask. The gas outlet tube led to an inverted funnel closely positioned above the surface of an aqueous solution of NaOH in a large beaker. The system was flushed with Ar immediately prior to introduction of HBr. Bromine solutions for TMS dibromide conversion experiments were prepared in oven-dried volumetric flasks by weighing added quantities of Br₂ and adding solvent under flow of Ar to the inscribed volume line. Bromine stock solutions were dispensed by syringe/Ar or N₂ pressure after careful and rapid exchange on volumetric flasks of glass stoppers (long-term storage) with rubber septa (dispensing period). TMSBr, allyl bromide, 1,2,3-tribromopropane, and allyltrimethylsilane were newly purchased from Aldrich for the present study and were used as received for conversion experiments (TMSBr), synthesis (allyltrimethylsilane), or for ¹H NMR spectral comparison (allyl bromide, and 1,2,3-tribromopropane).

4.3.2 Experimental Details

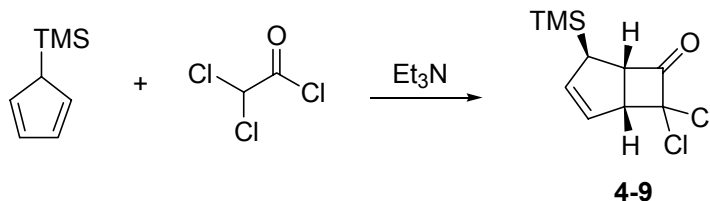
(3-Bromo o-propenyl)-trimethylsilane, (1-Bromo o-allyl)-trimethylsilane, and (2,3-Dibromo-propyl)-trimethylsilane



Allyl trimethylsilane (1.199 g, 0.0105 mol) and N-bromosuccinimide (1.869 g, 0.0105 mol) were dissolved in reagent grade CCl_4 and stirred in a round-bottom flask fitted with a condenser. The reaction was irradiated by an adjacent 150 W incandescent lamp, the assembly was wrapped in aluminum foil, and the reaction mixture was brought to reflux by the light source for 2 hours, 20 minutes. The reaction was cooled, filtered, successively washed with water (30 mL) and brine (30 mL), dried (Na_2SO_4), and concentrated *in vacuo*. Assessment by ^1H NMR spectroscopy indicated the presence of both title allylic bromide isomers in an approximate ratio of 3:1 (**4-4**:**4-23**), as well as a trace quantity of the title dibromide. The mixture was submitted, without purification, to the next reaction on the expectation of degenerate respective $\text{S}_{\text{N}}2$ and $\text{S}_{\text{N}}2'$ substitution reactions of anionic ring-opened adduct **4-3** with **4-4** and **4-23** to give cationic cyclization substrate **4-5**. The successful generation of **4-5** was indicated by ^1H NMR spectroscopy, but its cationic cyclization was set aside when the present study was undertaken.

(2,3-Dibromo-propyl)-trimethylsilane

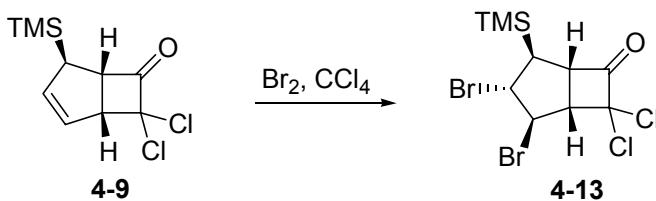
A solution of Br₂ (18.61 g, 0.116 mol) in dry CH₂Cl₂ (120 mL) was added slowly dropwise from an addition funnel over five hours to a solution of allyltrimethylsilane (19.88g, 0.174 mol) in CH₂Cl₂ (240 mL) at -10 °C. The reaction mixture was concentrated *in vacuo* and the residue was distilled through a short path Vigreux distillation apparatus under high vacuum (bp 74 °C). The material was spectroscopically identical to material prepared by Gamini Weeratunga (unpublished results). ¹H NMR (CDCl₃, 500 MHz) δ 4.25 (1 H, dddd, *J* = 10.3, 8.5, 4.6, 4.2 Hz, TMSCH₂CHBrCH₂Br), 3.83 (1 H, dd, *J* = 10.2, 4.6 Hz, TMSCH₂CHBrHCHBr), 3.61 (1 H, dd, *J* = 10.2, 8.5 Hz, TMSCH₂CHBrHCHBr), 1.74 (1 H, dd, *J* = 15.1, 4.2 Hz, TMSHCHCHBrCH₂Br), 1.27 (1 H, dd, *J* = 15.1, 10.3 Hz, TMSHCHCHBrCH₂Br), 0.09 (9 H, s, -Si(CH₃)₃); ¹³C NMR (CDCl₃, 75 MHz) δ 50.2, 40.6, 26.1, -0.1; Anal. Calcd. for C₆H₁₄SiBr₂: C, 26.29; H, 5.15; Br, 58.30. Found: C, 26.50; H, 5.20; Br, 58.46.

7,7-Dichloro-4-trimethylsilanyl-bicyclo[3.2.0]hept-2-en-6-one

To a stirred solution of 5-trimethylsilylcyclopentadiene (1.8 g, 0.013 mol) and triethylamine (3.288 g, 0.0325 mol) in dry CCl₄ at 0 °C under Ar was added dichloroacetyl chloride (4.79 g, 0.0325 mol) in dry CCl₄ (15 mL) dropwise over three hours. The mixture was suction-filtered and the cake of Et₃NHCl was washed with hexane. The filtrate was

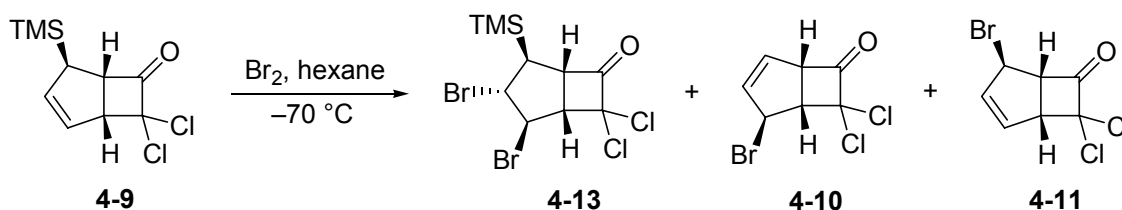
concentrated *in vacuo* and passed through a silica gel plug to give a clear golden oil. Silica gel column chromatography (230–400 mesh, 99:1 hexane:EtOAc) gave 1.35 g (41.7 %) of material sufficiently pure for direct synthetic use.

2-exo-3-endo-Dibromo-7,7-dichloro-4-exo-trimethylsilanyl-bicyclo[3.2.0]heptan-6-one



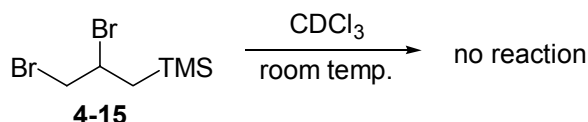
To a stirred solution of **4-9** (0.200 g, 0.804 mmol) in dry CCl_4 (25 mL) under Ar and in a 0 °C bath was added a CCl_4 solution of Br_2 (0.914 M, 0.041 mL) slowly dropwise from a syringe over 6 minutes. The reaction was stirred at 0 °C for three hours and allowed to warm to room temperature as it stirred overnight. An aqueous solution of NaHSO_3 (10 % w/v, 10 mL) was added and the mixture was stirred for 5 minutes. The reaction mixture was successively washed with water (15 mL) and brine (20 mL) and dried over Na_2SO_4 . Concentration *in vacuo* gave a yellow oil, determined to be largely **4-13** by ^1H NMR spectroscopy. Dissolved in minimal hexane and cooled in the refrigerator, the crude material deposited pure crystals (0.031 g, 9.5 %). The material was spectroscopically identical to material prepared by V. Freer in this laboratory, from which a crystal suitable for study by single crystal X-ray analysis had been obtained. ^1H NMR (CDCl_3 , 300 MHz) δ 4.23 (1 H, dd, $J = 9.5, 7.3$ Hz), 3.96–3.84 (2 H, m), 3.54 (1 H, dd, $J = 9.3, 7.3$ Hz), 1.82 (1 H, dd, $J = 11.6, 8.3$ Hz).

Attempted synthesis of 4-13 in hexane

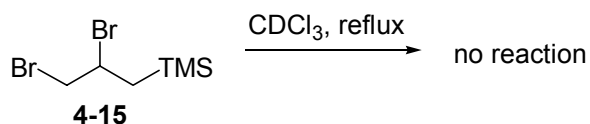


Experiment adapted slightly from reference 2. Bicyclic allylsilane **4-9** (250 mg, 1.00 mmol) was dissolved in dry hexane (1 mL) and stirred at $-70\text{ }^\circ\text{C}$ under Ar. A solution of Br_2 in hexane (0.40 mL of a 2.50 M solution, 1.00 mmol) was added via a syringe mounted in a syringe pump over 30 minutes. The stock solution of Br_2 in hexane became opaque brown within several minutes and formed a brown film on the flask walls. The vapour in the flask was withdrawn by syringe and expelled onto wet pH paper, thereby proving acidic. The reaction mixture was stored at $-20\text{ }^\circ\text{C}$ overnight, after which the yellow supernatant was withdrawn from the deposited white crystals. The crystals were washed with 2 mL of hexane, dissolved in CDCl_3 , and thoroughly concentrated *in vacuo*. The crude ^1H NMR spectrum (CDCl_3 , 300 MHz) evidenced the presence of **4-13** and the known compounds **4-10** and **4-11**.

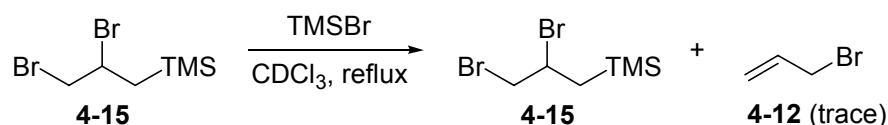
Attempted elimination of TMSBr from 4-15 in CDCl_3 at room temperature



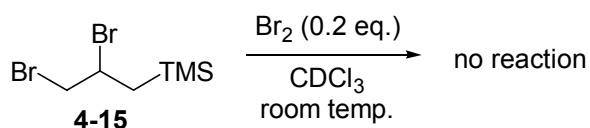
A small quantity of **4-15** was dissolved in CDCl_3 and stored in an NMR tube at room temp. for periodic assessment by ^1H NMR spectroscopy. After 389 hours of monitoring, no reaction had been observed.

Attempted elimination of TMSBr from 4-15 in CDCl₃ at reflux

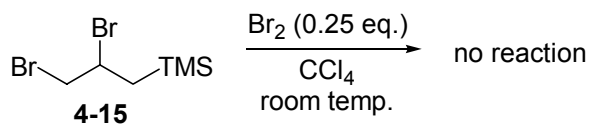
TMS dibromide **4-15** (0.4518 g, 1.65 mmol) was dissolved in CDCl₃ (8 mL) and heated to reflux under Ar. An aliquot removed at 47 hours and assessed by ¹H NMR spectroscopy revealed no reaction.

Attempted elimination of TMSBr from 4-15 with TMSBr in CDCl₃ at reflux

To **4-15** (0.3414 g, 1.25 mmol) were added CDCl₃ (10 mL) and TMSBr (58 mg, 0.379 mmol, 0.30 equiv.). The reaction mixture was heated at reflux for a total of 47 hours, during which time a trace quantity of allyl bromide was generated.

Attempted elimination of TMSBr from 4-15 with Br₂ in CDCl₃ at room temp.

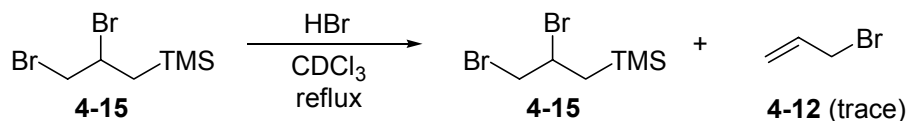
Molecular bromine (49 mg, 0.307 mmol, 0.2 equiv. with respect to **4-15**) and **4-15** (420 mg, 1.53 mmol) were combined in CDCl₃ (8 mL) and stirred at room temp. under Ar to a total of 70 hours, during which time no reaction was observed by ¹H NMR spectroscopy.

Attempted elimination of TMSBr from 4-15 with Br₂ in CCl₄ at room temp.

To a CCl₄ (10 mL) solution of **4-15** (0.4342 g, 1.58 mmol) was added Br₂ (0.43 mL of a 0.914 M CCl₄ solution, 0.397 mmol, 0.25 equiv.) and the reaction was stirred at room temperature for 2 hours 25 minutes, at which time a 0.5 mL aliquot was removed by syringe. The sample was stored at room temp. in an NMR tube for periodic examination. The substrate proved unreactive to a total of 163 hours.

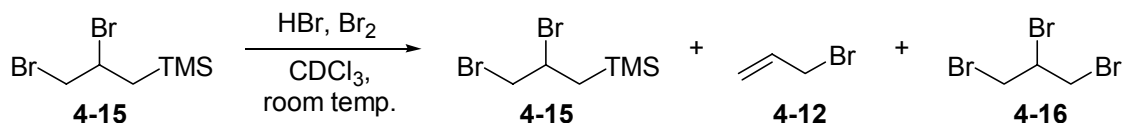
Attempted elimination of TMSBr from 4-15 with HBr in CDCl₃ at room temp.

Compound **4-15** (15 mg, 0.547 mmol) was dissolved in approximately 0.5 mL of CDCl₃ in an NMR tube. To this solution was added one drop of CDCl₃ saturated with HBr. The NMR tube was capped and periodically examined by ¹H NMR spectroscopy. No reaction was noted after 68 hours.

Attempted elimination of TMSBr from 4-15 with HBr in CDCl₃ at reflux.

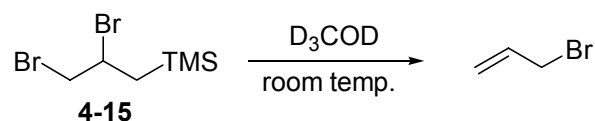
Compound **4-15** (0.4768 g, 1.74 mmol) was dissolved in a saturated HBr/CDCl₃ solution (10 mL) and refluxed under Ar. After 71 hours, ¹H NMR spectroscopy of an aliquot revealed only a trace quantity of allyl bromide.

Attempted elimination of TMSBr from 4-15 with HBr and Br₂ in CDCl₃ at room temp.



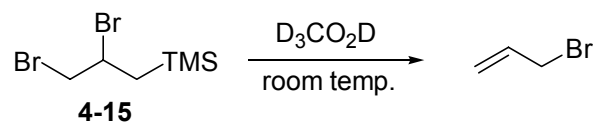
To **4-15** (29.9 mg, 0.109 mmol) were added catalytic quantities of Br₂ and saturated HBr/CDCl₃. The reaction was transferred to an NMR tube and maintained at room temperature. By 71 hours, **4-15** had declined to 17.3 mol % of the resultant mixture with **4-12** and **4-16**.

Conversion of 4-15 to allyl bromide in methanol-d₄



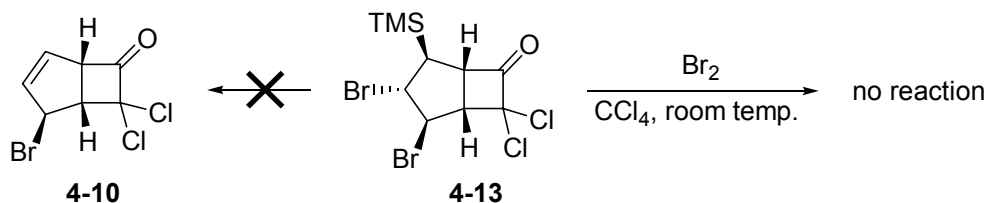
Approximately 15 mg of **4-15** was dissolved in methanol-d₄ from a freshly opened ampule. The room temp. solution was assessed periodically by ¹H NMR spectroscopy. By 2 hours 48 minutes, **4-15** had declined to less than 5 mol % of the mixture with allyl bromide, and had been completely consumed at some point before the next examination at 19 hours.

Conversion of 4-15 to allyl bromide with acetic acid-d₄



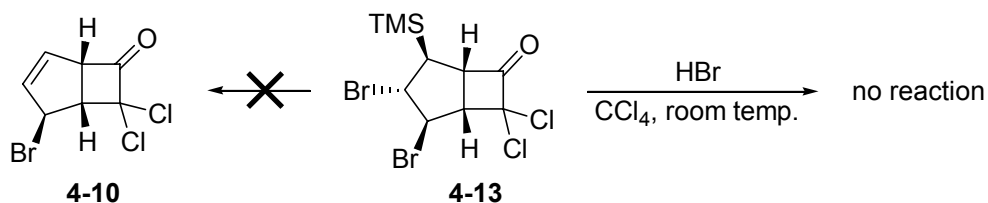
Approximately 15 mg of **4-15** was dissolved in acetic acid-d₄ from a freshly opened ampule. The quantity of **4-15** had declined to 52 mol % of the mixture with allyl bromide by 8 hours. The smooth conversion to allyl bromide was complete before the next assessment by ¹H NMR spectroscopy at 3 days.

Attempted elimination of TMSBr from 4-13 with Br₂ in CCl₄ at room temp.



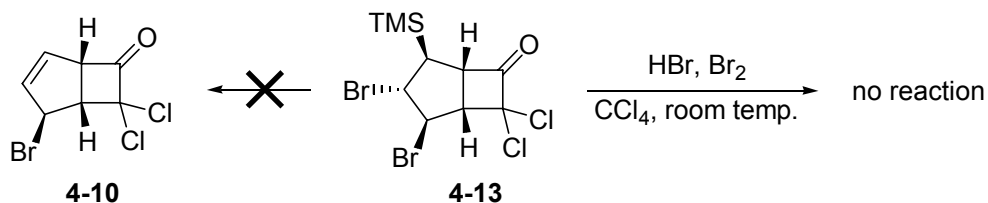
To a solution of bicyclic TMS dibromide **4-13** (8.7 mg, 0.0213 mmol) in CCl₄ (1 mL) was added Br₂ (0.17 mL of a 32.2 mM solution in CCl₄, 0.0055 mmol, 0.25 equiv.) and the mixture was stirred at room temp. under Ar. An aliquot was removed by syringe and stored in an NMR tube for further monitoring. No reaction was observed at 96 hours.

Attempted elimination of TMSBr from 4-13 with HBr in CCl₄ at room temp.



To approximately 4 mg of **4-13** in dry CCl₄ (1 mL) was added two drops of saturated HBr/CCl₄, and the reaction was stirred at room temp. under Ar. No reaction was observed by ¹H NMR spectroscopy over the course of 96 hours.

Attempted elimination of TMSBr from 4-13 with HBr and Br₂ in CCl₄ at room temp.



To approximately 4 mg of **4-13** in dry CCl₄ (1 mL) were added successively Br₂ (0.16 mL of a 32.2 mM solution in CCl₄, 0.0052 mmol, approx. 0.5 equiv.) and two drops of saturated HBr/CCl₄ and the reaction was stirred at room temp. under Ar. An aliquot was removed at 24 hours and periodically monitored by ¹H NMR spectroscopy. No reaction was observed over 96 hours

References

1. Sommer, L. H.; Tyler, L. J.; Whitmore, F. C. *J. Am. Chem. Soc.* **1948**, *70*, 2872-2874.
2. Fleming, I.; Au-Yeung, B.-W. *Tetrahedron* **1981**, *37*, 13-24.
3. Thandi, M. S. Master of Science, University of Waterloo, 1981.
4. Chan, T. H.; Fleming, I. *Synthesis* **1979**, 761-786.
5. Carre, F.; Corriu, R.; Henner, B. *J. Organomet. Chem.* **1970**, *22*, 589-598.
6. Tanner, D. D.; Ochiai, T.; Rowe, J.; Pace, T.; Takiguchi, H.; Samal, P. W. *Can. J. Chem.* **1977**, *55*, 3536-3543.
7. Hart, L. S.; Whiting, M. C. *J. Chem. Soc., Perkin Trans. 2* **1983**, 1087-1092.
8. Boeyens, J. C. A.; Denner, L.; Howard, A. S.; Michael, J. P. *S. Afr. J. Chem.* **1986**, *39*, 217-220.

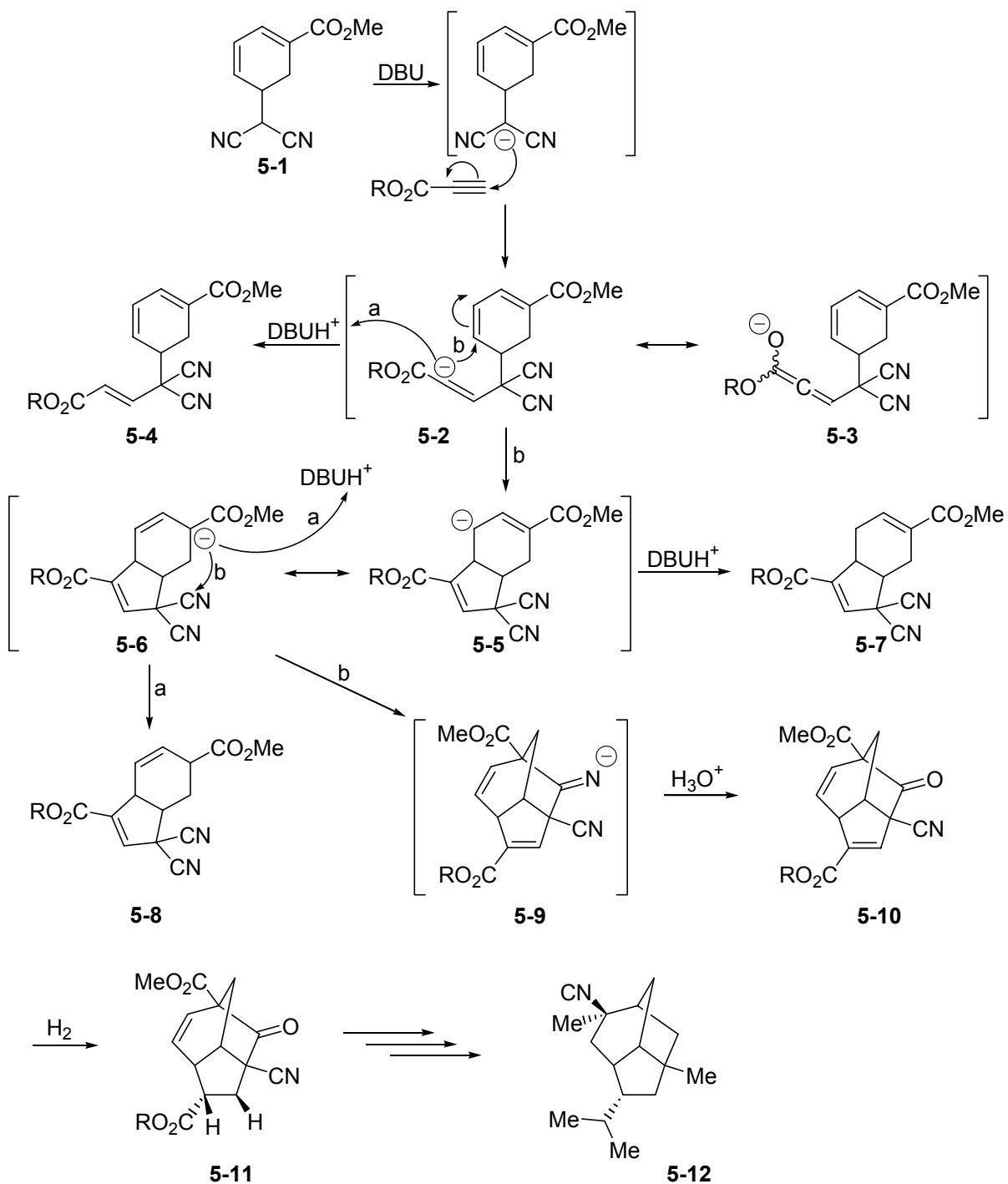
Chapter 5

Novel Reactivity of the Adducts of the Ring-Opened Adduct and Alkyl Propiolates

5.1 Introduction

In light of the well-established utility of propiolate esters in Michael reactions, we sought to explore their reactivity with the anion of our ring-opened Diels-Alder adduct. We envisioned the possibility of the propiolates exhibiting the same tandem Michael-Michael cascade that ultimately furnishes the homobrendane imine in high yield with the doubly-activated acceptor di-*tert*-butyl methylenemalonate, and in modest and vanishing yields with the singly-activated acceptors methyl vinyl ketone and cyclopenten-3-one, respectively. The symmetrical propiolates held the unique attraction over singly-activated or asymmetrically doubly-activated Michael acceptors of avoiding the diastereoisomerism established upon the first Michael addition to these kinds of double bond acceptors. Failing progress through the complete homobrendane-generating cascade, we reasonably expected termination at products of the first two steps of the cascade (Scheme 5-1). The initial adduct anion **5-2**, depicted with its allenolate resonance partner **5-3**, might simply have protonated to furnish the adduct **5-4**. Alternatively, **5-2** might have further undergone 1,6-addition to the $\alpha,\beta,\gamma,\delta$ -unsaturated π -system of the parent ring to furnish the allylic anionic resonance pair **5-5** and **5-6**, concluding with protonation to furnish conjugated (**5-7**) or deconjugated (**5-8**) bicyclic systems, respectively. Finally, intermediate **5-6** might have added to the proximal nitrile to

give the homobrendane imine anion, which could be hydrolyzed to the 8-oxo-homobrendane **5-10** with aqueous acid.



Scheme 5-1. Expected products of Michael addition of ring-opened adduct anion to propiolate esters.

Examination of the X-ray crystal structures obtained for our C3-acetyl- and C3-di-*t*-butoxycarbonyl-homobrendanes supported the expectation, on steric grounds, that any subsequent reduction of the cyclopentene double bond of a propiolate-derived homobrendane would deliver hydrogen from the “*exo*” surface of the molecule, establishing the future isopropyl group stereochemistry required for further elaboration toward isocyanopupa-keanene (Scheme 1, **5-11** → **5-12**).

5.2 Results and Discussion

5.2.1 Structure Elucidation of Novel Product

Our initial attempt at this reaction involved treatment of a mixture of the ring-opened adduct and methyl propiolate in CH₃CN with 0.1 equivalents of DBU at -10 °C. The bright yellow colour that developed instantly upon addition of base persisted for several minutes, but faded over several seconds to a pale straw colour. An aliquot removed and worked up (aq. NH₄Cl/EtOAc partition) at this stage was later assessed by ¹H NMR spectroscopy, which revealed that the reaction had already cleanly proceeded to completion. The whole reaction was worked up a few hours later and provided a ¹H NMR spectrum that contained more side products than were evident in the early sample. The experiment was repeated with ethyl propiolate, and it generated the same identity and distribution of the dominant and minor products. The main product (> 75 %) produced unfamiliar ¹H NMR signals (Figure 5-1; ethyl propiolate case), based on our previous experience with the ring-opened adduct. The ring vinyl proton pattern of the starting material and of its simple adducts at the side-chain dicyano carbon was absent, but was not replaced by signals typical of bicyclic adducts of

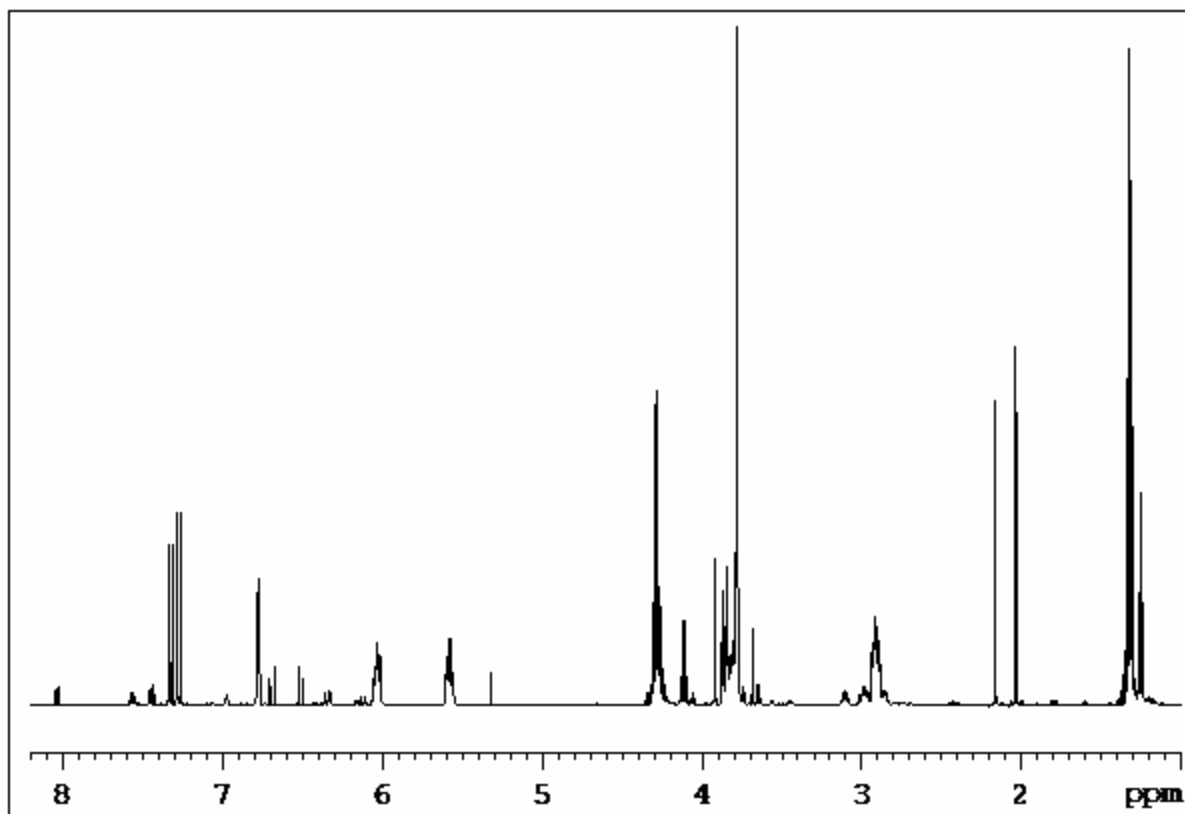


Figure 5-1. ^1H NMR spectrum (500 MHz, CDCl_3) of product of reaction of ring-opened adduct with ethyl propiolate.

types **5-7** and **5-8** seen as side-products in our previous homobrendane-generating reactions, or by those of a homobrendane system. Mass spectra were obtained for the methyl propiolate-derived product mixture. Whereas the electrospray mass spectrum evidenced a very weak signal for the molecular ion (m/z 286), the chemical ionization mass spectrum contained as its base peak the $(M + 18)^+$ (m/z 304) signal expected of an adduct of **5-1** and methyl propiolate. Considered in light of the novel ^1H NMR spectrum, the MS data indicated that the major product was likely an isomer of the products expected in the chain of tandem reactions available to this system.

Most ^1H NMR spectral signals of the main constituent were broad and complex, and the methyl ester protons evidenced two distinct peaks, visible at higher line resolution, as did

the ethyl ester methyl proton triplets; moreover, the separate and exceptionally far downfield vinyl proton doublets at 7.32 and 7.27 ppm (respective 10.5 and 10.6 Hz J) were of half the intensity of the upfield vinyl protons (6.77, 6.03, and 5.58 ppm), and were isolable unrelated protons, as revealed in separate ^1H - ^1H TOCSY spectra (Figure 5-2) derived from their individual irradiations, rather than a doublet of doublets comprising large couplings. These data indicated diastereoisomerism in the unknown product.

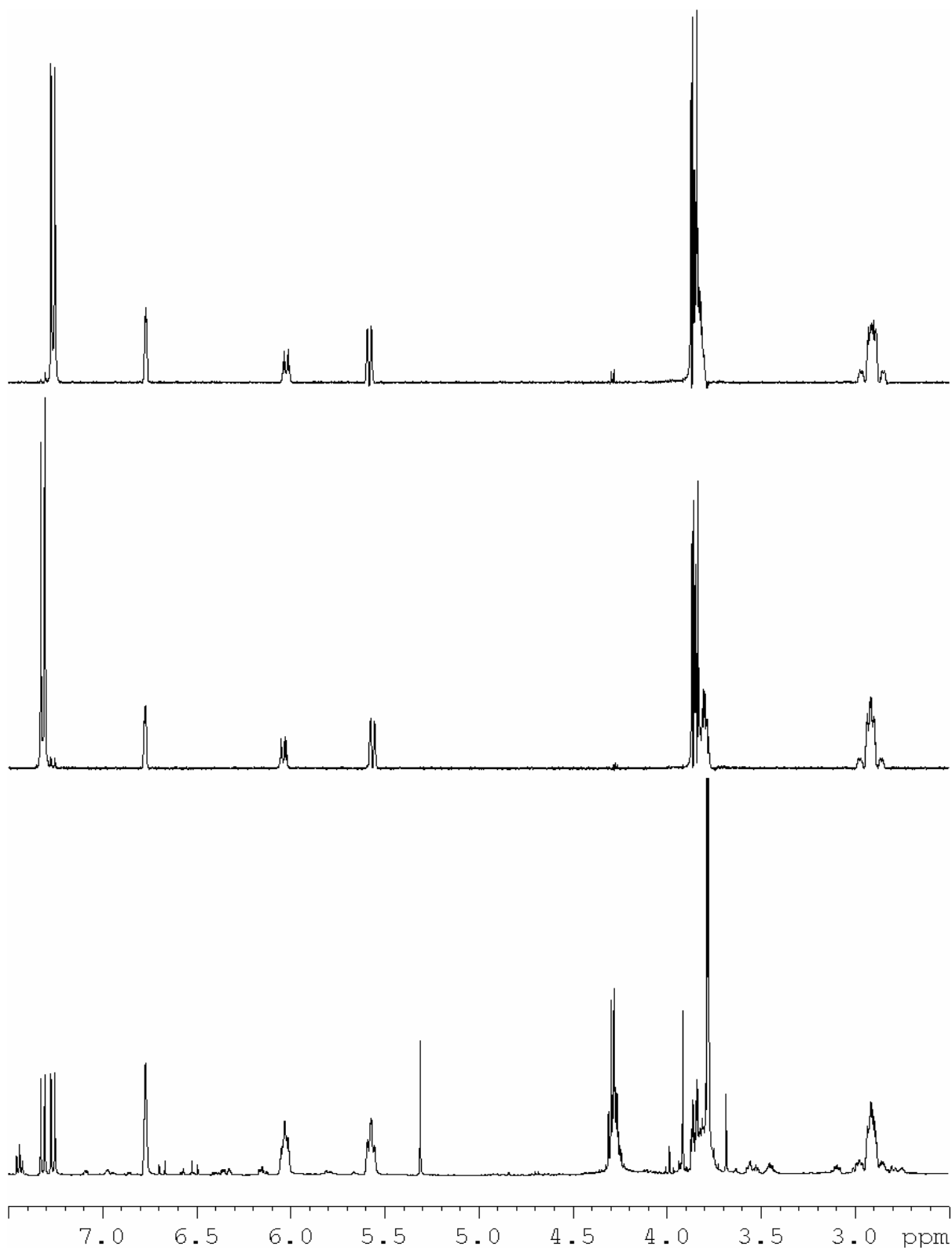


Figure 5-2. ^1H NMR spectrum (bottom) of ethyl propiolate-derived Cope product, and ^1H - ^1H TOCSY spectra based upon irradiation of isolated one-proton signals at δ 7.32 (middle) and δ 7.27 (top).

A ^1H - ^1H COSY spectrum revealed a strong coupling between the vinyl protons at δ 6.03 and δ 5.58 ppm and the total isolation of this pair from the vinyl protons at δ 7.32 and δ 7.27 ppm, each likely a diastereotopic proton of the novel compound. The δ 6.77 and δ 5.58 signals did reveal a trace correlation at extreme vertical expansion. The downfield doublets (δ 7.32/7.27) evidenced as their sole correlation a strong cross peak associated with the downfield region of the complex multiplet spanning δ 3.77–3.87. This broad superimposed signal, which also contained the methyl ester proton signals, integrated to suggest the inclusion of two protons from each diastereomer. Though impossible to discern in the ^1H NMR spectrum, these complex and slightly offset one-proton signals were made clear in the separate ^1H - ^1H TOCSY spectra (Figure 5-3).

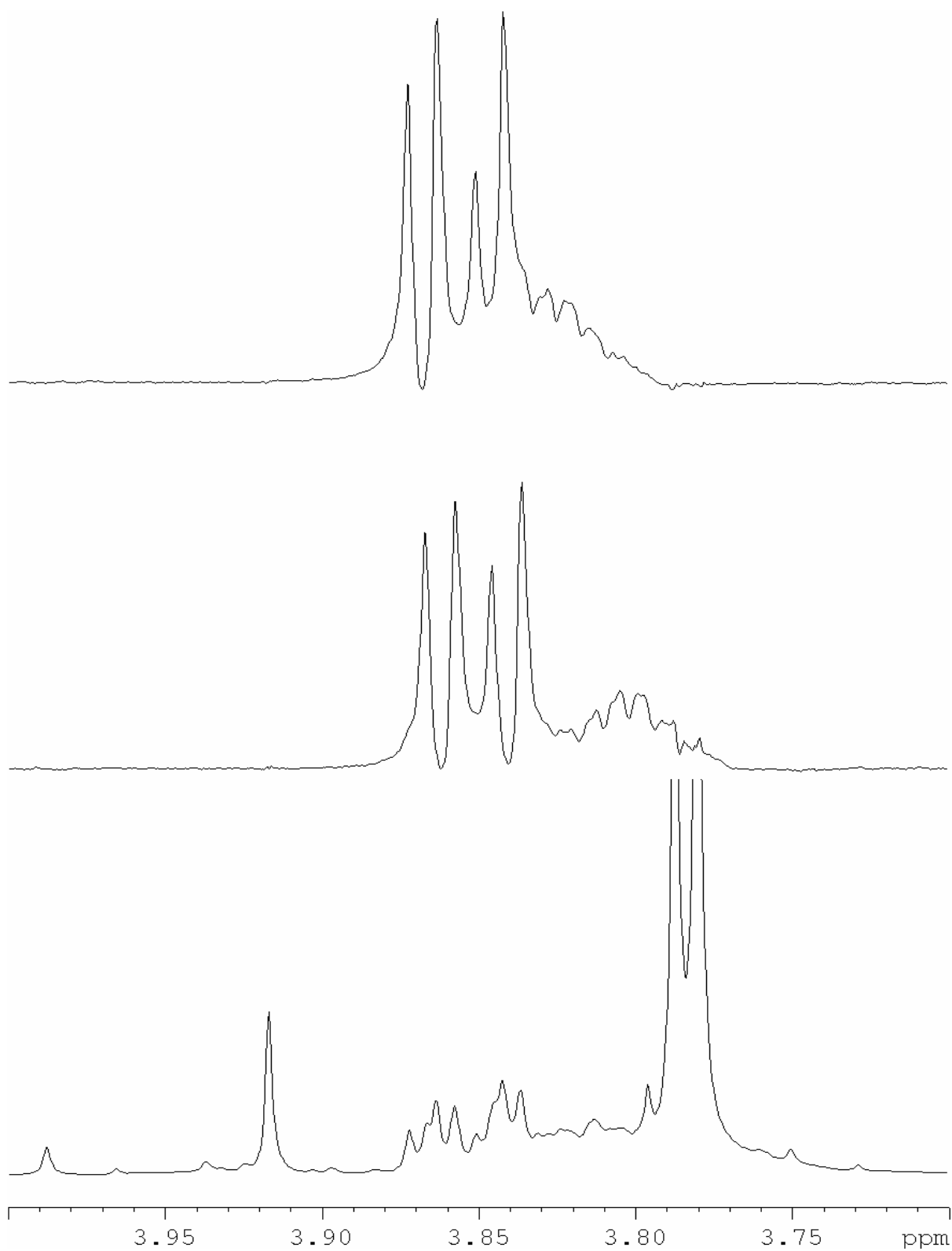


Figure 5-3. Scale-expanded ^1H NMR spectrum (bottom) of ethyl propiolate-derived Cope product, and ^1H - ^1H TOCSY spectra based upon irradiation of isolated one-proton signals at δ 7.32 (middle) and δ 7.27 (top).

Their chemical shift range was appropriate for deshielded protons at sp^3 centers. As illustrated in the scale expansions of the 1H - 1H TOCSY spectra, the downfield region of the superimposed signal resolves as a doublets-of-doublets from each diastereomer, each expressing vicinal magnitude couplings (δ 3.86, dd, $J = 10.7, 4.6$ Hz; δ 3.85, dd, $J = 10.6, 4.8$ Hz). One coupling partner is accounted for as the vicinal vinyl proton, requiring another vicinal proton. This relationship permits the formulation of the partial structure indicated in Figure 5-4.

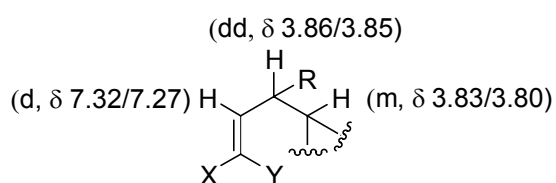


Figure 5-4. Initial partial structure of novel compound.

The second vicinal coupling partner is assigned as the diastereotopic proton multiplets (δ 3.83/3.80) that constitute the balance of the broad signal under consideration. In the 1H - 1H COSY spectrum, the only obvious off-diagonal correlation apparent for the downfield (δ 3.86/3.85) region is to the downfield doublets at δ 7.32/7.27. An expanded view of this region in the 1H - 1H COSY spectrum revealed suggestive peaks slightly displaced from the diagonal that indicated coupling, within the broad combined signal, of the downfield doublets-of-doublets to the upfield multiplets. The vicinal disposition of these protons was conclusively established by a series of 1H - 1H TOCSY spectra based upon irradiation of the doublet at δ 7.32 with varying mixing times. At 35 msec mixing time, only the δ 3.85 doublet-of-doublets is evident. With increasing mixing times, the subsequent spectra witness the evolution of the upfield multiplet (δ 3.80) in advance of any other peaks.

The presence of two methyl ester proton signals indicated that the ring-opened adduct's carbomethoxy moiety was unaltered; coupled with the presence of three interrelated vinyl protons — two on one double bond (δ 6.03, 5.58) and the third (δ 6.77) very weakly correlated to one proton of the pair — and the reasonable presumption that the ring was intact, these data suggested a doubly-substituted deconjugated cyclohexadiene, with one substituent on a double bond and the other at one of the intervening sp^3 carbons. The two-proton signal at δ 2.92 showed a strong correlation to this region, leading to its speculative assignment as the ring methylene proton pair demonstrating the 5J coupling (to the proton at the substituted position) typical of cyclohexa-1,4-dienes.^{1,2} This tentative formulation is supported by the 1H - 1H COSY data. The two multiplets (δ 3.83/3.80) exhibit four clear correlations aside from the apparent vicinal correlation in contact with the diagonal signals. Strong and weak cross peaks to the vinyl protons at δ 5.58 and 6.03, respectively, associate the δ 3.93/3.80 signals with the unsubstituted vinyl fragment. A moderate intensity correlation to the vinyl proton at δ 6.77 establishes the substituted double-bond as another attachment to the methine carbon, conclusively extending the partial formulation to comprise the further elements in Figure 5-5.

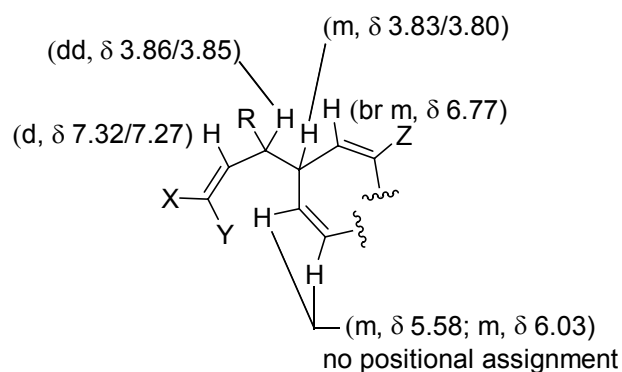
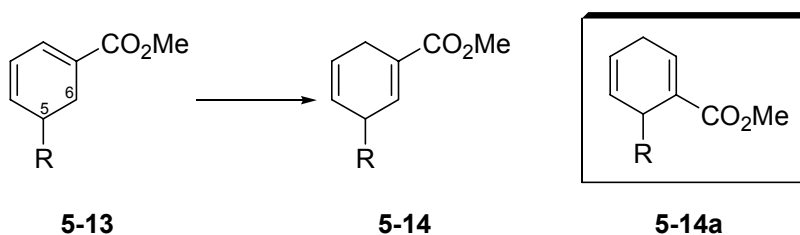


Figure 5-5. Expanded partial structure of novel compound.

The two proton multiplet centered at δ 2.92 exhibits a strong correlation to the vinyl signal at δ 6.03, and a weaker correlation to that at δ 6.77. Absent is a correlation to the vinyl proton at δ 5.58, indicating the absence of either vicinal or allylic coupling. An additional strong correlation relates the signals at 2.92 and δ 3.83/3.80. As indicated, this correlation is a striking feature of cyclohexa-1,4-diene systems, reflective of the unusually large 5J coupling available to the protons at the sp^3 centers at C3 and C6. The association of the methylene group with both vinyl fragments definitively closes the six-membered ring as per the overall ring arrangement already ventured.

The lack of a strong vinyl proton correlation for the signal at δ 6.77 indicated its participation in the substituted double bond. Its chemical shift was consistent with the double-bond substituent being electron-withdrawing. A reasonable ring assignment at this stage was that the double bond was conjugated to the carbomethoxy group carbonyl as in the starting material, but that the double bond had allylicly isomerized to install the correct double-bond arrangement (Scheme 5-2).



Scheme 5-2. Allylic isomerization to the likely ring arrangement of the unidentified product.

At this stage, the possibility was recognized that a structure **5-14a**, isomeric with **5-14**, had been generated in which the ring carbomethoxy group was situated at the other end of the double-bond. Recourse to the connectivity information provided by the HMBC spectrum did not unambiguously distinguish between the two regioisomeric possibilities;

however, closer consideration of the coupling information evident in the ^1H NMR spectrum settled the positional question in favour of partial structure **5-14**. It was reasoned that both systems **5-14** and **5-14a** should exist in a boat-like conformation with the R group in the stereochemically less-hindered position, as is expected for 1,4-cyclohexadiene systems that are substituted at the sp^3 positions, unlike the normally planar unsubstituted system. The orientation of the R group cannot be definitively decided upon as either pseudoaxial or pseudoequatorial, as the literature concerning the conformations of these systems details the considerable experimental difficulties inherent to these determinations as well as numerous ambiguities in the results. It suffices for the current issue to observe that the decisive ^1H NMR resonance at δ 6.77 is a broad singlet, revealing multiple finely spaced shoulders in expanded views of carefully obtained high resolution spectra. If the functional disposition were as in **5-14a**, it would be expected that the δ 6.77 hydrogen would experience a dihedral relationship to one of the vicinal methylene hydrogen atoms that would be evidenced as a substantial vicinal magnitude coupling (Figure 5-6). The absence of such a coupling indicates that the diagnostic proton has only one vicinal coupling partner on an sp^3 center, but that the fixed dihedral relationship drastically reduces the magnitude of the coupling constant.

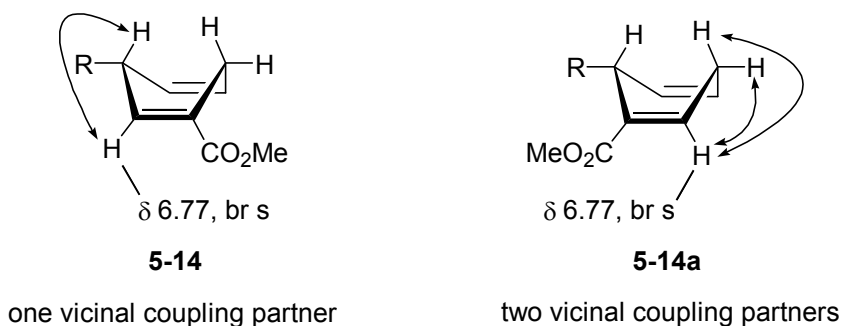
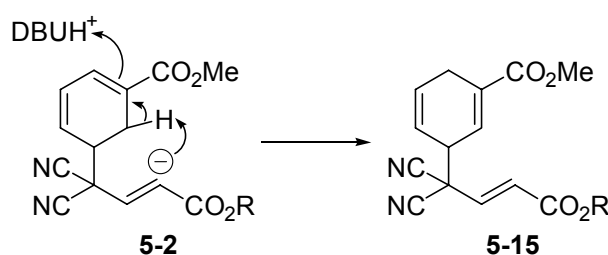


Figure 5-6. Determination of ring substitution pattern through observed ^1H – ^1H coupling pattern to decisive δ 6.77 resonance.

The smooth conversion to the main product of general type **5-14** did not seem consistent with DBU-induced double-bond migration; indeed, the C5 proton is expected to be more acidic than that at C6, due to its allylic relationship to the π -system in conjugation with the C1 α -carbonyl and residence at a position substituted with the strongly electron-withdrawing side-chain, as compared to the C6 proton situated in allylic cross-conjugation to the C1 α -carbonyl. If allylic isomerization was the pathway to the observed product, intramolecular reaction of the intermediate adduct anion seemed more likely to furnish almost exclusively a single product (Scheme 5-3).



Scheme 5-3. Intramolecular mechanism for ring allylic isomerization.

Such a result would nevertheless be remarkable in that subtle electronic or geometric factors inherent to the vinyl anion/allenolate intermediate **5-2** would be sufficiently powerful to constrain it to six- rather than five-centered deprotonation (of the C5 proton), and to preclude tandem conjugate addition; in addition, intramolecular reaction would be sufficiently favourable to outpace proton abstraction from DBUH^+ . Moreover, further reaction would have to occur in the side-chain to generate a product consistent with the spectral data: only one vinyl proton can be assigned to the side-chain, whereas that of **5-15** contains two (Figure 5-7). In addition, structure **5-15** does not exist as diastereomers.

Taking into account several reasonable shift equivalences, the ^{13}C JMOD spectrum indicated that the unknown product was a direct adduct, and had suffered no elimination. The presence of two nitrile carbon signals for each diastereomer, the large coupling constant of the side chain vinyl proton doublet (> 10 Hz), and its correlation to a midfield signal (ca. δ 3.8) called for a proton on an sp^3 carbon vicinal to the vinyl proton. It was imagined that the compliant structure might have been generated through 1,3-nitrile migration within the side-chain. The double-bond position was assigned on the basis of the ^1H - ^1H TOCSY spectrum, which revealed that both ca. δ 3.8 one-proton signals had further vicinal-magnitude couplings for which to account (Figure 5-7).

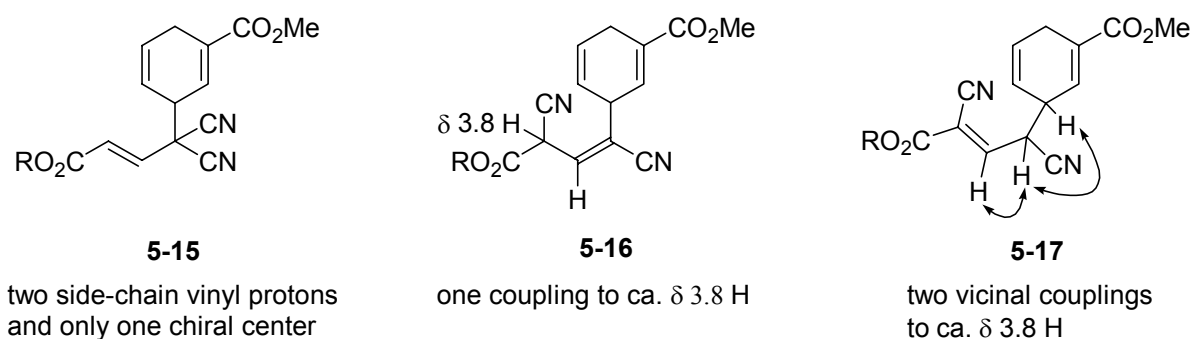
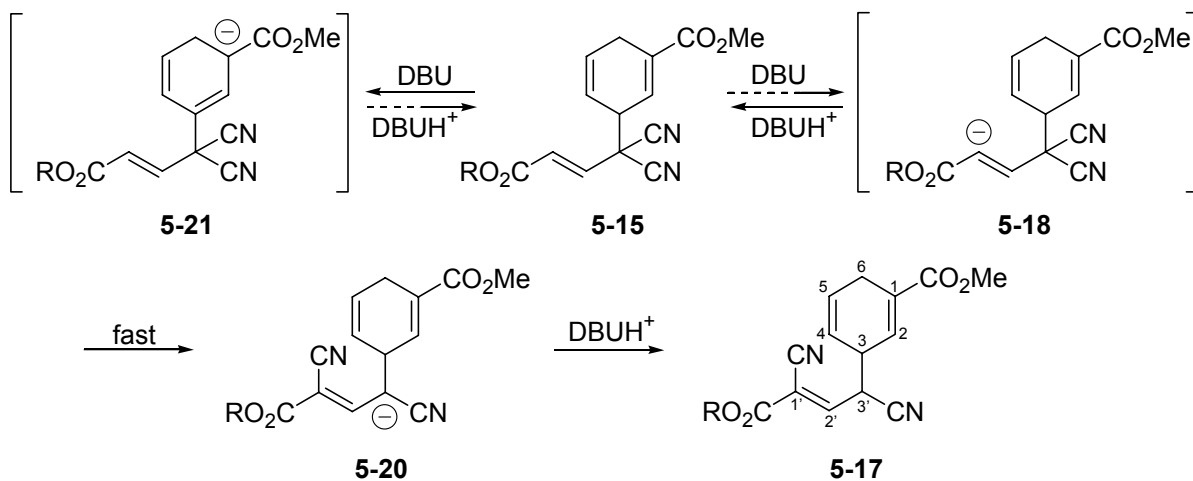


Figure 5-7. Potential double-bond position and substitution assignment to **5-17** on the basis of side-chain vinyl proton count and vicinal proton coupling pattern.

Such a 1,3-transfer of a nitrile group would have to occur by an anionic mechanism (Scheme 5-4), which is depicted as proceeding from an already-established ring double-bond isomerization. Vinyl anion **5-18** would be available by either of two means: by its survival from initial adduct formation, throughout the previously described DBU-induced allylic isomerization; or, by regeneration by DBU after having been neutralized in its role in intramolecular allylic isomerization of the ring as per Scheme 5-3. Its 4-*exo*-dig addition to the nitrile (to generate imine anion **5-19**) to the exclusion of 5-*exo*-trig cyclization onto the ring C2 would have to arise from the same geometric constraint that has been invoked to explain

either the unreactivity of **5-21** (Scheme 5-5) or the reversibility of its reactions, and the fast and irreversible reaction of any equilibrium quantity of **5-18** formed via neutral **5-15**, to give the anion **5-20** of putative identity **5-17**.



Scheme 5-5. Pathway to putative identity **5-17** via side-chain vinylic deprotonation.

Whatever the dubious selectivities inherent to its generation, **5-17** seemed to satisfy the available characterization data and was mechanistically feasible. It met the demand of two quaternary (C1 and C1') and four singly-substituted vinyl carbons (C2', C2, C4, and C5) indicated by the $^1\text{H}-^1\text{H}$ COSY and ^{13}C JMOD spectra, and the single coupling and far-downfield position of one vinyl proton (C2'-H), heavily deshielded at its position on a double-bond in conjugation with two electron-withdrawing groups. The C2'-H (δ 7.32 and 7.37) had the expected HMBC correlations to both nitrile carbons and the side chain ethyl ester carbonyl carbon, which was distinguished from that of the methyl ester by its HMBC correlations to its ester ethyl methylene protons. On a correlational basis, stepwise deduction appeared to permit complete assignment of the proton and carbon signals in confirmation of **5-17** as the identity of the unknown product, allowing for the inability of the two partially superimposed diastereotopic pairs of tertiary one-proton signals at ca. δ 3.8 to play a

definitive role, since the large number of HMBC cross-peaks directed at this region could not be individually assigned, and their vicinal disposition put both in range for many of the same correlations.

Closer consideration of the ^{13}C JMOD peaks brought to our attention the unusually far-upfield position of the quaternary vinyl carbon signal at ca. 92 ppm, which was assigned as side-chain C1' on the basis of its correlation to C2'-H. Typical incremental chemical shift-prediction schemes would not ascribe to its single nitrile substituent the shielding power to push the vinyl carbon signal so far upfield; moreover, the predicted proton chemical shift for C2'-H cis to the C1'-carbomethoxy group is ca. 7.5 ppm, downfield of the observed positions (7.32 and 7.27 ppm). We noted that the data would more closely agree with empirical prediction tools by exchanging the positions of the C1'-carbomethoxy group and C3'-nitrile, although such an exchange was not conclusively demanded on the sole basis of the α -olefinic chemical shift (Figure 5-6).

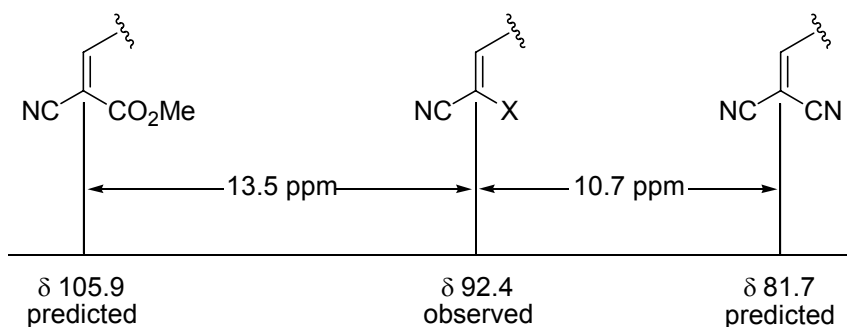


Figure 5-8. Observed olefinic ^{13}C resonance for side-chain C1' of novel compound and estimated resonances for side-chain bearing potential substitutions, as predicted by ChemNMR Pro functionality of CS ChemDraw Ultra®.

Though favouring slightly the geminal dicyano-bearing substitution pattern and prompting further detailed consideration, the observed average (of two diastereomers) chemical shift of δ 92.4 could not unambiguously be assigned as such. The influence of the

contending substitution patterns on the C2' vinyl carbon was therefore considered in turn, again with recourse to the incremental shift prediction tool (Figure 5-7). In this instance, the observed chemical shift more reasonably compels the assignment of substituent X as a nitrile.

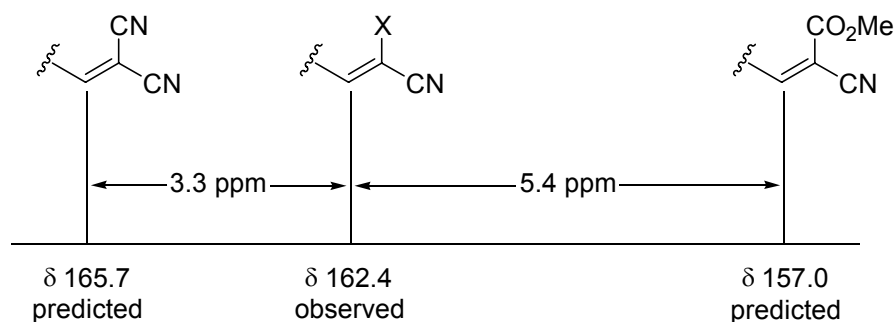
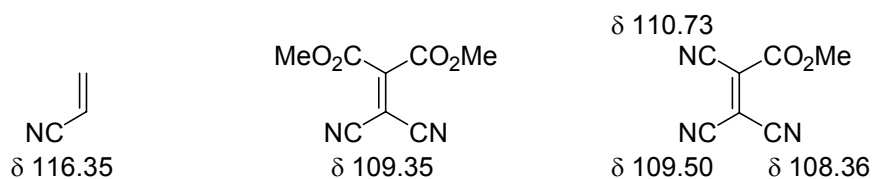


Figure 5-9. Observed olefinic ^{13}C resonance for side-chain C2' of novel compound and estimated resonances for side-chain bearing potential substitutions, as predicted by ChemNMR Pro functionality of CS ChemDraw Ultra®.

The final relevant feature of the available ^{13}C NMR evidence that certifies a geminal dinitrile arrangement is the chemical shift data pertaining to the nitrile carbons. The four nitrile carbons in the diastereomeric mixture of the novel compound resonate in the range 111.3 to 109.9 ppm. It has been demonstrated that the chemical shifts of nitriles at vinyl positions are shifted upfield by geminal nitrile neighbours. For example, in a ^{13}C NMR study of olefins and the additivity relationships and chemical shift influence of nitrile and carbomethoxy substituents, Barfield and co-workers disclosed chemical shift values for olefins bearing geminal nitriles as well as nitrile/carbomethoxy pairings.³ Lone nitrile carbons (acrylonitrile) resonated at δ 116.35. In the geminal nitrile/carbomethoxy case, the nitrile carbon was shifted to δ 110.73, and in a geminal dinitrile case, to δ 109.30. Whereas the nitrile/carbomethoxy pair and the dinitrile pair exhibit nitrile carbon resonances in mutual proximity, the observation that all nitrile carbon resonances for the novel compound are found in this upfield range indicates a geminal vinylic arrangement. If arranged as in **5-17**, two of the nitrile carbon resonances would be observed at ca. δ 117 (Figure 5-8).

Empirical nitrile carbon chemical shifts:



Comparison of novel compound formulations:

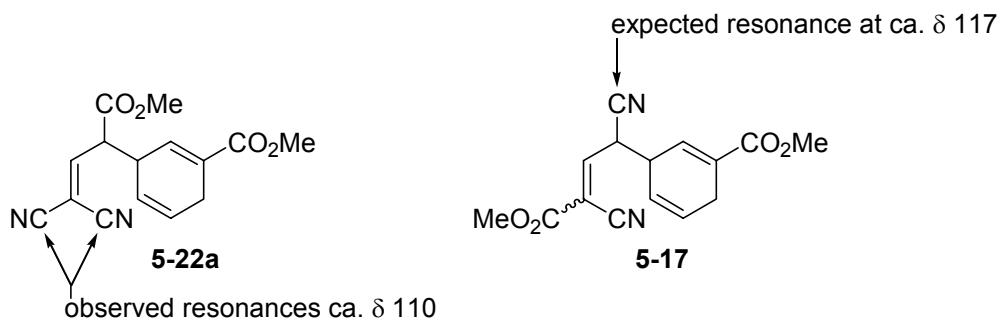


Figure 5-10. Ultimate structural assignment of novel compound as **5-22** on the basis of nitrile carbon chemical shifts.

The EI mass spectrum was interpreted in light of the structural formulation **5-22a** (derived from methyl propiolate; **5-22b** derived from ethyl propiolate) (Figure 5-9). An interesting feature of the peak assignments is the initial fragmentation, which produces methyl benzoate and the side-chain fragment bearing an additional hydrogen derived from the aromatization of the ring. Cleavage and aromatization of the Cope product will be treated in detail and is central to the mechanistic interpretation (see section 5.2.7) that permits discernment of the identity of the reactive species in the rearrangement.

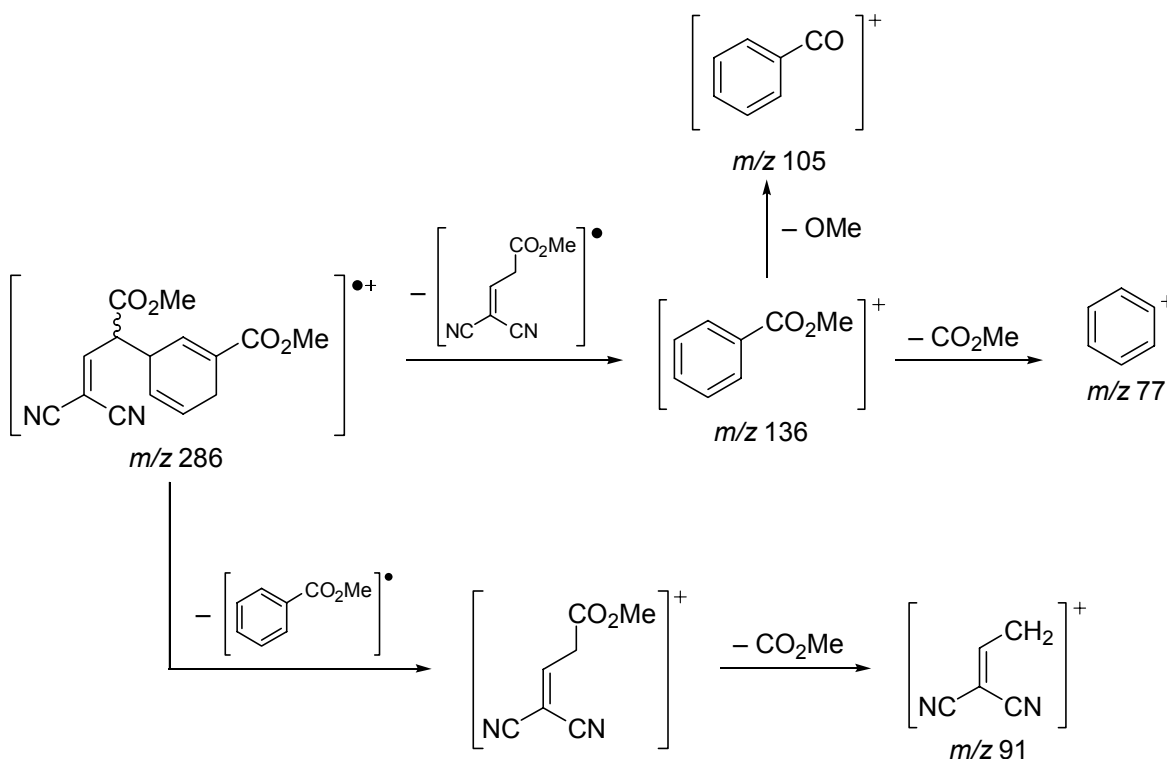
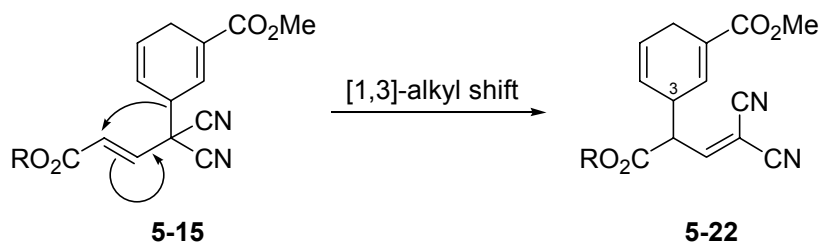


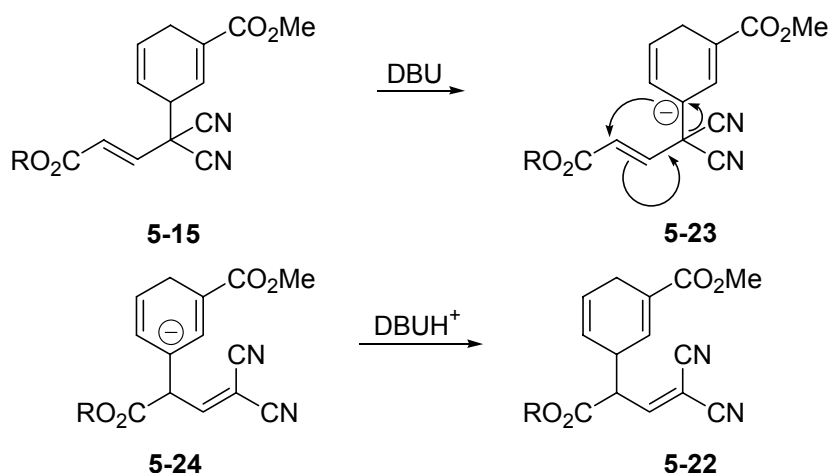
Figure 5-11. Fragmentation of methyl propiolate-derived rearrangement product in EI mass spectrum.

The rapid and nearly quantitative completion of the drastic stepwise sequence of rearrangements required within the side-chain to produce **5-22a** was deemed unlikely, so the exhaustive mechanistic consideration of conceivable reaction pathways that had been undertaken at the initial encounter with the novel compound was reinitiated. Once even remote anionic schemes had been explored, attention was turned to the possibility of a pericyclic process generating **5-22a**. For example, the retention of geminal nitriles, their situation on the double bond and the positioning of the carbomethoxy group on the allylic carbon could be envisioned to arise from the general neutral direct adduct **5-4** by [1,3]-sigmatropic shift of the ring attachment carbon (Scheme 5-6).



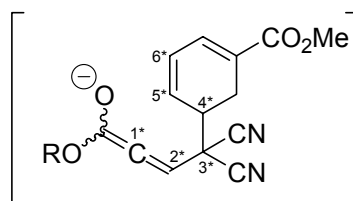
Scheme 5-6. Generation of **5-22** by formal [1,3]-alkyl shift.

Although the presence of geminal nitriles is known to account for remarkably facile, often symmetry-forbidden pericyclic processes, including a variety of unexpected [1,3]-sigmatropic shifts⁴ (*vide infra*), the low temperature ($-10\text{ }^{\circ}\text{C}$) and short reaction time ($< 20\text{ min.}$) in this case suggested that another process was at work. Neither was it concluded that the analogous anionic process was responsible (Scheme 5-7), which would begin with ring C3 deprotonation. The mechanistically cyclic flow of electrons that would bring about the formal σ -bond shift would include a 4-*endo*-trig step that is disfavoured by Baldwin's rules and involves attack at the less electrophilic end of the side-chain double-bond; furthermore, the more expected 3-*exo*-trig attack is available to **5-23**, an outcome later observed and exploited in the exploration of this propiolate chemistry (*vide infra*).

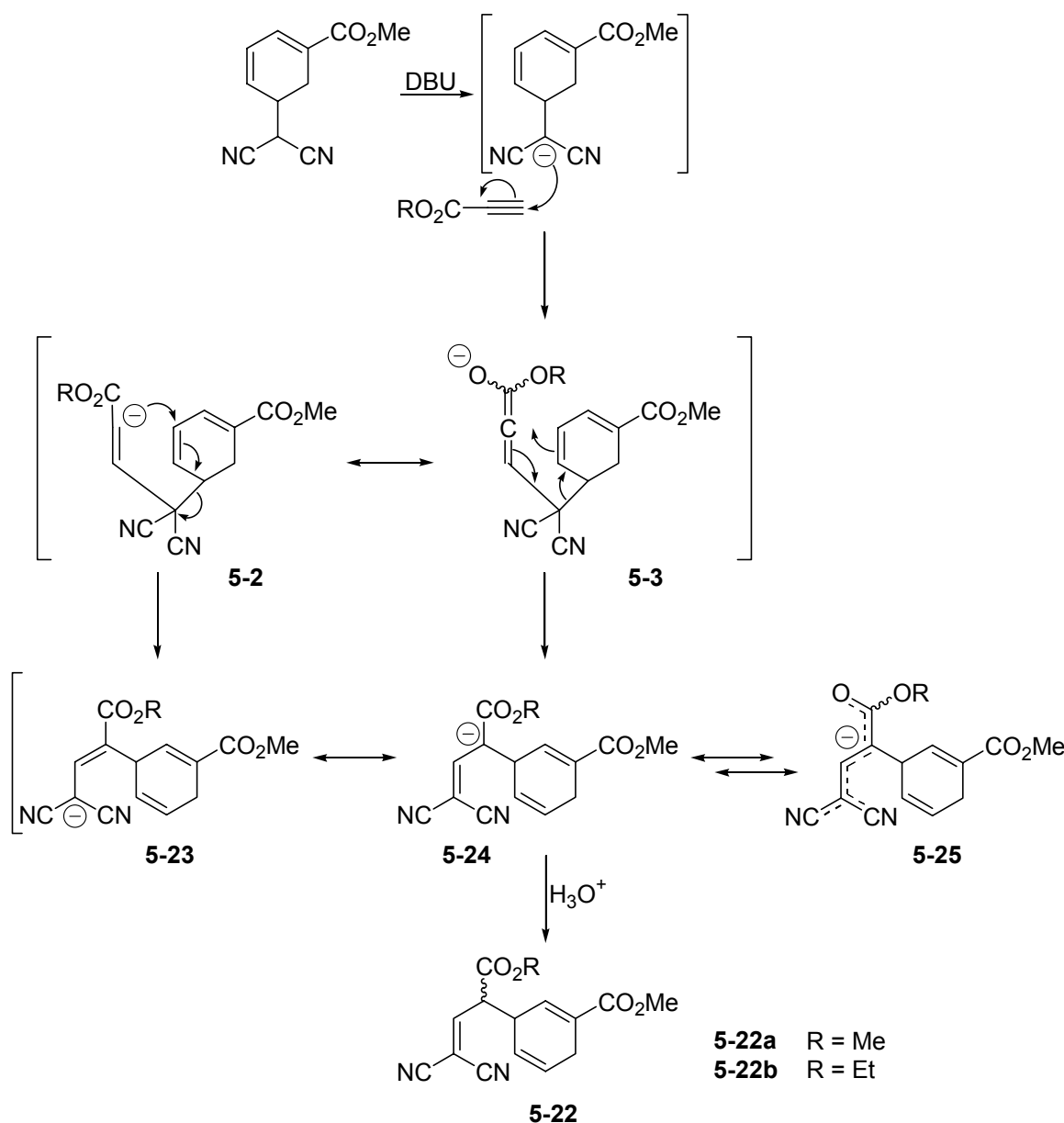


Scheme 5-7. Anionic formal 1,3-shift of C3-C3' bond to generate identity **5-22**.

Still considering a pericyclic route to **5-22**, and keeping in mind the allenolate contributor to resonance hybrid **5-2** ↔ **5-3** of the initial adduct anion, the six-bond array with vinyl termini spanning the allenolate and ring C3–C4 double bond was noted (Figure 5-10).

**5-3****Figure 5-12.** Initial adduct intermediate.

This prompted the ultimate conclusion concerning the process that generates the major product: that the anionic intermediate undergoes a formal allenolate Cope rearrangement to give an enolate that protonates without facial selectivity to give the diastereomeric mixture of **5-22**. Depicted in Scheme 5-8 are two formally equivalent mechanistic possibilities for the conversion: a polar mechanism implicating a discrete vinyl anion (**5-2** → **5-23**), and a sigmatropic rearrangement implicating the allenolate (**5-3** → **5-24**), which respectively furnish resonance contributors **5-23** and **5-24**.



Scheme 5-8. Formal allenolate Cope rearrangement to generate **5-22**.

The possibility that the rearrangement involved an allenol **5-26** or the neutral adduct **5-4** was also recognized (Figure 5-13). The mechanistic implications of later data in the study of this remarkably facile transformation supported a painstaking assessment of the nature of the reactive species within the context of a securely identified formal [3,3]-sigmatropic rearrangement.

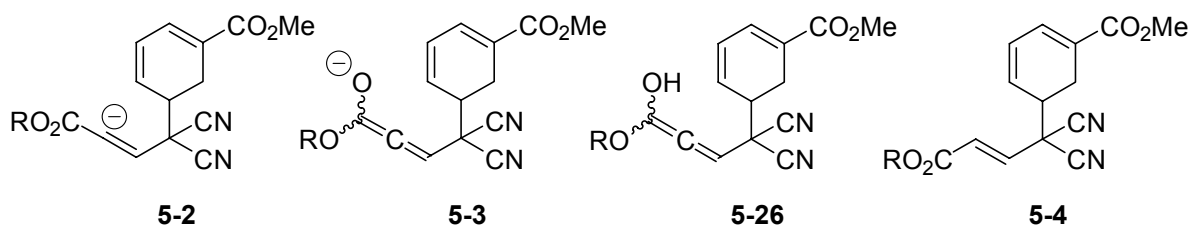


Figure 5-13. Set of potential reactive species in formal [3,3]-sigmatropic rearrangement.

This mechanistic conclusion is appealing because it proceeds from initial adduct formation to the observed product by a mode that establishes all of the considerable structural alterations in a single step. It requires no recourse to combined steps functioning with regio- and chemospecificity. The structural assignment **5-22** is consistent with the comprehensive NMR spectral assignment. The results of this analysis and a representation of the NMR correlation data are presented in Table 1, for the rearrangement product **5-22b** derived from reaction of **5-1** with ethyl propiolate, with reference to the numbering in Figure 5-14.

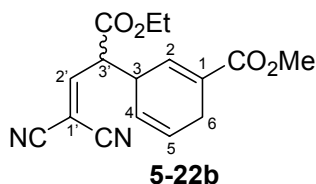


Figure 5-14. Numbering of allenolate Cope rearrangement product cited in Table 5-1.

Table 5-1. NMR spectral correlations (^1H - ^1H COSY, HMQC, HMBC) and positional assignments for formal Cope product **5-22b**.^a

Position	^{13}C JMOD	^{13}C $\delta^{\text{b,c}}$	$^1\text{H}^{\text{b,c}}$											$^1\text{H}\delta$	# ^d	Position		
			7.32	7.27	6.77	6.03	5.58	4.28	3.83	3.79	3.78	2.92	1.33				1.32	
CO ₂ Et	Up	167.31	3	3				3	•, 2							7.32	1	(CN) ₂ CCH
CO ₂ Me	Up	165.99			3	5			•	3	3	3				7.27	1	(CN) ₂ CCH
(CN) ₂ C-C2'	Down	162.49	1 ^f	1				•	•, 2			•				6.77	2	C2-H
(CN) ₂ C-C2'	Down	162.44	1	1				•	•, 2			•				6.03	2	C4-H
C2	Down	134.09			•, 1	•	2		•, 3			3				5.58	2	C5-H
C2	Down	132.52			1		2		3			3	•	•		4.28	4	CO ₂ CH ₂ CH ₃
C1-CO ₂ Me	Up	131.58	•	•	•	•, 4	•		3			•, 2				3.83	4	C3-H, C3'-H
C1-CO ₂ Me	Up	131.06				4			3			2				3.79	3	CO ₂ CH ₃
C4	Down	128.74				1						3				3.78	3	CO ₂ CH ₃
C4	Down	128.16				1			•			3				2.92	4	C6-H ₂
C5	Down	122.56			4		1	•	4			2				1.33	3	CO ₂ CH ₂ CH ₃
C5	Down	120.71			4		1	•	4			2				1.32	3	CO ₂ CH ₂ CH ₃
CN	Up	111.33	3	3														
CN	Up	111.31	3	3														
CN	Up	110.14	3	3														
CN	Up	109.95	3	3														
(CN) ₂ C	Up	92.48	2	2						3								
(CN) ₂ C	Up	92.35	2	2						3								
CO ₂ CH ₂ CH ₃	Up	62.43						1					2	2				
HC3'-CO ₂ Et	Down	52.56					3		1				4					
HC3'-CO ₂ Et	Down	52.42					3		1				4					
CO ₂ CH ₃	Down	51.82									1	1						
C3	Down	39.87	2	2	2	2	3		1, 2				5					
C3	Down	39.61	2	2	2	2	3		1, 2				5					
C6	Up	25.45			3	3	2						1					
CO ₂ CH ₂ CH ₃	Down	13.90						2						1	1			

^a Positional assignments refer to numbered structure in Figure 5-14 (*vide supra*). ^b ^1H and ^{13}C NMR spectra were recorded at 300 and 75 MHz, respectively. ^c Spectra were obtained on a racemic mixture of diastereomers. Six equivalences occurred in the ^{13}C spectrum. ^d Column labelled # indicates proton counts per signal: "1" refers to an isolated one proton signal from one diastereomer; "2" to doubled one-proton signals due to overlap; "3" to discernable one-diastereomer methyl signals; "4" to a doubled two-proton signal (δ 4.28) or to a doubling of two overlapping one-proton multiplets (δ 3.83). Some proton signals will therefore have multiple HMQC correlations. ^e Correlations: "1" refers to one-bond HMQC correlations; values >1 to HMBC correlations; "•" to ^1H - ^1H COSY correlations. ^f Boxed regions cite all possible correlations within a 2D signal if 1D line spacings are too closely spaced to permit unambiguous assignments.

5.2.2 Identification of Minor Components of Cope Product Mixture

Having secured the identity of the major product of our reactions of the ring-opened adduct with methyl and ethyl propiolates, and proposed a mechanism for its formation, we turned our attention to the identification of the minor components of the product mixtures. Based on the consistency of their integrations, we were able to associate the broad, finely-coupled multiplets at δ 6.97 and δ 6.32 with the AB quartet signals at δ 6.6 and δ 6.5 (Figure 5-15).

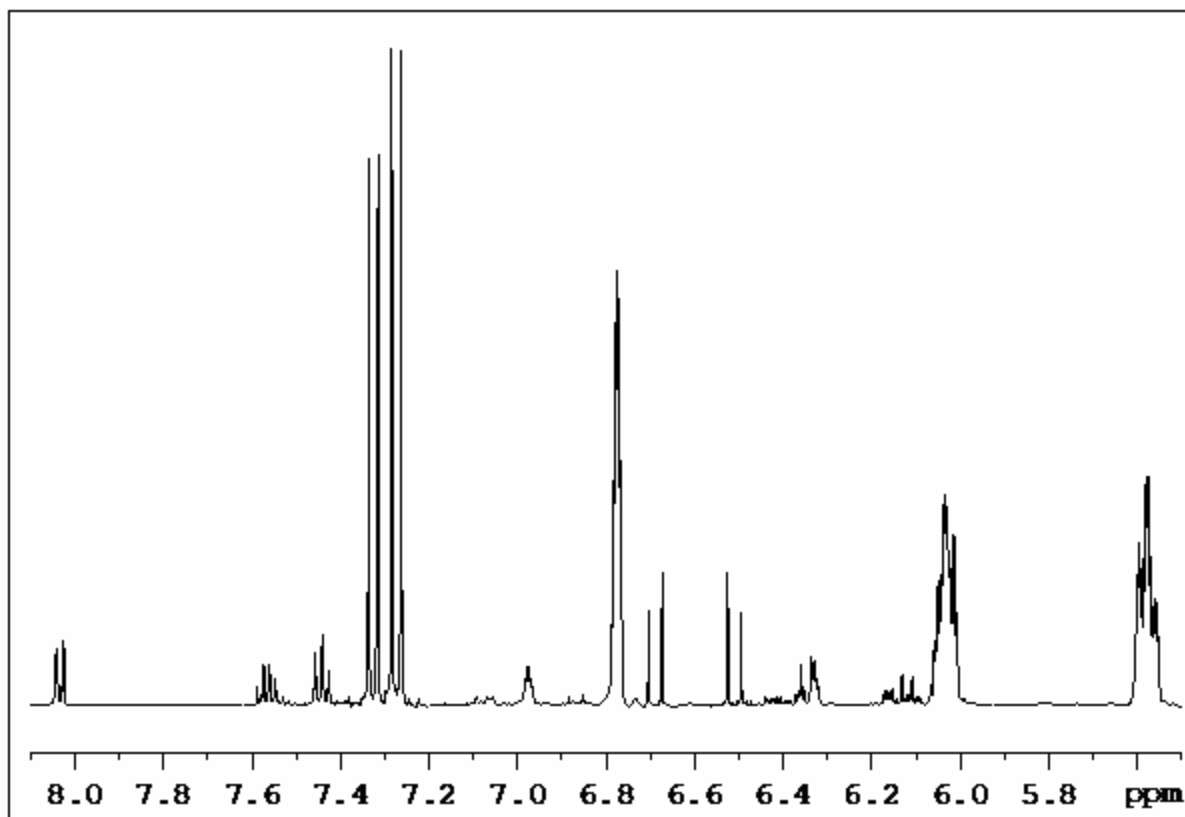
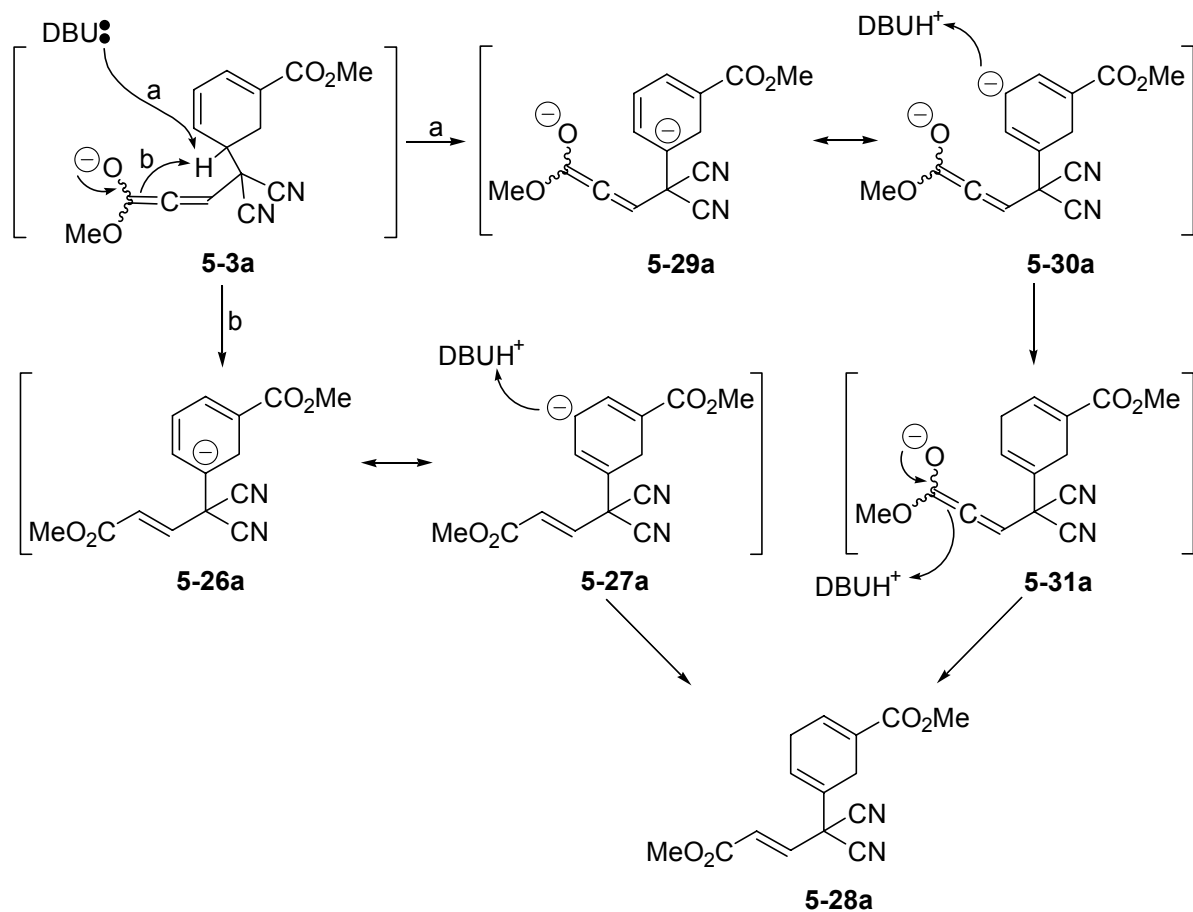


Figure 5-15. Expansion of ¹H NMR spectrum (500 MHz, CDCl₃) of ethyl propiolate Cope product mixture.

The large coupling constant (15.5 Hz) of the slanted pair of doublets, their lack of further coupling, and their chemical shifts immediately suggested a trans-substituted double bond within the side-chain. The far downfield chemical shift of one proton was consistent with that of the C3-vinyl proton of a conjugated ester; the upfield doublet's δ 6.3 shift position could be accounted for by the inductive electron-withdrawing effect of the allylic nitriles. Together, these data suggested a Michael adduct structure for the appendage. In considering the structure of the ring, it was noted that the broad, extremely finely-coupled multiplets at δ 6.97 and δ 6.32 suggested the same ring arrangement that had been encountered as a side product of the alkylation of the ring-opened adduct with 2-iodo-benzyl bromide to generate the substrate for the study of intramolecular Heck reactions. In assigning the parent ring structure of that side product, ^1H NMR spectral support was discovered for the structural formulation as a 1,5-disubstituted cyclohexadiene in a literature report of a 1-trifluoromethylcarbonyl-5-methyl-substituted cyclohexa-1,4-diene generated in a study of the Diels-Alder reactions of β -trifluoroacetylvinylsulfones.¹ The vinyl protons of that and other known compounds of this type demonstrate vicinal and allylic couplings of a magnitude sufficient only to broaden their signals into unresolved complex multiplets, in this literature instance (at 400 MHz) referred to as broad singlets. In that study, the two pairs of ring methylene protons are superimposed and so do not clearly reveal the second remarkable spectral characteristic typical of these systems: large mutual 5J couplings of the two pairs of methylene group protons. The close similarity of the ^1H NMR spectral features of the minor product's ring protons to those encountered in the Heck reaction substrate and the literature compound supported the structural assignment as a deconjugated adduct (**5-28a**) of the ring-opened compound and the propiolate ester. The ^1H NMR signal of one ring-methylene

proton pair is completely obscured by main product signals (Table 5-2 notes: assigned as C6-protons); whereas the other ring proton pair signal (Table 5-2: C3-H₂) is superimposed on the C5-H signal of the lesser quantity of the ring-opened adduct, it nevertheless evidences sufficient broadness and coupling to indicate the cited long-range coupling and to further support our assignment.

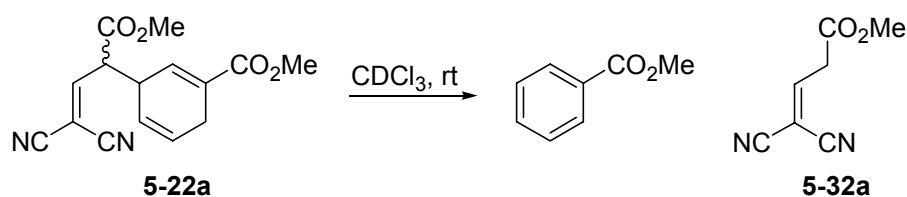
The deconjugated adduct is depicted in Scheme 5-9 as arising by two possible pathways: by the first (path a), intramolecular neutralization of the adduct allenolate **5-3a** by the ring C5-proton would generate the ring-carbanionic intermediate **5-26a** ↔ **5-27a**, which would protonate at ring C3 to give **5-28a**; by the second (path b), DBU deprotonates the ring C5-proton during the lifetime of the allenolate to give intermediate **5-29a** ↔ **5-30a**, followed by ring-deconjugative protonation to **5-31a** and allenolate neutralization. A reasonable alternative is stepwise intermolecular neutralization of **5-3a** by DBUH⁺ to give the direct adduct **5-4a**, followed by DBU-catalyzed allylic isomerization.



Scheme 5-9. Formation of deconjugated adduct **5-28a**.

The shift positions and intensities of the aromatic proton signals at δ 8.05, 7.56, and 7.44 indicate that this component is methyl benzoate, a conclusion that was not immediately clear. The EI mass spectrum contains strong signals at m/z 136 (methyl benzoate), 105 (benzoyl fragment), 77 (phenyl ion) and 59 (carbomethoxy fragment). The ¹H NMR spectrum of the crude mixture did not disclose signals that could definitively indicate the presence or structure of the free moiety whose cleavage allowed the generation of methyl benzoate. It is possible that acid workup either brings about a reaction of the side-chain whose product contains no vinyl protons, or that the side-chain fragment or its products are largely extracted by the acidic aqueous phase. Indeed, the integral of the ¹H NMR signal of the C4-proton of methyl benzoate is not perfectly consistent with the two double-intensity

signals of the remaining pairs of ring protons, and close examination at high expansion does reveal further lines, but it is not certain that these arise from the trace presence of the free moiety. We ultimately did observe the clean production of increasing quantities of the methyl benzoate/stable free moiety pair from the neutral formal Cope product (Scheme 5-10) in NMR samples retained in CDCl_3 at room temperature over the course of several days. This cleavage/aromatization reaction and the susceptibility of the cleaved side-chain or its deprotonated DBUH^+ salt to reaction with acid to produce complex product mixtures elicited further experimental and mechanistic scrutiny.



Scheme 5-10. Products of cleavage/aromatization of the formal Cope product.

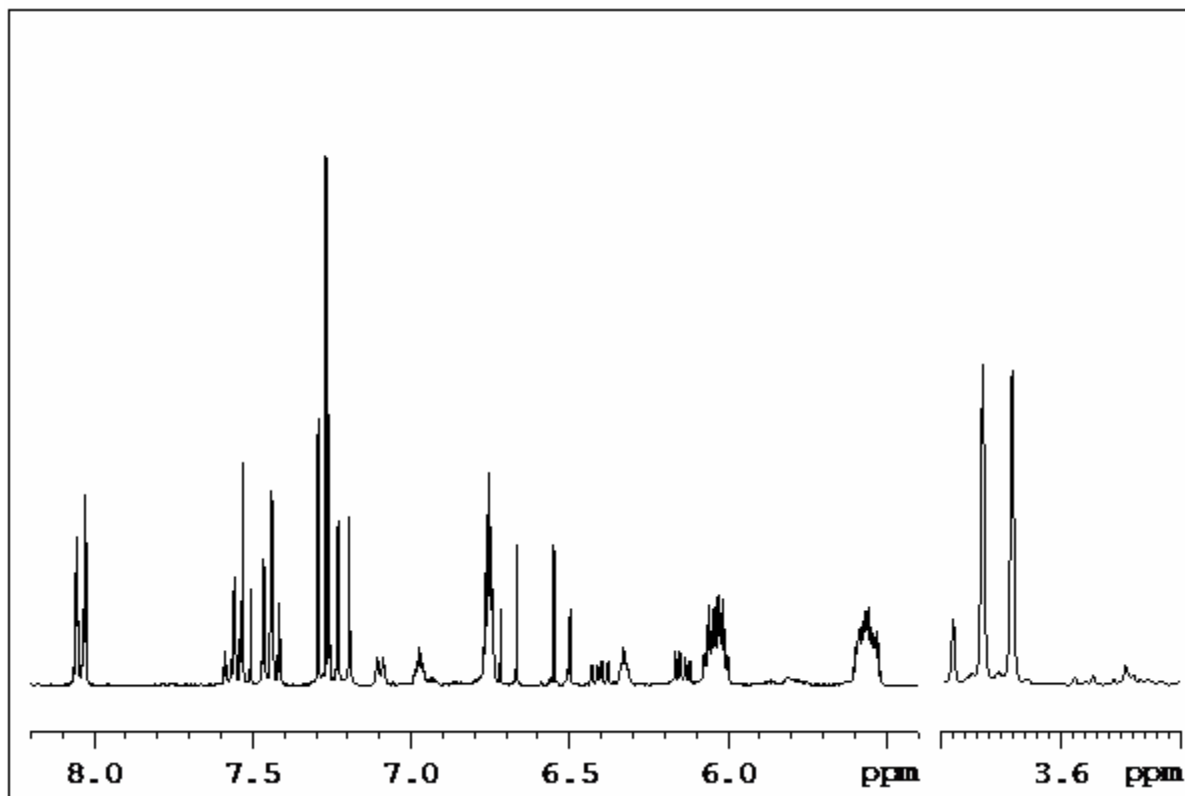


Figure 5-16. Expansion of ^1H NMR spectrum (300 MHz, CDCl_3) of methyl propiolate Cope product mixture after several days' retention at room temp. in CDCl_3 .

The identity of **5-32a** as a discrete compound was not immediately evident when we examined ^1H NMR spectra of samples in which CDCl_3 incubation had brought about its generation stoichiometrically with respect to methyl benzoate. We initially failed to appreciate the difference between spectra of the crude mixtures, whose δ 7.6–7.5 signal had approximately the expected one-half intensity with respect to the two related two-proton aromatic signals, and aged samples (in the case of Figure 5-16 a sample retained in CDCl_3 after column chromatography had removed the aromatic component) which had a broader and more complex signal of an intensity equal to the other aromatic proton signals. Considered in isolation and prior to the assignment of methyl benzoate as a constituent of the crude mixtures, the ^1H - ^1H COSY spectrum of the aged sample led us to briefly associate the

δ 7.6–7.5 signal with the equal-intensity doublet at δ 3.65 (differently-scaled inset signal in Figure 5-16). We were immediately forced to reconsider by the unreasonably large coupling constant (7.3 Hz) of the construed benzylic proton to the ring proton. The integral expansions of the sole 500 MHz ^1H NMR spectrum (Figure 5-17) from among our qualitative time-course observations of the Cope product-to-aromatic/cleaved moiety **5-32a** conversion confirmed our suspicion that we were confronted with two discrete components with lower field ^1H signal overlap in the aromatic region: the higher field spectrum resolved the multiplet into a perfect triplet (δ 7.53, $J = 7.3$ Hz) and the triplet-of-triplets (δ 7.56) of what we could now assign as methyl benzoate.

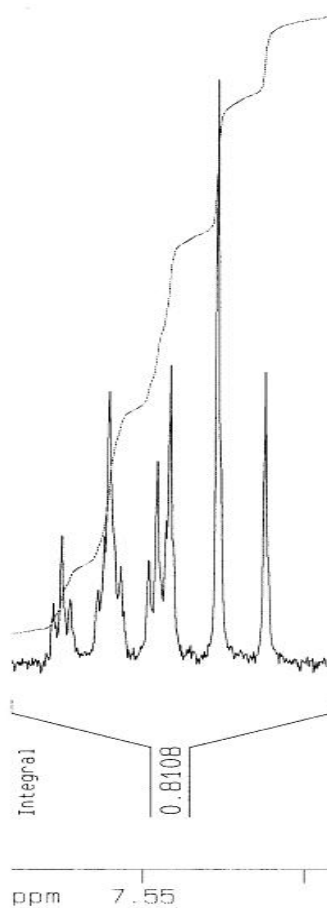
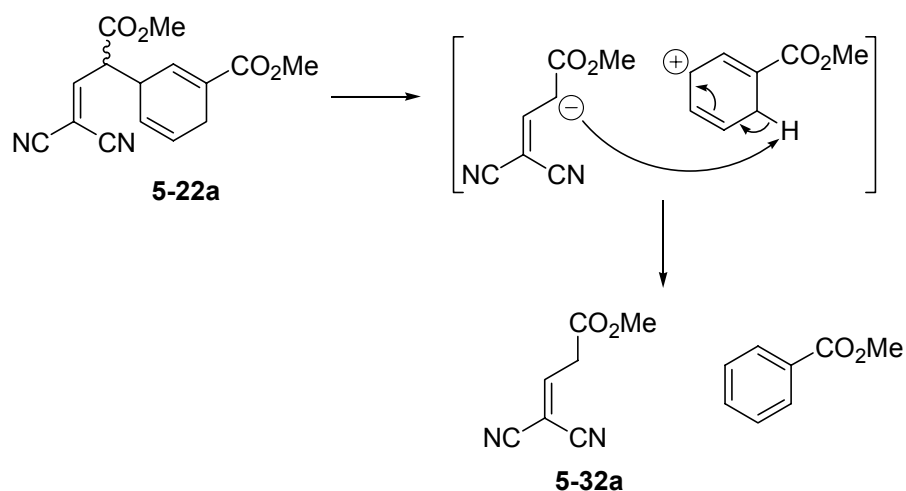


Figure 5-17. ^1H NMR spectral expansion reveals discrete signals of methyl benzoate and **5-32**.

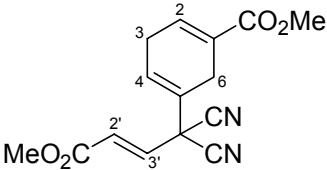
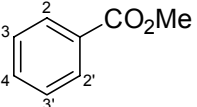
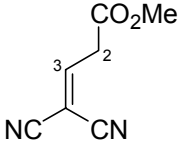
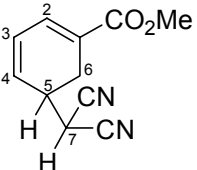
The extreme downfield chemical shift of the necessarily vinylic proton triplet made it clear that, as in the Cope product, **5-32a** contained a geminal-dinitrile-substituted methyldene arrangement, and that the vinylic proton was now coupled to two allylic protons. The cleaved side-chain structure **5-32a** can be considered to formally arise by heterolytic cleavage with proton transfer to the departing side-chain anion from a ring methylene proton, and concluding with bond rearrangement to aromatize the ring (Scheme 5-11). Specific mechanistic possibilities are also examined (*vide infra*).



Scheme 5-11. A formal mode of cleavage and aromatization of **5-22a**.

The final minor constituent evident in Figure 5-16 and to a lesser extent in Figure 5-15 is a small quantity of the ring-opened adduct. Table 5-2 presents the ¹H NMR spectral details of the minor constituents of the Cope product mixtures.

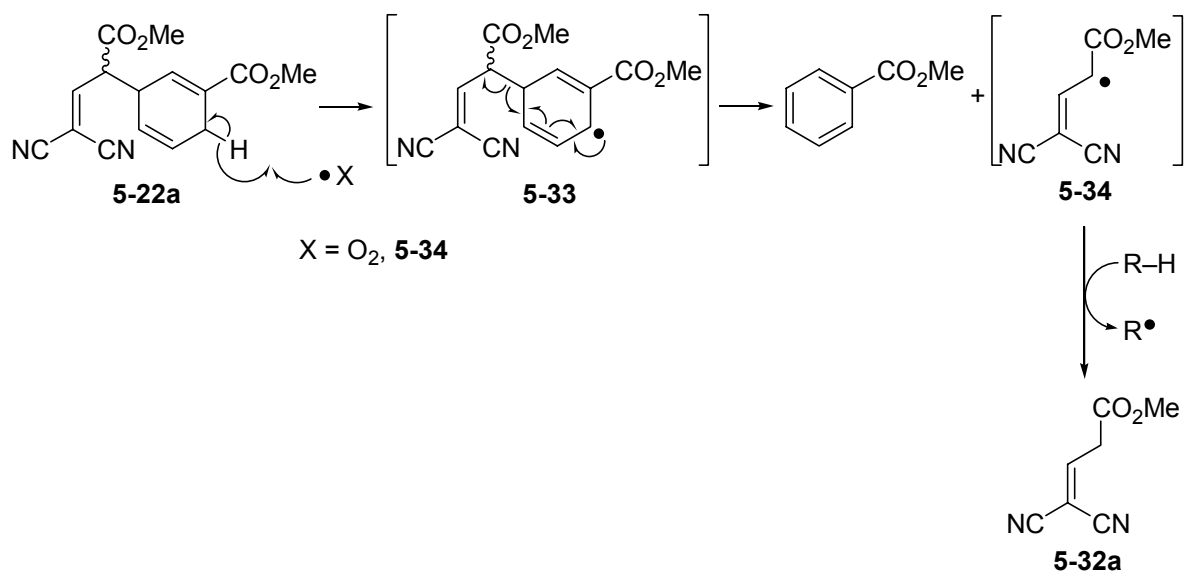
Table 5-2. Minor constituents^a of the formal allenolate Cope reaction product mixture.

Compound	Ratio ^c	Selected ¹ H NMR data ^b				
		δ (ppm)	Number of protons	Coupling pattern	J (Hz)	Assignment
 5-28a	0.20	6.98 6.69 6.52 6.33 3.23	1 1 1 1 2	m d d m br m	15.4 15.4	C2-H ^d C3'-H ^d C2'-H ^d C4-H ^d C3-H ₂ ^{d, e}
	0.33	8.05 7.56 7.44	2 1 2			C2-H, C2'-H H C4-H C3-H
 5-32a	0.33	7.53 3.79 3.65	1 1 2	t s d	7.3 7.3	C3-H CO ₂ CH ₃ C2-H
 5-1	0.18	7.07 6.38 6.12 3.78 3.69 3.11 2.79	1 1 1 3 1 1 2	d ddd dd s d br m dd	5.5 9.5, 5.5, 1.4 9.5, 4.5 8.1 8.4, 1.6	C2-H C4-H C3-H CO ₂ CH ₃ C7-H C5-H ^e C6-H ₂

^a With reference to Figure 5-16: product from reaction with methyl propiolate. Sample incubated in CDCl₃ at room temp. for 11 days prior to recording of spectrum. ^b Recorded at 300 MHz in CDCl₃. In most cases, only isolated signals are cited. ^c Ratios with respect to 1 for single-proton signals of **5-22a**. ^d Assignments for **5-28a**: discrimination between ¹H signals for C2 and C4; C3 and C6; and C2' and C3' by chemical shift considerations alone. C6-protons are obscured by signals from **5-22a** and are not listed, but were observed by ¹H selective TOCSY at δ 3.0. ^e Compound **5-28a** C3 methylene protons and ring-opened adduct C5-proton overlapped: discussion in main text.

5.2.3 Cleavage and Aromatization of Cope Product 5-22

An immediate possibility for the means of the slow, room temperature conversion of **5-22a** to methyl benzoate and **5-32a** in CDCl_3 is a radical mechanism (Scheme 5-12), perhaps initiated by molecular oxygen, which was neither removed by sparging the solvent with inert gas in advance, nor rigorously excluded from the plastic-capped NMR tube for the duration of the observations.



Scheme 5-12. Radical mechanism for the conversion of **5-22a** to methyl benzoate and **5-32a**.

Homolytic cleavage of the C6–H bond would furnish cyclohexadienyl radical **5-33**, which would undergo ring bond rearrangement to aromatize and release allylic radical **5-34**, and the process would conclude with hydrogen atom abstraction, in a chain-propagating step, from **5-22a**.

The observation that the progress of the cleavage/aromatization reaction was much faster for one of the diastereomers of **5-22a** (Figure 5-18) demonstrated that substrate stereochemistry was influential, which seemed to argue against a radical mechanism insofar as a role for diastereochemical discrimination is not readily apparent.

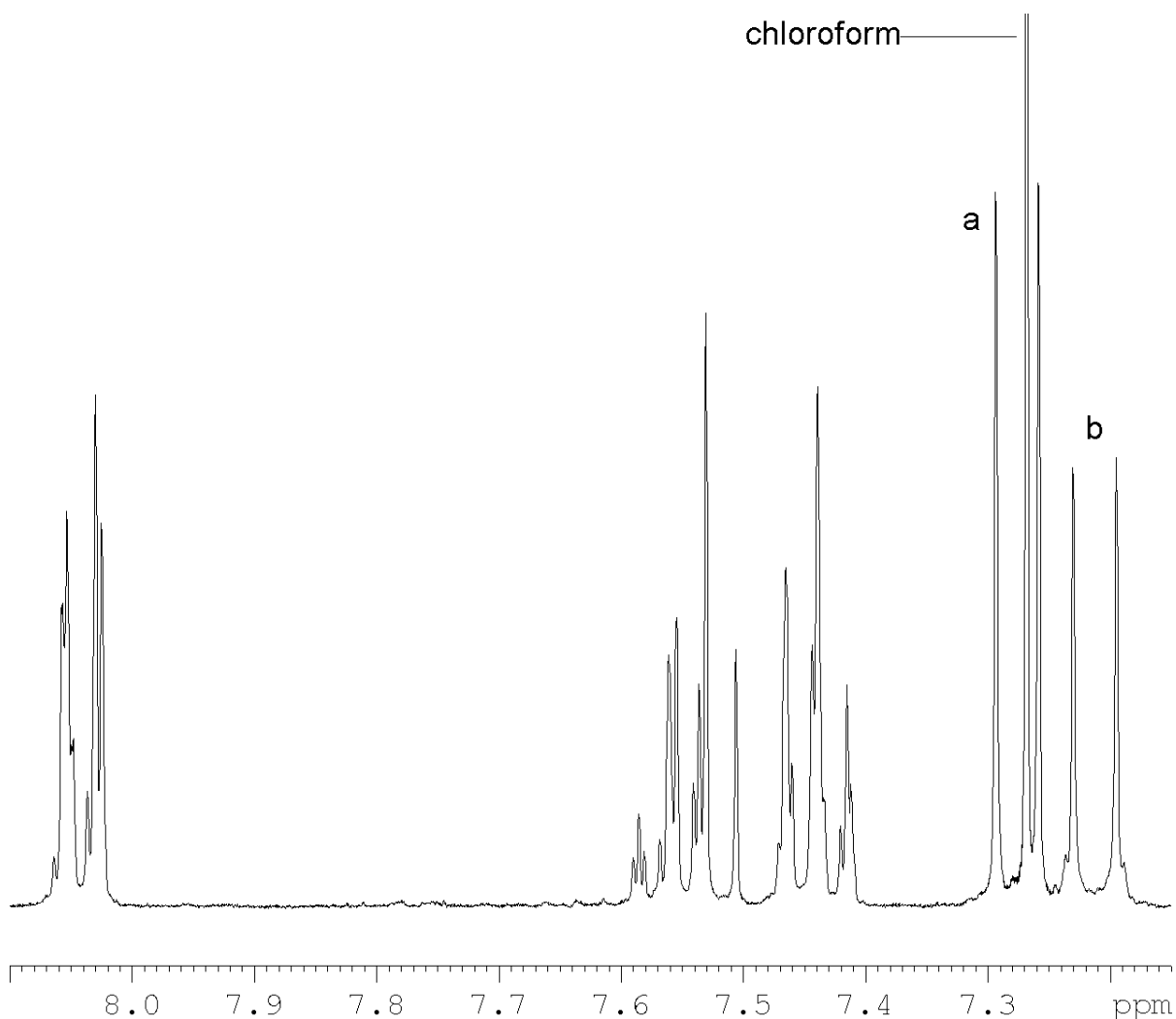
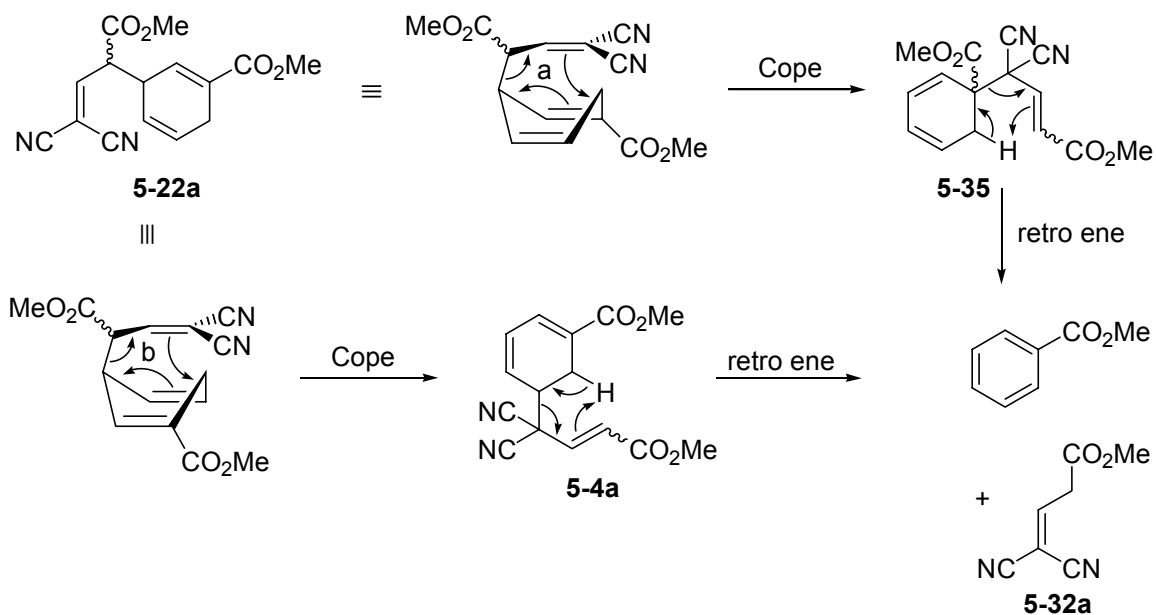


Figure 5-18. ^1H NMR spectrum (300 MHz, CDCl_3) of methyl propiolate Cope product after several days' aging in CDCl_3 . The two diastereomers were nearly equimolar initially, but one diastereomer (doublet b; relative stereochemistries unassigned) has declined to a greater extent than the other (doublet a).

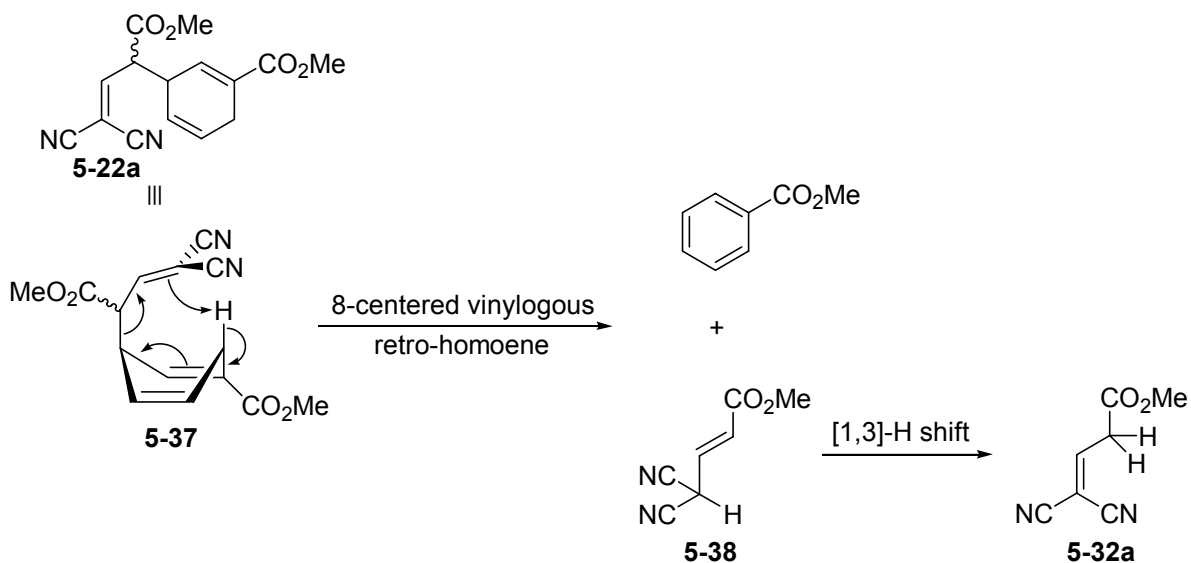
We therefore considered the possibility that a stereochemically sensitive intramolecular reaction was at work. One possibility (Scheme 5-13) is that an initial Cope reaction occurs with the involvement of one of the ring double-bonds to bring about rearrangement and side-chain migration to either C1 (**5-35**) or C5 (**5-4a**, the neutral direct adduct not observed in the forward reaction). By either pathway, **5-32a** would be freed by a retro-ene reaction through a six-atom array ending with a ring-methylene proton. Granted

the generation of **5-35** or **5-4a**, the retro-ene reaction would have to be fast, as ^1H NMR spectra of the samples undergoing these conversions contain no discernable signals for the Cope products.



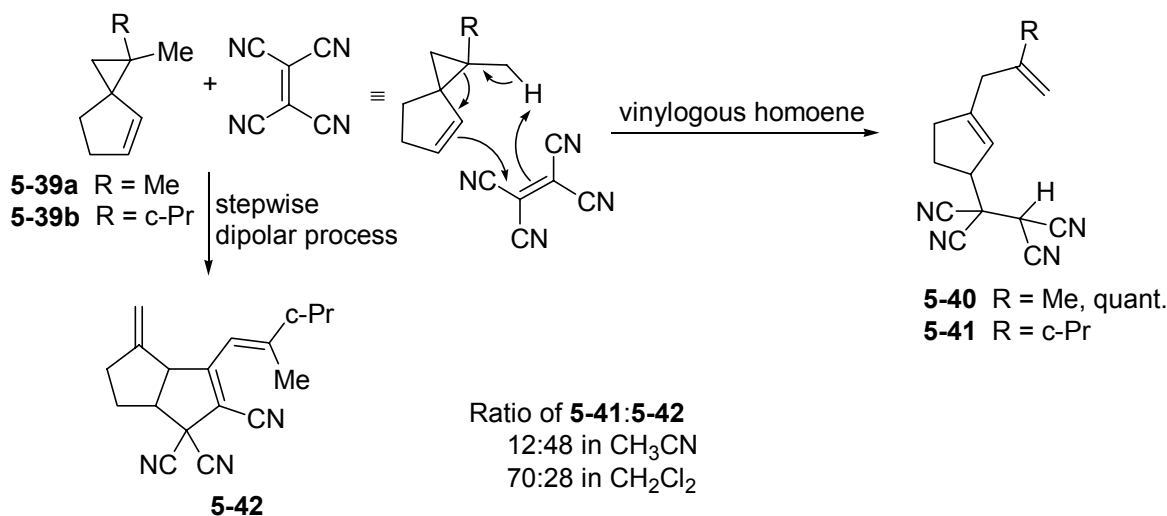
Scheme 5-13. Generation of methyl benzoate and **5-32a** from **5-22a** by alternative Cope/retro-ene reaction sequences.

An intriguing, if remote, speculation would posit a direct, one-step mechanism from **5-22a** to methyl benzoate (Scheme 5-14). Observation of a model of **5-22a** in the boat conformation (**5-37**) that places the C3-substituent in the axial position, as is expected for 1,3-disubstituted 1,4-cyclohexadienes,⁵ such that the dinitrile-bearing carbon of the side-chain overlies the axial C6-proton, establishes a bond alignment suggestive of an eight-centered pericyclic reaction that would simultaneously aromatize the ring and release the new free moiety **5-38**.



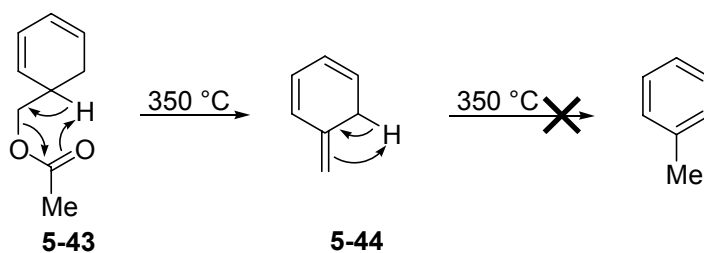
Scheme 5-14. Generation of methyl benzoate and **5-32a** from **5-22a** by an eight-centered reaction and [1,3]-H shift.

The conversion of **5-22a** to methyl benzoate and **5-38**, which would represent a vinylogous retro-homoene reaction, might be novel. The sole instance in the literature of a related eight-centered reaction — a forward vinylogous homoene reaction — was described in reluctant terms by Nishida and co-workers⁶ as a potentially concerted process (Scheme 5-15). In their study of rearrangements resultant from reactions of tetracyanoethylene with substituted spiro[2.4]hept-4-enes, they observed only the generation of **5-40** from the 1,1-dimethyl-substituted spiro substrate **5-39a**; moreover, the 1-cyclopropyl-1-methyl derivative **5-39b** gave mixtures of **5-41**, perhaps by concerted reaction, and **5-42**, which was concluded to have formed by a stepwise dipolar process, the potential homoene product being formed in greater quantities in less polar solvents. On the basis of its being unprecedented and thus requiring closer scrutiny, the authors chose to describe the generation of **5-40** and **5-41** as proceeding, like the generation of **5-42**, by a stepwise mechanism through cyclopropyl-opening rearrangement of a zwitterionic adduct intermediate, neutralization by intramolecular proton transfer, and tautomerization.

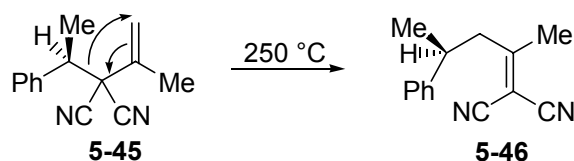


Scheme 5-15. Literature example of a putative vinylogous homoene reaction.

Were the eight-centered concerted cleavage and aromatization of **5-22a** occurring, it would release the unobserved 4,4-dicyano crotonate **5-38**, which would have to be converted to **5-32a**, perhaps by DCI-catalyzed tautomerization in CDCl₃. Scheme 5-14 alternatively cites a sigmatropic hydrogen shift as furnishing **5-32a**. Whereas suprafacial [1,3]-hydrogen migrations are symmetry forbidden (e.g. **5-44**, which is stably synthesized by pyrolysis of **5-43**,⁴ Scheme 5-16), and the symmetry allowed antarafacial hydrogen migrations are geometrically untenable, the presence of strongly electron-withdrawing substituents can bring about suprafacial [1,3]-shifts, with retention of configuration in the case of chiral migrating groups. For example, the presence of geminal nitriles in **5-45** permits the thermal [1,3]-alkyl shift that gives **5-46** to proceed without inversion (Scheme 5-17).⁴



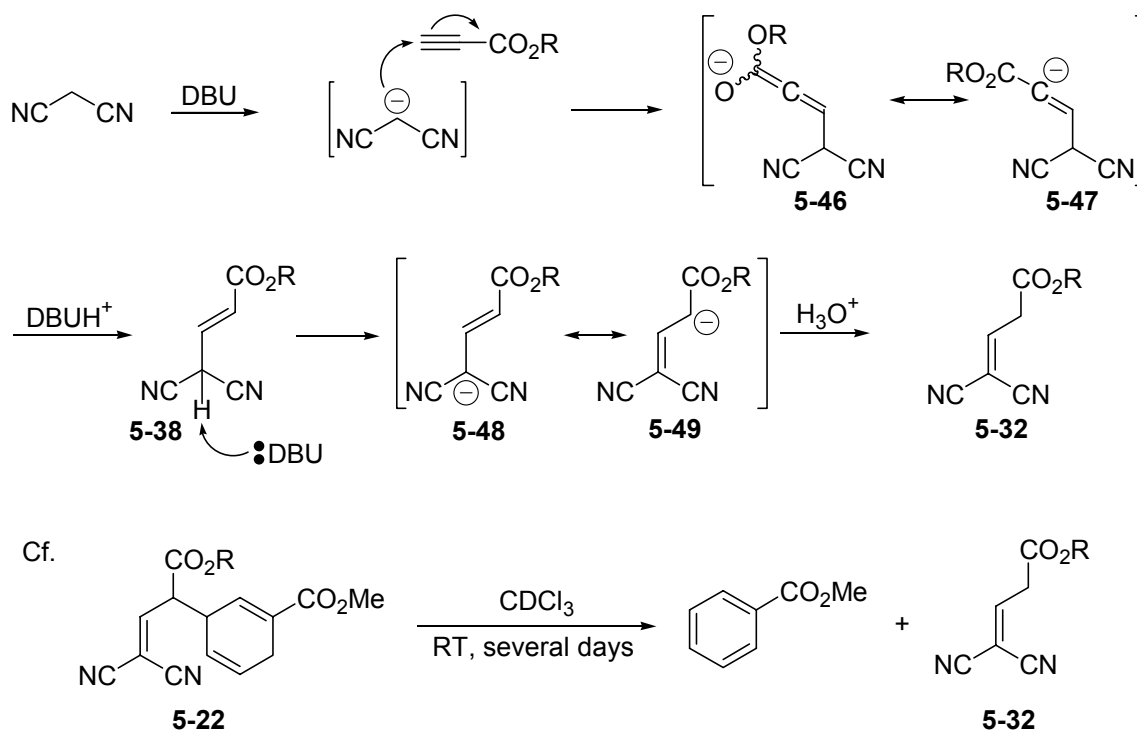
Scheme 5-16. Resistance of methylenecyclohexadienes to aromatization by [1,3]-H shift.



Scheme 5-17. A suprafacial, configuration-retaining [1,3]-alkyl shift.

5.2.4 Reactivity of Anionic 5-32

To confirm the structure assigned to **5-32**, a separate synthesis by base-induced conjugate addition of malononitrile to a propiolate was undertaken (Scheme 5-18). It was also felt that such an exploration might yield valuable insight into the intrinsic reactivity of the unusual side-chain present in **5-22**.



Scheme 5-18. Expected synthesis of **5-32**.

It was expected that although the initial conjugate addition of malononitrile to the propiolate would furnish the allenolate/vinyl anion species **5-46** \leftrightarrow **5-47**, either DBU-H⁺ or intramolecular proton transfer would neutralize it to give **5-38**. The anion **5-48** \leftrightarrow **5-49** was expected to arise by a sequence of protonation/deprotonation, leading to the more conjugated dicyanomethylidene-bearing isomer **5-32**.

In the initial experiment, one equivalent of DBU and stoichiometric malononitrile and methyl propiolate were employed, and the reaction was carried out in CH₃CN at 0 °C. After five hours, the reaction was quenched with 6% aq. HCl and extracted with CH₂Cl₂. The complex mixture included **5-32a** as an appreciable component as well as multiple unidentified components with both far-downfield vinylic and complex upfield signals.

This result suggested the possibility that stoichiometric base was prone to induce unintended reactions, prompting a second experiment with catalytic DBU. It was reasoned that the rearranged anionic adduct **5-49** would be neutralized by DBU-H⁺, permitting the reaction to continue to completion, as it had when the analogous fragment was a newly established moiety in the original allenolate Cope reaction. Under the same reaction conditions, only 0.05 equivalent of DBU was added. After 128 minutes, the reaction was partitioned, this time between saturated aq. NH₄Cl (due to the alternative concern that strong acid had induced the mixed reactions of the first experiment) and CH₂Cl₂, and examined by ¹H NMR, which revealed mostly starting material accompanied by a trace quantity of **5-32a** visible only at high vertical expansion, and a slightly greater quantity of a new species. The unknown constituent, which differed from those of the first experiment, evidenced an aromatic-region signal familiar from the vinyl proton on the dicyanomethylidene double-bonds of **5-22** and **5-32**, suggesting the involvement of this substructure. The new compound

also contained protons resonating in the region spanning δ 5–2.5, although the result was not explored at the time beyond the practical conclusion that DBU was not recycled after the initial conversion.

It was now considered useful to carry out a carefully controlled and monitored experiment to clarify the factors limiting the production of **5-32** in the preceding experiments. This experiment again employed stoichiometric DBU, and the anion of malononitrile was prepared ahead of the introduction of ethyl propiolate. A few minutes later, a small aliquot was removed and concentrated by rotary evaporator and high vacuum pump at room temperature prior to preparation of an NMR sample in CDCl_3 . A second aliquot was later removed and neutralized with 6% aq. HCl, and, finally, the remaining reaction mixture was later divided for separate workup by 6% aq. HCl and saturated aq. NH_4Cl . The unquenched sample would prove to merit consideration, but assessment of the other samples at the time only revealed a limited quantity of **32** in the HCl-treated reaction, almost completely obscured in the ^1H NMR spectrum, and none in the HCl-treated early aliquot or the NH_4Cl -quenched reaction.

The unquenched sample furnished a clean ^1H NMR spectrum containing resonances at δ 7.15 and δ 5.15, doublets with a mutual coupling of 14.3 Hz. The spectrum also contained single signals for the ethyl ester and the protons of protonated DBU, for which we had previously obtained a reference spectrum by generating the stoichiometric DBU-H^+ salt of malononitrile. The resonances of the two coupled fragment protons provided strong evidence for the operation of the mechanism in Scheme 5-18, indicating the sole presence of the DBU-H^+ salt of **5-49b**. The chemical shifts, one far downfield as in the analogous proton of **5-32** and one upfield at the carbon that carries the localized electron pair in **5-49**, were in

line with expectation. Moreover, the large coupling was consistent with a *trans* configuration about the bond, which in the resonance hybrid model of the anion possesses double-bond character.

The sample was retained in CDCl₃ solution and later observed for further reaction toward the multiple products observed in the other samples from the same and previous experiments. The second ¹H NMR spectrum, obtained after three days, contained no new species, but intriguingly revealed reduced signal intensity for the vicinal doublets with a concomitant increase in the intensity of the CHCl₃ proton signal, demonstrating slow H–D exchange between **5-49b** and the solvent. After several more days, the proton signals had declined to 30% of their starting intensity, and a new signal that had started to appear within the downfield doublet with the first evidence of exchange now exceeded its intensity. The timecourse of NMR spectra are reproduced in Figure 5-19.

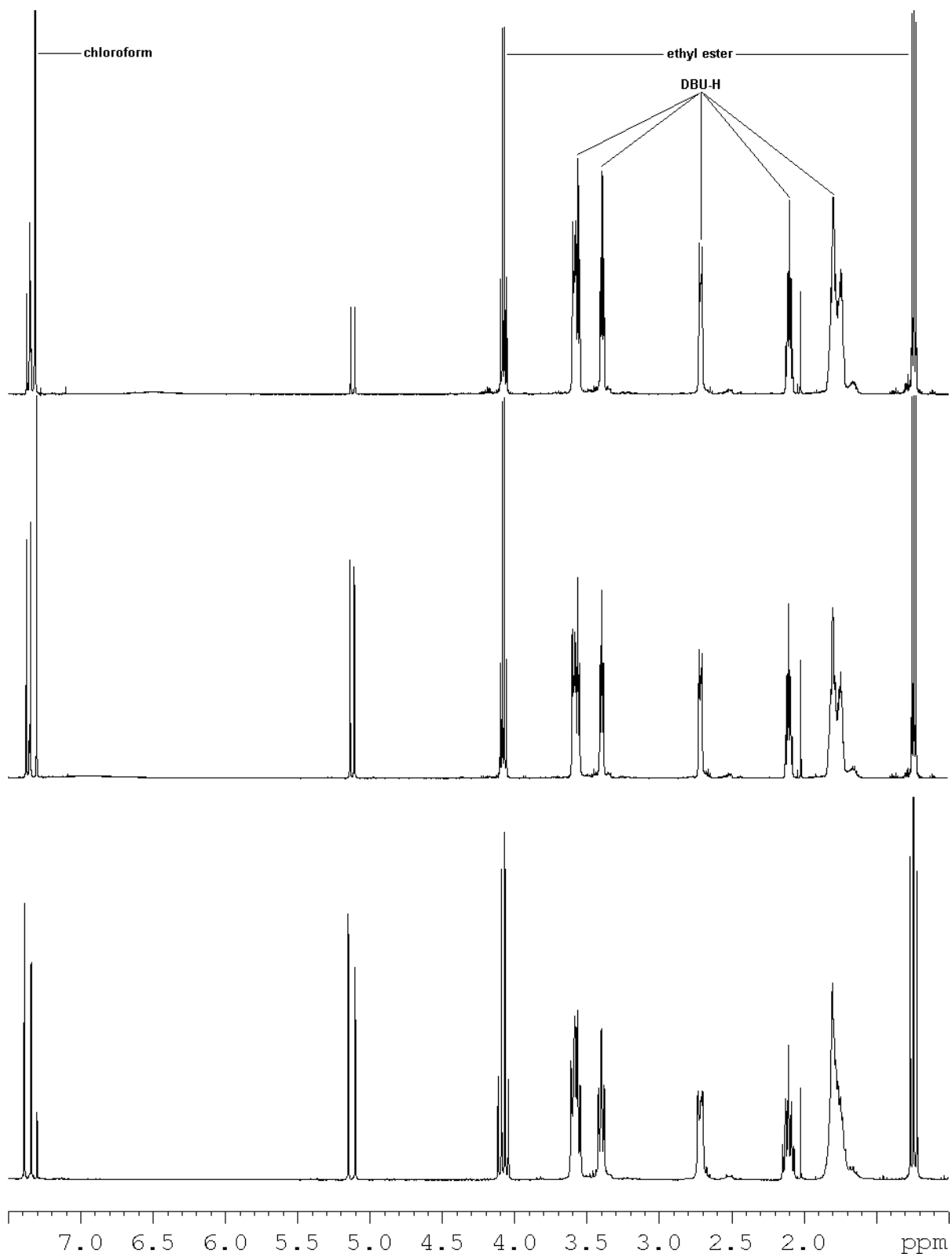


Figure 5-19. ^1H NMR spectra of CDCl_3 solution of DBU- H^+ salt of **5-49b**. Bottom spectrum (300 MHz): initial; middle spectrum (500 MHz): 67 hours; top spectrum (500 MHz): 147 hours.

If both protons of **5-49b** were capable of exchange, the ^1H NMR spectrum of a mixed population of unexchanged and both singly-exchanged species would contain signals for the diminished starting anion, and signals for the remaining protons in either of the single deuterium-bearing species. Some technical considerations include the slight upfield shift (approximately 0.0005 ppm) the deuterium would cause in the vicinal proton, and the vicinal coupling constant 6.5 times less than the parent H–H coupling, derived from the ratio of the magnetogyric ratios of the two isotopes.^{7,8} In addition, the three equally populated spin states for spin 1 deuterium would split the vicinal proton resonance into a 1:1:1 triplet if perfectly resolved. Figure 5-20 depicts an idealized ^1H NMR spectrum of the signals in question.

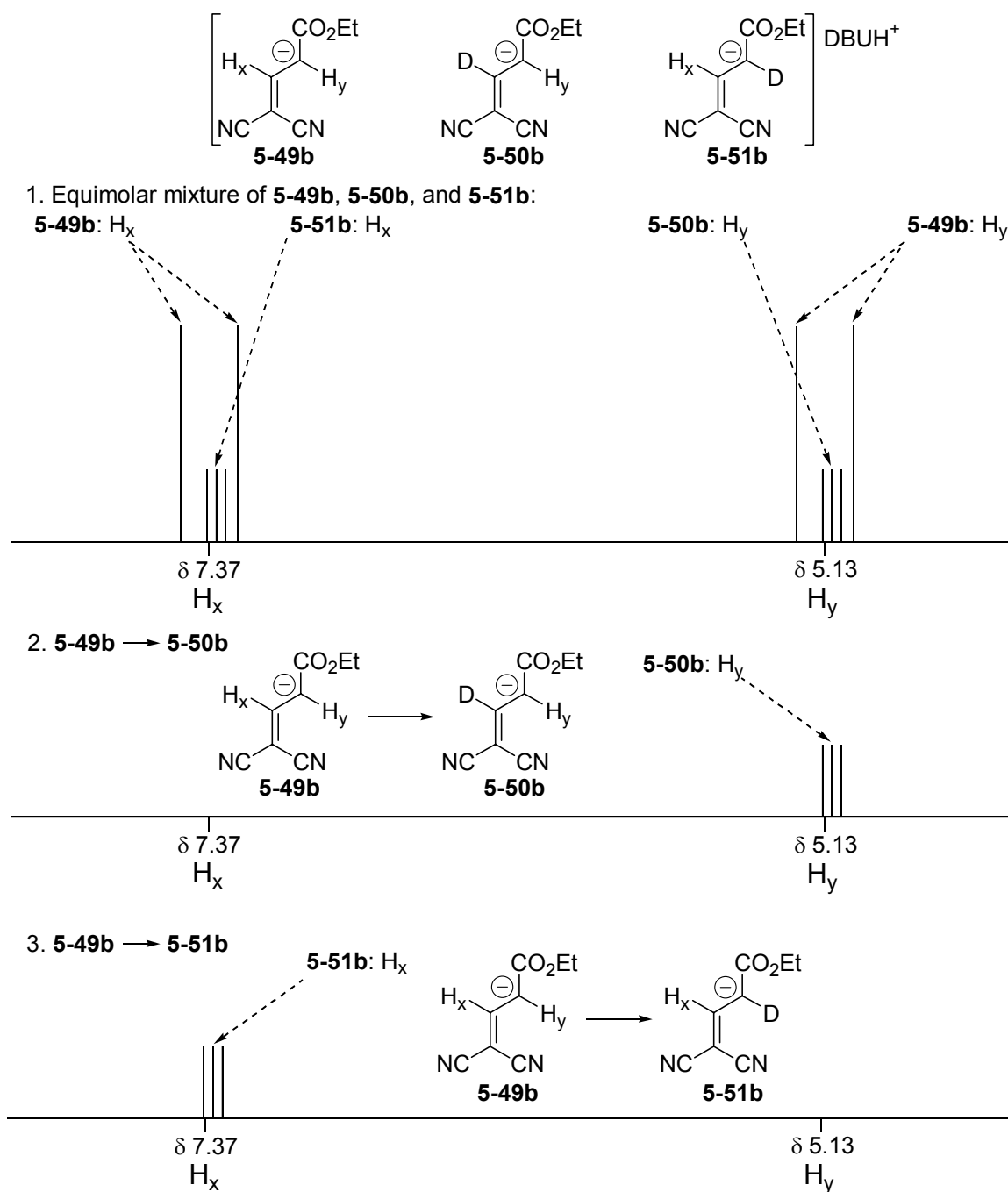


Figure 5-20. Schematic ^1H NMR spectra for an equally-populated mixture of species **5-49b**, **5-50b**, and **5-51b** (top); exchange product **5-50b** (middle); and exchange product **5-51b** (bottom).

The observed ^1H NMR spectra of the exchange process contain no signal for the upfield proton of Figure 19, species **5-50b**. An examination of the resonance contributors of **5-49b** reveals a distribution of sites of electron-pair localization that does not include the

carbon bearing the downfield proton (Figure 5-21). In light of this, the absence of species **5-50b** in the mixture is readily accepted.

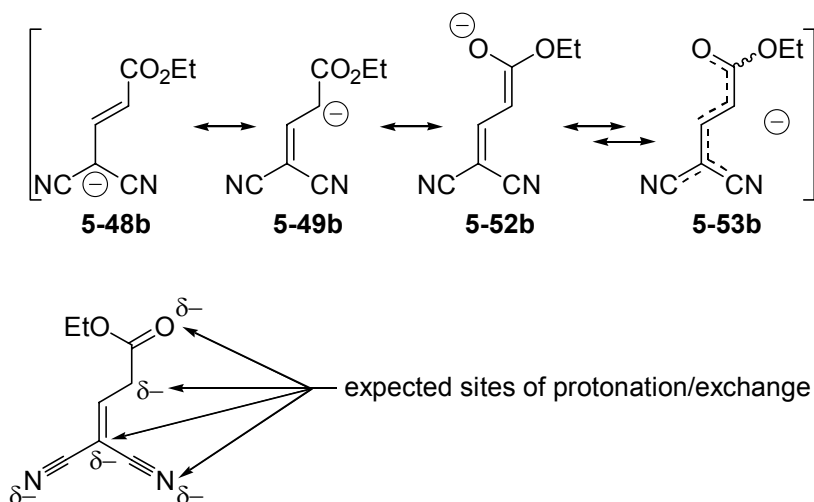


Figure 5-21. Resonance contributors and hybrid of fragment anion, and expected sites of D exchange at sites of electron-pair localization.

An expanded view of the downfield region reveals the increasing new signal within the δ 7.37 resonance to be a broad singlet, slightly off-center to the upfield side. Whereas this signal reveals no trace of the calculated 2.2 Hz splitting, it is nevertheless reasonably identified as the exchange product **5-51b** (Figure 5-22).

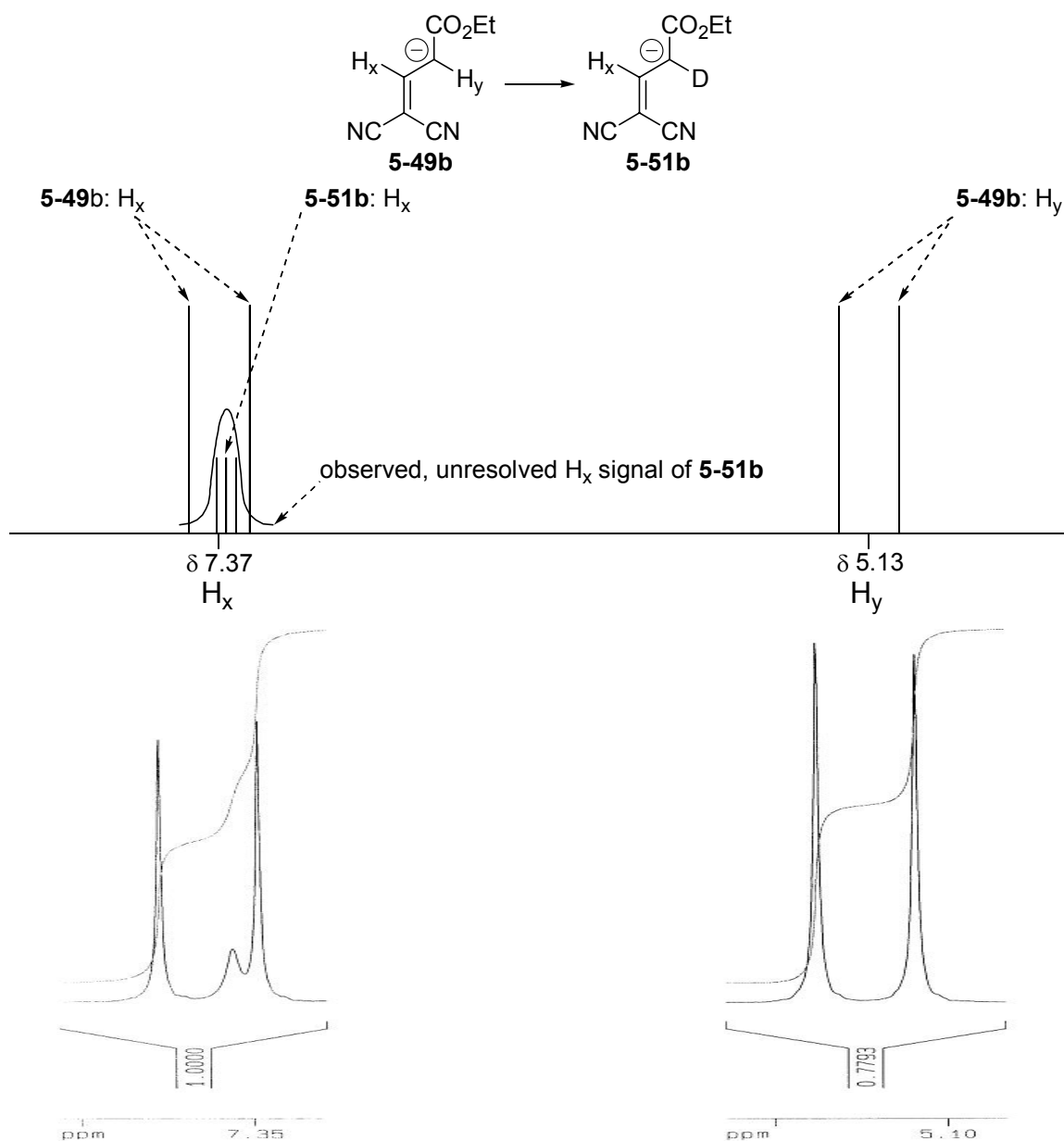
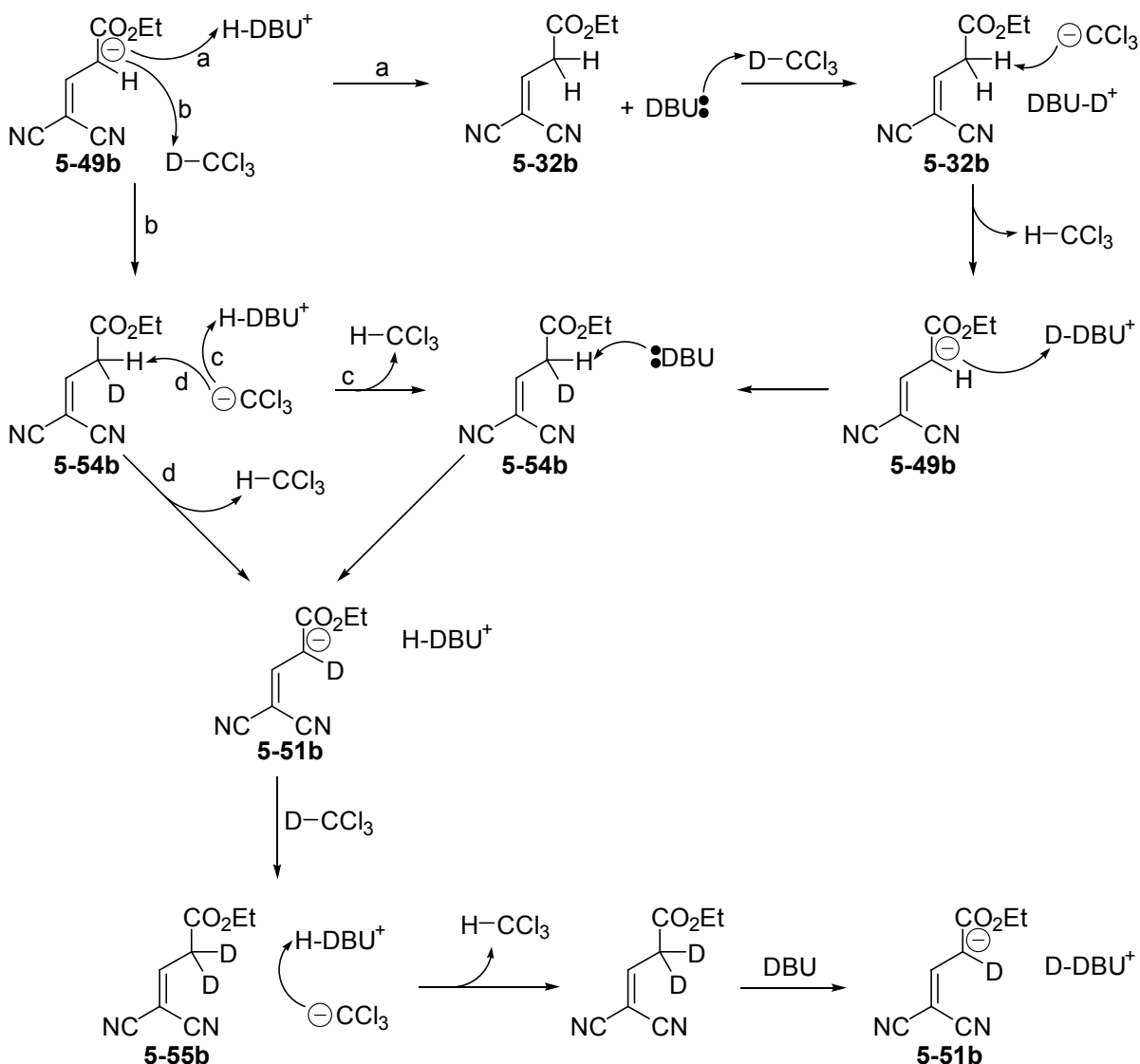


Figure 5-22. Schematic and observed 1H NMR spectra reflecting conversion of species **5-49b** to deuterated species **5-51b**.

The loss of intensity of the exchanging protons of **5-49b** had reached 70% by the third observation; the measured integral was 0.3, referenced to the starting value of 1 for either single proton. The corresponding increase in the intensity of the $CHCl_3$ proton signal was 1.85 “protons,” a seemingly high figure but in reasonable agreement with the value of

1.7, representing the sum of 0.7 provided by **5-49b** and 1 provided by total exchange of protonated DBU (Scheme 5-19).



Scheme 5-19. Available exchange pathways for exhaustive H–D exchange of **5-49b** and DBU-H^+ .

An exchange mechanism involving only **5-49b** and CDCl_3 can be envisioned in which neutralization of the carbanion by a deuteron is simultaneously accompanied by the conclusion of exchange by deprotonation of **5-32b** by the departing trichloromethyl anion (Scheme 5-19, path b, followed by path d); however, the aforementioned account of the ^1H

NMR spectral intensity of the CHCl_3 proton upon 70 mole percent conversion of **5-49b** to **5-51b** demands the inclusion of exchange of the DBU iminium proton. To this end, path a (Scheme 5-19) depicts an indirect exchange pathway, in which DBU-H^+ neutralizes **5-49b** and then dedeuterates CDCl_3 , becoming the agent that delivers the deuteron to **5-49b** once it is regenerated by the trichloromethyl anion. Alternatively, a role for DBU emerges in path b/path c, in which the trichloromethyl anion is neutralized by DBU-H^+ before the pathways converge on **5-51b**, en route to the conclusion of exhaustive H–D exchange upon one salt molecule. The exchange mechanisms are schematically depicted as entailing two possible directions of electron flow in Figure 5-23.

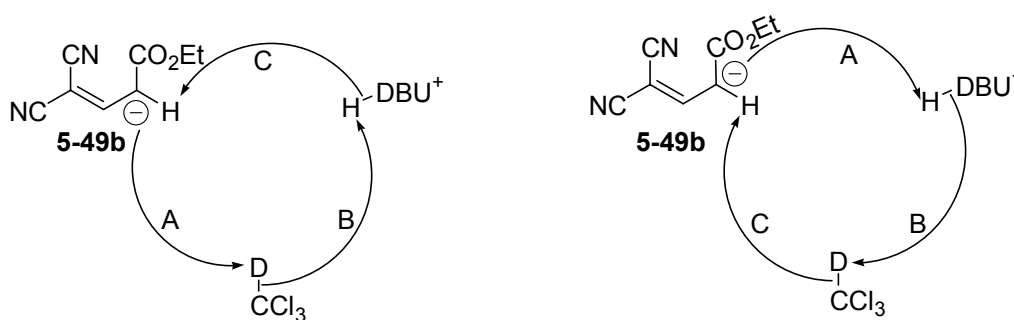
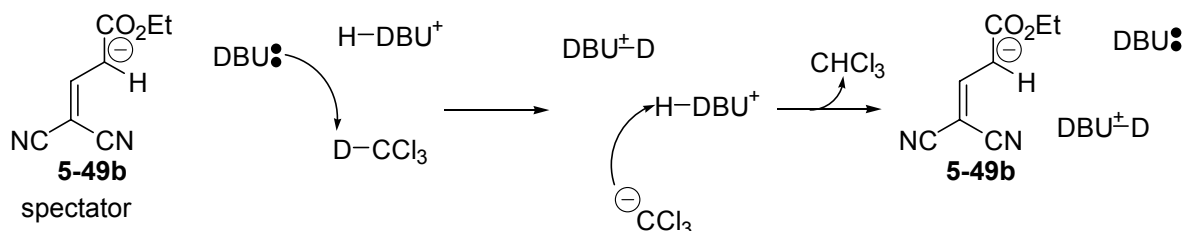


Figure 5-23. Schematic mechanism of H–D exchange of **5-49b**/ DBU-H^+ salt. Two cycles (A→B→C) with one intervening replacement of CDCl_3 conclude the exchange process.

The apparent increase in the intensity of CHCl_3 of 1.85 protons, while necessarily including exchange of the DBU proton, is not accounted for by the mechanism in Scheme 5-19: it does not provide a means of exchange that uncouples the exchange of a proton on the fragment from the exchange of the proton carried by DBU, indicating a limit for the increase in intensity of the CHCl_3 proton of 1.40 (two times the measured decline of proton-bearing **5-49b**). Even a scheme involving counterion exchange among differently isotopomerically substituted organic salt pairs does not address the necessary difference. This suggests that a slight excess of DBU is present, which provides a catalyst for exchange at DBU-H^+

independent of **5-49b**, affording different extents of exchange among the fragment anion and DBU, that is, 0.7 equivalent H–D exchange of **5-49b** and one equivalent exchange of DBU–H⁺ (Scheme 5-20).



Scheme 5-20. Catalytic excess DBU permits total H–D exchange of DBU–H⁺ counterion independent of 70 mol percent exchange of **5-49b**.

The persistence of **5-49b** for seven days in solution at room temperature, aside from isotopic exchange, indicated that the generation of the multiple side-products in the other experiments was not the result of either stoichiometric base or of any reactions prior to workup: acid treatment itself was responsible for reactions subsequent to the generation of **5-49b**. To determine whether **5-32b** (or its isotopomers) could be generated *in situ*, a drop of acetic acid (0.25 equivalent) was added to the NMR sample and the effects on the ¹H spectrum were observed. A striking effect evident within the few minutes needed to obtain the first spectrum was the consumption of the new downfield singlet relative to the remaining proton signal of **5-49b**, and the appearance of a new singlet at δ 7.415 (Figure 5-24). Neither of the isotopomers of **5-32b** was observed.

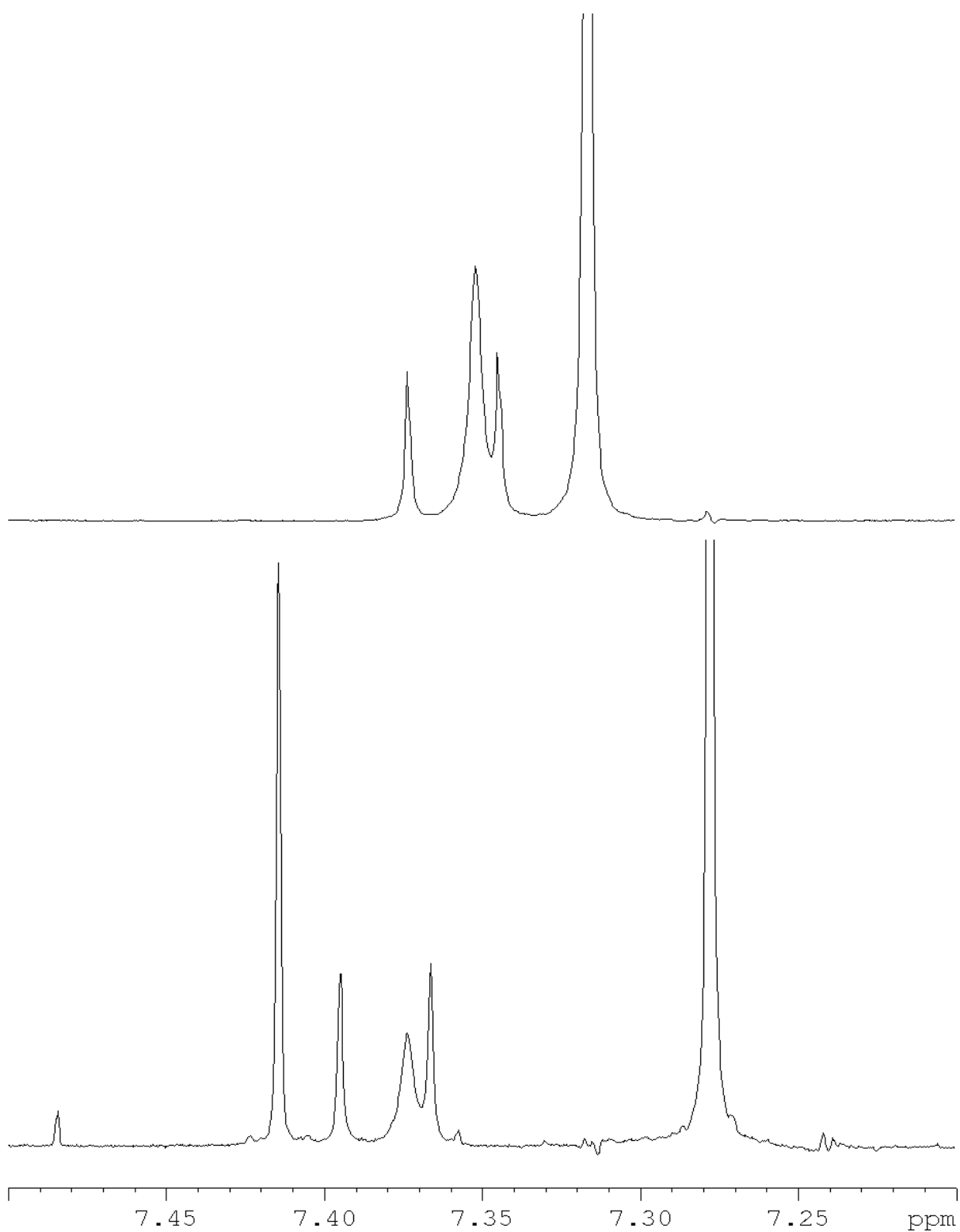
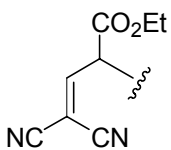


Figure 5-24. Expanded ^1H NMR spectra (500 MHz, CDCl_3) of the downfield region of **5-49b** at the last observed stage of H–D exchange (top) and after addition of acetic acid. Spectra plotted on matching scales: chemical shift alterations are observed.

In addition to the new downfield singlet, several new signals at intermediate field appeared (4.8, 4.5, 3.0, and 2.8 ppm). The chemical shifts of all the new signals were consistent with those of the unknown compound generated in the NH_4Cl -treated reactions, differing only in ratios of intensity among themselves and in observed coupling patterns. This prompted a more detailed assessment, including structure determination, of the two instances of workup with saturated aqueous NH_4Cl , one involving catalytic DBU, and the other the one-equivalent DBU case that provided the early aliquot of **5-49b**.

The δ 7.415 singlet immediately brought to mind an analogous signal in the ^1H NMR spectrum (Figure 5-25) of the DBU-H^+ salt of Cope product **5-22b**, which was generated in experiments to be discussed later. A second similarity was the shift position of a proton at approximately δ 4.5, which had been pushed downfield in the salt relative to the neutral species. Taken together, these signals suggested that a partial structure of the unknown could be formulated as a substituted adduct of **5-32b** (inset).



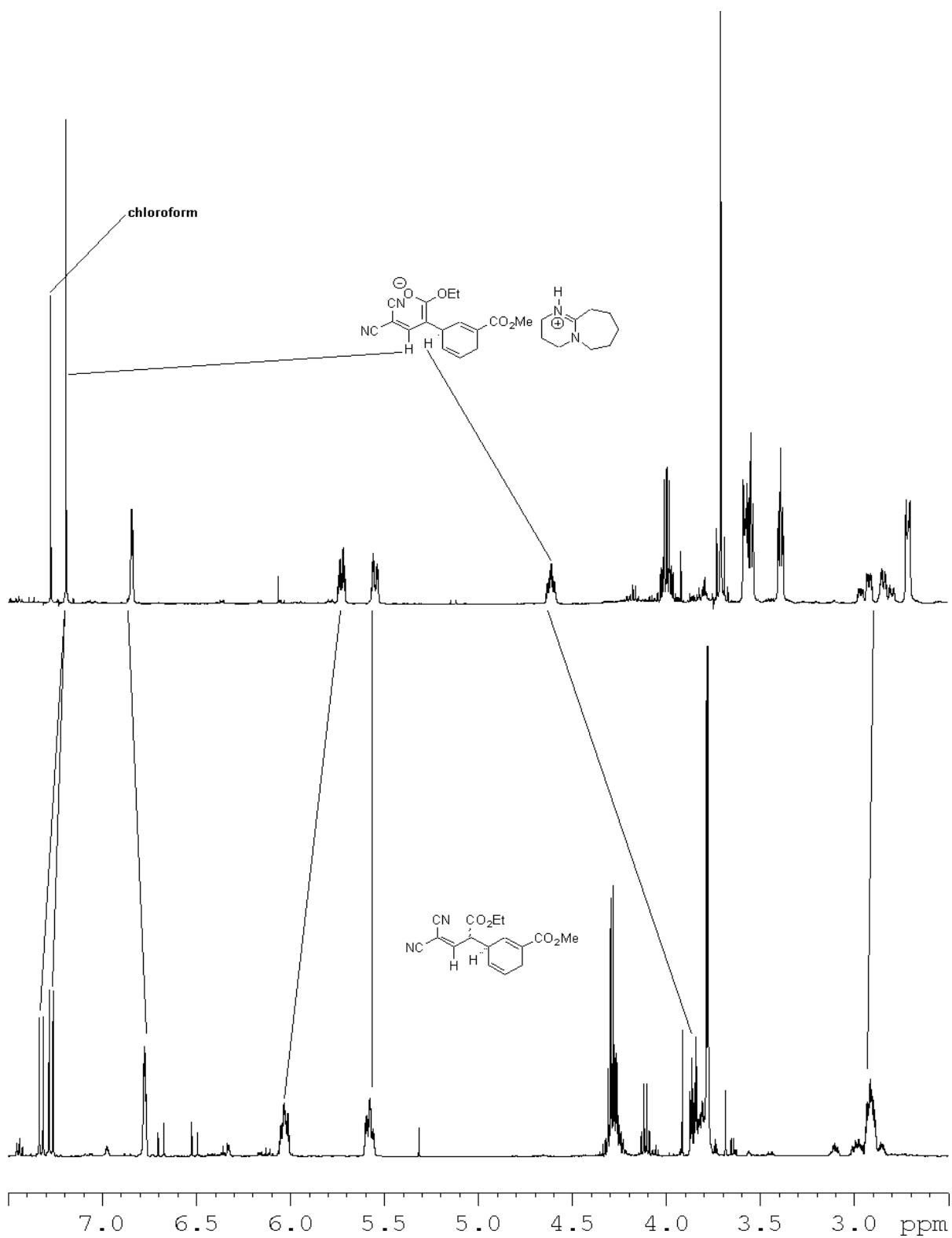


Figure 5-25. ¹H NMR spectra (500 MHz, CDCl₃) of neutral Cope product **5-22b** (bottom) and Cope product/DBU-H⁺ salt. Lines associate signals derived from identical protons in both species. Two protons of the salt significant in the current structural determination are indicated.

The NMR sample of the stoichiometric DBU reaction worked up with saturated aqueous NH_4Cl precipitated to a large extent, providing a spectrum of poor quality. The precipitate was completely soluble in deuterated acetone and furnished a high quality spectrum (Figure 5-26) that was crucial to further structural assignment.

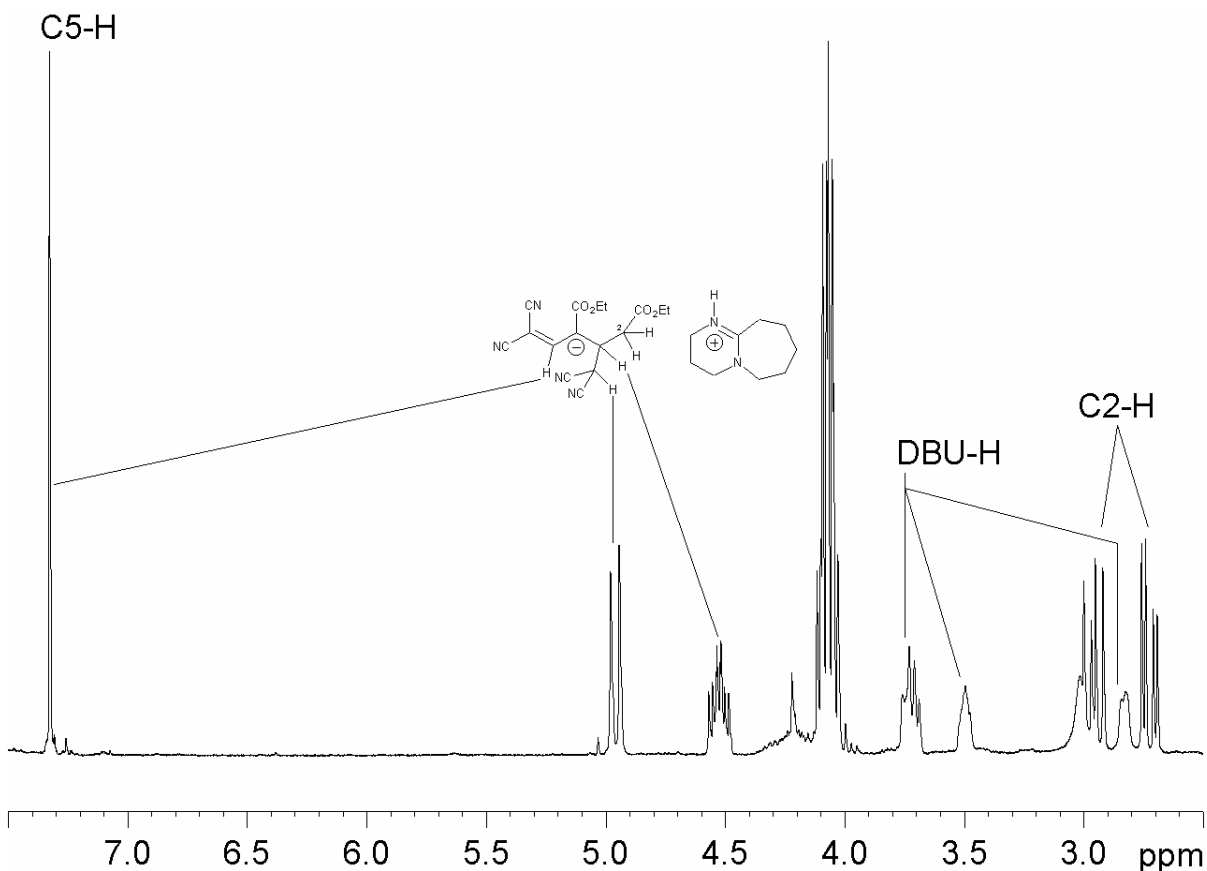
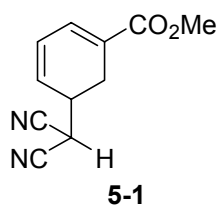


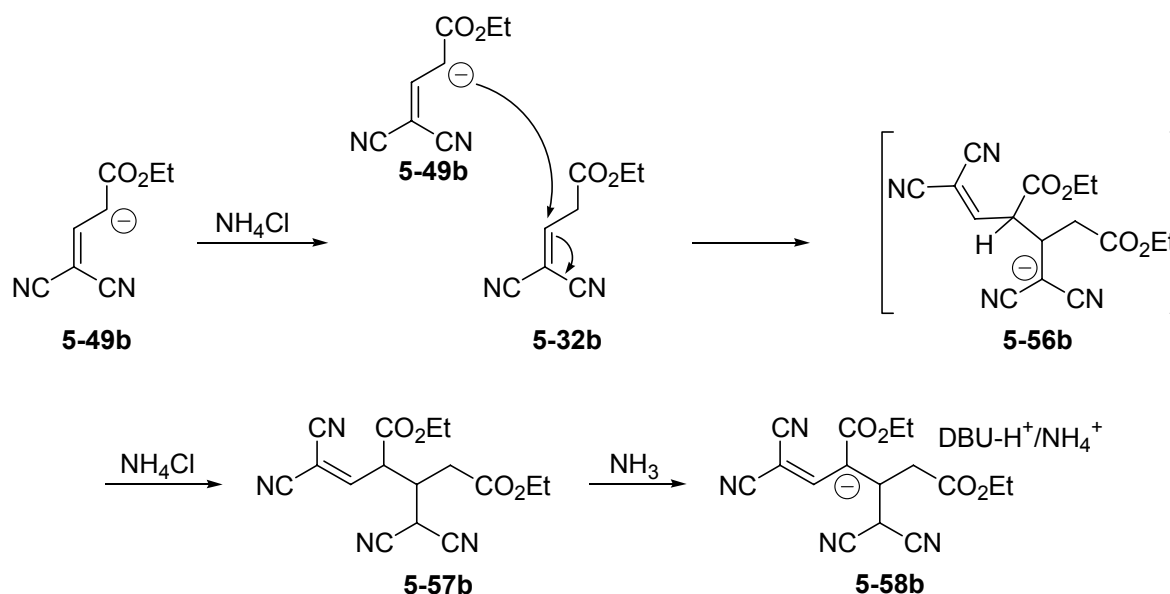
Figure 5-26. Partial ^1H NMR spectrum (300 MHz, $\text{CO}(\text{CD}_3)_2$) of **5-53b** precipitated from CDCl_3 solution. Broad signal superimposed upon C2-H signal at δ 3.0 is the protons of NH_4^+ .

Identical large line spacings of the signals at δ 2.96 and δ 2.73 (14.7 Hz) indicated moderately deshielded geminal protons. Their differing vicinal couplings (9.4 and 5.0 Hz



observed line spacings) to the complex proton signal at δ 4.53 indicated an ABX partial spin system. The X proton had a further coupling to the doublet at δ 4.96 of 10.8 Hz, whose shift position was comparable to that

in acetone-d₆ (δ 4.64) of the dicyanomethyl methine proton of the ring-opened adduct **5-1**. This disposition of protons along a three-carbon unit, along with the likely dicyano substitution of the terminal carbon, suggested that a dimer of **5-49b** had formed. Furthermore, the conclusion that one substructure was the C2-substituted fragment anion supported the conclusion that the dimer had formed by conjugate addition of **5-49b** to **5-32b**, formed by neutralization of **5-49b** on mild acid workup (Scheme 5-21).



Scheme 5-21. Dimerization of **5-49b** and **5-32b** by conjugate addition during mild acid workup.

The quantity of the protonated DBU counterion relative to **5-58b** was observed to be less (25 mol % relative to **5-58b**) in the ¹H NMR spectrum in deuterated acetone (obtained from the precipitate from the CDCl₃ sample) than in the initial spectrum obtained in CDCl₃ (61 mol %). The balance of the counterion in either instance is provided by NH₄⁺, indicating that the ammonium salt of **5-58b** is less soluble in CDCl₃ than the more highly organic salt involving protonated DBU. That the initial quantity of DBU-H⁺ observed in the ¹H NMR spectrum was less than stoichiometric indicates that ammonium is capable of competing with

DBU-H⁺ as counterion to **5-58b**, but that its pK_a sufficiently exceeds that of the conjugate C-4 acid of **5-58b** that no neutral species is observed in either NMR solution.

The acidity of saturated aqueous NH₄Cl is necessarily high enough to protonate **5-49b** to generate at least a quantity of the conjugate acceptor **5-32b**, otherwise dimerization could not proceed. It evidently cannot do so at a diffusion-controlled rate, or at a rate sufficiently hastened by the large excess of NH₄Cl to produce a population of **5-32b** that at some stage in the dimerization outnumbers the remaining population of **5-49b**, otherwise a quantity of **5-32b** would be observed. The clean dimerization of the fragment anion to give **5-58b** supports a kinetic account of the brief workup period in which the slowly generated **5-32b** represents a powerful electrophile that is attacked by **5-49b** at a high, and perhaps diffusion-controlled, rate to give **5-56b**, which equilibrates by a sequence of protonation/deprotonation to the stable extended enolate **5-58b**.

The nitrile and carboethoxy substituents of the acceptor-derived region of **5-58b** are somewhat remote from the acidic C-4 carbon, but must nevertheless exert an inductive electron-withdrawing effect capable of reducing the pK_a of the conjugate acid relative to the analogous acidic site of the Cope product **5-22** (Figure 5-27).

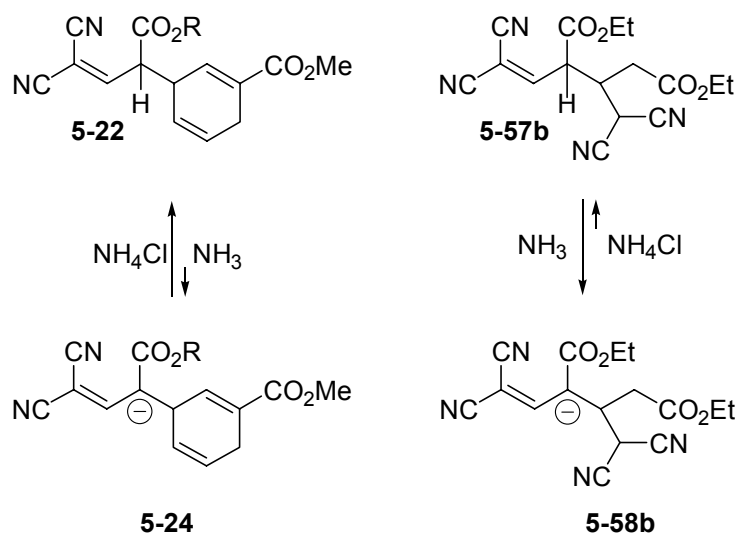
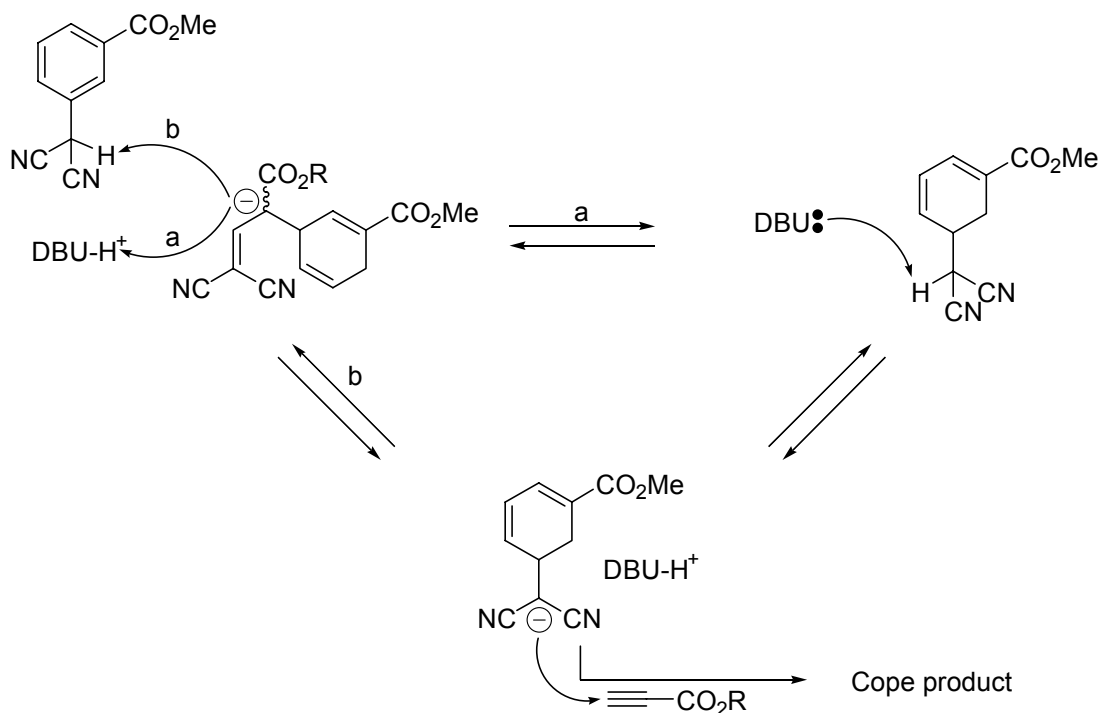


Figure 5-27. Differences in pK_a of analogous acidic protons in **5-22** and **5-57b** as revealed by differential neutralization by saturated aqueous NH₄Cl of anions **5-24** and **5-58b**.

Whereas ammonium can only function as a counterion to **5-58b**, it can neutralize the anion of **5-22**, which indicates that the inductive electron-donation of the substituted 1,4-cyclohexadienyl moiety of **5-22** to the side-chain's acidic carbon increases its pK_a relative to that of **5-57b**. The implication of this difference is that the Cope reaction would not be able to proceed to completion with only catalytic base if the pK_a of the acidic product carbon were slightly lower, a finding supported by the failure of the attempted synthesis of **5-32** with catalytic DBU. The Cope carbanion is basic enough either that there is some direct equilibration to neutral **5-22** and DBU after the Cope reaction, which permits continuation of the reaction, or that the Cope product equilibrates to some extent with the ring-opened adduct to furnish its anion to propiolate and then the Cope conversion, so that DBU is not involved in a catalytic cycle (Scheme 5-22).



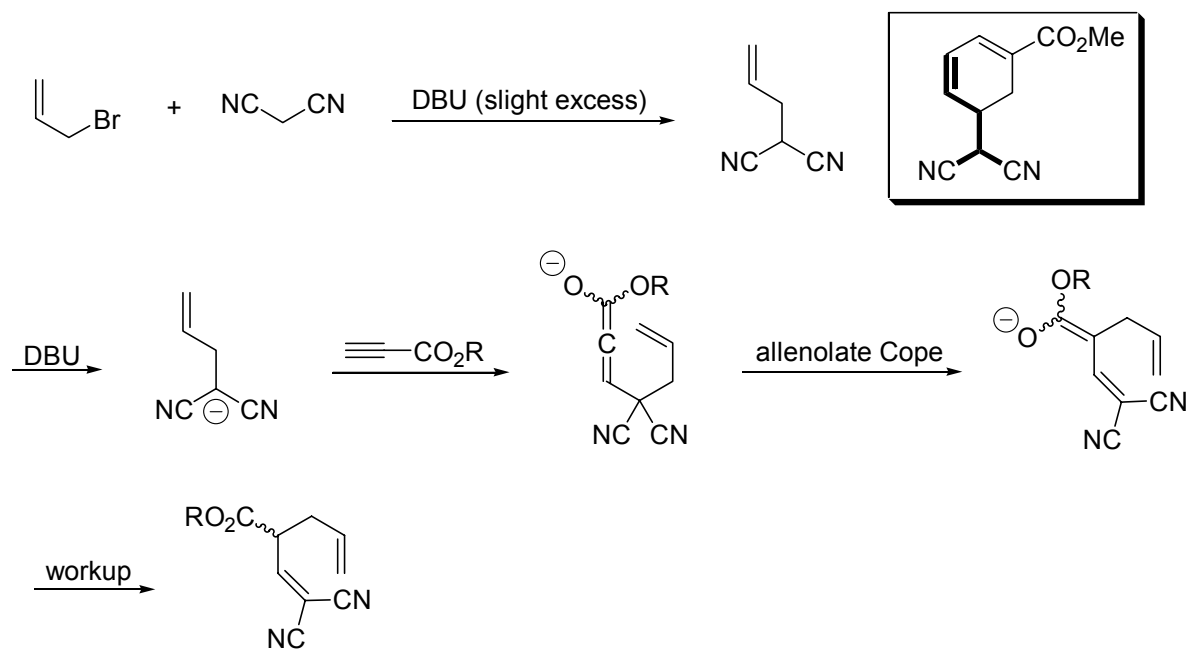
Scheme 5-22. Continuation of Cope reaction by neutralization of Cope product enolate.

5.2.5 Attempted Generalization of Allenolate Cope Reactions

In an effort to assess the generality of the allenolate Cope reactions, simpler model systems were devised in the hopes of distinguishing the minimal structural requirements for successful rearrangements. Of particular interest was the determination of whether the driving elements of the successful reaction in the parent system were located solely in the model “side-chain,” namely the incipient conjugated dinitrile and the allenolate moiety, or whether the substitution pattern of the ring’s reactive double-bond was necessary to the process.

The simplest possible model system, derived from allyl bromide and malononitrile, was chosen as a starting point. It was initially envisaged that an efficient experimental approach to the problem could be implemented through a cumulative one-pot process

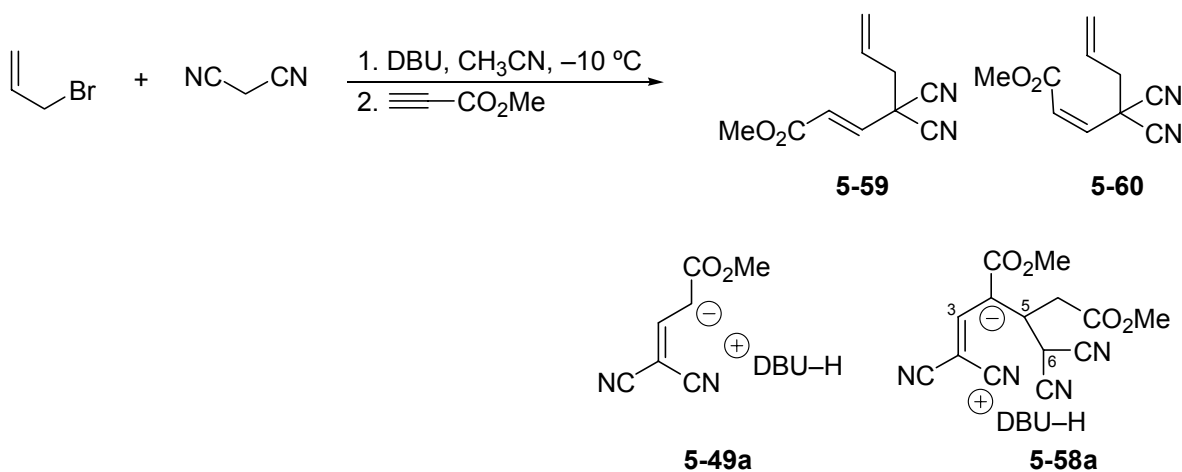
comprising both the generation of the model substrate and the subsequent introduction of an alkyl propiolate, the base catalysis being provided by the initial introduction of a slight excess of DBU in the substrate-generating step (Scheme 5-23).



Scheme 5-23. Planned one-pot Cope rearrangement of a model substrate derived from allyl bromide.

To this end, malononitrile and propenyl bromide were dissolved in CH_3CN at $-10\text{ }^\circ\text{C}$ and 1.1 equivalents of DBU were added, the ten mole percent greater than stoichiometric DBU in accord with the catalytic quantity of base employed in the parent Cope rearrangements. After 15 minutes, methyl propiolate was added in a slow dropwise fashion from a stock CH_3CN solution. Several hours' reaction time was arbitrarily allowed to elapse before the reaction was worked up with saturated aqueous NH_4Cl and partitioned with CH_2Cl_2 .

Assessment of the crude reaction mixture by ^1H NMR spectroscopy revealed the presence of four constituents (Scheme 5-24).



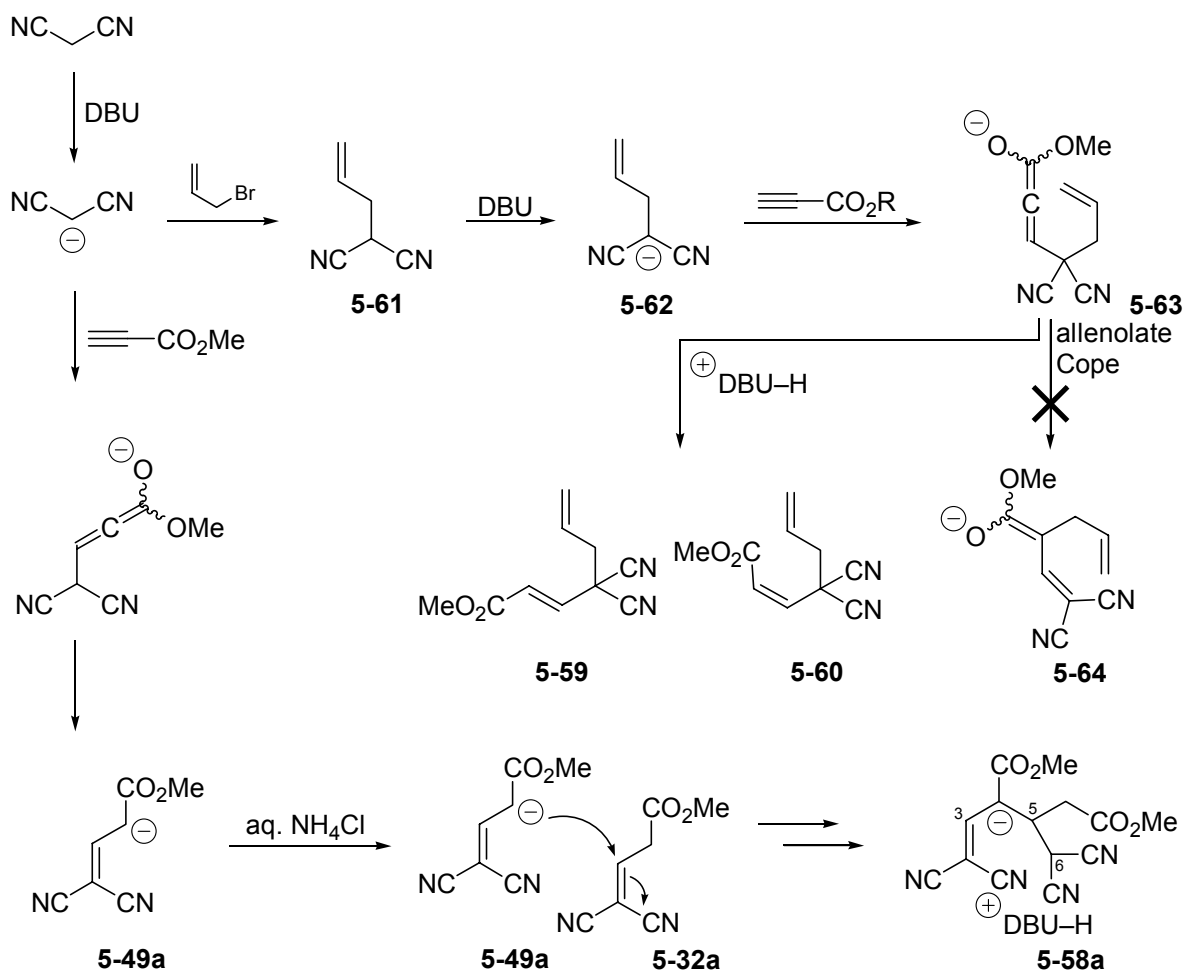
Scheme 5-24. Products of initial model Cope rearrangement.

Consistency among the proton integral values readily provided for association of the signals derived from the direct tripartite adduct **5-59**. The appropriate shift positions and coupling constants for a *trans*-configured ester-conjugated double-bond (δ 6.75 and δ 6.43, 15.4 Hz J) were in evidence for the structure as formulated. The signals were associated with a methyl ester proton singlet resonance at δ 3.82. Also in evidence was an isolated two-proton signal (δ 2.69) assigned to the symmetrically disposed allylic methylene proton pair, expressing a coupling constant of 7.2 Hz to the vicinal vinyl proton, a value consistent with expectation for such an arrangement. The remaining three vinyl protons displayed overlapping multiplets arising from two mixture components from δ 6.00–5.80 and from δ 5.52–5.38.

Structure **5-60** was assigned on the basis of the upfield shift of the slanted pair of doublets for the ester-conjugated vinyl group protons (δ 6.30 and δ 6.06) relative to those of the *trans* isomer. Also supportive of the assigned *cis* configuration was the smaller coupling constant (11.2 Hz) of the vicinal vinyl protons, along with the upfield shift a standard feature in the comparison of vinyl *E* and *Z* vinyl isomers.

Fragment **5-49a** was identified by the recognition of the two doublets (δ 7.37 and δ 5.13, 14.4 Hz J) observed in isolation in the already-discussed synthesis of the ethyl ester analogue. Finally, the previously recognized dimer **5-58a** (also as the ethyl ester analogue) was identified by its diagnostic isolated doublets at δ 4.82 (10.7 Hz J , C6-H) and at δ 4.48 (multiplet, C5-H) and by the partially obscured singlet of the C3 proton.

Neither the Cope product anion nor the neutral Cope product was observed. It is apparent from the products generated that insufficient time was permitted for the completion of the alkylation of malononitrile with propenyl bromide prior to the addition of methyl propiolate. The quantity of unreacted malononitrile readily reacted with methyl propiolate to generate anionic adduct **5-49a**, which, either upon acidic workup or by proton transfer from the large quantity of DBU-H⁺, formed a highly electrophilic population of neutral **5-32a**, which rapidly dimerized to **5-58a**, as in the experiment specifically addressed to the synthesis of **5-32b**. A quantity of **5-49a** also survived workup without coupling or neutralizing to **5-32a** (Scheme 5-25).



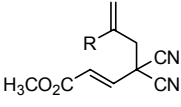
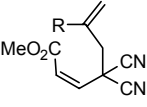
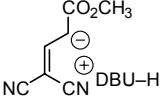
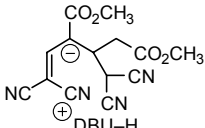
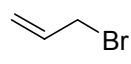
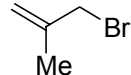
Scheme 5-25. Mode of generation of product distribution observed in attempted one-pot model Cope rearrangement.

The extent of alkylation prior to the introduction of methyl propiolate was approximately 64 percent. The population of anion **5-62** also reacted readily with methyl propiolate to give allenolate **5-63**, but rather than undergoing an allenolate Cope rearrangement to give **5-64**, the adduct was neutralized in a ratio of 4.2 to 1 in favour of the *E* isomer.

The same result, differing only in the varying quantities of the four constituents of the crude mixture, was observed for the attempted one-pot model allenolate Cope experiment concurrently undertaken with 3-bromo-2-methylpropene, although the extent of alkylation of

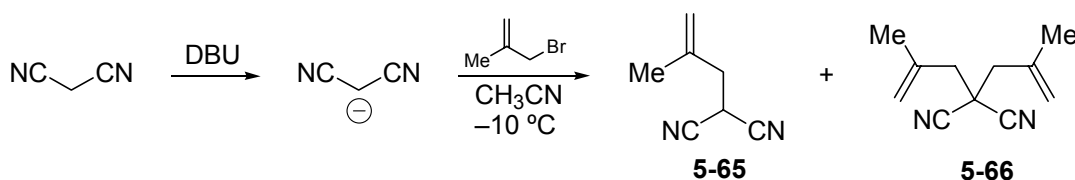
malononitrile with the bromide was only 40 percent. Table 5-3 reproduces the results of the two one-pot model experiments.

Table 5-3. Product distributions in attempted one-pot model allenolate Cope reactions.

Allylic substrate	R in product	Product ratio ^a			
					
	H	1.00	0.26	0.30	0.21
	Me	1.00	0.23	0.78	0.41

^a ¹H NMR integral ratios.

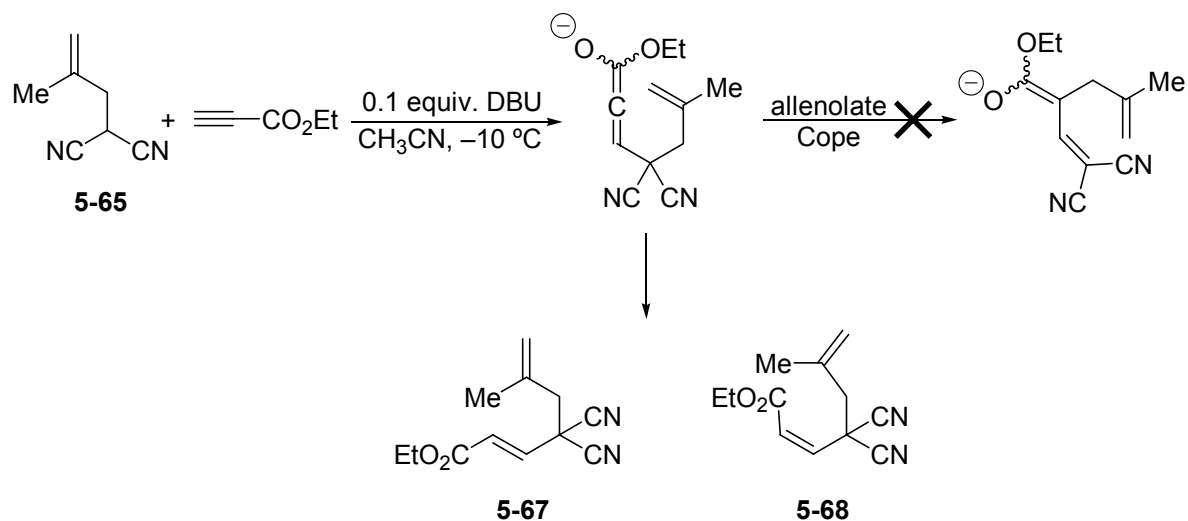
A two-step approach, starting with the generation and isolation of adduct **5-65** (Scheme 5-26), was implemented to ensure that a homogenous supply of alkylated Cope substrate would be present upon introduction of base and alkyl propiolate. Equimolar quantities of malononitrile and 3-bromo-2-methylpropene were treated at $-10\text{ }^{\circ}\text{C}$ with one equivalent of DBU, and the reaction mixture was allowed to warm to room temperature over the course of several hours. Column chromatography of the crude mixture removed the bis-alkylated side-product **5-66** and furnished a pure supply of model Cope substrate **5-65** in 42 % yield.



Scheme 5-26. Generation of model Cope substrate **5-65**.

Compound **5-65** was treated in a fashion identical (differing only in alkyl propiolate) to the attempted one-pot experiments, with ten mole percent of DBU and one equivalent of ethyl propiolate at $-10\text{ }^{\circ}\text{C}$ in CH_3CN . The allenolate intermediate failed to undergo Cope

rearrangement, instead neutralizing as previously to deliver neutral adducts **5-67** and **5-68** with an *E/Z* ratio of 4/1 (Scheme 5-27). An experiment conducted at room temperature afforded the same result, and one conducted with NaH (at excess due to difficulties encountered in accurate dispensing at small scale) afforded a complex mixture whose ^1H NMR spectrum did not evidence the far-downfield vinyl proton signal diagnostic of the Cope product.



Scheme 5-27. Attempted allenolate Cope rearrangement of preformed substrate **5-65**.

These findings illustrated that the success of the allenolate Cope reaction observed in the original substrate could not be solely identified with the cumulative influence of the dicyanomethyl and allenolate moieties. Evidently, factors inherent to the ring contribute indispensably to the success of the rearrangement. The specific structural features of the ring are discussed (in section 5.2.7) in the context of the contribution of double-bond substituents to the success of Cope reactions. In the interest of other investigative priorities, an experimental series entailing stepwise elaboration of the model system toward closer analogy with the parent Cope substrate was not undertaken.

5.2.6 Attempted Allenolate Cope Rearrangements with Stoichiometric and Excess Bases

5.2.6.1 Attempted Allenolate Cope Rearrangement with Stoichiometric DBU Followed by Acidic Workup

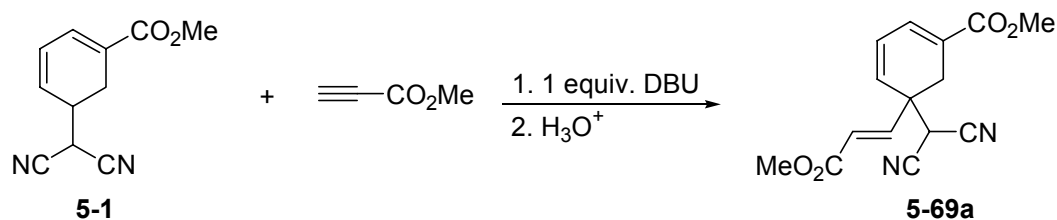
Immediately following the first observation of adduct formation and Cope rearrangement of methyl propiolate and the ring-opened adduct under conditions of catalytic DBU, it was deemed potentially instructive to conduct an experiment to observe the effect of employing stoichiometric base. Of particular interest was the influence of base concentration upon the extent of side-product generation. To this end, one equivalent of DBU was added slowly to a cooled solution of ring-opened adduct and methyl propiolate. After twenty minutes, the reaction was worked up by organic partition against saturated aqueous NH_4Cl . Whereas the complicated product mixture contained the Cope rearrangement product, a number of new constituents were observed in the ^1H NMR spectrum which did not immediately yield to interpretation. Previously identified components also included the ring-deconjugated propiolate adduct **5-28a** and methyl benzoate.

The presence of a considerable quantity of DBU-H^+ indicated the likelihood of an organic salt representing a substantial fraction of the crude mixture. An obvious candidate was the conjugate base of the Cope product, deprotonated at the side-chain sp^3 carbon. A singlet at δ 7.19 was appropriate for the side chain vinyl proton, now absent a vicinal coupling partner ($(\text{CN})_2\text{CCH-}$). Signals of intensities consistent with the first appeared at positions offset to those of the neutral Cope product's ring vinyl protons. A peak was observed at δ 4.5 with an intensity that could only group it with those under consideration, suggesting a downfield-shifted Cope product ring methine proton. Moreover, slightly upfield of the ring methylene proton pair was a partially obscured signal with resolved geminal-scale

coupling, suggestive of the analogous methylene protons of the anion. This assignment would later be confirmed by treatment of a sample of the Cope product with one equivalent of DBU followed by immediate partition between water and EtOAc. The concentrated organic-soluble material furnished a ^1H NMR spectrum (Figure 5-25, presented in the context of elucidation of the side-chain dimer anion structure **5-58b**) containing, aside from very minor impurity, only the Cope product anion-DBU- H^+ salt.

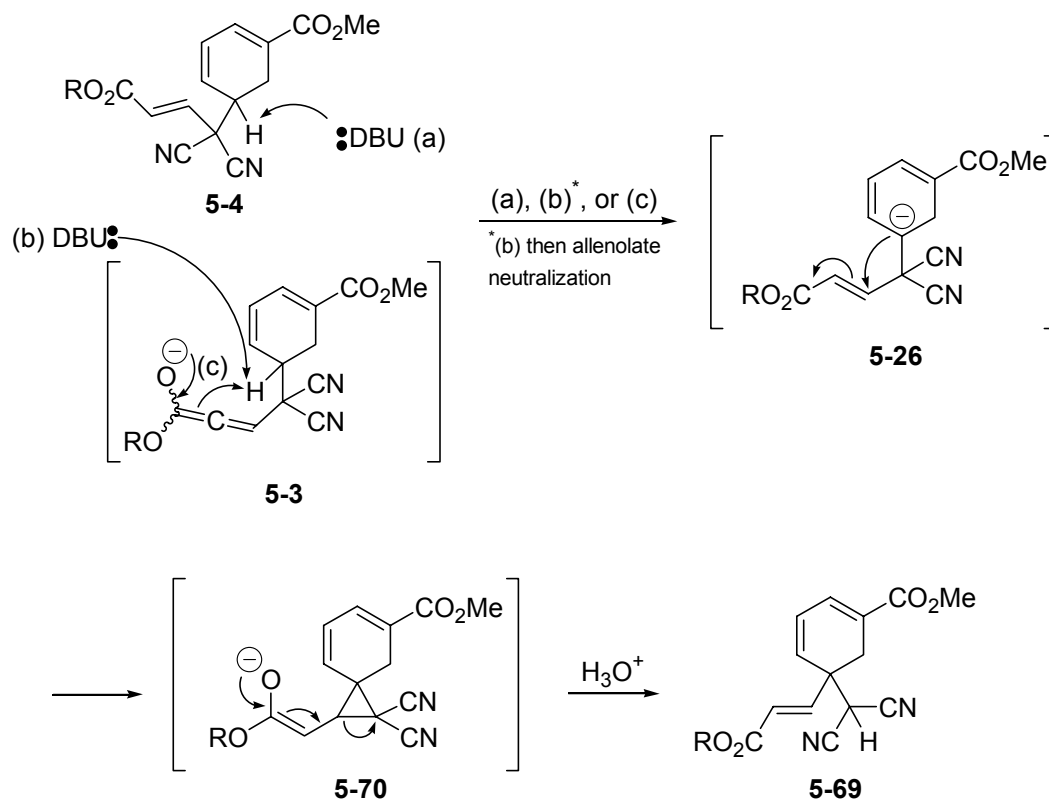
The peaks of the remaining major constituent were now easily mutually associated by their integrals and measured coupling constants. Three proton signals in the vinyl region were highly reminiscent of those of the ring vinyl protons of the ring-opened adduct, although they exhibited simpler coupling patterns (δ 7.10, br d, $J = 5.6$; δ 6.47, dd, $J = 9.5$, 5.6; and 6.06, d, $J = 9.5$). The upfield-most proton of the ring-opened adduct exhibited a doublet-of-doublets, reflecting its two vicinal partners, one a vinyl proton and the other the methine proton at C5; the central vinyl proton a doublet-of-doublets-of-doublets, due to its vicinal vinyl protons and its allylic relationship to the C5-proton. The pattern at hand suggested the same ring-vinyl proton disposition, absent the C5-proton. The isolation of the propiolate-derived vinyl protons indicated that their attachment to the rest of the molecule was at a site bearing no protons. A pair of slightly leaning doublets of high coupling constant (15.77 Hz), the upfield one superimposed upon another smaller J value doublet, was appropriate for the isolated vinyl protons of a *trans*-substituted, ester-conjugated double-bond. Formulation of the structure as the substrate ring-opened adduct substituted by the propiolate at ring C5, rather than at the dicyanomethyl carbon appeared to satisfy the data (Scheme 5-28). The association of the peaks assigned to the isomeric adduct was later

confirmed both on the neutral form and the anionic DBU-H⁺ salt by ¹H-¹H TOCSY experiments.



Scheme 5-28. New ring-opened adduct-propiolate adduct **5-69a** observed in reaction conducted with stoichiometric base.

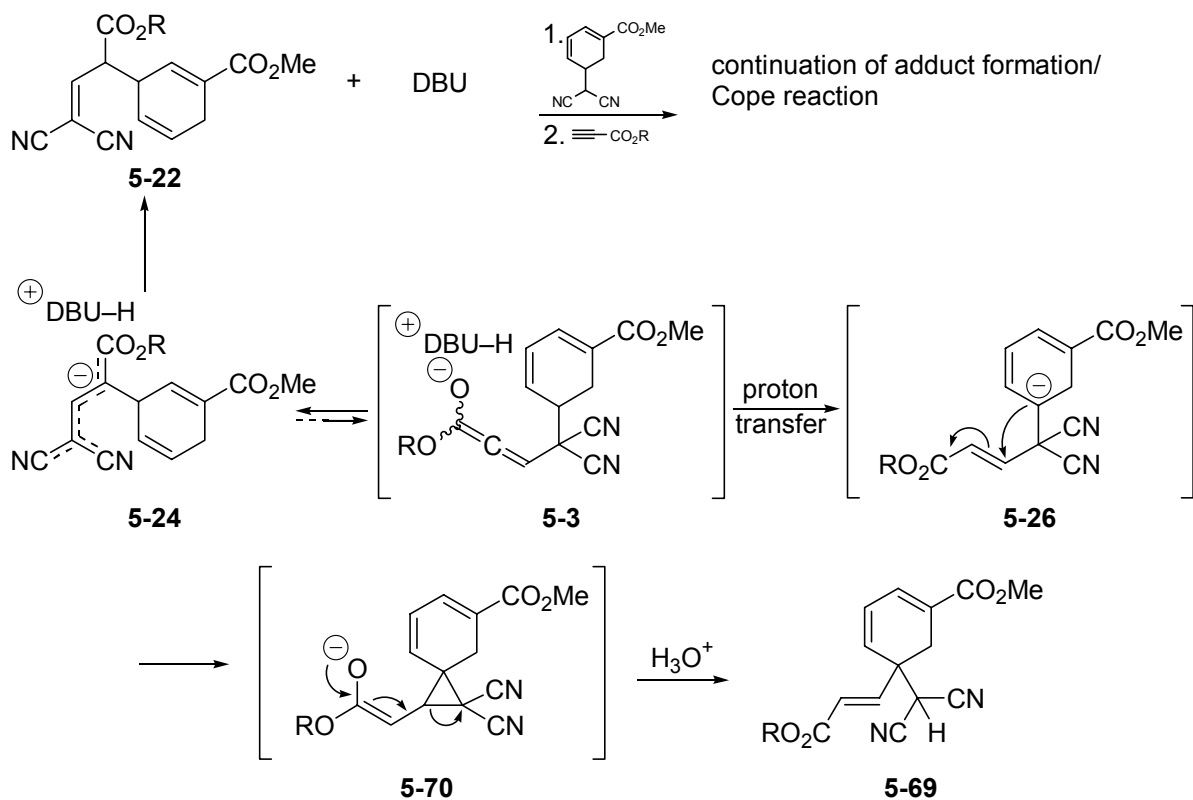
The ability of an increased concentration of base to bring about the generation of the adduct isomer raised the issues of mechanism and competing kinetics in the alternative reactions. The fundamental mechanistic features of the conversion were readily determined. It appeared necessary that an initial adduct (either the allenolate **5-3** or the neutral adduct **5-4**) of **5-1** and the alkyl propiolate was the starting point and that deprotonation of ring C5 would generate a species (**5-26**) set up for a 3-*exo*-trig addition-elimination pathway (via **5-70**) to the isomer anion and, upon workup, to **5-69** (Scheme 5-29).



Scheme 5-29. Conversion of direct adducts to adduct isomer **5-69a**.

Two views of the reaction made possible by higher quantities of base were considered. The first entertained the possible reversibility of the Cope rearrangement. If the Cope rearrangement proceeded from the allenolate intermediate **5-3**, it appeared that a low concentration of base was not able to bring about a great extent of ring C5 deprotonation in advance of rearrangement. At the end of the short reaction time, only a small population of Cope product anion, equivalent to the quantity of catalytic DBU, would be present, offering less potential for the reverse rearrangement. The reaction effected with stoichiometric base would, however, produce a large population of anionic Cope product, favouring a greater occurrence of Cope reversal. The now greater population of pre-Cope adduct would afford the opportunity for ring C5 deprotonation and the subsequent steps toward the adduct isomer,

which in this case would represent the thermodynamic product in comparison with **5-22** (Scheme 5-30).



Scheme 5-30. Generation of adduct isomer **5-69** by pathway involving a reverse allenolate Cope rearrangement.

To probe the potential of the reaction to undergo reverse rearrangement, the rearrangement product **5-22b** (from ethyl propiolate) was treated in separate experiments with stoichiometric and catalytic DBU. In neither case was the Cope rearrangement found to be reversible, indicating the generation of **5-69b** during the progress toward the rearrangement. The implication of this finding is that whatever the Cope-reactive species, it is intercepted by base and deprotonated at ring C5 before rearrangement.

5.2.6.2 Attempted Allenolate Cope Rearrangement with Stoichiometric DBU Without Acidic Workup

A second allenolate Cope experiment was conducted with stoichiometric DBU, but it was deemed potentially instructive to observe the reaction mixture by ^1H NMR spectroscopy without acidic workup. To this end, the anion of the ring-opened adduct was stoichiometrically generated by slow addition of DBU at $-10\text{ }^\circ\text{C}$, followed by the addition of one equivalent of ethyl propiolate. After 7.5 min., the reaction mixture was concentrated *in vacuo* at room temperature, and stored at $-20\text{ }^\circ\text{C}$ prior to NMR sample preparation. The CDCl_3 solution of the crude mixture was assessed within minutes of preparation and was monitored with subsequent spectra over the course of several hours. Figure 5-28 depicts the evolution of the sample through the initial, an intermediate, and the last of five total spectra.

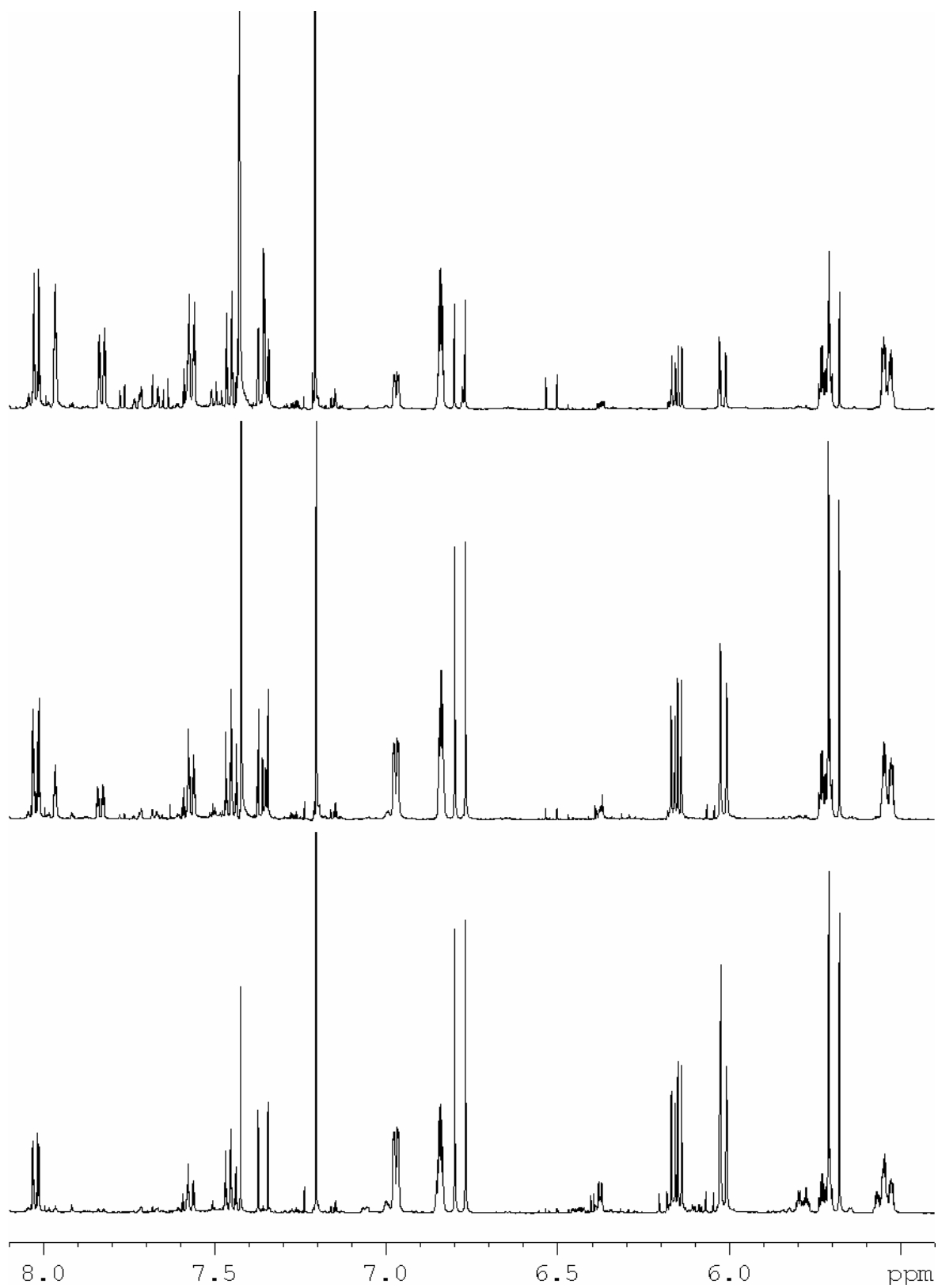
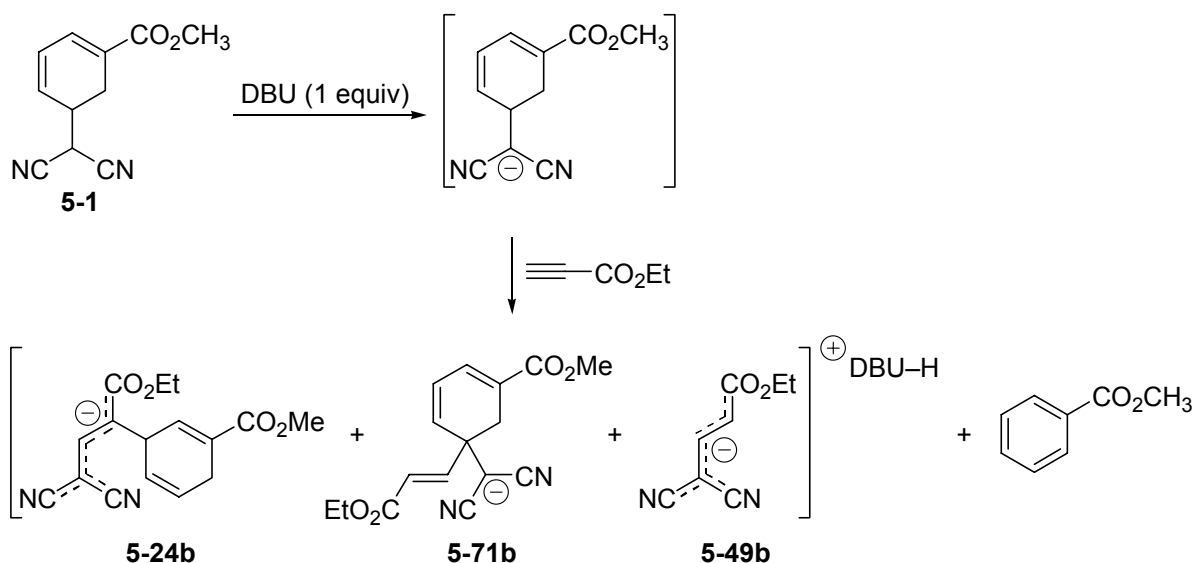


Figure 5-28. Sequential ^1H NMR spectra of attempted stoichiometric DBU Cope reaction isolated without acidic workup. Bottom spectrum - initial; middle - 190 min.; top - 20 hrs.

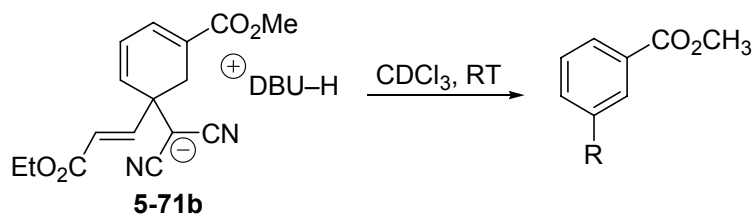
All but one of the constituents of the mixture were easily recognized from the structural formulations derived from previous experiments. Present initially were the anions of the Cope product **5-24b**, the side-chain fragment **5-49b**, and the adduct isomer **5-71b**, as well as methyl propiolate and trace quantities of structures whose identities were not pursued (Scheme 5-31).



Scheme 5-31. Initial constituents of the product mixture derived from formal allenolate Cope reaction employing one equivalent of DBU without acidic workup.

Of particular significance, as in the parallel experiment worked up with mild acid, is the large quantity of methyl propiolate and the side-chain anion **5-49b**, as compared to the minor quantity of these constituents in experiments conducted with catalytic base. The aromatic region signals at δ 7.97 and δ 7.83, which arose over the course of the NMR observations, were taken as diagnostic for *meta*-substituted aromatic compounds derived from the ring-opened adduct, encountered at various stages of this and previous workers' research. The overlap of other signals in the aromatic region precluded complete assignment of the ring protons; furthermore, a complete structural formulation was not considered crucial

to the issue under consideration. A careful analysis of the signal integral intensities allowed for the association of the development of the *meta*-substituted compound with the decline of the adduct isomer **5-71b** (Scheme 5-32).



Scheme 5-32. Development of a *meta*-substituted aromatic compound through aromatization of adduct isomer **5-71b**.

Of particular interest was the complete loss, by the time of the second ^1H NMR spectrum, of certain signals noted in the first (Figure 5-29).

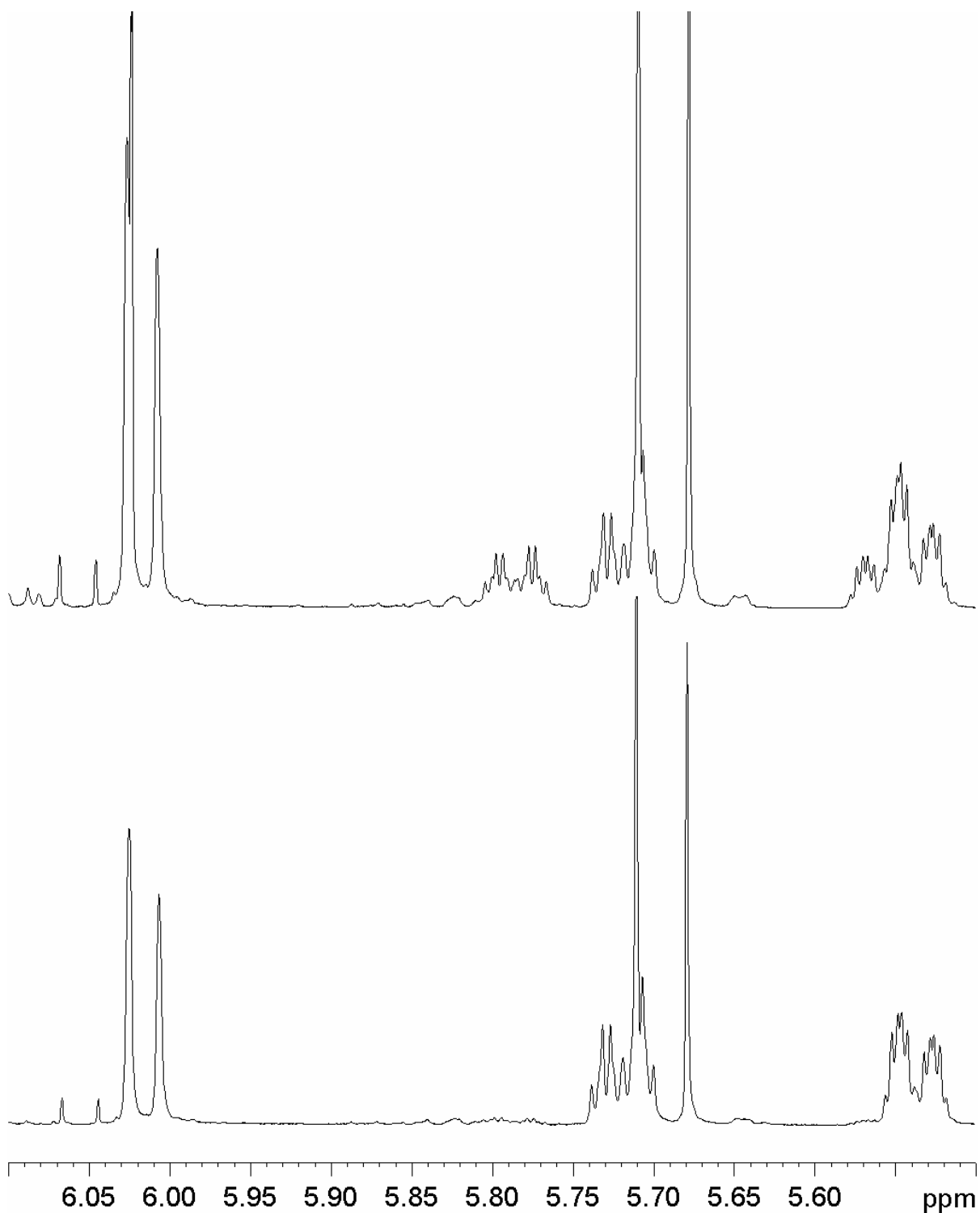
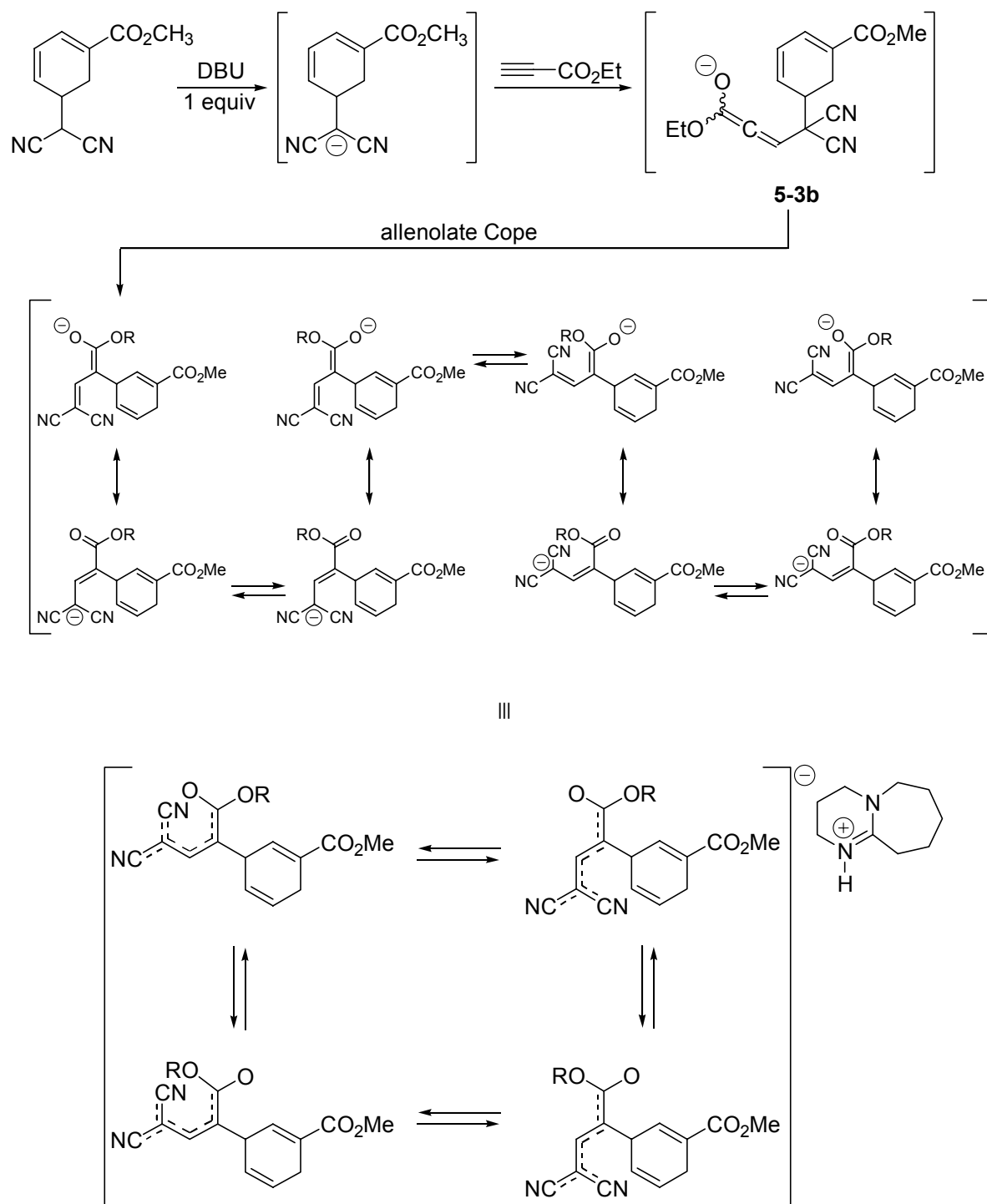


Figure 5-29. Elimination of vinyl ^1H NMR signals upon isomerization of side-chain of Cope product anion. Lost intensity of partially obscured singlet at δ 6.022 is added to singlet at δ 7.21. Multiplet at δ 5.785 contributes to multiplet at δ 5.719. Upfield partially obscured multiplet (visible downfield component at δ 5.569) contributes to multiplet at δ 5.539.

Scrupulous attention to the relevant integral intensities indicated that the intensity of three visible signals in the vinyl and aromatic region (two obscured and one baseline resolved) was contributed, in their disappearance, to other signals initially present. In particular, the singlet at δ 6.19 contributed its intensity to the singlet at δ 7.19, already established as the side-chain vinyl proton of Cope product anion **5-24b**. The multiplets at δ 5.785 and δ 5.569 (visible downfield portion of signal) declined concomitantly to the intensity gain of the ring vinyl proton multiplets at δ 5.719 and δ 5.539, respectively. Collectively, the data suggest the initial presence of two isomeric Cope product anions that experienced equilibration to the thermodynamically more stable form. That the equilibration occurred slowly enough to be followed over the course of 75 min. suggests a considerable energy barrier separating the observable isomers.

Reasonable candidates for the interconvertible species would be among the ensemble of side-chain geometric isomers resident in various stable configurations due to the considerable double-bond character imparted across the entire σ -bonded system by delocalization of anionic charge. Scheme 5-33 depicts the set of equilibria among the various isomerically related pairs of species differing by single configuration changes established by rotation about single bonds formally assigned in the resonance contributors to the relevant sites.



Scheme 5-33. Geometric isomerism within the side-chain of the Cope rearrangement product.

The presence of signals for only two anionic species configurations despite the presence of four isomers suggests two possibilities: that the visible resonances are sensitive

only to the configuration change about one of the side-chain bonds, such that pairs of isomers generate shift equivalent signals (Figure 5-30); or that the steric relationships among the side chain moieties demand that isomerization of one partial double-bond drives the isomerization of the other such that two of four isomers depicted in the lower portion of Scheme 5-33 do not occur at an observable quantity.

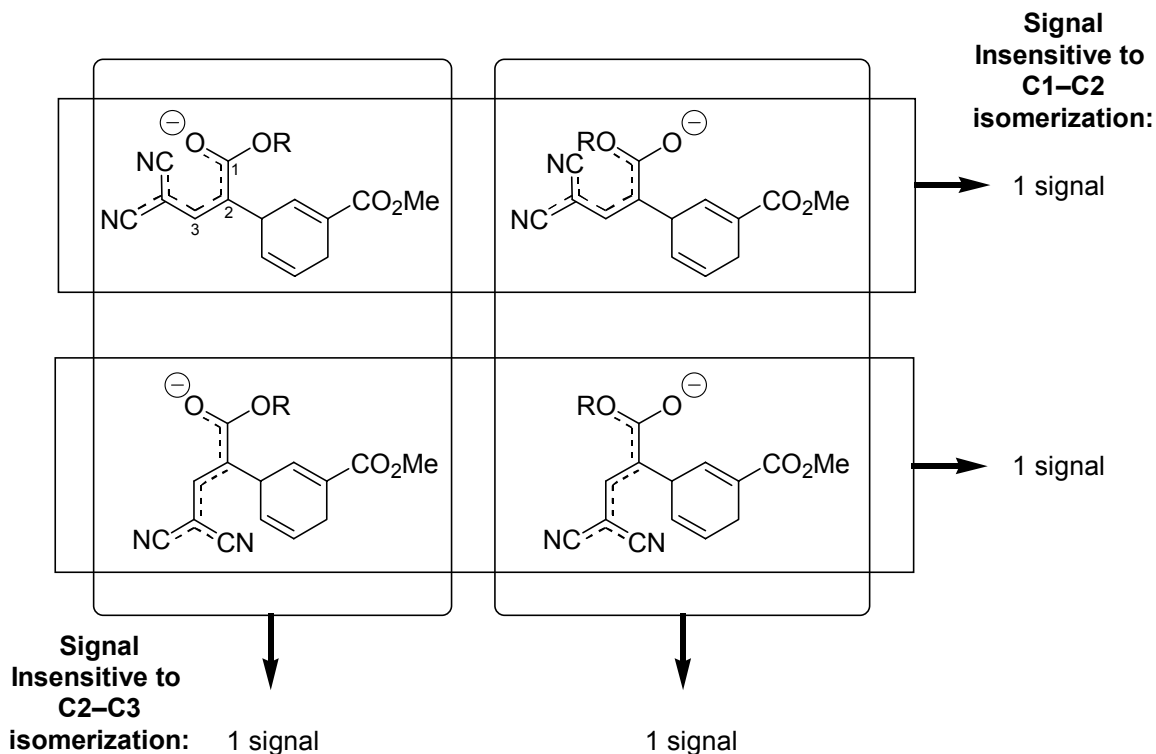
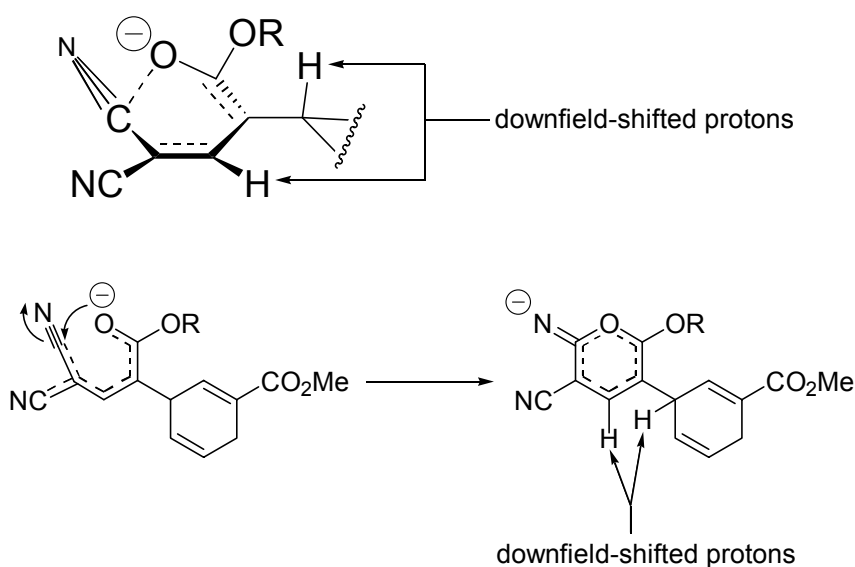


Figure 5-30. Sources of two observed signals for isomers of anionic Cope product based upon accidental chemical shift equivalence of indicated pairs of isomers.

Promising candidates for the species visible in the ^1H NMR spectra are the C2-C3 *cis* and *trans* isomers. An allenolate Cope rearrangement would deliver the *trans* isomer. An intriguing indication of the identity of the thermodynamically more stable isomer is its downfield shift of the side-chain-C3' (δ 6.022 to δ 7.21) proton relative to the initial isomer. The C2-C3 *cis* isomer would have to adopt the conformation of a helical segment with slight out-of-plane twisting of the terminal groups to accommodate the seven or greater atoms

(dependent upon the alkoxy carbonyl moiety's configuration) in proximity at the side-chain termini. A potential outcome of this arrangement is that the oxygen and nitrile carbon atoms will be correctly situated to establish an electronic relationship about the entire "ring" that effectively operates as a ring current and effects a downfield shift of the indicated protons. A corollary possibility is that the *cis* isomer cyclizes by attack of oxygen on the nitrile carbon, establishing a conventional ring current (Scheme 5-34). It has been repeatedly demonstrated that the anionic Cope product in the thermodynamically more stable isomeric form neutralizes as **5-22**.



Scheme 5-34. Downfield shift in protons of thermodynamically more stable side-chain isomer by possible ring-current-like effect, or by ring current established through cyclization.

Comprehensive information regarding the conformation of the ring and the side-chain of the neutral Cope product **5-22** was obtained through a ¹H NMR nOe experiment which, when considered in light of ¹H NMR spectral data obtained through deprotonation of preformed **5-22**, strongly supports the isomerization hypothesis for the anionic side-chain as well as the isomer identities. Irradiation of the upfield side-chain vinyl proton at δ 7.27 elicited a nOe involving the second proton of the side-chain as well as a proton of the two-

proton multiplet at ring C6. A redundant experiment, based upon irradiation of the ring C6 multiplet, confirmed mutual proximity of the proton of the ring methylene (syn to the C3 substituent) and the side-chain protons. This relationship confirms that the ring adopts a boat conformation that situates the side-chain in the pseudo-axial position: a boat conformation that situates the side-chain in the pseudo-equatorial position would sufficiently distance the diagnostic protons that no nOe would be possible. At the same time, the mutual proximity of the side-chain protons indicates that it resides in a conformation destined to establish the *Z*-isomer of the side-chain anion upon deprotonation: indeed, treatment of the Cope product with stoichiometric DBU, followed by immediate assessment by ^1H NMR spectroscopy (following sample concentration *in vacuo*, both with and without initial partition between water and EtOAc) revealed only the presence of the thermodynamically more stable isomer. Conversely, the stoichiometric anionic Cope product derived directly from the allenolate Cope rearrangement, as observed in the timecourse of spectra already presented, is initially present as the thermodynamically less stable isomer and only reaches equilibrium with the more stable isomer at some point in the range of 43 to 81 minutes (the times of the first two ^1H NMR spectra after complete introduction of ethyl propiolate to the ring-opened adduct anion).

The support for the structural formulations of the two interconvertible side-chain anion isomers obtained from the combination of the nOe experiments and the ^1H NMR spectral observations following base treatment of preformed **5-22** afford plausible insight into the geometry of the allenolate Cope reaction. It appears likely that the allenolate Cope reaction proceeds via a chair transition state. Study of a physical model of the incipient formally conjugated enolate product of the allenolate Cope rearrangement in the chair

conformation for the reverse reaction makes it clear that the dihedral angle between the depicted double-bonds (Figure 5-31) better positions the side-chain to achieve complete π -delocalization by adopting the *E* configuration than by rotation through a considerable angle to the *Z* configuration. Conversely, it is tempting to ascribe to an allenolate Cope rearrangement via a boat transition state a direct adoption of the *Z* side-chain configuration, as the π -bonds are more nearly orthogonal and there is a severe steric interaction between one nitrile and the proximal ring methylene hydrogen

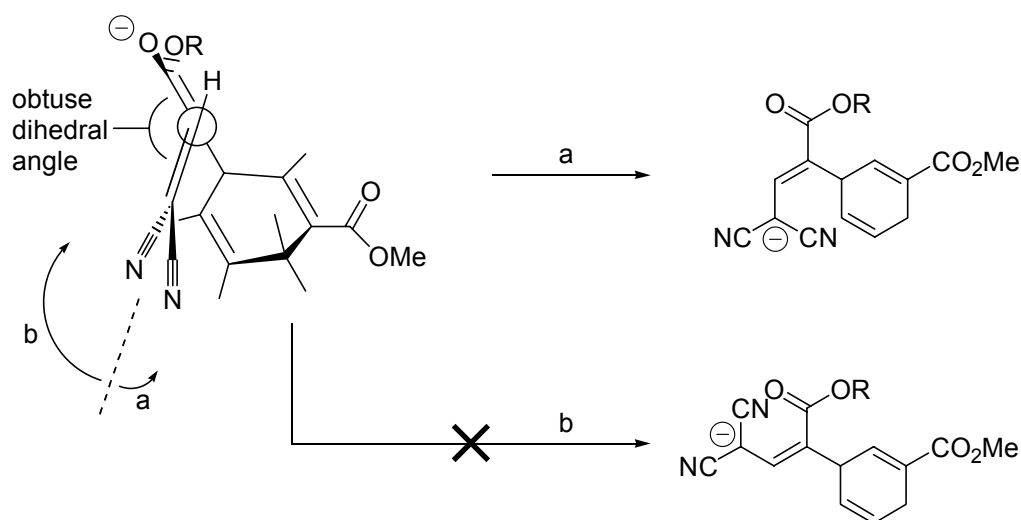


Figure 5-31. Generation of initial anionic side-chain *E* isomer by slight rotation of formal σ -bond in Cope enolate product derived via putative chair transition state.

A depiction of the relationship between the conformational data derived from NOE observations and the isomeric assignments upon deprotonation, as well as the reasonable geometric implication of these findings for the allenolate Cope rearrangement, are summarized in Figure 5-32.

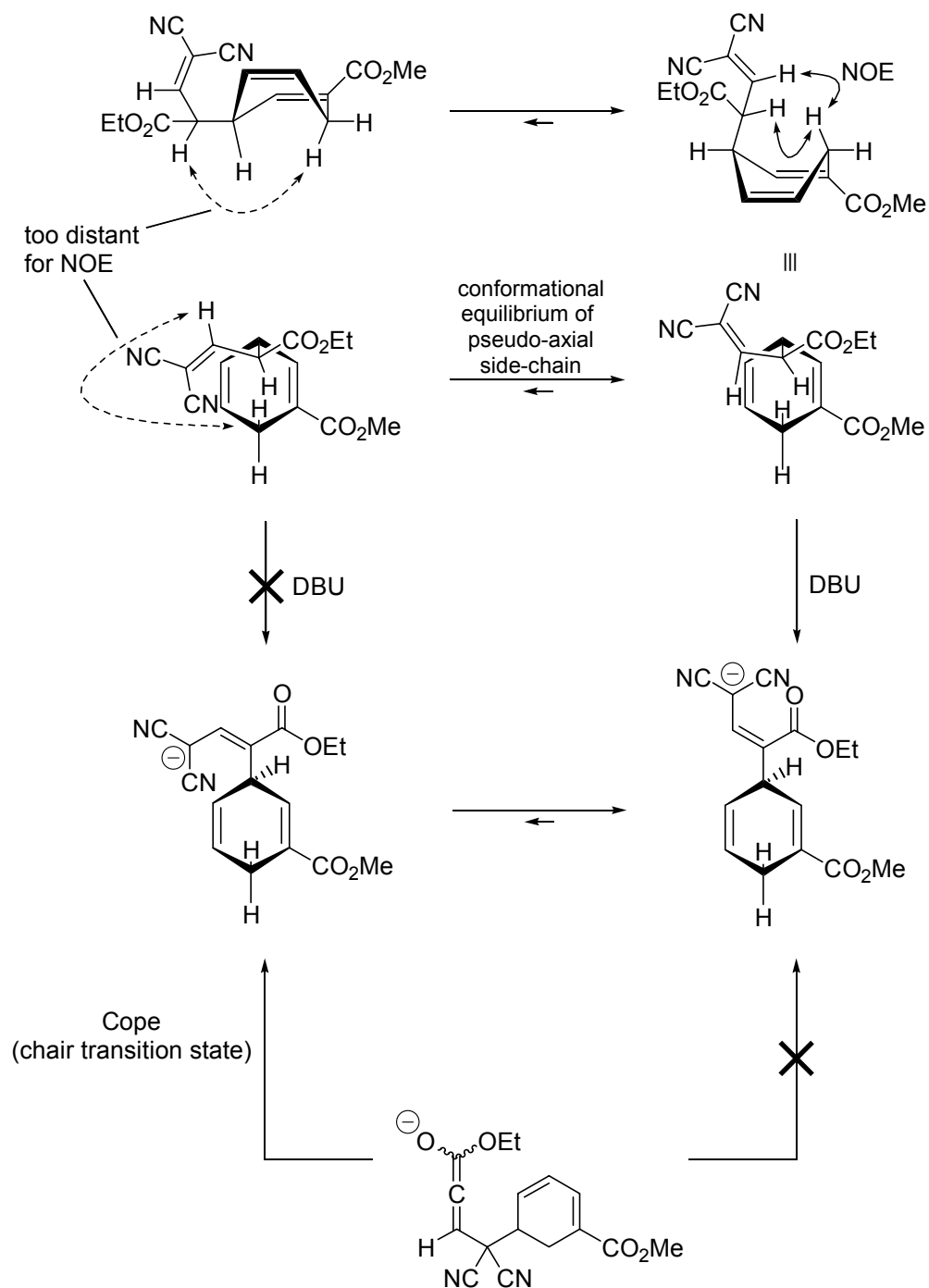
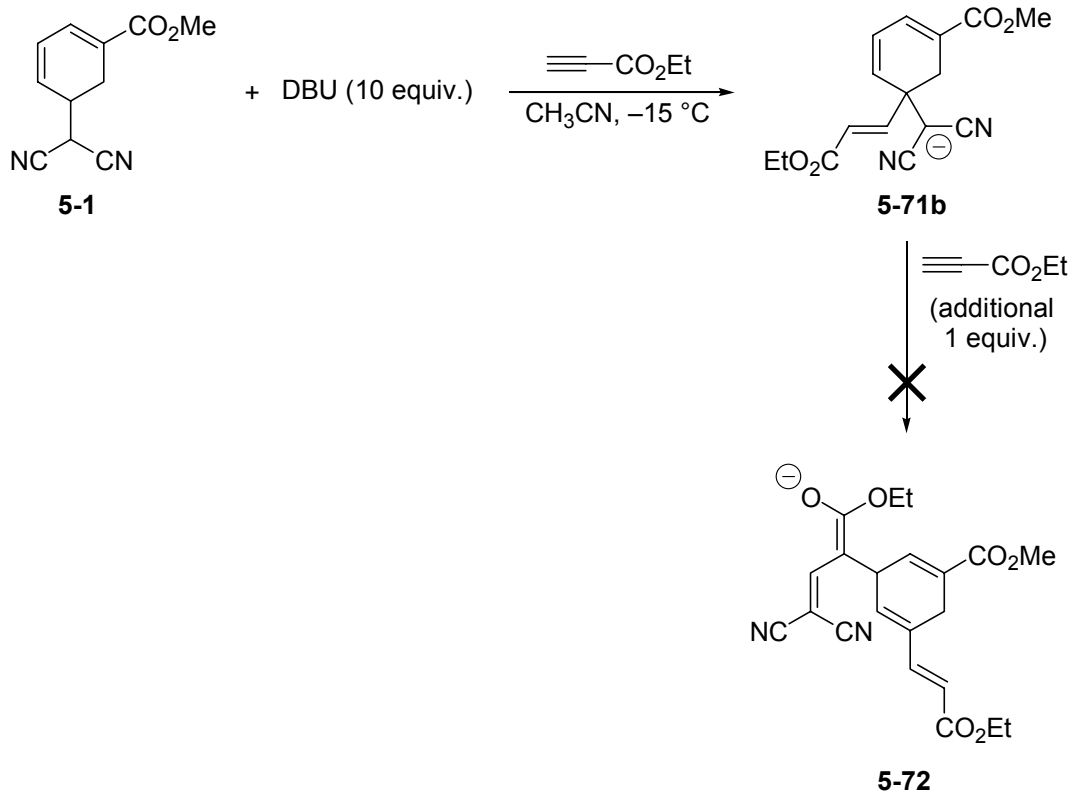


Figure 5-32. Relationship between conformation of Cope product and isomerism of side-chain anion, and tenable implication for the geometry of rearrangement.

5.2.6.3 Attempted Allenolate Cope Rearrangement with Excess Base

The observation of the novel adduct isomer **5-69** in reactions of **5-1** with alkyl propiolates and stoichiometric base, and the conclusion that **5-69** arises by interception of the Cope substrate by base, suggested that a further increase in the quantity of base would increase the quantity of **5-69** generated, to the relative exclusion of cleavage/aromatization and allenolate Cope rearrangement. Thus, **5-1** was treated with 10 equiv. of DBU at $-15\text{ }^{\circ}\text{C}$ in CH_3CN , followed by one equiv. of ethyl propiolate. An aliquot was removed at 20 min. and assessed by ^1H NMR spectroscopy without acidic workup. The sole species, aside from a trace quantity of methyl benzoate and starting material, was **5-71b**, which offered further evidence of the proposed mechanism. We sought to capitalize upon its nearly stoichiometric generation, and so a second equivalent of ethyl propiolate was added in the hope that an allenolate Cope reaction might occur to generate a substituted Cope rearrangement product (**5-72**), but the intermediate proved unreactive (Scheme 5-35).



Scheme 5-35. Nearly quantitative generation of **5-71b** by treatment of **5-1** with a large excess of DBU.

5.2.6.4 Attempted Allenolate Cope Rearrangements with Strong Base

In the interest of exploring the breadth of conditions capable of inducing the allenolate Cope rearrangement, it was deemed potentially instructive to employ stoichiometric amide base. A planned benefit of strong base, as opposed to DBU, was the potential to observe the Cope rearrangement absent the possibility of proton transfer to the incipient allenolate adduct by protonated base. It was anticipated that this restriction could provide insight into the generation of side-products evident in experiments conducted with stoichiometric DBU. Very interesting, and at the time, very puzzling differences in the

outcome of the anionic addition to ethyl propiolate were found when the reaction was performed with lithium and potassium hexamethyldisilazide in place of DBU.

The reactions of **5-1** with stoichiometric quantities of either LHMDS or potassium hexamethyldisilazide (KHMDs) exposed divergent extents of reactivity of its anion toward ethyl propiolate, although both sets of conditions favoured the generation of alternative adduct **5-69b** as the main product. Treatment of **5-1** in THF with commercial KHMDs in toluene at low temperature caused extensive precipitation of the resultant anion that warming and exposure to ultrasonic bath failed to reverse. The amorphous suspension darkened considerably upon slow dropwise introduction of a THF solution of ethyl propiolate, turning the reagent stream black upon direct contact with exposed solid above the solvent surface, and ultimately furnishing an opaque reaction mixture. The reaction nevertheless proceeded at a reasonable pace to consume the starting material and to provide a high recovery of converted material. A second experiment with KHMDs carried out at room temperature also brought about a great extent of precipitation, but the precipitate similarly underwent reaction. ¹H NMR spectra of the crude reaction mixtures clearly revealed a preponderance of a *meta*-substituted aromatic compound along with **5-69b** (approx. 2:1 of *m*-aromatic:**5-69b**).

Two parallel experiments with LHMDS (1 equiv.) witnessed no precipitation and exhibited very slow rates of reaction. An aliquot removed at 45 min. revealed the generation of approximately 16 mol % of **5-22b**, and a trace of **5-69b**, but both products declined in the second aliquot fifty min. later. Transfer to a 0 °C bath brought about rapid reaction, such that the quantity of **5-69b** increased to 44 mol % within one hour. The reaction was concluded at room temperature and at a total of 3.5 hours, but the ratio of **5-1** to **5-69b** was found to have changed little from earlier aliquots. A second experiment was conducted over several days

with the temperature continuously maintained at $-78\text{ }^{\circ}\text{C}$. In this case, 21 mol % of Cope product **5-22b** was produced.

These observations were very intriguing and led to a more detailed consideration of the possible mechanistic considerations which might explain the difference in result observed in the reactions with LHMDS and KHMDS versus that with DBU where no *meta*-substituted aromatic products were observed in reactions that were promptly quenched. The potential of the DBU-induced allenolate Cope reaction to branch into substantial extents of side reactions has been detailed for experiments employing stoichiometric DBU. Prolonged observation of the stoichiometric DBU reaction mixture by ^1H NMR spectroscopy, as already described, provided the sole instance of generation, in DBU experiments, of a presumably anionic *meta*-substituted aromatic compound and demonstrated conclusively its derivation from the anionic alternative adduct anion **5-71b**. It is reasonably concluded that the *meta*-substituted aromatic compounds observed as the major product in the KHMDS reactions and as a minor product in the LHMDS reactions also derive from **5-71b**.

In attempting to discern the factors at work in bringing about such divergent outcomes in the DBU and strong base experiments, a very interesting set of observations and conclusions was unearthed in an analysis of the literature related to the conformational preference of C-5-substituted 1,3-cyclohexadienes. It has been shown that 1,3-cyclohexadienes prefer a pseudoaxial orientation of the C-5 substituent at higher temperatures and a pseudoequatorial orientation at lower temperatures (Figure 5-33).⁵

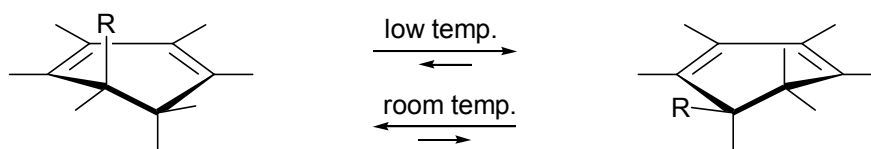


Figure 5-33. Temperature-dependent conformational preferences of substituted 1,3-cyclohexadienes.

The studies that led to this conclusion concerned the temperature-conformation relationship for 5-isopropyl-1,3-cyclohexadiene and attributed the pseudoaxial preference at room temperature to the greater entropy associated with the freedom of rotation of the substituent in the pseudoaxial position. It was thought that differences in conformation could be implicated in the reactions of **5-1** under different base conditions, whereby the base, and thus the counterion to deprotonated **5-1**, would encourage different reactions through their influence on the conformation of the reactive species. There is not a clear temperature-conformation relationship at work in the present system that can invoke that applicable to 5-isopropyl-substituted cyclohexadienes, although the influence of the counterion on the reaction course was considered carefully in terms of conformation. Experiments at the alkylation stage began at low temperature (LHMDS) and were continued at temperatures ranging from $-78\text{ }^{\circ}\text{C}$ to room temperature. The KHMDS experiments were conducted at as high as room temperature after the introduction of ethyl propiolate. If anything, it would be tempting to devise a rationale for the varying reactivities observed in the present study that is the reverse of the stated temperature-conformation trend, were temperature the sole variable at work.

It is possible that the entropy gain in the isopropyl substituent, which is a combination of free rotation about the ring-attachment C–C bond as well as methyl group rotation, is greater on going to the pseudoaxial conformation than that for the dicyanomethyl, where rotation about the C–CN sigma axis wouldn't be expected to make a contribution as substantial as methyl rotation. This could mean that the pseudoequatorial conformation could dominate at higher temperatures than for the bulkier isopropyl.

A second conformational possibility, and one with more compelling implications for the present system, is detailed in Figure 5-34, in which the nature of the counterion has a significant effect on the conformation. Potentially, metal counterions are small enough to associate with both the anionic center and conjugated system of ring, favouring the pseudoaxial conformation. A physical model also suggests the ability of the ester carbonyl to participate in complexation with a metal ion over the ring, bridging to a nitrile nitrogen atom. The steric bulk of DBU-H^+ may demand a position away from the surface of the ring, especially in pseudoaxial conformation.

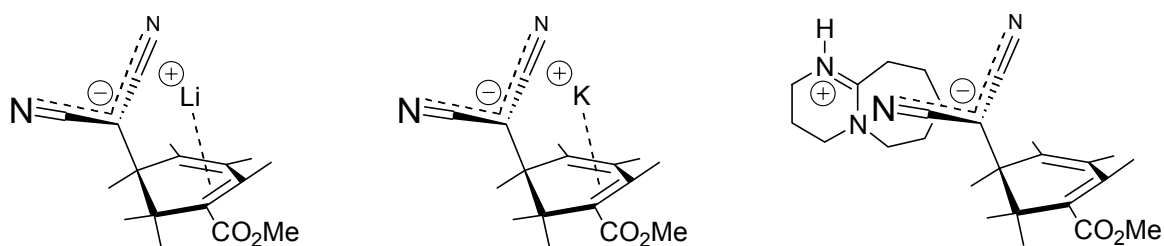
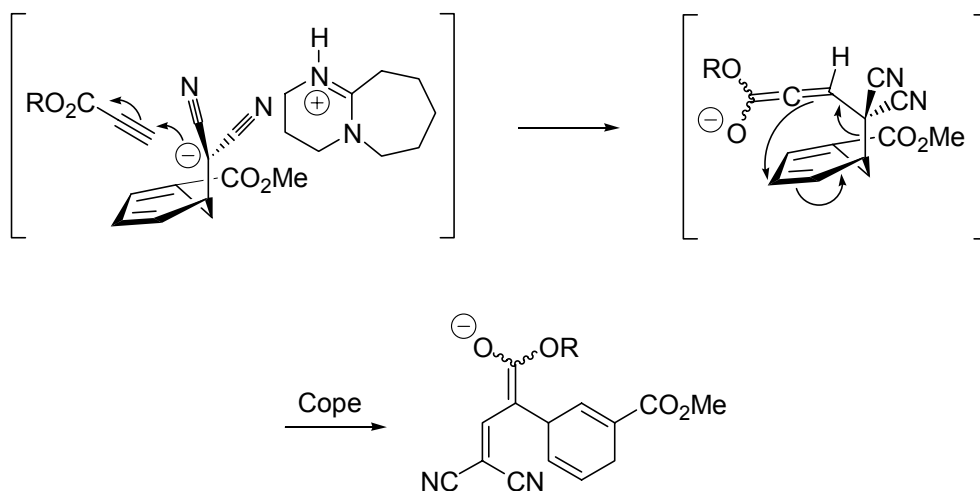


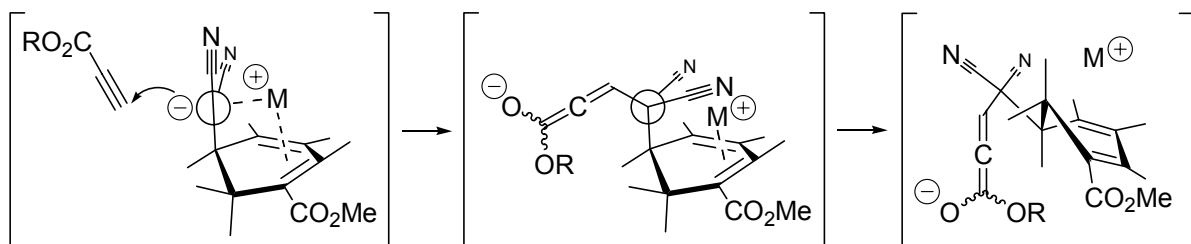
Figure 5-34. Potential relationships of ring face of anionic ring-opened adduct to counterions in the pseudoaxial conformation.

In light of these possibilities, the conjugate addition stage in the DBU experiment may favour immediate Cope reaction because of the ideal site of alkylation. The combination of a pseudoaxial orientation and the positioning of the DBU-H^+ counterion on the anionic face of the dicyanomethyl group opposite the ring may bring about conjugate addition to alkyl propiolates directly over the ring, permitting immediate Cope reaction to the near exclusion of ring C-5 deprotonation (Scheme 5-36).



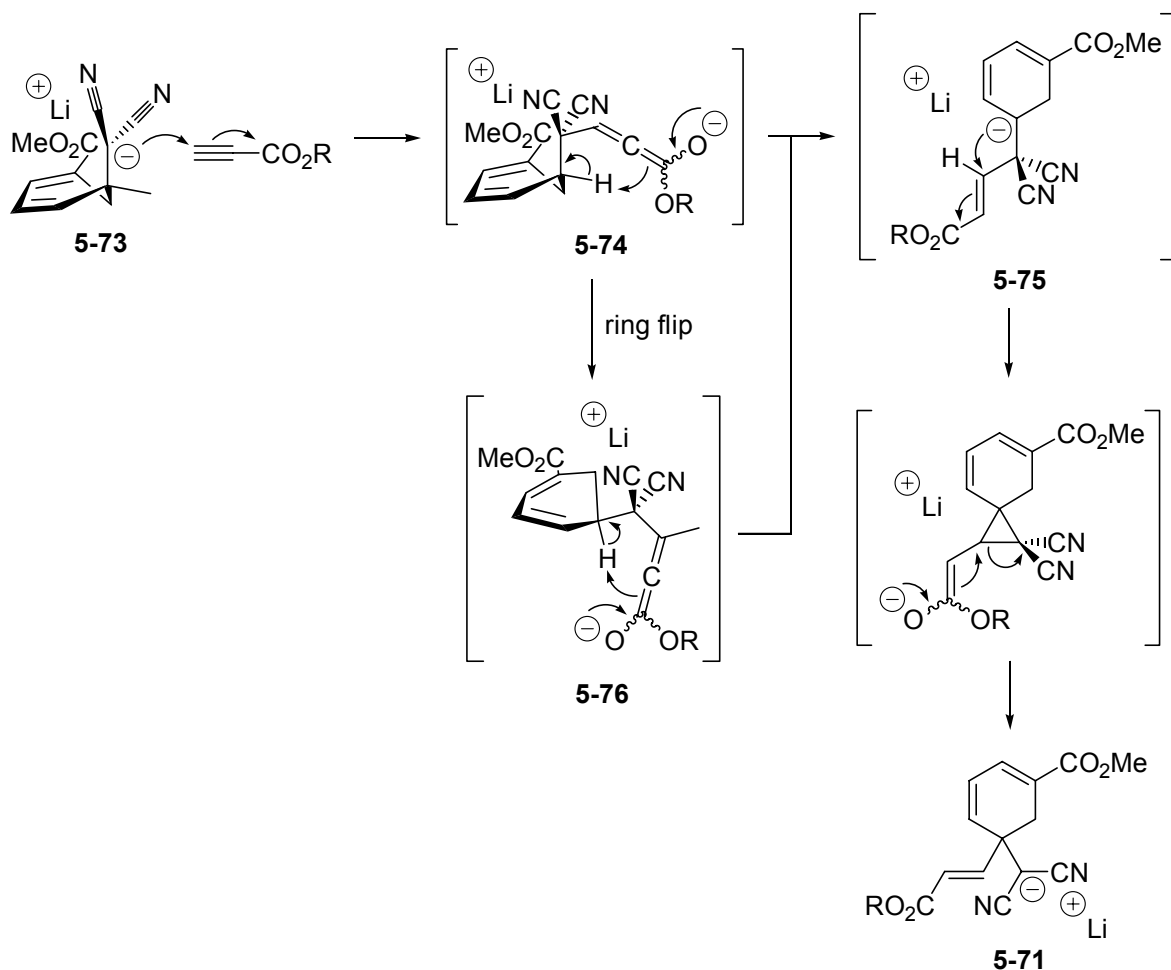
Scheme 5-36. Postulated role of conformation in allenolate Cope experiments conducted with DBU.

Whereas the ring-opened adduct anion may readily adopt the conformation that situates the anionic dicyanomethyl substituent in the pseudoaxial position, whatever the counterion, it is reasonably suggested that conjugate addition to an alkyl propiolate in the case of metal counterions favours a ring flip due to the increased steric interactions of the nitriles with the ring π system and the syn ring methylene hydrogen as the formerly anionic carbon takes on sp^3 hybridization (Scheme 5-37). Compounding the steric crowding is the posited involvement of the metal ion between the dicyanomethyl moiety and the ring surface, which is impinged upon by the folding over of the nitriles.



Scheme 5-37. Proposed steric interactions upon conjugate addition promoting conformation change to position side-chain in pseudo-axial orientation.

The kinetic acidity of the ring C5 proton may be increased in the pseudoequatorial conformation, as the then pseudoaxial C–H bond would be parallel to the ring π -system. This could explain the great propensity of the system in the KHMDS experiment to deprotonate C5 and generate **5-69b**, as the larger counterion would experience greater steric crowding over the ring, thus favouring a conformational change. At low temperature, LHMDS favoured slow allenolate Cope reaction, whereas at 0 °C, **5-69b** was rapidly generated. This could indicate a temperature-conformation trend for the lithium-associated anionic species in which, at low temperature, conjugate addition is well positioned for allenolate Cope rearrangement, whereas, at higher temperature, the counterion association is disrupted such that ring-flip of lithium anion **5-73** occurs (to **5-76**) and the route to **5-69** (via **5-75**) comes into play (Scheme 5-38). It also cannot be ruled out that ring C5 deprotonation occurs from the pseudoaxial orientation (**5-74**): it may be that higher temperature hastens this kinetically less favourable reaction.



Scheme 5-38. Possible conformational features at work in generation of **5-71**.

5.2.7 Mechanistic Considerations and Assessment of Reactive Species in Formal Allenolate Cope Rearrangements

5.2.7.1 Introduction

The sigmatropic rearrangement of adducts of **5-1** and alkyl propiolates has so far been carefully referred to as a formal allenolate Cope rearrangement. Whereas two experimental lines of evidence described below argue for the allenolate as Cope substrate, it has been borne in mind throughout the consideration of this process that ironclad experimental

evidence of the nature of the reactive species has not been available and that several criteria for discernment of the reactive entity — allenolate, allenol, or a neutral adduct — apparently implicit in the available data were necessarily deemed problematic by countervailing interpretations. So too have subtle potentialities frustrated the devising of new experiments to put this issue to rest. This constraint limits the interpretation to pointing out the preponderance of evidence in support of one overall model among the three (each based upon one of the three Cope substrate species) that account for the observed species and their quantities. The question of how the Cope rearrangement, the cleavage/aromatization reaction, and the generation of the adduct isomers occur are related in the context of processes involving the scrutinized propiolate-centered tautomeric and ionic states is best informed by consideration of the factors which are known to influence the Cope rearrangement in general. These substituent effects apply to all the mechanistic models to be considered.

5.2.7.2 Mechanism of Cope Rearrangement and Influence of Substituents

Examination of the literature concerning the Cope rearrangement⁹ reveals that there has been considerable debate concerning the mechanism of this process, even for the prototypical degenerate rearrangement of 1,5-hexadiene (Figure 5-35).

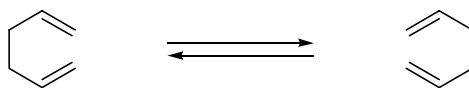


Figure 5-35. Cope rearrangement of 1,5-cyclohexadiene.

The reaction has been variously described as a concerted [3.3] sigmatropic shift with a single transition state (**5-77**) possessing aromatic character and as a diradicaloid process. In particular, a cyclohexane-1,4-diyl transition state (**5-78**) has been considered as well as a loosely associated bis-allyl radical (**5-79**, Figure 5-36).

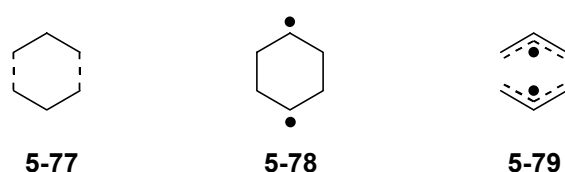


Figure 5-36. Transition state models for the Cope rearrangement.

Some of the earlier uncertainty concerning mechanism arose from the inadequacy of either semi-empirical molecular orbital or Hartree-Fock ab initio methods employing lower basis sets and excluding configuration interaction. More recent theoretical treatments involving newer theoretical methods suggest that the transition state is best considered to be a resonance hybrid of the three species (Figure 5-37).¹⁰⁻¹²

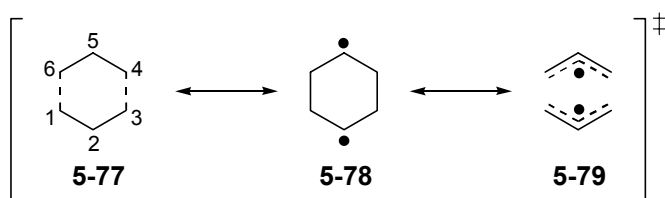


Figure 5-37. Resonance hybrid model of Cope rearrangement transition state.

Such a model allows for a reasonable interpretation of the influence of various substituents on the nature of the transition state structure. For example, substituents at C2 or C5 which stabilize radical character are expected to favour a transition state geometry similar to **5-78**, whereas substituents at C1, C3, C4 and C6 which stabilize radical character would be expected to favour a transition state geometry analogous to **5-79** with elongated bonds between the termini of the allyl radical-like components.

In this context, the Cope rearrangement of interest in the present study can be considered to be one in which the parent 1,5-hexadiene system is substituted at C1, C3, C4 and C-6 and it is instructive to analyze the expected influence of each of the substituents on the transition state for this unusually facile Cope rearrangement (Figure 5-38).

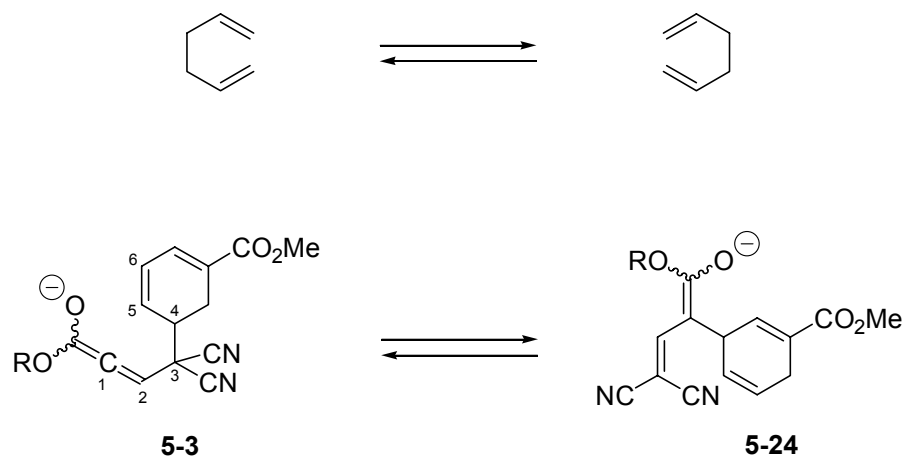


Figure 5-38. Consideration of formal allenolate Cope rearrangement in terms of substituent effects at C1, C3, C4, and C6.

Influence of Cyano Substituents at C3

Ab initio molecular orbital calculations employing Density Functional Theory using the B3LYP/6-31G* method shed some light on the expected influence of the cyano substituents at C3 on the transition state for the reaction of 3,3-dicyano-1,5-hexadiene.¹¹ In that study, it was found that the predicted chair-like Cope transition state was of the bis-allyl radical type (**5-82**) with rather elongated partial bonds between the termini of the allyl systems as shown below (Figure 5-39).

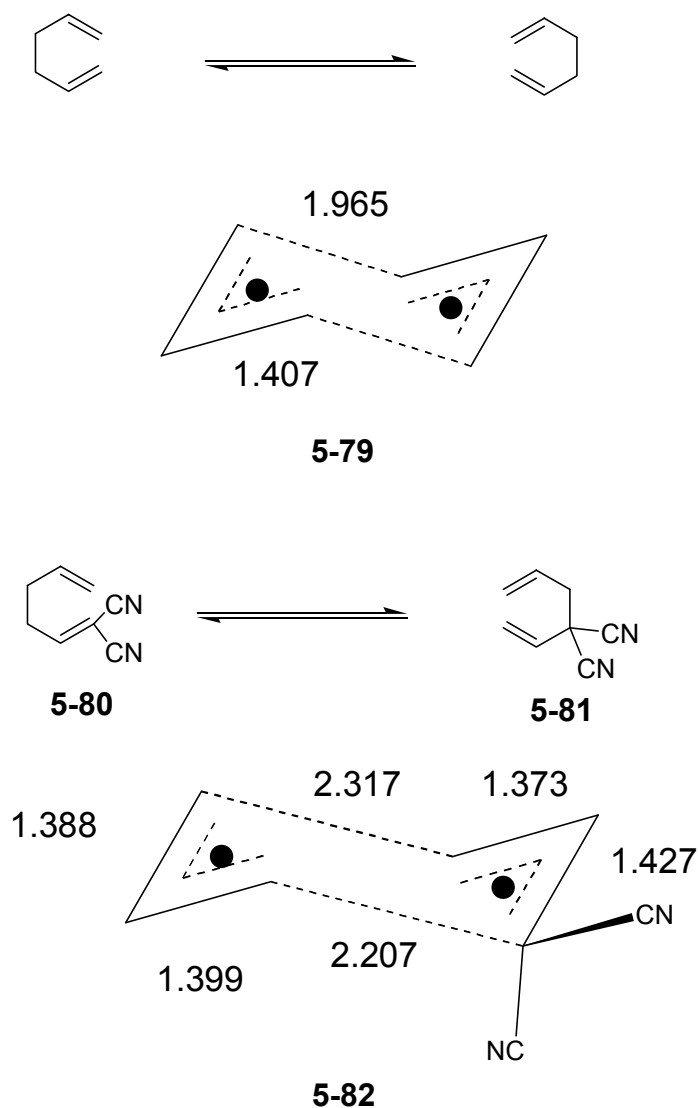
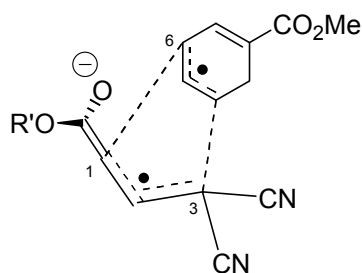


Figure 5-39. Bis-allyl radical character in the transition state of the Cope rearrangement of 3,3-dicyano-1,5-hexadiene.

The cyano substituents appear to stabilize allyl-type radical character in the transition state and, thus, it is reasonable to suggest that a similar interaction in the transition state for conversion of **5-3** to **5-24** favours a bis-allyl radical type geometry (**5-83**) for that Cope rearrangement (Figure 5-40).



5-83

Figure 5-40. Bis-allyl radical character in the transition state of the formal allenolate Cope rearrangement.

Of further interest is the prediction that the conversion of **5-81** to **5-80** should be exothermic to the extent of 11.6 kcal/mol and that the average enthalpy of activation for equilibration of 3,3- and 1,1-dicyano-1,5-hexadiene is 4.1 kcal/mol lower than that computed for the parent Cope rearrangement. As a result, the cyano groups in **5-3** are expected to make a significant contribution to the ease of rearrangement to **5-24**; however, the presence of the geminal nitriles is not sufficient to account for the ease of the observed Cope rearrangements, as the simpler allylic models of the original rearrangement failed to undergo the reaction.

Influence of Substitution at C4 and C6

Since vinyl and alkyl substituents are known to stabilize radicals, it is reasonable to assume that the sigma C–C (ring) bond at C4 (according to the numbering of the reactive carbon array) and the π -bond at C-6 would both contribute to the stabilization of the bis-allyl radical character of the transition state **5-83**. Vinyl substitution at C6 would be expected to act analogously to the cyano substituents and extend the conjugative stabilization of the allylic radical character of the contiguous reactive centers in the transition state through an additional two double-bonds to include the carbonyl of the ring substituent (Figure 5-41). The alkyl substitution at C4 is expected to impart some extent of inductive stabilization to the same allyl radical-like fragment.

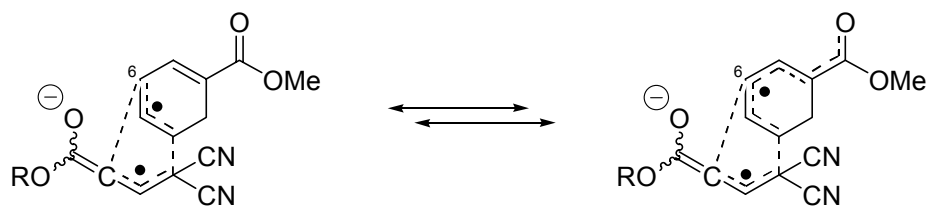


Figure 5-41. Delocalization of allyl radical character by C6 substituent in Cope rearrangement transition state.

Influence of enolate at C1

The C1 enolate, as part of the allenolate moiety, is expected to contribute the same driving force to the conversion of **5-3** to **5-24** that has been observed in the Cope ring expansions of the allenyl analogs of divinylcyclohexanes to 1,5-cyclodecadienes, due to the “decumulation” of the allene subunit to a conjugated 1,3-diene arrangement. Whereas the Cope ring expansion of divinylcyclohexanes (**5-84** to **5-85**) is unfavourable ($\Delta G^\circ = 8.5 \text{ kcal mol}^{-1}$ at 40°C ; $K_{\text{eq}} = 1.3 \times 10^{-6}$), that of 1-allenyl-2-vinylcyclohexane occurs with complete conversion in the case of the *cis* isomer (**5-86** to **5-87**) and with a highly favoured equilibrium in the case of the *trans* isomer (**5-88** to **5-89**) (Figure 5-42). The allenyl/vinyl Cope rearrangement is noted to occur with a lower activation energy than that of the divinyl case, presumably because some of the thermodynamic advantage of decumulation is realized in the transition state.¹³ It is reasonable to surmise that the same influence attends the formal allenolate Cope rearrangement of **5-3** to **5-24**.

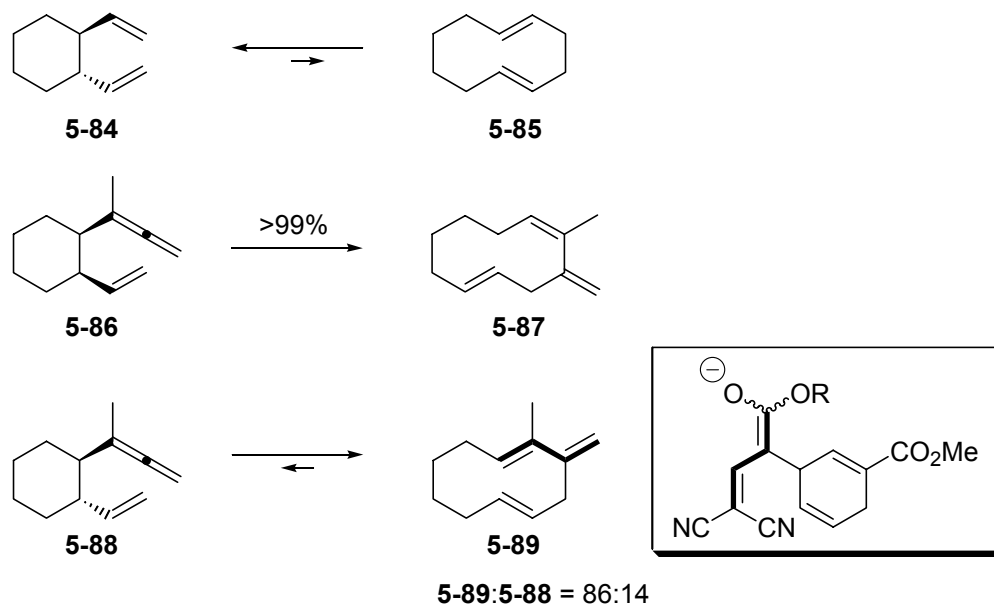
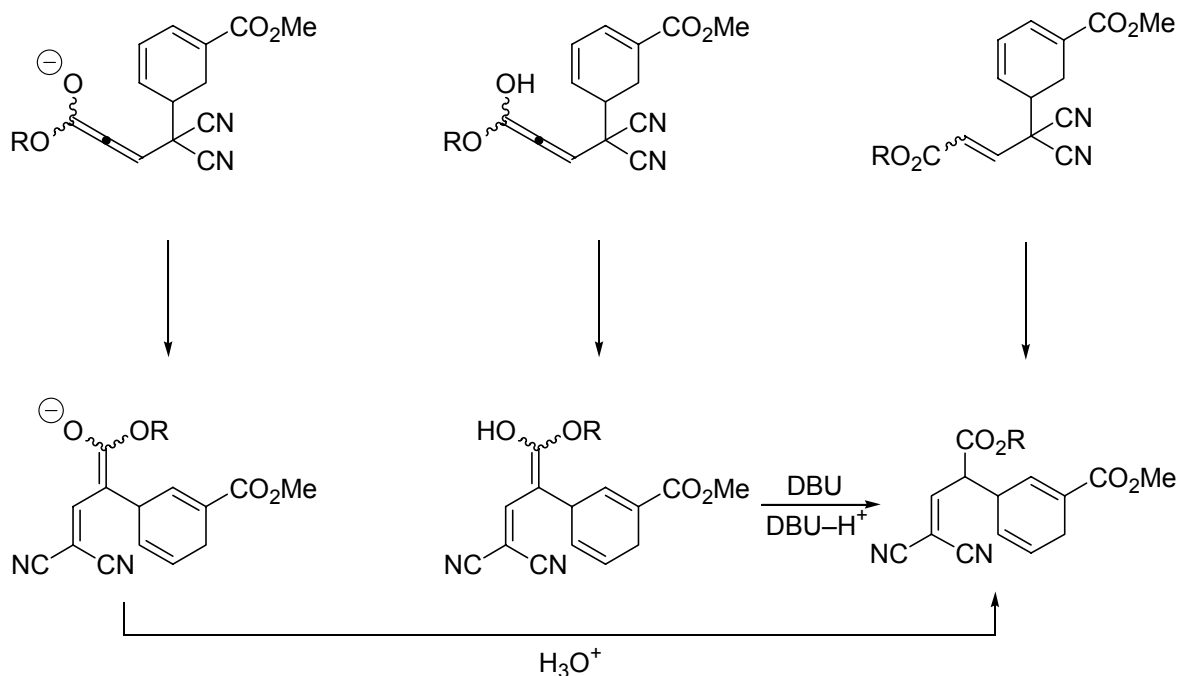


Figure 5-42. The Cope ring expansion of 1-allenyl-2-vinylcyclohexanes driven by decumulation of the allenyl subunit.

The Cope rearrangement of **5-3** experiences a sufficient accumulation of beneficial substituent effects to occur under facile conditions ($-10\text{ }^{\circ}\text{C}$, < 20 minutes). Evidently, the difference in substitution between the original system based on ring-opened adduct **5-1** and the model allyl system, that is, the C4 alkyl substitution and the C6 vinyl substitution, is required to drive the Cope rearrangement. If the Cope rearrangement occurs from a neutral substrate, the two additional substituent effects hasten the reaction sufficiently to occur at low temperature, in contrast to the model systems, which fail to demonstrate rearrangement at room temperature. If an allenolate Cope is in operation, the additional substitutions are required to bring about rearrangement ahead of the allenolate neutralization that is observed to terminate the model reactions.

5.2.7.3 Assessment of the Reactive Species

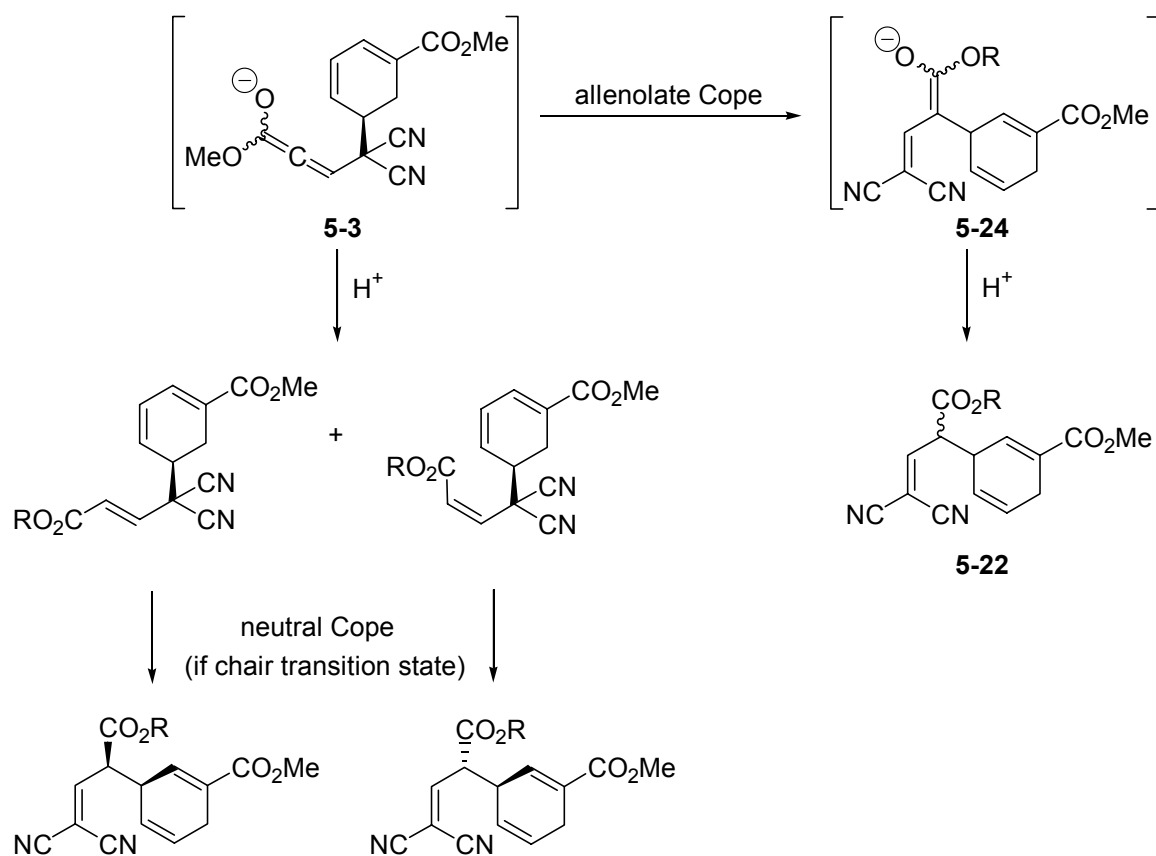
Extensive effort has been directed toward discerning in the available data conclusive evidence for the reactive species. It would be significant to determine whether the reaction represents a completely novel allenolate or allenol Cope rearrangement, or is conventional (neutral), though remarkably facile (Scheme 5-39).



Scheme 5-39. Potential reactive species in Cope rearrangement of adduct of **5-1** and alkyl propiolates.

It was initially thought that the equal populations of the two diastereomers of the Cope product **5-22** provided evidence of an allenolate Cope rearrangement. The experiments aimed at assessing the generality of the Cope rearrangement, through the substitution of the ring component of the parent experiment by simpler acyclic vinyl components, failed to produce the rearrangement product. Instead, the allenolate intermediate was neutralized, furnishing a simple adduct. The protonation of the allenolate was observed by ^1H NMR spectroscopy to furnish *cis* and *trans* double-bond isomers in a ratio of one to five. If this

diastereoselectivity can reasonably be expected of the comparable neutralization of the allenolate intermediate **5-3**, then the population of neutral adduct **5-4**, though never observed, can be expected to have comprised a similar distribution of double-bond isomers. If the observed formal Cope rearrangement proceeded from the neutral adduct, the stereospecificity of the conversion with respect to the double-bond isomer would impart the same diastereomeric ratio to the population of carboalkoxy-bearing carbon epimers (C2). It was thought that an observation of the Cope product at this stage would therefore distinguish between a neutral Cope mechanism, and rearrangement of the allenolate. If the ratio of the intensities of the isolated side-chain vinyl protons of the product matched the ratio of *cis-trans* double-bond isomers of the neutral adduct, a neutral Cope mechanism would be confirmed (Scheme 5-40).



Scheme 5-40. Diastereomeric product ratio as possible evidence of allenolate Cope rearrangement.

Alternatively, the Cope rearrangement of the allenolate intermediate **5-3** would deliver an extended enolate product, which would protonate kinetically, either *in situ* in the successful catalytic DBU experiments to permit the reaction to continue, or upon protonation at workup of the $\text{LiN}(\text{TMS})_2$ experiment. In either case, the observed ratio of product epimers would reflect the facial selectivity in protonation of the enolate, offering no mechanistic evidence if the neutralization exhibited high stereochemical preference, or confirming the allenolate mechanism if equal quantities of neutral diastereomers were produced. The neutralization of the enolate does not, in fact, exhibit any selectivity. Treatment of the Cope product with stoichiometric DBU in experiments probing the

reversibility of the rearrangement produced an enolate population that was later worked up with 6% aqueous HCl and that generated equal quantities of the two epimers.

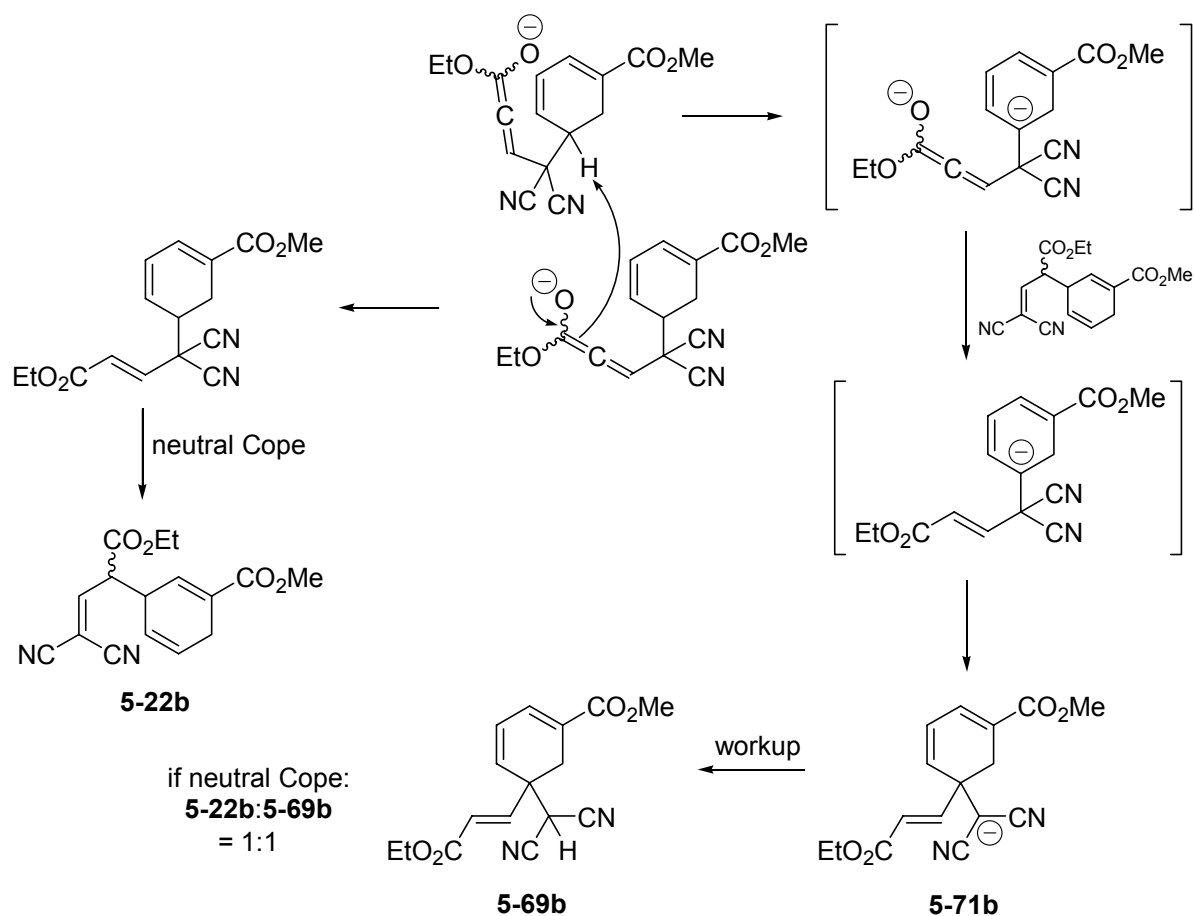
The observation of nearly equal quantities of diastereomers in the catalytic DBU experiments would seem to confirm the allenolate-based rearrangement, but the stated criteria for mechanistic discrimination are upset in this instance by the possibility of stereochemical scrambling of an initially unequal distribution of diastereomeric neutral Cope products at the epimeric site by rapid acid-base reactions among DBU-H^+ or neutral product and product enolate.

One experiment involving stoichiometric LiN(TMS)_2 (which appears to have contained BuLi in excess) generated a small quantity of rearrangement product. At first, this experiment appeared ideally suited to evidencing one of the mechanisms under consideration. In this case, the reaction contains, at each stage, stoichiometric anion, first of the ring-opened adduct and then of the allenolate adduct, without an apparent proton source to neutralize the intermediate, and so would appear to support the allenolate Cope mechanism. Unfortunately, if a Cope reaction of the neutral adduct is operating, it cannot be ruled out that the rearrangement might happen upon workup. The other criterion available, the preservation of the isomeric ratio in the Cope product, is here confounded by the quality of the ^1H NMR spectroscopic data: there was only a small extent of conversion and all four lines of the two diagnostic vinyl proton doublets are of different intensities due to contamination by impurity peaks. Whereas the pattern does not appear to approach an integral ratio of five to one, no conclusion can be made.

Perhaps the clearest support for the Cope occurring from the allenolate is the observation that over the course of two days at low temperature, the quantity of **5-22**

generated did indeed increase in the course of assessment of aliquots and the crude mixture, indicating that the Cope product was present in the reaction mixture and did not appear upon workup of extant allenolate. It would be expected that, over the course of several days, equilibrium between the lithiated ring-opened adduct anion and ethyl propiolate would be achieved at the outset if the Cope were a neutral process and so a workup-induced Cope rearrangement would not be observed to generate increased product (relative to starting material ^1H NMR spectral signals) over time.

A necessary component of this support for the allenolate mechanism is offered by the observed ratio of Cope product to adduct isomer **5-69b** in the LHMDS experiments. In each case, the quantity of Cope product generated exceeded the quantity of **5-69b**, in one case at a ratio of 2:1, and in the other by an apparently much greater ratio (unintegrated trace **5-69b**). The generation of **5-69b** requires deprotonation of the allenolate intermediate. Either the base function must be provided by the ring-opened adduct anion or by another allenolate. In either case, one allenolate is thereby neutralized, either by direct deprotonation of ring C5 of the other allenolate or by the intermediary ring-opened adduct. In the case of an allenolate Cope, one can envision base catalysis of the allenolate-to-**5-71b** conversion (**5-71b**: the anion *in situ*) being carried out by the ring-opened adduct anion alone, and the presumably small equilibrium quantity of allenolate undergoing Cope rearrangement independently. However, the operation of a neutral Cope rearrangement, coupled with the observation of increasing quantities of product over time, requires that each neutralization and Cope reaction be accompanied by one conversion to **5-71b**. That the Cope product accumulates at a higher rate than **5-71b** strongly suggests that the two processes are not coupled and that an allenolate Cope mechanism is at work (Scheme 5-41)

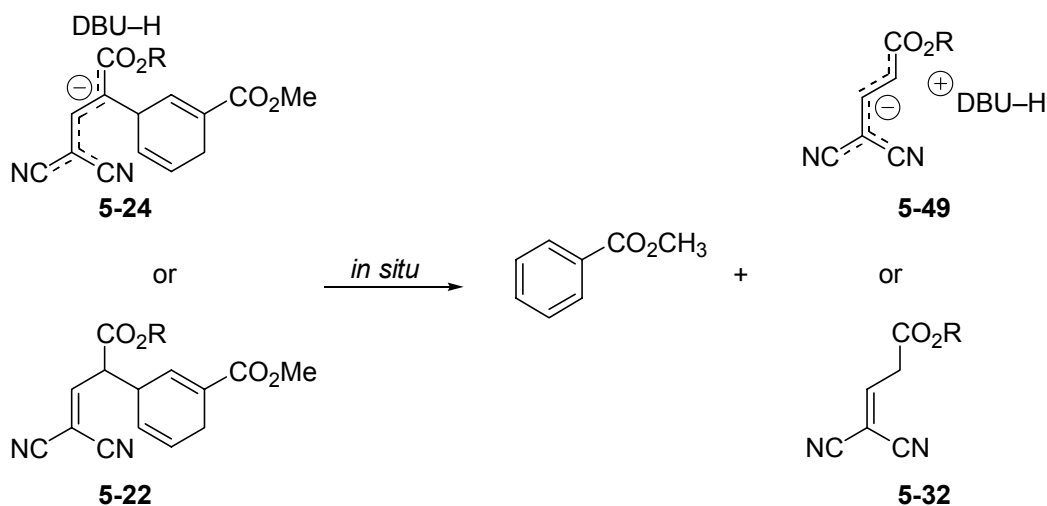


Scheme 5-41. Coupling of neutral Cope rearrangement to generation of **5-69b** in LHMDs experiments.

The available data do provide for the development of comprehensive mechanistic accounts of the Cope rearrangement and the attendant generation of side-products under various sets of conditions. Each of these models centers around the possible reactive species and each invokes an ensemble of factors with respect to the acid-base behaviour of the reactive adducts and the mode of cleavage and aromatization. In consideration of these issues, two experimental results have the same implication for all of the models. The first, the finding that the adduct isomer **5-69** does not arise from the reversal of the Cope rearrangement, has already been described. The second concerns the cleavage/aromatization

process which generates varying quantities of methyl benzoate and **5-32**, depending on the conditions.

Throughout the course of experimental study of the formal allenolate Cope reactions, the generation of methyl benzoate and the side-chain fragment **5-32** during the course of the conversion has reasonably been interpreted to have been a reaction of the rearrangement product, either from the neutral or the anionic state (Scheme 5-42)

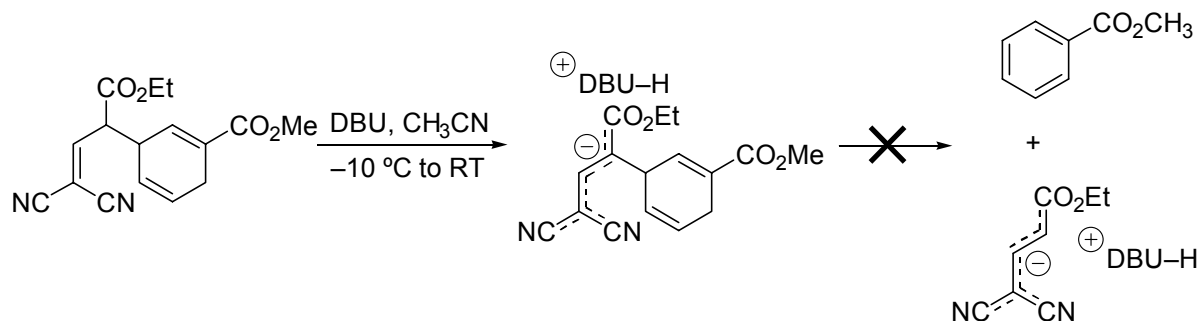


Scheme 5-42. Reasonably expected aromatization/cleavage substrates for conversion observed during adduct formation/allenolate Cope reaction.

The aromatization of the neutral species has been clearly demonstrated on standing in CDCl_3 solution over the course of several days. The rapid cleavage/aromatization that occurs to a small extent in experiments employing catalytic DBU [approximately ten percent, assuming minimal loss of methyl benzoate (bp $199.6\text{ }^\circ\text{C}$) *in vacuo*], and which is revealed in ^1H NMR spectra of the crude material, has reasonably been thought to favour a mechanism proceeding from the anion. Unless the reaction is brought about by NH_4Cl quench, the conversion must occur during the period that the reaction mixture is in CH_3CN at $-10\text{ }^\circ\text{C}$.

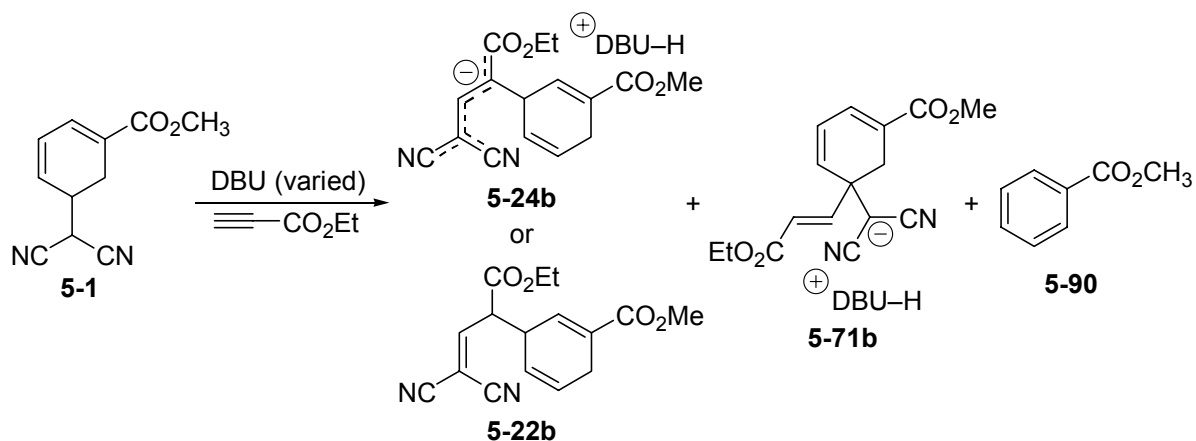
Two experiments aimed at establishing whether the generation of the isomeric adduct **5-69** is preceded by reversal of the Cope rearrangement demonstrated that the reaction occurs

by the intervention of DBU before the adduct of the ring-opened adduct and the alkyl propiolate can undergo Cope rearrangement. An incidental observation of those experiments, one conducted with catalytic and one with stoichiometric DBU, both of which, like the Cope reactions, were carried out in CH_3CN , was that prolonged exposure to DBU, even at room temperature, did not bring about cleavage and aromatization (Scheme 5-43).



Scheme 5-43. Cope product anion is not observed to generate methyl benzoate and fragment anion.

Methyl benzoate is invariably observed in these Cope reactions, under all conditions employed (the fragment is not observed with consistent intensity in ^1H NMR spectra when the reaction is worked up with saturated aqueous NH_4Cl , which may reflect aqueous solubility of the fragment dimer anion **5-58**, *vide supra*). Three experiments conducted at different base concentrations provide decisive insight into the cleavage process, with the salient features of each product distribution being the neutral or anionic Cope products, the adduct isomer anion, and methyl benzoate (Table 5-4).

Table 5-4. Product distributions in allenolate Cope reaction at varied quantities of DBU.

Quantity of DBU (equiv.)	Temp.	Time ^a (min.)	Workup	Relative quantities			
				5-24b	5-22b	5-71b	5-90
0.1	-10 °C	26	Aq. NH ₄ Cl/CH ₂ Cl ₂	n/a	0.95	0	0.05
1.0	-10 °C	7	Conc'd <i>in vacuo</i>	0.41	n/a	0.41	0.18
10	-15 °C	18	Water/EtOAc partition	0	n/a	0.92	0.08

^a Total time from end of addition of final reagent to workup. Orders of reagent addition to ring-opened adduct: cat. DBU expt. – ethyl propiolate, DBU; stoichiometric DBU expt. – DBU, ethyl propiolate; excess DBU expt. – DBU, ethyl propiolate.

In the several Cope reactions conducted with catalytic DBU and both methyl and ethyl propiolate, whatever the reaction time permitted, a small extent of aromatization is observed. The stoichiometric DBU experiment, which provided anionic constituents because of the absence of acidic workup, generated large and equal quantities of the adduct isomer and the Cope product, as well as a considerable quantity of methyl benzoate. Finally, the experiment conducted with excess DBU generated almost solely the adduct isomer, along with a small quantity of methyl benzoate. The Cope product is not observed. This experiment has already been invoked in conjunction with the aforementioned attempted Cope reversal experiments to account for the generation of the adduct isomer by a second deprotonation en route to the Cope product. Because the anionic Cope product does not

exhibit cleavage and aromatization, the small amount of methyl benzoate and fragment anion observed in the excess DBU experiment does not arise from substrates that have successfully advanced through the Cope process; therefore, the high concentration of base is sufficient to intervene upon the adduct, permitting only rearrangement to the isomeric adduct. This accounts for the observed trend that, whereas increasing base steadily increases the quantity of **5-71b** and steadily decreases the quantity of Cope product, the degree of cleavage/aromatization at first increases and then decreases. At stoichiometric DBU, a competitive balance is realized between the effect of increased base on the allenolate (which leads to cleavage: two interpretations of the consequence of higher DBU concentration are offered below) and the deprotonation of ring C5 (leading to **5-71b**). At a high excess of DBU, the base almost always intervenes upon the allenolate intermediate to generate **5-71b** before any other reaction can happen.

The observation that the Cope product anion is not the substrate for the cleavage/aromatization reaction, together with the product distributions observed in the Cope reactions at varying quantities of DBU, provide the key data in the formulation of the mechanism of the Cope transformation and the mechanisms and kinetics of the formation of the other products. Of particular significance in this regard are the absence of Cope product and the slight extent of cleavage and aromatization in the experiment employing ten equivalents of DBU.

That the cleavage/aromatization process does not follow the Cope rearrangement constrains the overall process relating the Cope and the cleavage reactions: if the Cope rearrangement substrate is the neutral adduct **5-4**, then methyl benzoate and fragment **5-32** derive from the allenolate; if the rearrangement substrate is the allenolate, then the

cleavage/aromatization proceeds from the neutral adduct. The allenol case does not hold to this inversion and is slightly more complex with respect to the acid/base kinetics and their influence upon the available reaction pathways.

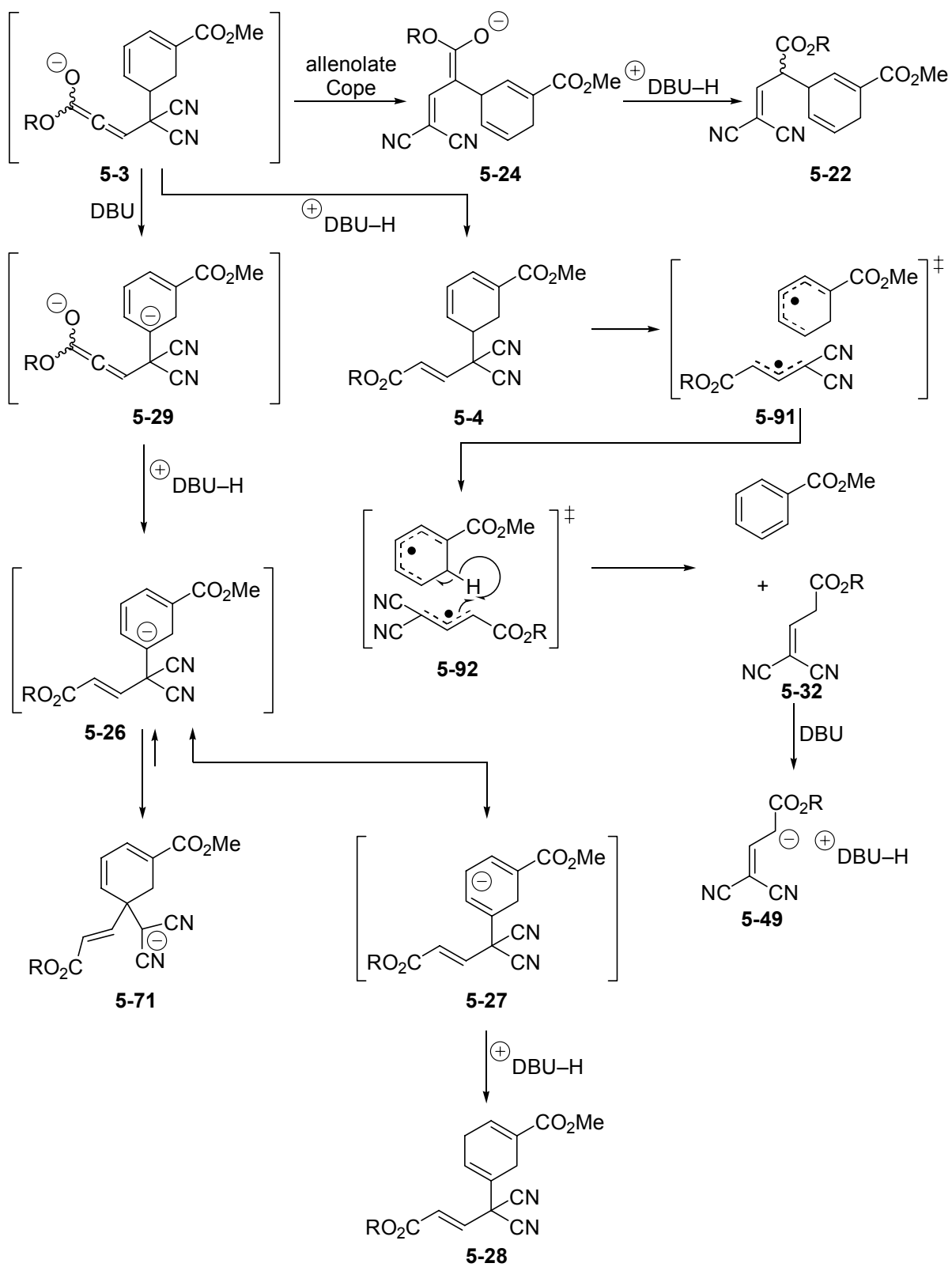
Allenolate Cope Rearrangement

If the allenolate is the cleavage substrate, then the rise in cleavage products observed with stoichiometric DBU is inconsistent with expectation for the degree of generation of the Cope product. If every instance of adduct formation were accompanied by allenolate neutralization by the associated protonated DBU, then the presence of either catalytic or stoichiometric anionic ring-opened adduct should be immaterial to the kinetics of neutralization/Cope rearrangement within each allenolate/DBU-H⁺ counterion pair. In this scenario, a longer-lived allenolate is the basis of increased cleavage, whereas individual allenolate lifespan would not be contingent upon the concentration of the overall population.

The alternative rearrangement, involving the adduct allenolate, is reasonably suggested by the data. In this instance, the cleavage/aromatization process is undergone by the neutral adduct **5-4**, and thus, increased neutralization of the allenolate is associated with a greater extent of cleavage. In the experiment employing catalytic DBU, the least cleavage is observed, indicating that the neutral ring-opened adduct is kinetically a poor proton source, despite the greater basicity of the allenolate than the dicyanomethyl system; therefore, the allenolate Cope rearrangement for the most part occurs more quickly than the intermediate can be neutralized, although a small extent of neutralization and attendant cleavage are observed.

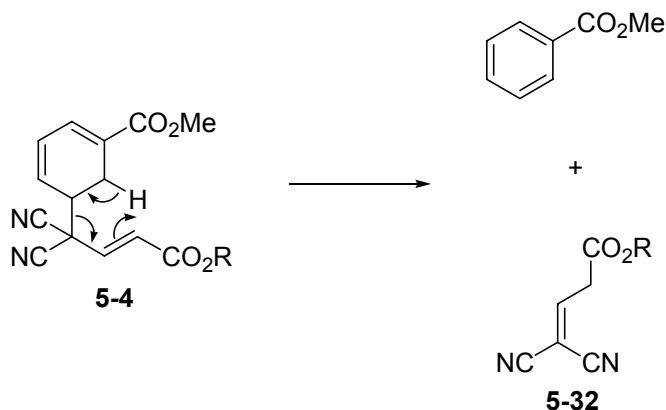
The small extent of deconjugated adduct isomer **5-28** generated is linked to the generation of the alternative adduct **5-69**, insofar as both products are the outcome of ring C5 deprotonation. The generation of the intermediate dianion is depicted in Scheme 5-43 as deriving from deprotonation of allenolate **5-3** by DBU. Two additional potential routes to the adduct C5-anion **5-26** involve intramolecular deprotonation by the allenolate, or neutralization of the allenolate to **5-4**, followed by ring C5 deprotonation by DBU prior to cleavage. In the catalytic base experiment, the alternative adduct **5-69** is not observed, indicating that the deconjugated adduct is the result of kinetic protonation once the anion is formed. At high concentrations of base, the opportunity is present for the favourable equilibration toward alternative adduct **5-69** to occur. This conclusion is supported by the conversion of **5-28** to **5-69** by treatment of Cope product mixtures with DBU.

It is reasonably concluded that, like the allenolate, the neutral adduct **5-4** is capable of undergoing the Cope rearrangement. The mechanistic considerations previously advanced, which locate in the present system several elements capable of stabilizing Cope transition states involving a loosely associated bis-allyl radical structure, may apply in the cleavage reaction as well. It is possible that the neutral adduct enters a Cope-like transition state **5-91**, but that the dissociating allyl radical moieties prove sufficiently stable that complete fragmentation results. A second transition structure **5-92** involving the transfer of the ring C6-hydrogen atom to the departing fragment is encountered, concluding with the release of methyl benzoate and fragment **5-32**. In basic conditions, **5-32** is present in its deprotonated form **5-49** (Scheme 5-44).



Scheme 5-44. Processes involved in allenolate Cope rearrangement.

Alternative to the radical mechanism of cleavage is the possibility that the neutral adduct undergoes a facile retro-ene reaction. It has been demonstrated (*vide supra*) that the presence of a suitably positioned malononitrile moiety is capable of increasing the rate of pericyclic processes that conclude with an unsaturation in conjugation with the nitriles (Scheme 5-45).



Scheme 5-45. Aromatization of neutral adduct **5-4** by retro-ene reaction.

The greater extent of cleavage observed at stoichiometric DBU is due to the neutralization of the allenolate by protonated DBU associated with the ring-opened adduct anion. In contrast to the sluggish neutralization afforded by neutral ring-opened adduct under catalytic base conditions, the proton associated with the heteroatom of DBU proves a kinetically favourable proton donor. The difference in the extent of cleavage between the catalytic and stoichiometric experiments reflects differing extents of neutralization. Analogous to the consideration of neutralization within counterion pairs applied to the rejection of the allenolate as the cleavage substrate, this difference indicates that the DBU-H⁺ associated with ring-opened adduct, and not that associated with the allenolate, is the main proton donor that opens the pathway to cleavage. It is reasonably asserted that the combination of the brief intermediacy of the allenolate prior to Cope rearrangement and the distance that develops between the counterionic charge centers on alkylation of the propargyl

reagent is responsible for the slight extent of neutralization brought about by allenolate-associated DBU-H⁺. The planar dicyanomethyl anion of the ring-opened adduct is expected to have DBU-H⁺ associated with one face of the delocalized five atom system. The alkyl propiolate approaches the reactive site from the opposite face, resulting in electron delocalization into the remote carboalkoxy group (Figure 5-43). The interval between alkylation and movement of the protonated DBU into position to neutralize the enolate carbon is sufficiently long that the Cope rearrangement cannot be prevented

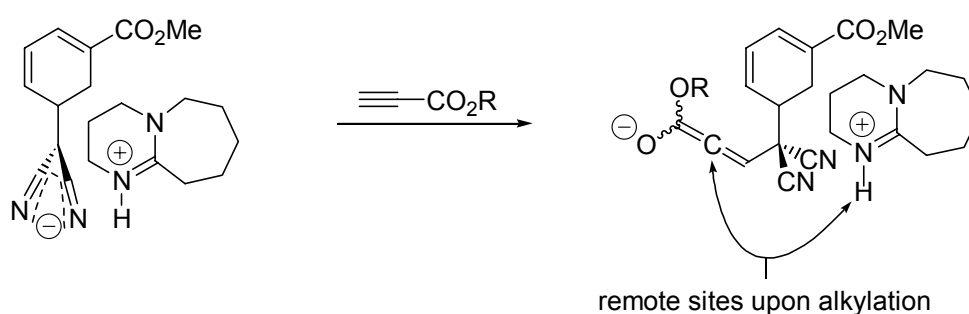
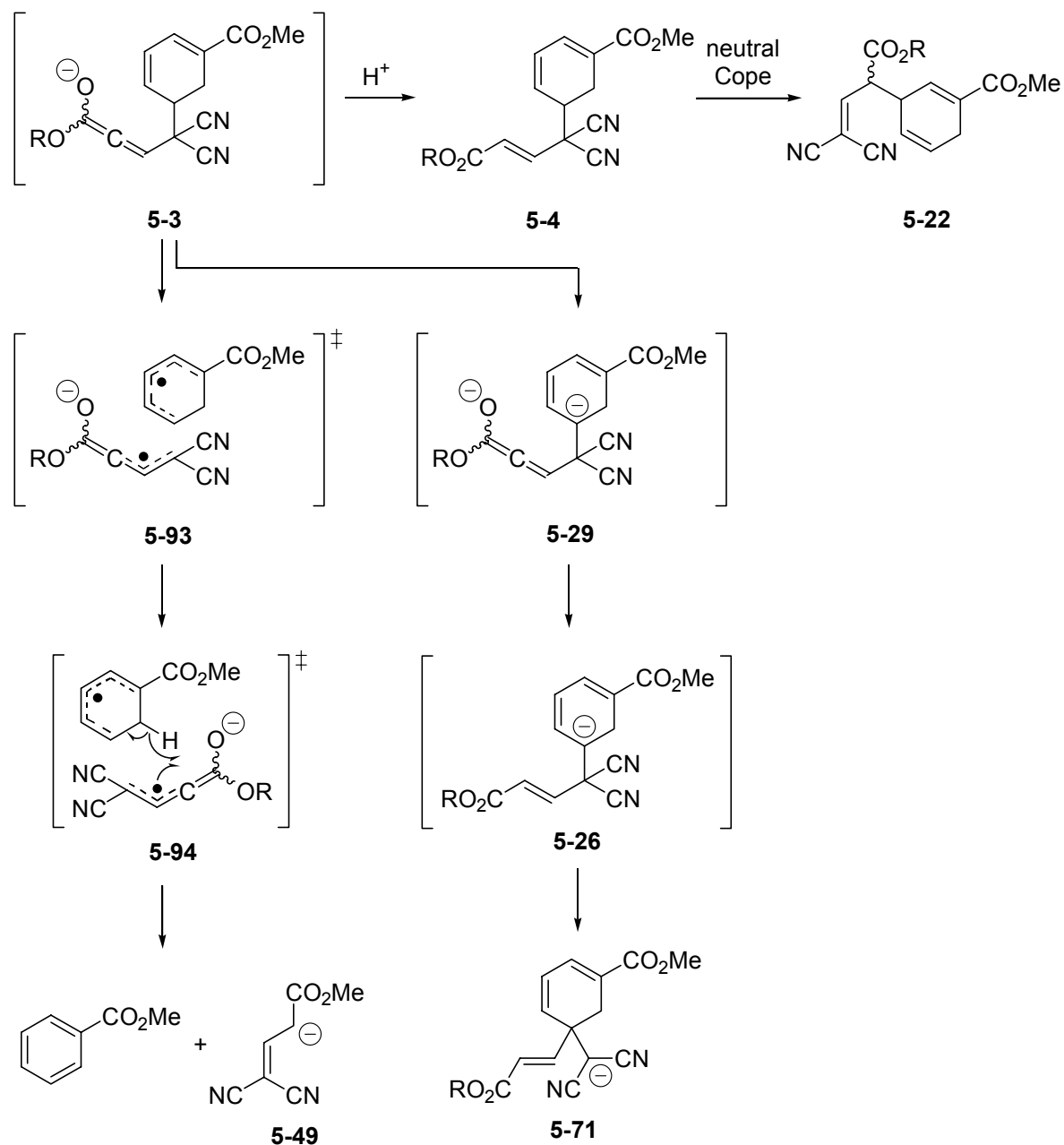


Figure 5-43. Counterionic centers of the allenolate intermediate are at sufficient separation to provide opportunity for Cope rearrangement prior to neutralization.

Neutral Cope Rearrangement

The possible, if unlikely, operation of a neutral Cope rearrangement implies several reversals of claims made for the allenolate Cope. In this case, the catalytic DBU experiment, which generates a high yield of **5-22**, would require either that associated DBU-H⁺ or **5-1** is a rapid proton donor and that almost stoichiometric neutralization of **5-3** occurs, thus bringing about rearrangement; furthermore, the allenolate would now be considered the cleavage/aromatization substrate (Scheme 5-46). Therefore, a more persistent allenolate at stoichiometric DBU would account for the high degree of cleavage. This could be accounted for in one of two ways: either the usual proton source to neutralize **5-3** is **5-1** and at stoichiometric DBU there is thus no source to rapidly neutralize **5-3**; or, the ionic

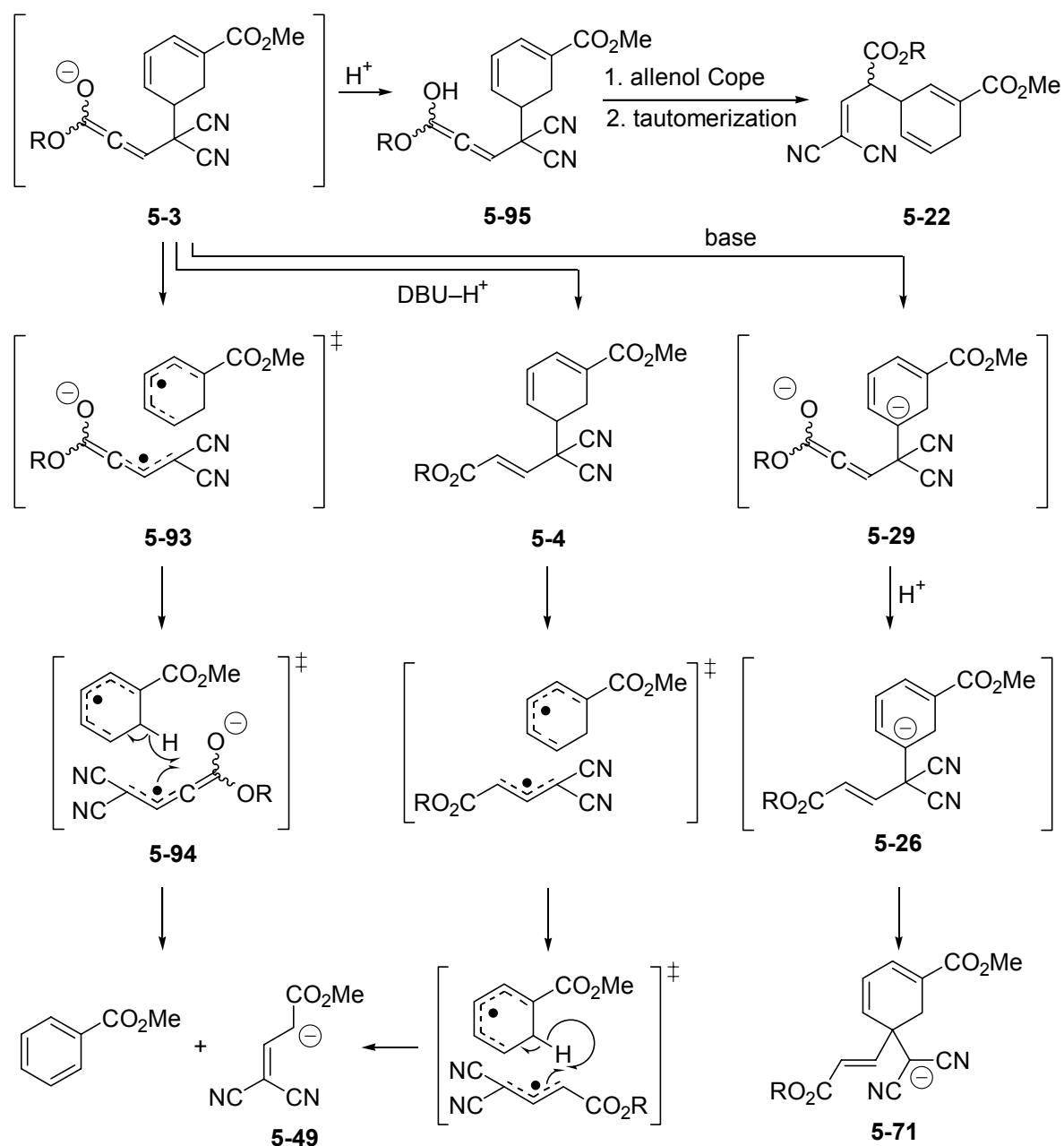
environment of the reaction in the case of stoichiometric substrate anion/DBU-H⁺ salt involves counterion solvation in aggregates that prevents the usual acidic behaviour of DBU-H⁺ toward the allenolate. It could be suggested that the allenolate undergoes cleavage in the same fashion as posited for the neutral adduct **5-4**: either by dissociation from a Cope transition state, or by an anionically-accelerated retro-ene reaction.



Scheme 5-46. Processes involved in neutral Cope rearrangement.

Allenol Cope Rearrangement

The possible allenol Cope does not offer an obvious choice for the cleavage substrate. In this case, two possibilities must be admitted to account for the product distributions at catalytic versus stoichiometric DBU. Foremost is the necessity that protonation at oxygen of the allenolate represents the usual course of Cope rearrangement in this scenario; moreover, the proton source can be identified as **5-1**. If DBU-H^+ were the proton source, the quantity of Cope product on advancing from catalytic to stoichiometric DBU would not be expected to decline, as the quantity of DBU-H^+ is greater under stoichiometric conditions and so the Cope route would be readily available. To account for greater cleavage at stoichiometric DBU, it must be concluded that **5-1** neutralizes the allenolate; therefore, at stoichiometric DBU, there is a lesser quantity of kinetically available protons to bring about rearrangement. Thus, either the cleavage reaction increases in prominence due to greater persistence of the allenolate, or the reaction occurs from neutral adduct **5-4**, neutralized on the carbon atom preferentially by DBU-H^+ (Scheme 5-47).



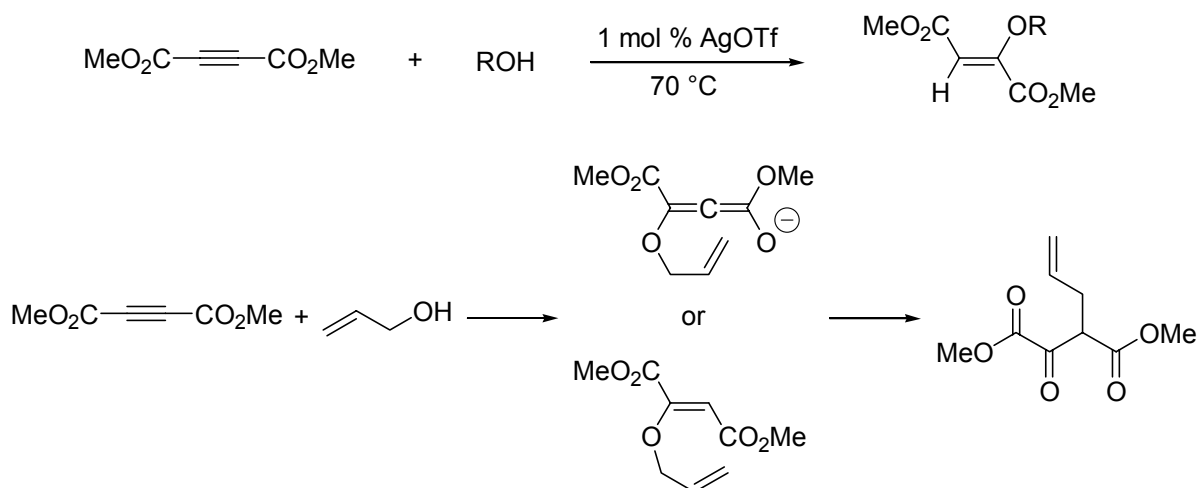
Scheme 5-47. Processes involved in the allenol Cope rearrangement.

5.2.7.4 Other Examples of Allenolate-Based [3,3]-Rearrangements

To the best of our knowledge, the allenolate Cope rearrangement of the present study is the first such facile all carbon [3,3]-sigmatropic rearrangement from an allenolate intermediate, that is, one arising from the reaction of a carbon nucleophile with an activated

acetylene compound. Heteroatom examples arising from the reaction of activated acetylenic compounds and allylic alcohols, allylic thiols,^{14,15} and allylamines, respectively giving rise to Claisen and thio- and aza-Claisen rearrangements, are already well-established. Apparently, the aza-Claisen has so far undergone the most extensive study.

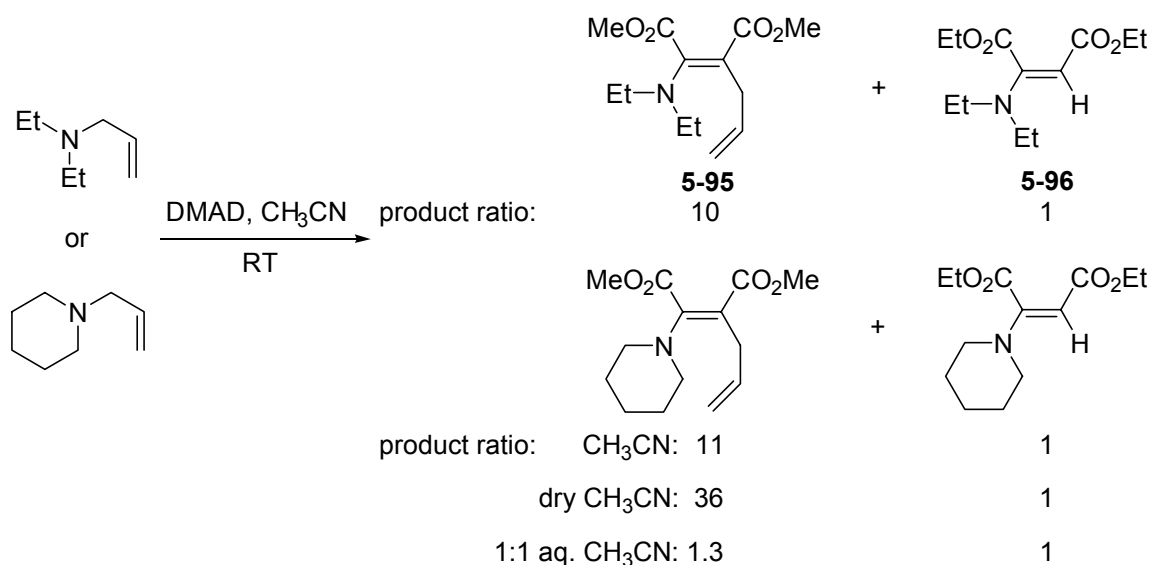
The Claisen rearrangement following reaction of allylic alcohols and acetylenic esters appears to be limited to only two examples that have not been studied in any detail. For example, in a study of the stereoselective addition of alcohols to dimethyl acetylenedicarboxylate (DMAD) catalyzed by silver trifluoromethanesulfonate (AgOTf), Kataoka et al. noted that the reaction with allyl alcohol gave the Claisen rearrangement product (Scheme 5-48).¹⁶



Scheme 5-48. Claisen rearrangement in the addition of allyl alcohol to DMAD.

Studied in much greater detail have been the reactions of allylamines with acetylenic esters. Beyond their specialized applications, for example in total synthesis, several groups have demonstrated the generality of the reaction in simpler cases and have determined some of the governing factors involved in the transformation.

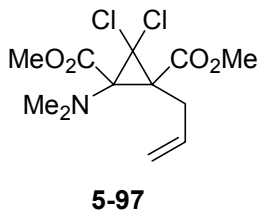
Kandeel and Vernon have demonstrated formal [3,3]-sigmatropic shifts, amounting to allyl rearrangement and N,C-transfer, in the addition of allylamines to DMAD.¹⁷ Whereas the reaction failed in dry Et₂O, a mixture of aza-Claisen product **5-95** and deallylated enamine adduct **5-96** was obtained when the reaction was carried out in CH₃CN. The authors deemed the reaction to have involved the zwitterionic intermediate, depicted in their work as a vinyl anion (Scheme 5-49).



Scheme 5-49. Aza-Claisen rearrangements in reactions of allylamines with DMAD.

Schwan and Warkentin's contemporary report extended the reaction with DMAD to a series of alkyl substituted allylamines.¹⁸ In their study, equimolar solutions of DMAD and allylamines were refluxed in CH₃CN, which generated the rearranged products as well as considerable extents of N-C (allyl) cleavage. In both studies, the respective authors posit that neutralization of the zwitterionic intermediate was the cause of cleavage, rationalized as the outcome of either S_N2 or S_N2' displacement of the ammonium nitrogen from the allyl fragment by either water (or hydroxide) or deprotonated solvent. Kandeel and Vernon found that cleavage was minimized when the CH₃CN was rigorously dried, arising in a 1 to 36 ratio

with the aza-Claisen product. Schwan and Warkentin observed the generation of the



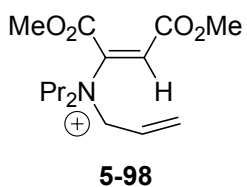
dichlorocarbene adduct **5-97** from aza-Claisen product in reactions performed in CHCl_3 , verifying the deprotonation of solvent.

Chloroform was thought to bring about greater cleavage than CH_3CN because of its lower $\text{p}K_a$. The role of neutralization of the intermediate was subtle: parallel experiments in CHCl_3 (or CDCl_3) and CH_2Cl_2 revealed reduced reactivity in the latter solvent, possibly due to the lack of acidic protons; however, the addition of benzoic acid in other experiments, on the grounds of activating DMAD as a conjugate acceptor, reduced the yield of aza-Claisen product. Vedejs and Gingras in a later study¹⁹ found evidence for the beneficial role of adventitious acid cited by Schwan and Warkentin with an experiment involving DMAD and allyl-di-*n*-propylamine in which the CDCl_3 solvent was filtered through alumina, resulting in less than 2 % conversion after 24 hours.

The later study by Vedejs and Gingras revived the possibility of successful acid catalysis of allylamine additions to DMAD. An experiment involving methyl propiolate and a mixture of allyl-*n*-propylamine and allyl-*n*-propylammonium chloride generated the Claisen product in greater than 90 % yield. This prompted a series of trials involving substituted allylamine conjugate additions to DMAD catalyzed by various acids. The previous authors' observation of reduced yield with benzoic acid catalysis was repeated and accounted for as the result of benzoate acting as a nucleophile toward the allyl fragment. Allyl benzoate (74 %) was isolated from the reaction mixture.

Other acids proved better catalysts, namely triflic acid, toluenesulfonic acid (TsOH), and TFA, and high yields of aza-Claisen products (as high as 99 %) were obtained with little cleavage. Vedejs and Gingras suggested that acid catalysis supported the rearrangement by

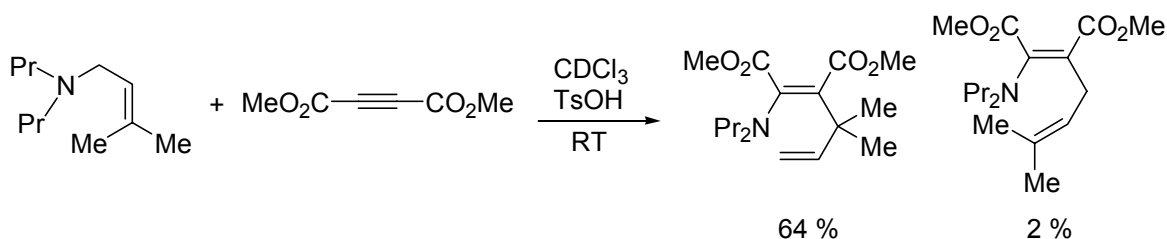
activating DMAD toward addition of the amine, and that reaction occurred from a cationic intermediate, that is, from a neutralized allenolate. Their experiments without acid catalysis also generated aza-Claisen products, albeit at lower yields that were improved in more polar solvents. In these examples, it was suggested that rearrangement occurred from the zwitterion. A low temperature ^1H NMR experiment with DMAD and allyl-*n*-propylamine, catalyzed by 10 % TsOH, evidenced the rapid generation of a cationic intermediate **5-98** and



the early persistence of starting materials and a small quantity of product. Enammonium adduct **5-98** was noted to be kinetically incompetent in the generation of the aza-Claisen product, indicating an

alternative route from starting materials to product. The authors therefore proposed that the allenol may be the most reactive intermediate in the aza-Claisen reaction. To test the hypothesis that an allenyl moiety represented the most reactive species, Lewis acid-catalyzed experiments were conducted that generated aza-Claisen products and confirmed reaction via the allenolate.

In one experiment, a product was isolated that resulted from allyl transfer without rearrangement, indicating heterolysis of the intermediate and recombination of the allyl cation fragment at its less hindered end (Scheme 5-50). This finding reveals the potential operation of cleavage and recombination as a mode of allyl transfer.



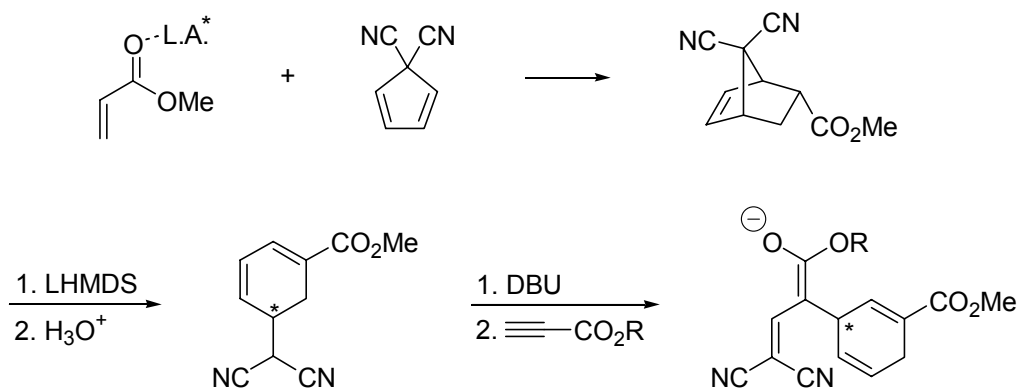
Scheme 5-50. Minor generation of allyl transfer product without allylic isomerization.

This may offer an account of the several strains of results among the three reports cited. Vedejs and Gingras demonstrate the benefit of acid catalysis and that rearrangement occurs from a cationic intermediate. Cumulatively, the three papers demonstrate uncatalyzed reaction from the zwitterion, which is also demonstrated in the Lewis acid-catalyzed experiments. Lower yields in CH₃CN are obtained from refluxing than from room temperature conditions. Schwan and Warkentin also demonstrate that higher concentration in refluxing CH₃CN reduces the yield of aza-Claisen products. It is possible that, as Vedejs and Gingras suggest, acid-catalyzed rearrangements proceed from the allenol. At room temperature, zwitterionic [3,3]-rearrangements may dominate to deliver aza-Claisen products in the highest possible uncatalyzed yields. At reflux, heterolysis and recombination may come increasingly into prominence as the mode of allyl transfer. Higher concentrations may thus allow interception of the briefly dissociated allyl cation fragment by various nucleophilic species. Allyl transfer without double-bond isomerization¹⁹ confirms the intermediacy of dissociated fragments and relative translation of the reactive centers, opening the possibility in other heterolytic cases of intermolecular reactions. The apparent necessity of adventitious acid in CHCl₃ reactions, along with the extensive cleavage, may reflect a balance between the beneficial acidic activation of the acceptor (and catalysis of the rearrangement) and the cited detrimental nucleophilic attack on the allyl unit: HCl may be intermediate in effect between the almost completely beneficial TsOH and the highly nucleophilic carboxylate of benzoic acid.

5.3 Conclusions and Future Work

The remarkably facile Cope rearrangement of the adducts of the ring-opened adduct and alkyl propiolates has been demonstrated. The evidence permits the reasonable assertion that the rearrangement proceeds from an allenolate intermediate, delivering a highly delocalized anionic side-chain moiety that isomerizes at room temperature slowly enough to be observed by ^1H NMR spectroscopy. High base concentrations intercede in the process and bring about rearrangement of the adduct to the isomer **5-69**. Both processes represent unexpected modes of tandem reactivity for the ring-opened adduct.

Whereas the present study has largely been concerned with mechanistic understanding of the various processes at work, the smooth generation either of Cope product **5-22** or adduct isomer **5-69** in high yields, determined solely by variation of base concentration, suggests the promise of these transformations in synthetic applications. An immediately apparent potential lies in the possibility of using the Cope rearrangement as a mode of chirality transfer. Enantioselective synthesis of the Diels-Alder adduct precursor to the ring-opened adduct would permit generation and isolation of that key substrate as a single enantiomer. The allenolate Cope rearrangement would then produce a single enantiomer stereospecifically (Scheme 5-51).



Scheme 5-51. Potential for allenolate Cope rearrangement from optically pure ring-opened adduct as a 1,3-chirality transfer process.

Whereas the anionic Cope product proved unreactive toward MeI at room temperature, further exploration of the reaction of the delocalized side-chain anion with electrophiles is also recommended.

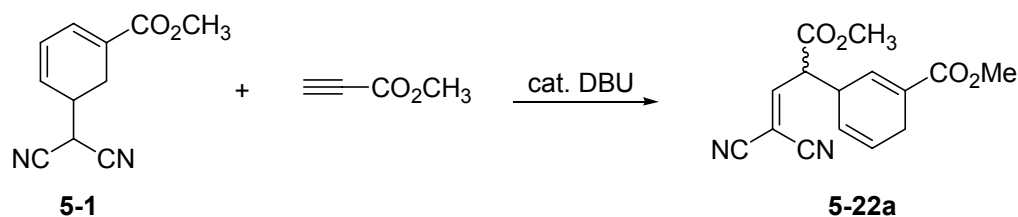
5.4 Experimental

5.4.1 Supplementary General Experimental

Acetonitrile was reagent grade and was used as received. When substrate and DBU solutions were dispensed by syringe, gas-tight™ syringes were used to obtain precise measurements.

5.4.2 Experimental Details

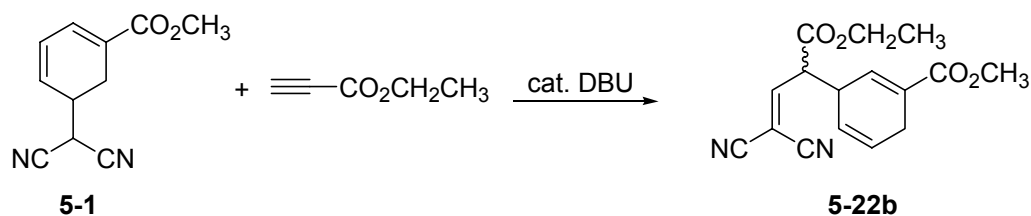
3-(3,3-Dicyano-1-methoxycarbonyl-allyl)-cyclohexa-1,4-dienecarboxylic acid methyl ester



The ring-opened adduct (83.6 mg, 0.413 mmol) and methyl propiolate (1.68 mL of a 20.7 mg/mL CH₃CN solution, 0.413 mmol) were dissolved in 4 mL of CH₃CN and stirred at -10 °C. DBU (0.17 mL of a 38.6 mg/mL CH₃CN solution, 0.0413 mmol, 0.1 equiv) was added over 82 seconds, turning the reaction yellow. After 23 minutes, an aliquot (0.25 mL) was removed by syringe and partitioned between saturated aqueous NH₄Cl (1 mL) and EtOAc (1 mL), passed through a filter pipette containing Na₂SO₄ and concentrated *in vacuo*. The sample provided a ¹H NMR spectrum of high purity 5-22a. After two hours of total reaction time, the remainder of the reaction mixture was partitioned between saturated aqueous NH₄Cl (50 mL) and successive portions of CH₂Cl₂ (3 × 20 mL). The combined organic portions were dried (Na₂SO₄) and concentrated *in vacuo*, furnishing a golden oil. TLC (40:60 EtOAc:hexanes) revealed a broadly diffused product spot that was superimposed

over several impurities, and that turned yellow after drying. Column chromatography (12 g of 230–400 mesh silica, 1.43×18 cm bed, 20:80–40:60 EtOAc:hexanes) failed to isolate the title compound from the minor impurities. The NMR sample of the initial aliquot was retained in CDCl_3 in the NMR tube at room temp for several days during which ^1H NMR spectra were periodically recorded to monitor the conversion of the Cope rearrangement product to methyl benzoate and 4,4-dicyano-but-3-enoic acid methyl ester. ^1H NMR (CDCl_3 , 300 MHz) δ 7.27 (1 H, d, $J = 10.5$ Hz), 7.21 (1 H, d, $J = 10.7$ Hz), 6.76[†] (2 H, m), 6.03[†] (2 H, m), 5.58[†] (2 H, m), 3.84 (3 H, s, CO_2CH_3), 3.82 (3 H, s, CO_2CH_3), 3.79 (3 H, s, CO_2CH_3), 3.78 (3 H, s, CO_2CH_3), 3.87–3.78[†] (4 H, m), 2.92[†] (4 H, m) [†] Superimposed signals from each diastereomer.

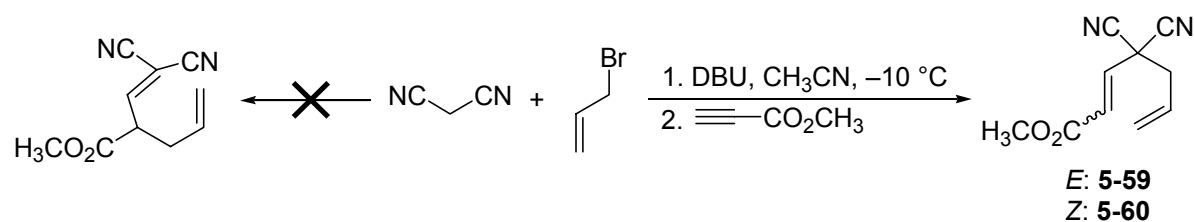
3-(3,3-Dicyano-1-ethoxycarbonyl-allyl)-cyclohexa-1,4-dienecarboxylic acid methyl ester



The ring-opened adduct (0.1057 g, 0.523 mmol) and ethyl propiolate (1.43 mL of a 36.0 g/mL solution, 0.523 mmol) were dissolved in CH_3CN (4 mL) and stirred at -10 °C. DBU (0.16 mL of a 50.15 mg/mL solution, 0.0523 mmol) was added dropwise over 70 seconds. After 26 minutes, the reaction was added to saturated aqueous NH_4Cl (50 mL) and extracted with CH_2Cl_2 (3×25 mL). The combined organic phases were dried (Na_2SO_4) and concentrated *in vacuo*, yielding a yellow oil. See table 5-1 for complete NMR spectral data.

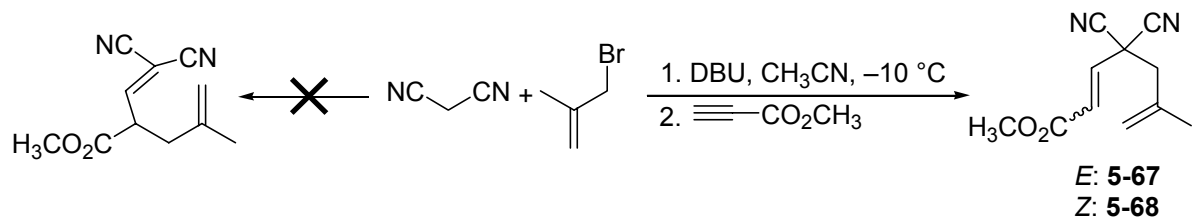
Attempted Cope Reaction on Generalized Substrates Prepared *in situ*:

1. Attempted Synthesis of 2-Allyl-4,4-dicyano-but-3-enoic acid methyl ester

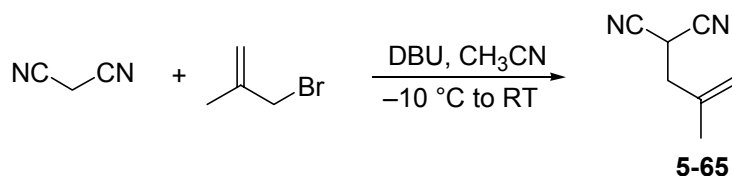


Malononitrile (0.0362 g, 0.548 mmol) was dissolved in CH₃CN and stirred at -10 °C. Allyl bromide (1.1 mL of a 60.0 mg/mL solution in CH₃CN, dispensed by syringe) was added, followed by DBU (1.83 mL of a 45.6 mg/mL solution in CH₃CN, dispensed slowly dropwise by syringe). After 15 minutes, methyl propiolate (2.23 mL of a 20.7 mg/mL solution in CH₃CN, dispensed by syringe) was added over the course of 95 seconds. The salt-ice water bath was allowed to slowly warm to room temperature over the course of six hours, at which time the reaction mixture was neutralized by partition between saturated aqueous NH₄Cl (60 mL) and CH₂Cl₂ (20 mL), followed by further CH₂Cl₂ extractions (2×20 mL). The combined organic extracts were dried (Na₂SO₄) and concentrated *in vacuo*. The crude ¹H NMR spectrum revealed largely the adducts **5-59** and **5-60** in a ratio of 4.07:1, which were formulated on the basis of isolated diagnostic ¹H NMR signals, and small quantities of side-chain anion **5-49a** and anionic dimer **5-58a**. Purification of the crude mixture was not performed. **5-59**: ¹H NMR (CDCl₃, 300 MHz) δ 6.75 (1 H, d, *J* = 15.4 Hz, C3-H), 6.43 (1H, d, *J* = 15.4 Hz, C2-H), 6.0–5.76[†] (1 H, m, C6-H), 5.51–5.36[†] (2 H, m, C7-H), 3.82 (3 H, s, CO₂CH₃), 2.69 (2 H, br d, *J* = 6.5 Hz, C5-H₂); **5-60**: ¹H NMR (CDCl₃, 300 MHz) δ 6.30 (1 H, d, *J* = 11.2 Hz, C3-H), 6.06 (1 H, d, *J* = 11.2 Hz, C2-H), 6.0–5.76[†] (1 H, m, C6-H), 5.51–5.36[†] (1 H, m, C7-H), 3.87 (3 H, s, CO₂CH₃), 2.84 (2 H, br d, *J* = 7.3 Hz, C5-H₂)[†] Superimposed signal from both isomers.

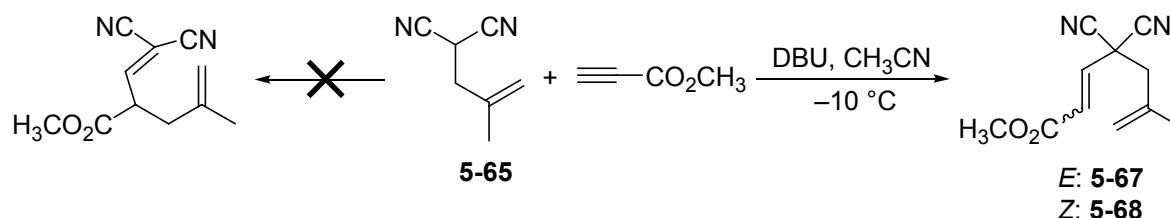
2. Attempted Synthesis of 4,4-Dicyano-2-(2-methyl-allyl)-but-3-enoic acid methyl ester



Freshly opened 2-bromo-3-methylpropene (0.0658 g) was dispensed by syringe into a round-bottom flask, dissolved in CH₃CN (3 mL), suspended in a -10 °C bath, and stirred under Ar. Stoichiometric malononitrile was added (1.60 mL of a 20.1 mg/mL solution, dispensed by syringe), followed by the dropwise addition of DBU (1.63 mL of a 50.2 mg/mL solution, mmol, 1.1 equivalents, dispensed by syringe) over four minutes, 30 seconds. After 20 minutes, methyl propiolate (1.18 mL of a 34.9 mg/mL solution, mmol, dispensed by syringe) was added over three minutes. After four hours (unmonitored), the reaction was partitioned between saturated aqueous NH₄Cl (60 mL) and successive portions of CH₂Cl₂ (3×20 mL). The combined organic portions were dried (Na₂SO₄) and concentrated *in vacuo* to give a dark yellow oil (0.1061 g) that was determined, on the basis of the crude ¹H NMR spectrum, to contain largely the adduct isomers **5-67** and **5-68** as well as the anion **5-49a** and the anionic dimer **5-58a**. Purification of the crude mixture was not performed. **5-67**: ¹H NMR (CDCl₃, 300 MHz) δ 6.79 (1 H, d, *J* = 15.4 Hz, C4-H), 6.45 (1 H, d, *J* = 15.4 Hz, C5-H), 5.25–5.1[†] (2 H, m, C1-H₂), 3.82 (3 H, s, CO₂CH₃), 2.79 (2 H, s, CH₂), 1.94 (3 H, s, CH₃); **5-68**: ¹H NMR (CDCl₃, 300 MHz) δ 6.31 (1 H, d, *J* = 11.3 Hz, C5-H), 6.14 (1 H, d, *J* = 11.3 Hz, C6-H), 5.25–5.1[†] (2 H, m, C1-H₂), 3.86 (3 H, s, CO₂CH₃), 2.99 (2 H, s, CH₂), 1.98 (3 H, s, CH₃)[†] Superimposed signal from both isomers.

2-(2-Methyl-allyl)-malononitrile

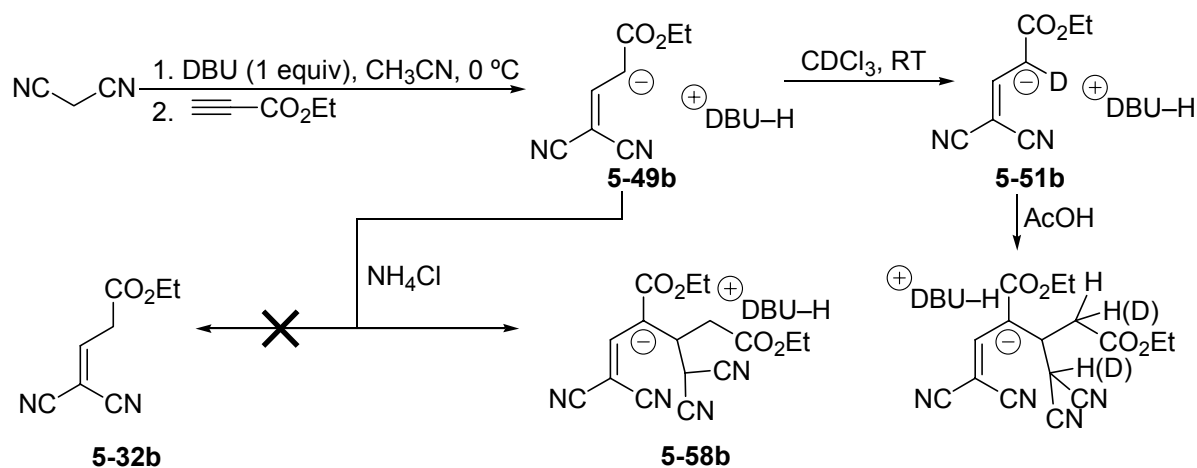
An CH₃CN (10 mL) solution of 3-bromo-2-methylpropene (446.9 mg, 3.31 mmol) was stirred at -10 °C. Malononitrile (218.7 mg, 3.31 mmol) was added, followed by the dropwise addition of DBU (0.495 mL, 3.31 mmol) over three minutes. The reaction was allowed to slowly warm to room temperature, at which time it was partitioned between saturated aqueous NH₄Cl (60 mL) and multiple portions of CH₂Cl₂ (3 × 20 mL). The combined organic extracts were dried (Na₂SO₄) and concentrated *in vacuo*. Column chromatography (21 g of 230–400 mesh silica, 2.58 × 9.6 cm bed, 15:85, 25:75 EtOAc:hexanes) furnished the title compound and bisalkylated material. The product (165.2 mg, 41.5 %) was evacuated at high vacuum only for one minute at each stage of isolation to minimize material loss. ¹H NMR (CDCl₃, 300 MHz) δ 5.10 (1 H, br s, C1-H), 5.01 (1 H, br s, C1-H), 3.91 (1 H, t, *J* = 7.35 Hz, HC(CN)₂), 2.71 (2 H, d, *J* = 7.35 Hz, C3-H), 1.83 (3 H, s, CH₃).

Attempted Cope Rearrangement of Adduct 5-65 and Methyl Propiolate:

To a stirred CH₃CN (2 mL) solution of nn (0.0457 g, 0.380 mmol) and methyl propiolate (0.92 mL of a 0.0349 g/mL solution in CH₃CN, 0.3803 mmol) at -10 °C was

added DBU (0.135 mL of a 42.7 mg/mL solution, 0.0380 mmol) dropwise over 50 seconds. After 100 minutes, the reaction was partitioned between saturated aqueous NH_4Cl (60 mL) and successive portions of CH_2Cl_2 (3×20 mL), and the combined organic phases were dried (Na_2SO_4) and concentrated *in vacuo*. Workup turned the yellow reaction solution pink, and the colour darkened during handling and storage. The crude ^1H NMR spectrum revealed the generation of **5-67** and **5-68** as in the one-pot experiment.

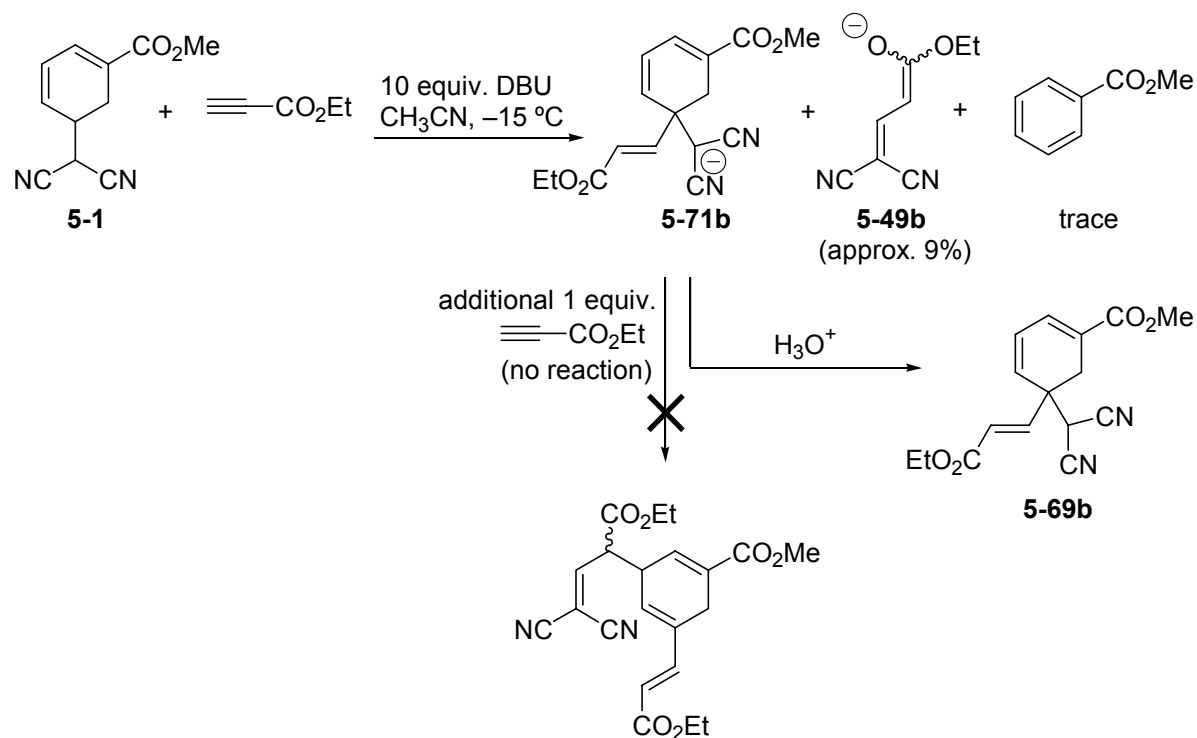
Attempted Synthesis of 4,4-Dicyano-but-3-enoic acid ethyl ester **5-32**.



To a stirred CH_3CN (1 mL) solution of malononitrile (0.1057 g, 1.60 mmol) at $0\text{ }^\circ\text{C}$ was added DBU (5.7 mL of a 42.7 mg/mL solution, 1.60 mmol) dropwise over three minutes. Ethyl propiolate (4.36 mL of a 36.0 g/mL solution, 1.60 mmol) was added dropwise over 50 seconds. After three minutes, an aliquot (1 mL) of **5-49b** was removed by syringe, concentrated *in vacuo*, and dissolved in CDCl_3 for assessment by ^1H NMR spectroscopy. The sample was retained at room temperature and periodic ^1H NMR spectra obtained over several days recorded the H–D exchange that furnished **5-51b**. After 47 minutes of total reaction time, the remainder of the reaction mixture was partitioned between saturated aqueous NH_4Cl (30 mL) and multiple portions of CH_2Cl_2 (3×20 mL). The combined

organic phases were dried (Na_2SO_4) and concentrated *in vacuo*. The crude material was poorly soluble in CDCl_3 , but the precipitate from the CDCl_3 preparation was completely soluble in acetone- D_6 . Both preparations furnished spectra of **5-58b** that differed in the relative quantities of DBU-H^+ and NH_4^+ counterions. After 7 days, the aliquot that had been monitored for H-D exchange was dissolved in CDCl_3 to a total volume of 2 mL and cooled to 0 °C. One drop of AcOH was added, and after 2 min., an aliquot was removed for assessment by ^1H NMR. The sample revealed individually more complex signals than **5-58b** at shift positions suggestive of the deuterated dimer depicted in the scheme. **5-49b**: ^1H NMR (CDCl_3 , 500 MHz) δ 7.37 (1 H, d, $J = 14.3$ Hz, C3-H), 5.13 (1 H, d, $J = 14.3$ Hz, C4-H), 4.08 (2 H, q, $J = 7.1$ Hz, $\text{CO}_2\text{CH}_2\text{CH}_3$), 1.24 (3 H, t, $J = 7.1$ Hz, $\text{CO}_2\text{CH}_2\text{CH}_3$); **DBU-H⁺**: 3.57 (4 H, m), 3.40 (2 H, br t, $J = 5.9$ Hz, C9-H), 2.71 (2 H, m, $J = \text{Hz}$), 2.11 (2 H, br qn, $J = 5.9$ Hz, C10-H), 1.85–1.68 (6 H, m); **5-58b** (signals not derived from DBU-H^+): ^1H NMR (CDCl_3 , 300 MHz) δ 7.33 (1 H, s), 4.96 (1 H, d, $J = 10.8$ Hz), 4.51 (1 H, m), 4.07 (4 H, m, $2 \times \text{CO}_2\text{CH}_2\text{CH}_3$), 2.95 (1 H, dd, $J = 14.7, 9.4$ Hz), 2.72 (1 H, dd, $J = 14.7, 5.0$ Hz); **5-51b**: ^1H NMR (CDCl_3 , 300 MHz) δ 7.35 (1 H, br s).

5-Dicyanomethyl-5-(2-ethoxycarbonyl-vinyl)-cyclohexa-1,3-dienecarboxylic acid methyl ester

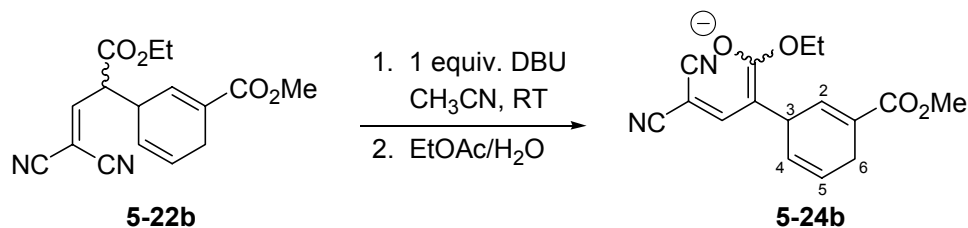


To a stirred solution of **5-1** (105.0 mg, 0.519 mmol) in CH₃CN (5 mL) at -15 °C was added neat DBU (0.78 mL) by glass syringe dropwise over two minutes, which caused the reaction to progressively change from yellow to dark orange by the end of the addition. One equivalent of ethyl propiolate (1.30 mL of a 39.1 mg/mL solution, 0.519 mmol) was added dropwise over two minutes, darkening the reaction mixture slightly. After 18 minutes, an aliquot (1 mL) was removed by syringe and partitioned between water (4 mL) and successive volumes of EtOAc (3 × 1.5 mL). The combined EtOAc portions were dried (Na₂SO₄) and concentrated *in vacuo* to furnish a light brown/orange oil. Assessment by ¹H NMR spectroscopy (500 MHz, CDCl₃) revealed the presence of anionic side-chain fragment **5-49b** (approx. 9 %) and of anionic adduct isomer **5-71b** and small quantities of methyl benzoate (trace: slight loss *in vacuo*). One minute after the first aliquot, a second (1 mL) was removed

by syringe and neutralized by partition between saturated aqueous NH_4Cl (3 mL) and EtOAc (3×1.5 mL). The dried (Na_2SO_4) combined organics were concentrated *in vacuo* and examined by ^1H NMR spectroscopy (500 MHz, CDCl_3), this time revealing the neutral adduct isomer **5-69b**. An additional one equivalent of ethyl propiolate (1.30 mL of a 0.03908 g/mL solution, 0.5193 mmol) was slowly (85 seconds) added 31 minutes after the addition of the first equivalent. After 26 minutes, two more aliquots (1 mL each) were removed. The first was partitioned between water (4 mL) and EtOAc (3×1.5 mL), and the second was neutralized by partition between saturated aqueous NH_4Cl (3 mL) and EtOAc (3×1.5 mL). In both cases, the combined organics were dried (Na_2SO_4), concentrated *in vacuo*, and dissolved in CDCl_3 for ^1H NMR spectroscopy (500 MHz). Both spectra revealed the persistence of the adduct isomer, either as the anion **5-71b** (aqueous workup) or as the neutral species **5-69b** (acidic workup), as well as unidentified impurities. Signals diagnostic of a novel substituted Cope rearrangement product derived from the second equivalent of ethyl propiolate were not observed. The remaining reaction mixture was allowed to warm up to room temperature and was stirred overnight. The mixture was added to ice-cold 6 % aqueous HCl (60 mL) and was extracted with CH_2Cl_2 (3×20 mL). The dried (Na_2SO_4), combined CH_2Cl_2 portions were concentrated *in vacuo* to furnish a brown foam that was revealed by ^1H NMR spectroscopy (CDCl_3 , 300 MHz) to contain **5-69b** as the major product, as well as DBU-HCl, trace aromatic compounds, and additional complex signals in the regions of the ethyl ester proton signals. An overall reaction yield was not calculated and characterization was performed on the reasonably pure earliest aliquots. Anionic adduct isomer **5-71b**: ^1H NMR (CDCl_3 , 500 MHz) δ 6.98 (1 H, dt, $J = 5.5, 1.0$ Hz, C2-H), 6.80 (1 H, d, $J = 15.7$ Hz, EtO_2CCHCH), 6.14 (1 H, dd, $J = 9.4, 5.5$ Hz, C3-H), 6.04 (1 H, d, $J = 9.4$ Hz, C4-H), 5.71 (1

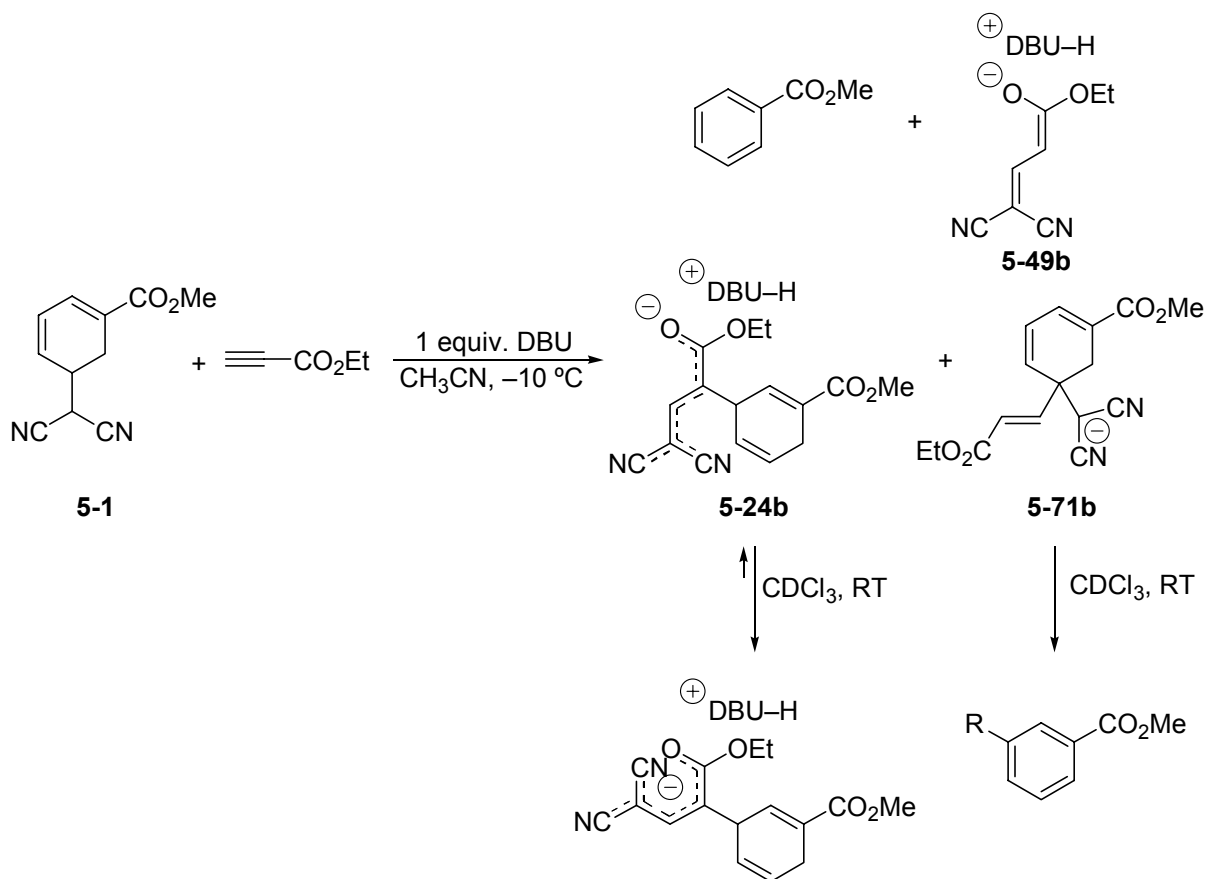
H, d, $J = 15.7$ Hz, EtO₂CCH), 4.13 (2 H, q, $J = 7.1$ Hz, CO₂CH₂CH₃), 3.74 (3 H, s, CO₂CH₃), 2.70 (2 H, m, C6-H₂), 1.26 (3 H, t, $J = 7.1$ Hz, CO₂CH₃); neutral adduct isomer **5-69b**: ¹H NMR (CDCl₃, 500 MHz) δ 7.10 (1 H, br d, $J = 5.5$ Hz, C2-H), 6.87 (1 H, d, $J = 15.8$ Hz, EtO₂CCHCH), 6.47 (1 H, dd, $J = 9.5, 5.5$ Hz, C3-H), 6.06 (1 H, d, $J = 9.5$ Hz, C4-H), 6.04 (1 H, d, $J = 15.8$ Hz, EtO₂CCH), 4.22 (2 H, q, $J = 7.1$ Hz, CO₂CH₂CH₃), 3.81 (3 H, s, CO₂CH₃), 3.80 (1 H, s, HC(CN)₂), 2.96 (1 H, dd, $J = 17.9, 1.8$ Hz, C6-H), 2.90 (1 H, dd, $J = 17.9, 1.6$ Hz, C6-H), 1.31 (3 H, t, $J = 7.1$ Hz, CO₂CH₂CH₃); ¹³C JMOD (CDCl₃, 125 MHz) δ 165.8 (u), 164.9 (u), 142.2 (d), 131.5 (d), 129.5 (d), 128.3 (d), 126.3 (u), 124.9 (d), 110.6 (u), 110.3 (u), 61.0 (u), 52.2 (d), 44.1 (u), 31.2 (d), 30.1 (u), 14.0 (d).

Generation of Cope product DBU-H⁺ salt **5-24b**



To a stirred room temperature solution of **5-22b** in CH₃CN (5 mL) was added one equiv. of DBU. An aliquot was withdrawn by syringe and the mixture was immediately partitioned between water and EtOAc, which effected a slight degree of purification of the starting mixture and furnished a sample of greater purity than direct concentration of a separate aliquot *in vacuo* without extraction. The extracted sample was concentrated *in vacuo*, dissolved in CDCl₃, and immediately assessed by ¹H NMR spectroscopy. **5-24b**: ¹H NMR (CDCl₃, 500 MHz) δ 7.19 (1 H, s, (NC)₂CH), 6.84 (1 H, m, C2-H), 5.72 (1 H, m, C4-H), 5.55 (1 H, m, C5-H), 4.61 (1 H, m, C3-H), 4.00 (2 H, m, CO₂CH₂CH₃), 3.71 (3 H, s, CO₂CH₃), 3.0–2.79 (2 H, m, C6-H₂).

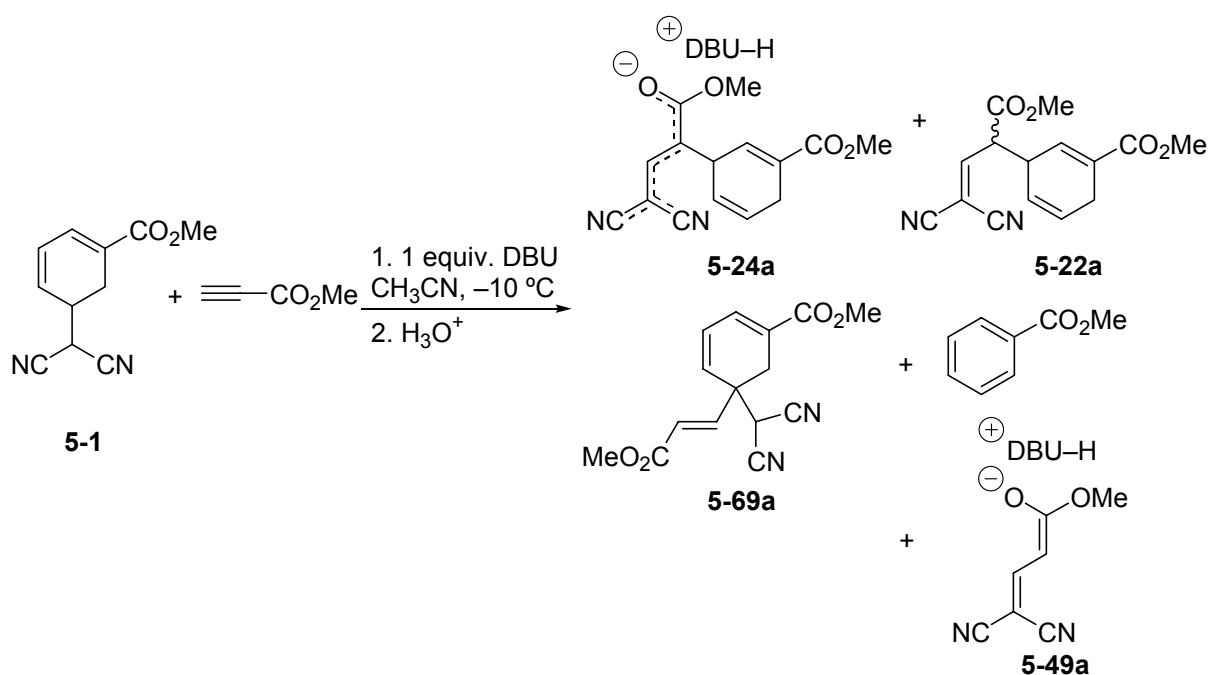
Synthesis of 3-(3,3-Dicyano-1-ethoxycarbonyl-allyl)-cyclohexa-1,4-dienecarboxylic acid methyl ester with stoichiometric DBU and without acidic workup



To a stirred solution of **5-1** (91.6 mg, 0.453 mmol) in CH₃CN (3 mL) at -10 °C was added stoichiometric DBU (1.61 mL of a 42.7 mg/mL CH₃CN solution, 0.453 mmol, 1 equiv.) over 86 seconds. Within a few minutes, ethyl propiolate (1.23 mL of a 36.0 mg/mL CH₃CN solution, 0.453 mmol, 1 equiv.) was added over 36 seconds. After seven minutes, the reaction was concentrated *in vacuo* and stored at -20 °C prior to assessment by ¹H NMR spectroscopy. The concentrated crude mixture was dissolved in CDCl₃ and a ¹H NMR spectrum was obtained (500 MHz), evidencing the generation of the Cope rearrangement product–protonated DBU salt **5-24b**, as well as methyl benzoate and the anionic fragment **5-49b**, and anionic adduct isomer **5-71b**. Spectra were obtained periodically over several

hours, revealing the postulated geometric isomerization of the Cope rearrangement product (putative isomeric relationship depicted), and the appearance and increase of an apparently *meta*-substituted aromatic compound derived from the ring C5-disubstituted adduct isomer **5-71b**.

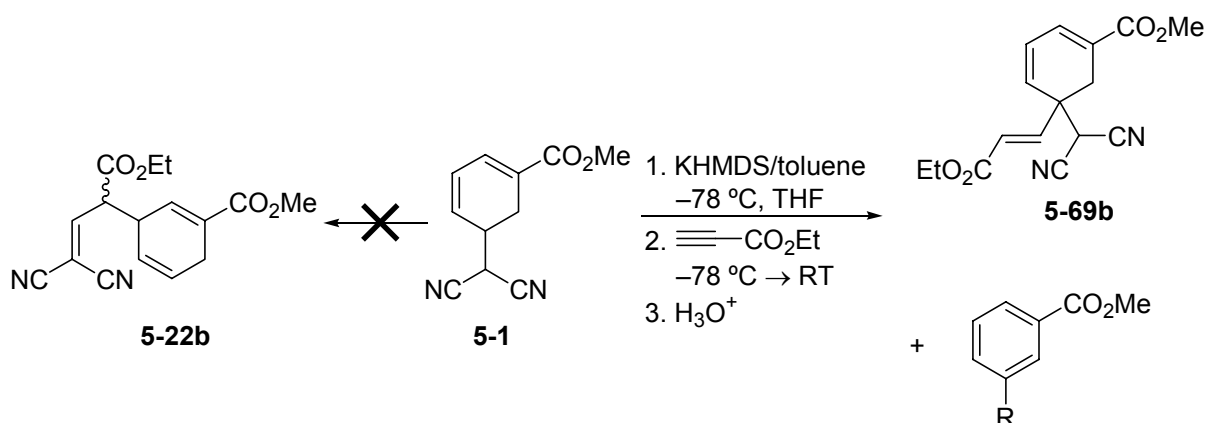
Synthesis of 3-(3,3-Dicyano-1-methoxycarbonyl-allyl)-cyclohexa-1,4-dienecarboxylic acid methyl ester with stoichiometric DBU and acidic workup



To a stirred solution of **5-1** (86.5 mg, 0.428 mmol) in CH₃CN (4 mL) at -10 °C was added stoichiometric methyl propiolate (1.74 mL of a 20.7 mg/mL CH₃CN solution, 0.428 mmol). One equivalent of DBU (1.71 mL of a 38.1 mg/mL CH₃CN solution, 0.428 mmol) was added slowly over five minutes, causing the reaction mixture to become yellow. After 21 minutes, the reaction mixture was poured into saturated aqueous NH₄Cl (80 mL) and partitioned against CH₂Cl₂ (3 × 20 mL), dried (Na₂SO₄), and concentrated *in vacuo*. At this stage of the study, the identities of the adduct isomer **5-69a** and the Cope product anion

5-24a were not characterized, and column chromatography on silica was unsuccessful. Later efforts individually identified the various products and enabled an assignment of the mixture constituents from the ^1H NMR spectrum of the crude product.

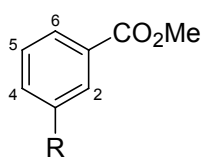
Attempted Cope rearrangement of ring-opened adduct/ethyl propiolate allenolate generated with stoichiometric potassium hexamethyldisilazide



To 3 mL of dry, freshly distilled THF at $-78\text{ }^\circ\text{C}$ was added commercial KHMDS (2.41 mL of a 0.5 M solution in toluene, 1.21 mmol). A solution of **5-1** in THF (2 mL) was added slowly over 4.5 minutes, followed by a 0.5 mL THF rinse of the solution source flask over 45 seconds. The reaction mixture turned yellow with the addition of base, and later became orange. During the transfer of the reaction flask to a $0\text{ }^\circ\text{C}$ bath, extensive heterogeneous precipitation was noticed, comprising fine yellow precipitate and dark orange amorphous aggregates within the orange solution. After several minutes at $0\text{ }^\circ\text{C}$, the mixture was immersed in an ultrasonic bath for several minutes at room temperature, which failed to dissolve the solids. The flask was again mounted in the $0\text{ }^\circ\text{C}$ bath and ethyl propiolate (2.71 mL of a 43.7 mg/mL solution in THF, 1.21 mmol) was added over 2.5 minutes, causing the reaction mixture to become brown/black and opaque. An additional period of immersion in an ultrasonic bath was unsuccessful. The reaction was removed from the $0\text{ }^\circ\text{C}$ bath and

allowed to warm to room temperature. After 1.5 hours, the reaction mixture was added to ice-cold 6 % aqueous HCl (60 mL) and extracted with CH₂Cl₂ (3 × 20 mL). The combined CH₂Cl₂ portions were dried (Na₂SO₄) and concentrated *in vacuo*, and the crude mixture was dissolved in CDCl₃ for examination by ¹H NMR spectroscopy (CDCl₃, 300 MHz), evidencing the presence of adduct isomer **5-69b** and a greater quantity of a compound partially formulated as a *meta*-substituted aromatic derivative of **5-1** (ratio of *meta*-substituted aromatic to **5-69a** approximately 1:0.9).

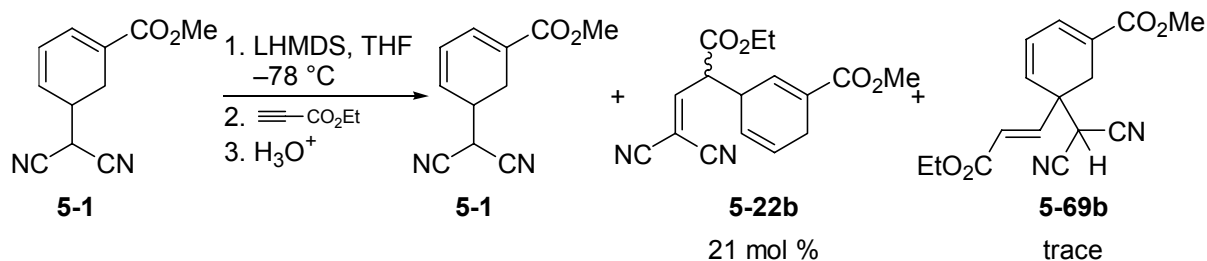
The reaction was repeated under comparable conditions, but was carried out entirely at room temperature; nevertheless, opacity of the reaction mixture and extensive amorphous precipitation again were observed. The reaction was stirred for 2.2 hours after the addition of ethyl propiolate and was worked up as before. Late in the reaction, it appeared as though the suspended precipitate had dissolved. The remaining adsorbed precipitate was water soluble and generated a yellow aqueous solution. Assessment of the crude mixture by ¹H NMR spectroscopy (CDCl₃, 300 MHz) revealed the same products as previously, but with a greater proportion of the aromatic compound (ratio of *meta*-substituted aromatic to **5-69b** approximately 1:0.7). Isolated ¹H NMR signals of *meta*-substituted aromatic product (signals



qualified as broad evidenced extremely fine additional *meta* couplings insufficiently resolved to merit designation: ¹H NMR (CDCl₃, 300 MHz) δ 8.19 (1 H, br s, C2-H), 8.15 (1 H, br d, $J = 7.8$ Hz, C6-H), 7.74 (1 H, br d, J

$= 7.8$ Hz, C4-H), 7.61 (1 H, t, $J = 7.8$ Hz, C5-H).

Attempted Cope rearrangement of ring-opened adduct/ethyl propiolate allenolate generated with stoichiometric lithium hexamethyldisilazide



To dry THF at $-50\text{ }^{\circ}\text{C}$ were added successively $\text{HN}(\text{TMS})_2$ (0.117 mL, 0.552 mmol), and *n*-BuLi (0.528 mL, 0.552 mmol). The reaction flask was immersed in a $0\text{ }^{\circ}\text{C}$ bath for 15 min. and then placed in a $-78\text{ }^{\circ}\text{C}$ bath. A THF (2 mL) solution of **5-1** (111.7 mg, 0.552 mmol) was added dropwise by syringe over 3 min. 20 sec., followed by a 0.7 mL rinse of the source flask over 1 min. 45 sec. Ethyl propiolate (1.24 mL of a 43.7 mg/mL THF solution, 54 mg, 0.552 mmol) was added by syringe over 3 min. 25 sec. and the reaction was allowed to stir at $-78\text{ }^{\circ}\text{C}$ for 1 hr. 40 min., at which time approx. half of the reaction was withdrawn by 5 mL syringe and quickly transferred to a dry reaction flask immersed in a $0\text{ }^{\circ}\text{C}$ bath. The remainder of the reaction was stirred at $-78\text{ }^{\circ}\text{C}$ for 3 days and monitored by the withdrawal and aq. acidic workup of small aliquots. The crude reaction mixture was partitioned between saturated aqueous NH_4Cl (60 mL) and 6 % aq. HCl and CH_2Cl_2 (3×20 mL). The combined organics were dried (Na_2SO_4) and concentrated *in vacuo*. Assessment of the crude mixture by ^1H NMR spectroscopy revealed the generation of 21 mol % of **5-22b** and trace **5-69b**. The parallel $0\text{ }^{\circ}\text{C}$ portion was allowed to warm to room temp. and stir overnight, at which time it was worked up in the same way as the $-78\text{ }^{\circ}\text{C}$ portion. The crude ^1H NMR spectrum contained trace **5-69b**, aromatic minor products, and none of Cope product **5-22b**.

References

1. Krasovsky, A. L.; Nenajdenko, V. G.; Balenkova, E. S. *Tetrahedron* **2001**, *57*, 201-209.
2. Garbisch Jr., E. W.; Griffith, M. G. *J. Am. Chem. Soc.* **1968**, *90*, 3590-3592.
3. Barfield, M.; Gotoh, T.; Hall Jr., H. K. *Magn. Res. Chem.* **1985**, *23*, 705-709.
4. Miller, B. *Advanced Organic Chemistry: Reactions and Mechanisms*; Prentice-Hall, Inc.: Upper Saddle River, 1998.
5. Eliel, E. L.; Wilen, S. H.; Mander, L. N. *Stereochemistry of Organic Compounds*; John Wiley & Sons: New York, 1994.
6. Nishida, S.; Asanuma, N.; Murakami, M.; Tsuji, T.; Imai, T. *J. Org. Chem.* **1992**, *57*, 4658-4663.
7. Becker, E. D. *High Resolution NMR: Theory and Chemical Applications*; Academic Press, Inc.: New York, 1980.
8. Saunders, J. K. M.; Hunter, B. K. *Modern NMR Spectroscopy: A Guide for Chemists*; Oxford University Press, Inc.: New York, 1993.
9. Foster, E. G.; Cope, A. C.; Daniels, F. *J. Am. Chem. Soc.* **1947**, *69*, 1893-1896.
10. Navarro-Vázquez, A.; Prall, M.; Schreiner, P. R. *Org. Lett.* **2004**, *6*, 2981-2984.
11. Hrovat, D. A.; Beno, B. R.; Lange, H.; Yoo, H.-Y.; Houk, K. N.; Borden, W. T. *J. Am. Chem. Soc.* **1999**, *121*, 10529-10537.
12. Staroverov, V. N.; Davidson, E. R. *J. Am. Chem. Soc.* **2000**, *122*, 7377-7385.
13. Vedejs, E.; Cammers-Goodwin, A. *J. Org. Chem.* **1994**, *59*, 7541-7543.
14. Hayakawa, K.; Kamikawakaji, Y.; Kanematsu, K. *Tetrahedron Lett.* **1982**, *23*, 2171-2174.
15. Hayakawa, K.; Kamikawakaji, Y.; Wakita, A.; Kanematsu, K. *J. Org. Chem.* **1984**, *49*, 1985-1989.
16. Kataoka, Y.; Matsumoto, O.; Tani, K. *Chem. Lett.* **1996**, 727-728.
17. Kandeel, K. A.; Vernon, J. M. *J. Chem. Soc., Perkin Trans. 1* **1987**, 2023-2026.
18. Schwan, A.; Warkentin, J. *Can. J. Chem.* **1988**, *66*, 1686-1694.

19. Vedejs, E.; Gingras, M. *J. Am. Chem. Soc.* **1994**, *116*, 579-588.

APPENDIX

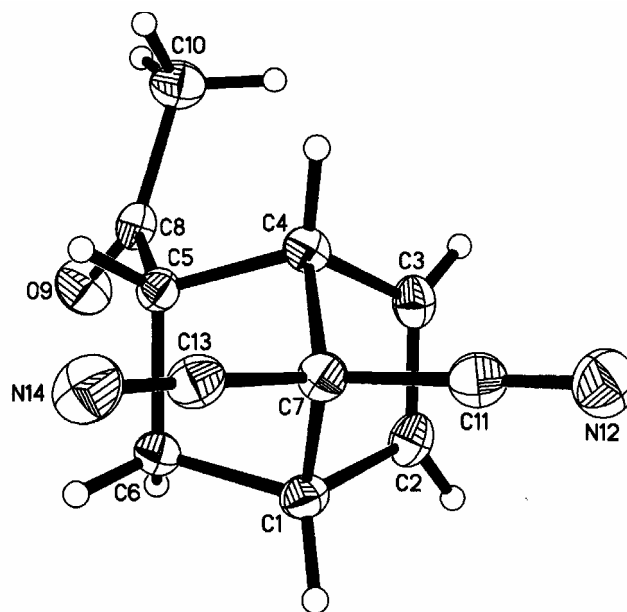
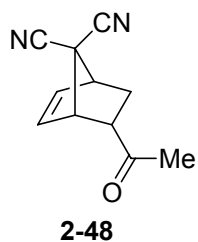


Table 1. Crystal data and structure refinement for **2-48**.

Empirical formula	$C_{11}H_{10}N_2O$	
Formula weight	186.21	
Temperature	150(1) K	
Wavelength	0.71073 Å	
Crystal system	Orthorhombic	
Space group	Pbca	
Unit cell dimensions	$a = 8.3151(3)$ Å	alpha = 90°
	$b = 16.5039(7)$ Å	beta = 90°
	$c = 13.4183(5)$ Å	gamma = 90°
Volume, Z	$1841.41(12)$ Å ³ , 8	
Density (calculated)	1.343 Mg/m ³	
Absorption coefficient	0.089 mm ⁻¹	
F(000)	784	
Crystal size	0.46 × 0.38 × 0.30 mm	

θ range for data collection	2.47 to 30.03°
Limiting indices	$-11 \leq h \leq 11, -23 \leq k \leq 23, -18 \leq l \leq 18$
Reflections collected	21381
Independent reflections	2689 ($R_{\text{int}} = 0.0514$)
Completeness to $\theta = 30.03^\circ$	100.0 %
Absorption correction	None
Refinement method	Full-matrix least-squares on F^2
Data / restraints / parameters	2689 / 0 / 157
Goodness-of-fit on F^2	2.490
Final R indices [$I > 2\sigma(I)$]	$R1 = 0.0520, wR2 = 0.1229$
R indices (all data)	$R1 = 0.0556, wR2 = 0.1239$
Extinction coefficient	0.011(2)
Largest diff. peak and hole	0.325 and $-0.356 \text{ e}\text{\AA}^{-3}$

Table 2. Atomic coordinates [$\times 10^4$] and equivalent isotropic displacement parameters [$\text{\AA}^2 \times 10^3$] for **2-48**. $U(\text{eq})$ is defined as one third of the trace of the orthogonalized U_{ij} tensor.

	x	y	z	$U(\text{eq})$
C(1)	2283(1)	1995(1)	1031(1)	21(1)
C(2)	4092(1)	1939(1)	1126(1)	23(1)
C(3)	4566(1)	1212(1)	813(1)	22(1)
C(4)	3070(1)	742(1)	505(1)	19(1)
C(5)	2111(1)	570(1)	1490(1)	18(1)
C(6)	1581(1)	1424(1)	1842(1)	21(1)
C(7)	2041(1)	1458(1)	83(1)	19(1)
C(8)	3024(1)	71(1)	2257(1)	20(1)
O(9)	2906(1)	215(1)	3142(1)	31(1)
C(10)	4010(1)	-630(1)	1886(1)	27(1)
C(11)	2735(1)	1818(1)	-829(1)	24(1)
N(12)	3244(1)	2098(1)	-1542(1)	32(1)
C(13)	342(1)	1252(1)	-109(1)	23(1)
N(14)	-984(1)	1106(1)	-239(1)	31(1)

Table 3. Bond lengths [Å] for **2-48**.

C(1)-C(2)	1.5126(13)
C(1)-C(6)	1.5533(14)
C(1)-C(7)	1.5632(13)
C(2)-C(3)	1.3317(15)
C(3)-C(4)	1.5230(13)
C(4)-C(7)	1.5641(13)
C(4)-C(5)	1.5701(13)
C(5)-C(8)	1.5216(13)
C(5)-C(6)	1.5504(13)
C(7)-C(13)	1.4752(14)
C(7)-C(11)	1.4779(14)
C(8)-O(9)	1.2153(12)
C(8)-C(10)	1.5020(14)
C(11)-N(12)	1.1439(13)
C(13)-N(14)	1.1420(13)

Table 4. Bond angles (°) for **2-48**.

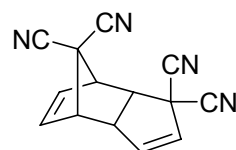
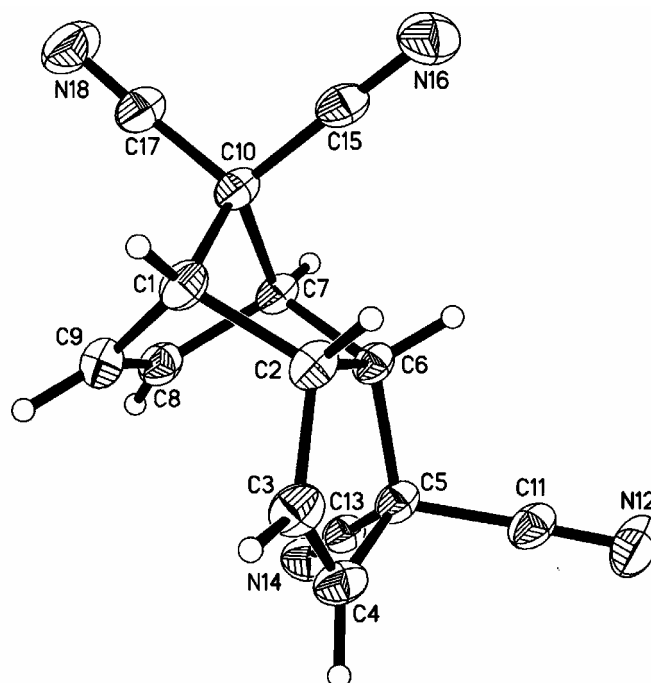
C(2)-C(1)-C(6)	106.15(8)
C(2)-C(1)-C(7)	99.35(7)
C(6)-C(1)-C(7)	100.26(8)
C(3)-C(2)-C(1)	108.77(8)
C(2)-C(3)-C(4)	107.64(8)
C(3)-C(4)-C(7)	99.25(7)
C(3)-C(4)-C(5)	106.17(7)
C(7)-C(4)-C(5)	99.41(7)
C(8)-C(5)-C(6)	115.31(8)
C(8)-C(5)-C(4)	114.47(8)
C(6)-C(5)-C(4)	103.66(8)
C(5)-C(6)-C(1)	103.36(7)
C(13)-C(7)-C(11)	108.77(8)
C(13)-C(7)-C(1)	113.31(8)
C(11)-C(7)-C(1)	113.27(8)
C(13)-C(7)-C(4)	114.41(8)
C(11)-C(7)-C(4)	112.96(8)
C(1)-C(7)-C(4)	93.62(7)
O(9)-C(8)-C(10)	121.27(9)
O(9)-C(8)-C(5)	120.98(9)
C(10)-C(8)-C(5)	117.68(8)
N(12)-C(11)-C(7)	178.74(11)
N(14)-C(13)-C(7)	178.30(11)

Table 5. Anisotropic displacement parameters [$\text{\AA}^2 \times 10^3$] for **2-48**. The anisotropic displacement factor exponent takes the form: $-2\pi^2 [(ha^*)^2U_{11} + \dots + 2hka^*b^*U_{12}]$

	U11	U22	U33	U23	U13	U12
C(1)	22(1)	17(1)	23(1)	-2(1)	0(1)	-1(1)
C(2)	21(1)	24(1)	24(1)	3(1)	-3(1)	-5(1)
C(3)	17(1)	26(1)	21(1)	4(1)	0(1)	-1(1)
C(4)	19(1)	20(1)	17(1)	0(1)	0(1)	2(1)
C(5)	19(1)	18(1)	18(1)	0(1)	0(1)	-1(1)
C(6)	22(1)	20(1)	22(1)	-3(1)	3(1)	0(1)
C(7)	18(1)	20(1)	21(1)	1(1)	-2(1)	0(1)
C(8)	19(1)	21(1)	21(1)	2(1)	0(1)	-4(1)
O(9)	35(1)	38(1)	20(1)	1(1)	-1(1)	4(1)
C(10)	29(1)	25(1)	27(1)	2(1)	-3(1)	5(1)
C(11)	23(1)	23(1)	24(1)	2(1)	-3(1)	3(1)
N(12)	34(1)	33(1)	30(1)	8(1)	1(1)	4(1)
C(13)	24(1)	20(1)	24(1)	1(1)	-3(1)	1(1)
N(14)	27(1)	30(1)	37(1)	1(1)	-8(1)	-2(1)

Table 6. Hydrogen coordinates ($\times 10^4$) and isotropic displacement parameters ($\text{\AA}^2 \times 10^3$) for **2-48**.

	x	y	z	U(eq)
H(10X)	4970	-424	1546	41
H(10Y)	3369	-952	1419	41
H(10Z)	4334	-969	2451	41
H(1)	1825(13)	2540(7)	1003(8)	24(3)
H(2)	4717(14)	2353(8)	1453(10)	27(3)
H(3)	5646(15)	991(8)	883(9)	30(3)
H(4)	3187(13)	278(7)	43(8)	17(3)
H(5)	1206(14)	228(7)	1321(9)	27(3)
H(6X)	2053(14)	1562(7)	2483(10)	31(3)
H(6Y)	407(16)	1465(8)	1857(8)	26(3)

**2-41****Table 1.** Crystal data and structure refinement for **2-41**.

Empirical formula	$C_{14}H_8N_4$	
Formula weight	232.24	
Temperature	180(2) K	
Wavelength	0.71073 Å	
Crystal system	Monoclinic	
Space group	$P2_1/c$	
Unit cell dimensions	$a = 12.8296(11)$ Å	$\alpha = 90^\circ$
	$b = 6.6455(7)$ Å	$\beta = 96.583(5)^\circ$
	$c = 13.9896(13)$ Å	$\gamma = 90^\circ$
Volume, Z	$1184.88(19)$ Å ³ , 4	
Density (calculated)	1.302 Mg/m ³	
Absorption coefficient	0.083 mm ⁻¹	
$F(000)$	480	

Crystal size	0.68{010} × 0.36{001} × 0.22{100} mm
θ range for data collection	2.93 to 29.99°
Limiting indices	0 ≤ h ≤ 18, 0 ≤ k ≤ 9, -19 ≤ l ≤ 19
Reflections collected	3463
Independent reflections	3454 (R _{int} = 0.0106)
Completeness to θ = 29.99°	100.0 %
Absorption correction	Integration
Max. and min. transmission	0.9811 and 0.9690
Refinement method	Full-matrix least-squares on F ²
Data / restraints / parameters	3454 / 0 / 196
Goodness-of-fit on F ²	1.918
Final R indices [I > 2σ (I)]	R1 = 0.0381, wR2 = 0.0777
R indices (all data)	R1 = 0.0502, wR2 = 0.0787
Extinction coefficient	0.0158(11)
Largest diff. peak and hole	0.274 and -0.198 eÅ ⁻³

Table 2. Atomic coordinates [$\times 10^4$] and equivalent isotropic displacement parameters [$\text{\AA}^2 \times 10^3$] for **2-41**. U(eq) is defined as one third of the trace of the orthogonalized U_j tensor.

	x	y	z	U (eq)
C(1)	1442(1)	-791(2)	1715(1)	25(1)
C(2)	1849(1)	-313(2)	2792(1)	23(1)
C(3)	2306(1)	-2048(2)	3370(1)	28(1)
C(4)	3318(1)	-1852(2)	3660(1)	28(1)
C(5)	3747(1)	157(2)	3345(1)	22(1)
C(6)	2789(1)	1134(2)	2709(1)	20(1)
C(7)	2848(1)	1267(2)	1602(1)	21(1)
C(8)	3098(1)	-786(2)	1223(1)	25(1)
C(9)	2282(1)	-1984(2)	1292(1)	28(1)
C(10)	1638(1)	1302(2)	1262(1)	23(1)
C(11)	4062(1)	1432(2)	4201(1)	27(1)
N(12)	4289(1)	2372(2)	4876(1)	41(1)
C(13)	4699(1)	-126(2)	2850(1)	23(1)
N(14)	5438(1)	-388(1)	2488(1)	30(1)
C(15)	1071(1)	2990(2)	1650(1)	26(1)
N(16)	652(1)	4332(2)	1947(1)	36(1)
C(17)	1414(1)	1342(2)	202(1)	29(1)
N(18)	1225(1)	1436(2)	-614(1)	42(1)

Table 3. Bond lengths [Å] for **2-41**.

C(1)-C(9)	1.5127(14)	C(1)-C(10)	1.5602(14)	C(1)-C(2)	1.5698(13)
C(2)-C(3)	1.4891(15)	C(2)-C(6)	1.5562(13)	C(3)-C(4)	1.3212(14)
C(4)-C(5)	1.5283(14)	C(5)-C(13)	1.4838(13)	C(5)-C(11)	1.4844(14)
C(5)-C(6)	1.5731(13)	C(6)-C(7)	1.5610(12)	C(7)-C(8)	1.5116(15)
C(7)-C(10)	1.5710(12)	C(8)-C(9)	1.3269(15)	C(10)-C(15)	1.4738(14)
C(10)-C(17)	1.4783(13)	C(11)-N(12)	1.1415(14)	C(13)-N(14)	1.1385(12)
C(15)-N(16)	1.1439(14)	C(17)-N(18)	1.1416(13)		

Table 4. Bond angles (°) for **2-41**.

C(9)-C(1)-C(10)	98.80(8)	C(9)-C(1)-C(2)	107.94(8)	C(10)-C(1)-C(2)	99.07(8)
C(3)-C(2)-C(6)	105.00(8)	C(3)-C(2)-C(1)	115.57(9)	C(6)-C(2)-C(1)	103.22(7)
C(4)-C(3)-C(2)	113.72(10)	C(3)-C(4)-C(5)	111.79(9)	C(13)-C(5)-C(11)	106.69(8)
C(13)-C(5)-C(4)	111.51(8)	C(11)-C(5)-C(4)	109.87(8)	C(13)-C(5)-C(6)	114.81(7)
C(11)-C(5)-C(6)	110.10(8)	C(4)-C(5)-C(6)	103.85(8)	C(2)-C(6)-C(7)	103.61(7)
C(2)-C(6)-C(5)	105.35(8)	C(7)-C(6)-C(5)	117.44(7)	C(8)-C(7)-C(6)	109.50(8)
C(8)-C(7)-C(10)	98.56(8)	C(6)-C(7)-C(10)	98.17(7)	C(9)-C(8)-C(7)	108.37(9)
C(8)-C(9)-C(1)	108.51(10)	C(15)-C(10)-C(17)	107.90(8)	C(15)-C(10)-C(1)	114.86(8)
C(17)-C(10)-C(1)	113.66(8)	C(15)-C(10)-C(7)	114.34(8)	C(17)-C(10)-C(7)	112.07(8)
C(1)-C(10)-C(7)	93.65(7)	N(12)-C(11)-C(5)	177.96(12)	N(14)-C(13)-C(5)	177.98(11)
N(16)-C(15)-C(10)	178.27(11)	N(18)-C(17)-C(10)	177.67(12)		

Table 5. Anisotropic displacement parameters [$\text{\AA}^2 \times 10^3$] for **2-41**. The anisotropic displacement factor exponent takes the form: $-2\pi^2 [(ha^*)^2U_{11} + \dots + 2hka^*b^*U_{12}]$

	U11	U22	U33	U23	U13	U12
C(1)	19(1)	31(1)	23(1)	0(1)	0(1)	-5(1)
C(2)	17(1)	33(1)	20(1)	1(1)	4(1)	-3(1)
C(3)	30(1)	32(1)	23(1)	6(1)	6(1)	-5(1)
C(4)	29(1)	33(1)	21(1)	6(1)	3(1)	2(1)
C(5)	18(1)	31(1)	18(1)	0(1)	2(1)	1(1)
C(6)	16(1)	26(1)	16(1)	-1(1)	2(1)	0(1)
C(7)	16(1)	28(1)	17(1)	1(1)	1(1)	-1(1)
C(8)	24(1)	33(1)	18(1)	-2(1)	2(1)	4(1)
C(9)	32(1)	29(1)	22(1)	-4(1)	0(1)	0(1)
C(10)	19(1)	30(1)	18(1)	0(1)	0(1)	0(1)
C(11)	19(1)	41(1)	21(1)	-1(1)	0(1)	4(1)
N(12)	34(1)	62(1)	28(1)	-12(1)	-1(1)	4(1)
C(13)	21(1)	26(1)	22(1)	1(1)	-2(1)	2(1)
N(14)	24(1)	34(1)	34(1)	4(1)	5(1)	4(1)
C(15)	17(1)	35(1)	24(1)	4(1)	0(1)	0(1)
N(16)	27(1)	41(1)	41(1)	2(1)	6(1)	6(1)
C(17)	24(1)	36(1)	24(1)	1(1)	-1(1)	1(1)
N(18)	43(1)	58(1)	25(1)	2(1)	-4(1)	6(1)

Table 6. Hydrogen coordinates ($\times 10^4$) and isotropic displacement parameters ($\text{\AA}^2 \times 10^3$) for **2-41**.

	x	y	z	U(eq)
H(1)	733(8)	-1306(16)	1599(7)	24(3)
H(2)	1299(9)	350(16)	3089(8)	27(3)
H(3)	1914(10)	-3255(19)	3505(9)	41(3)
H(4)	3773(8)	-2783(17)	4035(8)	29(3)
H(6)	2662(8)	2486(17)	2944(7)	22(3)
H(7)	3224(8)	2445(16)	1404(7)	17(3)
H(8)	3762(9)	-1140(18)	1004(8)	35(3)
H(9)	2240(9)	-3428(19)	1159(8)	35(3)

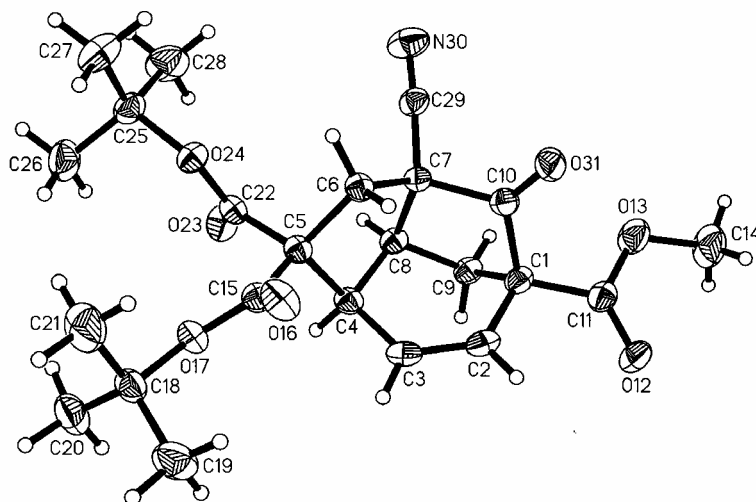
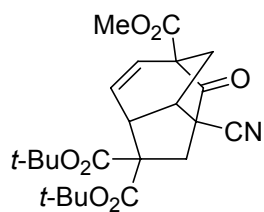


Table 1. Crystal data and structure refinement for **2-74**.

Empirical formula	$C_{23}H_{29}NO_7$	
Formula weight	431.47	
Temperature	180(2) K	
Wavelength	0.71073 Å	
Crystal system	Monoclinic	
Space group	$P2_1/c$	
Unit cell dimensions	$a = 10.9275(8)$ Å	$\alpha = 90^\circ$
	$b = 15.8444(13)$ Å	$\beta = 104.172(4)^\circ$
	$c = 13.3389(10)$ Å	$\gamma = 90^\circ$
Volume, Z	$2239.2(3)$ Å ³ , 4	
Density (calculated)	1.280 Mg/m ³	
Absorption coefficient	0.095 mm ⁻¹	
$F(000)$	920	
Crystal size	0.90 × 0.60 × 0.60 mm	
θ range for data collection	2.03 to 27.00°	
Limiting indices	$0 \leq h \leq 13, 0 \leq k \leq 20, -17 \leq l \leq 16$	
Reflections collected	5113	

Independent reflections	4861 ($R_{\text{int}} = 0.0396$)
Completeness to $\theta = 27.00^\circ$	99.4 %
Absorption correction	Integration
Max. and min. transmission	0.9552 and 0.9432
Refinement method	Full-matrix least-squares on F^2
Data / restraints / parameters	4861 / 0 / 281
Goodness-of-fit on F^2	2.597
Final R indices [$I > 2\sigma(I)$]	$R1 = 0.0390$, $wR2 = 0.1013$
R indices (all data)	$R1 = 0.0445$, $wR2 = 0.1020$
Extinction coefficient	0.0059(9)
Largest diff. peak and hole	0.297 and $-0.188 \text{ e}\text{\AA}^{-3}$

Table 2. Atomic coordinates [$\times 10^4$] and equivalent isotropic displacement parameters [$\text{\AA}^2 \times 10^3$] for **2-74**. $U(\text{eq})$ is defined as one third of the trace of the orthogonalized U_{ij} tensor.

	x	y	z	U(eq)
C(1)	6590(1)	593(1)	1556(1)	25(1)
C(2)	5836(1)	-218(1)	1484(1)	27(1)
C(3)	4667(1)	-227(1)	1602(1)	27(1)
C(4)	4014(1)	544(1)	1876(1)	23(1)
C(5)	3866(1)	477(1)	3006(1)	22(1)
C(6)	5218(1)	612(1)	3665(1)	22(1)
C(7)	5826(1)	1222(1)	3003(1)	21(1)
C(8)	4864(1)	1327(1)	1933(1)	22(1)
C(9)	5662(1)	1311(1)	1139(1)	25(1)
C(10)	6992(1)	810(1)	2717(1)	23(1)
C(11)	7662(1)	523(1)	1027(1)	29(1)
O(12)	7789(1)	-39(1)	462(1)	41(1)
O(13)	8439(1)	1185(1)	1258(1)	40(1)
C(14)	9474(2)	1217(1)	757(1)	51(1)
C(15)	3330(1)	-372(1)	3234(1)	24(1)
O(16)	3949(1)	-934(1)	3708(1)	35(1)
O(17)	2089(1)	-382(1)	2821(1)	26(1)
C(18)	1291(1)	-1093(1)	3015(1)	29(1)
C(19)	1673(2)	-1893(1)	2553(1)	45(1)
C(20)	-18(1)	-820(1)	2433(1)	44(1)
C(21)	1401(2)	-1157(1)	4160(1)	57(1)
C(22)	2977(1)	1172(1)	3210(1)	24(1)
O(23)	2400(1)	1654(1)	2566(1)	33(1)
O(24)	2962(1)	1156(1)	4207(1)	26(1)
C(25)	2234(1)	1786(1)	4649(1)	30(1)
C(26)	846(1)	1681(1)	4145(1)	46(1)
C(27)	2545(2)	1539(1)	5782(1)	46(1)
C(28)	2724(2)	2662(1)	4504(1)	50(1)
C(29)	6166(1)	2026(1)	3543(1)	26(1)
N(30)	6389(1)	2647(1)	3983(1)	42(1)
O(31)	7979(1)	666(1)	3314(1)	34(1)

Table 3. Bond lengths [Å] for **2-74**.

C(1)-C(11)	1.5129(17)	C(1)-C(2)	1.5167(17)	C(1)-C(9)	1.5341(16)
C(1)-C(10)	1.5422(16)	C(2)-C(3)	1.3249(18)	C(3)-C(4)	1.5052(16)
C(4)-C(8)	1.5405(16)	C(4)-C(5)	1.5579(16)	C(5)-C(15)	1.5284(16)
C(5)-C(22)	1.5353(16)	C(5)-C(6)	1.5382(15)	C(6)-C(7)	1.5633(16)
C(7)-C(29)	1.4653(16)	C(7)-C(10)	1.5597(16)	C(7)-C(8)	1.5606(15)
C(8)-C(9)	1.5285(16)	C(10)-O(31)	1.1945(14)	C(11)-O(12)	1.1955(16)
C(11)-O(13)	1.3370(16)	O(13)-C(14)	1.4493(16)	C(15)-O(16)	1.1996(14)
C(15)-O(17)	1.3334(14)	O(17)-C(18)	1.4861(14)	C(18)-C(21)	1.505(2)
C(18)-C(19)	1.5122(19)	C(18)-C(20)	1.5142(19)	C(22)-O(23)	1.2048(14)
C(22)-O(24)	1.3340(14)	O(24)-C(25)	1.4859(14)	C(25)-C(26)	1.5105(19)
C(25)-C(27)	1.517(2)	C(25)-C(28)	1.5179(19)	C(29)-N(30)	1.1410(17)

Table 4. Bond angles (°) for **2-74**.

C(11)-C(1)-C(2)	112.25(10)	C(11)-C(1)-C(9)	113.81(10)
C(2)-C(1)-C(9)	107.73(10)	C(11)-C(1)-C(10)	114.96(10)
C(2)-C(1)-C(10)	105.68(9)	C(9)-C(1)-C(10)	101.50(9)
C(3)-C(2)-C(1)	121.76(11)	C(2)-C(3)-C(4)	123.24(11)
C(3)-C(4)-C(8)	110.49(10)	C(3)-C(4)-C(5)	110.35(9)
C(8)-C(4)-C(5)	102.22(9)	C(15)-C(5)-C(22)	107.87(9)
C(15)-C(5)-C(6)	111.69(9)	C(22)-C(5)-C(6)	111.13(9)
C(15)-C(5)-C(4)	112.84(9)	C(22)-C(5)-C(4)	110.03(9)
C(6)-C(5)-C(4)	103.29(9)	C(5)-C(6)-C(7)	104.19(9)
C(29)-C(7)-C(10)	111.12(9)	C(29)-C(7)-C(8)	112.96(10)
C(10)-C(7)-C(8)	103.24(9)	C(29)-C(7)-C(6)	110.58(9)
C(10)-C(7)-C(6)	111.38(9)	C(8)-C(7)-C(6)	107.32(9)
C(9)-C(8)-C(4)	113.07(10)	C(9)-C(8)-C(7)	105.11(9)
C(4)-C(8)-C(7)	102.85(9)	C(8)-C(9)-C(1)	101.53(9)
O(31)-C(10)-C(1)	127.96(11)	O(31)-C(10)-C(7)	125.13(10)
C(1)-C(10)-C(7)	106.83(9)	O(12)-C(11)-O(13)	124.38(12)
O(12)-C(11)-C(1)	124.80(12)	O(13)-C(11)-C(1)	110.81(10)
C(11)-O(13)-C(14)	116.41(11)	O(16)-C(15)-O(17)	126.52(11)
O(16)-C(15)-C(5)	124.36(11)	O(17)-C(15)-C(5)	109.12(9)
C(15)-O(17)-C(18)	121.11(9)	O(17)-C(18)-C(21)	108.91(11)
O(17)-C(18)-C(19)	109.41(10)	C(21)-C(18)-C(19)	113.33(13)
O(17)-C(18)-C(20)	102.37(10)	C(21)-C(18)-C(20)	111.74(13)
C(19)-C(18)-C(20)	110.50(12)	O(23)-C(22)-O(24)	126.18(11)
O(23)-C(22)-C(5)	124.86(11)	O(24)-C(22)-C(5)	108.97(9)
C(22)-O(24)-C(25)	121.41(9)	O(24)-C(25)-C(26)	109.09(11)
O(24)-C(25)-C(27)	102.20(10)	C(26)-C(25)-C(27)	111.75(12)
O(24)-C(25)-C(28)	108.90(11)	C(26)-C(25)-C(28)	113.01(13)
C(27)-C(25)-C(28)	111.29(13)	N(30)-C(29)-C(7)	177.13(13)

Table 5. Anisotropic displacement parameters [$\text{\AA}^2 \times 10^3$] for **2-74**. The anisotropic displacement factor exponent takes the form: $-2\pi^2 [(ha^*)^2U_{11} + \dots + 2hka^*b^*U_{12}]$

	U11	U22	U33	U23	U13	U12
C(1)	28(1)	28(1)	20(1)	-2(1)	6(1)	3(1)
C(2)	35(1)	25(1)	21(1)	-4(1)	4(1)	3(1)
C(3)	34(1)	25(1)	20(1)	-3(1)	2(1)	-3(1)
C(4)	23(1)	27(1)	18(1)	1(1)	2(1)	-1(1)
C(5)	21(1)	24(1)	20(1)	2(1)	3(1)	0(1)
C(6)	21(1)	26(1)	20(1)	2(1)	3(1)	0(1)
C(7)	22(1)	23(1)	18(1)	-2(1)	4(1)	-1(1)
C(8)	25(1)	23(1)	18(1)	1(1)	4(1)	2(1)
C(9)	29(1)	27(1)	18(1)	1(1)	6(1)	2(1)
C(10)	25(1)	23(1)	22(1)	-1(1)	6(1)	-1(1)
C(11)	28(1)	36(1)	21(1)	0(1)	5(1)	7(1)
O(12)	38(1)	53(1)	35(1)	-17(1)	11(1)	6(1)
O(13)	43(1)	40(1)	44(1)	-5(1)	27(1)	-5(1)
C(14)	48(1)	60(1)	56(1)	2(1)	34(1)	-4(1)
C(15)	24(1)	26(1)	21(1)	1(1)	4(1)	-1(1)
O(16)	30(1)	31(1)	40(1)	12(1)	0(1)	0(1)
O(17)	22(1)	26(1)	31(1)	3(1)	4(1)	-2(1)
C(18)	27(1)	29(1)	32(1)	1(1)	9(1)	-7(1)
C(19)	41(1)	29(1)	61(1)	-5(1)	6(1)	-3(1)
C(20)	26(1)	44(1)	60(1)	0(1)	9(1)	-4(1)
C(21)	56(1)	81(1)	38(1)	6(1)	19(1)	-23(1)
C(22)	21(1)	24(1)	26(1)	2(1)	5(1)	-3(1)
O(23)	32(1)	37(1)	31(1)	10(1)	8(1)	10(1)
O(24)	29(1)	26(1)	24(1)	0(1)	8(1)	5(1)
C(25)	32(1)	27(1)	33(1)	-4(1)	12(1)	4(1)
C(26)	31(1)	59(1)	49(1)	-2(1)	14(1)	8(1)
C(27)	60(1)	47(1)	33(1)	-4(1)	18(1)	13(1)
C(28)	67(1)	29(1)	57(1)	-10(1)	19(1)	-4(1)
C(29)	30(1)	27(1)	22(1)	0(1)	9(1)	-1(1)
N(30)	61(1)	31(1)	38(1)	-8(1)	15(1)	-6(1)
O(31)	24(1)	51(1)	26(1)	-4(1)	4(1)	5(1)

Table 6. Hydrogen coordinates ($\times 10^4$) and isotropic displacement parameters ($\text{\AA}^2 \times 10^3$) for **2-74**.

	x	y	z	U(eq)
H(2)	6204	-722	1352	33
H(3)	4229	-736	1512	33
H(4)	3195	631	1386	28
H(6X)	5674	81	3784	27
H(6Y)	5213	864	4326	27
H(8)	4381	1852	1895	27
H(9X)	6099	1842	1124	30
H(9Y)	5153	1185	451	30
H(14X)	9969	1715	976	77
H(14Y)	9145	1232	20	77
H(14Z)	9995	726	942	77
H(19X)	1585	-1814	1825	68
H(19Y)	1140	-2349	2659	68
H(19Z)	2536	-2024	2881	68
H(20X)	-53	-785	1708	66
H(20Y)	-204	-277	2679	66
H(20Z)	-626	-1225	2542	66
H(21X)	1148	-632	4408	85
H(21Y)	2260	-1277	4511	85
H(21Z)	864	-1602	4291	85
H(26X)	684	1842	3431	68
H(26Y)	362	2033	4491	68
H(26Z)	608	1102	4193	68
H(27X)	3432	1612	6076	69
H(27Y)	2322	959	5844	69
H(27Z)	2078	1890	6142	69
H(28X)	3608	2693	4837	75
H(28Y)	2273	3073	4803	75
H(28Z)	2602	2776	3779	75

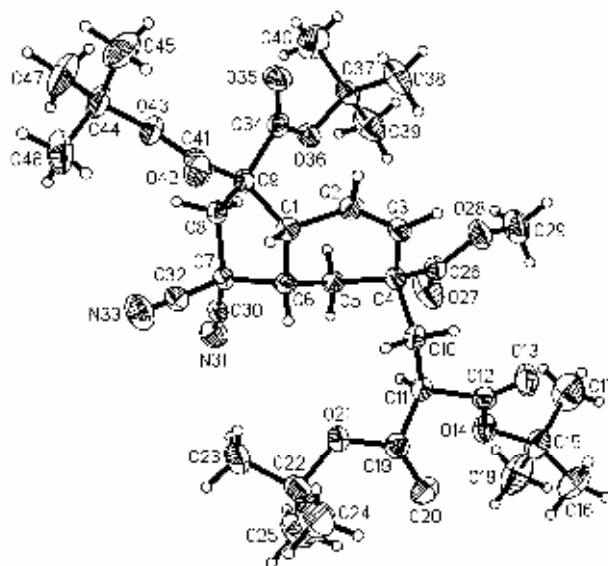
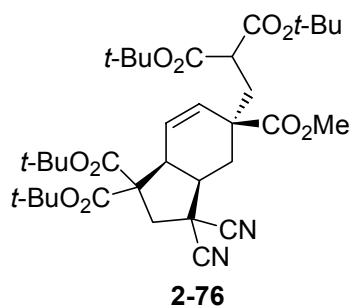


Table 1. Crystal data and structure refinement for **2-76**.

Empirical formula	$C_{35}H_{50}N_{2}O_{10}$	
Formula weight	658.77	
Temperature	180(2) K	
Wavelength	0.71073 Å	
Crystal system	Orthorhombic	
Space group	Pbca	
Unit cell dimensions	$a = 19.532(2)$ Å	alpha = 90°
	$b = 12.1828(15)$ Å	beta = 90°
	$c = 30.950(3)$ Å	gamma = 90°
Volume, Z	7364.8(15) Å ³ , 8	
Density (calculated)	1.188 Mg/m ³	
Absorption coefficient	0.087 mm ⁻¹	
F(000)	2832	
Crystal size	0.96{010} × 0.64{100} × 0.54{001} mm	

θ range for data collection	2.08 to 27.00°
Limiting indices	$0 \leq h \leq 24, 0 \leq k \leq 15, 0 \leq l \leq 39$
Reflections collected	7963
Independent reflections	7963
Completeness to $\theta = 27.00^\circ$	99.1 %
Absorption correction	Integration
Max. and min. transmission	0.9572 and 0.9485
Refinement method	Full-matrix least-squares on F^2
Data / restraints / parameters	7963 / 0 / 425
Goodness-of-fit on F^2	1.791
Final R indices [$I > 2 \sigma(I)$]	$R1 = 0.0426, wR2 = 0.0863$
R indices (all data)	$R1 = 0.0668, wR2 = 0.0878$
Extinction coefficient	0.00132(7)
Largest diff. peak and hole	0.257 and $-0.211 \text{ e}\text{\AA}^{-3}$

Table 2. Atomic coordinates [$\times 10^4$] and equivalent isotropic displacement parameters [$\text{\AA}^2 \times 10^3$] for **2-76**. $U(\text{eq})$ is defined as one third of the trace of the orthogonalized U_{ij} tensor.

	x	y	z	U(eq)
C(1)	3548(1)	272(1)	4294(1)	27(1)
C(2)	4289(1)	61(1)	4203(1)	31(1)
C(3)	4615(1)	410(1)	3857(1)	31(1)
C(4)	4286(1)	1066(1)	3500(1)	27(1)
C(5)	3634(1)	1636(1)	3670(1)	27(1)
C(6)	3177(1)	838(1)	3916(1)	26(1)
C(7)	2569(1)	1422(1)	4146(1)	28(1)
C(8)	2898(1)	1882(1)	4566(1)	28(1)
C(9)	3394(1)	969(1)	4715(1)	26(1)
C(10)	4130(1)	250(1)	3126(1)	30(1)
C(11)	3874(1)	771(1)	2704(1)	28(1)
C(12)	4445(1)	900(1)	2373(1)	32(1)
O(13)	4979(1)	416(1)	2388(1)	49(1)
O(14)	4258(1)	1617(1)	2072(1)	39(1)
C(15)	4711(1)	1870(2)	1702(1)	45(1)
C(16)	4829(1)	844(2)	1438(1)	57(1)
C(17)	5372(1)	2363(2)	1875(1)	67(1)
C(18)	4291(1)	2705(2)	1455(1)	73(1)
C(19)	3286(1)	133(1)	2504(1)	33(1)
O(20)	3297(1)	-296(1)	2154(1)	52(1)
O(21)	2760(1)	130(1)	2780(1)	38(1)
C(22)	2087(1)	-362(2)	2667(1)	42(1)

Table 2 continued

	x	y	z	U(eq)
C(23)	1691(1)	-224(2)	3087(1)	58(1)
C(24)	2168(1)	-1563(2)	2556(1)	68(1)
C(25)	1777(1)	304(2)	2307(1)	68(1)
C(26)	4750(1)	1969(1)	3322(1)	33(1)
O(27)	4546(1)	2757(1)	3134(1)	61(1)
O(28)	5413(1)	1774(1)	3384(1)	44(1)
C(29)	5867(1)	2606(2)	3206(1)	57(1)
C(30)	2246(1)	2300(1)	3888(1)	31(1)
N(31)	2005(1)	2990(1)	3692(1)	46(1)
C(32)	2038(1)	602(1)	4260(1)	36(1)
N(33)	1655(1)	-52(1)	4361(1)	61(1)
C(34)	4060(1)	1425(1)	4908(1)	29(1)
O(35)	4333(1)	1025(1)	5219(1)	44(1)
O(36)	4288(1)	2268(1)	4676(1)	30(1)
C(37)	4954(1)	2818(1)	4770(1)	34(1)
C(38)	5533(1)	2009(2)	4721(1)	52(1)
C(39)	4989(1)	3671(2)	4417(1)	56(1)
C(40)	4921(1)	3328(2)	5211(1)	78(1)
C(41)	3080(1)	216(1)	5063(1)	29(1)
O(42)	3080(1)	-767(1)	5044(1)	39(1)
O(43)	2814(1)	820(1)	5380(1)	36(1)
C(44)	2517(1)	278(2)	5767(1)	45(1)
C(45)	3068(1)	-357(2)	5998(1)	67(1)
C(46)	1916(1)	-433(2)	5630(1)	75(1)
C(47)	2282(1)	1248(2)	6033(1)	73(1)

Table 3. Bond lengths [Å] for 2-76.

C(1)-C(2)	1.498(2)	C(1)-C(6)	1.539(2)	C(1)-C(9)	1.584(2)
C(2)-C(3)	1.316(2)	C(3)-C(4)	1.506(2)	C(4)-C(26)	1.528(2)
C(4)-C(5)	1.5432(19)	C(4)-C(10)	1.556(2)	C(5)-C(6)	1.524(2)
C(6)-C(7)	1.556(2)	C(7)-C(30)	1.476(2)	C(7)-C(32)	1.483(2)
C(7)-C(8)	1.554(2)	C(8)-C(9)	1.546(2)	C(9)-C(34)	1.536(2)
C(9)-C(41)	1.542(2)	C(10)-C(11)	1.538(2)	C(11)-C(19)	1.519(2)
C(11)-C(12)	1.520(2)	C(12)-O(13)	1.1992(18)	C(12)-O(14)	1.3288(19)
O(14)-C(15)	1.4792(19)	C(15)-C(18)	1.514(3)	C(15)-C(16)	1.513(2)
C(15)-C(17)	1.521(3)	C(19)-O(20)	1.2029(19)	C(19)-O(21)	1.3357(18)
O(21)-C(22)	1.4865(19)	C(22)-C(25)	1.505(2)	C(22)-C(24)	1.512(3)
C(22)-C(23)	1.520(2)	C(26)-O(27)	1.1915(19)	C(26)-O(28)	1.3301(19)
O(28)-C(29)	1.4544(19)	C(30)-N(31)	1.1389(19)	C(32)-N(33)	1.137(2)
C(34)-O(35)	1.2024(17)	C(34)-O(36)	1.3301(17)	O(36)-C(37)	1.4900(17)
C(37)-C(38)	1.509(2)	C(37)-C(40)	1.502(2)	C(37)-C(39)	1.510(2)
C(41)-O(42)	1.1998(17)	C(41)-O(43)	1.3299(18)	O(43)-C(44)	1.4870(19)
C(44)-C(45)	1.505(3)	C(44)-C(47)	1.513(2)	C(44)-C(46)	1.519(3)

Table 4. Bond angles (°) for **2-76**.

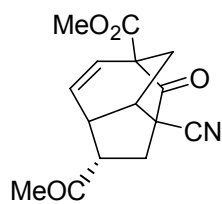
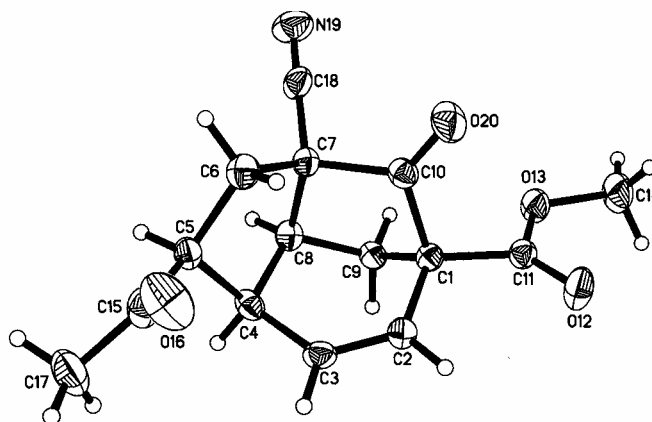
C(2)-C(1)-C(6)	112.88(12)	C(2)-C(1)-C(9)	115.48(12)
C(6)-C(1)-C(9)	107.20(12)	C(3)-C(2)-C(1)	124.45(14)
C(2)-C(3)-C(4)	124.15(14)	C(3)-C(4)-C(26)	113.13(13)
C(3)-C(4)-C(5)	109.91(12)	C(26)-C(4)-C(5)	106.81(12)
C(3)-C(4)-C(10)	106.81(12)	C(26)-C(4)-C(10)	108.00(12)
C(5)-C(4)-C(10)	112.25(12)	C(6)-C(5)-C(4)	111.57(12)
C(5)-C(6)-C(1)	112.90(12)	C(5)-C(6)-C(7)	112.54(12)
C(1)-C(6)-C(7)	102.52(11)	C(30)-C(7)-C(32)	108.55(13)
C(30)-C(7)-C(8)	111.58(12)	C(32)-C(7)-C(8)	109.41(12)
C(30)-C(7)-C(6)	114.23(12)	C(32)-C(7)-C(6)	109.49(12)
C(8)-C(7)-C(6)	103.43(11)	C(9)-C(8)-C(7)	104.44(12)
C(34)-C(9)-C(41)	106.28(12)	C(34)-C(9)-C(8)	112.73(12)
C(41)-C(9)-C(8)	112.74(12)	C(34)-C(9)-C(1)	110.74(12)
C(41)-C(9)-C(1)	109.36(12)	C(8)-C(9)-C(1)	105.02(11)
C(11)-C(10)-C(4)	115.61(12)	C(19)-C(11)-C(12)	109.50(13)
C(19)-C(11)-C(10)	112.32(13)	C(12)-C(11)-C(10)	112.15(12)
O(13)-C(12)-O(14)	126.11(15)	O(13)-C(12)-C(11)	124.16(15)
O(14)-C(12)-C(11)	109.74(13)	C(12)-O(14)-C(15)	121.02(13)
O(14)-C(15)-C(18)	101.93(14)	O(14)-C(15)-C(16)	109.77(14)
C(18)-C(15)-C(16)	111.39(16)	O(14)-C(15)-C(17)	108.53(15)
C(18)-C(15)-C(17)	111.87(16)	C(16)-C(15)-C(17)	112.76(17)
O(20)-C(19)-O(21)	126.03(15)	O(20)-C(19)-C(11)	125.09(15)
O(21)-C(19)-C(11)	108.88(14)	C(19)-O(21)-C(22)	122.14(13)
O(21)-C(22)-C(25)	108.17(14)	O(21)-C(22)-C(24)	110.53(15)
C(25)-C(22)-C(24)	113.25(17)	O(21)-C(22)-C(23)	101.84(13)
C(25)-C(22)-C(23)	111.61(16)	C(24)-C(22)-C(23)	110.81(16)
O(27)-C(26)-O(28)	122.68(16)	O(27)-C(26)-C(4)	123.85(15)
O(28)-C(26)-C(4)	113.43(14)	C(26)-O(28)-C(29)	114.45(14)
N(31)-C(30)-C(7)	178.85(18)	N(33)-C(32)-C(7)	176.52(19)
O(35)-C(34)-O(36)	126.59(14)	O(35)-C(34)-C(9)	122.66(14)
O(36)-C(34)-C(9)	110.70(13)	C(34)-O(36)-C(37)	122.28(12)
O(36)-C(37)-C(38)	109.95(13)	O(36)-C(37)-C(40)	109.07(13)
C(38)-C(37)-C(40)	113.12(16)	O(36)-C(37)-C(39)	102.01(12)
C(38)-C(37)-C(39)	110.06(15)	C(40)-C(37)-C(39)	112.05(16)
O(42)-C(41)-O(43)	126.10(15)	O(42)-C(41)-C(9)	123.93(14)
O(43)-C(41)-C(9)	109.97(13)	C(41)-O(43)-C(44)	120.07(13)
O(43)-C(44)-C(45)	109.43(15)	O(43)-C(44)-C(47)	102.14(14)
C(45)-C(44)-C(47)	111.14(16)	O(43)-C(44)-C(46)	109.25(15)
C(45)-C(44)-C(46)	113.10(18)	C(47)-C(44)-C(46)	111.21(17)

Table 5. Anisotropic displacement parameters [$\text{\AA}^2 \times 10^3$] for **2-76**. The anisotropic displacement factor exponent takes the form: $-2\pi^2 [(ha^*)^2U_{11} + \dots + 2hka^*b^*U_{12}]$

	U11	U22	U33	U23	U13	U12
C(1)	30(1)	25(1)	26(1)	0(1)	0(1)	0(1)
C(2)	32(1)	34(1)	27(1)	1(1)	-3(1)	10(1)
C(3)	24(1)	36(1)	33(1)	-4(1)	-3(1)	7(1)
C(4)	24(1)	28(1)	28(1)	0(1)	1(1)	1(1)
C(5)	27(1)	27(1)	26(1)	1(1)	0(1)	2(1)
C(6)	24(1)	27(1)	26(1)	-2(1)	-1(1)	1(1)
C(7)	23(1)	32(1)	29(1)	1(1)	1(1)	-1(1)
C(8)	27(1)	32(1)	26(1)	0(1)	2(1)	2(1)
C(9)	24(1)	28(1)	26(1)	2(1)	1(1)	0(1)
C(10)	30(1)	29(1)	29(1)	1(1)	4(1)	3(1)
C(11)	28(1)	29(1)	27(1)	0(1)	4(1)	2(1)
C(12)	33(1)	35(1)	29(1)	1(1)	2(1)	-3(1)
O(13)	34(1)	71(1)	42(1)	12(1)	9(1)	13(1)
O(14)	41(1)	44(1)	34(1)	10(1)	9(1)	2(1)
C(15)	55(1)	44(1)	36(1)	9(1)	17(1)	-5(1)
C(16)	76(1)	60(1)	34(1)	-1(1)	9(1)	2(1)
C(17)	69(1)	57(1)	76(2)	1(1)	23(1)	-27(1)
C(18)	106(2)	63(1)	49(1)	24(1)	24(1)	19(1)
C(19)	33(1)	36(1)	31(1)	4(1)	4(1)	0(1)
O(20)	50(1)	69(1)	37(1)	-15(1)	8(1)	-13(1)
O(21)	28(1)	53(1)	33(1)	-1(1)	5(1)	-6(1)
C(22)	31(1)	54(1)	43(1)	8(1)	-3(1)	-13(1)
C(23)	34(1)	83(2)	56(1)	6(1)	9(1)	-12(1)
C(24)	69(1)	58(1)	75(2)	-1(1)	8(1)	-26(1)
C(25)	45(1)	98(2)	63(1)	27(1)	-14(1)	-8(1)
C(26)	28(1)	37(1)	34(1)	-6(1)	3(1)	-2(1)
O(27)	42(1)	48(1)	94(1)	31(1)	5(1)	-4(1)
O(28)	27(1)	52(1)	54(1)	0(1)	5(1)	-7(1)
C(29)	36(1)	62(1)	74(2)	-5(1)	12(1)	-20(1)
C(30)	22(1)	39(1)	32(1)	-4(1)	1(1)	3(1)
N(31)	40(1)	49(1)	48(1)	3(1)	-7(1)	12(1)
C(32)	26(1)	45(1)	36(1)	1(1)	-1(1)	1(1)
N(33)	41(1)	72(1)	69(1)	8(1)	4(1)	-21(1)
C(34)	28(1)	29(1)	29(1)	-1(1)	3(1)	4(1)
O(35)	36(1)	59(1)	36(1)	16(1)	-9(1)	-6(1)
O(36)	25(1)	31(1)	34(1)	4(1)	-2(1)	-3(1)
C(37)	26(1)	34(1)	43(1)	-3(1)	-2(1)	-6(1)
C(38)	29(1)	50(1)	77(2)	11(1)	2(1)	3(1)
C(39)	38(1)	45(1)	86(2)	19(1)	-7(1)	-11(1)
C(40)	70(2)	98(2)	66(2)	-44(1)	12(1)	-39(1)
C(41)	23(1)	36(1)	29(1)	4(1)	-1(1)	1(1)
O(42)	45(1)	35(1)	37(1)	6(1)	7(1)	-1(1)
O(43)	39(1)	41(1)	29(1)	3(1)	10(1)	2(1)
C(44)	46(1)	56(1)	34(1)	9(1)	17(1)	5(1)
C(45)	83(2)	81(2)	36(1)	16(1)	7(1)	23(1)
C(46)	52(1)	94(2)	79(2)	11(1)	28(1)	-20(1)
C(47)	91(2)	80(2)	47(1)	5(1)	35(1)	23(1)

Table 6. Hydrogen coordinates ($\times 10^4$) and isotropic displacement parameters ($\text{\AA}^2 \times 10^3$) for **2-76**.

	x	y	z	U(eq)
H(1)	3330	-445	4334	32
H(2)	4536	-344	4404	37
H(3)	5077	241	3831	37
H(5X)	3763	2235	3860	32
H(5Y)	3381	1941	3429	32
H(6)	2999	281	3717	31
H(8X)	3144	2558	4508	34
H(8Y)	2552	2021	4784	34
H(10X)	4543	-163	3064	35
H(10Y)	3787	-268	3226	35
H(11)	3704	1507	2773	34
H(16X)	5097	331	1602	85
H(16Y)	5069	1031	1177	85
H(16Z)	4397	517	1366	85
H(17X)	5623	1811	2030	101
H(17Y)	5266	2960	2066	101
H(17Z)	5643	2628	1639	101
H(18X)	4224	3345	1631	109
H(18Y)	3854	2393	1383	109
H(18Z)	4528	2906	1195	109
H(23X)	1901	-659	3309	86
H(23Y)	1227	-461	3045	86
H(23Z)	1695	534	3171	86
H(24X)	2367	-1944	2796	101
H(24Y)	2462	-1635	2308	101
H(24Z)	1728	-1873	2491	101
H(25X)	1737	1055	2397	103
H(25Y)	1331	20	2239	103
H(25Z)	2065	260	2056	103
H(29X)	6334	2408	3263	86
H(29Y)	5768	3302	3337	86
H(29Z)	5797	2657	2899	86
H(38X)	5527	1707	4435	78
H(38Y)	5480	1428	4928	78
H(38Z)	5961	2376	4769	78
H(39X)	4617	4180	4450	84
H(39Y)	4956	3318	4140	84
H(39Z)	5416	4058	4436	84
H(40X)	4543	3829	5224	117
H(40Y)	5340	3716	5268	117
H(40Z)	4861	2763	5424	117
H(45X)	3208	-967	5823	100
H(45Y)	2893	-623	6269	100
H(45Z)	3453	113	6050	100
H(46X)	1583	13	5484	112
H(46Y)	1711	-760	5881	112
H(46Z)	2073	-999	5439	112
H(47X)	1933	1641	5878	109
H(47Y)	2663	1727	6087	109
H(47Z)	2100	993	6303	109

**2-79****Table 1.** Crystal data and structure refinement for **2-79**.

Empirical formula	C ₁₅ H ₁₅ NO ₄	
Formula weight	273.28	
Temperature	295(2) K	
Wavelength	0.71073 Å	
Crystal system	Monoclinic	
Space group	P2 ₁ /n	
Unit cell dimensions	<i>a</i> = 9.2003(7) Å	alpha = 90°
	<i>b</i> = 8.9051(6) Å	beta = 96.194(2)°
	<i>c</i> = 16.3638(12) Å	gamma = 90°
Volume, <i>Z</i>	1332.85(17) Å ³ , 4	
Density (calculated)	1.362 Mg/m ³	
Absorption coefficient	0.099 mm ⁻¹	
F(000)	576	
Crystal size	0.42 × 0.16 × 0.15 mm	
θ range for data collection	2.43 to 25.03°	
Limiting indices	-10 ≤ <i>h</i> ≤ 10, -10 ≤ <i>k</i> ≤ 10, -19 ≤ <i>l</i> ≤ 19	
Reflections collected	9072	

Independent reflections	2355 ($R_{\text{int}} = 0.0519$)
Completeness to $\theta = 25.03^\circ$	100.0 %
Absorption correction	None
Refinement method	Full-matrix least-squares on F^2
Data / restraints / parameters	2355 / 0 / 183
Goodness-of-fit on F^2	3.003
Final R indices [$I > 2\sigma(I)$]	$R1 = 0.1070$, $wR2 = 0.1911$
R indices (all data)	$R1 = 0.1135$, $wR2 = 0.1920$
Largest diff. peak and hole	0.459 and $-0.273 \text{ e}\text{\AA}^{-3}$

Table 2. Atomic coordinates [$\times 10^4$] and equivalent isotropic displacement parameters [$\text{\AA}^2 \times 10^3$] for **2-79**. $U(\text{eq})$ is defined as one third of the trace of the orthogonalized U_{ij} tensor.

	x	y	z	U(eq)
C(1)	8075(3)	2215(4)	1456(2)	32(1)
C(2)	7958(4)	2389(4)	2362(2)	36(1)
C(3)	6775(4)	2014(4)	2687(2)	41(1)
C(4)	5418(3)	1393(4)	2197(2)	38(1)
C(5)	4135(4)	2512(4)	2117(2)	37(1)
C(6)	4542(4)	3670(4)	1488(2)	43(1)
C(7)	5503(3)	2753(4)	934(2)	36(1)
C(8)	5693(3)	1165(4)	1296(2)	36(1)
C(9)	7263(3)	752(4)	1172(2)	36(1)
C(10)	7097(3)	3386(4)	993(2)	37(1)
C(11)	9609(4)	2405(4)	1224(2)	36(1)
O(12)	10566(3)	3060(3)	1635(2)	58(1)
O(13)	9718(2)	1851(3)	483(2)	48(1)
C(14)	11098(4)	2074(5)	163(3)	67(1)
C(15)	3786(4)	3176(5)	2921(3)	51(1)
O(16)	4120(4)	4435(4)	3122(2)	85(1)
C(17)	3012(5)	2175(6)	3465(3)	74(2)
C(18)	4923(4)	2696(4)	67(3)	45(1)
N(19)	4512(4)	2561(4)	-614(2)	65(1)
O(20)	7464(3)	4529(3)	705(2)	61(1)

Table 3. Bond lengths [Å] for **2-79**.

C(1)-C(2)	1.506(4)
C(1)-C(11)	1.510(4)
C(1)-C(10)	1.525(5)
C(1)-C(9)	1.548(4)
C(2)-C(3)	1.306(4)
C(3)-C(4)	1.514(5)
C(4)-C(8)	1.536(5)
C(4)-C(5)	1.539(5)
C(5)-C(15)	1.508(5)
C(5)-C(6)	1.532(5)
C(6)-C(7)	1.562(4)
C(7)-C(18)	1.461(5)
C(7)-C(8)	1.537(4)
C(7)-C(10)	1.565(4)
C(8)-C(9)	1.525(4)
C(10)-O(20)	1.185(4)
C(11)-O(12)	1.200(4)
C(11)-O(13)	1.324(4)
O(13)-C(14)	1.439(4)
C(15)-O(16)	1.199(5)
C(15)-C(17)	1.493(6)
C(18)-N(19)	1.144(5)

Table 4. Bond angles (°) for **2-79**.

C(2)-C(1)-C(11)	113.8(3)	C(2)-C(1)-C(10)	108.5(3)
C(11)-C(1)-C(10)	108.4(3)	C(2)-C(1)-C(9)	107.4(3)
C(11)-C(1)-C(9)	116.9(3)	C(10)-C(1)-C(9)	100.7(2)
C(3)-C(2)-C(1)	121.7(3)	C(2)-C(3)-C(4)	123.6(3)
C(3)-C(4)-C(8)	110.2(3)	C(3)-C(4)-C(5)	112.9(3)
C(8)-C(4)-C(5)	102.0(3)	C(15)-C(5)-C(6)	114.4(3)
C(15)-C(5)-C(4)	114.4(3)	C(6)-C(5)-C(4)	104.6(3)
C(5)-C(6)-C(7)	103.5(3)	C(18)-C(7)-C(8)	110.9(3)
C(18)-C(7)-C(6)	114.3(3)	C(8)-C(7)-C(6)	107.7(3)
C(18)-C(7)-C(10)	108.3(3)	C(8)-C(7)-C(10)	104.0(3)
C(6)-C(7)-C(10)	111.2(3)	C(9)-C(8)-C(7)	103.9(2)
C(9)-C(8)-C(4)	114.6(3)	C(7)-C(8)-C(4)	103.0(3)
C(8)-C(9)-C(1)	101.0(2)	O(20)-C(10)-C(1)	127.3(3)
O(20)-C(10)-C(7)	126.2(3)	C(1)-C(10)-C(7)	106.5(3)
O(12)-C(11)-O(13)	124.8(3)	O(12)-C(11)-C(1)	124.3(3)
O(13)-C(11)-C(1)	110.7(3)	C(11)-O(13)-C(14)	116.0(3)
O(16)-C(15)-C(17)	121.3(4)	O(16)-C(15)-C(5)	122.3(4)
C(17)-C(15)-C(5)	116.5(4)	N(19)-C(18)-C(7)	175.5(4)

Table 5. Anisotropic displacement parameters [$\text{\AA}^2 \times 10^3$] for **2-79**. The anisotropic displacement factor exponent takes the form: $-2\pi^2 [(ha^*)^2U_{11} + \dots + 2hka^*b^*U_{12}]$

	U11	U22	U33	U23	U13	U12
C(1)	31(2)	32(2)	34(2)	-1(2)	4(1)	2(1)
C(2)	36(2)	36(2)	35(2)	-6(2)	5(1)	-1(1)
C(3)	44(2)	50(2)	28(2)	0(2)	4(2)	9(2)
C(4)	44(2)	31(2)	42(2)	5(2)	14(2)	0(2)
C(5)	33(2)	43(2)	36(2)	-3(2)	8(1)	-3(1)
C(6)	43(2)	42(2)	47(2)	-3(2)	8(2)	7(2)
C(7)	32(2)	43(2)	35(2)	0(2)	6(1)	2(2)
C(8)	36(2)	30(2)	41(2)	-5(2)	5(2)	-3(1)
C(9)	38(2)	34(2)	37(2)	1(2)	8(2)	-1(1)
C(10)	39(2)	36(2)	36(2)	0(2)	9(2)	3(2)
C(11)	33(2)	36(2)	39(2)	1(2)	5(2)	2(1)
O(12)	37(1)	78(2)	61(2)	-19(2)	7(1)	-11(1)
O(13)	38(1)	70(2)	39(2)	-6(1)	12(1)	0(1)
C(14)	45(2)	102(4)	57(3)	-5(3)	24(2)	-1(2)
C(15)	42(2)	61(3)	52(2)	-12(2)	10(2)	1(2)
O(16)	121(3)	66(2)	74(2)	-28(2)	39(2)	-18(2)
C(17)	70(3)	103(4)	55(3)	-7(3)	28(2)	-20(3)
C(18)	34(2)	55(2)	46(2)	-2(2)	5(2)	8(2)
N(19)	71(2)	81(3)	41(2)	0(2)	-6(2)	13(2)
O(20)	54(2)	39(2)	93(2)	17(2)	17(2)	1(1)

Table 6. Hydrogen coordinates ($\times 10^4$) and isotropic displacement parameters ($\text{\AA}^2 \times 10^3$) for **2-79**.

	x	y	z	U(eq)
H(2)	8750	2774	2699	43
H(3)	6765	2135	3251	49
H(4)	5124	445	2436	46
H(5)	3264	1975	1874	45
H(6X)	5091	4496	1756	52
H(6Y)	3677	4064	1168	52
H(8)	4991	458	1015	43
H(9X)	7364	530	600	43
H(9Y)	7607	-98	1510	43
H(14X)	11299	3130	136	100
H(14Y)	11059	1648	-378	100
H(14Z)	11859	1593	517	100
H(17X)	2993	2642	3992	111
H(17Y)	3517	1232	3530	111
H(17Z)	2029	2008	3221	111

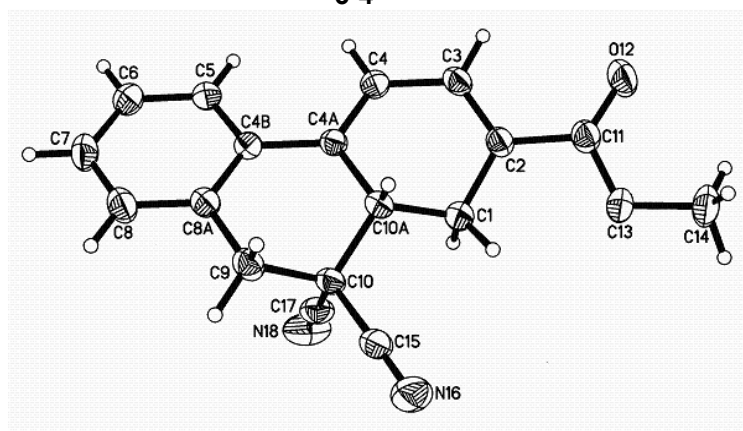
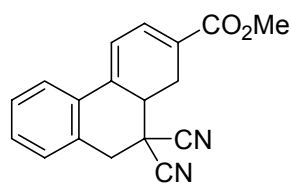


Table 1. Crystal data and structure refinement for **3-4**.

Empirical formula	$C_{18}H_{14}N_2O_2$	
Formula weight	290.31	
Temperature	150(1) K	
Wavelength	0.71073 Å	
Crystal system	Monoclinic	
Space group	$P2_1/c$	
Unit cell dimensions	$a = 10.4271(6)$ Å	$\alpha = 90^\circ$
	$b = 6.7971(4)$ Å	$\beta = 96.513(1)^\circ$
	$c = 20.6619(11)$ Å	$\gamma = 90^\circ$
Volume, Z	$1454.94(14)$ Å ³ , 4	
Density (calculated)	1.325 Mg/m ³	
Absorption coefficient	0.088 mm ⁻¹	
$F(000)$	608	
Crystal size	0.31 × 0.30 × 0.14 mm	
θ range for data collection	1.97 to 27.88°	
Limiting indices	$-13 \leq h \leq 13, -8 \leq k \leq 8, -27 \leq l \leq 27$	
Reflections collected	14917	
Independent reflections	3473 ($R_{int} = 0.0523$)	
Completeness to $\theta = 27.88^\circ$	100.0 %	
Absorption correction	None	

Refinement method	Full-matrix least-squares on F ²
Data / restraints / parameters	3473 / 0 / 201
Goodness-of-fit on F ²	2.201
Final R indices [I > 2σ (I)]	R1 = 0.0601, wR2 = 0.1100
R indices (all data)	R1 = 0.0691, wR2 = 0.1115
Extinction coefficient	0.0063(11)
Largest diff. peak and hole	0.340 and -0.241 eÅ ⁻³

Table 2. Atomic coordinates [$\times 10^4$] and equivalent isotropic displacement parameters [$\text{\AA}^2 \times 10^3$] for **3-4**. U(eq) is defined as one third of the trace of the orthogonalized U_{ij} tensor.

	x	y	z	U(eq)
C(1)	-917(1)	2092(2)	890(1)	31(1)
C(2)	-2096(1)	2623(2)	1197(1)	27(1)
C(3)	-1990(1)	2976(2)	1840(1)	29(1)
C(4)	-751(1)	2943(2)	2234(1)	28(1)
C(4A)	373(1)	2960(2)	1956(1)	24(1)
C(4B)	1661(1)	3072(2)	2334(1)	25(1)
C(5)	1835(1)	2798(2)	3012(1)	28(1)
C(6)	3046(1)	2919(2)	3358(1)	35(1)
C(7)	4115(1)	3310(2)	3040(1)	41(1)
C(8)	3973(1)	3566(2)	2373(1)	38(1)
C(8A)	2757(1)	3448(2)	2017(1)	28(1)
C(9)	2642(1)	3725(2)	1289(1)	31(1)
C(10)	1529(1)	2465(2)	959(1)	27(1)
C(10A)	264(1)	3075(2)	1225(1)	32(1)
C(11)	-3374(1)	2701(2)	809(1)	32(1)
O(12)	-4355(1)	3251(2)	1008(1)	51(1)
C(13)	-3321(1)	2121(2)	192(1)	42(1)
C(14)	-4494(2)	2311(3)	-249(1)	49(1)
C(15)	1420(1)	2786(2)	243(1)	32(1)
N(16)	1355(1)	3073(2)	-303(1)	45(1)
C(17)	1792(1)	353(2)	1088(1)	33(1)
N(18)	1986(2)	-1260(2)	1206(1)	53(1)

Table 3. Bond lengths [Å] for **3-4**.

C(1)-C(2)	1.4904(18)
C(1)-C(10A)	1.4998(18)
C(2)-C(3)	1.3436(18)
C(2)-C(11)	1.4763(18)
C(3)-C(4)	1.4469(18)
C(4)-C(4A)	1.3619(18)
C(4A)-C(4B)	1.4761(17)
C(4A)-C(10A)	1.5045(18)
C(4B)-C(5)	1.4037(18)
C(4B)-C(8A)	1.4046(18)
C(5)-C(6)	1.3813(18)
C(6)-C(7)	1.382(2)
C(7)-C(8)	1.380(2)
C(8)-C(8A)	1.3943(18)
C(8A)-C(9)	1.5074(18)
C(9)-C(10)	1.5374(18)
C(10)-C(17)	1.480(2)
C(10)-C(15)	1.4877(18)
C(10)-C(10A)	1.5417(18)
C(11)-O(12)	1.2040(16)
C(11)-C(13)	1.3402(16)
C(13)-C(14)	1.4461(17)
C(15)-N(16)	1.1398(17)
C(17)-N(18)	1.1359(19)

Table 4. Bond angles (°) for **3-4**.

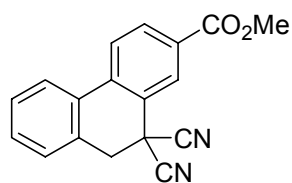
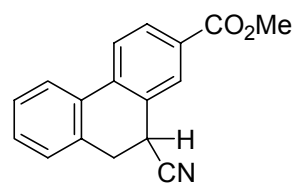
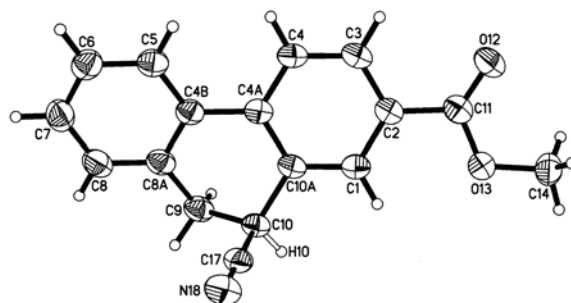
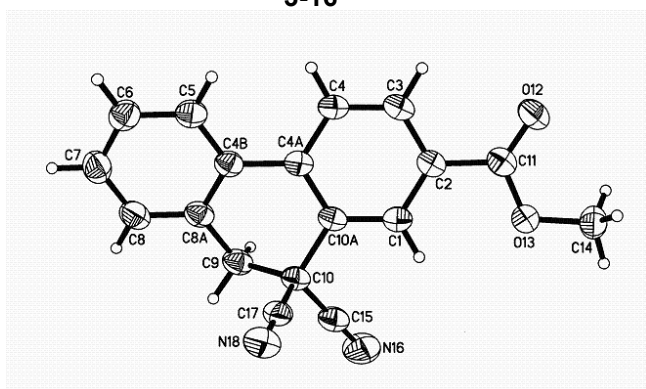
C(2)-C(1)-C(10A)	111.68(11)	C(3)-C(2)-C(11)	119.92(12)
C(3)-C(2)-C(1)	119.04(12)	C(11)-C(2)-C(1)	121.01(12)
C(2)-C(3)-C(4)	121.40(12)	C(4A)-C(4)-C(3)	121.32(12)
C(4)-C(4A)-C(4B)	123.53(12)	C(4)-C(4A)-C(10A)	116.93(12)
C(4B)-C(4A)-C(10A)	119.25(11)	C(5)-C(4B)-C(8A)	118.00(12)
C(5)-C(4B)-C(4A)	121.85(11)	C(8A)-C(4B)-C(4A)	120.15(11)
C(6)-C(5)-C(4B)	121.09(12)	C(5)-C(6)-C(7)	120.27(13)
C(8)-C(7)-C(6)	119.86(13)	C(7)-C(8)-C(8A)	120.54(13)
C(8)-C(8A)-C(4B)	120.24(12)	C(8)-C(8A)-C(9)	118.99(12)
C(4B)-C(8A)-C(9)	120.77(11)	C(8A)-C(9)-C(10)	110.06(11)
C(17)-C(10)-C(15)	108.25(11)	C(17)-C(10)-C(9)	110.20(11)
C(15)-C(10)-C(9)	109.11(11)	C(17)-C(10)-C(10A)	110.23(11)
C(15)-C(10)-C(10A)	110.05(11)	C(9)-C(10)-C(10A)	108.99(11)
C(1)-C(10A)-C(4A)	113.88(11)	C(1)-C(10A)-C(10)	113.96(11)
C(4A)-C(10A)-C(10)	111.94(11)	O(12)-C(11)-C(13)	122.99(13)
O(12)-C(11)-C(2)	125.07(13)	C(13)-C(11)-C(2)	111.92(12)
C(11)-C(13)-C(14)	116.70(11)	N(16)-C(15)-C(10)	178.28(16)
N(18)-C(17)-C(10)	177.96(15)		

Table 5. Anisotropic displacement parameters [$\text{\AA}^2 \times 10^3$] for **3-4**. The anisotropic displacement factor exponent takes the form: $-2\pi^2 [(ha^*)^2U_{11} + \dots + 2hka^*b^*U_{12}]$

	U11	U22	U33	U23	U13	U12
C(1)	25(1)	42(1)	26(1)	-2(1)	3(1)	1(1)
C(2)	22(1)	31(1)	29(1)	2(1)	3(1)	1(1)
C(3)	21(1)	35(1)	31(1)	1(1)	7(1)	2(1)
C(4)	27(1)	34(1)	24(1)	1(1)	4(1)	1(1)
C(4A)	23(1)	25(1)	23(1)	0(1)	3(1)	2(1)
C(4B)	24(1)	26(1)	25(1)	-2(1)	2(1)	1(1)
C(5)	27(1)	32(1)	26(1)	-1(1)	4(1)	0(1)
C(6)	34(1)	44(1)	25(1)	0(1)	-1(1)	2(1)
C(7)	26(1)	62(1)	34(1)	-3(1)	-6(1)	-1(1)
C(8)	24(1)	55(1)	36(1)	1(1)	4(1)	-2(1)
C(8A)	24(1)	34(1)	27(1)	0(1)	4(1)	1(1)
C(9)	24(1)	39(1)	31(1)	4(1)	6(1)	-1(1)
C(10)	23(1)	37(1)	23(1)	1(1)	6(1)	4(1)
C(10A)	22(1)	48(1)	27(1)	-6(1)	5(1)	4(1)
C(11)	25(1)	40(1)	30(1)	4(1)	3(1)	0(1)
O(12)	24(1)	89(1)	39(1)	0(1)	4(1)	9(1)
C(13)	27(1)	68(1)	30(1)	-6(1)	-4(1)	4(1)
C(14)	32(1)	77(1)	36(1)	2(1)	-10(1)	2(1)
C(15)	28(1)	40(1)	29(1)	1(1)	7(1)	6(1)
N(16)	48(1)	58(1)	30(1)	5(1)	8(1)	10(1)
C(17)	35(1)	40(1)	26(1)	0(1)	10(1)	3(1)
N(18)	76(1)	43(1)	45(1)	3(1)	21(1)	13(1)

Table 6. Hydrogen coordinates ($\times 10^4$) and isotropic displacement parameters ($\text{\AA}^2 \times 10^3$) for **3-4**.

	x	y	z	U(eq)
H(1X)	-1033	2486	426	37
H(1Y)	-796	647	909	37
H(3)	-2746	3253	2041	35
H(4)	-720	2909	2695	34
H(5)	1109	2524	3236	34
H(6)	3145	2733	3817	42
H(7)	4946	3401	3280	49
H(8)	4710	3825	2155	46
H(9X)	3460	3338	1124	37
H(9Y)	2479	5129	1181	37
H(10A)	155	4505	1119	39
H(14X)	-5237	1969	-20	74
H(14Y)	-4458	1423	-620	74
H(14Z)	-4582	3671	-405	74

**3-16****3-17****Table 1.** Crystal data and structure refinement for **3-16** and **3-17**.

Empirical formula	$C_{17.90}H_{12.10}N_{1.90}O_2$	
Formula weight	285.79	
Temperature	200(1) K	
Wavelength	0.71073 Å	
Crystal system	Monoclinic	
Space group	C2/c	
Unit cell dimensions	$a = 15.3039(8)$ Å	$\alpha = 90^\circ$
	$b = 12.3670(7)$ Å	$\beta = 94.876(1)^\circ$
	$c = 14.8618(8)$ Å	$\gamma = 90^\circ$
Volume, Z	$2802.6(3)$ Å ³ , 8	
Density (calculated)	1.355 Mg/m ³	
Absorption coefficient	0.090 mm ⁻¹	
F(000)	1190	
Crystal size	0.46 × 0.27 × 0.23 mm	
θ range for data collection	2.12 to 27.47°	
Limiting indices	$-19 \leq h \leq 19, -16 \leq k \leq 16, -19 \leq l \leq 19$	
Reflections collected	13966	
Independent reflections	3208 ($R_{\text{int}} = 0.0382$)	
Completeness to $\theta = 27.47^\circ$	100.0 %	
Absorption correction	None	

Refinement method	Full-matrix least-squares on F^2
Data / restraints / parameters	3208 / 0 / 201
Goodness-of-fit on F^2	2.278
Final R indices [$I > 2\sigma(I)$]	R1 = 0.0432, wR2 = 0.1033
R indices (all data)	R1 = 0.0512, wR2 = 0.1043
Extinction coefficient	0.0023(5)
Largest diff. peak and hole	0.248 and -0.189 e \AA^{-3}

Table 2. Atomic coordinates [$\times 10^4$] and equivalent isotropic displacement parameters [$\text{\AA}^2 \times 10^3$] for **3-16** and **3-17**. $U(\text{eq})$ is defined as one third of the trace of the orthogonalized U_{ij} tensor.

	x	y	z	U(eq)
C(1)	1493(1)	3089(1)	758(1)	35(1)
C(2)	2104(1)	3739(1)	370(1)	34(1)
C(3)	1857(1)	4283(1)	-428(1)	38(1)
C(4)	1012(1)	4205(1)	-823(1)	37(1)
C(4A)	382(1)	3575(1)	-437(1)	32(1)
C(4B)	-531(1)	3504(1)	-846(1)	34(1)
C(5)	-890(1)	4284(1)	-1447(1)	39(1)
C(6)	-1745(1)	4196(1)	-1823(1)	44(1)
C(7)	-2256(1)	3334(1)	-1598(1)	48(1)
C(8)	-1913(1)	2555(1)	-998(1)	45(1)
C(8A)	-1054(1)	2629(1)	-618(1)	37(1)
C(9)	-656(1)	1768(1)	-1(1)	41(1)
C(10)	-29(1)	2267(1)	760(1)	36(1)
C(10A)	648(1)	2999(1)	350(1)	33(1)
C(11)	3012(1)	3870(1)	787(1)	38(1)
O(12)	3567(1)	4407(1)	470(1)	53(1)
O(13)	3150(1)	3316(1)	1554(1)	46(1)
C(14)	4013(1)	3406(1)	2021(1)	48(1)
C(15)	423(1)	1393(1)	1301(1)	44(1)
N(16)	775(1)	722(1)	1708(1)	68(1)
C(17)	-544(1)	2910(1)	1372(1)	38(1)
N(18)	-951(1)	3400(1)	1836(1)	50(1)

Table 3. Bond lengths [Å] for **3-16** and **3-17**.

C(1)-C(10A)	1.3858(17)
C(1)-C(2)	1.3945(17)
C(2)-C(3)	1.3866(18)
C(2)-C(11)	1.4815(18)
C(3)-C(4)	1.3776(18)
C(4)-C(4A)	1.4009(17)
C(4A)-C(10A)	1.3996(17)
C(4A)-C(4B)	1.4779(17)
C(4B)-C(5)	1.3961(18)
C(4B)-C(8A)	1.4038(17)
C(5)-C(6)	1.3827(18)
C(6)-C(7)	1.379(2)
C(7)-C(8)	1.385(2)
C(8)-C(8A)	1.3894(18)
C(8A)-C(9)	1.5008(19)
C(9)-C(10)	1.5468(18)
C(10)-C(15)	1.483(2)
C(10)-C(17)	1.4842(18)
C(10)-C(10A)	1.5403(16)
C(11)-O(12)	1.2044(15)
C(11)-O(13)	1.3319(16)
O(13)-C(14)	1.4426(16)
C(15)-N(16)	1.136(2)
C(17)-N(18)	1.1419(17)

Table 4. Bond angles (°) for **3-16** and **3-17**.

C(10A)-C(1)-C(2)	119.93(12)	C(3)-C(2)-C(1)	119.28(12)
C(3)-C(2)-C(11)	118.86(11)	C(1)-C(2)-C(11)	121.86(12)
C(4)-C(3)-C(2)	120.62(11)	C(3)-C(4)-C(4A)	121.16(12)
C(10A)-C(4A)-C(4)	117.65(12)	C(10A)-C(4A)-C(4B)	120.76(11)
C(4)-C(4A)-C(4B)	121.59(11)	C(5)-C(4B)-C(8A)	119.08(12)
C(5)-C(4B)-C(4A)	121.97(11)	C(8A)-C(4B)-C(4A)	118.95(11)
C(6)-C(5)-C(4B)	120.76(12)	C(7)-C(6)-C(5)	119.98(13)
C(6)-C(7)-C(8)	120.07(13)	C(7)-C(8)-C(8A)	120.69(13)
C(8)-C(8A)-C(4B)	119.41(12)	C(8)-C(8A)-C(9)	121.51(12)
C(4B)-C(8A)-C(9)	119.02(12)	C(8A)-C(9)-C(10)	110.94(10)
C(15)-C(10)-C(17)	107.79(11)	C(15)-C(10)-C(10A)	110.16(11)
C(17)-C(10)-C(10A)	109.69(10)	C(15)-C(10)-C(9)	109.71(11)
C(17)-C(10)-C(9)	109.45(11)	C(10A)-C(10)-C(9)	110.00(10)
C(1)-C(10A)-C(4A)	121.28(11)	C(1)-C(10A)-C(10)	120.58(11)
C(4A)-C(10A)-C(10)	118.13(11)	O(12)-C(11)-O(13)	123.55(12)
O(12)-C(11)-C(2)	124.32(12)	O(13)-C(11)-C(2)	112.13(11)
C(11)-O(13)-C(14)	116.37(10)	N(16)-C(15)-C(10)	179.19(18)
N(18)-C(17)-C(10)	179.07(15)		

Table 5. Anisotropic displacement parameters [$\text{\AA}^2 \times 10^3$] for **3-16** and **3-17**. The anisotropic displacement factor exponent takes the form: $-2\pi^2 [(ha^*)^2U_{11} + \dots + 2hka^*b^*U_{12}]$

	U11	U22	U33	U23	U13	U12
C(1)	40(1)	31(1)	34(1)	2(1)	7(1)	1(1)
C(2)	36(1)	30(1)	37(1)	-2(1)	9(1)	-1(1)
C(3)	41(1)	36(1)	40(1)	1(1)	12(1)	-6(1)
C(4)	44(1)	34(1)	33(1)	5(1)	8(1)	-3(1)
C(4A)	39(1)	28(1)	31(1)	-2(1)	7(1)	-2(1)
C(4B)	37(1)	35(1)	29(1)	-4(1)	8(1)	-1(1)
C(5)	44(1)	38(1)	34(1)	-2(1)	8(1)	0(1)
C(6)	45(1)	51(1)	36(1)	-1(1)	6(1)	7(1)
C(7)	37(1)	66(1)	40(1)	-6(1)	4(1)	-2(1)
C(8)	43(1)	55(1)	39(1)	-5(1)	10(1)	-12(1)
C(8A)	41(1)	39(1)	32(1)	-4(1)	9(1)	-5(1)
C(9)	47(1)	36(1)	41(1)	-1(1)	9(1)	-11(1)
C(10)	40(1)	34(1)	36(1)	5(1)	8(1)	-4(1)
C(10A)	38(1)	28(1)	34(1)	0(1)	10(1)	-3(1)
C(11)	40(1)	31(1)	42(1)	-4(1)	9(1)	-2(1)
O(12)	44(1)	54(1)	62(1)	11(1)	7(1)	-13(1)
O(13)	38(1)	58(1)	42(1)	8(1)	1(1)	-7(1)
C(14)	39(1)	59(1)	45(1)	-3(1)	-1(1)	-4(1)
C(15)	48(1)	40(1)	46(1)	10(1)	10(1)	-7(1)
N(16)	75(1)	54(1)	73(1)	29(1)	7(1)	1(1)
C(17)	39(1)	40(1)	34(1)	6(1)	5(1)	-9(1)
N(18)	54(1)	52(1)	47(1)	2(1)	14(1)	-5(1)

Table 6. Hydrogen coordinates ($\times 10^4$) and isotropic displacement parameters ($\text{\AA}^2 \times 10^3$) for **3-16** and **3-17**.

	x	y	z	U(eq)
H(1)	1656	2709	1302	42
H(3)	2274	4712	-704	46
H(4)	854	4586	-1368	44
H(5)	-543	4883	-1600	46
H(6)	-1981	4728	-2236	53
H(7)	-2844	3275	-1855	57
H(8)	-2268	1965	-846	54
H(9X)	-328	1250	-353	49
H(9Y)	-1128	1365	269	49
H(14X)	4457	3279	1595	72
H(14Y)	4078	2868	2506	72
H(14Z)	4089	4132	2280	72
H(10)	280	1673	1111	36